

https://dspace.org/

Stratigraphy and sedimentary environments of the Late Permian Dicynodon Assemblage Zone (Karoo Supergroup, South Africa) and implications for basin development

Viglietti, Pia Alexa

2016

http://hdl.handle.net/10539/21691

Viglietti, Pia Alexa (2016) Stratigraphy and sedimentary environments of the Late Permian Dicynodon Assemblage Zone (Karoo Supergroup, South Africa) and implications for basin development, University of Witwatersrand, Johannesburg, <http://wiredspace.wits.ac.za/handle/10539/21691>

Downloaded from a DSpace repository. https://dspace.org/

Stratigraphy and sedimentary environments of the Late Permian *Dicynodon* Assemblage Zone (Karoo Supergroup, South Africa) and implications for basin development



Pia Alexa Viglietti

A thesis submitted to the Faculty of Science, University of the Witwatersrand, Johannesburg in fulfilment of the requirements for the degree of Doctor of Philosophy

June 2016

Supervisors: Prof. Bruce S. Rubidge and Prof. Roger M.H. Smith

Declaration

I declare that this thesis is my own, unaided work, except where specified in the text. It is being submitted for the Degree of Doctor of Philosophy in the University of the Witwatersrand, Johannesburg. This work has not been previously submitted to any other University or academic institution.



(Signature of candidate)

1st day of June 2016

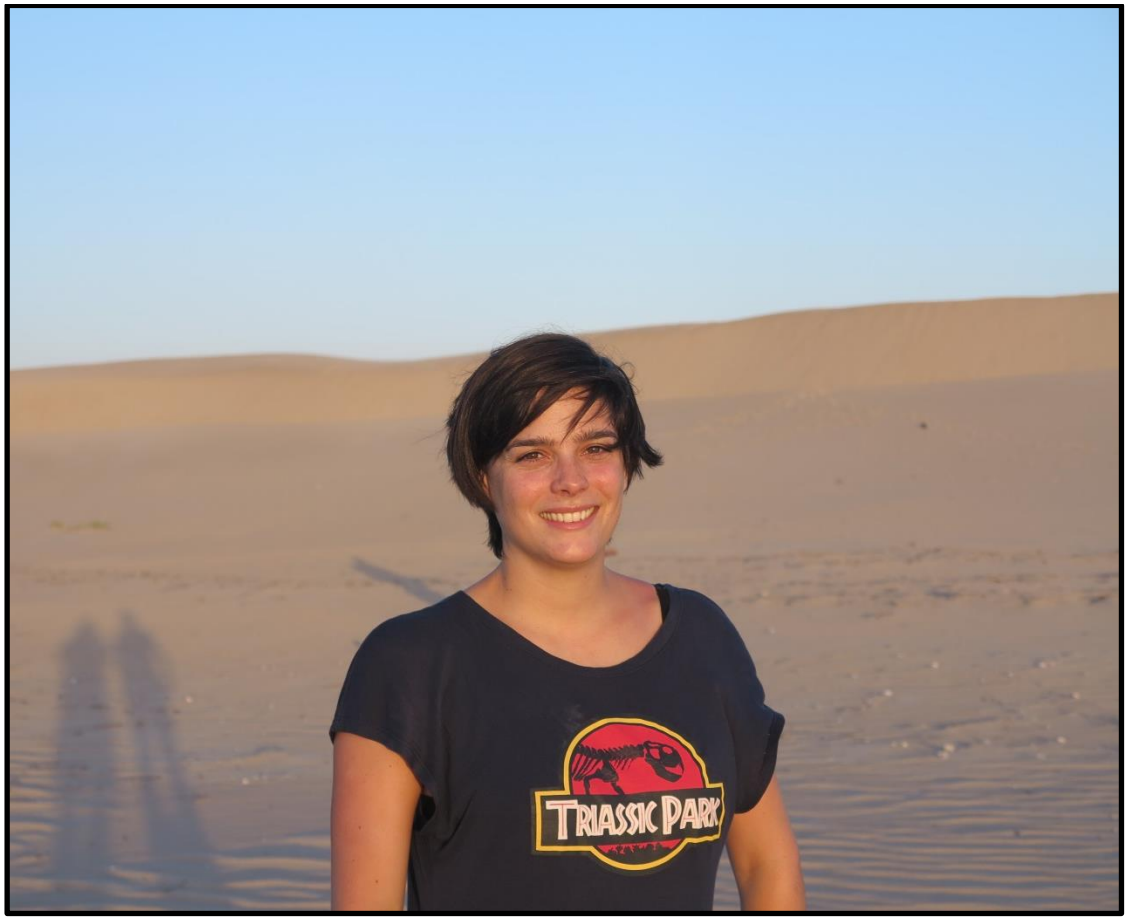

Abstract

The *Dicynodon* Assemblage Zone (DiAZ) spans the last three million years of the Late Permian (Lopingian) Beaufort Group (Karoo Supergroup). Fluvio-lacustrine conditions covered the entire Karoo Basin during this period, preserved as the rocks of the Balfour, Teekloof, and Normandien formations. However widely separated exposures and few dateable horizons make correlating between lithostratigraphic subdivisions difficult. Here a revised litho- and biostratigraphic framework is provided for the Upper Permian DiAZ. The Balfour Formation's Barberskrans Member (BM) is renamed due to identifying the Oudeberg Member and not the BM at the current type locality (Barberskrans Cliffs). It is renamed Ripplemead member (RM) after Ripplemead farm 20 km north of Nieu Bethesda where it outcrops. The Teekloof Formation's Javanerskop member and Musgrave Grit unit in the central Free State Province are regarded mappable units whereas the Boomplaas sandstone (BS) may represent a unit that is a lateral equivalent to the Oudeberg Member. Palaeontological and detrital zircon data suggest none of these locally persistent sandstone horizons correlate temporally.

Three index fossils that currently define the DiAZ (*Dicynodon lacerticeps*, *Theriognathus microps*, and *Procynosuchus delaharpeae*) appear below its lower boundary and disappear below the Permo-Triassic Boundary (PTB), coincidentally with the appearance of *Lystrosaurus maccaigi*. The base of the DiAZ is redefined, with the revived *Daptocephalus leoniceps* and *T. microps* re-established as the index fossil for the newly proposed *Daptocephalus* Assemblage Zone (DaAZ), and is subdivided into two subzones. *Da. leoniceps* and *T. microps'* appearance define the lower and *L. maccaigi* defines the base of the upper subzone. The same patterns of disappearance are observed at the same stratigraphic interval throughout the basin, despite the thinning of strata northward. Additionally wetter floodplain conditions prevailed in the Lower DaAZ than in the Upper DaAZ which likely reflects climatic changes associated with the Permo-Triassic mass extinction (PTME).

Palaeocurrent and detrital zircon data demonstrate a southerly source area, and recycled orogen petrography indicates the Cape Supergroup is the source of Upper Permian strata. Dominant late Permian zircon population supports the foreland nature of the Karoo Basin. Orogenic loading/unloading events are identified by two fining-upward cycles, separated by a diachronous third-order subaerial unconformity at the base of the RM and Javanerskop members. Sediment progradation northwards was out-of-phase with the south and wedge-shaped. Distributive fluvial systems depositing sediment within a retroarc foreland basin best explains these observations. Lithostratigraphic beds and members are recommended for use as local marker horizons only in conjunction with other proxies, such as index fossils or radiometric dates in future studies.

Acknowledgements

Submitting a PhD such as this one would not be possible without support from many people along the way. Therefore, I cannot go any further without extending my gratitude to my supervisors Prof. Bruce Rubidge and Prof. Roger Smith. I thank Bruce for his guidance, encouragement, and helping me to see my potential in becoming an independent researcher. Bruce's knowledge of the Karoo was invaluable in this project and it will always be a privilege to have worked with someone who has a passion for Karoo palaeontology and a family with such a steeped history in the field. I also want to thank Roger for his mentorship over the years. I met Roger as an undergraduate when I was investigating an honours project in Palaeontology, and since then we have had many discussions over coffee at Iziko South African Museum where he shared his inexhaustive knowledge of the Karoo. Some of my first fossil collecting trips were with Roger and his unfailing field team (Zaituna Erasmus, Annelize Crean, Georgina Farrell, Nolusindiso Matalana , Sibusiso Mtungata, Paul October, Mike Strong, Derik Wolfaardt, Derik Ohland), who not only fostered my keen interest in the rocks and fossils of the Karoo but also made the work great fun.

Funding was also a very important component to the success of this PhD, so I am very grateful to the National Research Foundation (NRF), African Origins Platform (AOP), DST/NRF Centre of Excellence in Palaeosciences (CoE in Palaeosciences), and Palaeontological Scientific Trust (PAST) for their generous financial support during the completion of this thesis. The funding also paid for the detrital zircon dating I conducted during this study, which would not have been possible without the help of Dr. Dirk Frei from the Central Analytical Facility at Stellenbosch University, who processed and dated all of my samples. Funding also helped to pay for thin section samples, so a big thanks you to Musa Cebekhulu from Wits School of Geosciences who cut and polished all of my thin sections samples.

Fieldtrips I needed to complete for this investigation would have not been successful without all the different personalities who made the fieldwork all the more fun and/or fossiliferous by their presence. I'd like to thank Dr. Michael Day, Marc Van Den Brandt, Cameron Penn-Clarke, Gina Viglietti, Guy Thomas, Rachel Anderson, Dr. Aurore Val, and Dr. Paloma De la Peña. I am indebted to you all for your company, discussions, guidance, and sense of humour, especially during times when I nearly lost mine.

The hospitality and kindness of people that I met in the Karoo throughout my fieldwork was incredible, and without it much of the work would have been near impossible to do. Many of these individuals are deserving of special recognition for providing me not only with the

opportunity to work on their land, but also for providing shelter, sometimes even in their own homes. My first fieldtrip I conducted was a solo trip to Nieu Bethesda where I stayed with Sunet and Kosie Wolfaardt at Onverwags. It was through them that I was introduced to the Saturday night tennis club parties in the town and in this way met many other farmers in the area who then allowed me access onto their properties. Other farmers from the Nieu Bethesda area who were also of great help during fieldwork were Leonard Kingwill of Ripplemead, and James Brodie from Doornplaats.

Near Cradock I had the pleasure of meeting Alex, Barrie, David, and Taryn Pringle from Eildon who accommodated me on three occasions in the Baviaansrivier Valley. Additionally farmers from the Cradock and Baviaansriver Valley who were also very accommodating were Ernest and Anne Pringle from Huntly Glen. Ernest has an amazing knowledge for the natural world and kindly shared this knowledge. Ernest houses the largest amateur butterfly collection in the southern hemisphere and I highly recommend visiting it. I would also like to thank Andrew and Roxanne Pringle from Kelso, Vivian and Clive Kaywood from Lower Clifton, Noel and Janet Ross from Craig Rennie, Francois Marais from Skelmkloof, and Fanie Fererra from Hales Owen.

The farmers from Gariep Dam and Jagersfontein were also very welcoming and accommodating when I needed to measure sections and prospect for fossils on their land. They included Marcel Mellet from Inhoek, Meyer and Carina van Der Walt from Schalkwykskraal and Tierhoek, and Charlie van Der Heefer from van Wyksfontein. Neels Visser from Excelsior was also very helpful in gaining access to Boomplaas Hill near Jagersfontein. Returning from fieldtrips with lots of heavy fossils and equipment meant help from Sifelani Jirah, Charlton Dube, Gerry Germishuizen, Pepson Mukanela, Thilivhali Nemavhundi, Gilbert Mokgethoa, and Gladys Mokoma did not go unnoticed. I am grateful to all the technical staff for helping me pack and put equipment away, check the vehicles, and also for the preparation and accessioning of fossils.

Finally thank you to my family, loved ones, and friends who have always supported me and my career choice over these years. Your support has resulted in putting up with my frequent absences due to fieldtrips and conferences in order to pursue my studies, so I will always be grateful for your encouragement to achieve my goals.

Table of Contents

Chapter 1: Literature Review 1

1.1 Background to this study 1

1.2 Lithostratigraphic Review of the Upper Permian (Lopingian) Beaufort Group 6

1.3 Lithological properties of the Balfour, Teekloof, and Katberg formations 10

1.4 Thickness of the Balfour and Teekloof formations 22

1.5 Review of the biostratigraphy of the Upper Permian Beaufort Group 23

Chapter 2: Present Investigation 26

2.1 Aims 26

2.2. Preliminary work 27

2.3 Materials and methods 27

Chapter 3: Results 40

3.1 Status of the Barberskrans Member 41

3.2 Stratigraphic sections 44

3.3 Biostratigraphic investigation 86

3.4 Palaeocurrent investigation 110

3.5 Petrography 114

3.6 Detrital zircon age populations of rock samples from the Beaufort Group 122

Chapter 4: Facies and architectural element analysis 168

4.1 Lithofacies 168

4.2 Facies associations 172

4.3 Architectural element analysis 188

4.4 Recognition of architectural types in the study area 190

4.5. Interpretation of identified architectural types 207

Chapter 5: Discussion 214

5.1 New stratigraphic framework for the Upper Permian Karoo Basin 215

5.2 Distribution of Lopingian fauna within the Balfour and Teekloof formations 217

5.3 Palaeoenvironmental interpretation of the Daptocephalus Assemblage Zone 220

5.4 Provenance of the Upper Permian – Lower Triassic Beaufort Group 227

5.5 Basin Development model for the Lopingian Karoo Basin 234

Chapter 6: Conclusions 242

Chapter 7: References 246

Chapter 1: Literature Review

1.1 Background to this study

The Upper Carboniferous to Middle Jurassic sedimentary succession of the South African Karoo Supergroup has a maximum thickness of approximately 6 km (Lindeque et al. 2007; 2011; Scheiber-Enslin et al. 2015). It is known worldwide for its unique record of some of the earliest established terrestrial ecosystems (Sumida and Martin, 1997), evolution of major tetrapod groups, and also the greatest known biotic crisis at the end of the Permian (Smith, 1995; Smith and Ward, 2001; Smith and Botha, 2005; Botha and Smith, 2006; Shen et al. 2011; Bottjer, 2012; Sun et al. 2012; Fröbisch, 2013; Ruta et al. 2013; Benton and Newell, 2014; Burgess et al. 2014; Smith and Botha-Brink, 2014). Additionally smaller en-echelon rift basins within southern Africa created by Permo-Carboniferous crustal extension, and Triassic strike-slip movements preserve sedimentary deposits that correlate with the main Karoo Basin and have warranted further investigation (De Wit et al. 1988; Smith et al. 1993; Zerfass et al. 2004; Catuneanu et al. 2005; Abdala et al. 2013).

The Karoo Basin of South Africa is supported by the Kaapvaal Craton in the northeast and the Namaqua-Natal Metamorphic Belt (NNMB) in the southwest (Catuneanu et al. 1998; Tankard et al. 2009). Many theories have been used in the past to explain the origin of accommodation in the Karoo Basin and its significant distance from the Palaeo-Pacific subduction zone to the south (> 1500 km) (Pysklywec and Mitrovica, 1999) which include activation of the Southern Cape Conductive Belt, a crustal geophysical anomaly (De Wit et al. 1988), fault controlled subsidence (Turner, 1999; Tankard et al. 2009), and even continent-continent collision with south dipping subduction zone (Lindeque et al. 2011). Currently, it is generally accepted that flexural tectonics (imposed by orogenic loading) and dynamic subsidence (imposed by flat slab subduction) were the two most important controls on accommodation in the main Karoo Basin (Visser and Dukas, 1979; Lock, 1980; Cole, 1992; Visser, 1992, 1993; Le Roux, 1995; Pysklywec and Mitrovica, 1999; Uličný, 1999; Catuneanu et al. 1998, 2002, 2004b, 2005; Isbell et al. 2008; Miall et al. 2008).

Depocentres within the Karoo foreland basin were greatly controlled by pulses of orogenic loading in the Cape Fold Belt (also known as the Gondwanan Mobile Belt) (Lock, 1978; Söhnge and Hälbich, 1983). Orogenic loading was the initial subsidence mechanism acting on the Karoo Basin (Catuneanu et al. 1998, 2005) and flexural tectonics partitioned the Karoo Basin into the foredeep, forebulge, and backbulge flexural provinces (Catuneanu et al. 1997, 1998). Orogenic loading and unloading caused changes in position of the forebulge and foredeep. This resulted in

deposition in the proximal (with reference to the Gondwanan Mobile Belt) or distal regions of the Karoo Basin (Catuneanu et al. 1998). Flat slab subduction (dynamic subsidence) had a greater influence over subsidence rates and depocentres later in the evolution of the Karoo Basin. Because this dynamic subsidence was controlled by the drag force generated by viscous mantle corner flow coupled to the low-angled subducting plate (the flat slab condition) (Mitrovica et al. 1989; Gurnis, 1992; Holt and Stern, 1994; Burgess et al. 1997), the time-lag between initiation of subduction and tectonic loading is due to the time it takes for the subducting slab to reach far enough beneath the overriding plate to generate a viscous corner flow (Mitrovica et al. 1989; Catuneanu et al. 2005). This caused loading and subsidence to happen out-of-phase throughout the Karoo Basin, thus many of the upper and lower boundaries of the lithostratigraphic groups are diachronous (eg. Dwyka–Ecca, Ecca–Beaufort etc.), and have proximal and distal equivalents (eg. Whitehill and Vryheid formations) (Rubidge et al. 1995, 2000; Catuneanu et al. 1998, 2005).

Deposition and accumulation of the Karoo Supergroup began with the Dwyka Group (320-280 Ma) once accommodation had been created, coincident with the end of the Gondwanan glacial period (Catuneanu, 2004a). The Dwyka Group was followed by the dominantly marine Ecca, and non-marine to terrestrial sequences the Beaufort (fluvio-lacustrine), and Stormberg (fluvio-lacustrine, aeolian), finally terminating after more than 100 million years of sedimentation with the early Jurassic-aged Karoo volcanics (SACS, 1980; Tankard et al. 1982; Cole, 1992; Smith et al. 1993; Duncan et al. 1997; Catuneanu et al. 1998, 2005; Catuneanu and Elango, 2001) (Figure 1.1). South Africa's Beaufort Group (part of the Karoo Supergroup) is unique because it preserves, with relatively little tectonic disturbance, a near continuous sequence of non-marine deposits ranging from the late Guadalupian (Capitanian) to the middle Triassic (Anisian). The abundant fossil tetrapods from the Beaufort Group have enabled biostratigraphic subdivision into six Permian (*Eodicynodon*, *Tapinocephalus*, *Pristerognathus*, *Tropidostoma*, *Cistecephalus*, *Dicynodon*) and two Triassic (*Lystrosaurus*, *Cynognathus*) assemblage zones (AZs) (Rubidge et al., 1995).

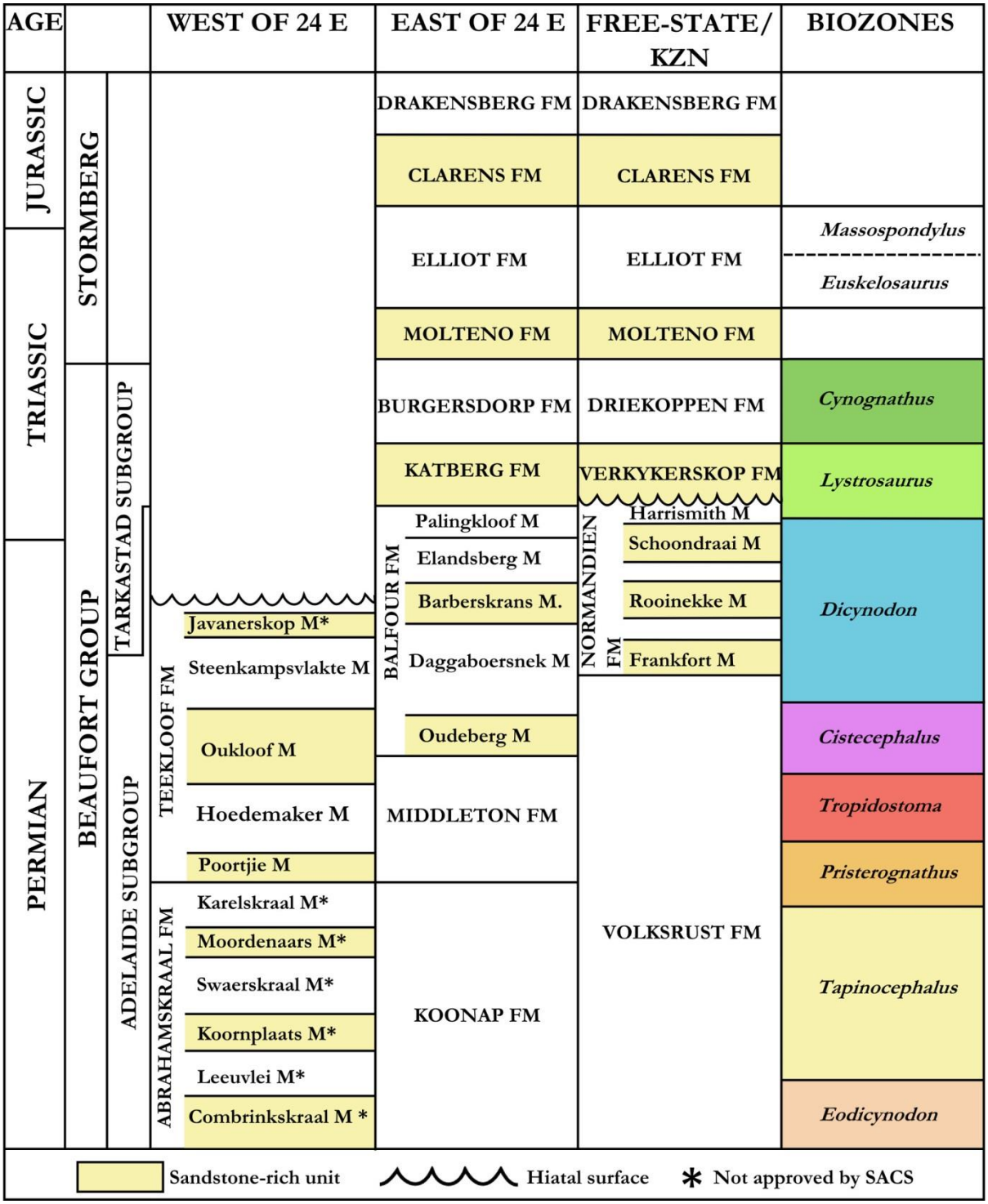

Figure 1.1: Stratigraphy of South Africa's main Karoo Basin as currently accepted by SACS (1980). Data sourced from Kitching and Raath (1984), Le Roux (1985); Jordaan (1990); Loock (1993); Rubidge et al. (1995); and Cole and Wipplinger (2001).

The fossils of the Beaufort Group have a long history of being used as chronostratigraphic correlative tools (Bain, 1845; Owen, 1845; Dunn, 1887; Seeley, 1892; Broom, 1906a, b, 1907a; Watson, 1914; Broom, 1932; Hotton and Kitching, 1963; Kitching, 1970, 1977; Keyser and Smith, 1979b; Rubidge, 1990; Rubidge et al. 1995; Viglietti et al. 2016), and as a result have potential in playing a major role in refining basin development models for the Karoo Basin in the absence of well-defined lithological marker horizons (Hancox and Rubidge, 1997; Rubidge et al. 2000; Rubidge, 2005). Although mainly defined by the first appearance datum (FADs) of therapsid fauna, other notable fossil fauna from the Beaufort Group includes early diapsid reptiles (Carroll, 1987; Smith and Evans, 1996; Botha-Brink and Modesto, 2009), amphibians (Latimer et al. 2002; Damiani and Rubidge, 2003; Marsicano et al. 2015), fish (Bender, 2001), and flora (Bamford, 1999, 2000, 2004; Prevec et al. 2010). Apart from its record of the Permo-Triassic extinction, new radiometric dates (Rubidge et al. 2013) have recently made possible the identification of a mid-Permian (end-Guadalupian) extinction event in the terrestrial realm at 260 Ma (upper *Tapinocephalus* Assemblage Zone, Abrahamskraal Formation, Day et al. 2015). However for many of the other Beaufort assemblage zones the available stratigraphic range data of tetrapods are not up to date and need to be re-evaluated before an accurate picture of faunal composition and turnover patterns can be discerned.

The *Dicynodon* Assemblage Zone (DiAZ) is the uppermost Permian biozone of the Beaufort Group, encompassing strata of the Upper Permian (Lopingian), and is currently defined by the first appearance datum (FAD) of the therapsids *Dicynodon lacerticeps* (Dicynodontia), *Theriognathus microps* (Therocephalia), and *Procynosuchus delaharpeae* (Cynodontia). The Lopingian is an important time in Earth's history as by this stage of the Permian all the world's continents had coalesced into a single supercontinent (Pangea) which was surrounded by a global ocean (Panthalassa). This had significant climatic implications. The extensive subpolar coal forests of the early to middle Permian had given way to drier continental climates, and this is believed to have been a major driver in the evolution and diversification of the amniotes (Sahney et al. 2010). In the terrestrial realm, the Permian is best known for its radiation of non-mammalian synapsids (including the therapsids, the synapsid subclade containing mammals as their extant representatives). This was the golden age of the therapsids, which were at the peak of their ecological domination by this time, occupying almost every available niche, although they began to relinquish this position during the Permo-Triassic mass extinction (PTME) (Benton and Twitchett, 2003; Erwin, 2006; Fröbisch, 2013; Benton and Newell, 2014; Smith and Botha-Brink, 2014). Events immediately prior to this great extinction and its aftermath in the terrestrial realm have received deserved attention from varied scientific disciplines including sedimentology and

taphonomy (Smith, 1995; Smith and Ward, 2001; Smith and Botha, 2005; Ward et al. 2005; Botha and Smith, 2006; Viglietti et al. 2013); global climate and ocean modelling (Wignall and Twitchett, 1996; Bottjer, 2012; Sun et al. 2012; Rey et al. 2015); and disparity, ecology, and ecosystem modelling (Benton et al. 2004; Roopnarine et al. 2007; Sahney and Benton, 2008; Ruta et al. 2013). Recent work has proven that the current definition of the DiAZ is problematic because all three index species (*Di. lacerticeps*, *T. microps*, and *P. delaharpeae*) are reported to have FADs that predate the traditionally-recognized base of the DiAZ (Botha-Brink and Abdala, 2008; Kammerer et al. 2011; Huttenlocker, 2014).

The current manifestation of the DiAZ is one of the thickest and most widely distributed of the Beaufort Group's biozones and recent radiometric dates suggest that it spans approximately three million years (Rubidge et al. 2013). The DiAZ roughly coincides with the lithologically defined Balfour Formation in the east, upper Teekloof Formation in the west (foredeep), and Normandien Formation in the north of the basin (backbulge), but the temporal relationship of these lithological units is poorly understood. This is in part due to the monotonous nature of the Beaufort Group rocks which comprise multiple mega-cycles of mudrock and subordinate sandstone, sometimes reaching up to 500 m in thickness (Visser and Dukas, 1979). This coupled with significant lateral lithological variation that is evident throughout the Beaufort Group, makes lateral correlation of these megacycles difficult over more than one or two hundred kilometres, let alone individual sandstone or mudstone units.

Episodic tectonism and uplift (orogenic loading/unloading cycles) in the provenance areas to the west, south, and eastern Karoo Basin may have produced these megacycles (Le Roux, 1993), with each event causing progradation of sandy sediment, followed by source-ward retrogradation of muddy sediment, as the gradients of rivers declined (Catuneanu et al. 1998). It is also possible that these allocycles accumulated due to differential fault-controlled subsidence and sedimentation rates between adjacent areas of the basin, causing the migration of major fluvial systems in different parts of the basin (Smith, 1981, 1989; Turner, 1999; Tankard et al. 2009, 2012).

Many of these mudstone and sandstone-rich units have been given member status by virtue of their apparent utility as local marker horizons; however, the regional extent and distribution of most of these units has not been well-documented. Consequently the focus of this study is to identify potential marker horizons that could serve to correlate Upper Permian deposits in different parts of the main Karoo Basin. The Balfour Formation, occurring in the eastern part of the basin, includes the most thoroughly studied exposures of the DiAZ and therefore was the

one focus of this investigation. An arenaceous unit in the middle of the mostly argillaceous Balfour Formation, called the Barberskrans Member (BM), has been highlighted by previous workers as a potential marker horizon in the uppermost Permian in the main Karoo Basin (Johnson, 1966; 1976; Tordiffe, 1978). Therefore the revision of the litho- and biostratigraphic framework of the Upper Permian Karoo Basin strata became the main focus of this investigation. In order to provide further context to this study, a brief stratigraphic review of the Upper Permian Beaufort Group will be discussed. A broader review of the Beaufort Group stratigraphy can be found in previous works by Theron (1970), Hancox (1998), Neveling (2002), and Day (2013a,b).

1.2 Lithostratigraphic Review of the Upper Permian (Lopingian) Beaufort Group

The Upper Permian Beaufort Group is part of the Adelaide Subgroup (SACS, 1980), but the stratigraphy is divided into three main depocentres or transport systems which are referred to as the following: east of 24^0 E, west of 24^0 E, and the Free State/Kwa-Zulu Natal lithostratigraphic provinces (SACS, 1980) (see Figure 1.1). They are defined by palaeocurrent directions and position east or west of 24^0 E in the main Karoo Basin (Theron, 1970; Groenewald, 1990; Cole and Wipplinger, 2001). These lithostratigraphic provinces will now be discussed in the context of the most up to date literature. Table 1.1 in Section 1.3 lists lithological properties of all lithostratigraphic units important to this study.

Lithostratigraphy east of 24^0 E

The successively deposited Koonap, Middleton, and Balfour formations are documented east of 24^0 E and form part of Cole and Wipplinger's (2001) northwesterly fluvial transport system of the Karoo Basin's foredeep between the Eastern Cape and the southern Free State Province. The Balfour Formation represents the uppermost Permian part of the stratigraphy and correlates mainly with the Lopingian *Dicynodon* Assemblage Zone but also contains strata assigned to the uppermost *Cistecephalus* and lowermost *Lystrosaurus* assemblage zones. Johnson (1966) was the first to divide the Beaufort Group stratigraphically in this area, using previous definitions of the Ecca/Beaufort Boundary made by Mountain (1946). Johnson (1966) created the Middle Permian Koonap, and Upper Permian Middleton and Balfour Formations, which later formed part of the Adelaide Subgroup (Johnson, 1976). South of Cradock, he further subdivided the Balfour Formation into Zones 1, 2, and 3, which later became the Oudeberg (Zone 1), Daggaboersnek (Zone 2), Elandsberg, and Palingkloof members (Zone 3). Tordiffe (1978) made a minor adjustment to Johnson's (1966, 1976) Zone 3 by separating a local laterally continuous sandstone

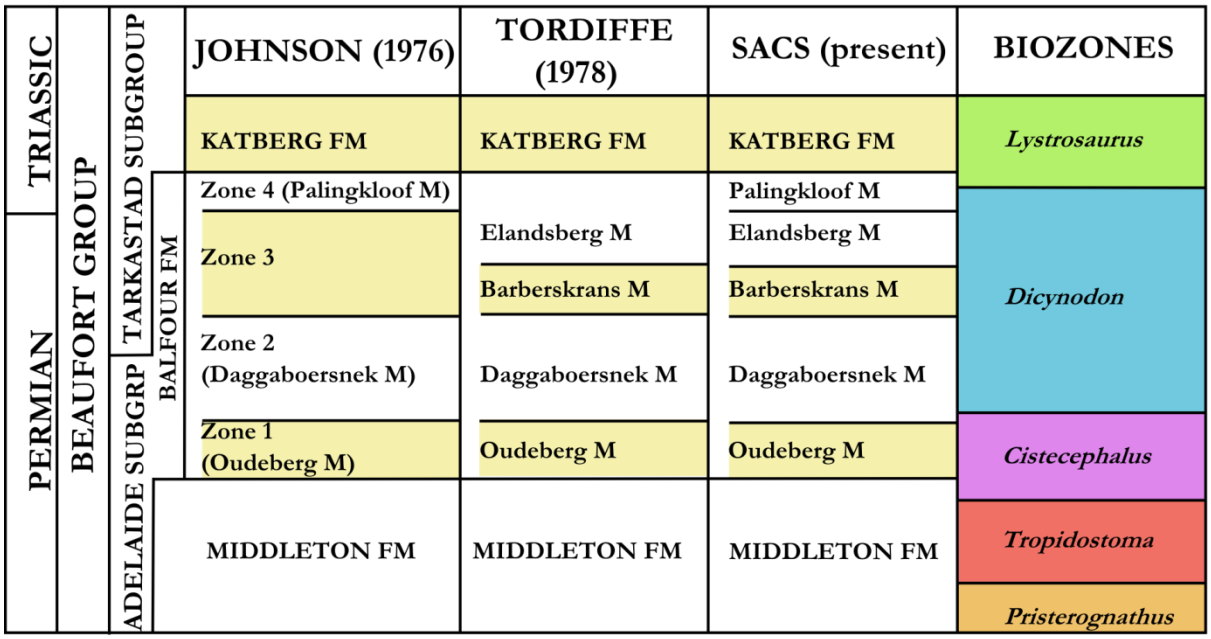

Figure 1.2: Subdivisions of the Balfour Formation by Johnson (1976), Tordiffe (1978), and the currently accepted subdivisions (SACS, 1980).

unit from the argillaceous Elandsberg Member and naming it the Barberskrans Member (BM) (see Figure 1.2). Tordiffe (1978) also removed Johnson's (1976) Palingkloof Member which was later reinstated by Smith (1995) during his work on the PTME. Previous workers such as Johnson (1966, 1976), Tordiffe (1978), Visser and Dukas (1979), and Smith (1995) subdivided the Balfour Formation into the Oudeberg, Daggaboersnek, Barberskrans, Elandsberg, and Palingkloof members. These units are particularly well-exposed in the Winterberg and Sneeuberg ranges near Cradock, Graaff-Reinet, and Nieu Bethesda (See Table 1.1). Work conducted by Smith and Botha (2005); Botha and Smith (2006); Smith and Botha-Brink (2014) on the PTME in the southern Free State Province has identified only some of these lithological units in the Bethulie area. The most recent sedimentological work conducted on the Balfour Formation was by Catuneanu and Elango (2001) who measured a total thickness for the Balfour Formation of 2150 m in the Fort Beaufort area of the Eastern Cape. The authors did not assess the lithostratigraphy but identified six, unconformity-bound third-order fluvial depositional sequences.

Lithostratigraphy west of 24^0E

The Abrahamskraal and Teekloof formations form part of the northeasterly fluvial transport system in the Karoo Basin's foredeep between the Western Cape and southern Northern Cape (Cole and Wipplinger, 2001). Best outcrop is visible along the escarpment Between Sutherland and Beaufort West in the Nuweveld range, Roggeveld, and the Koup. The Abrahamskraal Formation represents the middle Permian deposits and is divided into six informal members:

Combrinkskraal, Leeuvlei, Koonplaats, Swaerskraal, Moordenaars, and Karelskraal members (Le Roux, 1985; Jordaan, 1990; Loock, 1993; Cole and Wipplinger, 2001). The Teekloof Formation represents the Middle (Guadalupian) and Late (Lopingian) Permian period in this part of the basin and is divided into Poortjie, Hoedemaker, Oukloof, and Steenkampsvlakte members (see Figure 1.1). Stear (1980) provided names for the argillaceous members above and below the Oukloof Member, being the Steenkampsberg and Hoedemaker members, respectively. Later the Steenkampsberg Member was changed to the Steenkampsvlakte Member after the Farm Steenkampsvlakte 416 because the Steenkampsberg Formation of the Pretoria Group had priority (SACS, 1980). The base of the Steenkampsvlakte Member coincides with the *Dicynodon* Assemblage Zone and although dominantly argillaceous, it does contain some sandstone-rich zones which in places form thin isolated packages of limited lateral extent (Keyser and Smith, 1979a; Smith, 1987). One of these sandstone-rich intervals was noted in the Steenkampsberg area by Le Roux (1985) which he informally named the Javanerskop member after a koppie on Oukloof Pass. This unit has also been identified by Smith (pers. comm. 2013) north of Beaufort West as being a potential lateral equivalent of the Barberskrans Member of the Balfour Formation (See Table 1.1).

Lithostratigraphy of the Free State/Kwa–Zulu Natal

According to SACS (1980), the boundary between the Adelaide and Tarkastad subgroups can be followed throughout the Karoo Basin however this becomes increasingly difficult in the central and northern Free State Province. Very little work on the stratigraphy of the Free State or Kwa-Zulu Natal provinces has been undertaken, mostly due to poor outcrop (Figure 1.1). As a result, the stratigraphy in this part of the basin has been difficult to define or correlate with the south. Theron (1970), Rutherford (2009), and Rutherford et al. (2015) have conducted the most significant work in the central Free State Province, which represents the most distal foredeep of the Karoo Basin. Based on palaeocurrent directions and provenance studies, Theron (1970) divided the Beaufort Group in this part of the Free State Province into four formations: the Lower Beaufort Formation, Northern Beaufort Formation, the Middle and Upper Beaufort formations. Botha and Linström (1977) and Csaky and Wachsmuth (1971) equated the Northern Beaufort formations of Theron (1970) with the upper part of the Adelaide Subgroup and to this day this has not been challenged.

A more recent study of the geology of the Thaba Nchu area by Rutherford et al. (2015) recognized Theron's (1970) previous subdivisions but gave those informal names. In Rutherford (2009) and Rutherford et al.'s (2015) work, Theron's (1970) Lower Beaufort, Northern Beaufort,

Middle Beaufort, and Upper Beaufort formations are referred to as the Dubbeldam Mudrocks, Musgrave Grit, Middle Sandstone Units (which includes the Sepenare's Hoek sandstone and Townland fines unit and upper Eden Sandstone Member) respectively. Rutherford et al.'s (2015) Musgrave Grit is a single sandstone in the uppermost Dubbeldam mudrock, but a series of coarse-grained sandstones within the Dubbeldam are referred to as the Musgrave unit, and previously the Northern Beaufort Formation of Theron (1970). These have been correlated to the Balfour (Dubbeldam Mudrocks, Musgrave unit) and Katberg (Sepenare's Hoek sandstone, Townland fines, Eden sandstone) formations (Rutherford, 2009; Rutherford et al. 2015). Interestingly all the palaeocurrent directions for these northern units show a distinct north-westerly flow direction (338^0-342^0) except for the Musgrave unit which shows a distinct south-westerly flow direction (~230^0) (Rutherford et al. 2015).

In the north eastern Free State Province, part of the Karoo Basin's backbulge, the Adelaide Subgroup comprises the Normandien and Estcourt formations (Figure 1.1). Poor exposure and uncertain correlation with southern Karoo Basin stratigraphy are reasons that the Normandien Formation is poorly constrained temporally. However, Catuneanu et al. (1998, 2005) suggest that it is representative of only the uppermost Permian. Groenewald (1989, 1990) and Rubidge et al. (1995) had correlated the Normandien Formation with the Balfour Formation further to the south, but Catuneanu et al. (1998) hypothesized that the Normandien Formation only correlates with the upper portion of the Balfour Formation. Botha and Lindstrom (1978) identified the Estcourt Formation as the lateral equivalent of the Balfour Formation in north-west KwaZulu-Natal. Later Johnson et al. (1997) argued for the absorption of the Estcourt Formation into the Normandien Formation.

The Normandien Formation comprises three arenaceous and three argillaceous units (Groenewald, 1989, 1990). The basal Member of this formation (the Frankfort Member) nonconformably overlies the Volksrust Formation of the Ecca Group and consists of upward-coarsening coarse-grained feldspathic sandstone and green shale (Groenewald, 1990). The remaining arenaceous members (Rooinek and Schoondraai members) are fining-upward successions of fine-grained sandstone and mudstone. The Rooinek Member consists principally of lenses of very coarse to very fine-grained feldspathic sandstone, which pinch out laterally over short distances (Groenewald, 1990). Coarse-grained feldspathic sandstone, containing pieces of silicified wood, forms the erosional base of stacked units of upward-fining sandstone of the Schoondraai Member (Groenewald, 1990). The three argillaceous members succeed each of the sandstone rich members. The lower two consist primarily of green mudstone whilst the

uppermost member of the Normandien Formation is a red mudstone package which Groenewald (1990) named the Harrismith Member. Groenewald (1989, 1996) divided the Tarkastad Subgroup in the northern Free State into a lower Verkykerskop Formation and an upper Driekoppen Formation, whilst Botha and Linstrom (1978) subdivided the succession in north western KwaZulu-Natal into the upper Otterburn and lower Belmont formations. SACS (1980) questioned the division of the Tarkastad Subgroup north of 31^0S into two formations however, Neveling (2002) found that the subgroup was represented by two distinct formations in the south-eastern Free State and favoured the retention of the terms Katberg and Burgersdorp formations. Groenewald (1990) correlated the Verkykerskop and Driekoppen formations in the north eastern Free State with the Katberg and Burgersdorp formations of the Eastern Cape. A similar correlation was made between the Belmont and Otterburn formations in KwaZulu-Natal.

1.3 Lithological properties of the Balfour, Teekloof, and Katberg formations

The lithostratigraphic units of the Balfour, Teekloof, and Katberg formations that are under investigation during this study have their rank, source of name, type localities, stratigraphic position, and lithological properties summarized in Table 1.1. Their distinguishing features were documented by previous workers, or during this study and are used to distinguish these different lithostratigraphic units from one another in the field. This table will also be referred to in proceeding chapters when the lithostratigraphic units are discussed with reference to field observations in this study.

Table 1.1: Lithostratigraphic units of the Balfour, Teekloof, and Katberg formations. Formation (F), member (M), and bed (B) status, proposer, type location, stratigraphic position, and lithological properties are summarized. An asterisk(*) next to the rank means the unit is not formally accepted by the South African Committee for Stratigraphy.

Unit	Rank	Source of name	Proposer(s)	Stratotype (S) Type Locality (L) Type area (A)	Stratigraphic position/age	Thickness and boundaries	Lithological features
Balfour	F	Village north of Fort Beaufort.	Johnson (1966)	Fort Beaufort-Balfour road (S)	Late Permian (Lopingian) in age (255-252 Ma) (Rubidge et al. 2013). Overlies the Middleton F (Adelaide Subgroup) and underlies the Lower Triassic Katberg F (Tarkastad Subgroup). Correllates to the upper Teekloof F in the west and Normandien F in the northeast, as well as the *Dicynodon* Assemblage Zone (Rubidge et al. 1995).	Maximum thickness 2150 m but average thickness between 450-500 m (Johnson, 1976; Visser and Dukas, 1979; Rubidge et al. 1995). The lower boundary is sharp and drawn at the base of the Oudeberg M (SACS, 1980). The upper boundary is sharp with the base of the Katberg F (Catuneanu et al. 1998).	Sandstone (20-25%): Mean thickness 5 m. Maximum thickness 40 m. Fine to medium grained, moderatley sorted, crossbedded, horizontally laminated, massive, ripple cross-lamiated, pale olive (10Y 6/2) or greenish grey (5G 6/1) tabular or lenticular sublitharenites. Average palaeocurrent direction ~ 291°. Mudstone (75-80%): Mean thickness 20 m. Structureless or finely laminated red (4YR 10/1) or green (5GY 5/2, 5G 4/1) mudstone. Pedogenic and diagenetic carbonate nodules, plant, vertebrate, and ichno fossils common. Comprises alternating mudstone and subordinate lense to tabular shaped laterally discontinuous sandstones. Subdivided into the Oudeberg, Daggaboersnek, Barberskrans, Elandsberg, and Palingkloof members. Well-exposed in the Winterberg and Sneeuberg ranges near Cradock, Graaff-Reinet, and Nieu Bethesda.

Katberg	F	Katberg Pass north of Fort Beaufort.	Johnson (1966)	Katberg Pass to Poplar Grove along the Fort Beaufort-Queenstown road (S)	Lower Triassic in age. Overlies the Balfour F and underlies the Burgersdorp F. Correlates to the *Lystrosaurus* Assemblage Zone (Rubidge et al. 1995).	Reaches maximum thickness of 1000 m according to Hiller and Stavrakis (1984) but average thickness ~ 200 m (Cole and Wipplinger, 2001). Lower boundary is sharp (see Balfour F) while the upper boundary is gradational with the argillaceous Burgersdorp F.	Sandstone (90-95%): Fine to medium grained, moderatley sorted, crossbedded, horizontally laminated, massive, ripple cross-lamiated, pale olive or greenish grey tabular subarkose sandstones. Average palaeocurrent direction ~ 342°. Mudstone (10-25%): Structureless or horizontally laminated, medium to thick bedded red and minor green mudstone. Pedogenic and diagenetic carbonate nodules, plant, vertebrate, and ichnofossils common. Thin mudstone beds are present, with red mudstone beds increasing in abundance towards the upper boundary of the formation as it grades into the Burgersdorp F (Johnson, 1976; Johnson et al. 2006).

Teekloof	F	Pass in Nuweveld south of Fraserburg.	Keyser and Johnson pers. comm.	Road cuttings, Teekloof Pass (S)	Middle Permian (Guadalupian) to Late Permian (Lopingian) in age. Overlies the Abrahamskraal F and its upper bounding surface is a regional unconformable surface. Spans the *Pristerognathus*, *Tropidostoma*, *Cistecephalus*, and *Dicynodon* assemblage zones (Rubidge et al. 1995).	Maximum total thickness is estimated to be between 400 and 500 m (Smith, 1993; Cole and Wipplinger, 2001). The lower boundary is sharp and conformable, defined as the base of the arenaceous Poortjie M. The upper boundary represents a regional unconformity as it is an erosional hiatus.	Sandstone (20-25%): Mean thickness 5 m. Maximum thickness 30 m. Fine to medium grained, moderatley sorted, crossbedded, horizontally laminated, massive, ripple cross-lamiated, pale olive or greenish grey tabular or lenticular litharenites. Average palaeocurrent direction ~ 58 ° .Mudstone (75-80%): Mean thickness 20 m. Generally structureless or horizontally laminated, medium to thick bedded red or minor green mudstone. Pedogenic and diagenetic carbonate nodules, plant, vertebrate, and ichnofossils common. Four subdivisions correlate to four biostratigraphic zones: Poortjie (*Pristerognathus* AZ), Hoedemaker (*Tropidostoma* AZ), Oukloof (*Cistecephalus* AZ), and Steenkampsvlakte (Dicynodon AZ) members. Uranium mineralisation locally abundant (Turner, 1978; Le Roux, 1985). Outcrops in the Nuweveld escarpment near Beaufort West and Fraserburg but grades into the Balfour F to the east (Turner, 1981).

Oudeberg	M	Pass northwest of Graaff-Reinet.	Keyser 1973b	The pass (L)	Lopingian in age. It overlies the Middleton F and is the lowermost member of the Balfour F. The overlying member is the argillaceous Daggaboersnek M. Correllates to the *Cistecephalus* Assemblage Zone (Rubidge et al. 1995).	Maximum thickness is 50 m (Visser and Dukas, 1979) but an average thickness of 40 m is recorded in the Cradock area by Tordiffe (1978). The lower contact is sharp with the underlying Middleton F, but the upper boundary is gradational with the overlying argillaceous Daggaboersnek M. Both are conformable boundaries.	Sandstone (70-75%): Maximum thickness 50 m. Average 40 m. Several fine to medium grained tabular to lenticular, massive or trough crossbedded, ripple cross-laminated pale olive sublitharenites. Mudstone (30-25%): Subordinate green mudstone is structureless and other features (eg. fossils, rootlets nodules) rare. Individual sandstones can be traced over tens of kilometres. Pedogenic nodule conglomerates common at bases. Fossils of *Cistecephalus microrhinus* are found above the unit (Keyser, 1973; Kitching, 1977). Good outcrops of the unit can be found on Oudeberg Pass and north of Cookhouse, although it can be traced east to East London and northwest to Richmond (Johnson, 1976; Tordiffe, 1978; Visser and Dukas, 1979).

Daggaboersnek	M	Saddle (nek) 23 km north of Cookhouse.	Johnson (1976)	Road cutting hill slopes at Daggaboersnek (L)	Lopingian in age. It overlies the Oudeberg M and underlies the Barberskrans M, both arenaceous units in comparison to the Daggaboersnek M. The lower third correllates to the *Cistecephalus* Assemblage Zone, while the upper two thirds correlates to the *Dicynodon* Assemblage Zone.	A Maximum thickness of 1200 m was estimated by Tordiffe (1978) in the Cradock/Cookhouse area but an average thickness varies between 300 and 440 m (Visser and Dukas, 1979; Cole and Wipplinger, 2001). Its lower boundary is gradational as sandstone content decreases in the uppermost Oudeberg M. Its upper boundary with the overlying Barberskrans M is transitional although, sandstone content rapidly increases (Tordiffe, 1978).	Sandstone (20-25%): Maximum thickness 3 m. Average thickness 1.5 m. Dark greenish grey (5GY 4/1) or pale olive lithofeldspathic sandstone ripple crosslaminated lenses are encountered but in general crossbedded units are uncommon. Mudstone (75-80%): Average thickness 20 m. Regularly bedded, varve-like tabular green and minor red mudstone beds. Interbedded with thin wave-rippled shales and sandstones. In the Cradock area pedogenic nodules are rare in comparison to where it outcrops near Nieu Bethesda. Vertebrate fossils are encountered but this unit is most well known for its plant fossils, in particular leaf impressions of Glossopteris. (Johnson 1976; Tordiffe, 1978; Johnson et al. 2006) Good outcrops of this unit can bee seen in the Daggaboer area between Cradock and Cookhouse, and also in the Graaff-Reinet area along the Murraysburg road. This unit thin rapidly northwards and is not present north of the Orange River.

Barberskrans	M	Cliff 10 km southeast of Cradock.	Tordiffe (1978)	The cliff (S)	Lopingian in age. It overlies the Daggaboersnek M and underlies the Elandsberg M. Correlates to the *Dicynodon* Assemblage Zone.	A maximum thickness of 190 m was estimated by Tordiffe (1978) near Cradock, but an average thickness of 60 m was obtained by Visser and Dukas (1979) on Platberg near Graaff-Reinet. The lower boundary with the Daggaboersnek M is gradational while the upper boundary with the Elandsberg M is relatively sharp (Visser and Dukas, 1979).	Sandstone (70-80%): Maximum thickness 40 m. Average thickness 20-25 m. Fine to medium-grained tabular pale olive, crossbedded, and ripple cross-laminated sublitharenites. Mudstone (20-30%): Maximum thickness 20 m thick. Green, structureless mudstone. Sometimes pedogenic nodules and rootlets encountered. Vertebrate fossils are also found in mudstones. A conspicuous sandstone rich unit that lies between the argillaceous Daggaboersnek and Elandsberg members.Sandstones are often paired and continue laterally for a few kilometres (Tordiffe, 1978). Mud pellet/feldspathic conglomerates, plant and fish fossils are common at sandstone bases, particularly in Nieu Bethesda (Bender, 2000). Cradock, Cookhouse and northwest of Nieu Bethesda have good exposure of this unit.

Elandsberg	M	Mountain 10 km east of Cradock.	Tordiffe (1978)	Flanks of Elandsberg (A)	Lopingian in age. It overlies the Barberskrans M and underlies the Palingkloof M. Correlates to the *Dicynodon* Assemblage Zone.	For many decades the Elandsberg and Palingkloof members were not distinguished from one another (Tordiffe, 1978; Cole and Wipplinger, 2001). However Smith and Botha-Brink (2014) determined that the maximum thickness is between 37-42 m. The lower bounding surface with the Barberskrans is sharp, whereas its upper boundary with the Palingkloof is gradational and determined by an increase in sandstone and red mudstone content (Johnson, 1976; Smith and Botha-Brink, 2014).	Sandstone (20-25%): Maximum thickness 3 m. Average thickness 1.5 m. Fine to medium-grained, crossbedded to ripple cross-laminated, greenish grey or pale olive sublitharenites. Average palaeocurrent direction ~ 291°. Mudstone (75-80%): Average thickness 20 m. Massivley bedded or horizontally laminated green or greenish greay mudstone Red mudstone is sometimes locally common. (Johnson, 1976). Mudstones rich in pedogenic and diagenetic carbonate nodules. In particular large brown weathering (10R 2/2) nodules with green mudstone pellets are a conspicuous feature (Smith and Botha-Brink, 2014). Tetrapod fossils are common as are plant impressions at the bases of the thin sandstone beds. Good outcrops can be seen on Elandsberg near Cradock, and also in the Nieu Bethesda area west of Compassberg.

Palingkloof	M	Farm Palingkloof 323, 24 km south of Tarkastad.	Johnson (1976)	Palingkloof area (A)	Transitional between Lopingian and Lower Triassic in age. The Permo-Triassic extinction event (PTME) and faunal transition between the *Dicynodon* and *Lystrosaurus* assemblage zones is preserved in this unit (Smith, 1995; Smith and Botha, 2005; Smith and Botha-Brink, 2014).	Total thickness has been documented by Smith and Botha-Brink (2014) to range between 46-60 m. Its lower boundary with the Elandsberg M is gradational and relates to a general increase in red mudstone and sandstone content (Tordiffe, 1978). The upper boundary with the Katberg F is transitional but is defined by a rapid change in abundance of sandstone and red mudstone (Johnson, 1966; 1976).	Sandstone (40-45%): Maximum thickness 3 m. Average thickness 1.5 m. Fine to medium-grained, crossbedded to ripple cross-laminated, greenish grey or pale olive sublitharenites with ubiquitous nodule conglomerates at their bases. Average palaeocurrent direction ~ 291°. Mudstone (55-60%): Average thickness 20 m. Massivley bedded or horizontally laminated red and minor green mudstone. (Johnson, 1976). Locally green mudstone can be dominant as observed in this study. Pedogenic nodule layers become very frequent as do large black or brown weathering diagenetic nodules. Fossil content is abundant and does not change throughout the unit even though the terrestrial PTME is documented (Smith and Botha-Brink, 2014).

Oukloof	M	Pass northwest of Beaufort West.	Turner 1979	The pass (L)	Lopingian in age. Has been correlated to the Oudeberg M and *Cistecephalus* Assemblage Zone.	Total thickness is approximately 125 m (Turner, 1981). Its lower boundary with the Hoedemaker M is erosive and sharp while its upper boundary with the Steenkampsvlakte M is gradational (Smith, 1993).	Sandstone (70-75%): Maximum thickness 28 m. Average thickness 18 m. Fine to medium-grained, crossbedded, horizontally laminated, ripple cross-laminated, greenish gray to pale olive sublitharenites with mudstone pellet conglomerates (Turner, 1981). Average palaeocurrent direction ~ 58°.The sandstones form prominent cliffs and ledges. Mudstone (25-30%): Average thickness 7 m. Red and green structureless or horizontally laminated mudstone. Vertebrate burrows, fossils, and carbonate nodules (pedogenic and diagenetic) common (Turner, 1981). Good outcrops on Oukloof and Teekloof Pass near Beaufort West.
Steenkampsvlakte	M	Farm Steenkampsvlakte 416 northwest of Beaufort West .	Stear (1980)	Steenkampsvlakte area (A)	Lopingian in age. Has been correlated to the Daggaboersnek M and *Dicynodon* Assemblage Zone. Overlies the Oukloof M and underlies the informal Javanerskop M of Le Roux (1985).	Total thickness is approximately 200 m if the informal Javanerskop M is included (Smith, 1993). Its lower boundary with the Oukloof is gradational (Turner, 1981) while its upper boundary with the Javanerskop M is sharp due to a rapid increase in sandstone content.	Sandstone (~20%): Fine to medium-grained crossbedded, horizontally laminated, ripple cross-laminated pale olive or greenish grey sublitharenite lenses. Average palaeocurrent direction ~41°. Mudstone (~80%): Average thickness ~ 20m. Red horizontally laminated mudstone very common. Rich in vertebrate fossils, pedogenic nodules, palaeosols, and rooted horizons. Good outcrop of this unit can be seen on Steenkampsberg on Oukloof Pass and north of Beaufort West in the highest parts of the escarpment.

Javanerskop	M*	Hill northwest of Beaufort West in Oukloof Pass.	Le Roux (1985)	Flanks of Javanerskop (A)	Lopingian in age. Has been tentatively correlated to the Barberskrans M and *Dicynodon* Assemblage Zone (Smith pers. comm.). It overlies the Steenkampsvlakte M and is overlain by a regional hiatus.	Occurs ~ 100 m within the Steenkampsvlakte M and its thickness and bounding surfaces require investigation.	Has been described by Le Roux (1985) as a series of ribbon-shaped sandstones in the Upper Steenkampsvlakte M. Is identified in outcrop by an increase in sandstone content relative to the underlying Steenkampsvlakte M and lower red mudstone content identified in this study.
Musgrave Grit	B*	Location within city of Bloemfontein.	Loock pers. comm.	Named after area in city of Bloemfontein (A)	Lopingian in age. Correlates to the *Dicynodon* Assemblage Zone (Rutherford, 2009; Rutherford et al. 2015). Is underlain by argillaceous Balfour F (informally named the Dubbeldam mudrocks) and overlian by the Lower Triassic Sepenareshoek sandstones (Rutherford et al. 2015).	Is a prominent bed (5 m) within the uppermost Lopingian strata of the Free State Balfour F (see section 1.2). Lower boundary sharp but upper boundary gradational (Rutherford, 2009; Rutherford et al. 2015).	Sandstone (~90%). Maximum thickness 5 m. Average thickness 2 m. Coarse-grained, trough/planar crossbedded sublitharenites rich in large quartz and feldspar clasts. Average palaeocurrent direction ~ 223°. Mudstone (~10%): Structureless greenish grey mudstone with brown weatherin nodules. Identified by significant increase in coare-grained sandstone and anomalous southwesterly palaeocurrent directions which are different to underlying and overlying units (Rutherford, 2009; Rutherford et al. 2015).

Boomplaas sandstone	M*	Boomplaas Hill east of Jagersfontein.	Viglietti, 2016	Named after hill (A).	Lopingian in age. Could correlate to *Cistecephalus* or *Dicynodon* assemblage zone stata.	A prominent (20 m) bed within Lopingian strata near Jagersfontein. Lower boundary sharp and upper boundary gradational.	Sandstone (80-90%): Maximum thickness 20 m. Coarse-grained, trough/planar crossbedded sublitharenite with gravel lags containing quartz and feldspar. Fossil plant stems, wood, and leaf fragments common. Average palaeocurrent direction ~ 255°. Mudstone (20-10%): Structureless greenish grey mudstone. Good outcrop on Boomplaas Hill on Buffelsboutfontein, Trifaldi Major, and Excelsior farms.

1.4 Thickness of the Balfour and Teekloof formations

The Balfour and uppermost Teekloof formations are the main focus of this study and therefore the thickness of lithological subdivisions documented by previous research are summarized in Table 1.2, showing the location or field site where the total thickness was documented.

Table 1.2: Thicknesses of lithological units of the Balfour and Teekloof formations from previous investigations.

Location/Field Site	Formation	Member/Unit	Thickness (m)	Source
King William's Town	Balfour	Total thickness	2350 m (± 500 m)	Johnson (1976)
Fort Beaufort	Balfour	Total thickness	2150 m (± 150 m)	Johnson (1976)
Cradock	Balfour	Total thickness	1220 m (± 150 m)	Johnson (1976)
Cradock	Balfour	Total thickness	1770 m	Tordiffe (1978)
Nieu Bethesda	Balfour	Total thickness	450 m	Johnson (1976)
Nieu Bethesda	Balfour	Total thickness	650 m	Visser and Dukas (1979)
Nieu Bethesda	Balfour	Total thickness	500 m	Rubidge et al. 1995
Thaba Nchu	Balfour	Total thickness	57 m	Rutherford et al. (2015)
Cradock	Balfour	Oudeberg	180 m	Tordiffe (1978)
Nieu Bethesda	Balfour	Oudeberg	50 m	Visser and Dukas (1979)
Cradock	Balfour	Daggaboersnek	1200 m	Tordiffe (1978)
Nieu Bethesda	Balfour	Daggaboersnek	440 m	Visser and Dukas (1979)
Nieu Bethesda	Balfour	Daggaboersnek	300 m	Cole and Wipplinger (2001)
Cradock	Balfour	Barberskrans	190 m	Tordiffe (1978)
Nieu Bethesda	Balfour	Barberskrans	60 m	Visser and Dukas (1979)
Cradock	Balfour	Elandsberg/ Palingkloof	200 m	Tordiffe (1978)
Nieu Bethesda	Balfour	Elandsberg/ Palingkloof	100 m	Visser and Dukas (1979)
Nieu Bethesda	Balfour	Elandsberg/ Palingkloof	100-150 m	Cole and Wipplinger (2001)
Nieu Bethesda	Balfour	Elandsberg	37-42 m	Smith and Botha-Brink (2014)
Bethulie	Balfour	Elandsberg	41 m	Smith and Botha-Brink (2014)
Nieu Bethesda	Balfour	Palingkloof	60 m	Smith and Botha-Brink (2014)
Bethulie	Balfour	Palingkloof	46 m	Smith and Botha-Brink (2014)
Thaba Nchu	Balfour	Musgrave Grit	1 m	Rutherford et al. (2015)
Beaufort West	Teekloof	Total thickness	~ 400 m	Smith (1993)
Beaufort West	Teekloof	Total thickness	500 m	Cole and Wipplinger (2001)
Beaufort West	Teekloof	Oukloof	~125 m	Turner (1981)
Beaufort West	Teekloof	Steenkampsvlakte	~ 200 m	Stear (1980)
Beaufort West	Teekloof	Javanerskop	unknown	Le Roux (1985)

Of particular interest in Table 1.2 is the thickness of the Balfour Formation and its lithostratigraphic units varying greatly depending on their position in the Karoo Basin and Johnson (1976) was one of the first to document this. Nevertheless, Johnson (1966, 1976) did not measure any vertical sections and estimated significant thicknesses for the Balfour

Formation. For example, if the dramatic thickness changes he documented are corroborated between Cradock and Nieu Bethesda, which are separated by only 122 km, this would be a rapid reduction in thickness over a short distance (~ 75 % decrease). Tordiffe (1978) also only estimated his thicknesses for the Balfour Formation in the Cradock and were later used by Catuneanu and Elango (2001).

In the Nieu Bethesda area Visser and Dukas (1979) and Cole and Wipplinger (2001) documented similar total thickness for the Balfour Formation. Smith and Botha-Brink's (2014) Permo-Triassic Boundary work in the Nieu Bethesda (Eastern Cape Province) and Bethulie (Free State Province) districts also resulted in thickness measurements for the upper subdivisions of the Balfour Formation and they did not show much change in thickness between these sites. Kitching (1977) had documented significant attenuation of the Balfour Formation in the Free State Province near Gariep Dam, although this was never quantified. Rutherford et al. (2015) also document an attenuated Balfour Formation in the far north west of the basin near Thaba Nchu which does agree with Kitching's (1977) observations.

1.5 Review of the biostratigraphy of the Upper Permian Beaufort Group

Currently the Beaufort Group comprises eight accepted vertebrate biozones, which are used to broadly correlate different formations and members within the Beaufort Group (see Figure 1.1). The names are derived from the most common tetrapod taxa defining the biostratigraphic interval. Recently Day (2013) and Day et al. (2015) have contributed further resolution on vertebrate ranges in the middle Permian portion of the main Karoo Basin. Smith and Botha (2005), Botha and Smith (2006), and Smith and Botha-Brink (2014) have also increased the resolution of faunal changes occurring before, during, an after the end-Permian mass extinction event. These recent studies do not address refined biostratigraphic resolution of the *Dicynodon* Assemblage Zone (AZ). Accordingly, this study aims to achieve this as a means of potential biostratigraphic correlation throughout the main Karoo Basin.

Dicynodon and the *Dicynodon* Assemblage Zone

Owen (1845) first described *Dicynodon* from a set of skulls collected by Andrew Geddes Bain who took great interest in the palaeontology and geology of the Great Karoo during his work as a road engineer near the Fort Beaufort area of the Karoo Basin (Bain, 1845, 1856). These were also some of the earliest records of vertebrate fossils from the Karoo Basin of South Africa. The sets of skulls sent by Andrew Geddes Bain to the Natural History Museum in London were made the type specimens of *Dicynodon lacerticeps*. As a result *Dicynodon* became the first of its kind to be referred to as a "mammal–like reptile". Later van Hoepen (1934) recognized that the larger

Dicynodon specimens were a new species and named these *Daptocephalus leoniceps* but also erected two other species of large *Dicynodon* (*D. ingens, D. perdiceps*). Haughton and Brink (1954) did not recognize *D. ingens, D. perdiceps*, but retained *Daptocephalus leoniceps*.

Kitching (1977) also treated *Daptocephalus* as valid and monotypic (but considered a number of large *Dicynodon* species to be junior synonyms), later using this species to erect the terminal Permian *Daptocephalus* Range Zone for stratigraphic levels above the *Cistecephalus* Range Zone and below the *Lystrosaurus* Range Zone. Cluver and Hotton (1981) considered *Daptocephalus* to be synonymous with *Dicynodon*, but retained the valid species *Dicynodon leoniceps*. Subsequent studies have either considered *Da. leoniceps* a valid species of *Dicynodon* (King, 1988) or a synonym of *Di. lacerticeps* (Brink, 1986), and as a result Kitching's '*Daptocephalus* Range Zone' was renamed the *Dicynodon* Assemblage Zone (DiAZ).

The *Daptocephalus* Range Zone was changed to the *Dicynodon* Assemblage Zone by Keyser and Smith (1979b) who introduced the assemblage zone concept to the Beaufort Group, although this work was aimed primarily in the southwest Karoo Basin after previous mapping in the east by Keyser (1973) and his work on the *Cistecephalus* Assemblage Zone (Day, 2013a). Additionally Keyser (1979) later adopted a scheme whereby two genera were used to define each assemblage which was adopted by SACS (1980) in order to conform to the International Subcomission on Stratigraphic Classification (ISSC, 1976) regulations on stratigraphic nomenclature. Thus the DiAZ became the *Dicynodon lacerticeps-Whaitsia* Assemblage Zone. However new recommendations by the ISSC (1994) meant Beaufort Group assemblage zones needed to be reverted back to use of a single genus in the name for the zone. Therefore in the most recent publication on the status of the Karoo biostratigraphic zones (Rubidge et al. 1995) the *Dicynodon-Whaitsia* Assemblage Zone reverted back to the *Dicynodon* Assemblage Zone.

Diycnodon sensu lato has a long history of being used for biostratigraphic correlations between the Karoo Basin and other areas (Anderson and Cruickshank, 1978; King, 1992; Lucas, 1997, 1998a, b, 2001, 2002, 2005, 2006), but it has been recognized for some time that the paraphyly of the traditionally recognized genus and taxonomic confusion at the species level made it a poor index fossil (Angielczyk and Kurkin, 2003a, b). Indeed, the change in nomenclature from the older *Daptocephalus* Zone (Kitching, 1977) to the current DiAZ (Rubidge et al. 1995) was driven entirely by obsolete taxonomy, which viewed *Daptocephalus* as a junior synonym of *Dicynodon* and expressed uncertainty as to whether *Da. leoniceps* was a junior synonym of *Di. lacerticeps* (Cluver and Hotton, 1981; Cluver and King, 1983; King, 1988).

Recently, Kammerer et al. (2011) undertook a comprehensive taxonomic revision of *Dicynodon*, reducing the 168 nominal species to 15 species in 14 genera and underscoring the paraphyly of *Dicynodon* sensu lato. In the Karoo Basin, Kammerer et al. (2011) recognized five valid species of basal (non-lystrosaurid, non-kannemeyeriiform) dicynodontoids: *Basilodon woodwardi*, *Daptocephalus leoniceps*, *Dicynodon lacerticeps*, *Dinanomodon gilli*, and *Sintocephalus alticeps*. Additionally, they erected new genera (*Keyseria* and *Euptychognathus*) for the Karoo-occurring former "*Dicynodon*" species "*D.*" *benjamini* and "*D.*" *bathyrhynchus*, which they recovered as a basal cryptodont and lystrosaurid, respectively. However, they expressed uncertainty about the stratigraphic ranges of some of these species and noted that *Da. leoniceps* might be a more appropriate index fossil for the DiAZ than *Di. lacerticeps*.

Beyond the uncertainty surrounding the stratigraphic occurrence of *Dicynodon* and its close relatives, the current definition of the DiAZ is also problematic because all three index species (*Di. lacerticeps*, *Theriognathus microps*, and *Procynosuchus delaharpeiae*) are reported to have FADs that predate the traditionally-recognized base of the DiAZ. *Dicynodon lacerticeps* is considered to first appear in *Cistecephalus* Assemblage Zone (CAZ) strata (Kammerer et al. 2011), as is *Theriognathus microps* (Huttenlocker, 2014). *Procynosuchus delaharpeae* has an even earlier FAD in the *Tropidostoma* Assemblage Zone (TAZ) (Botha-Brink and Abdala, 2008). Given these ranges, the first co-occurrence of these species would be in rocks traditionally assigned to the CAZ, requiring a redefinition of the zone. A similar problem occurs at the top of the zone, where *Lystrosaurus maccaigi* first appears in Upper Permian rocks that are below the traditional lower bound of the *Lystrosaurus* Assemblage Zone (LAZ) just after the Permo-Triassic boundary (PTB)(Botha and Smith, 2007).

Chapter 2: Present Investigation

2.1 Aims

The review has identified several uncertainties relating to the stratigraphy of the Upper Permian deposits of the Beaufort Group. Accordingly, this multi-disciplinary investigation of the Upper Permian strata of the Karoo Basin aims to:

• Revise the lithostratigraphic units that currently define the *Dicynodon* Assemblage Zone (DiAZ). By using Google Earth, field logging and data collection, geochemical and petrographic sampling this study also investigates the arenaceous Barberskrans Member (BM) as a potential marker horizon and tests its lateral continuity and synchroneity with other sandstone-rich units (eg. the Javanerskop member and the Musgrave Grit).

• Address the shortcomings of the current manifestation of the DiAZ. First, reassess the stratigraphic ranges of *Dicynodon lacerticeps*, other Upper Permian basal dicynodontoids, and additional DiAZ-occurring taxa in the Karoo Basin and test their utility as index fossils. Secondly, redefine the assemblage zone and resolve the biostratigraphic problem of the Lopingian FAD of *Lystrosaurus maccaigi*. Finally, provide an updated faunal list and set of stratigraphic ranges for the vertebrates of the DiAZ. The new stratigraphic ranges will be compared to Smith and Botha-Brink's (2014) three extinction phases of the Permo-Triassic mass extinction (PTME) in the uppermost boundary of the assemblage zone.

• Provide a basin development model for the Upper Permian Karoo Basin by integrating refined stratigraphic schemes, petrography, palaeocurrents, detrital zircon dates, facies and architectural element analysis, and interpreting them in the context of palaeoenvironmental and tectonic evolution of the basin.

2.2. Preliminary work

The following 1:250 000 geological maps were consulted (3226, King William's Town, 3224, Graaff-Reinet, 3220, Sutherland, 3222, Beaufort West, 3124, Middelburg, 3024, Colesburg, 2924, Koffiefontein, and 2926, Bloemfontein). These maps reflect the stratigraphy only at formation level, necessitating a review of existing subdivisions of the formations. Previous lithostratigraphic work done by Johnson (1966, 1976), Tordiffe (1978), Visser and Dukas (1979), Le Roux (1985), Smith (1993b, 1995, 2000), Cole and Wipplinger (2001), Smith and Botha (2005), Botha and Smith (2006), and Smith and Botha-Brink (2014) is also consulted in this study. At localities where stratigraphic sections were measured, lithostratigraphic units were traced out laterally in the field and on Google Earth. The study area encompasses much of the south central Karoo Basin and field sites were selected for outcrops that covered most of the stratigraphic range of the DiAZ. Detailed work was undertaken on outcrops from Cradock, Nieu Bethesda, Beaufort West, Gariep Dam, Jagersfontein, and Bloemfontein. The resulting thirteen numbered field sites that were selected for fieldwork and vertical section measuring are shown in Figure 2.1. The vertical sections and interpretation of field data collected at these thirteen sites is presented in Chapter 3 with the results.

2.3 Materials and methods

To determine whether the lithological units identified at the thirteen field sites could be correlated to represent the same stratigraphic intervals, a number of proxies were investigated as a means to characterize them and identify any similarities. The lithological investigations included collecting sandstone samples for detrital zircon dating and petrography, stratigraphic work was undertaken to gain additional information on lithological units such as thickness and also to plot the distribution of vertebrate fossil fauna to document possible faunal changes. Finally sedimentological studies were conducted for palaeoenvironmental and basin analysis which involved the identification of lithofacies, facies associations and architectural element analysis. The procedures involved in such investigations will now be briefly explained.

2.3.1 Stratigraphy

Lithostratigraphy

Lithostratigraphic investigations involved measuring thirteen vertical sections which were used to create five composite sections. They were measured during the course of several field excursions undertaken between 2013 and 2015. All sections measured during this study were undertaken

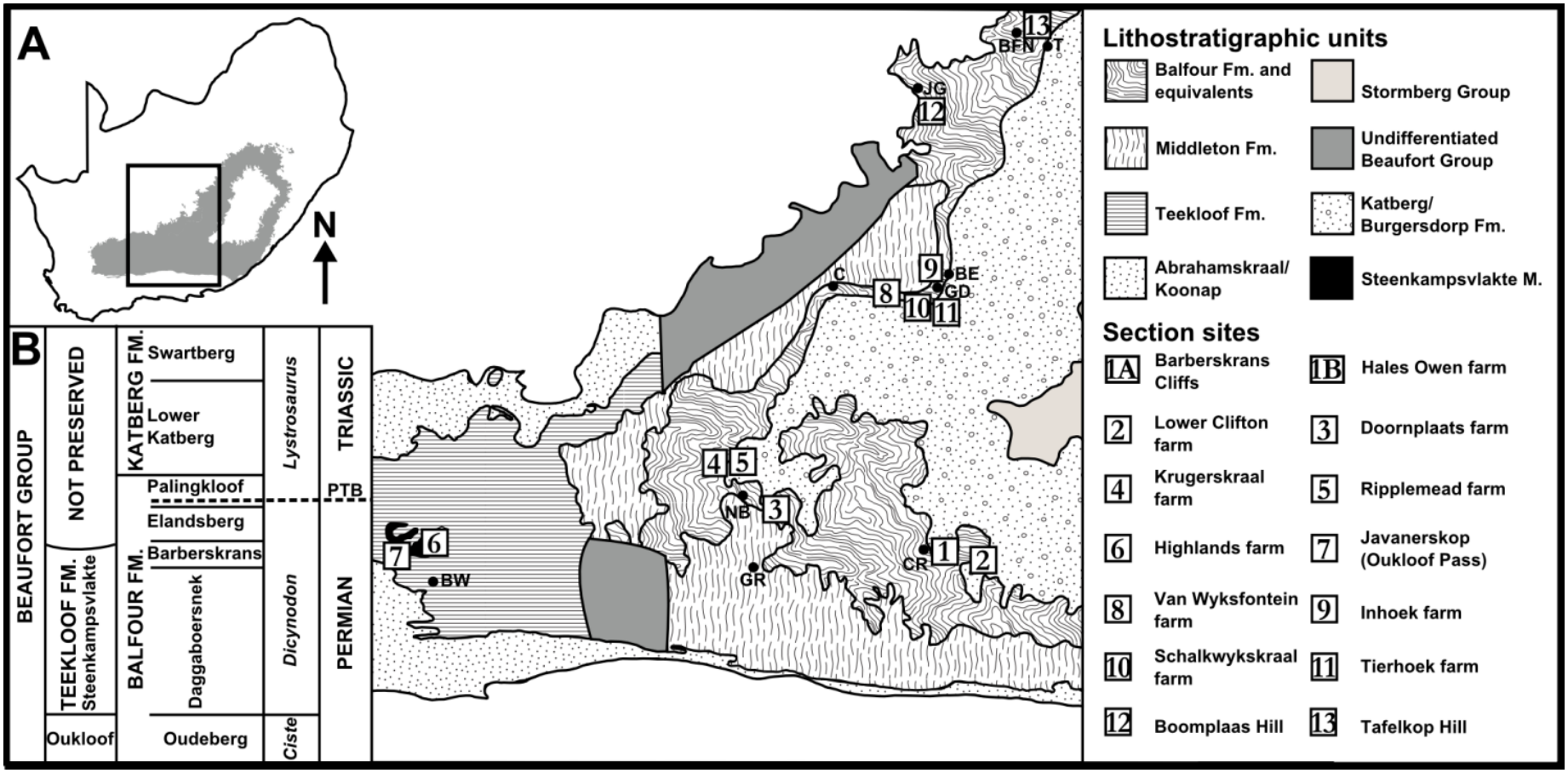

Figure 2.1: A) A map of South Africa showing the position of the field sites in the main Karoo Basin and close up of local geology and numbered field sites. The field sites are near ten major town and abbreviations for town names are: Thaba Nchu (T), Bloemfontein (BFN), Jagersfontein (JG), Bethulie (BE), Gariep Dam (GD), Colesburg (C), Cradock (CR), Nieu Bethesda (NB), Graaff-Reinet (GR), and Beaufort West (BW). B) Current lithostratigraphic subdivisions of strata correlated to the *Dicynodon* and *Lystrosaurus* assemblage zones.

using a Jacob's staff and Abney level. Wherever possible, vertically logged lithological units were followed out laterally for at least 50 m. Stratigraphic sections were measured through as much of the Balfour and Teekloof formations as possible and up to the first Katberg Formation sandstone, or from the upper contact of a recognized underlying unit (Oukloof or Oudeberg members). Features such as lithology, textures, colours, sedimentary structures, bounding surfaces, scours, nodules, fossils, and burrows were all included. The dip of strata is low throughout the study area (< 4 degrees) and thus no compensation for dip was required. Vectorial sedimentary structures were measured wherever possible to provide palaeocurrent data which has been presented either as rose diagrams or indicated by arrows on the vertical sections.

Lithostratigraphic units of the Beaufort Group vary greatly in lateral extent, and thickness (Johnson, 1976; Kitching, 1977; Keyser and Smith, 1979a; Groenewald, 1989, 1990; Jordaan, 1990) thus, changes in thickness of lithological units is also noted. All stratigraphic sections were digitized using Inkscape, Gimp, and Adobe Illustrator. The sections also show information concerning lithologies present, colour, fossils, carbonate nodules which were distinguished between pedogenic (occurring within palaeosol horizons) and diagenetic (disturbing surrounding bedding, concentric growth pattern, and lack of micrite) (Tabor et al. 2007). Also other interesting features encountered (eg. soft sediment deformation). See Figure 2.2 for the legend showing symbols used in the vertical sections. Use of the published geological maps allowed for the generation of more detailed maps of each field site (See Chapter 3.2, Figures 3.4, 3.9, 3.14, 3.15, 3.19, and 3.25) and prominent sandstones under investigation were marked on these maps. These locally occurring sandstones were identified as potentially representing the BM or equivalent by their stratigraphic position (eg. sandstones occurring between 150 and 80 m below the Katberg Formation) and also their lithological properties (See Table 1.1). The field sites do differ in size, but the maps show the extent of area studied for each field site in kilometre scale and can be found in Chapter 3.

Biostratigraphy

The biostratigraphic investigation used previous work conducted by Kammerer et al. (2011) who updated the taxonomy of the genus *Dicynodon* by re-examining specimens in local and global databases. The updated identifications of DiAZ fossil specimens from these databases had their stratigraphic positions and ranges investigated using vertical sections measured and fossils collected in this study. Prior to 1976, only farm names and elevations were used by collectors to record fossil localities in the Karoo Basin. As a result the majority of South African fossils in

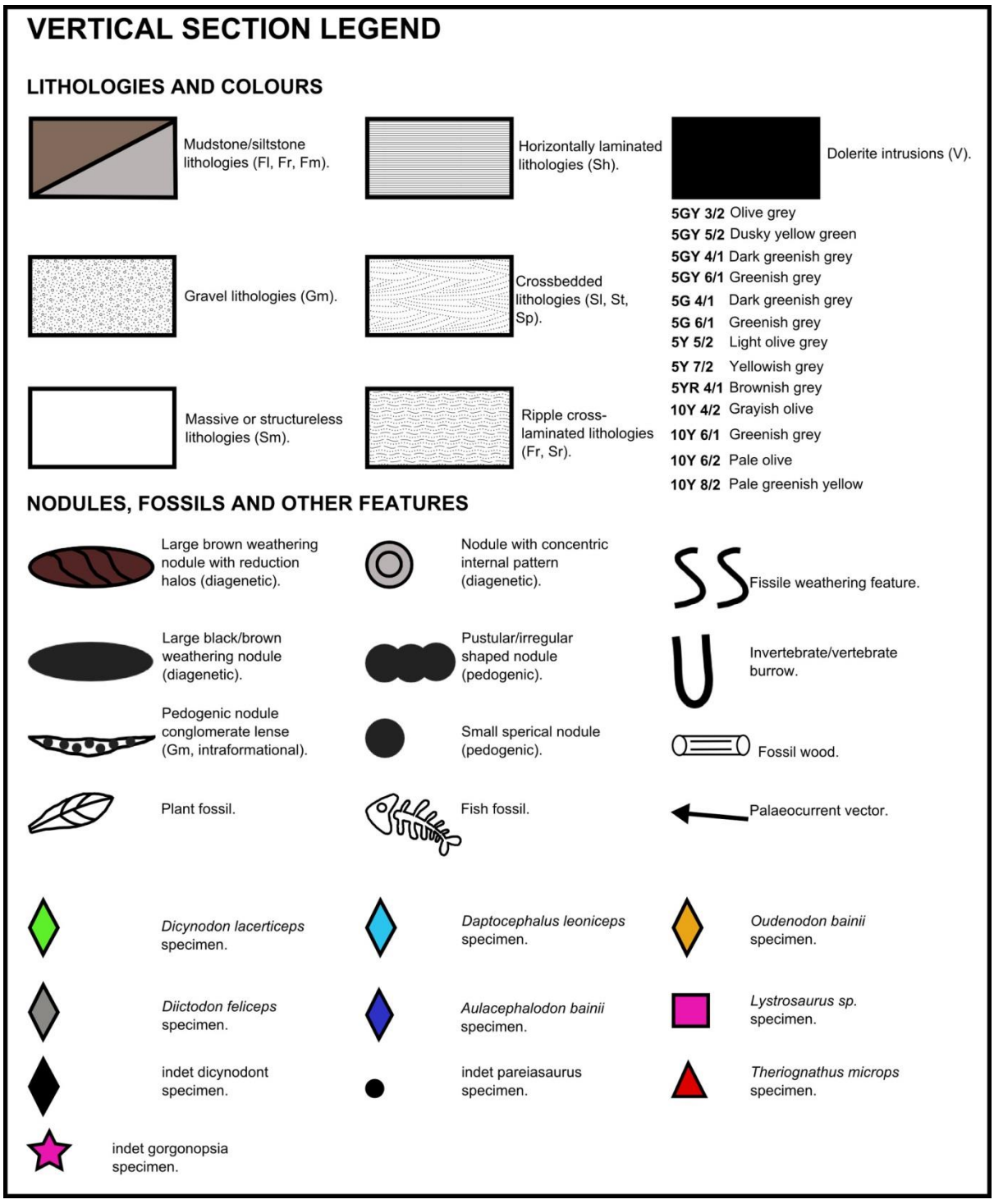

Figure 2.2: Legend showing symbols used to denote sedimentary and palaeontological features identified on the thirteen sections constructed for this study. See Chapter 3 for the vertical sections from each of the study sites.

museum collections have relatively poor provenance data which is limited to the resolution of farm names. A GIS database of all Karoo vertebrate fossils curated in South African museum collections is maintained by the Evolutionary Studies Institute (Nicolas, 2007; van der Walt et al. 2011). Historical specimens from these collections were utilized in this study only if the stratigraphy was well known in the area in which the fossils were found. For such specimens

rough locality and stratigraphic positions were assigned in this study using the farm centroids derived from Google Earth (van der Walt et al. 2011). However, much more accurate locality and biostratigraphic information was generated through systematic collecting of tetrapod fossils in the outcrops where detailed stratigraphic sections were logged by PAV (PV) and RMHS (RS). All recently discovered fossils have accurate GPS coordinates and have also been positioned on measured vertical sections, which allows for reliable first appearance datum (FAD) or last appearance datum (LAD) data of different species. In all 1212 fossils have been reliably provenanced to the upper CAZ or DiAZ and are stored at the following institutions: Albany Museum, Grahamstown (AM); American Museum of Natural History, New York, USA (AMNH); Bremner Collection (SAM satellite collection, Graaff-Reinet Museum) (B); Evolutionary Studies Institute, University of the Witwatersrand, Johannesburg (BP); Council for Geoscience (Geological Survey), Pretoria (CGS); Natural History Museum, London, UK (NHMUK); National Museum, Bloemfontein (NM); specimens collected during doctoral work for Pia Viglietti (PV); Rubidge Collection, Wellwood, Graaff-Reinet (RC); Roger Smith field specimens, not accessioned (RS); Iziko South African Museum, Cape Town (SAM-PK); Ditsong (Transvaal Museum) Pretoria (TM); University of California Museum of Paleontology, Berkeley, USA (UCMP); University Museum of Zoology, Cambridge, UK (UMZC); and the National Museum of Natural History, Washington, DC, USA (USNM).

Since the last biostratigraphic review of the Beaufort Group (Rubidge et al. 1995) the taxonomic assignment of many DiAZ tetrapods has been revised and therefore had to be updated for this study. To review the stratigraphic range of a fossil taxon three conditions need to be met (Day, 2013b): 1) thorough understanding of the lithostratigraphy throughout the basin; 2) robust taxonomic framework; and 3) re-identification of all relevant specimens in collections based on the most recent taxonomic framework. The first criterion has mostly been met through fieldwork and literature studies, although some fossils found in the Normandien Formation were excluded from consideration because the detailed stratigraphy of this Formation remains poorly understood.

Accordingly, all vertebrate taxa from the DiAZ of the Beaufort Group were investigated, and the stratigraphic ranges updated from this data pool. Additionally, the following taxa were investigated in further detail to assess their potential utility as DiAZ index fossils: the dicynodonts *Dicynodon lacerticeps*, *Daptocephalus leoniceps*, and *Lystrosaurus maccaigi*, and the therocephalians *Theriognathus microps*, and *Moschorhinus kitchingi*. Where possible the FAD and LAD were determined respectively for each species by the stratigraphically lowest and highest

occurring specimen in the database with reliable stratigraphic information. Because the taxonomic revision of *Dicynodon* is recent (Kammerer et al. 2011) many museum collections databases have not yet been updated and only specimens of *D. lacerticeps* and *D. leoniceps* that were directly re-examined by Christian F. Kammerer, Jörg Fröbisch, Kenneth D. Angielczyk were used. The hyper-abundant dicynodont *Diictodon feliceps*, and the comparatively rare cynodont *Procynosuchus delaharpeae*, were also investigated in further detail and their updated FADs, and LADs were compared to those of the index fossils and also the phased end Permian extinctions outlined by Smith and Botha-Brink (2014). Their inferred extinctions occur between 45–30 m below the PTB (phase 1), 20–0 m below the PTB (phase 2) and 30–45 m above the PTB (phase 3). The ranges of the five potential index taxa were also plotted relative to the local stratigraphy at the five main study areas and compared to positions of the inferred phased extinctions. The fossils are important relative dating tools to help infer whether laterally continuous sandstones at the field sites are penecontemporaneous.

Rarefaction

In addition a rarefaction analysis of the ranges of taxa was conducted to determine if a true representation of the diversity is being documented (see Chapter 3.3). Rarefaction allows the calculation of species richness for a given number of individual samples, based on the construction of rarefaction curves. For example rarefaction answers the question of how many species would you expect in a sample if you only got 25 specimens instead of 100. Rarefaction calculates the the estimated amount of species for a given sample by plotting a curve using the calculation below.

$$E(s) = \sum_{i-1}^{s} \left(1 - \frac{N - Ni}{N/n}\right)$$

E(s) is the expected number of species (which is what we want to calculate), N is the total number of individuals in the rarefaction sample (eg. 100), Ni is the number of individuals in the ith species, and n is the size of the smaller sample (eg. 25). The curve created is a plot of the number of species as a function of the number of samples. A steep slope indicates a large fraction of the species diversity remains to be discovered however, if the curve becomes flatter to the right, a reasonable number of individual samples have been taken and more sampling is unlikely to yield additional species. See Chapter 3.3 for the results of this investigation.

2.3.2 Sedimentology

Palaeocurrents

Palaeocurrent data was measured with a Silva compass and represented as vectors. In sedimentary rocks there are numerous features that allow for the reconstruction of ancient current directions in fluvial environments. Palaeocurrent indicators normally correlate with bedform or sand body orientation however, not all palaeocurrent indicators preserved in sedimentary rocks are reliable. Surface ripple marks and ripple cross-lamination, and in many cases, planar cross bedding are not very reliable as the bedforms that create them often do not orientate themselves to the dominant flow of the current (Collinson and Thompson, 1989). Trough crossbeds are a better indicator of downstream direction but the entire width of the bedform needs to be exposed in planview for accurate palaeocurrent readings. The sedimentary structures that provide the most reliable palaeocurrent readings in a fluvial environment are those formed near the thalweg of the main channels. These features include most sole markings at the base of the channel fill but especially longitudinal runnels, gutter and flute casts and current crescents in the upper phase plane beds which commonly give a trend and direction. Parting lineations, striations, wood and stem impressions orientated to the flow, and tool marks commonly only give trends but can be very accurate if used in association with other palaeocurrent vectorial indicators.

Palaeocurrent readings were collected for statistical analyses concerning palaeoenvironmental reconstruction (eg. fluvial style of channel deposits) (Boggs Jr, 2006) and also to identify changes in source area during deposition of the Balfour Formation as a whole. If significant changes in the source area can be identified between the field sites, these may have implications to understand the tectonic setting of the basin during the Lopingian, as well as other autogenic (synsedimentary changes in main flow directions due to avulsion) or even allogenic forces (eg. climate change).

Petrography

Sandstone samples for petrographic descriptions were collected from all localities where stratigraphic sections were measured. These samples were taken from arenaceous units within the DiAZ which include the upper Oudeberg Member, BM, Javanerskop member, and Musgrave Grit unit. The Lower Triassic Katberg Formation was also sampled for comparison. In some cases samples were taken from both the base and top of each outcrop in order to gain full understanding of the textures and grain sizes present in the sandstones. Petrographic descriptions of sandstone samples followed the methodology of Dickinson (1985) and Pettijohn

et al. (1987) noting the following features of sandstone grains: grain size, texture, roundness, sorting, and maturity. Any incidence of fabric and grain orientations and contacts, mineral composition, and the presence of matrix was also noted. This data was used to classify the sandstone petrography and interpret the provenance.

2.3.3 Detrital zircon analyses

Detrital zircon dating is also undertaken to assist characterization of the sandstone rich lithostratigraphic units under investigation. Source area determinations of the different zircon age populations were used to determine the maximum age of deposition. Samples were collected from sandstones correlated to the BM, Oudeberg, and Javanerskop members, Boomplaas sandstone (BS), and Musgrave Grit unit from the six study sites. Samples of the lowermost Katberg Formation were also obtained from some of the study areas for comparison. Sandstone samples were taken from the bases of the sandstone units as the densest minerals and largest particles accumulate at the bases of channels. At least 35-75 randomly selected grains are required to ensure the analysed sample is representative of the population (Dodson et al. 1988; Fedo et al. 2003) therefore samples collected had to be a minimum of 2 kg to ensure extraction of an accurate representative population of detrital zircon grains.

Once samples were collected they were taken for grain extraction to the Central Analytical Facility at the University of Stellenbosch. Zircons were extracted by heavy mineral separation and ages were determined by Laser Ablation Inductively Coupled Plasma Mass Spectrometry (LA-ICP-MS). This method uses a laser to ablate material from a grain mounted on a polished resin mount which is then isotopically analysed using a mass spectrometer. LA-ICP-MS is currently the most common method for analysing detrital zircons because it achieves the same precision and accuracy as an ion probe (Košler, 2007) but is considerably more efficient and cost effective (Gehrels, 2014).

The zirconium silicate, zircon ($ZrSiO_4$) forms in a wide variety of contrasting rock types, such as acid to intermediate igneous, volcanic and metamorphic rocks. Uranium ($U^{4+/6+}$) often substitutes Zirconium (Zr^{4+}) into its structure due to the similarity in size however, any initial Lead (Pb^{2+}) is excluded from the structure. Therefore any Pb present (^{206}Pb, ^{207}Pb) in the structure is assumed to have been the result of decay of initial U (^{238}U, ^{235}U) within the zircon crystal. Exhibiting high refractory behaviour and mechanical resistance under sedimentary conditions, zircons represent reliable closed systems that are important for obtaining accurate and precise U-Th-Pb ages concerning source rock petrology and chronology. Also, the radiometric age obtained for the youngest zircon grain within a population of detrital zircons is

considered to be a good indication as to the maximum age of the deposition of the sedimentary layer itself, or it can indicate the timing of metamorphism responsible for affecting sedimentary rocks after deposition (Zeh et al. 2008; Vorster, 2013). This makes zircons ideal mineral tracers in sedimentary systems, recording potential tectonic and sedimentary processes active in the geological past (von Eynatten and Dunkl, 2012).

What makes the U-Th-Pb dating system especially rigorous is its existence as three decay schemes. However the Thorium (Th) system is generally not used because of its rarity in zircons and its inability to measure on the Concordia diagram (Gehrels, 2014). Pb also has one other non-radiogenic isotope (^{204}Pb) but this is very rare in nature and since no initial Pb is present in zircons it is not normally a problem. ^{238}U decays to ^{206}Pb with the emission of 8 α particles and 6 β particles at 4.2 Mega-electronvolts (MeV) (half-life of 4.47 Ga), ^{235}U decays to ^{207}Pb at 7 α particles and 4 β particles at 4.2-4.6 MeV (half-life of 0.70 Ga), and ^{232}Th decays to ^{208}Pb at 6 α particles and 4 β particles 3.0-4.0 MeV (half-life of 14.01 Ga). The Isochron method of plotting age determinates can be used but more rigorous is combining the two U-Pb decay schemes to plot the Concordia curve of Wetherill (1956). Combining the decay schemes creates the following equation:

$$\frac{207\text{Pb}}{206\text{Pb}} = \frac{235\text{U}}{238\text{U}} \frac{(e^{\lambda 235t} - 1)}{(e^{\lambda 238t} - 1)}$$

Where **e** is the natural log, **λ** is the decay rate of Uranium, and ***t*** is age of the zircon we want to determine. The ^{235}U/^{238}U ratio is a natural constant and as a result is the assumed amount 132.82 (Heiss et al. 2012). The Concordia curve that results is caused by the locus of points for which the ^{206}Pb/^{238}U age equals the ^{207}Pb/^{235}U age (Wetherill, 1956). It is curved due to the different half-lives of ^{238}U and ^{235}U. Successive gaps between age increases back into time (value of ^{207}Pb/^{235}U higher than for ^{206}Pb/^{238}U). This is because the half-life of ^{238}U is much longer than ^{235}U so ^{235}U runs out faster, this also results in the curve steepening as it approaches younger geological ages and eventually the curve becomes asymptotic. This more rapid loss of ^{235}U causes loss of resolution as the curve approaches the modern day, therefore it is not a reliable dating method for very young rocks. Combining the decay schemes also allows for the identification of isotopic disturbances, or age underestimations due to resetting of the decay scheme in the zircon by reheating or recrystallization from Pb loss occurring in the system. This will be observed on the Concordia diagram as zircons plotting off the curve, usually below it. A discordia trajectory is then plotted through the discordant curves and where it intersects the Concordia, which tells you the actual age of crystallization (top intersect) and age of recrystallization (bottom intersect).

Lead loss due to recrystallization is often thought to be the most important mechanism to produce discordant age results (Wetherill, 1956). So not only can you receive accurate dates but you can attain precision by using the in–built correction mechanism of the paired decay scheme.

The presentation of the zircon dates in the Conchordia diagram is often not suitable for presenting data from a large number of grains. Probability density diagrams are the most popular means of representing detrital zircon age data because they allow easy visual comparison between large datasets (Košler, 2012). The area underneath the probability density curve has been normalized to 100%. The peak intensities of probability density diagrams could also be considered to reflect the precision of the age determination.

This was the manner in which detrital zircon dates were presented in this study, with referral to the Concordia diagrams and datasets where appropriate (see Chapter 3.5 and Appendix 1 on disc). The probability density plots only comprise zircons of a discordance that did not exceed 10%. This is because Pb-Pb ages with a discordancy of 5-10% are considered reliable enough for use in sedimentary provenance studies (Košler and Sylvester, 2003; Bowden, 2013). Metamorphic grains were also included in the probability density plots and investigation but Th/U values of < 0.07 differentiate metamorphic zircons from igneous ones (Rubatto, 2002). Additionally a representative of each major population identified in the 12 samples was compiled by use of CL images provided by Dr. Dirk Frei. Since the distribution of the grains on the mount is random, the compilation of the different population groups was undertaken manually. Descriptions and interpretations of the detrital zircon analysis and data followed the procedures of Vorster (2013) and Bowden (2013).

2.3.4 Palaeoenvironmental reconstruction

This was conducted for the purposes palaeoenvironment interpretation and basin evolution of strata assigned to the *Dicynodon* Assemblage Zone. The methodology in this section of the study involves facies analysis which is a discipline that aids in the identification and palaeoenvironmental interpretation of sedimentary rocks in the field. Facies analysis forms the framework for interpreting ancient depositional settings and was pioneered mainly in ancient fluvial deposits (Leopold and Wolman, 1957; Allen, 1983; Walker, 1984; Miall, 1996) however, its use in marine and lacustrine systems is also on the rise (Bellanca et al. 1992; Pemberton et al. 2003; Platt and Wright, 2009). In the context of interpretation of ancient fluvial systems, the core concept of facies analysis is that fluvial deposits are repeated, hierarchical, and predictable. The basic hierarchical building blocks of fluvial facies models are termed lithofacies, or facies elements, facies associations, and finally architectural elements.

Identifying these different ranked fluvial depositional features in the field involved the investigation of natural exposures on hillsides during the construction of vertical sections, but also artificial exposures such as road cuttings. These different types of outcrop allowed for the documentation of external and internal structures of the sedimentary rocks under investigation (either as a single vertical section or 2D panel section), and interpretation of the type of depositional setting. The methodology of the scaled facies analysis will now be briefly discussed.

Lithofacies and facies associations

Lithofacies and facies association classification schemes used in this study were compiled and defined according to methodologies of Reineck and Singh (1975), Reading (1978), Collinson and Thompson (1989), Miall (1977, 1985, 1988, 1996, 2014) , Colombera et al. (2013), and Wilson et al. (2014a). In addition Paiva (2015) also provided a useful framework for comparison in his un-published MSc thesis. Facies and facies associations have been the major tool in identifying and interpreting depositional environments for the sedimentary rocks of the Beaufort Group by previous workers and are still a standard component of the study of sedimentary rocks (Stear, 1983, 1985; Smith, 1990; Hancox, 1998; Rubidge et al. 2000; Neveling, 2002; Smith and Botha, 2005; Botha and Smith, 2006; Viglietti et al. 2013; Botha-Brink et al. 2014).

Reading (1978) defines a facies as a distinctive rock that forms under certain conditions of sedimentation, reflecting a particular process or environment. Meanwhile a facies association is defined by groups of lithofacies that form together under specific depositional circumstances such as channel or overbank environments (Miall, 1996).

Miall (1977) proposed a simple classification scheme when reviewing braided river deposits, making use of a two letter code to facilitate quick field and laboratory identification and documentation. Later use of this facies scheme by a number of workers showed that it could be applied to many kinds of fluvial deposits and not just the braided type. In Miall's (1996) scheme, a facies is given a facies code which includes a capital letter to indicate the dominant grain size (G=gravel, S=sand, F=fines including very fine sand, silt, and mud) and a lower case letter for the characteristic texture or structure of the lithofacies (eg. p=planar cross–bedding, h=horizontal lamination).

Architectural element analysis

A wealth of information is contained in many laterally extensive outcrops of fluvial deposits that are not captured by the conventional vertical section. Architectural elements are essentially a facies association with a distinctive 3D geometry and represent subenvironments in a particular

fluvial system. Their classification is founded on their lateral extent, internal geometry and organization of sedimentary facies (Miall, 1996; Colombera, 2013). Bounding surfaces and their nature are also key to their classification, which are ranked based on their lateral extent,

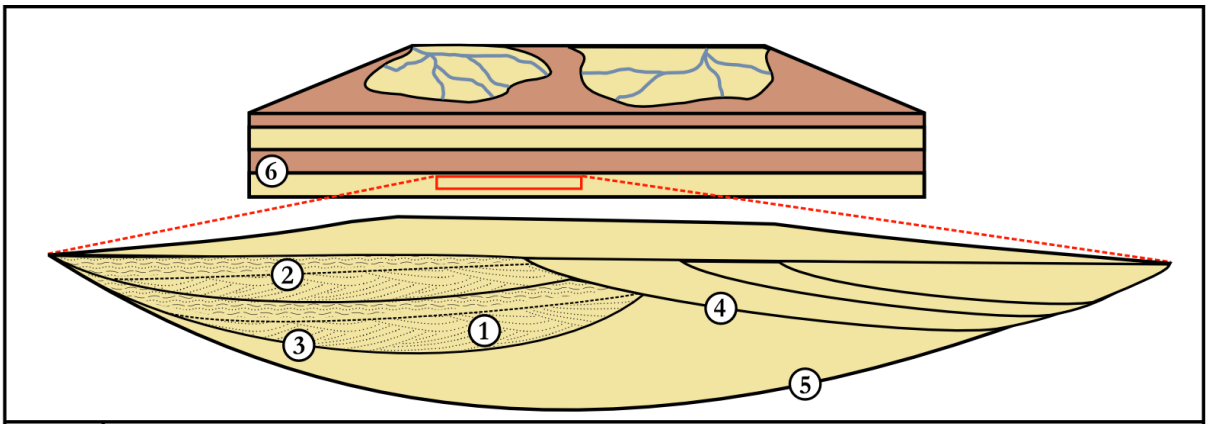

Order	Nature of surface
1st	Individual crossbed sets.
2nd	Separation between crossbed cosets.
3rd	Inclined erosion surface within coset or coset group.
4th	Separates unit with accretionary integrity (eg. lateral accretion barform).
5th	Surface with marked shift in grain size (eg. Shifting erosion on channel floor).
6th	Separated major channel sandbodies from other facies (eg. major base level or climatic change).

Figure 2.3: Diagram shows bounding surface and representstive illustrations within the context of a hypothetical continental fluvial system. Adapted from Miall (1996, 2014) and Paiva (2015).

erosional, or accretionary features. Bounding surfaces with illustrations are shown in Figure 2.3. Accordingly architectural elements were identified for the Barberskrans, and Javanerskop members, the Musgrave Grit unit, and potential lateral equivalents using the framework of Miall (1985, 1996, 2014). Architectural element studies on the Beaufort Group have been rare in the past (Stear, 1983; Smith, 1987, 1989; Smith and Ward, 2001; Smith and Botha, 2005; Botha and Smith, 2006; Smith and Botha-Brink, 2014) but recent work by Wilson et al. (2014) show that middle Permian channel sandstone deposits vary greatly in sinuosity, even on similar stratigraphic intervals. The fluvial style of the Barberskrans Member has been interpreted superficially in the past by previous workers (Tordiffe, 1978; Visser and Dukas, 1979; Cole and Wipplinger, 2001; Cole et al. 2004) who regarded them as representing distal braid plain environments by virtue of their tabular nature and higher sandstone:mudstone ratio. Regardless, no formal architectural element study on any of the sandstone units has since been conducted.

This study adopted existing terminology and methodology from earlier studies (Allen, 1983; Miall, 1985, 1996, 2014; Bridge, 2003, Colombera et al. 2013) and studies already done on the Beaufort Group (Wilson et al. 2014) using architectural element codes and bounding surface nomenclature. The type locality of the Barberskrans Member south of Cradock is well exposed and thus the most detailed panel was created here using photomosaics to study the architectural features preserved within the Barberskrans Member at its type locality. By recognition and classification of these ranked components of facies analysis in the field, fluvial systems are mainly divided into the channel and overbank (floodplain) deposits. Since subenvironments in the floodplain environment are difficult to decipher without good outcrop, and current nomenclature is not entirely applicable to floodplain deposits, often more emphasis is placed on the channel settings. This was why most of the emphasis was placed on sandstone rich units correlated to the BM, although where possible the floodplain sediments were investigated.

All the data is then synthesized into palaeoenvironmental reconstructions and a basin development model for the Lopingian *Dicynodon* Assemblage Zone in Chapter 5. Any differences identified between field sites were also documented. As fluvial style can change in response to a number of allogenic (tectonics and climate) and autogenic (gradient, aggradation, avulsion, discharge, bank strength, vegetation) influences (Leopold and Wolman, 1957; Schumm, 1968; Miall, 1996; Tooth, 2000; Catuneanu, 2006; Long, 2006; Ashworth and Lewin, 2012), it was never the assumption of this investigation to use fluvial style as the only means of characterization for the lithostratigraphic units under investigation. However, wherever fluvial style could be determined it was done in the context of bigger picture implications, such as the tectonic and palaeoenvironmental setting of the Lopingian Karoo Basin.

Chapter 3: Results

This chapter presents results of the investigation into the lithostratigraphic units of the Balfour and Teekloof formations at the main field sites (Cradock, Nieu Bethesda, Beaufort West/Fraserburg, Gariep Dam, Jagersfontein, and Bloemfontein) within strata of the *Dicynodon* Assemblage Zone (DiAZ).

The first part (Chapter 3.1) addresses the status of the Barberskrans Member because the discussion of observations and results otherwise becomes convoluted. The second part (Chapter 3.2) lists and discusses the stratigraphic sections used in the interpretation of the lithostratigraphy of the Lopingian DiAZ. Each field site is discussed separately with vertical sections measured at each field site presented showing the stratigraphic position of currently accepted lithological subdivisions (eg. the Oudeberg Member or Katberg Formation). The lithostratigraphic units are delimited using their stratigraphic position and also their lithological properties where appropriate. All the raw data are also presented on the vertical sections, and this is followed by the presentation and discussion of composite sections created for each field site (Chapter 3.2.1).

The third part (Chapter 3.3) presents the palaeontology and biostratigraphic data collected during this study. Most of these results are published in the Journal of African Earth Sciences (Viglietti, P. A. Smith, R. M. H., Angielczyk, K. D., Kammerer, C. F., Fröbisch, J., Rubidge, B. S., 2016. The *Daptocephalus* Assemblage Zone (Lopingian), South Africa: A proposed biostratigraphy based on a new compilation of stratigraphic ranges. Journal of African Earth Sciences, 113, 154-164 DOI 10.1016/j.jafrearsci.2015.10.011) and is included as the completed publication. Therefore the DiAZ is referred to as the *Daptocephalus* Assemblage Zone (DaAZ) from this point.

The fourth and fifth parts (chapters 3.4 and 3.5) presents sedimentological data whereby the lithostratigraphic units under investigation are compared using palaeocurrent vectors, petrographic descriptions that include mineral modal abundances, grain roundness, sorting, textural maturity, and inferred provenance. Additionally the sixth section (Chapter 3.6) includes detrital zircon dating results which not only help with refining interpretations on provenance and basin modelling, but also provide maximum depositional ages. Finally, the sedimentological data collected for palaeoenvironmental and basin analysis studies is presented in Chapter 4, showing identification of lithofacies, facies associations, and architectural element analysis. Finally an interpretation of fluvial style is made for the lithostratigraphic units of the Balfour and Teekloof formations.

3.1 Status of the Barberskrans Member

Johnson (1966) first identified a sandstone unit within his Zone 3 subdivision, but later Tordiffe (1978) named it the Barberskrans Member (BM). He used the Barberskrans Cliffs, 10 km south of Cradock in the Eastern Cape as the origin for its name because this is where a multi-storey sandstone correlated to the BM by Tordiffe (1978) is exposed along the Great Fish River (Figure 3.1). However, this study has identified that Tordiffe's (1978) BM cannot be correlated to the unit at the Barberskrans Cliffs because it is a sandstone of the Oudeberg Member.

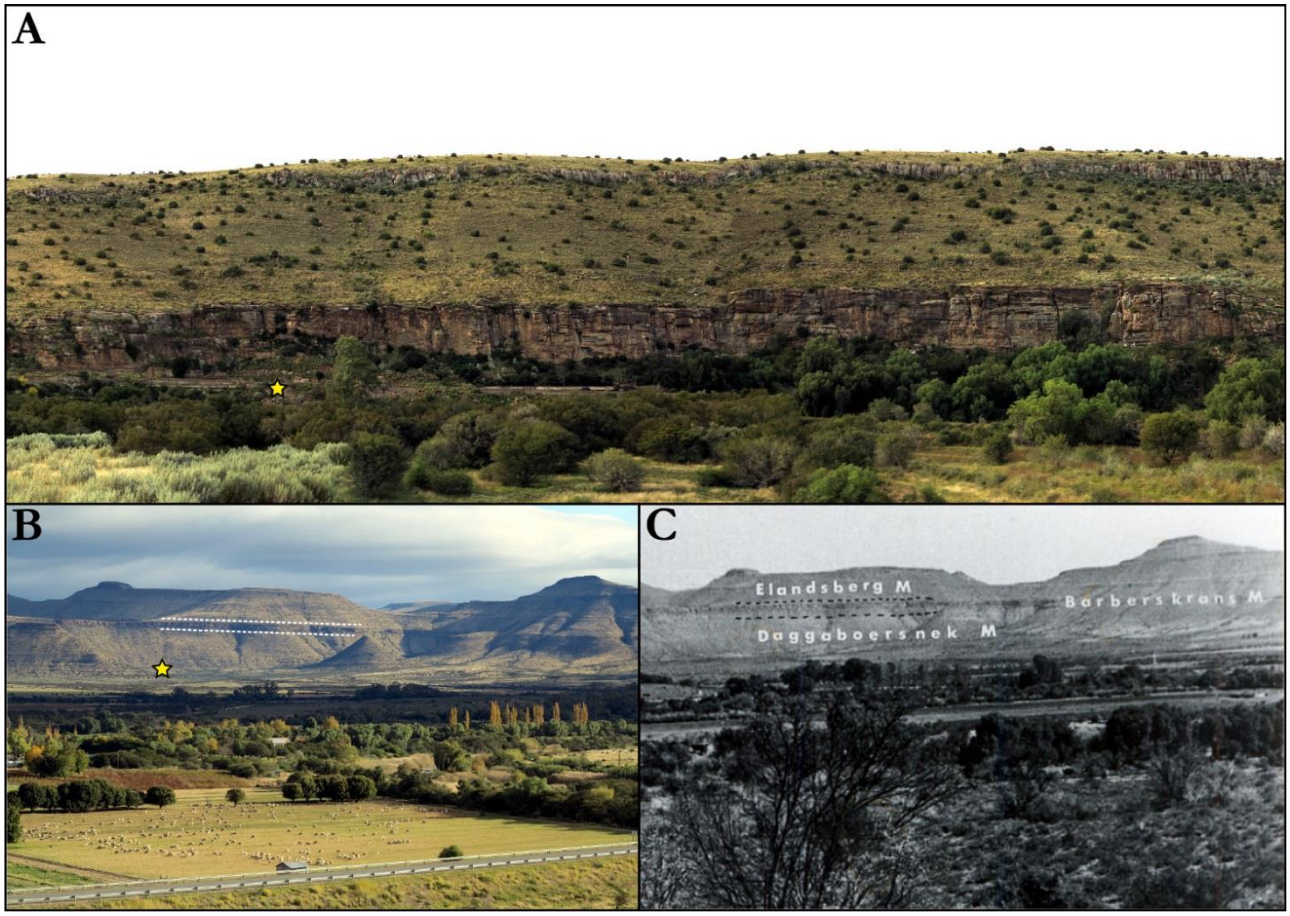

Figure 3.1: A) The current type locality of Tordiffe's (1978) Barberskrans Member (looking north) and position of section 1A (yellow star) 10 km south of Cradock along the N10 highway. B) View looking south from the Barberskrans Cliffs. A prominent sandstone unit (white dotted lines) is visible from this distance above Mortimer and this is Johnson's (1976) original Zone 3 which was renamed by Tordiffe's (1978) as the BM. Yellow star marks the position of section 1B. C) Tordiffe's (1978) photograph of the same unit he named the BM and correlated to the unit at the Barberskrans Cliffs. This study has shown that Tordiffe's (1978) BM is not the same unit at the Barberskrans Cliffs in (A). Firstly it is not at the same stratigraphic position and underlies the argillaceous Daggaboersnek Member. Secondly, while it is a sandstone-rich unit, it is a 40 m thick lense-shaped sandstone that is laterally continuous over a distance much like the sandstones of the Oudeberg Member described in the literature (Johnson, 1976; Tordiffe, 1978, see Table 1.1). Tordiffe's (1978) BM is a paired unit and the average maximum thickness attained for a single sandstone in this unit is between 20-25 m (although there are some exceptions). This study concludes that the unit at the Barberskrand Cliffs is the Ouderberg Member, which has priority (Johnson, 1976). Tordiffe's (1978) BM does not occur at the Barberskrans Cliffs, and therefore a new type location and name for this unit is given in this study.

The name of the Oudeberg Member has priority (Johnson, 1976) and thus should not be renamed. Nevertheless, Tordiffe's (1978) BM does not actually occur at its current type locality, and therefore requires a new type locality and a new name by lithostratigraphic definition of SACS (1980) and Johnson (1987).

A new lithostratigraphic subdivision

A new type area and name for Tordiffe's (1978) BM is proposed in this study. Ripplemead Farm 20 km north of Nieu Bethesda is chosen for the new type area for Tordiffe's (1978) BM and this study recommends the Ripplemead member (RM) as a new name for this unit. The RM is used to refer to Tordiffe's (1978) BM from this point on. The sandstone at the Barberskrans Cliffs has been identified as the Oudeberg Member and will also be referred to as such from this point on. Figure 3.2 shows the updated Upper Permian Beaufort Group lithostratigraphy. In addition, Table 3.1 gives a standardised lithostratigraphic description of the newly proposed Ripplemead member as outlined by SACS (1980) and Johnson (1987). The Ripplemead member is now investigated in regards to its lateral extent and whether it can be correlated to the Javanerskop member of Le Roux (1985) in the west, and Rutherford's (2009) Musgrave Grit in the north. The results of the stratigraphic sections will now discuss the outcome of this investigation.

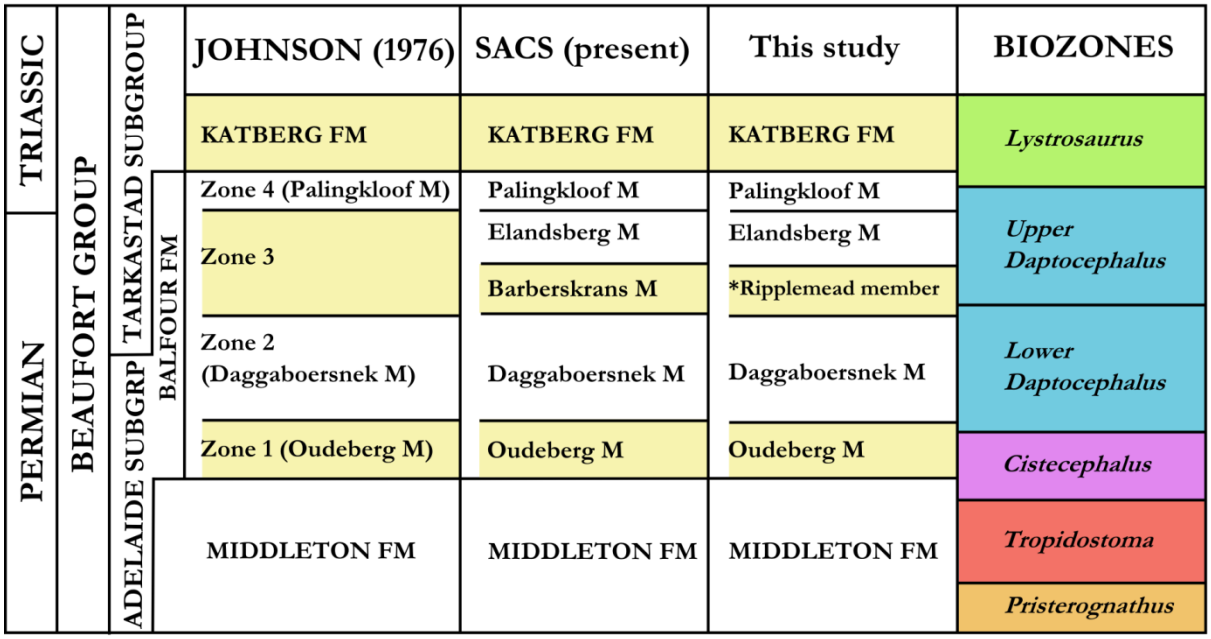

Figure 3.2: Subdivisions of the Balfour Formation by Johnson (1976), SACS (1980), and what has been identified during this study. Now that the Oudeberg Member and not Tordiffe's (1978) Barberskrans Member is identified at the current type locality (Barberskrans Cliffs) a new name has been given to this unit, which is the Ripplemead member. The unit is now named after a farm north of Nieu Bethesda (See Table 3.1). Note also the updated biostratigraphy is also shown after Viglietti et al. (2016).

Table 3.1: The formal lithostratigraphic definition of the newly proposed Ripplemead member. Since this unit refers to Tordiffe's (1978) old Barberskrans Member, its lithological properties have not changed. It is only the name, source of name, proposer, and type area for the unit which has changed.

Unit	**Rank**	**Source of name**	**Proposer**	**Stratotype (S) Type Locality(L) Type area (A)**	**Stratigraphic position/age**	**Thickness and boundaries**	**Lithological features**
Ripplemead	M*	Farm 20 km north of Nieu Bethesda.	Viglietti (2016)	Ripplemead Farm area (A).	Lopingian in age. It overlies the Daggaboersnek M and underlies the Elandsberg M. Correlates to the *Daptocephalus* Assemblage Zone (Viglietti et al. 2016).	A maximum thickness of 190 m was estimated by Tordiffe (1978) near Cradock, but an average thickness of 60 m was obtained by Visser and Dukas (1979) on Platberg near Graaff-Reinet. The lower boundary with the Daggaboersnek M is gradational while the upper boundary with the Elandsberg M is relatively sharp (Visser and Dukas, 1979).	Sandstone (70-80%): Maximum thickness 40 m. Average thickness 20-25 m. Fine to medium-grained tabular pale olive, crossbedded, and ripple cross-laminated sublitharenites. Mudstone (20-30%): Maximum thickness 20 m thick. Green, structureless mudstone. Sometimes pedogenic nodules and rootlets encountered. Vertebrate fossils are also found in mudstones. A conspicuous sandstone rich unit that lies between the argillaceous Daggaboersnek and Elandsberg members.Sandstones are often paired and continue laterally for a few kilometres (Tordiffe, 1978). Mud pellet/feldspathic conglomerates, plant and fish fossils are common at sandstone bases, particularly in Nieu Bethesda (Bender, 2000). Cradock, Cookhouse and northwest of Nieu Bethesda have good exposure of this unit.

3.2 Stratigraphic sections

As a basis for comparison of lithology, stratigraphy, and thickness of the sedimentary packages present at each field site, a total of 13 vertical sections were measured. Refer to Figure 2.2 in Chapter 2.3 for the vertical section legend. Each vertical section which detail the thicknesses of the lithologies encountered at each field site measured to an accuracy of 0.2 m, sedimentary structures, fossils (more information on fossils is shown in Appendix 2 on disc), palaeocurrents, petrography, and detrital zircon dates (stratigraphic position of all samples taken are shown). Lithofacies (eg. Sm, Sl, St) and facies association (eg. F1, F2) codes discussed in Chapter 4 are also shown on the vertical sections. Geological maps (see Figure 3.3 for map legend) and figures showing field relations are also referred to in this section. A brief description of each measured section is presented and is followed by five composite sections (Chapter 3.2.1) representing the complete stratigraphic succession in different sectors of the field area. These composite sections will later be discussed and compared in the context of the lithostratigraphy, biostratigraphy, palaeoenvironment, palaeocurrents, petrography, detrital zircon dates, and basin development model in Chapter 5. The southern-most field site (Cradock) is presented first then Nieu Bethesda, Beaufort West, and finally Gariep Dam, Jagersfontein, and Bloemfontein. Refer to Figure 2.1 in Chapter 2 for the positions of the field sites in the main Karoo Basin.

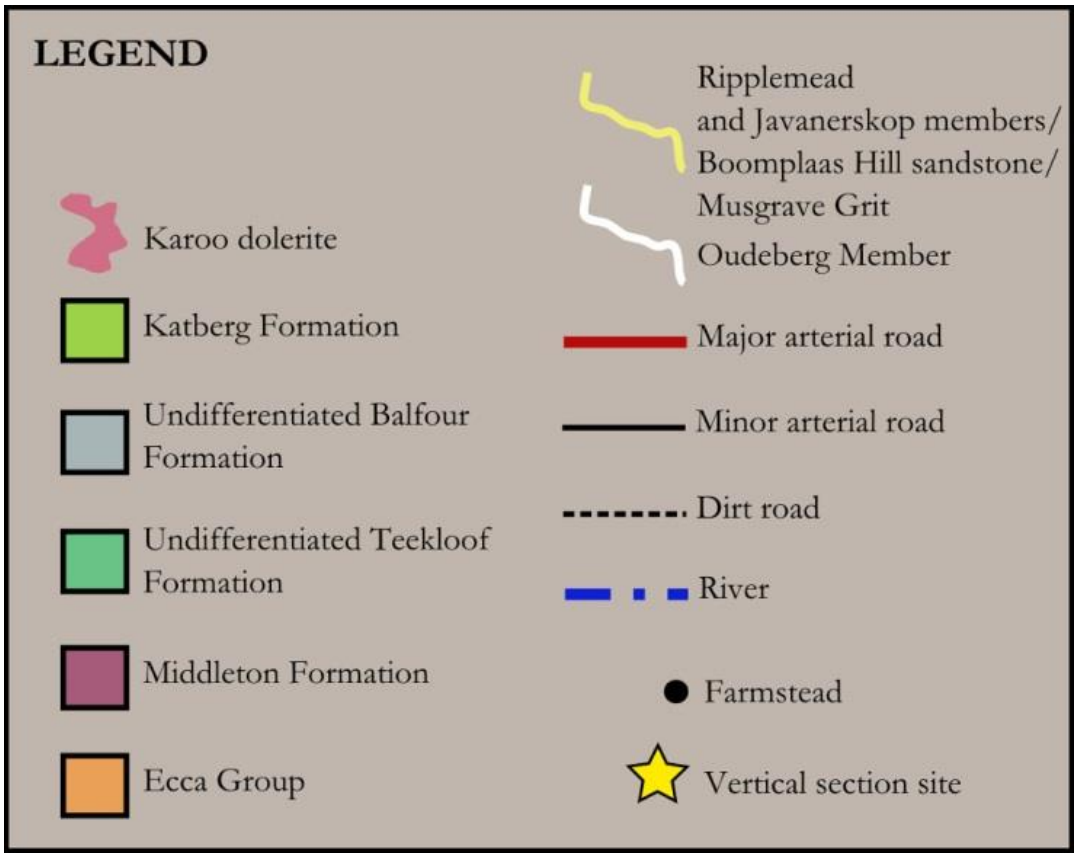

Figure 3.3: Legend of symbols used in maps created for the six main study sites of this investigation.

Cradock (Sections 1A, 1B, and 2)

Initially, the fieldwork focussed on the Barberskrans Cliffs about 10 km south of the town of Cradock on a portion of the old N10 Highway (Figures 3.1, 3.4) location of Tordiffe's (1978) type location for his BM (SACS, 1980). Here he recognized the BM as a 190 m thick arenaceous unit and although the sandstone in the area is well-exposed, the intervening mudrocks are concealed by significant vegetation cover or large doleritic intrusions. Stratigraphic section 1A (Figure 3.6) is measured at this site. Tordiffe (1978) also correlated this unit to a sandstone succession in the mountains surrounding the agricultural hub of Mortimer (Gannahoeksberg) on the farm Hales Owen, site of section 1B (Figure 3.7). However the sandstone at section 1A is now identified as the Oudeberg Member and because Tordiffe's (1978) BM is not present at this location the BM is now renamed the RM. In a road cutting along the N10 highway the same Oudeberg Member sandstone that is present at the Barberskrans Cliffs is outcropping below the RM and separated by the 300 m thick Daggaboersnek Member (Figure 3.5). Tordiffe (1978) also previously documented the Daggaboersnek Member to be 1200 m which is not observed anywhere in this study. The Daggaboernek Member was identified from its stratigraphic position, which overlies the Oudeberg Member and underlies the RM. In addition, regularly bedded varve-like mudstone with minor sandstone lenses, and rich fossil flora identifies the mudstone rich interval separating these units as the Daggaboersnek Member (see Table 1.1 for more information). The same stratigraphy is traced laterally to the Baviaansriver Valley near Bedford (Figure 3.5). Here suitable outcrop for detailed stratigraphic work is identified on Lower Clifton farm where section 2 is measured (Figure 3.8). The Oudeberg Member is also identified in the Baviaansrivier Valley at a similar altitude to the site of section 1A (between 865-900 m above sea level) and a similar stratigraphic relationship is identified with the RM (Figure 3.5, C). It is noteworthy to mention that this is the stratigraphic distance that Cole and Wipplinger (2001) documented between the Oudeberg Member and the RM near Murraysburg. The information gathered from the three vertical sections measured in this field area will now be briefly discussed.

Section 1A: Barberskrans Cliffs, N10, Cradock, Cradock district, Eastern Cape

This was the site of the type locality for Tordiffe's (1978) BM (Figures 3.1 and 3.6). Here Tordiffe (1978, pp 77) described a 190 m thick unit that comprises mainly sandstone in 20 m thick upward-fining cycles that grade into thin (2 m) layers of green mudstone. Upon visiting the type locality, which now overlooks an abandoned section of the old N10 highway, it is evident this unit, now identified as part of the Oudeberg Member is at most 40 m thick (Figure 3.1). The multi-storey sandstone which outcrops on the Barberskrans Cliffs extends laterally for

approximately 2000 m at an altitude of between 865 m and 900 m above sea level. The section was measured to the summit of the Barberskrans Cliffs where a dolerite sill caps the outcrop and there is no evidence for another sandstone unit outcropping at this site (section 1A, Figure 3.6). In addition, a 190 m thick arenaceous unit could not be identified at the type locality, or anywhere else in the Cradock area. During this study the Oudeberg Member sandstone at the Barberskrans Cliffs (section 1A) is traced along the Mortimer road (R390) where it forms a rocky promontory along the Fish River (Figure 3.5). The Oudeberg Member also outcrops at a similar altitude to a sandstone (~860-900 m above sea level) north of the town Cookhouse where the Oudeberg Member was identified by Johnson (1976) and Tordiffe (1978). In a personal communication to Visser and Dukas (1979) Tordiffe observed similarities in his BM to the Oudeberg Member which also makes this correlation compelling.

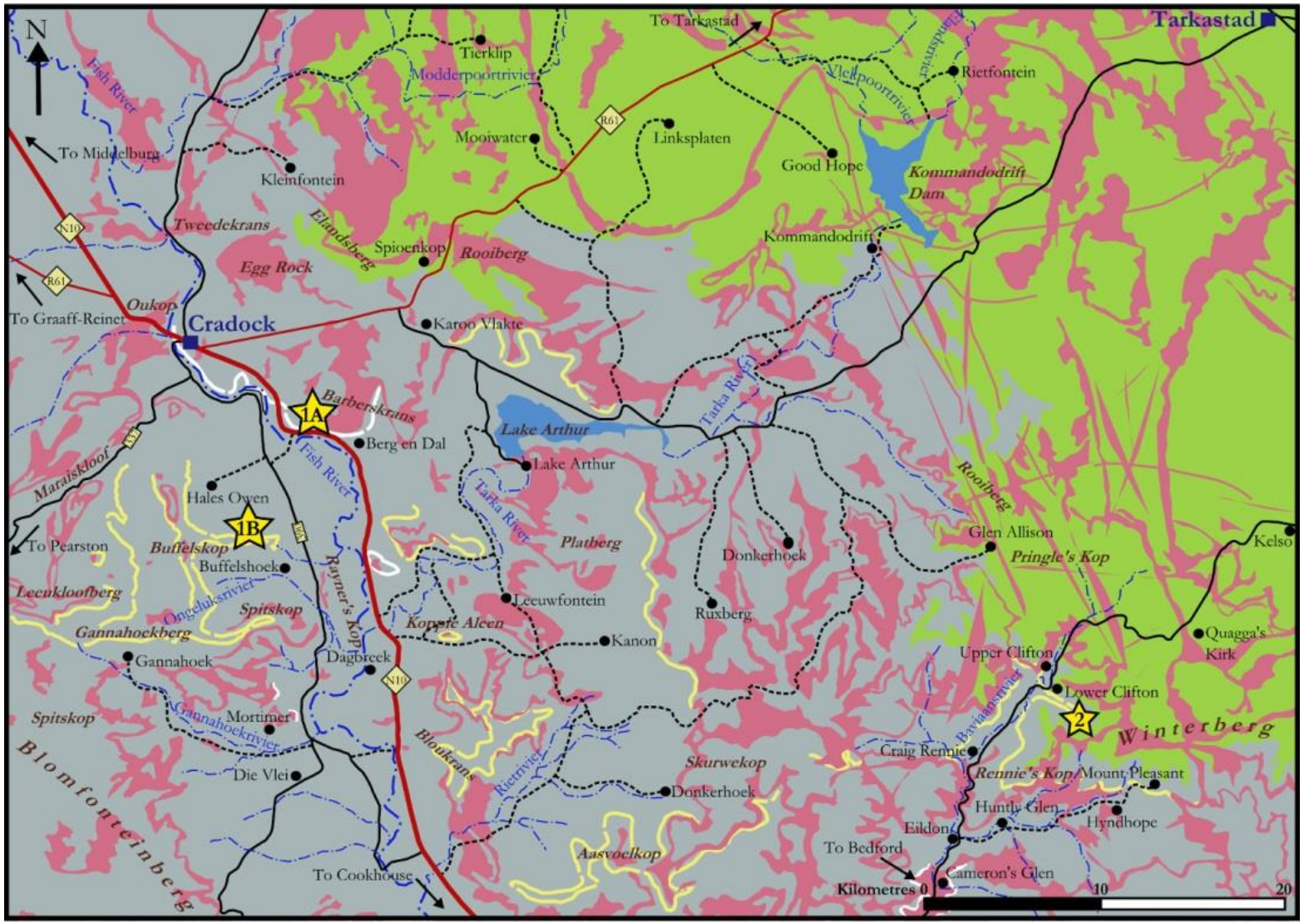

Figure 3.4: Map of the Cradock field site showing the distribution of the Oudeberg Member (white), the Ripplemead member (yellow), and the positions of vertical sections 1A, 1B, and 2.

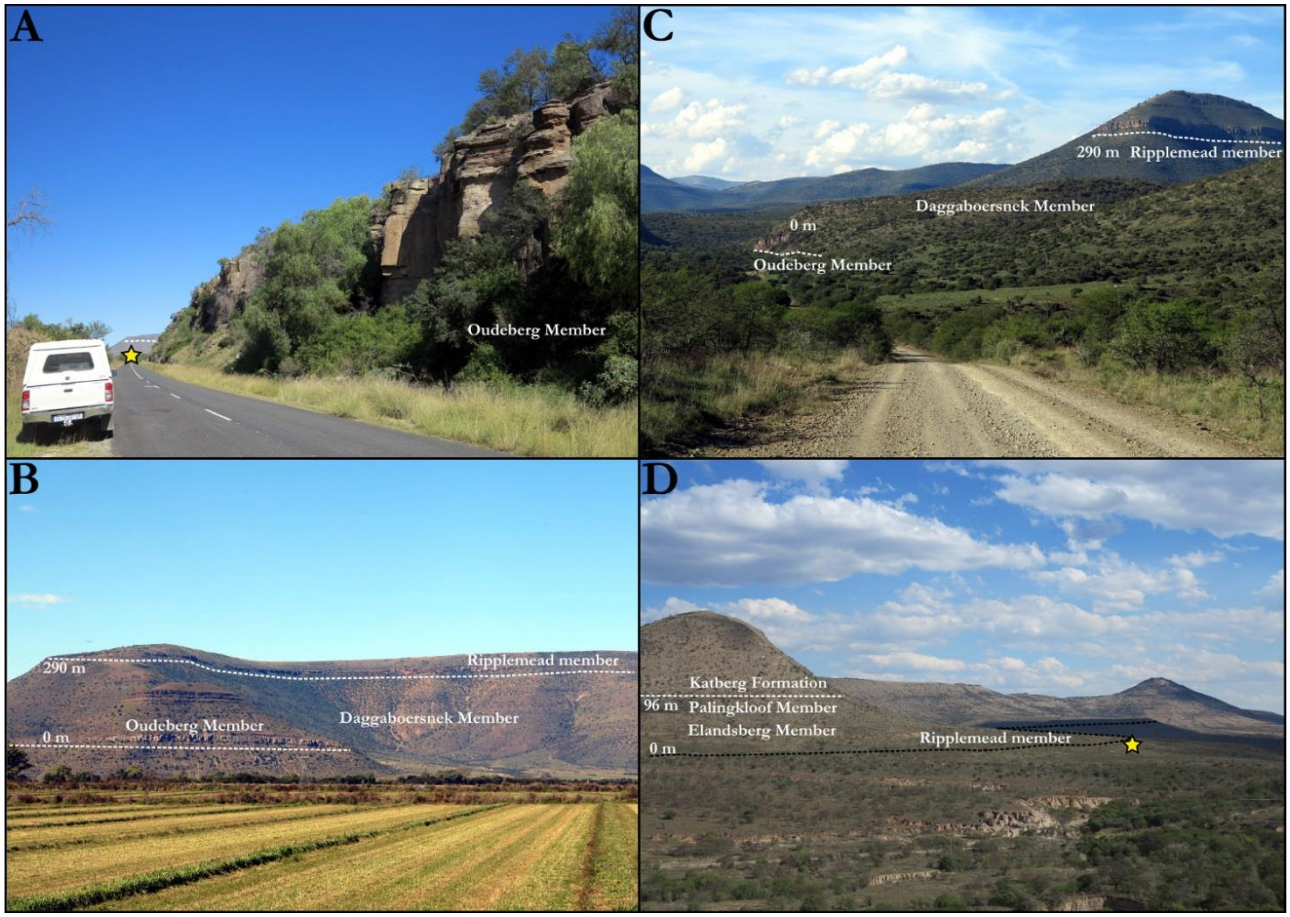

Figure 3.5: A) The Oudeberg Member sandstone identified on the Barberskrans Cliffs is shown outcropping along the R309 about 4 km north of Hales Owen Farm and site of vertical section 1B (yellow star). B) Photograph taken from the Mortimer road (R309) looking east towards Koppie Aleen and Rayner's kop. It shows the position of the Oudeberg Member and Ripplemead member which Tordiffe (1978) identified in the field area as belonging to the same unit and named the Barberskrans Member. They are in fact stratigraphically separated by 300 m of strata assigned to the Daggaboersnek Member. The RM does not occur at the Barberskrans Cliffs and thus Tordiffe's (1978) BM cannot retain its name. C) The same stratigraphy traced into the Baviaansrivier Valley in the Winterberg near Bedford. D) Lower Clifton farm in the Baviaansrivier Valley where vertical section 2 (Figure 3.8) was measured from the base of the RM to the base of the Katberg Formation (indicated by white dotted lines). Increased vegetation made photographing lithostratigraphic units difficult in the Baviaansrivier Valley. Yellow star indicate start point of vertical section 2.

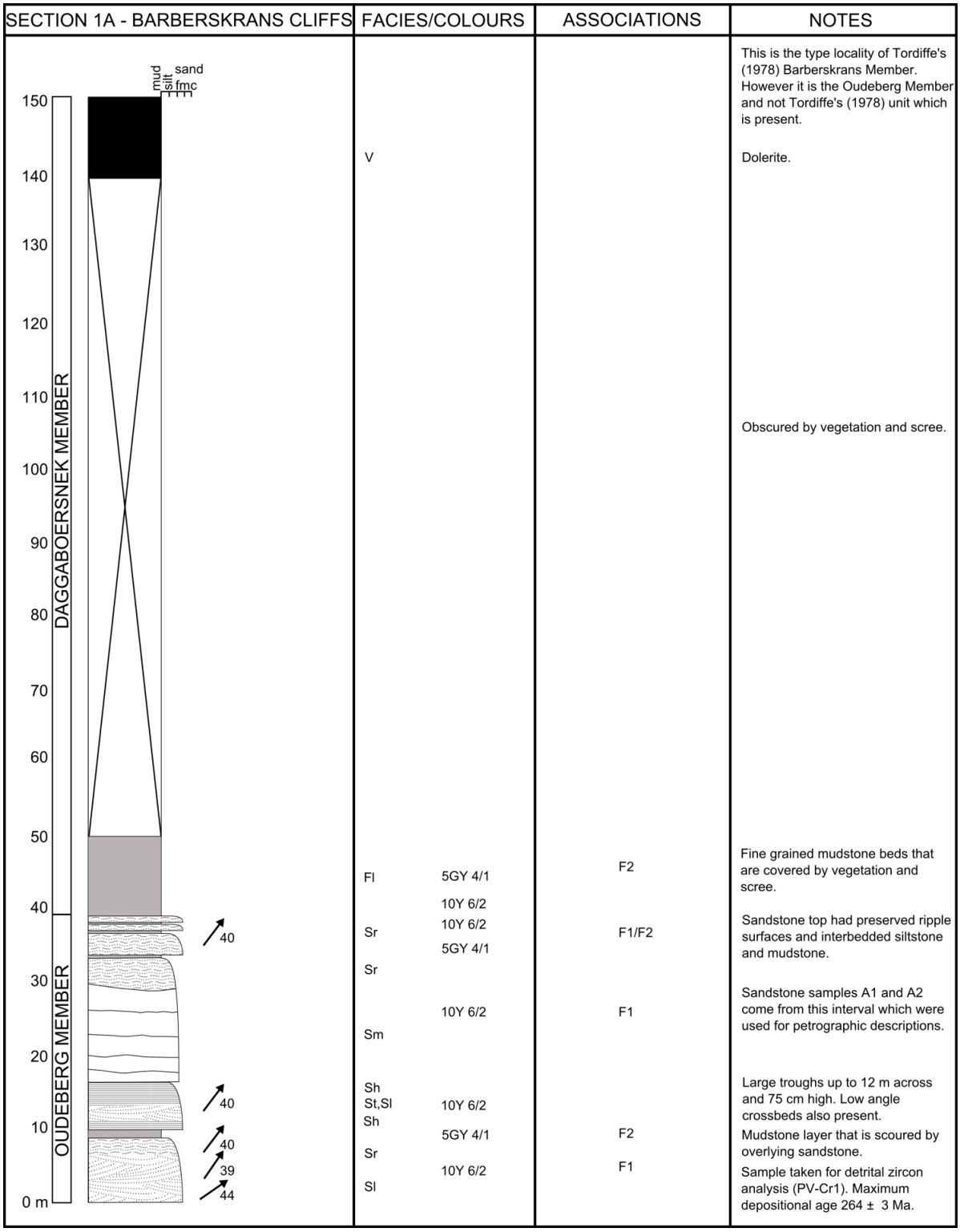

Figure 3.6: Vertical section 1A measured at the type locality of the Barberskrans Member named by Tordiffe (1978) on the Barberskrans Cliffs. Note that it is the Oudeberg Member present at this site.

Section 1B: Hales Owen farm, Cradock district, Eastern Cape

Here the prominent sandstone on the section is identified as the RM and does not correlate to the Oudeberg Member sandstone on section 1A (Figure 3.7). It is 290 m above the Oudeberg Member sandstone on section 1A, separated from it by the Daggaboersnek Member (See Table 1.1 and Figure 3.5, B). Here a single, sometimes paired and laterally continuous sandstone is identified in the section. The base of the measured section is approximately 82 m above the top of the Oudeberg Member at the Barberskrans Cliffs (section 1A), which was traced to the site along the Mortimer road (Figure 3.5). The section logs 170 m of the dominantly argillaceous Daggaboersnek Member and the arenaceous RM. Here the RM is split into two multi-storey sandstones separated by ~ 8 m of dark greenish grey siltstone (5GY 4/1), making it 67 m thick in total. The stratigraphic distance to the Katberg Formation could not be determined at this site however, the RM could be traced laterally southwards towards Bloukrans and Aasvoelkop and into the Baviaansrivier Valley on the farm Lower Clifton (Figure 3.5).

Section 2: Clifton farm, Baviaansriver Valley, Eastern Cape

Good outcrop on Lower Clifton enabled measurement of a stratigraphic section from the uppermost argillaceous Daggaboersnek Member to the dominantly arenaceous Katberg Formation (section 2, Figure 3.8). See Table 1.1 for lithological characteristics of these units. The 78 m thickness of RM is similar to the thickness logged for this unit on section 1B which consists of a paired unit interbedded dominantly by green mudstone and siltstone. Also the stratigraphic distance between the top of the RM and the base of the Katberg Formation is 94 m. This 94 m is occupied by the Elandsberg and Palingkloof members that are delineated by their lower sandstone content and greater green mudstone content (Elandsberg Member) or greater sandstone and red mudstone content (Palingkloof Member). These units were given a thickness of 48 and 46 m on the vertical section respectively.

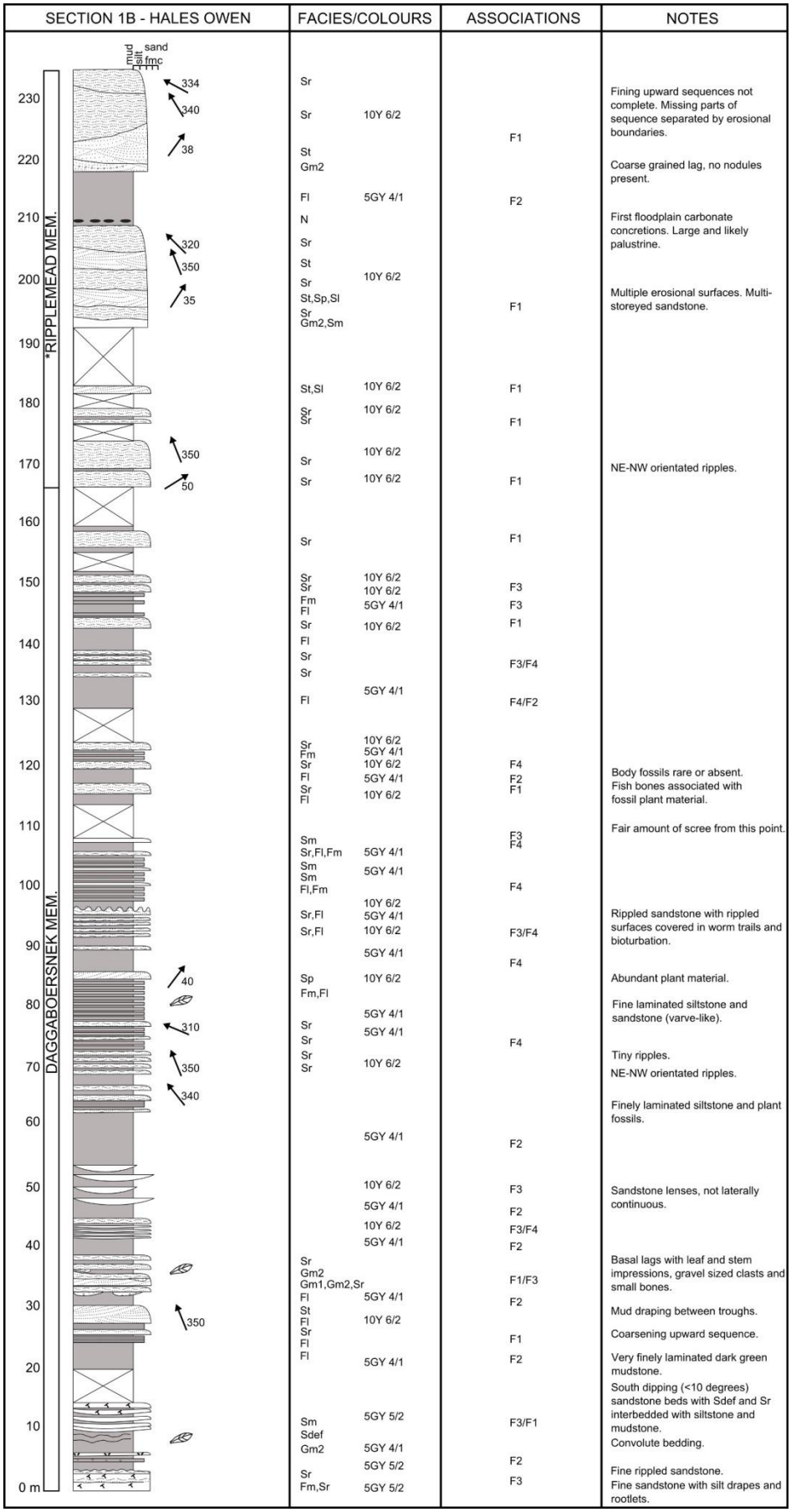

Figure 3.7: Vertical section 1B measured on Hales Owen farm south of Cradock.

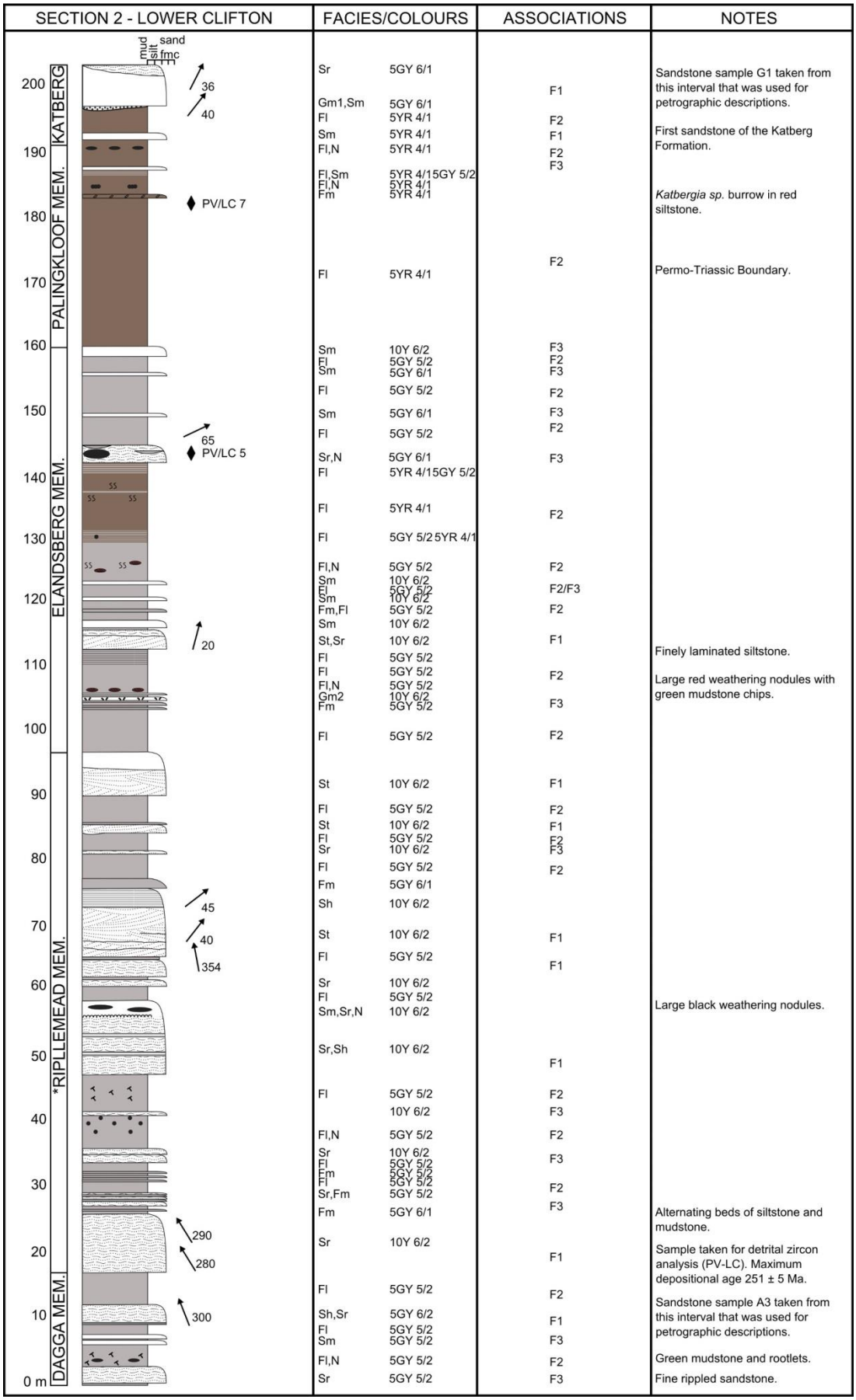

Figure 3.8: Vertical section 2 measured on Lower Clifton farm in the Baviaansrivier Valley.

Nieu Bethesda (Sections 3, 4, and 5)

Nieu Bethesds lies ~ 50 km north of Graaff-Reinet and 137 km west of Cradock in the Eastern Cape (Figure 3.9). Previous sedimentological and stratigraphic work by Visser and Dukas (1979 identified a sandstone rich interval near Nieu Bethesda as Tordiffe's (1978) BM. Subsequently Cole et al. (2004) also mapped this unit in the area, resulting in Smith and Botha-Brink (2014) also mapping this unit on their vertical sections for this site. However this unit, which overlies 300 m of argillaceous sediments that are characteristic of the Daggaboersnek Member, is renamed the RM after fieldwork conducted in the Cradock area confirmed that Tordiffe's (1978) BM is not present at the Barberskrans Cliffs (See Figures 3.2 and 3.5). The unit's new name and type area come from Ripplemead farm in this field area where this unit is well exposed and easily accessible (Figures 3.9 and 3.10). Together vertical sections measured at farms Doorplaats (section 3, Figure 3.11), Krugerskraal (section 4, Figure 3.12), and Ripplemead (section 5, Figure 3.13) near Nieu Bethesda and Graaff-Reinet together provided a complete composite section through the entire Balfour Formation in this part of the basin. The Oudeberg Member, which is present at the Barberskrans Cliffs near Cradock and Cookhouse, is present and its type location is Oudeberg Pass on the Murraysburg Road north of Graaff-Reinet (Johnson, 1976; SACS, 1980). It is also a sandstone rich unit but comprises normally three or four laterally continuous sandstone lenses over a 50 m interval in the field area (Visser and Dukas, 1979; Turner, 1981; Johnson et al. 2006). Unlike the RM fossils are uncommon within the Oudeberg Member and it only comprises green mudstone. It also underlies the argillaceous Daggaboersnek Member like in Cradock (See Table 1.1 for more detailed lithological decriptions on these units). Previous workers have measured sections at Krugerskraal (Visser and Dukas, 1979) and Ripplemead (Smith and Botha-Brink, 2014) but the more recent vertical sections (sections 3, 4, and 5) will now be briefly discussed in this context.

Section 3: Doornplaats farm, Graaff-Reinet, Eastern Cape

Platberg Hill on Doornplaats farm is the type location of DaAZ (Rubidge et al. 1995), and is a site where Tordiffe's (1978) BM was previously identified by Visser and Dukas (1979) on its summit (Figures 3.9 and 3.10). Section 3 (360 m in total) is measured here and begins at the Upper Oudeberg Member (Figure 3.11). The RM is now identified at the summit which overlies 320 m of Daggaboersnek Member, similar to Cole and Wipplinger's (2001) thickness (Table 1.2).Contrary to Visser and Dukas (1979) who documented a 60 m thick sandstone at the top of Platberg, this vertical section only documents a 40 m thick sandstone at the summit. It is underlain by two thinner sandstone units that are each ~ 5 m in total thickness.

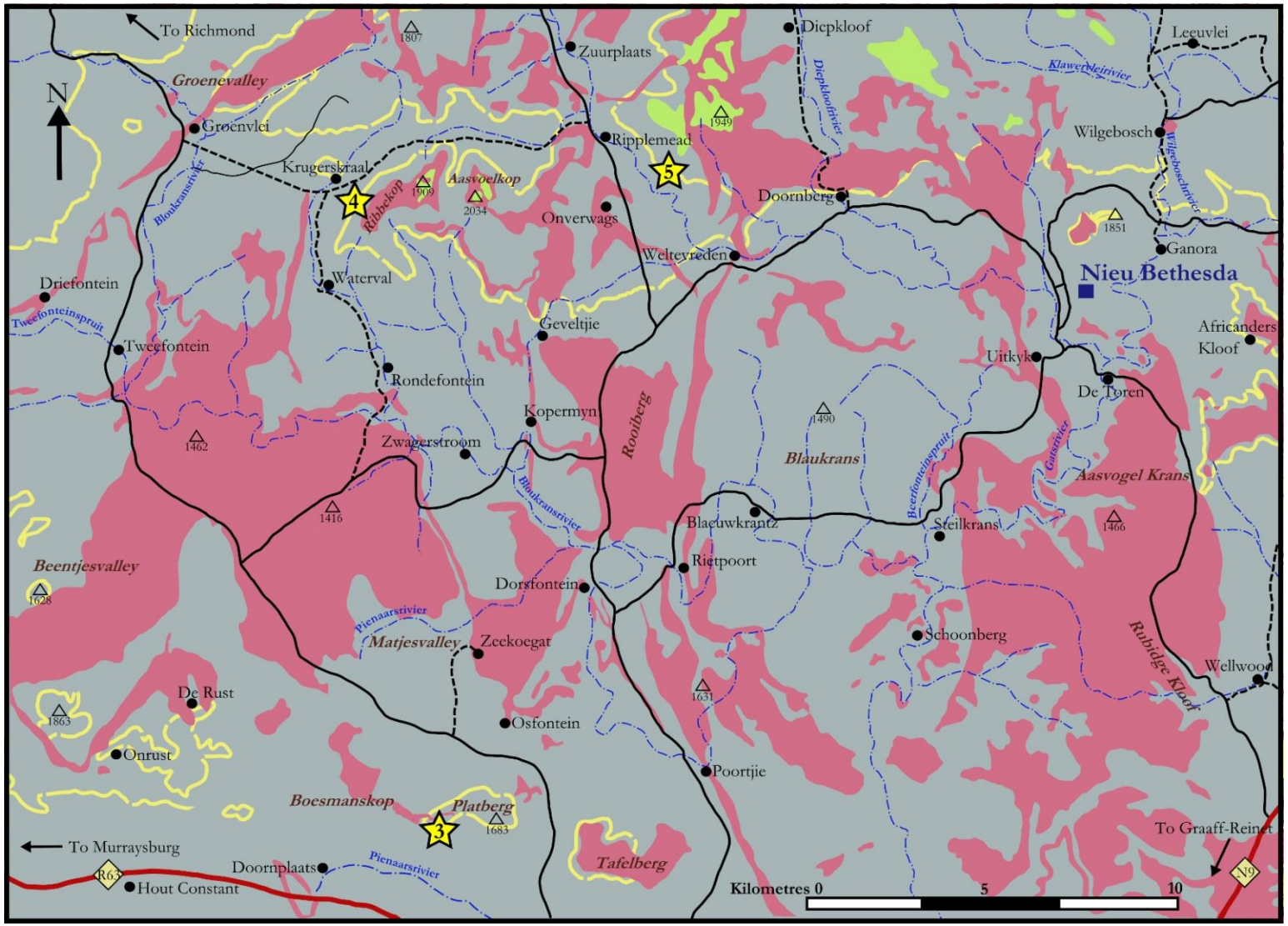

Figure 3.9: Map of the Nieu Bethesda field site showing the distribution of the Ripplemead member (yellow lines), and the positions of vertical sections 3 (Doornplaats farm), 4 (Krugerskraal farm), and 5 (Ripplemead farm).

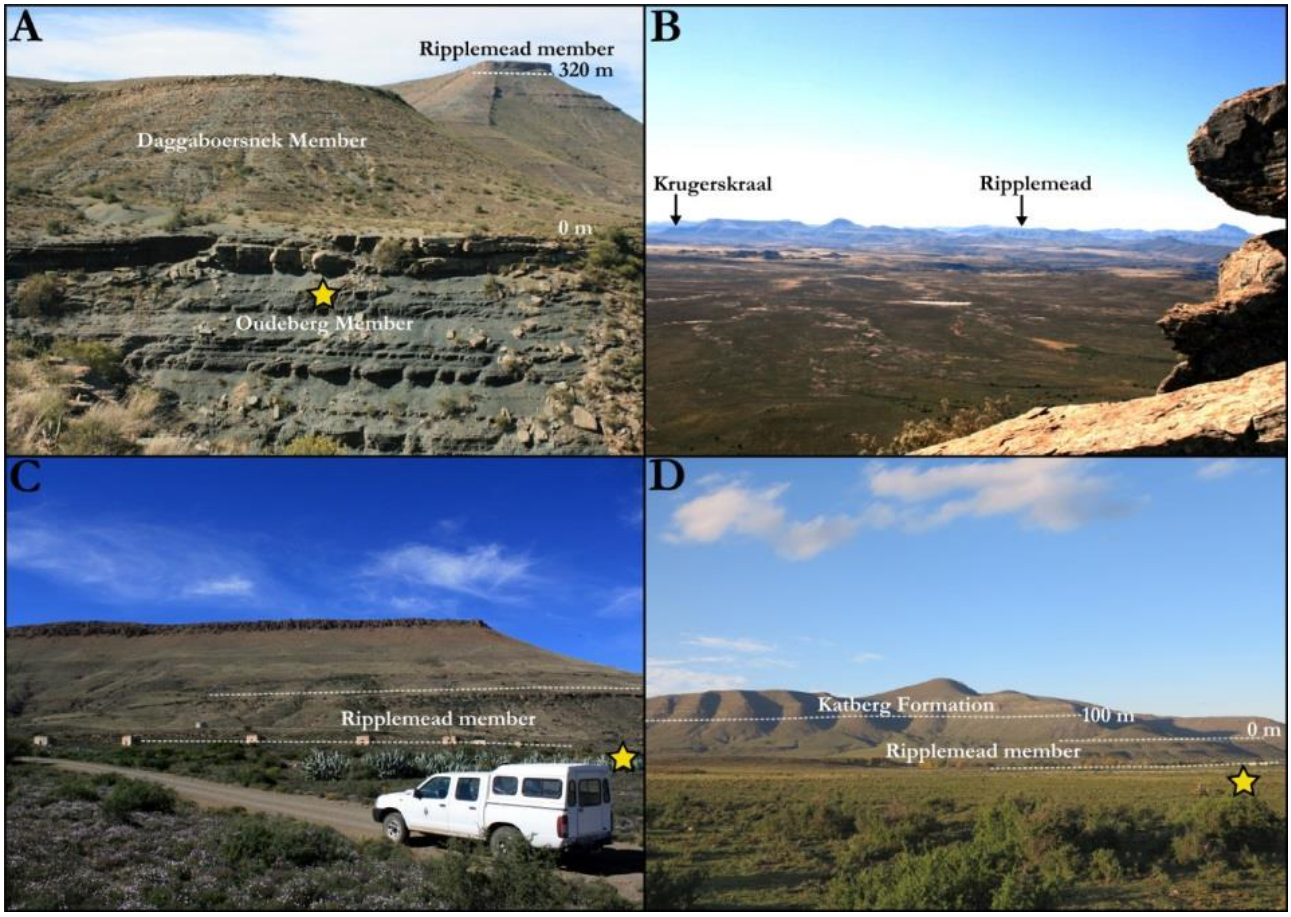

Figure 3.10: A) The site of vertical section 3 (Figure 3.11) on Doornplaats farm with a yellow star showing the start point of the section. Visser and Dukas (1979) identified a prominent sandstone on the top of Platberg as Tordiffe's (1978) Barberskrans Member which has now been renamed the Ripplemead member. B) Looking north from the summit of Platberg on Doornplaats farm showing the positions of Krugerskraal and Ripplemead farms where the RM can be traced from Doornplaats. C) Krugerskraal farm and the site of section 4 (Figure 3.12). Note the well exposed paired sandstone unit that is identified as the RM due to its lithological properties outlined in Table 1.2. D) A similar stratigraphy is identified on Ripplemead farm just east of Krugerskraal where section 5 (Figure 3.13) is measured. Note the position of the Elandsberg and Palingkloof members, and the Katberg Formation. The stratigraphic distance between the base of the RM and the Katberg Formation is 100 m, which similar to what is observed in the Cradock district.

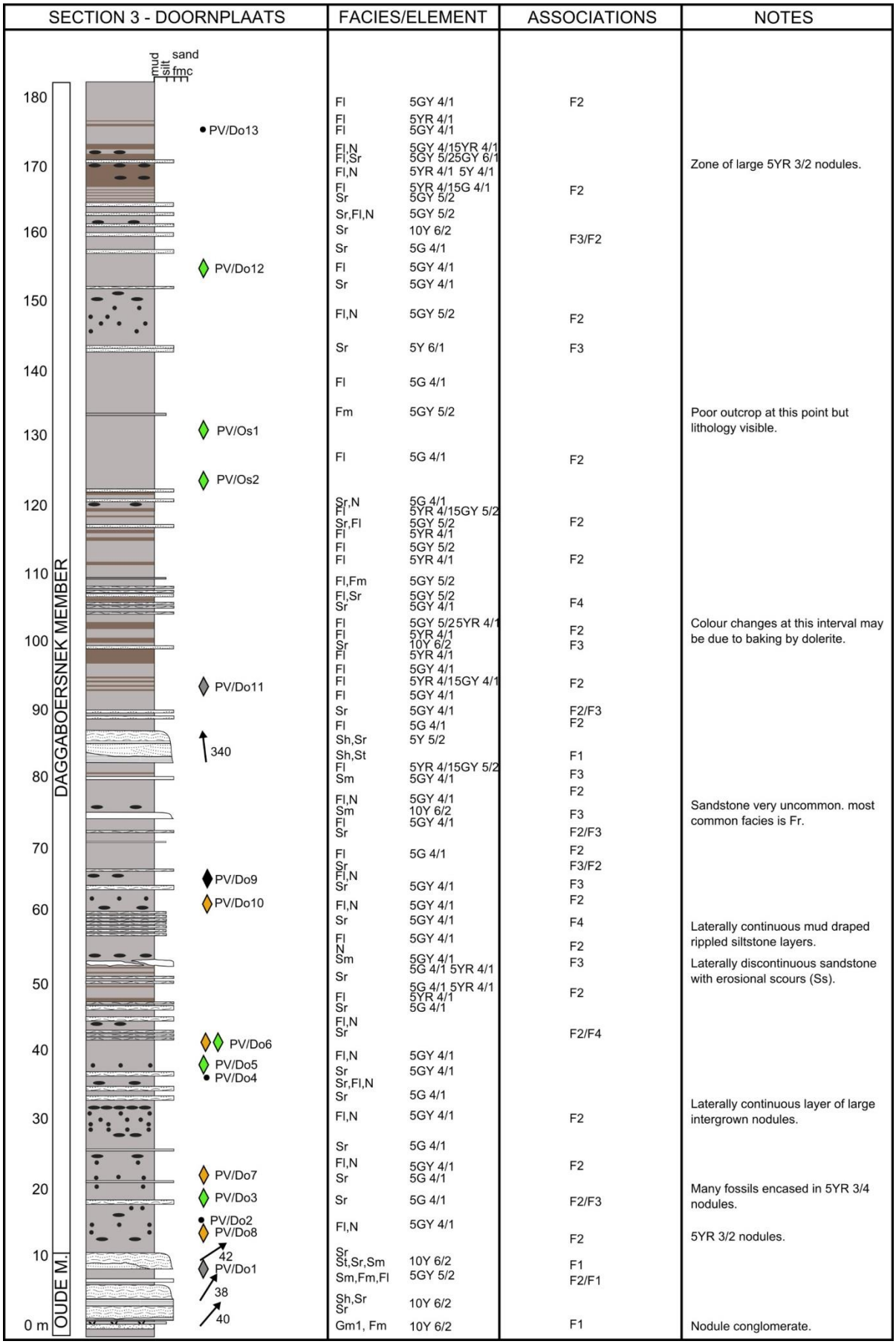

Figure 3.11: Section 3 measured on Doornplaats farm, near Graaff-Reinet.

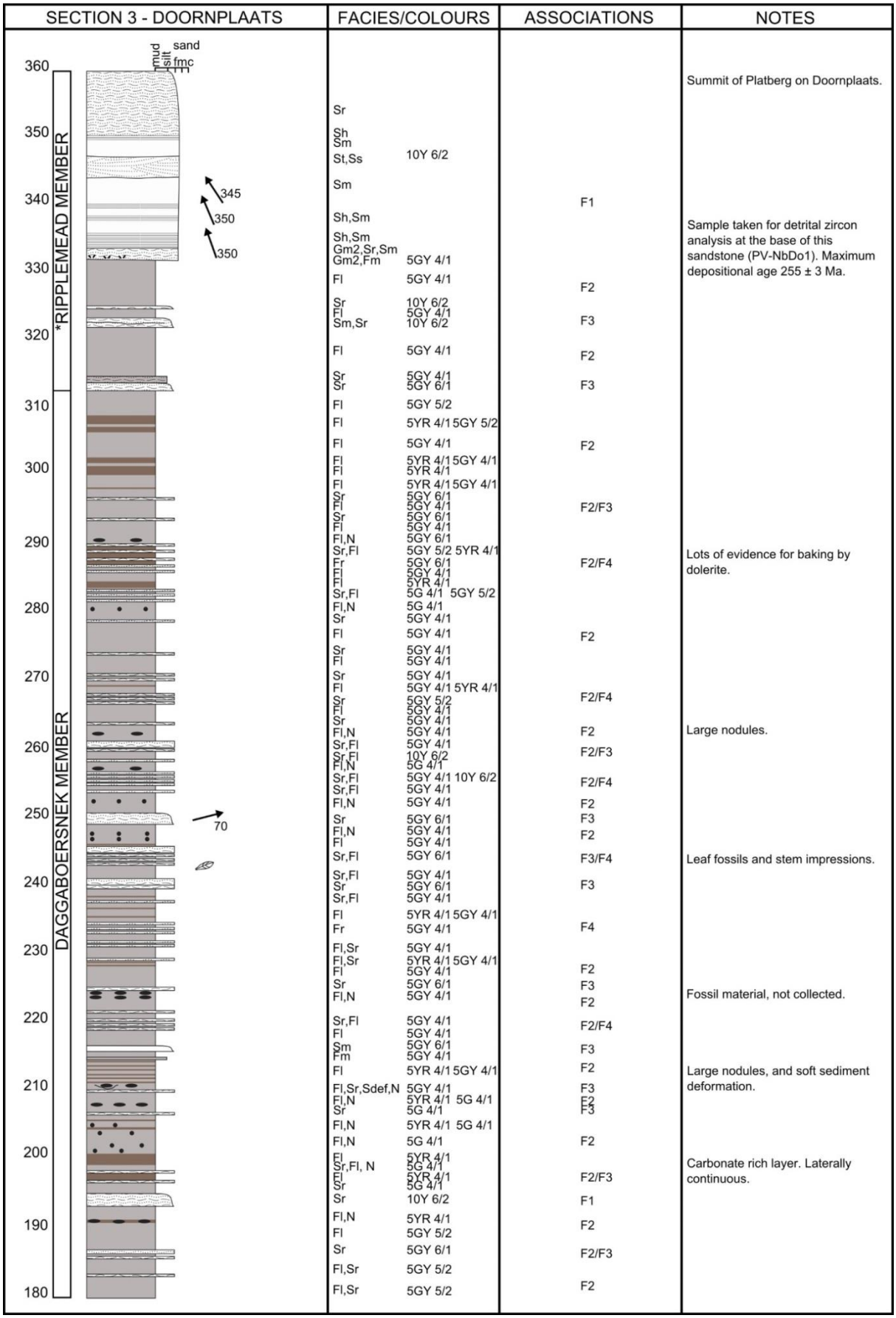

Figure 3.11 (continued)

As a result this sandstone is interpreted to represent the RM at this vertical section site. This sandstone was traced northwards to Krugerskraal and Ripplemead where sections 4 and 5 were measured (Figures 3.12 and 3.13).

Section 4: Krugerskraal farm, Nieu Bethesda, Eastern Cape

The Ripplemead member on the summit of Doornplaats farm is traced to Krugerskraal Farm where section 4 is measured (Figure 3.12). Visser and Dukas (1979) also identified the sandstones on Krugerskraal farm as belonging to Tordiffe's (1978) BM which is now renamed the RM after a farm 5 km away from this vertical section site. Only the uppermost portion of the argillaceous Daggeboersnek Member is exposed at this site, and instead of a single sandstone as documented at Doornplaats farm, there are two prominent sandstones (12 and 25 m thick respectively) within a 96 m interval. Although a stratigraphic distance from the top of the RM and the Katberg Formation cannot be determined at this site (a thick interval of scree and dolerite obscure this connection) the sandstones could be readily traced west to Ripplemead farm where a stratigraphic distance to the Katberg Formation can be logged (Figure 3.10).

Section 5: Ripplemead farm, Nieu Bethesda, Eastern Cape

This farm is now the new type area for the RM which is Tordiffe's (1978) old BM (see Table 3.1 and Figure 3.10). The two prominent RM sandstones at Krugerskraal farm are traced to the site of section 5 (Figure 3.13). On Ripplemead farm the units are thinner single-storey units within a 71m thick interval (see Figures 3.10 and 3.13). At this site the stratigraphic interval between the top of the RM and the base of the Katberg Formation is 100 m, similar to the distance measured on Lower Clifton farm in the Baviaansrivier Valley (see section 2, Figure 3.8). Smith and Botha-Brink (2014) also measured a vertical section on Ripplemead farm for their Permo-Triassic Boundary work, and this section was used to help place the positions of the Elandsberg and Palingkloof members, as well as the PTB. These workers did not document the entire thickness of the RM at this site (Figure 3.13).

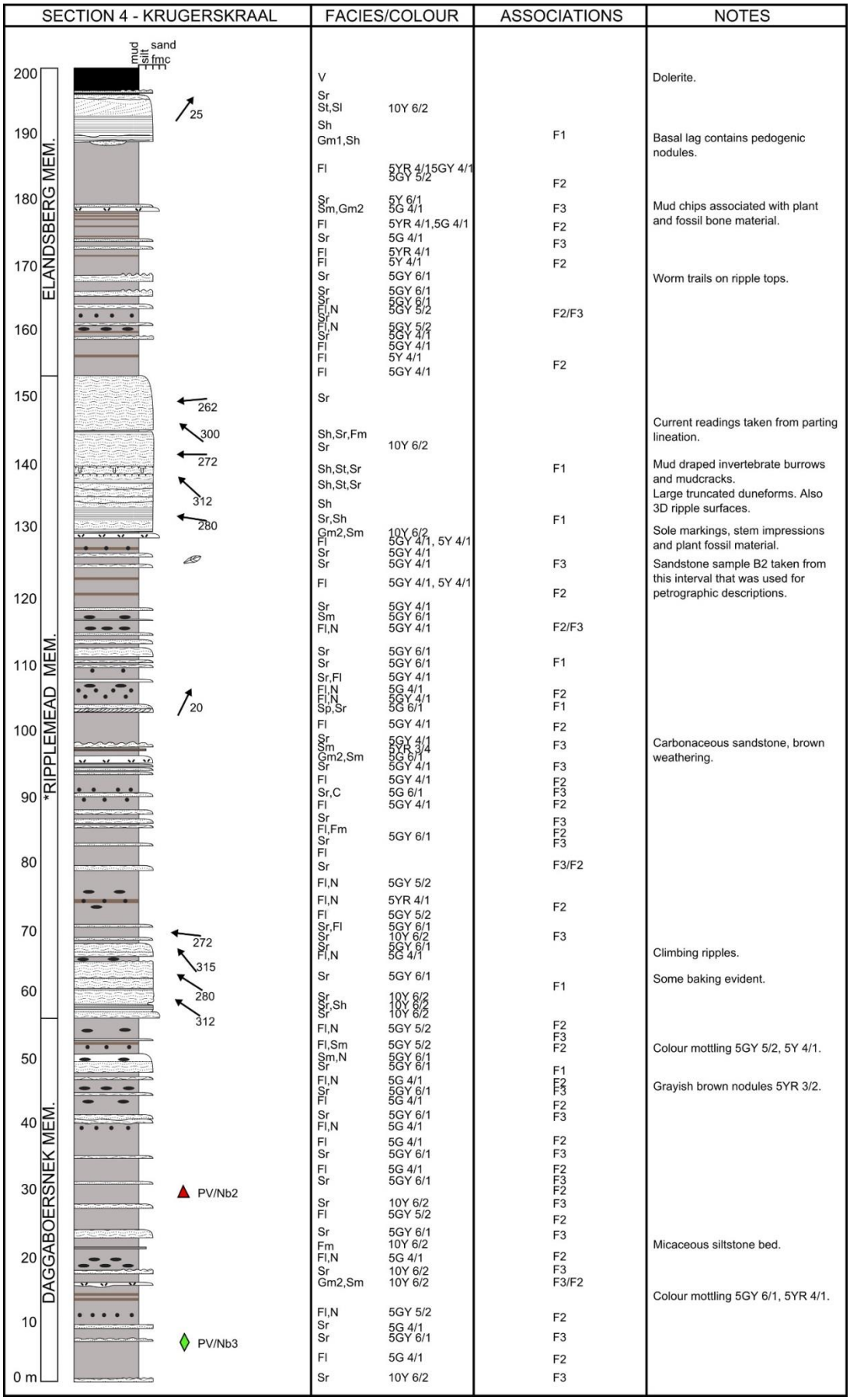

Figure 3.12: Section 4 measured on Krugerskraal farm near Nieu Bethesda.

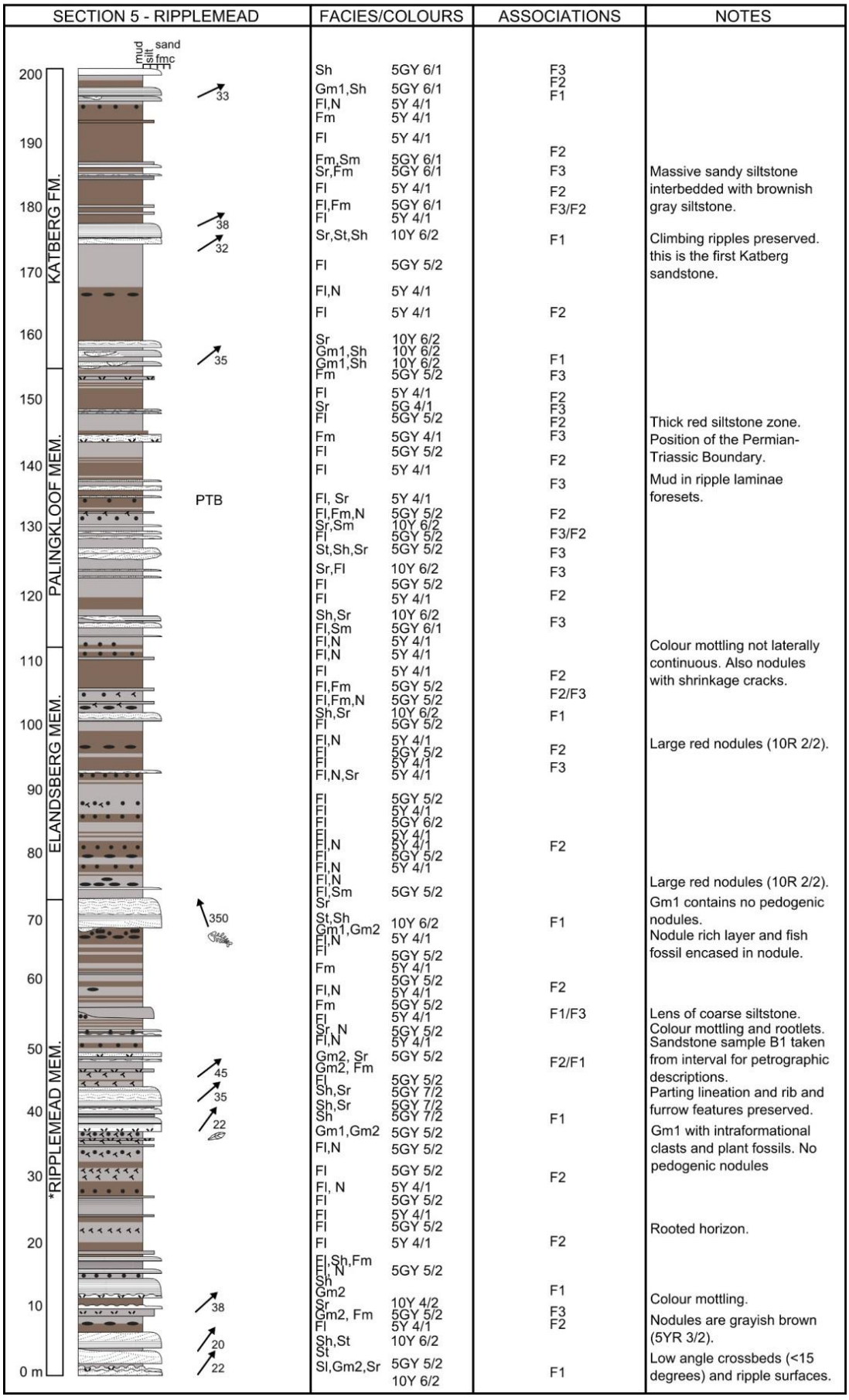

Figure 3.13: Section 5 measured on Ripplemead farm near Nieu Bethesda.

Beaufort West and Fraserberg (Sections 6 and 7)

This field site falls within Cole and Wipplinger's (2001) northeasterly fluvial transport system (See Figures 1.1, 3.14, and 3.15). Different lithostratigraphic units are present here however by using the biostratigraphic assemblage zones they have been correlated to other units found in the eastern parts of the main Karoo Basin (Smith, 1993b; Rubidge et al. 1995; Smith et al. 2012). Day (2013) and Jirah (2013) have recently conducted fieldwork in this part of the basin within the Abrahamskraal Formation and Lower Teekloof Formation in order to refine the stratigraphy in the area for middle Permian deposits. Smith (1993b) has also done extensive work on the Upper Permian Hoedemaker Member however little work has been conducted on the uppermost Permian strata of the Teekloof Formation (Steenkampsvlakte Member) in this part of the basin. The uppermost Permian strata are not continuous outcrops in this part of the basin due to their occurrence as erosive remnants only on the highest points of the escarpment.

A section was measured for this study on Highlands farm from the top of the Oukloof Member through the Steenkampsvlakte Member into an arenaceous unit (see Figures 3.14, 3.16 (A), and 3.17). Le Roux (1985) was the first to identify an arenaceous unit within the upper portion of the Steenkampsvlakte Member which he informally named the Javanerskop member. Thus this field site was investigated in order to ascertain if this sandstone rich horizon in the upper portions of the Steenkampsvlakte Member can be correlated to the Ripplemead member at Cradock and Nieu Bethesda. Two sites with prominent sandstones in the uppermost strata of the Steenkampsvlakte Member were earmarked for stratigraphic sections, one on Highlands farm near Beaufort West (section 6, Figures 3.14, 3.16 (A), and 3.17) and Javanerskop, Oukloof Pass, Fraserburg (section 7, Figures 3.15, 3.16 (B), and 3.18).

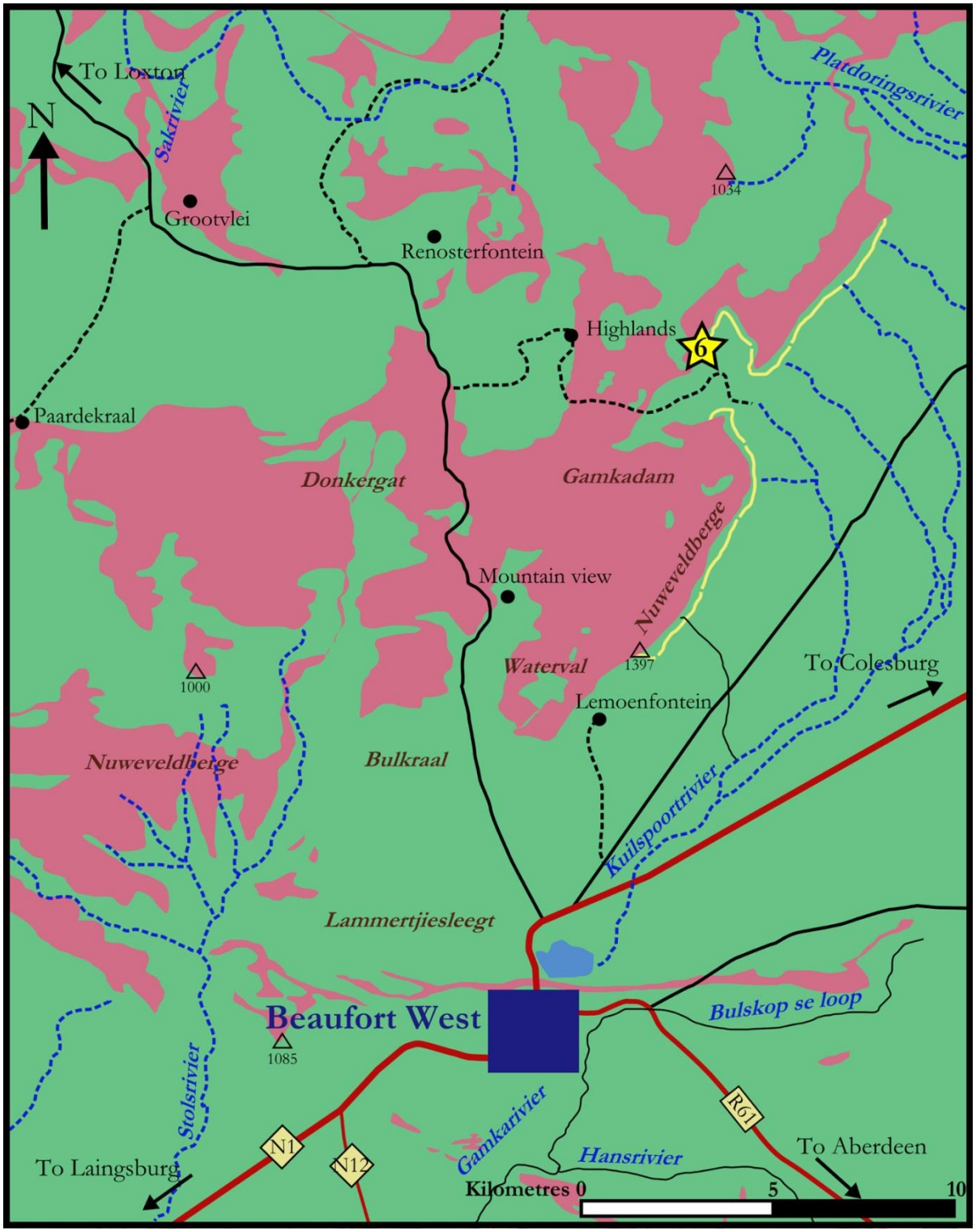

Figure 3.14: Map of the Beaufort West field site showing the Javanerskop member, a potential lateral equivalent (yellow lines) to the Ripplemead member in the uppermost Teekloof Formation (western depocentre of Cole and Wipplinger (2001). The position of vertical section 6 (Figure 3.17) (Highlands farm) is shown by yellow star.

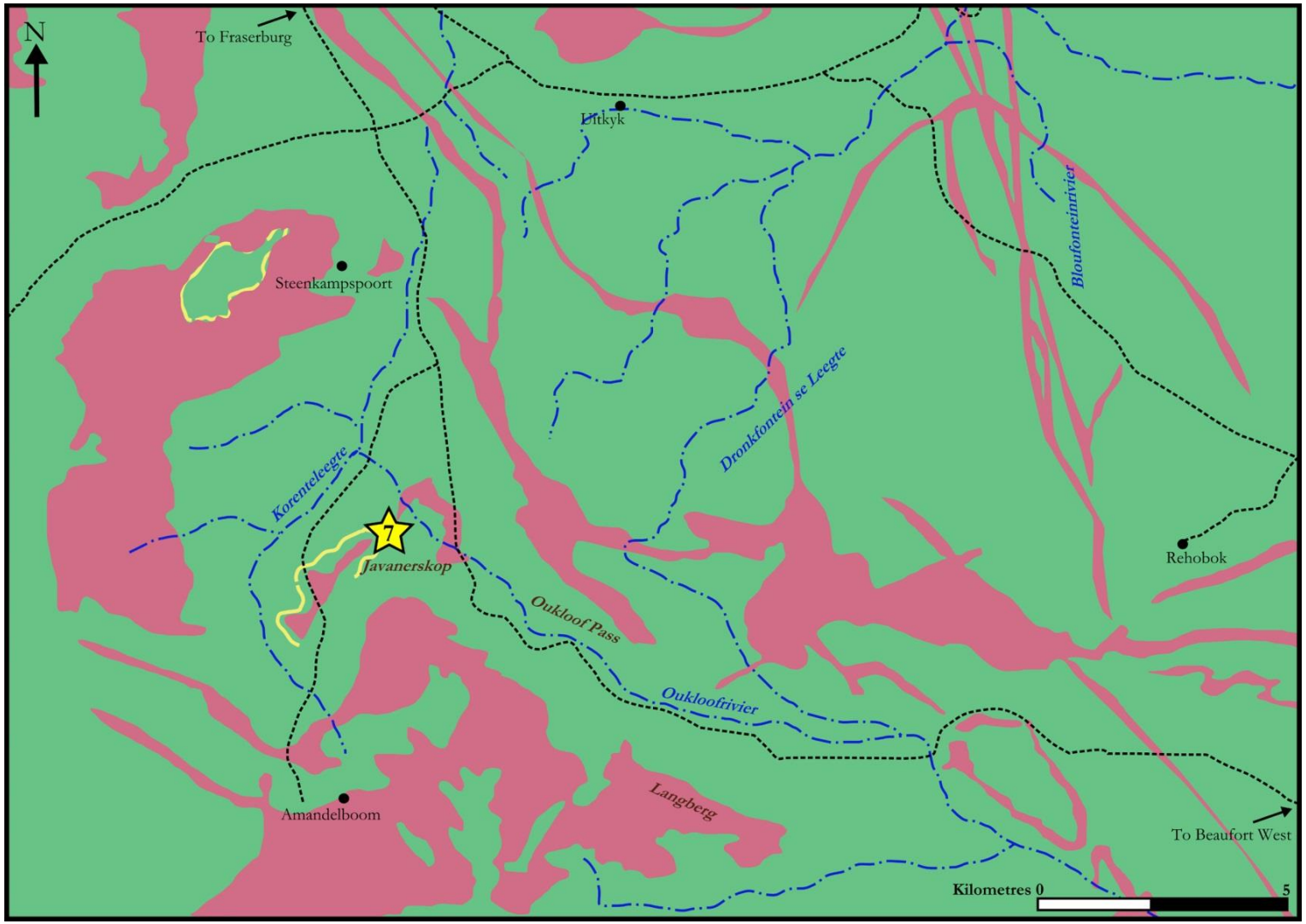

Figure 3.15: Map of the Fraserburg field site showing the Javanerskop member, a potential lateral equivalent (yellow lines) to the Ripplemead member in the uppermost Teekloof Formation (western depocentre of Cole and Wipplinger (2001)). The position of vertical section 7 (Figure 3.18) is shown by yellow star.

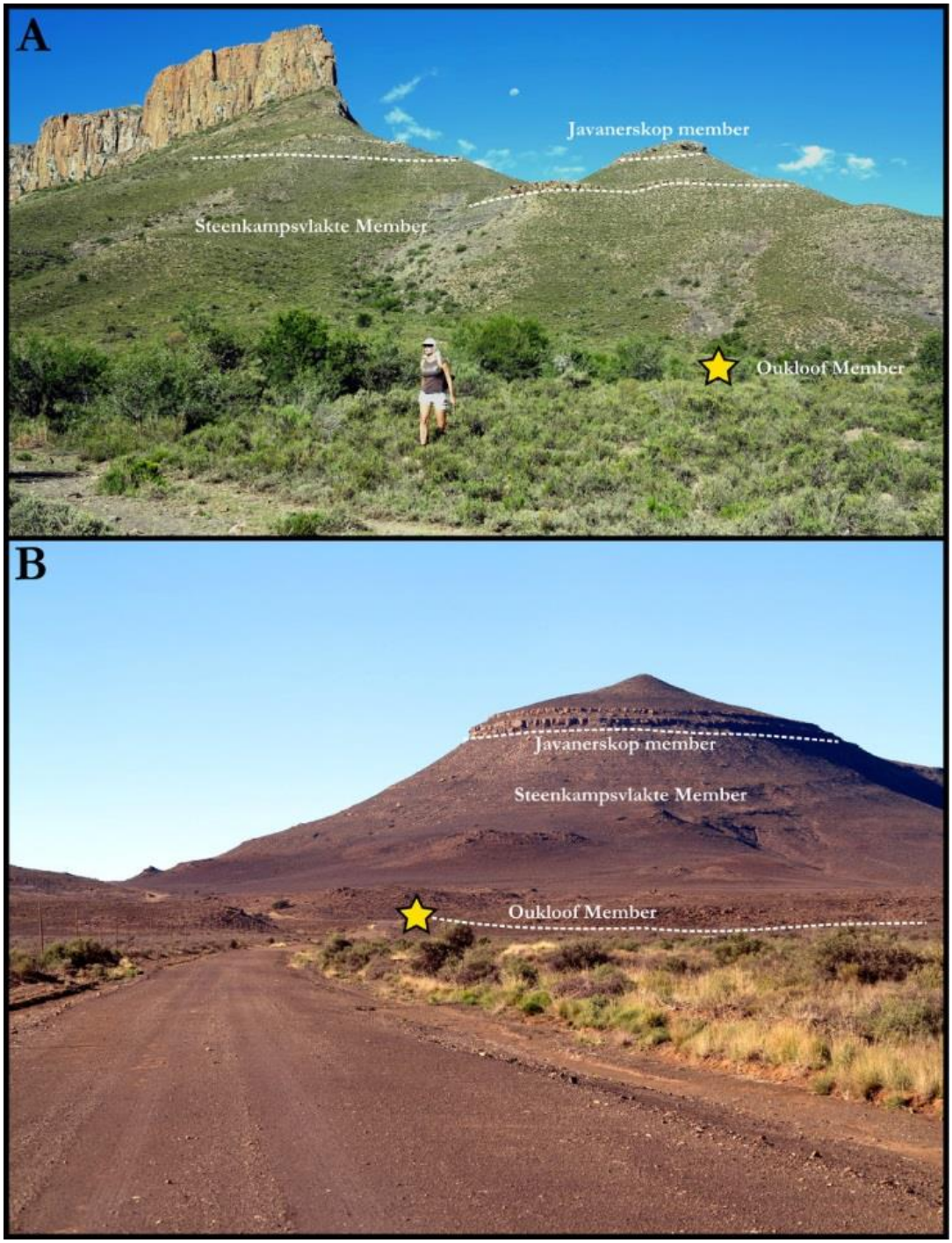

Figure 3.16: A) Highlands farm and the position of section 6 (Figure 3.17) is shown by a yellow star. Here a sandstone rich horizon is evident in the uppermost portions of the Teekloof Formation's largely argillaceous Steenkampsvlakte Member. B) Javanerskop on Oukloof Pass, near Fraserburg and the site of vertical section 7 (Figure 3.18). At the summit of the hill is the informal Javanerskop member identified by Le Roux (1985). This unit was investigated because it may represent a lateral equivalent to the Ripplemead member in the western portion of the Karoo Basin.

Section 6: Highlands farm, Beaufort West, Western Cape

Section 6 is measured on Highlands farm near Beaufort West (Figures 3.16 and 3.17). This section is in the Teekloof Formation, a lateral equivalent of the Balfour Formation that is present in this part of the basin. Section 6 (Figure 3.17) documents the Javanerskop member ~ 114 m from the top of the Oukloof Member, which occurs 10. 5 m below the start point of the vertical section (Figure 3.17). The Javanerskop member comprises the youngest strata preserved in this part of the Karoo Basin and consists of three sandstones within a 95 m thick interval. The individual sandstones are at most 10 m in thickness and single-storied, appearing as discontinuous couplets in outcrop. The sandstones are usually greenish grey (5GY 4/1) or pale olive (10Y 6/2) and contain many erosional boundaries which are lined with mudstone pellet conglomerates comprising dominantly red mudstone clasts. In addition the most common sedimentary structure is ripple cross-laminated sandstone (Figure 3.17). Le Roux (1985) first documented the Javanerskop member on Javanerskop (Oukloof Pass) near Fraserburg. The following section was logged at this site to determine whether the Highlands farm sandstones can be stratigraphically matched to Le Roux's Javanerskop member.

Section 7: Javanerskop, Oukloof Pass, Northern Cape

Section 7 (Figure 3.18), documents Le Roux's (1985) Javanerskop member on the summit of Javanerskop near Fraserburg (Figures 3.16 and 3.18). The base of Le Roux's (1985) first significant sandstone horizon is ~ 110 m above the Oukloof Member on the new measured section which is at a similar level to the base of the first sandstone documented on Highlands farm (Figure 3.17). Three sandstone-rich horizons are also present on Javanerskop, but in this case the second sandstone in this interval attains 30 m and is multi-storied. The sandstones are distributed over a 125 m thick interval in paired couplets which is slightly thicker than documented on Highlands but contain the same lithological characteristics. In addition, the stratigraphic position of the sandstones is near identical and therefore could be regarded as representing the same lithological unit (See Figure 3.16). The documentation of Le Roux's (1985) Javanerskop member at both study sites suggests that this arenaceous unit could be used as a local marker horizon in the western Karoo Basin. What needs to be tested is whether this unit can be correlated with the RM identified in the central-east Karoo Basin.

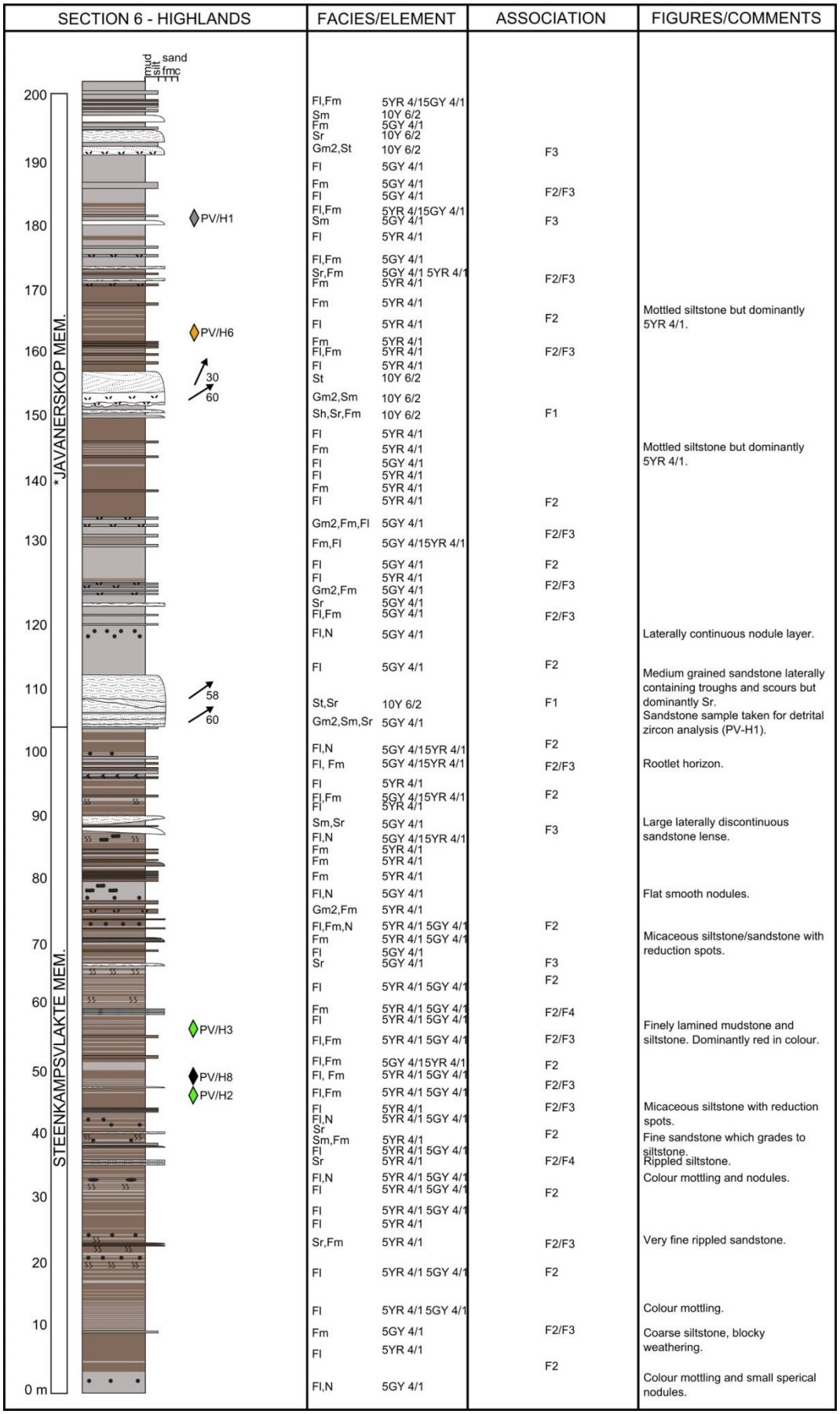

Figure 3.17: Section 6 measured on Highlands farm near Beaufort West.

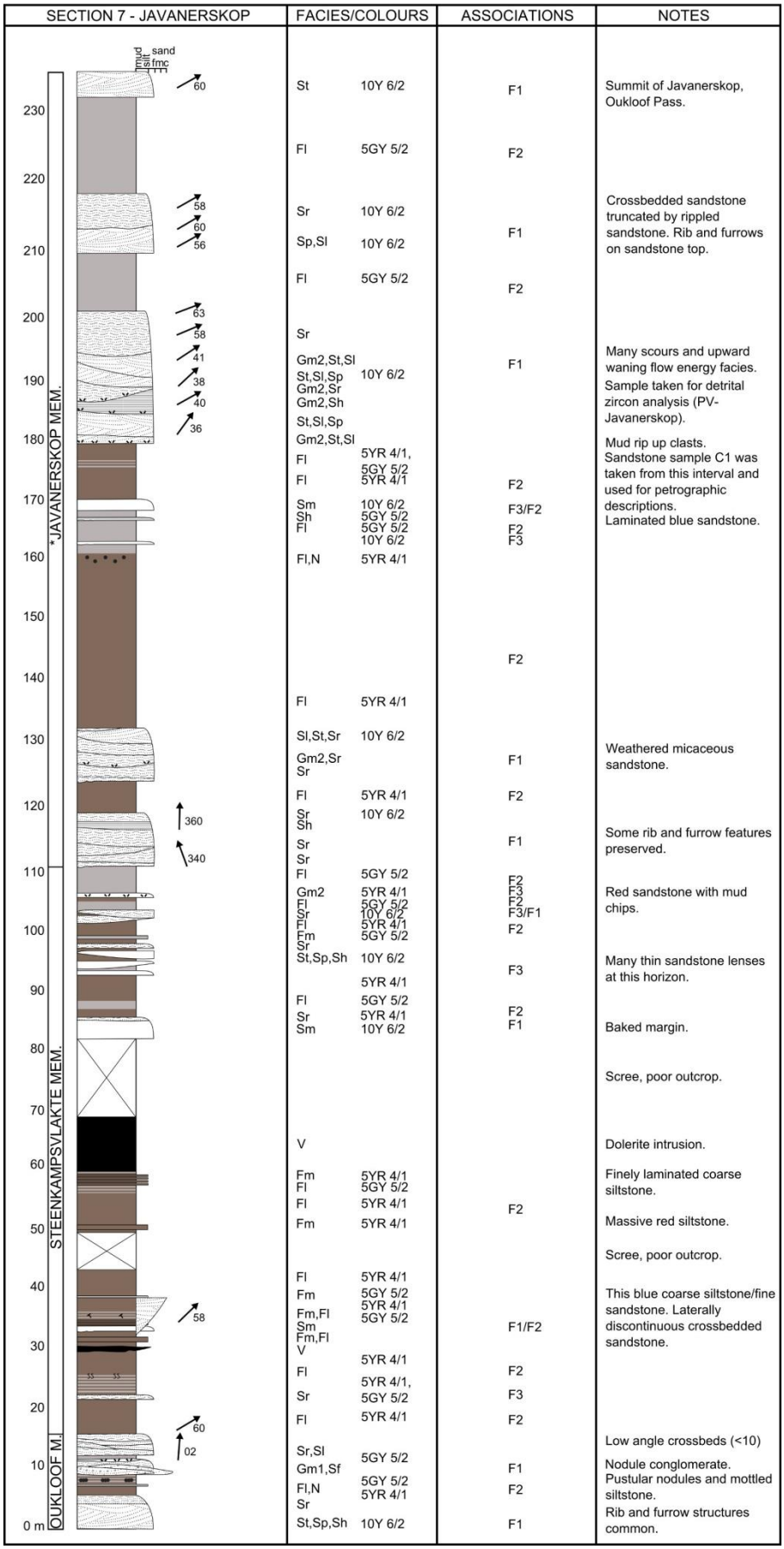

Figure 3.18: Section 7 measured on Javanerskop on Oukloof Pass, near Fraserburg.

Gariep Dam (Sections 8, 9, 10, and 11)

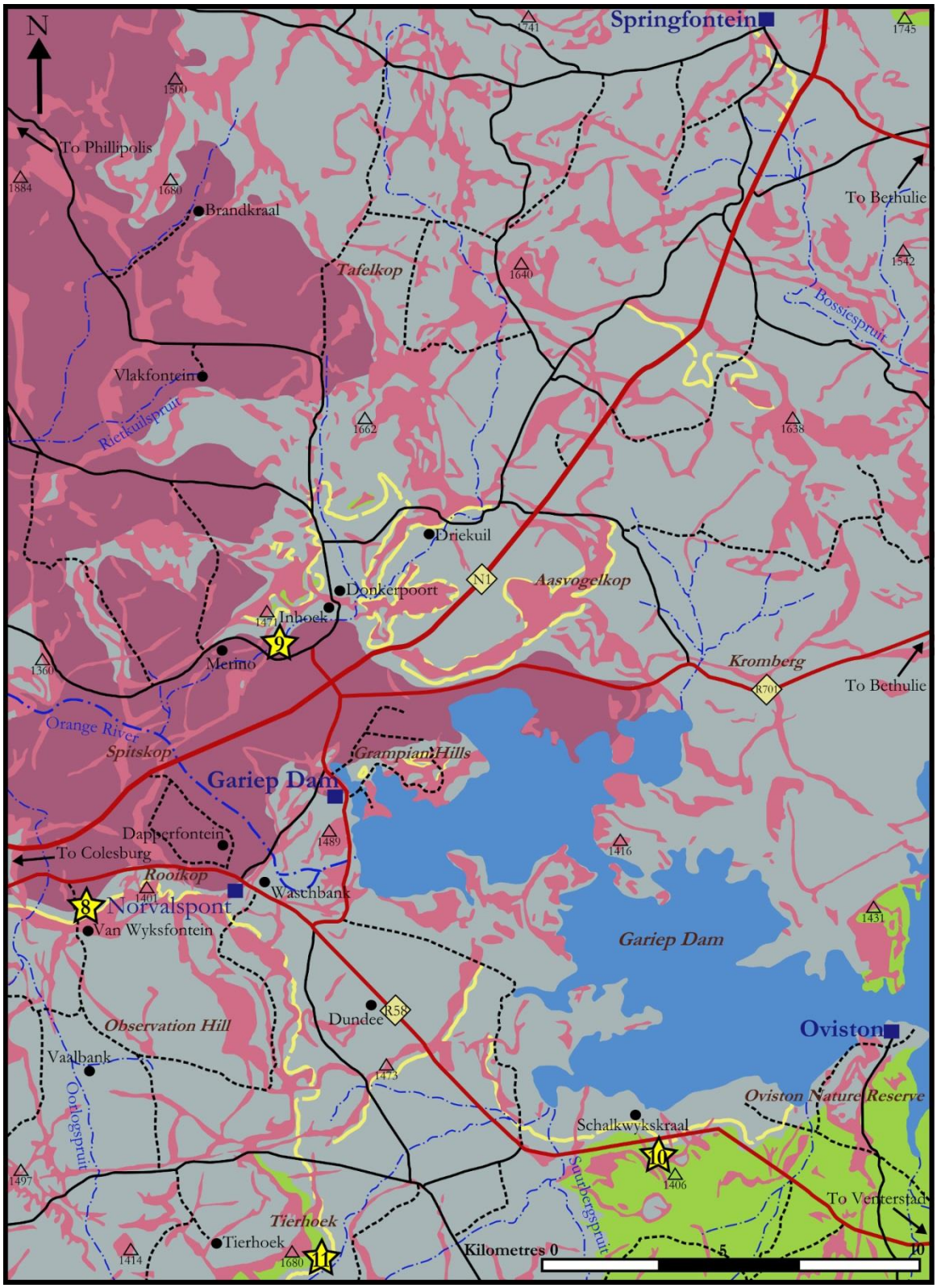

Figure 3.19: Map of the Gariep Dam field site showing the distribution of the Ripplemead member (yellow lines), and the positions of vertical sections 8 (van Wyksfontein farm), 9 (Inhoek farm), 10 (Schalkwykskraal farm) and 11 (Tierhoek farm).

Gariep Dam is a town and major dam in the southern Free State Province (Figure 3.19). During palaeontological survey and rescue collecting prior to the construction of the dam Kitching (1977, pg. 19) noted that the Beaufort stratigraphic succession in this part of the basin was "much attenuated". Smith and Botha (2005), Botha and Smith, (2006) and Smith and Botha–Brink (2014) recorded stratigraphic thicknesses similar to thicknesses of lithological units measured during their work in Nieu Bethesda, Wapadsberg, and Lootsberg Pass but did not document the Oudeberg or Todiffe's (1978) Barberskrans members in this part of the basin. Smith and Botha-Brink's (2014) section is measured at Bethel Canyon near Bethulie, about 70 km east of the field site for this study. The current study area has incorporated fossiliferous exposure with complete but attenuated Upper Beaufort Group.

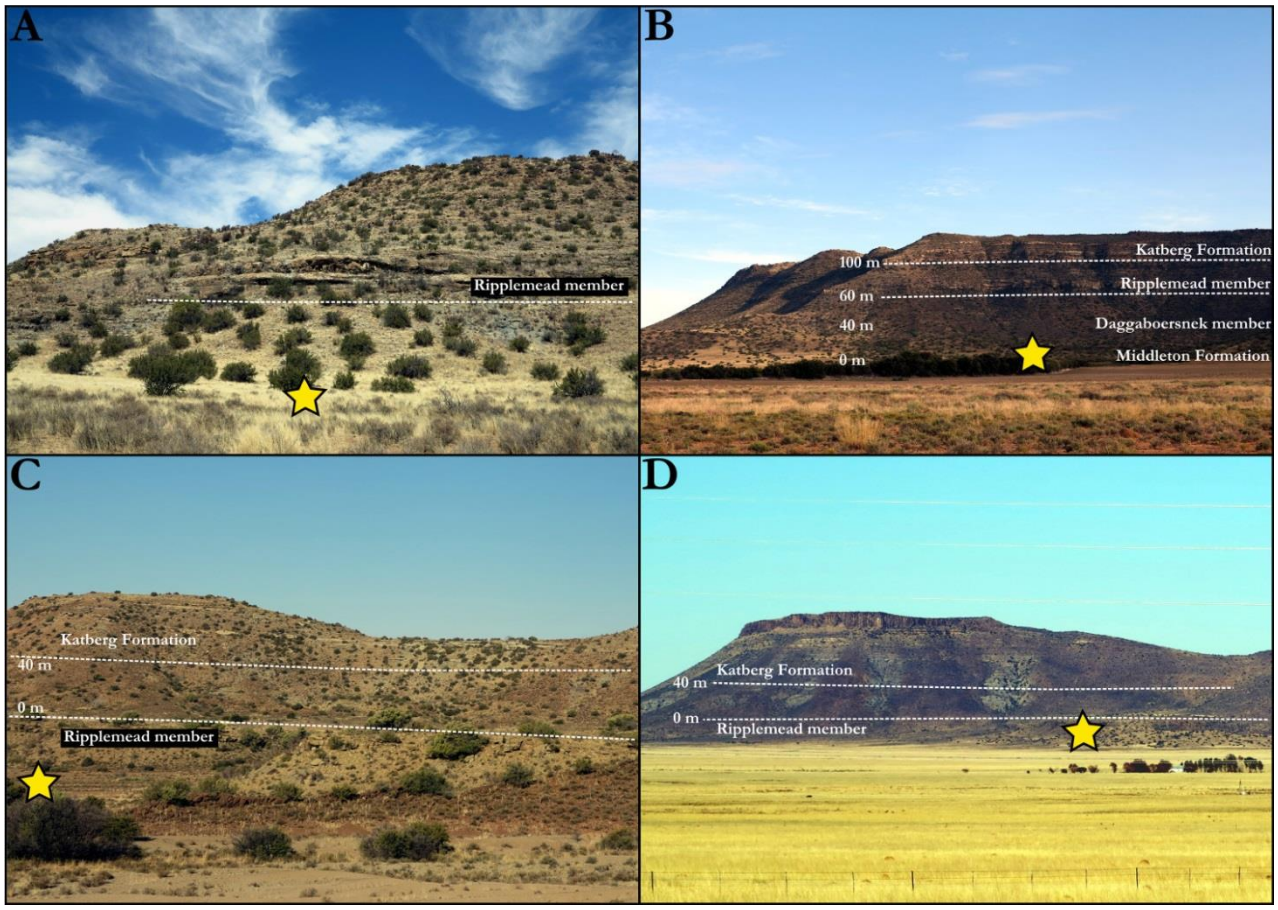

Figure 3.20: Field sites at Gariep Dam where vertical sections were measured into a sandstone rich unit that correlates with the Ripplemead member identified in Nieu Bethesda and Cradock. A) Van Wyksfontein and the site of section 8 (Figure 3.21). B) Inhoek farm and the site of section 9 (Figure 3.22). Here the Katberg Formation is identified for the first time and is currently mapped as Balfour Formation. C) The RM and its stratigraphic relationship with the Katberg Formation are well-demonstrated on Schalkwykskraal farm (section 10, Figure 3.23) and identical to what is observed at Inhoek. D) Tierhoek (section 11, Figure 3.24) demonstrates the same stratigraphic relationship. This relationship is an attenuated equivalent to what has been observed in the Cradock and Nieu Bethesda areas. This is demonstrated by the presence of two argillaceous units above the RM, one with more green mudstone and lower sandstone (Elandsberg Member), and another with abundant red mudstone and higher sandstone content (Palingkloof Member). See Table 1.1 for lithological descriptions.

A single prominent sandstone unit is laterally traceable in the area and is at the same stratigraphic level as the RM in the southern field sites (Cradock and Nieu Bethesda). It is regarded as an attenuated version of the RM due to lack of nodules in basal conglomerates that instead contain extrabasinal clasts and sometimes plant remains (See Table 3.1 for formal description). Stratigraphic sections were measured and fossils collected on the farms van Wyksfontein (section 8, Figure 3.21), Inhoek (section 9, Figure 3.22), Schalkwykskraal (section 10, Figure 3.23), and Tierhoek (section 11, Figure 3.24). See also Figures 3.19 and 3.20.

Section 8: Van Wyksfontein farm, Colesburg, Free State Province

A total of four vertical sections were measured in the Gariep Dam area because a sandstone documented as the RM is present in uppermost Permian strata in this part of the basin (Figures 3.20 and 3.21). From measuring sections in the Gariep Dam area, it became clear that the sedimentary package comprising the DaAZ is much thinner than in the southern field sites of Cradock and Nieu Bethesda. This was previously observed by Kitching (1977) but never quantified before this study. *Cistecephalus* Assemblage Zone strata occur on van Wyksfontein farm on the geological map, which was why this site was chosen for the first Gariep Dam vertical section (section 8, Figures 3.20 and 3.21). Kitching (1977) also collected *Cistecephalus microrhinus* in the low lying outcrops on van Wyksfontein. Due to this observation by Kitching (1977) the lowermost 10 m on section 8 was assigned to the CAZ. No evidence of the Oudeberg Member could be identified on the section or in the Gariep Dam area and the Daggaboersnek Member is highly attenuated and is difficult to distinguish from the Middleton Formation. However a single laterally extensive sandstone tentatively assigned to the RM (Figure 3.20) is present, but only ~ 20 m from the top of rocks assigned to the CAZ from Kitching's (1977) records. Although thin mudstone interbeds are evident, the total thickness of the RM is ~ 20 m, which demonstrates the significant attenuation in this part of the basin (Figures 3.20 and 3.21). The relative stratigraphic position of the RM could not be determined on van Wyksfontein however, it was easily traced out from this site to Inhoek, Schalkwykskraal, and Tierhoek farms where sections were measured that allowed for better stratigraphic resolution.

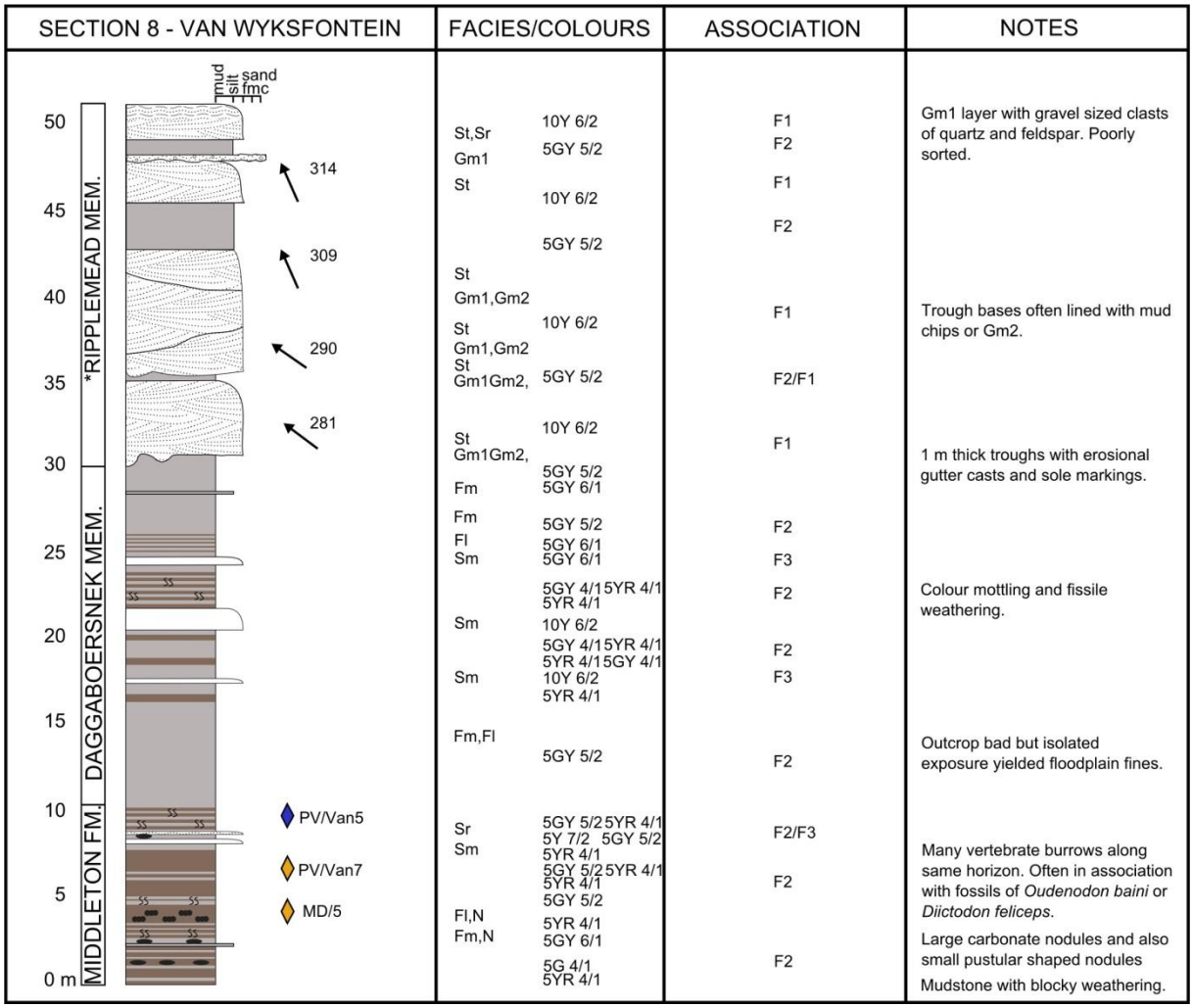

Figure 3.21: Section 8 measured on van Wyksfontein farm, near Colesburg.

Section 9: Inhoek farm, Gariep Dam, Free State Province

Kitching (1977) identified CAZ strata in low lying outcrops on Inhoek farm, which supports the geological maps for the area (Figures 3.19, 3.20, and 3.22). Here the RM sandstone which is present on van Wyksfontein outcrops as a ~ 20 m thick unit (section 9, Figure 3.22). Since the RM is present on van Wyksfontein where it is 20 m above strata assigned to the CAZ the same distance to the top of the CAZ was estimated for this section. However *C. microrhinus* was not found during the study so this could not be corroborated in the field although Kitching's (1977) records do show that this taxon has been found on Inhoek. Forty five metres above the top of the RM is the base of a sandstone-rich succession previously identified as part of the Balfour Formation on the geological maps (see 1:250 000 Geological Series; map sheet: Republic of South Africa 3024, Colesburg) and which is now identified as the Katberg Formation for a numder of reasons (Figures 3.19 and 3.20).

Firstly, the Katberg Formation which is the basal formation of the Tarkastad Subgroup, is characterised by a significant increase in the sandstone:mudstone ratio from 1:3 or 1:6 in the Adelaide Subgroup and 1:2 or 1:0.8 in the Tarkastad Subgroup. In percentages this is a jump from ~32% sandstone in the Balfour Formation to ~90-95% in the Katberg Formation (Johnson, 1976; Johnson and Keyser, 1976; Groenewald, 1996). The sandstones of the Katberg Formation are also tabular to sheet like in geometry and are mainly single-storey units with conglomerates comprising pedogenic nodules at their bases. They are frequently interbedded with thin floodplain deposits that are not always red in colour but almost always contain immature palaeosols, except where they amalgamate into the informally named Swartberg member (Neveling, 2002). In addition average palaeocurrents change from a northwesterly in the Balfour Formation to northeasterly in the Katberg Formation (Johnson, 1976). All these diagnostic features were identified in the uppermost sandstone package on Inhoek farm (See Table 1.1) and are also supported by the documentation of the Katberg Formation in a similar stratigraphic interval on vertical sections of Schalkwykskraal and Tierhoek farms (Figures 3.23 and 3.24). In addition, the uppermost Permian units present on Inhoek farm can be identified as attenuated versions of the Ripplemead, Elandsberg, and Palingkloof members (Figure 3.22). Although the Elandberg Member in section 9 does contain locally abundant red mudstone, and the Palingkloof Member contains locally abundant green mudstone, the general increase in sandstone content in this section indicates both are present (Figure 3.22). These units can be traced to Schalkwykskraal, and Tierhoek where the same stratigraphic relationships and lithological changes are documented. Therefore this study concludes that the Katberg Formation is indeed present in the highest points of Inhoek farm and section 9.

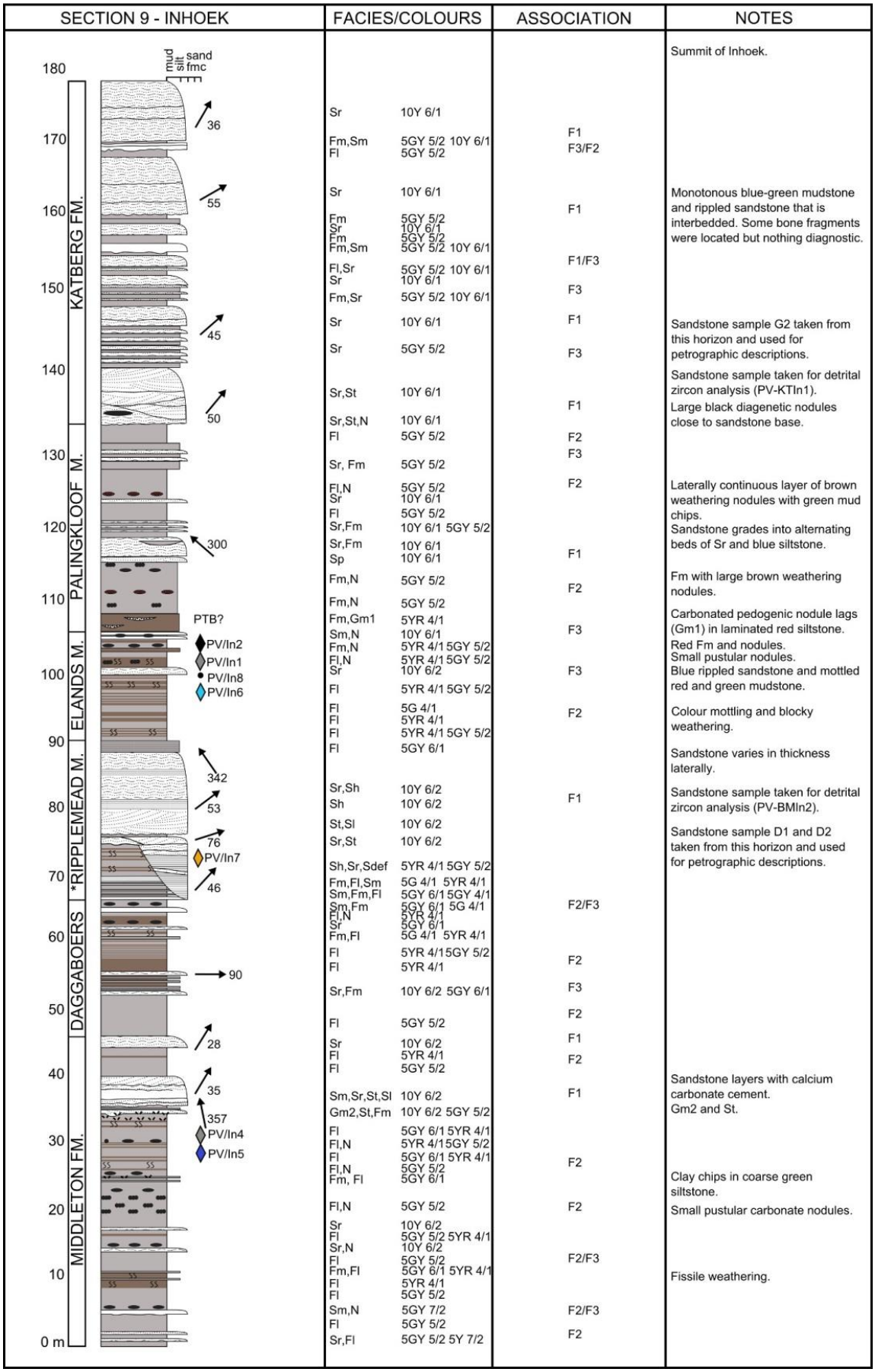

Figure 3.22: Section 9 measured on Inhoek farm, near Gariep Dam.

Section 10 and 11: Schalkwykskraal and Tierhoek farms, Venterstad, Eastern Cape

The stratigraphic succession exposed on Schalkwykskraal (section 10, Figure 3.23) is very similar to that on the upper portions of section 9 from Inhoek (Figure 3.22) and section 11 from Tierhoek (Figure 3.24). On Schalkwykskraal a 15 m thick sandstone in Upper Permian strata that was traced from Inhoek and van Wysfontein farm lies ~ 40 m below the first Katberg Formation sandstone which is similar to the stratigraphy at Tierhoek. The sedimentary succession is much thinner than in the south however, this stratigraphic separation of the Katberg Formation from a relatively thick Upper Permian sandstone unit is similar to the RM and Katberg Formation's stratigraphic relationship in Cradock and Nieu Bethesda (Figures 3.5, 3.10, and 3.20). It is proposed that this unit could represent the RM in the Gariep Dam area. No CAZ strata are exposed on Schalkwykskraal or Tierhoek farms and therefore a distance to the underlying strata could not be determined at these two sites.

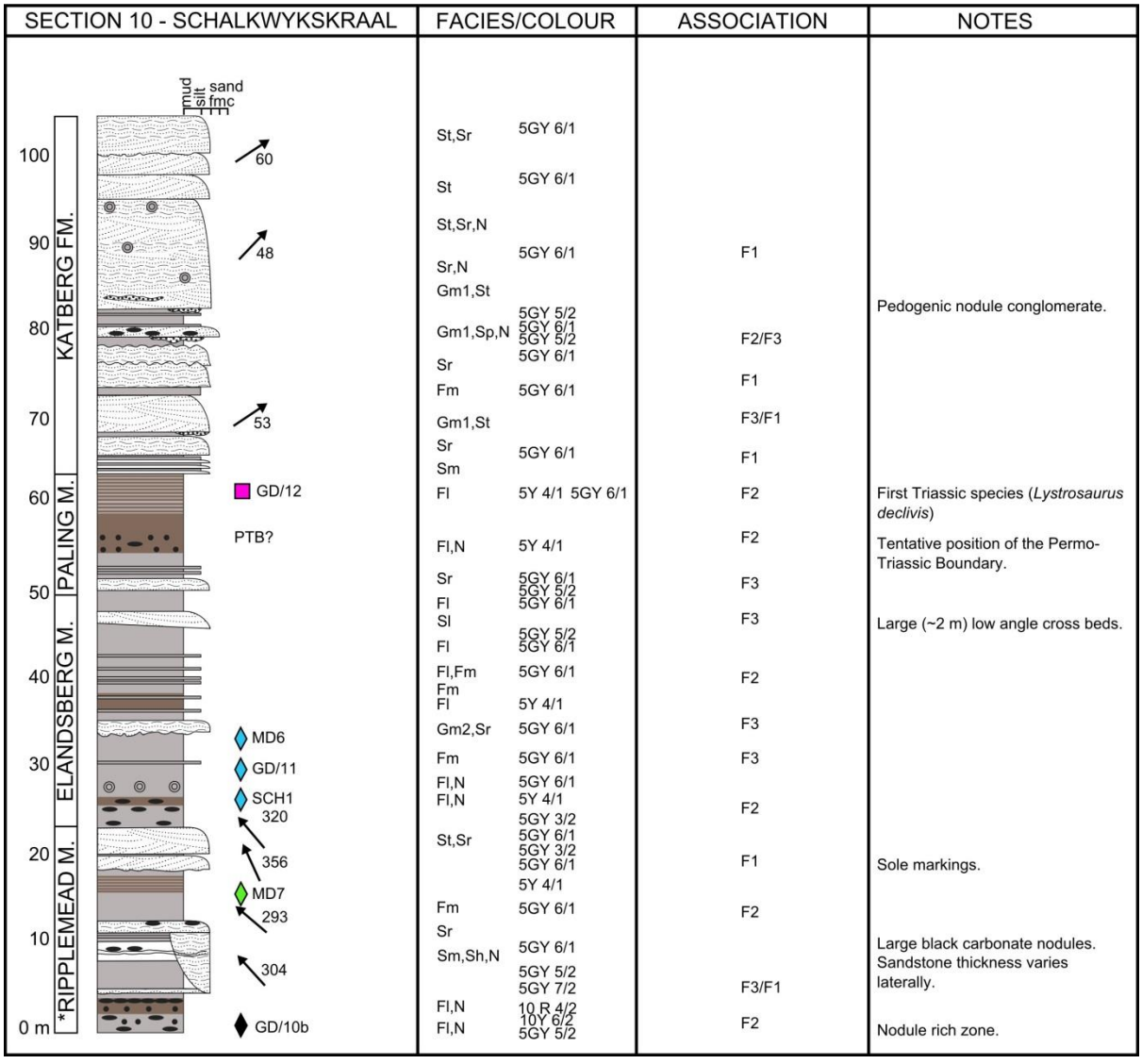

Figure 3.23: Section 10 measured on Schalkwykskraal farm, near Venterstad.

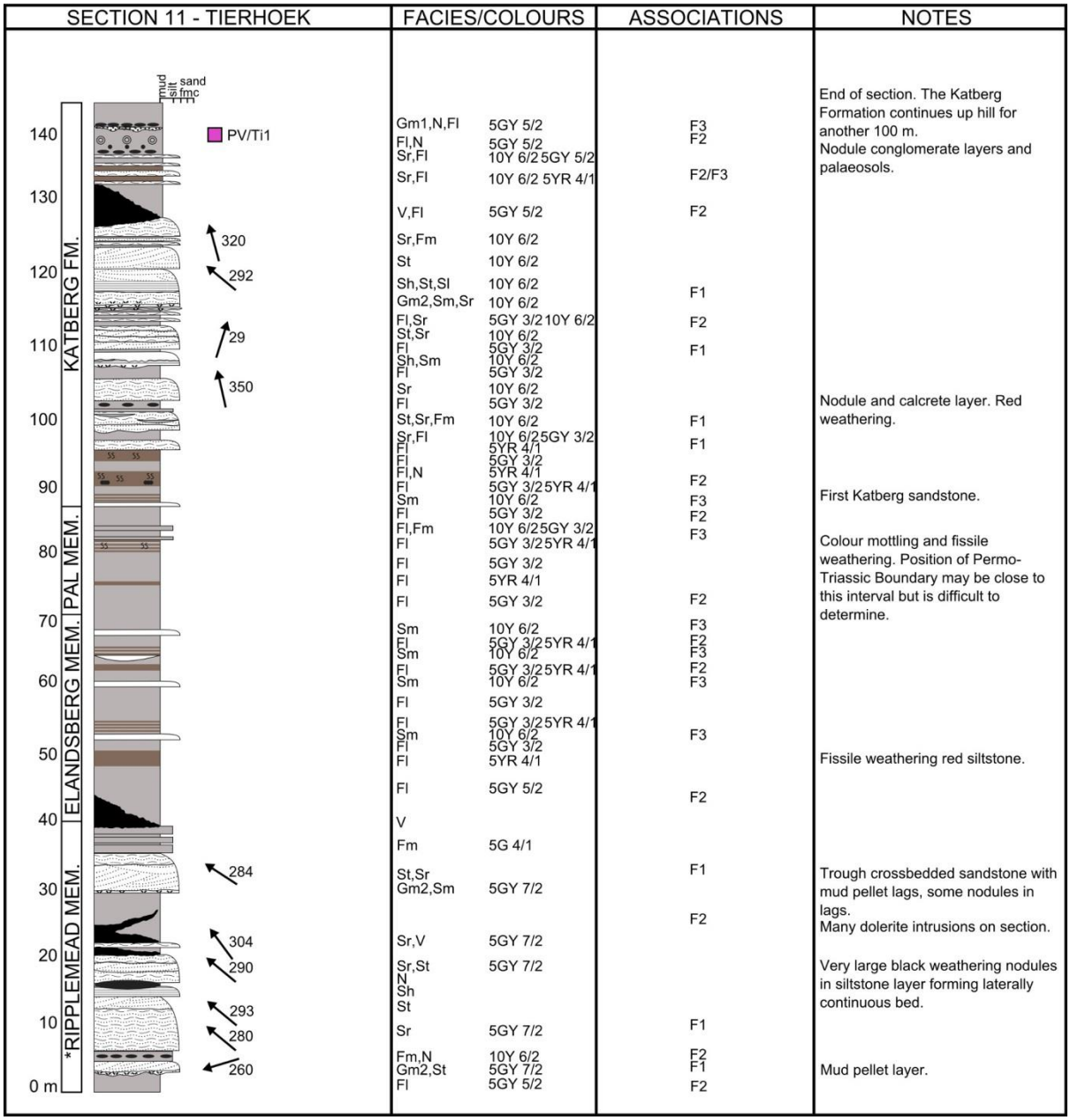

Figure 3.24: Section 11 measured on Tierhoek farm near Gariep Dam.

Central Free State Province (Sections 12 and 13)

Jagersfontein (Section 12)

The stratigraphy of the Beaufort Group in the central Free State Province (Jagersfontein and Bloemfontein districts) is poorly understood due to laterally restricted and poor outcrops. However fossils found in this part of the basin place the strata within the DaAZ and therefore these rocks are very relevant to the aims of this study. A prominent hill near the town of Jagersfontein on the Trompsburg road (R704) is well known as the site of the Battle of Boomplaas in 1848. Known as Boomplaas Hill in the area, the hill straddles three farms (Buffelsboutfontein, Trifaldi Major and Excelsior) and additionally straddles the edge of the Beaufort Group depositional margin (Figures 3.25 and 3.26). As a result the hill provided exposure in an otherwise featureless landscape to measure a vertical section extending from the Ecca Group (Tierberg Formation), which is present as small mudrock exposures in the flats, upwards into the Beaufort Group (see section 12, Figure 3.27). A single conspicuous sandstone near the top of the hill is investigated as a possible lateral equivalent to the Ripplemead member or Musgrave Grit (see Table 1.1 and Figure 3.26, A). In addition the Evolutionary Studies Institute database information shows that *Dicynodon lacerticeps* has been found on Boomplaas Hill (BP/1/5651; BP/1/5650) which tentatively confirms Lopingian strata at the site.

Section 12: Boomplaas Hill, Jagersfontein, Free State Province

The site of section 12 (Figure 3.27) is on the edge of the Beaufort Group close to the contact with the Ecca Group on Boomplaas Hill near Jagersfontein in the north central Free State Province. As outcrops in the Free State Province are isolated and tend to be preserved around dolerite sills and dykes it is difficult to trace out lithological units over long distances (Figures 3.25 and 3.26). The section measured on Boomplaas Hill (section 12, Figure 3.27) documents the presence of one prominent amalgamated sandstone unit that is informally referred to as the Boomplaas sandstone (BS). The BS has a heavily scoured base filled with coarse-grained gravel lags. Two other single-storey sandstones are also present higher in the stratigraphic column. The thick sandstone reaches a maximum thickness of 25 m and lies 120 m from the top of strata assigned to the Ecca Group. The top of the Ecca Group was defined by the first appearance of red mudstones on the section circumstantially as they represent oxidised soil conditions, but also by the disappearance of finely laminated dark green (5G 4/1) shales.

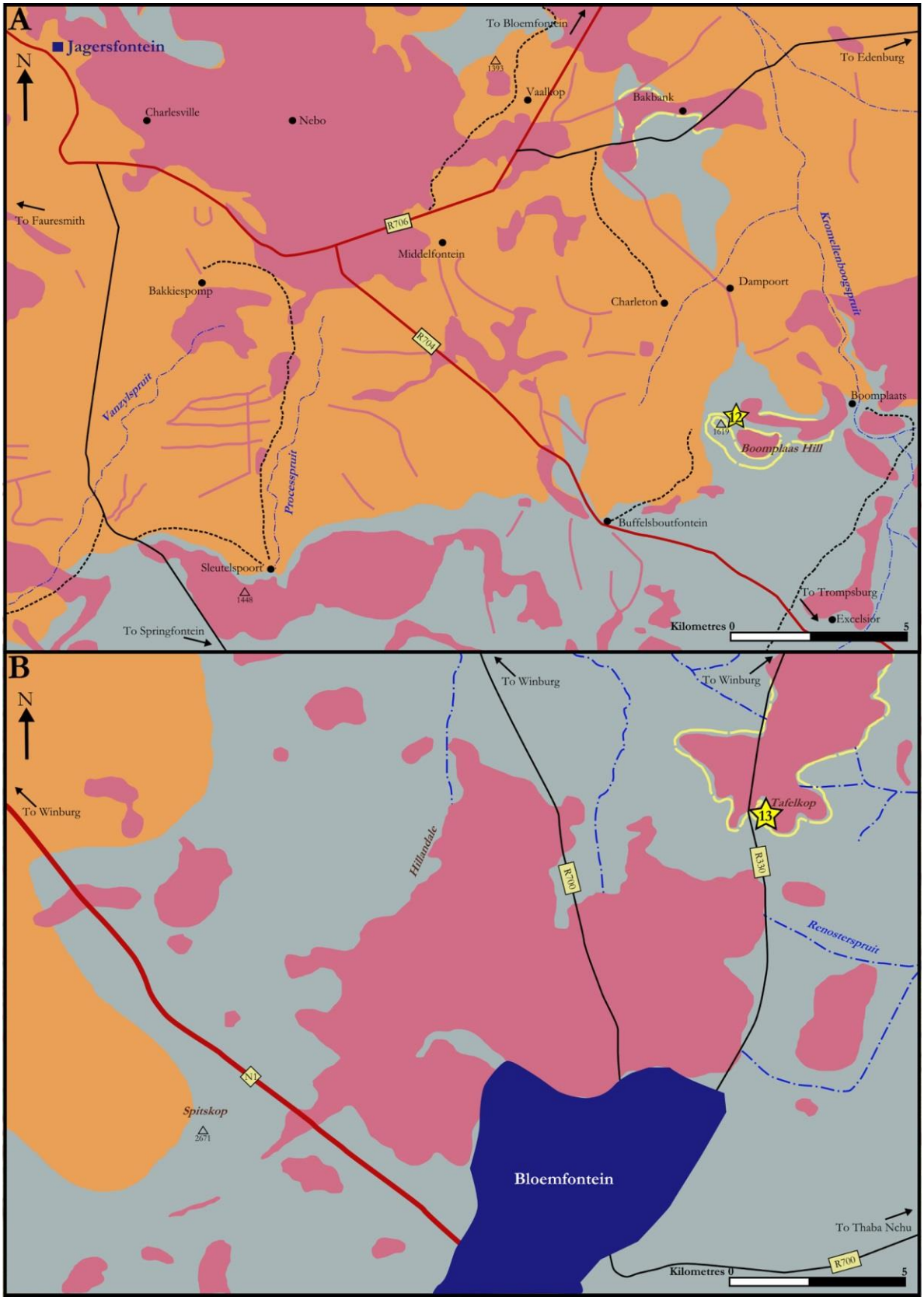

Figure 3.25: A) Map of the Jagersfontein field site showing the distribution of the Boomplaas Hill sandstone (yellow lines). The position of vertical section 12 (Boomplaas Hill) is shown by yellow star. B) Map of the Bloemfontein field site showing the distribution of potential lateral equivalents of the Ripplemead member within the Musgrave Grit unit. The position of vertical section 13 (Tafelkop) is shown by yellow star.

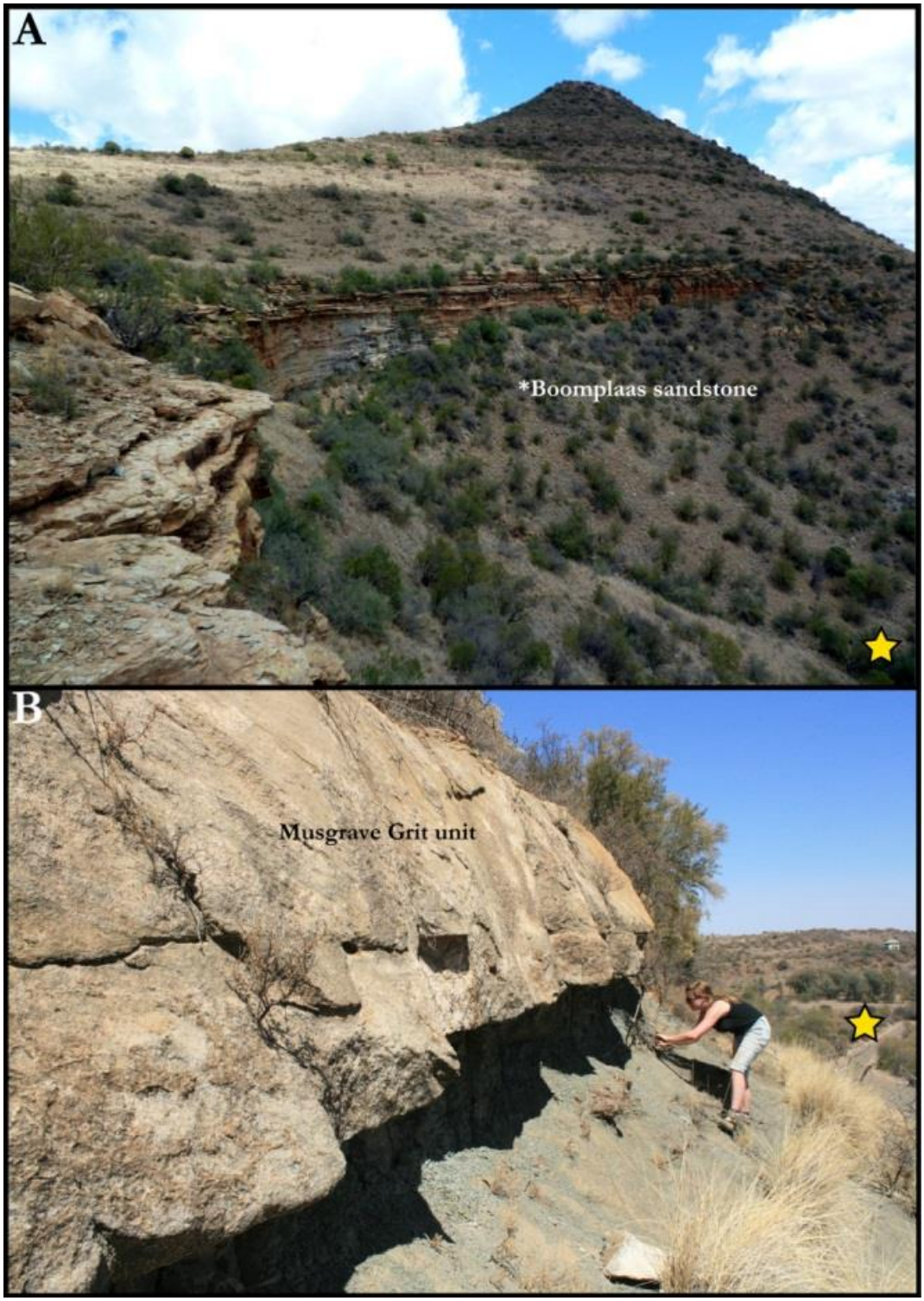

Figure 3.26: The final field sites studied in the central Free State Province, A) At the Jagersfontein (section 12, Figure 3.27) and B) Bloemfontein (section 13, Figure 3.28) field sites, the stratigraphy is poorly understood due to poor outcrop but at section 13 the Musgrave Grit unit has been identified by J.C Loock (pers. comm. 2013). The sandstone identified at section 12 is deemed indeterminate Balfour Formation but is informally referred to as the Boomplaas sandstone (BS) for this study. Nevertheless the stratigraphy at both sites is identified as Lopingian by the discovery of *Dicynodon lacerticeps* at Jagersfontein and *Theriognathus microps* on Tafelkop. J.C Loock (pers. comm. 2013) mentions the discovery of a *Lystrosaurus* fossil on the top of Tafelkop by James Kitching however this fossil could not be located in the collections at the ESI or the National Museum. Yellow stars indicate start point of vertical sections.

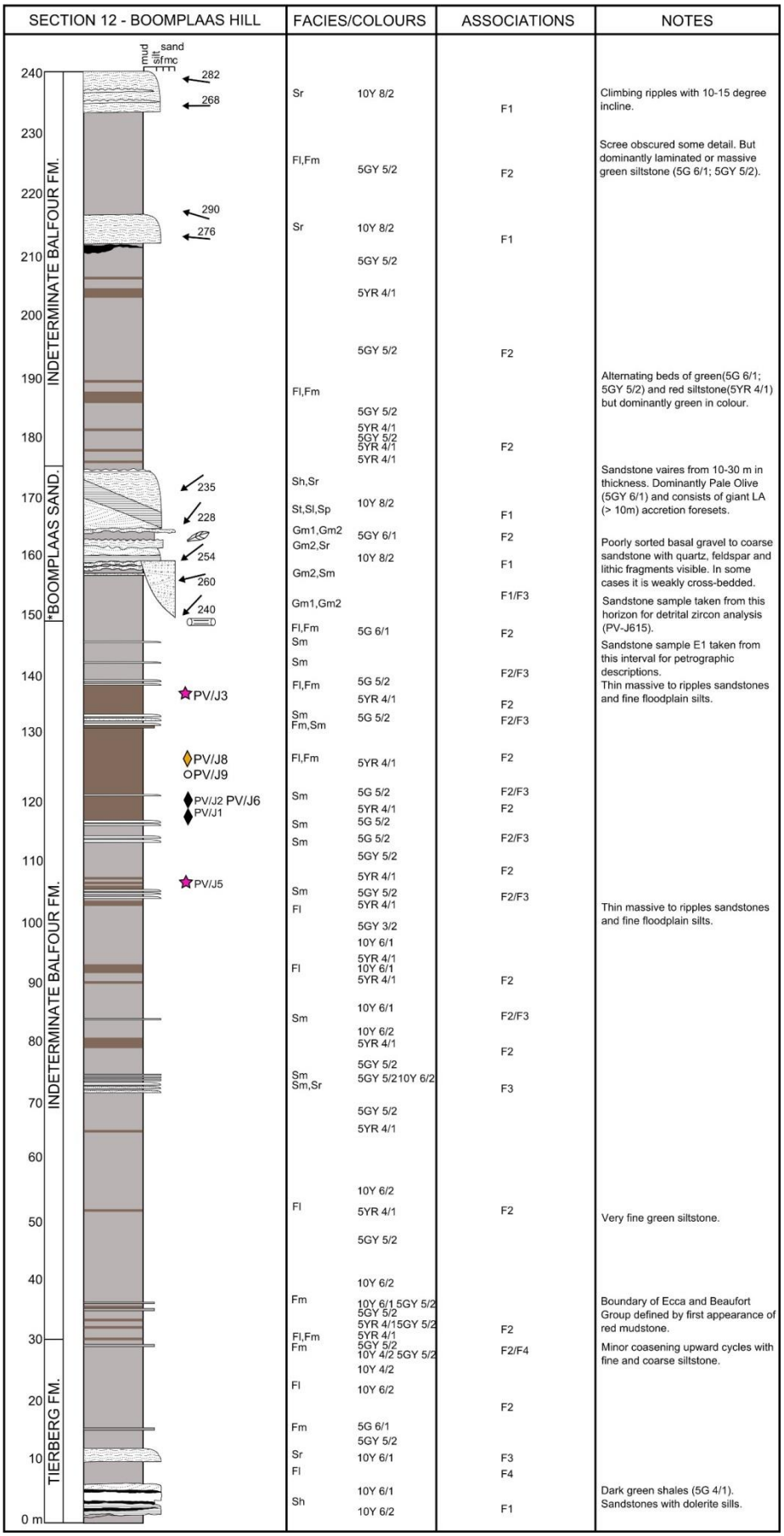

Figure 3.27: Section 12 measured on Boomplaas Hill near Jagersfontein.

Bloemfontein (Section 13)

A small koppie located on the R30 (Raymond Mhlaba drive) 10 km north of the city centre of Bloemfontein on a property called Tafelkop provided enough topography to measure a small vertical section where a sandstone rich interval is present attributed to belonging to the Musgrave Grit unit (Loock pers. comm. 2013) (Section 13, Figures 3.28). The sandstones of the Musgrave Grit unit were investigated in order to discover if they could be correlated to the Ripplemead member identified further south. The stratigraphy at this field site is poorly understood; however fossils of *Theriognathus microps* found on a small koppie in the property that are housed at the National Museum currently place these rocks within the Lopingian. Additionally, J.C Loock (pers. comm. 2013) claims a *Lystrosaurus* fossil was discovered by James Kitching on the top of the hill, although this has never been verified as the fossil is not recorded in local or global Karoo fossil collections. The Balfour Formation has been mapped in this area, but lithological units identified in the south are replaced by the Dubbeldam Mudrocks and the Musgrave Grit unit (Rutherford, 2009; Rutherford et al. 2015, see Chapter 1.2).

Section 13: Tafelkop, Bloemfontein, Free State Province

From palaeontological evidence (Chapter 2.2) the base of the locality at Tafelkop (section 13, Figure 3.28) is regarded as DaAZ age. Prominent sandstones are present (Figure 3.26) but they are difficult to trace out laterally. Work conducted by Rutherford et al. (2015) near Thaba Nchu identified a coarse-grained sandstone rich succession which is named the Musgrave Grit (see Chapter 1.2). The Musgrave Grit refers to a coarse-grained arenaceous unit that outcrops near the top of the Dubbeldam mudrock unit, however the Musgrave Grit unit is a series of coarse-grained sandstones within the Dubbeldam mudrock identified by J.C Loock, and named the Northern Beaufort Formation by Theron (1970) (Rutherford, 2009). Rutherford et al. (2015) describes the Musgrave Grit unit as being the only unit in the area with southerly palaeocurrent directions. Therefore this work could be used to provide stratigraphic context to section 13 because the same situation is observed in three sandstones at the base of Tafelkop (Figure 3.28). Therefore they are considered part of the Musgrave Grit unit. The top of this unit (the uppermost Musgrave Grit) is present ~ 50 m below the Katberg Formation at Thaba Nchu (Rutherford et al. 2015). The RM at Gariep Dam could not be traced further north into the Free State Province than the town of Springfontein, and therefore the stratigraphic relationship of the Musgrave Grit unit and the RM requires further work.

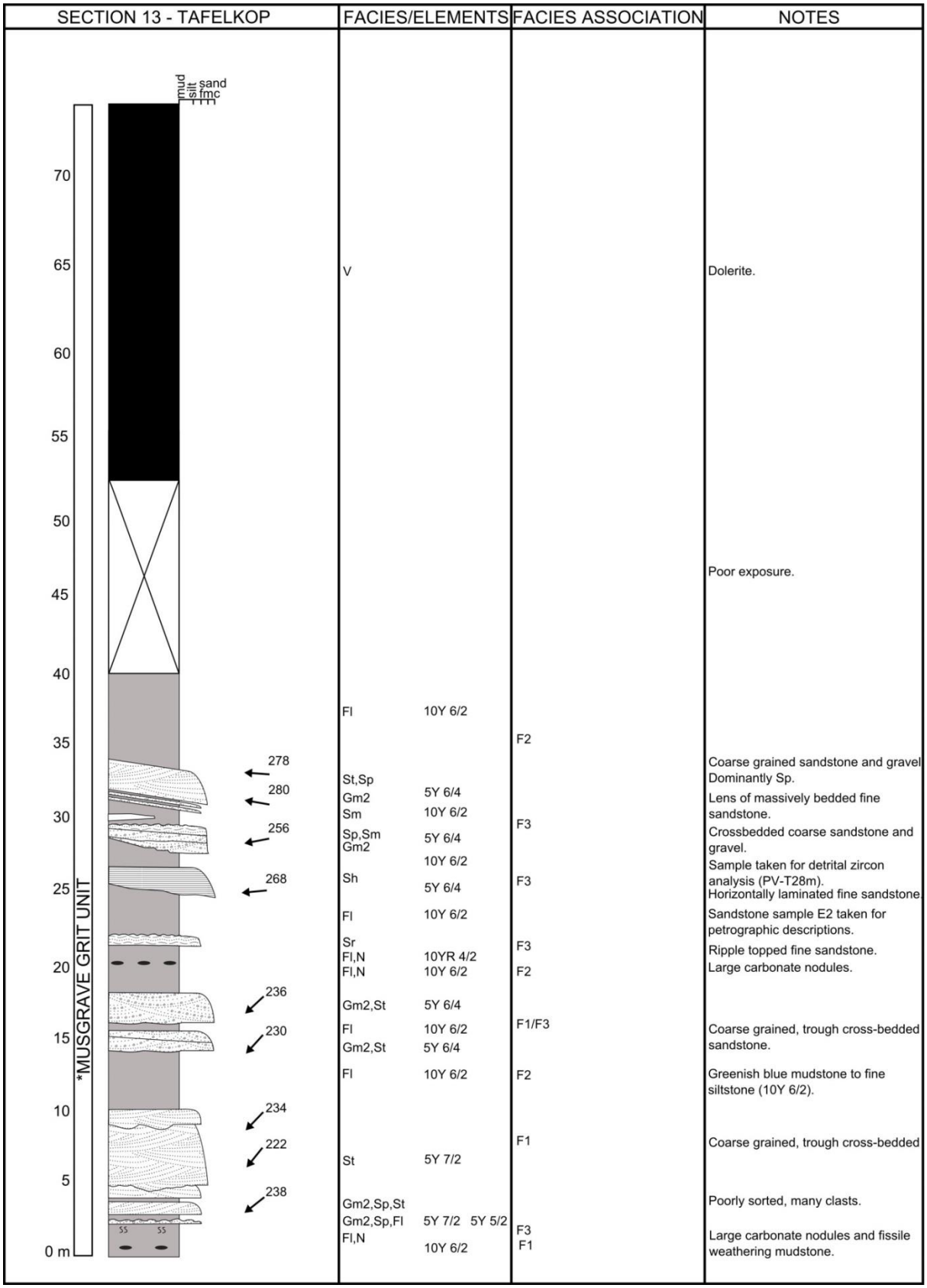

Figure 3.28: Section 13 measured on Tafelkop near Bloemfontein.

3.2.1 Composite sections

Twelve of the thirteen measured vertical sections measured near Cradock (1A, 1B, 2), Nieu Bethesda (3, 4, 5), Beaufort West (6, 7), Gariep Dam (8, 9, 10, 11), and Bloemfontein (13) allowed for the compilation of composite sections for strata assigned to the *Daptocephalus* Assemblage Zone (see Figure 3.29). Because of the difficulty in providing a stratigraphic framework for the Boomplaas sandstone, section 12 could not be incorporated into Figure 3.29. In addition a table summarizing the updated thicknesses for stratigraphic units from all the study sites are compared to previous workers (Table 3.2). The stratigraphic position of the Permo-Triassic Boundary was obtained by corroborating results of this study to those of Smith and Botha-Brink (2014). Later they will be used to correlate different lithostratigraphic units (eg. Ripplemead and Javanerskop members, and Musgrave Grit) using other proxies, such as biostratigraphy (Chapter 3.3), palaeocurrents (Chapter 3.4), and detrital zircon dates (Chapter 3.6). They will also be incorporated into Chapter 5 when palaeoenvironmental changes and basin model implications are discussed.

The composite sections demonstrate little change in thickness of the lithostratigraphic units between Cradock and Nieu Bethesda. They also show that thicknesses documented during this study are different to those recorded in previous studies (see Table 3.2). The implications are that thicknesses obtained by Johnson (1976), Tordiffe (1978), and Catuneanu and Elango (2001), are excessive for Cradock. It may be possible that thickness do increase to the east as suggested by Johnson (1976) however, the thicknesses these authors suggest are highly unlikely given the relatively short distance the strata would change from ~ 500 m to over 2000 m. In addition four stratigraphic sections measured in the Gariep Dam area confirm significant thinning of the Balfour Formation strata in this part of the basin (Table 3.2 and Figure 3.29). The absence of the Oudeberg Member an attenuated lithostratigraphic units of the Balfour Formation is likely due to longer and more frequent periods of non-deposition. Smith and Botha-Brink (2014) record thicknesses for the Elandsberg and Palingkloof members at Bethulie very similar to what was measured in Nieu Bethesda during this study, and do not match the thicknesses measured for these units in the Gariep Dam area. Maximum thicknesses for the DaAZ strata exposed in the Gariep Dam area are outlined in Table 3.2. This thickness (~ 91 m) is significantly thinner than in the southern field sites for the Balfour Formation, where it is ~ 500 m thick.

Table 3.2: Total thicknesses of formations and lithostratigraphic units from previous workers, and from this study (Viglietti, 2016). Note that for many of the units the total thicknesses are significantly less than previously documented.

Location/Field Site	Formation	Member/Unit	Thickness (m)	Source
King William's Town	Balfour	Total thickness	2350 m (± 500 m)	Johnson (1976)
Fort Beaufort	Balfour	Total thickness	2150 m (± 150 m)	Johnson (1976)
Cradock	Balfour	Total thickness	1220 m (± 150 m)	Johnson (1976)
Cradock	Balfour	Total thickness	1770 m	Tordiffe (1978)
Nieu Bethesda	Balfour	Total thickness	450 m	Johnson (1976)
Nieu Bethesda	Balfour	Total thickness	650 m	Visser and Dukas (1979)
Nieu Bethesda	Balfour	Total thickness	500 m	Rubidge et al. 1995
Thaba Nchu	Balfour	Total thickness	57 m	Rutherford et al. (2015)
Cradock	Balfour	Oudeberg	180 m	Tordiffe (1978)
Nieu Bethesda	Balfour	Oudeberg	50 m	Visser and Dukas (1979)
Cradock	Balfour	Daggaboersnek	1200 m	Tordiffe (1978)
Nieu Bethesda	Balfour	Daggaboersnek	440 m	Visser and Dukas (1979)
Nieu Bethesda	Balfour	Daggaboersnek	300 m	Cole and Wipplinger (2001)
Cradock	Balfour	Barberskrans	190 m	Tordiffe (1978)
Nieu Bethesda	Balfour	Barberskrans	60 m	Visser and Dukas (1979)
Cradock	Balfour	Elandsberg/ Palingkloof	200 m	Tordiffe (1978)
Nieu Bethesda	Balfour	Elandsberg/ Palingkloof	100 m	Visser and Dukas (1979)
Nieu Bethesda	Balfour	Elandsberg/ Palingkloof	100-150 m	Cole and Wipplinger (2001)
Nieu Bethesda	Balfour	Elandsberg	37-42 m	Smith and Botha-Brink (2014)
Bethulie	Balfour	Elandsberg	41 m	Smith and Botha-Brink (2014)
Nieu Bethesda	Balfour	Palingkloof	60 m	Smith and Botha-Brink (2014)
Bethulie	Balfour	Palingkloof	46 m	Smith and Botha-Brink (2014)
Thaba Nchu	Balfour	Musgrave Grit	1 m	Rutherford et al. (2015)
Beaufort West	Teekloof	Total thickness	~ 400 m	Smith (1993)
Beaufort West	Teekloof	Total thickness	500 m	Cole and Wipplinger (2001)
Beaufort West	Teekloof	Oukloof	~125 m	Turner (1981)
Beaufort West	Teekloof	Steenkampsvlakte	~ 200 m	Stear (1980)
Beaufort West	Teekloof	Javanerskop	unknown	Le Roux (1985)
Cradock	Balfour	Total thickness	513 m	Viglietti (2016)
Nieu Bethesda	Balfour	Total thickness	506 m	Viglietti (2016)
Gariep Dam	Balfour	Total thickness	91 m	Viglietti (2016)
Gariep Dam	Balfour	Oudeberg	not present	Viglietti (2016)
Cradock	Balfour	Daggaboersnek	300 m	Viglietti (2016)
Nieu Bethesda	Balfour	Daggaboersnek	330 m	Viglietti (2016)
Gariep Dam	Balfour	Daggaboersnek	20 m	Viglietti (2016)
Cradock	Balfour	Ripplemead	78 m	Viglietti (2016)
Nieu Bethesda	Balfour	Ripplemead	96 m	Viglietti (2016)
Gariep Dam	Balfour	Ripplemead	30 m	Viglietti (2016)
Cradock	Balfour	Elandsberg	63 m	Viglietti (2016)
Nieu Bethesda	Balfour	Elandsberg	37 m	Viglietti (2016)
Gariep Dam	Balfour	Elandsberg	26 m	Viglietti (2016)

Cradock	Balfour	Palingkloof	32 m	Viglietti (2016)
Nieu Bethesda	Balfour	Palingkloof	43 m	Viglietti (2016)
Gariep Dam	Balfour	Palingkloof	17 m	Viglietti (2016)
Beaufort West	Teekloof	Steenkampsvlakte	100 m	Viglietti (2016)
Beaufort West	Teekloof	Javanerskop	125 m	Viglietti (2016)

In the Beaufort West composite section, a stratigraphic package of 240 m comprises the upper Oukloof, Steenkampsvlakte, and Javanerskop members (Figure 3.29). The Steenkampsvlakte Member can be divided into a lower sandstone-poor (eg. the Steenkampsvlakte Member) and an upper sandstone rich succession (eg. the Javanerskop member). For the first time, the Javanerskop member has its total thickness documented, which is ~ 125 m. In addition it also has its lithological properties documented (see section 6 and 7, Figures 3.17 and 3.18). The Steenkampsvlakte Member is now considered to represent only the lower sandstone poor portion of DaAZ strata, and is ~ 110 m in total thickness. Correlation of the Javanerskop member with the RM is tentative at this stage because it requires the results of other investigations (eg. biostratigraphy, detrital zircons) to confirm.

Near Jagersfontein and Bloemfontein correllation of sandstone-rich horizons such as the BS is difficult due to poor exposure. Section 13 measured on Tafelkop Hill is correlated to a section measured by Rutherford (2009) and Rutherford et al. (2015) near Thaba Nchu and just east of Bloemfontein as is used as the composite section in this study (Figure 3.29). Rutherford (2009) identified the Musgrave Grit unit at the top of the Dubbeldam mudrocks during his investigation and is defined as a coarse-grained sandstone with distinct southerly palaeocurrent directions. Corroborating this information with results from the palaeocurrent and lithological properties during this study (Table 1.1, Figure 3.28) the sandstones on Tafelkop are defined as comprising part of the Musgrave Grit unit. The RM at Gariep Dam could not be traced further than the town of Springfontein and therefore the Musgrave Grit unit present at Tafelkop is only tentatively correlated with the RM at this point in the investigation. The next sections of the results (Chapters 3.3-3.6) will clarify the temporal nature of the Upper Permian lithostratigraphic units.

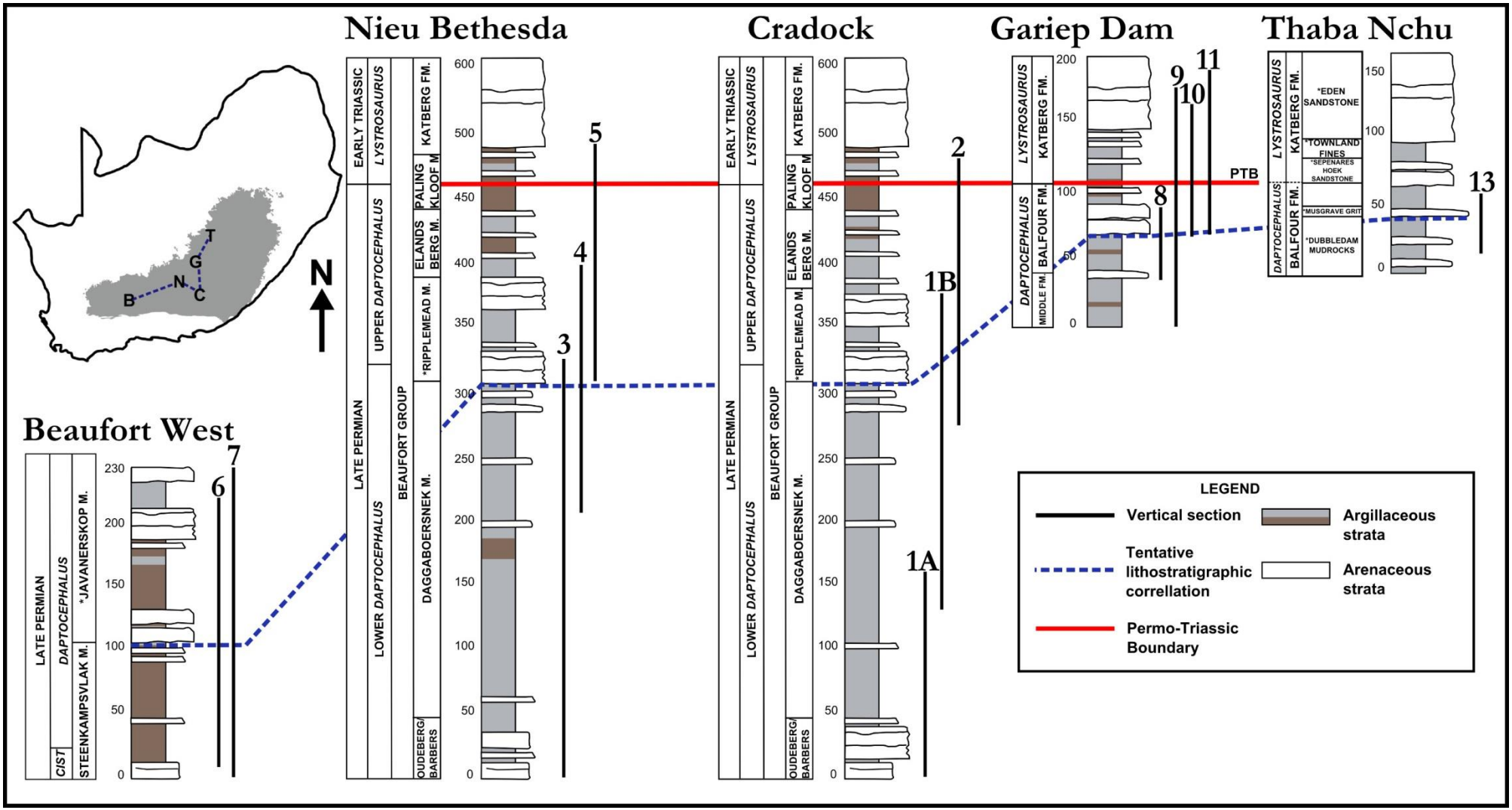

Figure 3.29: Five composite sections created using 12 out of 13 sections measured during this study. Numbered sections relate to same numbered sections discussed in Chapter 3.2. The map of South Africa and Karoo Basin show the position of the field sites Beaufort West (B), Nieu Bethesda (N), Cradock (C), Gariep Dam (G), and Thaba Nchu (T) which is just east of Bloemfontein. The Thaba Nchu composite section is adapted from Rutherford et al. (2015).

3.3 Biostratigraphic investigation

For this section a publication was completed and has been published (Viglietti, P. A., Smith, R. M. H., Angielczyk, K. D., Kammerer, C. F., Fröbisch, J., Rubidge, B. S., 2016. The *Daptocephalus* Assemblage Zone (Lopingian), South Africa: A proposed biostratigraphy based on a new compilation of stratigraphic ranges. Journal of African Earth Sciences, 113, 153-164 DOI 10.1016/j.jafrearsci.2015.10.011). As a result the *Dicynodon* Assemblage Zone (DiAZ) is no longer referred to in the thesis and instead is replaced by the *Daptocephalus* Assemblage Zone (DaAZ) as proposed in this chapter. Although the focus of the publication was the vertebrate fossils of the now newly proposed *Daptocephalus* Assemblage Zone, other notable fossil remains were also encountered during this investigation. These fossils included fossil fish, invertebrates, and plants. These fossils however are not useful for biostratigraphic correlation at this stage and therefore were not included in the publication. Their current status and occurrence in this investigation will be briefly discussed before the next section where the publication is presented. The fossils are referred to in Chapter 4 where their sedimentological context is discussed. Appendix 2 (on disc) can be referred to for more information on their provenance.

Fish (Actinopterygii)

Fossils of actinopterygians or ray-finned (Palaeoniscid) fish occur throughout the Beaufort Group succession however, their preservation is commonly localized which means their future biostratigraphic utility is questionable. Recently their taxonomy and biostratigraphy has been refined by Bender (2001, 2002), and Bender and Hancox (2003), which has facilitated a first attempt in using Beaufort Group fishes in conjunction with the vertebrate biozonation scheme. Bender (2001, 2002) demonstrates that certain taxa, such as *Atherstonia scutata, Atherstonia minor*, *Bethesdaicthys*, *Blourugia seeleyi* and *Namaicthys digitata* occur throughout the Permian Beaufort Group (with the exception of the *Eodicynodon* Assemblage Zone). *Westlepis kempeni* and *Kompasia delaharpi* are only known from the *Tapinocephalus* and *Daptocephalus* Assemblage Zones respectively. Additionally across the Permo-Triassic Boundary a marked change in taxonomic composition of the fish fauna is observed, which is possibly linked to palaeoclimatic changes that occurred over the extinction event (Bender and Hancox, 2003). In this study, fish fossils that were encountered were too fragmentary to make a confident identification to genus level. However a comment on their preservation is relevant. On Ripplemead farm (section 5, Figure 3.13) a single fish fossil was found encased in a pedogenic nodule. Fish fossils were also encountered as an apparent mass death in a single siltstone horizon on Eildon farm in the upper *Daptocephalus* Assemblage Zone (Figure 4.10, Chapter 4.2). A similar mode of preservation was described by Bender (2000) in the Abrahamskraal Formation (*Tapinocephalus* Assemblage Zone)

at Blourug near Victoria West, and the two sites in the Balfour Formation (*Daptocephalus* Assemblage Zone) on Wilgebosch near Nieu Bethesda from where he described his new species.

Invertebrates

The most common evidence of invertebrates encountered during this investigation was as trace fossils. There were mainly in the form of burrows (*Planolites*) or trackways (*Diplichnites*) that have been described by previous workers in the Beaufort Group (Anderson, 1975; Smith, 1993a). A noteworthy discovery during my study is freshwater bivalves in the Baviaansrivier Valley just above the BM, in the lowermost Daggaboersnek Member (Figure 4.12). Previous workers have identified freshwater bivalves in the Ecca Group (Cooper and Kensley, 1984), at the Ecca-Beaufort contact (Volksrust Formation) (Cairncross et al. 2005), in the Abrahamskraal and Teekloof formations (Rossouw, 1970; Smith, 1990; Rubidge et al. 2000), and early-middle Triassic Burgersdorp Formation in coprolites (Yates et al. 2012), and are rare localized occurrences. Bivalves have also been documented at the type locality of the *Cistecephalus* Assemblage Zone on Steilkrans farm near Nieu Bethesda (Smith, pers. comm. 2015). At this site they occur as laterally restricted deposits in sandy siltstone beds directly overlying the Oudeberg Member. The presence of bivalves could represent a particular facies association or subenvironment in the Beaufort Group, such as perennially subaqueous conditions, like standing water or lakes. The bivalves found during this study vary in size between 4 and 12 mm in length. The articulated bivalves occurred within isolated arenaceous and argillaceous calcareous pods within fine mudstone or siltstone. Disarticulated bivalves were found in thin fine-grained sandstone layers with rippled surfaces (Figure 4.12, Chapter 4.2). The last detailed descriptions of freshwater bivalves in the Beaufort Group were done by Rossouw (1970) who described them as belonging to the genus *Palaeanodonta*.

Fossil flora

The fossil floras of the Beaufort Group are diverse and are preserved in the fossil record as microfossils, macrofossils, and petrified wood (Bamford, 2004). Microflora include the pollen and spores of ferns and conifers (Barbolini, 2014) and the macroflora consist mainly of genera that include mosses (*Buthelezia*), sphenophytes or equisetum (*Sphenophyllum, Raniganjia, Phyllotheca, Schizoneura*), ferns (*Sphenopteris*), cordaitales (*Noeggerathiopsis*), and petrified woods (*Australoxylon, Prototawoxylon*) (Bamford, 2004). They occur as dense deposits when encountered but are never laterally or vertically continuous (Gastaldo et al. 2005). Fossil floras are also more frequently encountered in the north and eastern facies of the Beaufort Group (Normandien Formation) so their use for correlation into the west and central parts of the Beaufort Group has been difficult

(Anderson, 1977; Prevec et al. 2009). During this study leaf and stem impressions were the most commonly documented, particularly at the bases of multi and single-storey channel sandstones. In particular, sections 1B, 3, 4, 5, and 12 documented well preserved examples of this type of preservation. Rare siltstone horizons also contained fossil leaves and stems. In these examples the leaves or stems varied greatly in their degree of preservation, sometimes intact leaves and stems were found, but also chaotic broken chips of vegetable matter were also associated (Figure 4.2 (A)) . Additionally fossil rootlet horizons were also documented frequently within the overbank deposits (Figures 4.2 (G), and 4.3 (H)). At the site of section 12 (Figure 3.27) abundant blocks of fossil wood were found, but never in situ, and have not been identified at genus level.

3.3.1 Vertebrate biostratigraphy of the new *Daptocephalus* Assemblage Zone

This section presents the published manuscript Viglietti et al. 2016, which provides a newly proposed biostratigraphy for the latest Permian Karoo Basin. See Appendix 2 (on disc) for the specimen database rarefaction investigation.

The *Daptocephalus* Assemblage Zone (Lopingian), South Africa: A proposed biostratigraphy based on a new compilation of stratigraphic ranges

*Pia A. Viglietti[1], Roger M. H. Smith[1,2], Kenneth D. Angielczyk[1,3], Christian F. Kammerer[1,4], Jörg Fröbisch[1,5], Bruce S. Rubidge[1]

*Corresponding author (current address: Evolutionary Studies Institute, School for Geosciences, University of the Witwatersrand, Johannesburg, Private Bag 3 Wits 2050). pia.viglietti@gmail.com.

[1]Evolutionary Studies Institute, School for Geosciences, University of the Witwatersrand, Johannesburg, Private Bag 3 Wits 2050, pia.viglietti@gmail.com, (+27733760065), bruce.rubidge@wits.ac.za.

[2]Iziko South African Museum, P.O. Box 61, Cape Town, 8000 South Africa, rsmith@iziko.org.za.

[3]Integrative Research Center, Field Museum of Natural History, 1400 South Lake Shore Drive, Chicago, Illinois, 60605, USA, kangielczyk@fieldmuseum.org.

[4] Museum für Naturkunde, Leibniz-Institut für Evolutions- und Biodiversitätsforschung an der Humboldt-Universität zu Berlin, Invalidenstraße 43, 10115, Berlin Germany, christian.kammerer@mfn-berlin.de.

[5]Institut für Biologie, Humboldt-Universität zu Berlin Invalidenstraße 110, 10115 Berlin, Germany, joerg.froebisch@mfn-berlin.de.

Abstract

The *Dicynodon* Assemblage Zone (DiAZ) of South Africa's Karoo Basin is one of the eight biostratigraphic zones of the Beaufort Group. It spans the uppermost Permian strata (Balfour, Teekloof, and Normandien formations) and traditionally has been considered to terminate with the disappearance of *Dicynodon lacerticeps* at the Permo-Triassic Boundary. We demonstrate that the three index fossils currently used to define the *Dicynodon* Assemblage Zone (*Dicynodon lacerticeps*, *Theriognathus microps*, and *Procynosuchus delaharpeae*) have first appearance datum (FADs) below its traditionally recognized lower boundary and have ranges mostly restricted to the lower portion of the biozone, well below the Permo-Triassic Boundary. We propose re-establishing *Daptocephalus leoniceps* as an index fossil for this stratigraphic interval, and reinstating the name *Daptocephalus* Assemblage Zone (DaAZ) for this unit. Furthermore, the FAD of *Lystrosaurus maccaigi* in the uppermost reaches of the biozone calls for the establishment of a two-fold subdivision of the current *Dicynodon* Assemblage Zone. The biostratigraphic utility of *Da. leoniceps* and other South African dicynodontoids outside of the Karoo Basin is limited due to basinal endemism at the species level and varying temporal ranges of dicynodontoids globally. Therefore, we recommend their use only for correlation within the Karoo Basin at this time. Revision of the stratigraphic ranges of all late Permian tetrapods does not reveal a significant change in faunal diversity between the lower and upper DaAZ. However, the last appearance datum of the abundant taxa *Di. lacerticeps*, *T. microps*, *P. delaharpeae*, and *Diictodon feliceps* occur below the three extinction phases associated with the end-Permian mass extinction event. Due to northward attenuation of the strata, however, the stratigraphic position of the extinction phases may need to be reconsidered.

Keywords: *Dicynodon* Assemblage Zone, Late Permian, Karoo Biostratigraphy

1. Introduction

The Late Permian (Lopingian) is an important time in Earth's history. By this stage of the Permian all the world's continents had coalesced into a single supercontinent (Pangea), which was surrounded by a global ocean (Panthalassa), and this had significant climatic implications (Erwin, 1990; Parrish, 1993; Stampfli et al. 2013). The extensive subpolar coal forests of the early to middle Permian had given way to drier continental climates (Cairncross, 1989; Cadle et al. 1993). This is believed to have been a major driver in the evolution and diversification of the amniotes (Sahney et al. 2010). The Permian is best known for its radiation of non-mammalian synapsids (including the therapsids, the synapsid subclade containing mammals as their extant representatives). The Lopingian represents the golden age of the therapsids, which by this time

were at the peak of their ecological domination, occupying almost every available niche, although they began to relinquish this position during the end-Permian mass extinction (Benton and Twitchett, 2003; Erwin, 2006; Fröbisch, 2013; Benton and Newell, 2014; Smith and Botha-Brink, 2014). Events immediately prior to this great extinction and its aftermath in the terrestrial realm have received deserved attention from varied scientific disciplines including sedimentology and taphonomy (Smith, 1995; Smith and Ward, 2001; Smith and Botha, 2005; Ward et al. 2005; Botha and Smith, 2006; Viglietti et al. 2013); global climate and ocean modelling (Wignall and Twitchett, 1996; Bottjer, 2012; Sun et al. 2012); and disparity, ecology, and ecosystem modelling (Benton et al. 2004; Roopnarine et al. 2007; Sahney and Benton, 2008; Ruta et al. 2013).

South Africa's Beaufort Group (part of the Karoo Supergroup) is unique because it preserves, with little tectonic disturbance, a near continuous sequence of non-marine deposits documenting this radiation, ranging from the late Guadalupian (Capitanian) to the middle Triassic (Anisian). The abundant fossil tetrapods from the Beaufort Group have been divided into six Permian (*Eodicynodon*, *Tapinocephalus*, *Pristerognathus*, *Tropidostoma*, *Cistecephalus*, *Dicynodon*) and two Triassic (*Lystrosaurus*, *Cynognathus*) assemblage zones (AZs), biostratigraphic units based on therapsid index fossils. Apart from its record of the Permo-Triassic extinction, a new set of radiomentric dates (Rubidge et al. 2013) have recently made possible the identification of a mid-Permian (end-Guadalupian) extinction event in the terrestrial realm at 260 Ma (upper *Tapinocephalus* Assemblage Zone, Abrahamskraal Formation (Day et al. 2015). However for many of the other assemblage zones the available stratigraphic range data are not up to date and need to be re-evaluated before an accurate picture of faunal composition and turnover patterns can be discerned.

The *Dicynodon* Assemblage Zone (DiAZ) is the terminal Permian biostratigraphic assemblage zone of the Beaufort Group and is one of the thickest of the Beaufort Group's biozones (~ 500 m). During the time represented by this zone, the Karoo retroarc foreland system was in an overfilled phase and non-marine (molasse) environments occupied the entirety of the Karoo Basin for the first time in its history (Catuneanu et al. 1998; Smith et al. 2012). Recent radiometric dates suggest that it spans approximately three million years (Rubidge et al. 2013). It is currently defined by the first appearance datum (FAD) of the therapsids *Dicynodon lacerticeps* (Dicynodontia), *Theriognathus microps* (Therocephalia), and *Procynosuchus delaharpeae* (Cynodontia) (Rubidge et al. 1995), and is considered to terminate with the LAD of *D. lacerticeps*, associated with three extinction phases in a 70 m thick interval spanning the Permo-Triassic Boundary (Smith & Botha-Brink, 2014) (Figure 1). It roughly coincides with the lithologically defined

Balfour Formation in the east, Teekloof Formation in the west and Normandien Formation in the north of the basin.

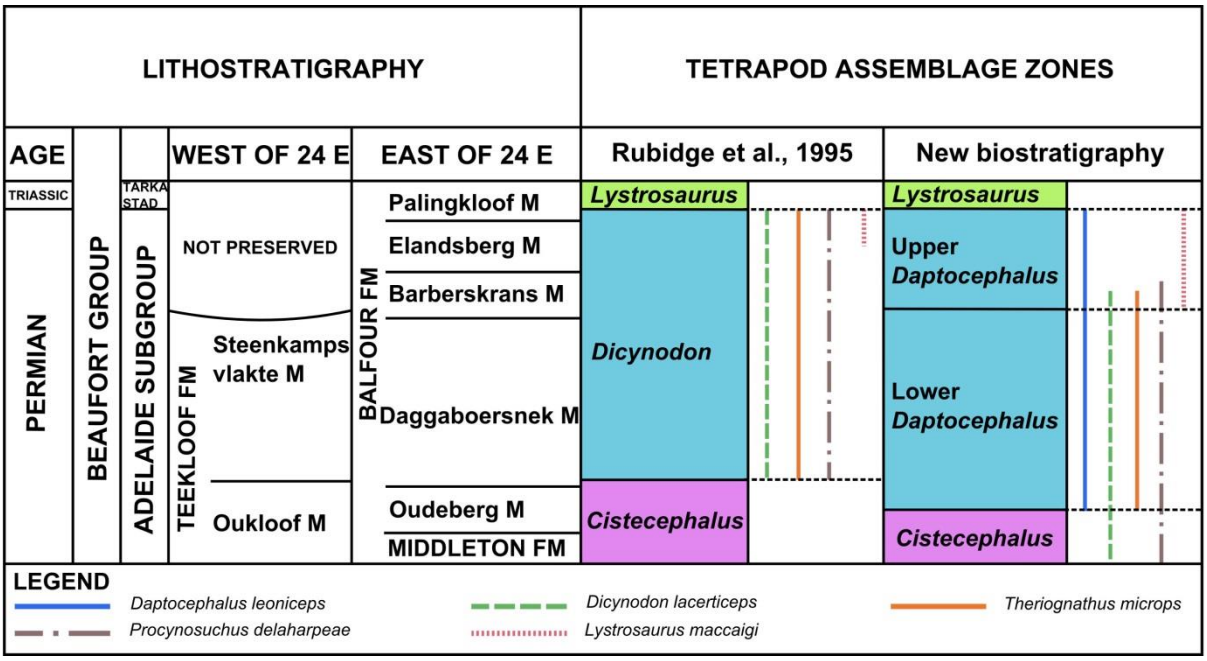

Figure 1: The current *Dicynodon* Assemblage Zone (sensu Rubidge et al. 1995) and our proposed *Daptocephalus* Assemblage Zone biostratigraphic schemes with lithostratigraphic subdivisions. Note the new range data for *Dicynodon lacerticeps*, *Theriognathus microps*, and *Procynosuchus delaharpeae*. In this new framework, the base of the lower *Daptocephalus* Assemblage Zone will be defined by the FAD of *Daptocephalus leoniceps* and *Theriognathus microps* and the base of the upper *Daptocephalus* Assemblage Zone will be defined by the FAD of *Lystrosaurus maccaigi*. The LAD of *Daptocephalus leoniceps* and *Lystrosaurus maccaigi* (and the upper boundary of the *Daptocephalus* Assemblage Zone) is within Smith and Botha-Brink's (2014) phase 2 extinction approximately at their stratigraphically defined Permo-Triassic Boundary.

Based on its use as an index fossil in the Karoo Basin, *Dicynodon* sensu lato has been used in the past to correlate various Karoo-aged basins within the Platbergian land vertebrate faunachron (LVF), a global biostratigraphic unit that covers the ages of the uppermost *Cistecephalus* Assemblage Zone (CAZ) and the entire DiAZ. The other LVFs are the Hoedemakeran (defined by the first appearance of *Tropidostoma*) and the Steilkransian (defined by the first appearance of *Cistecephalus*) (Lucas, 2006). As a result *Diycnodon* sensu lato has a long history of being used to make biostratigraphic correlations between the Karoo Basin and other areas such as Tanzania and Zambia (Anderson and Cruickshank, 1978; King, 1992; Lucas, 1997, 1998a, b, 2001, 2002, 2005; Rubidge, 2005; Lucas, 2006; Smith et al. 2012; Angielczyk et al. 2014a, b). However few definitive DiAZ strata have been found outside of the main Karoo Basin as many of these Karoo-aged basins are now believed to correlate with the CAZ (Angielczyk et al. 2014a, b). Nonetheless, a few places globally do have strata that correlate to the DiAZ, such as the Guodikeng Formation in northwestern China (Metcalfe et al. 2001) and the Sokolki fauna near Vyazniki and Gorokhovets on the Russian Platform (Newell et al. 2010). It has also been

recognized for some time that the paraphyly of the traditionally-recognized genus and taxonomic confusion at the species level made it a poor index fossil (Angielczyk and Kurkin, 2003a, b). Therefore *Dicynodon* sensu lato in various Karoo-aged basins do not represent the same taxon and as a result give no guarantee they had similar temporal ranges (Kammerer et al. 2011).

Recently, Kammerer et al. 2011 undertook a comprehensive taxonomic revision of *Dicynodon*, reducing the 168 nominal species to 15 species in 14 genera globally and underscoring the paraphyly of *Dicynodon* sensu lato. In the Karoo Basin, Kammerer et al. (2011) recognized five valid species of basal (non-lystrosaurid, non-kannemeyeriiform) dicynodontoids: *Basilodon woodwardi*, *Daptocephalus leoniceps*, *Dicynodon lacerticeps*, *Dinanomodon gilli*, and *Sintocephalus alticeps*. Additionally, they erected new genera (*Keyseria* and *Euptychognathus*) for the Karoo-occurring former "*Dicynodon*" species "*D.*" *benjamini* and "*D.*" *bathyrhynchus*, which they recovered as a basal cryptodont and lystrosaurid, respectively. However, they expressed uncertainty about the stratigraphic ranges of some of these species, noted that *Da. leoniceps* might be a more appropriate index fossil for the *Dicynodon* Assemblage Zone than *Di. lacerticeps*, and suggested that additional scrutiny was needed to fully understand the biostratigraphic utility of *Dicynodon* and its closest relatives. Indeed, the change in nomenclature from the older *Daptocephalus* Zone (Kitching, 1977) to the current *Dicynodon* Assemblage Zone (Rubidge et al. 1995) was driven entirely by obsolete taxonomy, which viewed *Daptocephalus* as a junior synonym of *Dicynodon* and expressed uncertainty as to whether *Da. leoniceps* was a junior synonym of *Di. lacerticeps* (Cluver and Hotton, 1981; Cluver and King, 1983; King, 1988).

Beyond the uncertainty surrounding the stratigraphic occurrences of *Dicynodon* and its close relatives, the current definition of the DiAZ is also problematic because all three index species (*Di. lacerticeps*, *T. microps*, and *P. delaharpeae*) are reported to have FADs that predate the traditionally-recognized base of the DiAZ. Therefore the use of *Dicynodon* sensu lato in the LVF biostratigraphic scheme is problematic in the Karoo Basin because it is considered to be concurrent with *Cistecephalus microrhinus* and therefore would overlap the Steilkransian LVF (Kammerer et al. 2011). *Theriognathus microps* is also regarded as present in the upper CAZ (Huttenlocker, 2014) and *P. delaharpeae* has an even earlier FAD in the Hoedemakeran LVF (*Tropidostoma* Assemblage Zone) (Botha-Brink and Abdala, 2008). Given these ranges, the first co-occurrence of these species would be in rocks traditionally assigned to the CAZ, requiring a redefinition of the zone such that it is based on a suite of taxa that do not also co-occur in other assemblage zones. A similar problem occurs at the top of the zone, where *Lystrosaurus maccaigi*

first appears in Late Permian rocks that are below the traditional lower bound of the *Lystrosaurus* Assemblage Zone (LAZ) just after the Permo-Triassic boundary (PTB) (Botha and Smith, 2007).

The aim of this investigation is to address the shortcomings of the current manifestation of the *Dicynodon* Assemblage Zone. First, we reassess the stratigraphic ranges of *Di. lacerticeps*, other basal dicynodontoids, and additional DiAZ-occurring taxa in the Karoo Basin and test their utility as index fossils. Second, we redefine the assemblage zone by replacing the DiAZ with the *Daptocephalus* Assemblage Zone (DaAZ) using a group of taxa that only occur within rocks assigned to this zone, and re-establishing *Da. leoniceps* as an index fossil for this stratigraphic interval (Figure 1). Third, we resolve the biostratigraphic problem of the Late Permian FAD of *L. maccaigi* by informally dividing the DaAZ into a lower and upper subzone. Fourth, we investigate the lower and upper DaAZ for differences in faunal diversity. Finally, we provide an updated faunal list and set of stratigraphic ranges for the vertebrates of the new *Daptocephalus* Assemblage Zone biostratigraphic scheme (Figure 2), and identify how their LADs relate to Smith and Botha-Brink's (2014) three extinction phases associated with the end-Permian mass extinction event.

2. Materials and Methods

2.1 Lithostratigraphy and study locations

The DaAZ coincides with three formations in the main Karoo Basin: the Teekloof Formation west of 24˚ E, the Balfour Formation east of 24˚ E, and the Normandien Formation in the northern Free State and Kwa-Zulu Natal provinces. The uppermost Steenkampsvlakte Member of the Teekloof Formation is assigned to the lower DaAZ and has been inferred as a lateral equivalent to the lower Balfour Formation (Cole and Wipplinger, 2001). Poor exposure and uncertain correlation with southern Karoo Basin stratigraphy are reasons that the Normandien Formation is poorly constrained temporally. However, based on sequence stratigraphy, Catuneanu et al. (2005) suggest that it is representative of only the latest Permian (see also Catuneanu et al. 1998).

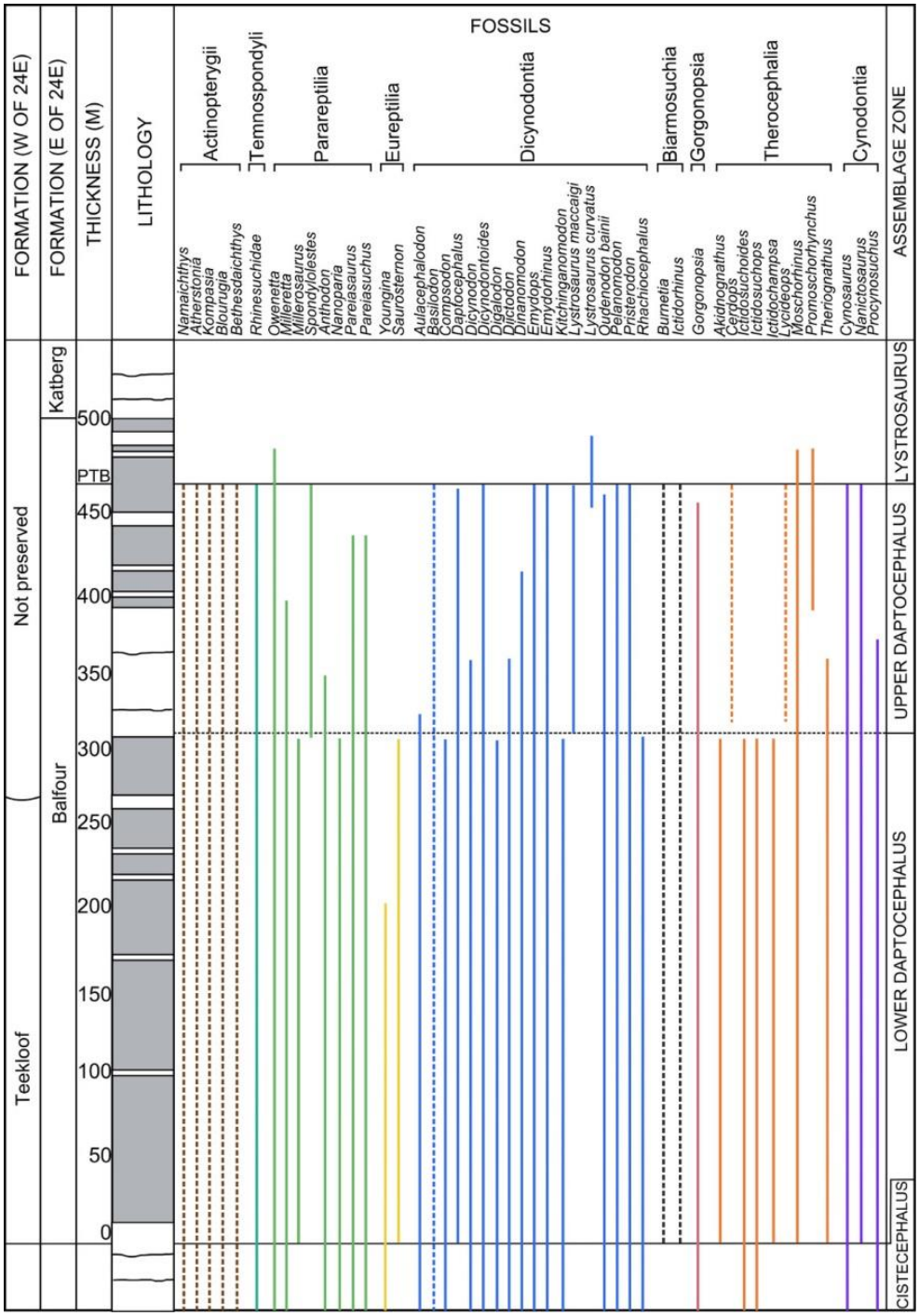

Figure 2: Updated stratigraphic ranges of vertebrate fauna of the newly proposed *Daptocephalus* Assemblage Zone. Note temnospondyls and gorgonopsians are represented by a single higher taxon due to taxonomic confusion and current lack of stratigraphic data available for them. Ranges of taxa at genus or species level that were not able to be verified in this study have dotted lines.

The Balfour Formation, occurring in the eastern part of the basin, includes the most thoroughly studied DaAZ exposures and therefore was the main focus of this investigation. It is currently divided into the Oudeberg, Daggaboersnek, Barberskrans, Elandsberg, and Palingkloof members (Figure 1). For ease of correlation and for the purpose of describing stratigraphic ranges within this study, the DaAZ has been split into "lower" and "upper" zones. The lower DaAZ is defined by the FADs of *Daptocephalus leoniceps* and *Theriognathus microps* and correlates to the upper Oudeberg Member of the Balfour Formation, and the Teekloof Formation's upper Oukloof and Steenkampsvlakte members. The upper DaAZ correlates approximately with the base of the Barberskrans Member, and terminates at the PTB in the lowermost Palingkloof Member. The upper DaAZ here is defined by the FAD of *Lystrosaurus maccaigi*, which is a maximum of ~ 150 m below the PTB (170 m below the Katberg Formation). Study sites were selected where strata of the DaAZ and underlying CAZ were exposed as well as the overlying *Lystrosaurus* Assemblage Zone (LAZ), or both. Vertical sections were measured and logged with a Jacob's staff and Abney level in the study area. Locations of the field sites are shown in Figure 3 and farm names are listed below:

1). Krugerskraal, Ripplemead, and Doornplaats, Graaff-Reinet District, Eastern Cape Province.

2). Hales Owen and Lower Clifton, Cradock District, Eastern Cape Province.

3). Inhoek, Schalkwykskraal, and van Wyksfontein, Gariep Dam area, Eastern Cape Province.

4). Oukloof Pass in the Beaufort West District, Western Cape Province.

Additional stratigraphic information was retrieved from the following publications: Bethulie, Free State and Lootsberg Pass, Eastern Cape (Botha and Smith, 2006; Botha-Brink et al. 2014; Smith and Botha-Brink, 2014). The combined lithostratigraphic information allowed for the creation of composite sections and for lateral correlation between field sites (Figure 5). There is a significant attenuation of the strata northwards, which was observed by Kitching (1977) in the Gariep Dam area, by Groenewald (1984) in the northern Free State Province (Normandien Formation), and also confirmed in this study.

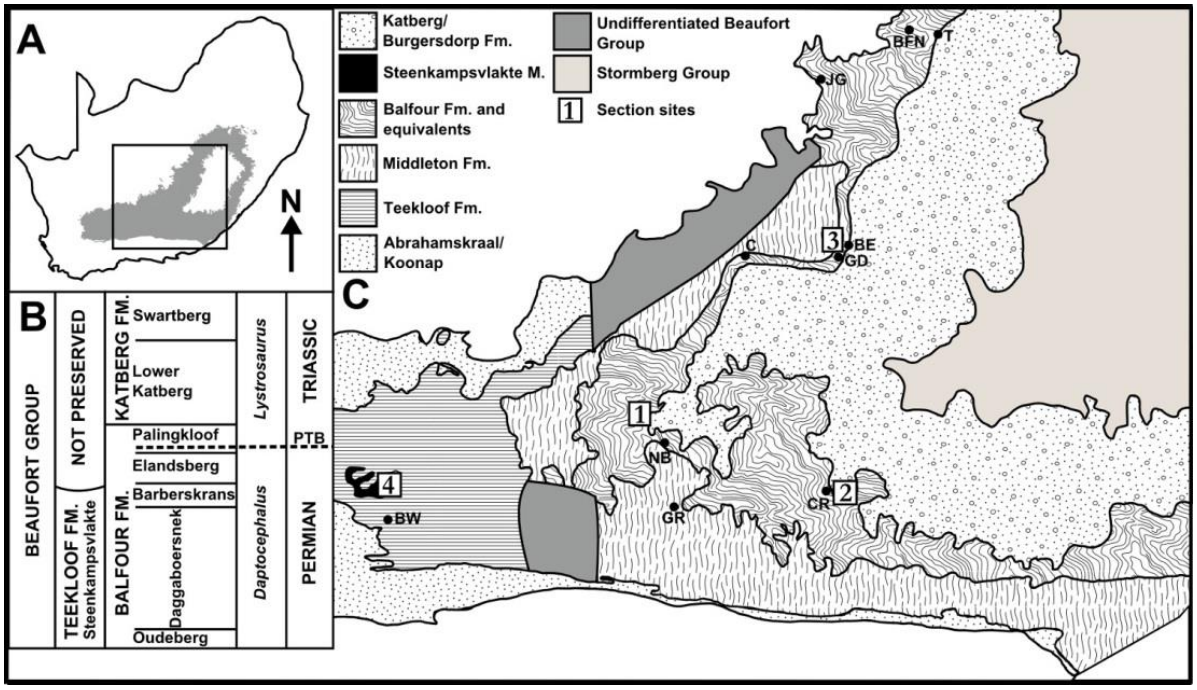

Figure 3: A) South Africa and the position of the Karoo Basin. B) Formal lithostratigraphic subdivisions of strata correlated to the *Daptocephalus* and *Lystrosaurus* assemblage zones. C) Map of the main Karoo Basin of South Africa showing the distribution of strata of the Beaufort and Stormberg groups. Numbered field sites where stratigraphic sections were measured are: 1) Krugerskraal, Ripplemead, and Doornplaats farms, Graaff-Reinet, Eastern Cape Province; 2) Hales Owen and Lower Clifton farms, Cradock, Eastern Cape Province; 3) Inhoek, Schalkwykskraal, and Van Wyksfontein farms, Gariep Dam, Eastern Cape Province; 4) Oukloof Pass, Beaufort West, Western Cape Province. Abbreviations for town names are: Thaba Nchu (T), Bloemfontein (BFN), Bethulie (BE), Gariep Dam (GD), Colesburg (C), Cradock (CR), Nieu Bethesda (NB), Graaff-Reinet (GR), Beaufort West (BW).

2.2 Determining stratigraphic positions of fossils used in this study

Prior to 1976, only farm names and elevations were used by collectors to record fossil localities in the Karoo Basin. As a result the majority of South African fossils in collections today have poor provenance data. Historical specimens from these collections were utilized in this study only if the stratigraphy was well known in the area in which the fossils were found. For such specimens rough locality and stratigraphic positions were assigned using the farm centroids derived from Google Earth (van der Walt et al. 2011). However, much more accurate locality and biostratigraphic information was generated through systematic collecting of tetrapod fossils in the outcrops where detailed stratigraphic sections were logged by PAV (PV) and RMHS (RS). More recently discovered fossils have accurate GPS coordinates and have also been positioned on measured vertical sections, which allows for some species to be assigned a reliable FAD or LAD. A total of 1212 fossils reliably provenanced to the upper CAZ or DaAZ were investigated. They are stored at the following institutions: Evolutionary Studies Institute, University of the Witwatersrand, Johannesburg (BP), Iziko South African Museum, Cape Town (SAM-PK), Rubidge Collection, Wellwood, Graaff-Reinet (RC), Albany Museum, Grahamstown (AM),

Ditsong (Transvaal Museum), Pretoria (TM), National Museum, Bloemfontein (NM), Council for Geoscience (Geological Survey), Pretoria (CGS), Bremner Collection (SAM satellite collection, Graaff-Reinet Museum) (B), RMHS field specimens, not accessioned (RS), specimens collected during doctoral work for PAV (PV), American Museum of Natural History, New York, USA(AMNH), Natural History Museum, London, UK (NHMUK), University of California Museum of Paleontology, Berkeley, USA (UCMP), University Museum of Zoology, Cambridge, UK, (UMZC), and the National Museum of Natural History, Washington, DC, USA, (USNM). A list of the specimens used in this study can be found in the supplementary datasheet.

2.3 Biostratigraphy

Since the last biostratigraphic review of the Beaufort Group (Rubidge et al. 1995) the taxonomy of many DaAZ occurring tetrapods has been revised. Although the dicynodont genera of the DaAZ have been the subject of extensive taxonomic revision the taxonomy of some other vertebrate groups is still in a state of flux, eg. Actinopterygii (Bender, 2001), Temnospondyli (Latimer et al. 2002; Damiani and Rubidge, 2003; Marsicano et al. 2015), Parareptilia (Gow and Rubidge, 1997; Lee, 1997; Jalil and Janvier, 2005; Cisneros et al. 2008), Therocephalia (Huttenlocker et al. 2011), and Gorgonopsia (Gebauer, 2007; Norton, 2012; Kammerer, 2015). Stratigraphic reassessment of all fauna in the DaAZ show the biozone contains 46 other taxa from nine different major vertebrate clades (Figure 2).

To review the stratigraphic range of a fossil taxon three conditions need to be met (Day, 2013b): 1) thorough understanding of the lithostratigraphy throughout the basin; 2) robust taxonomic framework; and 3) re-identification of all relevant specimens in collections based on the most recent taxonomic framework. The first criterion has mostly been met through fieldwork and literature studies, although some fossils found in the Normandien Formation were excluded from consideration because its temporal correlation remains poorly understood. Thus, all DaAZ taxa within temporally constrained strata from the basin were investigated, and the stratigraphic ranges updated from this data pool (Figure 2). Lingering taxonomic confusion associated with some DaAZ species meant that for two groups (Temnospondyli and Gorgonopsia) only the higher-level taxon was considered. Genus or species-level ranges could not be updated for these groups, pending revision. Additionally, difficulty in identifying parareptile specimens to species meant that we measured abundances in this group at higher taxonomic levels (Pareiasauria and Millerettidae). Six hundred and twenty-eight specimens from the DaAZ (477 lower DaAZ, 151 upper DaAZ) met the three criteria and were arranged according to rough stratigraphic position,

new higher taxon name or species where appropriate, and also as fossil taxa abundance pie charts for lower and upper DaAZ (Figure 4).

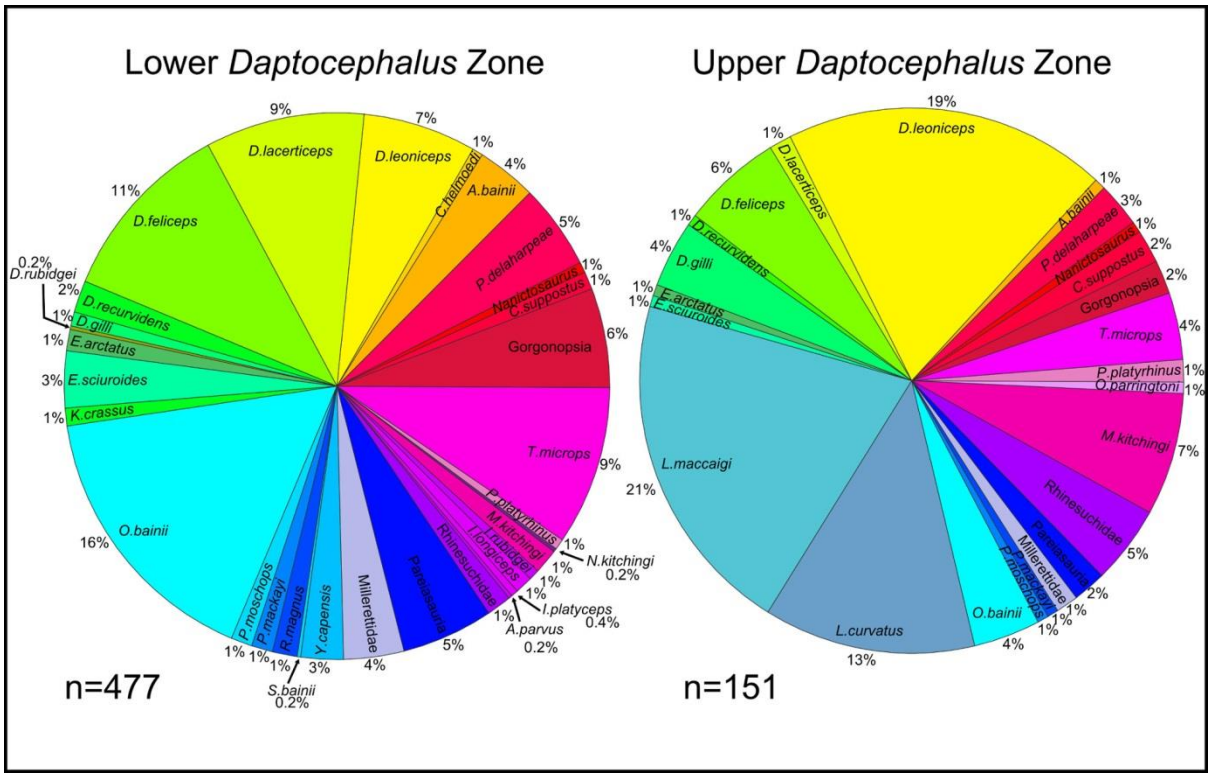

Figure 4: Pie charts representing percentages of different tetrapod taxa occurring in the lower and upper *Daptocephalus* Assemblage Zone. Note the changes in relative abundance in some species (i.e. *Dicynodon lacerticeps*) and also the number of fossil specimens in the lower (477) and upper (151) *Daptocephalus* Assemblage Zone for this study.

Additionally, the following taxa were investigated in further detail to assess their potential utility as DaAZ index fossils: the dicynodonts *Dicynodon lacerticeps*, *Da. leoniceps*, and *L. maccaigi* and the therocephalian *T. microps*, and the cynodont *P. delaharpeae*. Where possible, the FADs and LADs were determined for each species by the lowest and highest occurring specimen in the database with reliable stratigraphic information (Table 1). Because the taxonomic revision of *Dicynodon* is recent (Kammerer et al. 2011) many museum collections databases have not yet been updated and only specimens of *Di. lacerticeps* and *Da. leoniceps* that were directly re-examined by CFK, JF, and KDA were used. The hyper-abundant dicynodont *Diictodon feliceps*, and the PTB crossing therocephalian *Moschorhinus kitchingi* were also investigated in further detail and their updated FADs and LADs were compared to those of the index fossils and also the phased extinctions outlined by Smith and Botha-Brink (2014). The phased extinctions occur between 45–30 m below the PTB (phase 1), 20–0 m below the PTB (phase 2) and 30–45 m above the PTB (phase 3). The ranges of the five potential index taxa were also plotted relative to the local stratigraphy

at the four main study areas and compared to positions of the inferred phased extinctions (Figure 5).

2.4 Rarefaction analysis

An individual rarefaction analysis was conducted to ascertain whether or not the lower species richness of the upper DaAZ in comparison to the lower DaAZ reflects a real decrease in diversity, or a simple sampling bias (see Figure 4). Rarefaction is a common statistical tool used to assess species richness in modern and ancient communities (Erwin, 1990; Tarailo and Fastovsky, 2012; Croft, 2013; Guinot, 2013; Irmis et al. 2013; Oreska et al. 2013; Wilson et al. 2014b; Lindsey and Seymour, 2015; Vila et al. 2015). The analysis uses counts of individuals present in each taxon for two or more samples/localities/faunal horizons. In the present case, faunal horizons (i.e. upper and lower DaAZ) were used, so the analysis asks given the observed numbers of individuals and taxa in each horizon, what would the species richness of the larger sample (lower DaAZ) be if it was represented by the same number of specimens as are available for the smaller sample (upper DaAZ)?

This provides insight into whether the reduced species richness of the upper DaAZ is likely to be real or an artefact of sampling. Specimens and taxa are included for each subzone in the supplementary datasheet. For the data used in the test, only specimens and taxa that definitely were in the lower or upper DaAZ (i.e. only specimens that had lower or upper as their stratigraphic level) were considered. Indeterminate specimens were not included in the analysis, other than Rhinesuchidae indet. Altogether, 477 specimens in the lower DaAZ and 151 in the upper DaAZ were included. There are a total of 48 taxa in the dataset (45 in the lower DaAZ and 28 in the upper, although there is considerable overlap between the subzones). A rarefaction curve, with 95% confidence intervals was plotted for the lower and upper DaAZ datasets for comparison (Figure 6). The rarefaction analysis was carried out in PAST 2.17c (Hammer et al. 2001), which uses the algorithm of Krebs (1989) for individual rarefaction analyses.

3. Results

3.1 Significance of the revised biostratigraphic ranges

The new stratigraphic ranges of potential index fossils for the DaAZ (*Dicynodon lacerticeps*, *Daptocephalus leoniceps*, *Lystrosaurus maccaigi*, *Theriognathus microps*, and *Moschorhinus kitchingi*) along with other co-occurring species and higher taxa (*Aulacephalodon bainii*, *Diictodon feliceps*, *Oudenodon bainii*, *Cynosaurus suppostus*, *Nanictidops kitchingi*, *Nanictosaurus kitchingi*, *Procynosuchus delaharpeae*, Gorgonopsia, Parareptilia, Eureptilia, and Rhinesuchidae) are discussed in Table 1. These results

are then also compared to the traditional range of the DaAZ (see Figures 1 and 2) and also with reference to Smith and Botha-Brink's (2014) phased extinctions hypothesis (Figure 5). Note that for many taxa the metres above lower datum could not be determined due to poor provenance data available from the database.

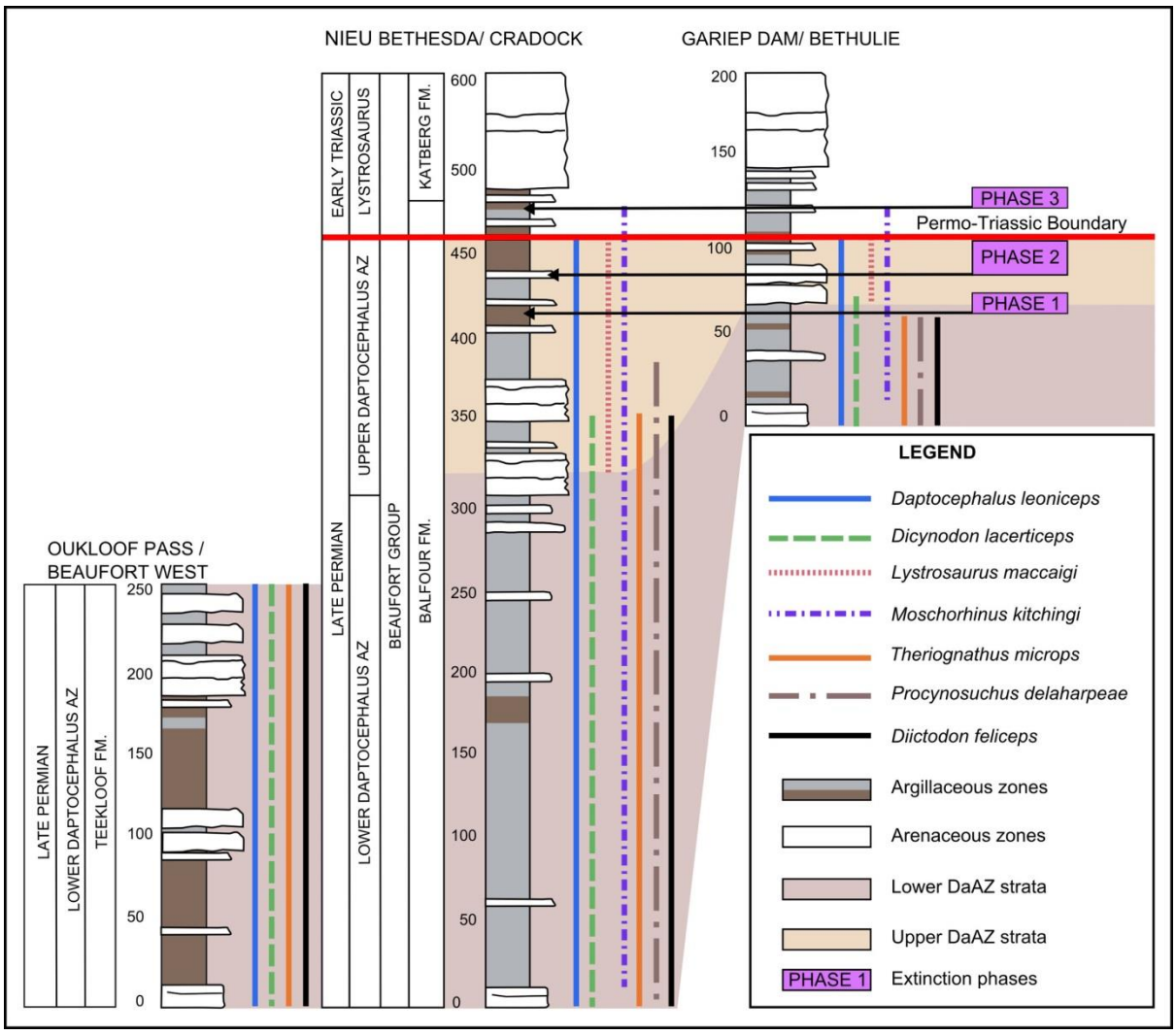

Figure 5: Composite sections showing the stratigraphic succession exposed near Beaufort West, Nieu Bethesda/Cradock, and Gariep Dam/Bethulie. Fossil specimens from the database were assigned a stratigraphic range using GPS positions or from stratigraphic collecting of fossils from Smith and Botha-Brink (2014), and from the current study. This allowed for a relatively accurate range determinates for *Daptocephalus leoniceps*, *Dicynodon lacerticeps*, *Lystrosaurus maccaigi*, *Moschorhinus kitchingi*, *Theriognathus microps*, *Procynosuchus delaharpeae*, and *Diictodon feliceps*. Strata assigned to lower and upper *Daptocephalus* Assemblage Zone have been highlighted with the current position of Smith and Botha-Brink's (2014) extinction phases on their Bethulie section. Note the attenuation of the stratigraphic units northwards (i.e. towards Gariep Dam/Bethulie) and the LADs of *Di. lacerticeps*, *T. microps*, *P. delaharpeae*, and *D. feliceps*.

Dicynodontia

Many of the dicynodont species in the DaAZ have long stratigraphic ranges and therefore were not considered useful as index fossils (see Figure 2). Nevertheless there were some surprises in

this group. Database information shows that *Dicynodon lacerticeps* occurs in the CAZ and is assumed to range throughout the biozone until a reliable FAD is determined (Table 1).

Table 1	FAD specimen	FAD position	LAD specimen	LAD position	Above lower datum (m)	Distance from PTB (m)
Dicynodontia						
Aulacephalodon bainii	PV/GD6	*Cistecephalus* AZ	RS 52	Upper DaAZ	131	−20
Daptocephalus leoniceps	RC 602	Lower DaAZ	SAM-PK-K10093	Upper DaAZ	Unknown	−10
Dicynodon lacerticeps	CGS WB 222 (CGP/1/479)	*Cistecephalus* AZ	SAM-PK-K9949	Upper DaAZ	Unknown	−25
Diictodon feliceps	Below DaAZ	*Tapinocephalus* AZ	RS 94	Upper DaAZ	Unknown	−105
Lystrosaurus curvatus	RS 92	Upper DaAZ	SAM-PK-K11045	*Lystrosaurus* AZ	64	+25
Lystrosaurus maccaigi	SAM-PK-10920	Upper DaAZ	SAM-PK-K10376	Upper DaAZ	148	−2
Oudenodon bainii	PV/GD5	*Cistecephalus* AZ	PV/GD19	Upper DaAZ	40	−3
Therocephalia						
Moschorhinus kitchingi	BP/1/2205	Lower DaAZ	SAM-PK-K10698	*Lystrosaurus* AZ	Unknown	+29
Theriognathus microps	SAM-PK-10981	Lower DaAZ	SAM-PK-K10505	Upper DaAZ	224	−96
Gorgonopsia						
Gorgonopsia	Below DaAZ	*Tapinocephalus* AZ	RS 19	Upper DaAZ	Unknown	−27
Cynodontia						
Cynosaurus suppostus	SAM-PK-05211	*Cistecephalus* AZ	BPI/1/5741	Upper DaAZ	Unknown	Unknown
Nanictosaurus kitchingi	RC 48	Lower DaAZ	TM 279	Upper DaAZ	Unknown	Unknown
Procynosuchus delaharpeae	SAM-PK-10138	*Tropidostoma* AZ	SAM-PK-K8142	Upper DaAZ	Unknown	−86
Parareptilia						
Parareptilia	SAM-PK-004020	*Tropidostoma* AZ	RS 12	Upper DaAZ	Unknown	−24
Eureptilia						
Youngina capensis	SAM-PK-K7710	*Tropidostoma* AZ	SAM-PK-K11289	Lower DaAZ	Unknown	−279
Temnospondyli						
Rhinesuchidae	Below DaAZ	*Tapinocephalus* AZ	SAM-PK-10506	Upper DaAZ	Unknown	−6

Table 1: FAD and LAD specimens for taxa investigated for stratigraphic utility in the *Daptocephalus* Assemblage Zone. Note that for many taxa poor stratigraphic data does not allow for calculation of range in metres above lower datum.

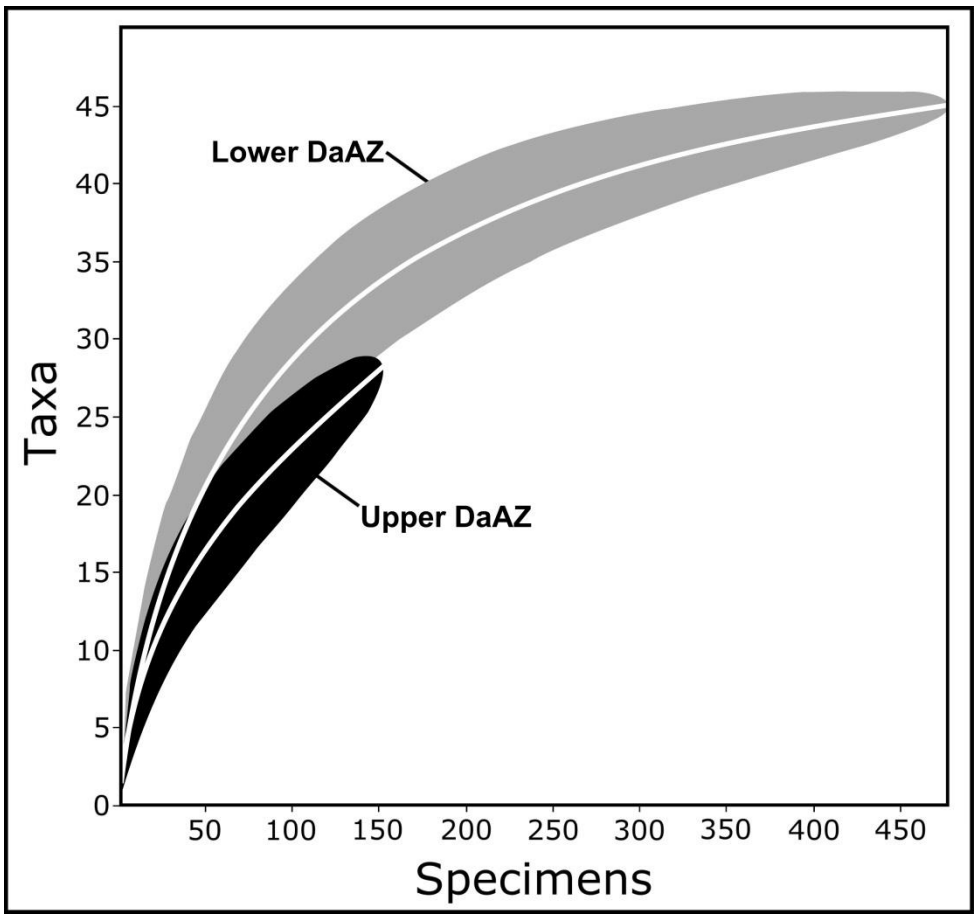

Figure 6: Individual rarefaction curves, with 95% confidence intervals for the lower and upper *Daptocephalus* Assemblage Zone. See text for more information.

Additionally *Dicynodon lacerticeps* does not range through the entire DaAZ because the LAD specimen is from 25 m below the PTB. This means it is only 5 m into the upper DaAZ due to the attenuation of the strata at the site of its collection, which is Bethel Canyon in the Free State Province (see Figure 5).

The FAD of *Daptocephalus leoniceps* is RC 602 a specimen that was located in the current upper CAZ. Therefore the lower boundary of the DaAZ had to be lowered. Since this specimen had poor stratigraphic data, at this stage the lower boundary is defined by the FAD of a reliably sourced *T. microps* specimen from Osfontein, Graaff-Reinet (See Table 1). *Daptocephalus leoniceps* is consistently present throughout the DaAZ and its LAD in the database is a stratigraphically well-defined specimen from Carlton Heights in the Eastern Cape Province. This specimen was collected 10 m below the PTB, which fits with Smith and Botha-Brink's (2014) observation that *Da. leoniceps* is involved in their phase 2 extinction.

Although not a biozone index fossil, *Aulacephalodon bainii* is a species which is ubiquitous in the CAZ and lower DaAZ, but is essentially absent from the upper DaAZ. The highest specimen with reliable stratigraphic data comes from Bethel Canyon and ~ 16 m into the upper DaAZ, although in this part of the basin attenuation must be taken into account (See Figure 5). *Diictodon feliceps* is frequently encountered in the lower biozones, but does not range far into the upper DaAZ (Figures 2 and 5), particularly in the Nieu Bethesda area. The LAD specimen is only 45 m into the upper DaAZ (~105 m from the PTB). This is 60 m below the beginning of Smith and Botha's (2014) extinction phase 1 (see Figure 5).

The FAD of *Lystrosaurus maccaigi* marks the beginning of the upper DaAZ. The FAD of *Lystrosaurus maccaigi* was previously documented as ~ 30 m below the PTB (Smith and Botha, 2007) from specimens collected close to or within the Bethulie section (RS 37, RS 40, RS 41, RS 48, RS 49, and SAM-PK-K9958 in database). More recently Botha-Brink et al. (2014) recorded their stratigraphically lowest *L. maccaigi* specimen (NMQR 3706) at 33 m below the PTB on Nooitgedacht 68 farm near the Bethulie section. However the FAD within the Graaff-Reinet area is ~150 m from the PTB (See Table 1). The stratigraphically highest *L. maccaigi* specimen in the current dataset is SAM-PK-K10376 which is recorded as 2 m below the PTB. Similarly Botha-Brink et al.'s (2014) LAD of *L. maccaigi* is ~ 1.5 m below the PTB. This study has revealed significant attenuation of the strata in this area so the stratigraphic positions of these specimens may require reinvestigation. *Lystrosaurus curvatus* has been documented previously as occurring between 8 m below and 30 m above the PTB (Botha and Smith, 2007; Smith and Botha-Brink, 2014), and our study is consistent with this result. At this stage *Lystrosaurus curvatus* is the only

Lystrosaurus species in the Karoo Basin that is present in both the Permian and Triassic (Botha and Smith, 2007), although *Lystrosaurus maccaigi* is also known from the earliest Triassic strata in Antarctica (Cosgriff et al. 1982; Collinson et al. 2006).

Therocephalia

Theriognathus microps is currently a DiAZ biozone indicator fossil but this study has identified that it also occurs also in strata currently assigned to the upper CAZ. The FAD specimen is from Osfontein farm, Graaff-Reinet (Table 1) and therefore the base of the new DaAZ is defined by the FAD of *T. microps* in co-occurrence with *Da. leoniceps* (see Figures 1 and 2). The LAD specimen with reliable stratigraphic is from 96 m below the PTB. This suggests that *T. microps* goes extinct below the extinction phase 1, which lies between 45–30 m below the PTB in the Gariep Dam/Bethulie area (Smith and Botha-Brink, 2014) (Figure 5).

Moschorhinus kitchingi has potential to serve as a useful index fossil in association with *Daptocephalus leoniceps*. However none of the lower DAZ specimens have reliable stratigraphic data which means the species distribution through the entire DAZ cannot be proven at this stage. According to Smith and Botha's (2014) observations, this species' LAD is within their phase 3 extinction event. The only reliable specimen from the Triassic is SAM-PK-K10698 and this specimen was located at ~ 29 m above the PTB, corroborating this observation.

Gorgonopsia

The Gorgonopsia comprise a large component of the latest Permian faunal assemblages (Smith et al. 2012), but their current taxonomy is highly confused. Therefore we did not attempt to reconstruct their ranges at the genus or species level. Smith and Botha-Brink (2014) recognized that all gorgonopsians go extinct within their extinction phases 1 and 2, but given the unreliability of the available identifications, any attempt to infer the extinction horizon of a particular gorgonopsian species would be speculative at this time. The LAD gorgonopsian in the database was located from Old Lootsberg Pass near Graaff-Reinet and 27 m below the PTB, therefore corroborating Smith and Botha-Brink's (2014) results (see Table 1).

Cynodontia

Three cynodont species are present in the DaAZ (Figure 2) but few specimens and little stratigraphic data means their ranges are not well constrained (Table 1). *Procynosuchus delaharpeae* is the only cynodont from the DaAZ to satisfy most of our criteria as there are 33 specimens available in the consulted collections. Huttenlocker et al. (2011) reported the presence of *P. delaharpeae* in the upper CAZ, and this is supported by work conducted by Botha-Brink and

Abdala (2008) who described SAM-PK-10138, a single specimen from the *Tropidostoma* Assemblage Zone (TAZ), Beaufort West. Accordingly *P. delaharpeae* is no longer regarded as a useful index fossil for the DaAZ. The LAD specimen was located 86 m below the PTB, below the phased extinction range of Smith and Botha-Brink (2014) (Table 1).

Parareptilia

The majority of the parareptiles are not unique to the DaAZ with many species first appearing as early as the TAZ (*Pareiasuchus peringueyi*, *Pareiasuchus nasicornis*, *Pareiasaurus serridens*, *Anthodon sp. Milleretta rubidgei*, *Millerosaurus nuffieldi*) and CAZ (*Nanoparia pricei*, *Owenetta rubidgei*). Only one procolophonoid (*Spondylolestes rubidgei*) and three pareiasaur specimens are known from the upper DaAZ. The uppermost pareiasaur specimen occurs 24 m below the PTB which fits with the extinction of pareiasaurs in Smith and Botha's (2014) extinction phase 2 (Table 1). The specimen is currently identified as *P. serridens* in the database, likely due to its size, but it consists of only a femur. This element is not diagnostic to the species level, so the femur could also represent *P. nasicornis*, *P. peringueyi*, or *Anthodon sp*. The uppermost *Anthodon sp.* in the database is SAM-PK-7841, which is approximately 109 m from the PTB from Zuurplaats farm near Nieu Bethesda in the Eastern Cape. *Nanoparia pricei* has one specimen in the database with a reliable stratigraphic position (SAM-PK-K10498), but this specimen comes from Beaufort West where only the lower DaAZ is known to be present. Therefore the LAD of this species is regarded as the uppermost lower DaAZ until further information can be gathered.

Eureptilia

Youngina capensis is not unique to the DaAZ and has also been found in the *Tropidostoma* and *Cistecephalus* assemblage zones (Smith and Evans, 1996). The apparent LAD of this species in the lower DaAZ is SAM-PK-K11289, a juvenile aggregation in a nodule from 279 m below the PTB (~129 m from upper DaAZ), found at Osfontein farm near Graaff-Reinet in the Eastern Cape.

Temnospondyli

Two species of temnospondyl amphibians (*Rhinesuchus muchos* and *Laccocephalus insperatus*) were known from the DaAZ at the time of the revision of the Karoo biostratigraphy by Rubidge et al. (1995). Subsequent taxonomic revisions (Latimer et al. 2002; Damiani and Rubidge, 2003; Marsicano et al. 2015) have revealed an updated list of DaAZ temnospondyls (including *Laccocephalus watsoni*, *Rhinesuchus capensis*, *Rhinesuchus waitsi*, and *Uranocentrodon senekalensis*) but the collections database has not yet been updated to reflect these changes. Therefore, the higher taxon Rhinesuchidae was used to represent all Late Permian temnospondyls in this study (Figure

2, Table 1). The uppermost DaAZ specimen from the database is from 6 m below the PTB and was found on Pienaarsbaken farm near Graaff-Reinet (SAM-PK-10506). Smith and Botha-Brink (2014) indicate from their study that *Rhinesuchus* sp. went extinct in extinction phase 2. Additionally Smith and Botha-Brink (2014) indicate *U. senekalensis* disappears in extinction phase 1, but with only one informally identified *U. senekalensis* specimen in the database (SAM-PK-10574), this is difficult to corroborate in our study. Furthermore, rhinesuchids are not restricted to the DaAZ because the clade is first known in the middle Permian in the Karoo Basin, and one taxon (*Broomistega putterilli*) occurs in the early Triassic LAZ (Shishkin and Rubidge, 2000). Revised identifications of the rhinesuchid specimens in collections will be necessary before we can comment on their ranges and potential roles in the Permo-Triassic extinction phases.

3.2 Lower versus upper *Daptocephalus* Assemblage Zone trophic structure

This investigation using 628 stratigraphically provenanced tetrapod fossil specimens revealed a distinct change in number of fossil specimens found in the lower (477 specimens) and upper (151 specimens) DaAZ (Figure 4). However, the disparity in numbers of specimens between lower and upper DaAZ does not seem to reflect a fundamental change in community structure leading up to the PTB. This means that the decrease in diversity as a result of the PTME was over a very short time interval, which is what has been outlined by previous workers (Smith and Botha-Brink, 2014).

The rarefaction analysis calculated an estimated richness for the lower DaAZ at around 33.8 for 150 specimens, with a 95% confidence interval that spans 29.3 -38.3. The upper DaAZ richness is estimated to be 27.9 species with a confidence interval of 27.3 - 28.5. Although the confidence intervals fail to overlap by a small amount at this sample size, these results still suggest that the upper DaAZ is not significantly less diverse than we would expect if its observed richness was simply an artefact of sampling. The rarefaction curves bear this out as well (see Figure 6); the upper DaAZ does not level off much and the confidence intervals for the two faunas mostly overlap for nearly all of their ranges. Based on these results, we cannot strongly reject the hypothesis that the lower richness of the upper DaAZ is based on the smaller sample size available for this portion of the assemblage zone. Therefore caution must be taken in how much the apparent lower diversity in upper DaAZ as a whole is interpreted.

4. Discussion

The index fossils, whose concurrent ranges are presently used to define the base of the DiAZ, *Dicynodon lacerticeps*, *Theriognathus microps* and *Procynosuchus delaharpeae* (Rubidge et al. 1995), are

considered to be present in strata currently within the CAZ due to their co-occurrence with *Cistecephalus microrhinus* in the Oudeberg Member. In addition *P. delaharpeae* is now confirmed to occur within the TAZ (Botha-Brink and Abdala, 2008). Together, these observations indicate that the current definition of the DiAZ is problematic. Therefore we propose redefining the base of the biozone and assign *Daptocephalus leoniceps* (Kammerer et al. 2011) as the index fossil. Kitching (1977) used *Da. leoniceps* as the index fossil for the original manifestation of the biozone (called the *Daptocephalus* Zone in that paper), which was only renamed *Dicynodon* Assemblage Zone by Keyser and Smith (1979b) because of the assumed synonymy of *Daptocephalus* with *Dicynodon* (Cluver and Hotton, 1981). Now that *Daptocephalus* has been resurrected by Kammerer et al. (2011), the original name of this unit should be restored. Furthermore, this taxon ranges well into the proposed DaAZ, unlike *Dicynodon lacerticeps*. We also recognize the subdivision of the DaAZ into lower and upper subzones, with the upper subzone being defined by the FAD of *Lystrosaurus maccaigi*. In this framework the base of the lower DaAZ would be defined by the FAD of *Da. leoniceps* and *Theriognathus microps* and the base of the upper DaAZ be defined by the FAD of *Lystrosaurus maccaigi*. The LAD of *Da. leoniceps* and *L. maccagi* (and the boundary of the DaAZ) is within Smith and Botha-Brink's (2014) phase 2 extinction approximately at their stratigraphically defined PTB (Figure 1).

4.1 Implications for Biostratigraphic Correlation

Previously interbasinal biostratigraphic correlations have been made using poorly provenanced specimens and poorly defined taxa. Taxonomic revision often reveals that the best index fossils have limited geographic distributions, which calls into question many previous correlations (e.g. Angielczyk and Kurkin 2003a; Angielczyk et al. 2014a). Kammerer et al. (2011) indicated that *Dicynodon* sensu lato should no longer be considered a useful correlation tool because even though most of the species previously assigned to this genus are closely related, most of them represent basinal endemics and may vary significantly in their temporal ranges. Therefore even if they are useful index fossils in the Karoo, they are not useful for biostratigraphic correlation beyond this basin. One exception is the dicynodontoid *Euptychognathus bathyrhynchus* (Kammerer et al. 2011), but this species is known from very few specimens and this extreme rarity does not make it an ideal biostratigraphic tool for correlation. Similar faunal compositions have also been described from the Guodikeng Formation in China where the dicynodontoid *Jimusaria sinkianensis* co-occurs with *Lystrosaurus* much like in the upper DaAZ (Metcalfe et al. 2001; Cao et al. 2008). Additionally the Russian Sokolki fauna may be another coeval deposit outside of the Karoo Basin, but again the temporal distribution of Russian dicynodontoids (*Delectosaurus arefjevi*, *Peramodon amalitzkii*, and *Vivaxosaurus trautscholdi*) may not be the same as *Dicynodon lacerticeps* or

Daptocephalus leoniceps. *Lystrosaurus maccaigi* has been described in Antarctica (Cosgriff et al. 1982) however, the only known specimen from Shenk Peak in Antarctica (AMNH 9509), is from earliest Triassic lower Fremouw Formation (Cosgriff et al. 1982; Collinson et al. 2006), suggesting the taxon may have persisted longer than previously thought.

4.2 Faunal turnovers in the latest Permian Karoo Basin

The base of the DAZ has been dated close to 255.22 ± 0.16 Ma (Rubidge et al. 2013). Bearing in mind that dates from the Global stratotype section at Meishan China define an end-Permian extinction interval of 251.941 ± 0.037 and 251.880 ± 0.031 Ma (60–48 ky) (Burgess et al. 2014), this means the temporal range of the DaAZ encompasses ~ 3 Ma. This is a significant amount of time for climatic and other environmental changes to occur, and concomitant changes in the populations of terrestrial tetrapods would be an expected outcome. Smith and Botha-Brink's (2014) phased extinctions span a 70 m stratigraphic interval, which they suggested represent about 120 000 y. If this estimate is correct then the most significant faunal and environmental changes appear to have occurred only in the uppermost DaAZ and perhaps just prior to the onset of the global end-Permian mass extinction event.

Recently the first high precision age of 253.48 ± 0.15 Ma (early Changhsingian) has been retrieved from strata close to the inferred PTB in South Africa from zircons in a silicified ash layer on Old Lootsberg Pass (Gastaldo et al. 2015). The authors also report on an apparent Permian dicynodontoid skull preserved in strata defined as earliest Triassic due to its presence in an intraformational conglomerate lag. The authors suggest this is evidence for the PTB and *Daptocephalus-Lystrosaurus* Assemblage Zone boundary being stratigraphically higher than is currently reported by the disappearance of taxa in the phased extinctions of Smith and Botha-Brink (2014). However, ash layers in the Beaufort Group often show evidence for significant reworking (Rubidge et al. 2013; McKay et al. 2015), and intraformational conglomerates are common in the upper DaAZ strata (Smith, 1995). Therefore the placement of the PTB by Gastaldo et al. (2015) is potentially questionable. Furthermore, the specimen in question is poorly preserved and due to its preservation within a conglomeritic lag this is not surprising as these deposits formed by the reworking of floodplain sediments (Smith, 1995; Viglietti et al. 2013; Smith and Botha-Brink, 2014). The specimen's poor preservation means any diagnostic affinity with *Dicynodon lacerticeps*, *Daptocephalus leoniceps*, or *Lystrosaurus maccaigi* is speculative. The preserved features of the specimen could also identify the specimen as the two Triassic *Lystrosaurus* species (*Lystrosaurus declivis* and *Lystrosaurus murrayi*), or *Lystrosaurus curvatus* which is known from latest Permian and earliest Triassic strata. Additionally it is now evident that

Lystrosaurus maccaigi survives the end-Permian mass extinction event in Antarctica (Cosgriff et al. 1982; Collinson et al. 2006) which means there is the possibility that *L. maccaigi* may have survived in the Karoo Basin as well. Consequently this data does not necessitate moving the current position of the PTB at this stage, or the boundary of the *Daptocephalus* and *Lystrosaurus* Assemblage Zones in the main Karoo Basin.

Our study has identified that the stratigraphic placement of Smith and Botha-Brink's (2014) phased extinctions mostly fits with the LADs of taxa in the DaAZ. However the stratigraphic succession in the south (Nieu Bethesda/Cradock sector), is much thicker than in the north (Gariep Dam/Bethulie sector), indicating great attenuation of the strata north of the Orange River. This is corroborated by the LADs of Di. lacerticeps, T. microps, P. delaharpeae, and D. feliceps occurring apparently lower than the extinction phases. This evidence suggests that the placement of the extinction phases may need to be reconsidered in the south where the Upper Permian lithostratigraphy has not been so greatly affected by attenuation. This does not mean that the time represented by the extinction phases will need to be reconsidered because thinning in the north has likely been due to increased hiatuses.

Conclusions

This study updates the stratigraphic ranges of Late Permian tetrapod fauna from the Karoo Basin, proposes a new biostratigraphic scheme (*Daptocephalus* Assemblage Zone), and provides the following conclusions.

The current manifestation of the *Dicynodon* Assemblage Zone (DiAZ) is problematic because the three index fossils currently used to define the DiAZ, *Dicynodon lacerticeps*, *Theriognathus Microps*, and *Procynosuchus delaharpeae*, have FADs below the traditionally recognized lower boundary. Therefore we redefine the assemblage zone by replacing the DiAZ with the *Daptocephalus* Assemblage Zone (DaAZ) where *Daptocephalus leoniceps* is reinstated as the index taxon for the DaAZ in co-occurrence with *T. microps*. We use the FAD of *Da. leoniceps* and *T. microps* to define the base of the DaAZ which incorporates strata previously defined as the uppermost *Cistecephalus* Assemblage Zone. It is further recommended that an informal two-fold lower and upper DaAZ subdivision be instated to reflect the appearance of *Lystrosaurus maccaigi* in the upper part of the zone only.

Dicynodon sensu lato has been used in the past to correlate various Karoo-aged basins within the Platbergian land vertebrate faunachron (LVF) yet it is now apparent it is unable to define a time unit finer than the Lopingian. This means Dicynodon sensu lato and the other South African

dicynodontoids have little biostratigraphic utility outside of the Karoo Basin at this stage because at this time they are not known to be present in other basins, are known from very few specimens (*Euptychognathus bathyrhynchus*), and vary significantly in their temporal ranges. *Daptocephalus leoniceps* in co-occurrence with *L. maccaigi* may provide correlation with Late Permian deposits in China (Guodikeng Formation) and the Sokolki fauna of Russia but further investigation is required. *Lystrosaurus maccaigi* on its own is not a useful correlation tool due to its survival into the early Triassic in Antarctica.

The more precisely determined stratigraphic ranges of all later Permian tetrapods do not reveal a significant change in faunal abundance between the lower and upper DaAZ which implies diversity drops attributed to the end-Permian mass extinction event were rapid and only occurring within the uppermost DaAZ. However the stratigraphic succession in the south (Nieu Bethesda/Cradock sector), is much thicker than in the north (Gariep Dam/ Bethulie sector), indicating great attenuation of the strata north of the Orange River. This is corroborated by the LADs of *Di. lacerticeps*, *T. microps*, *P. delaharpeae*, and *D. feliceps* occurring apparently lower than the extinction phases. Therefore it is further proposed that the position of the extinction phases be reconsidered in the south where the Late Permian lithostratigraphy has not been affected by attenuation to fit with the disappearances of, *Di. lacerticeps*, *T. microps*, *P. delaharpeae*, and *D. feliceps* in this interval.

Acknowledgements

This work was made possible by financial support to PAV and BSR from the Palaeontological Scientific Trust (PAST) and its Scatterlings of Africa programmes, as well as the National Research Foundation (NRF) ((AOGR)UID¼826103). The support of the DST/ NRF Centre of Excellence in Palaeosciences (CoE in Palaeosciences) towards this research is hereby acknowledged. CFK acknowledges the support of the Deutsche Forschungsgemeinschaft (Eigene Stelle KA 4133/1-1) and he and JF also acknowledge support from the Alexander von Humboldt Foundation (Sofja Kovalevskaja Award to JF). We thank Fernando Abdala, Luke Norton, and Adam Huttenlocker for invaluable discussions on the taxonomy and distribution of Late Permian Cynodontia, Gorgonopsia, and Therocephalia. Fossil finds by Jennifer Botha-Brink, Michael Day, Marc Van Den Brandt, Mike Strong, Derik Wolvaardt, and Ian Woods during fieldtrips contributed information to this study. We are grateful to Patrick Eriksson, Jennifer Botha-Brink, and Christian Sidor for valuable comments on the original manuscript.

3.4 Palaeocurrent investigation

Palaeocurrent vectors measured from strata of the Oudeberg, Ripplemead (RM), and Javanerskop members, the Boomplaas sandstone (BS), the Musgrave Grit unit, and Katberg Formation from the field sites are presented here as rose diagrams at both the formation and member level. Appendix 2 shows all raw palaeocurrent data collected from the vertical section sites. Palaeocurrent data was collected along distinct horizons either along a single upper surface or laterally along a cliff face (eg. Barberskrans Cliffs along cliff face or Ripplemead farm along upper surface). Composite sections from the field sites are then used to provide stratigraphic context for the palaeocurrent vectors later in the Chapter 5.4. All the data showed unidirectional flow, which is typical of continental fluvial deposits since aeolian and tidal deposits will show unimodal, bimodal and even polymodal current vectors (Boggs Jr, 2006). These data are presented in Figure 3.30 however subtle differences between the study sites were identified and are briefly discussed. Raw data for palaeocurrents is shown in Appendix 2 (see disc).

3.4.1 Cradock

At the Barberskrans Cliffs (section 1A) along a 450 m long road cutting a total of 134 palaeocurrent vectors were collected in the Oudeberg Member (Figure 3.30). The palaeocurrent data show a strong northeasterly (NE) direction (see Figure 3.30 and Appendix 2). The mean current vector for the type locality is ~32.30° (Figure 3.30). The Ripplemead member which is exposed on Hales Owen farm (seciont 1B) yielded a total 54 vectors. The vectors show a significantly different mean direction to the vectors from the unit at the Barberskrans Cliffs, supporting that they are different lithostratigraphic units (Figure 3.30). The mean direction is approximately ~324° but a four range from 280°-322°and two between 35°-38° respectively (Figure 3.30 and Appendix 2).

At Lower Clifton farm (section 2) in the Baviaansrivier Valley, palaeocurrent vectors were taken from the RM and also the Katberg Formation since there is good outcrop of both sandstone units at this site (Figure 3.30 and Appendix 2). Eighty vectors were obtained from the RM, mostly from rib and furrow features but some exposed trough crossbeds were also used along the same surface. These data were also to the NW, but with a slightly more westward inclination (average vector 290°). A total of eight vectors were to the NE (40°-48°) but these were the vectors taken from trough crossbeds and may be less reliable indicators (Miall, 1996). The Katberg Formation was better exposed in the area and 80 vectors were obtained from rib and furrow features (Appendix 2). These vectors showed a unimodal NE direction with an average direction of 57°.

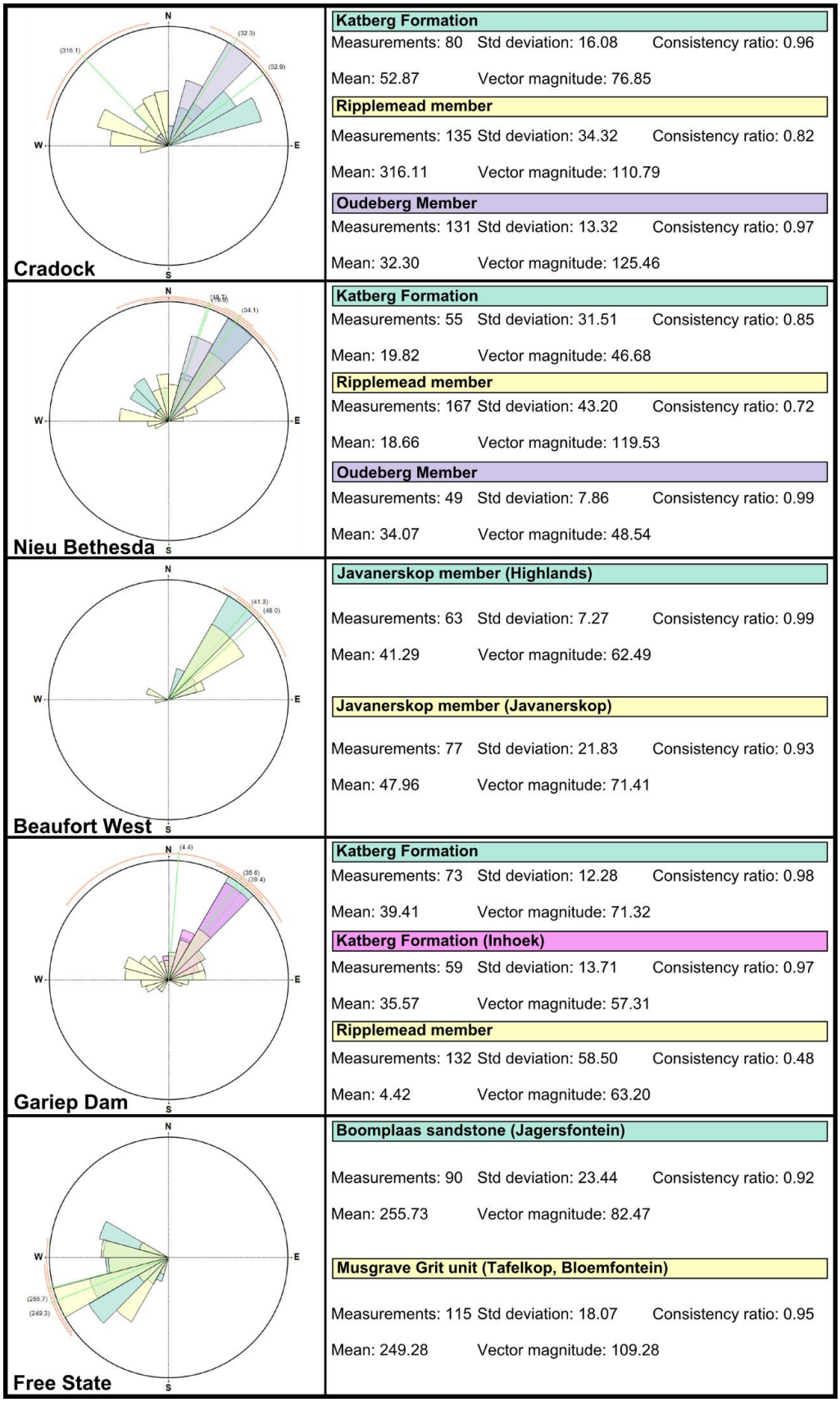

Figure 3.30: Rose diagrams with vector mean azimuths and stastitical data of sandstones studied in the field study area. This includes the Oudeberg, Ripplemead, and Javanerskop members, Boomplaas sandstone, Musgrave Grit unit, and the Katberg Formation. See Appendix 2 for more information on raw palaeocurrent data.

3.4.2 Nieu Bethesda

The RM on the top of Platberg on Doornplaats farm (section 3) yielded 49 vectors with a dominant NE direction (average palaeocurrent reading ~ 32°) (Figure 3.30 and Appendix 2). The distribution was slightly bimodal with another smaller population of NW orientation (312°-358°) (Appendix 2). On the Krugerskraal farm site (section 4) the RM yielded 63 readings which showed bimodal and different readings than elsewhere for this unit in Nieu Bethesda. Over half the readings showed a WNW direction (average 295°) and the rest a NE direction (average 48°).

The RM on Ripplemead farm yielded 54 readings (Appendix 2). The vectors are mainly unimodal and the average reading is ~40° (NE) although 21 readings range to the NNE (22°-35°) and NNW (308°-360°). The Katberg Formation on Ripplemead farm yielded 52 readings toward the NE (30°-40°) although 14 were to the NW (340°-350°) (Figure 3.30 and Appendix 2). Vectors were also taken from the Oudeberg Member on Oudeberg Pass as a means for comparison to the Oudeberg Member identified at the Barberskrans Cliffs in Cradock (section 1A). On the pass a total of 56 readings were measured and indicate a unimodal NE direction, with an average reading of approximately 35° (Figure 3.30 and Appendix 2).

3.4.3 Beaufort West

The Javanerskop member yielded a total of 65 palaeocurrent readings from section 6 (Highlands farm) and 80 from section 7 (Javanerskop) from rib and furrow features and trough crossbedding. Dominantly unimodal NE readings were obtained with an average of 41°and 58° obtained for this unit from section 6 and 7 respectively.

3.4.4 Gariep Dam

The RM on van Wyksfontein yielded 123 readings (Figure 3.30 and Appendix 2). The data yielded mostly unimodal NW palaeocurrent directions (average direction 302°-303°) which are different to the rest of the field sites in the Gariep Dam area. On Inhoek farm (section 9) 59 readings from the RM showed slight bimodality with 40 readings indicating a NE direction (average 50°) and 19 a NW direction (average 310°) (Appendix 2). The Katberg Formation identified on section 9 shows a mean palaeocurrent direction of 35.47° which is similar to readings collected from the Katberg Formation on Schalkwyskraal (section 10) and Tierhoek (section 11) which is 39.41° (Figure 3.30). At section 10 and 11 a total of 70 measurements indicated bimodal palaeocurrent directions with average reading toward NW (280°) and NE (66°) for sections 10 and 11 respectively (Appendix 2).

3.4.5 Jagersfontein and Bloemfontein

The BS on Boomplaas Hill (section 12) yielded 90 readings with a mean of 255.73°. This indicates a SW direction although, 28 readings did indicate a slight NW direction (282°-300°) (Figure 3.30 and Appendix 2). The Musgrave Grit unit on section 13 yielded 115 readings and mean of 249. 28° and this indicates a dominantly southwesterly palaeocurrent direction (SW).

Section 3.4.6: Summary

Palaeocurrent vectors collected during this study are plotted onto the field site map (Figure 3.31). Dominantly unimodal NE vectors are observed in the Oudeberg, RM, and Javanerskop members, and Katberg Formation (Figures 3.30 and 3.31). In the latter, similar vectors are observed throughout the field sites. Interestingly, the palaeocurrent directions of the RM sandstones show some variation. In Cradock, they are dominantly NW, Nieu Bethesda NE, and in Gariep Dam a combination of NW and NE vectors were observed. The vectors collected at Jagersfontein and at Bloemfontein in the Musgrave Grit unit show SW current directions. Vectors obtained during this study were also often different from those obtained by previous workers (Cole and Wipplinger, 2001) however no information on formation or stratigraphic positon of the data is provided by these authors.

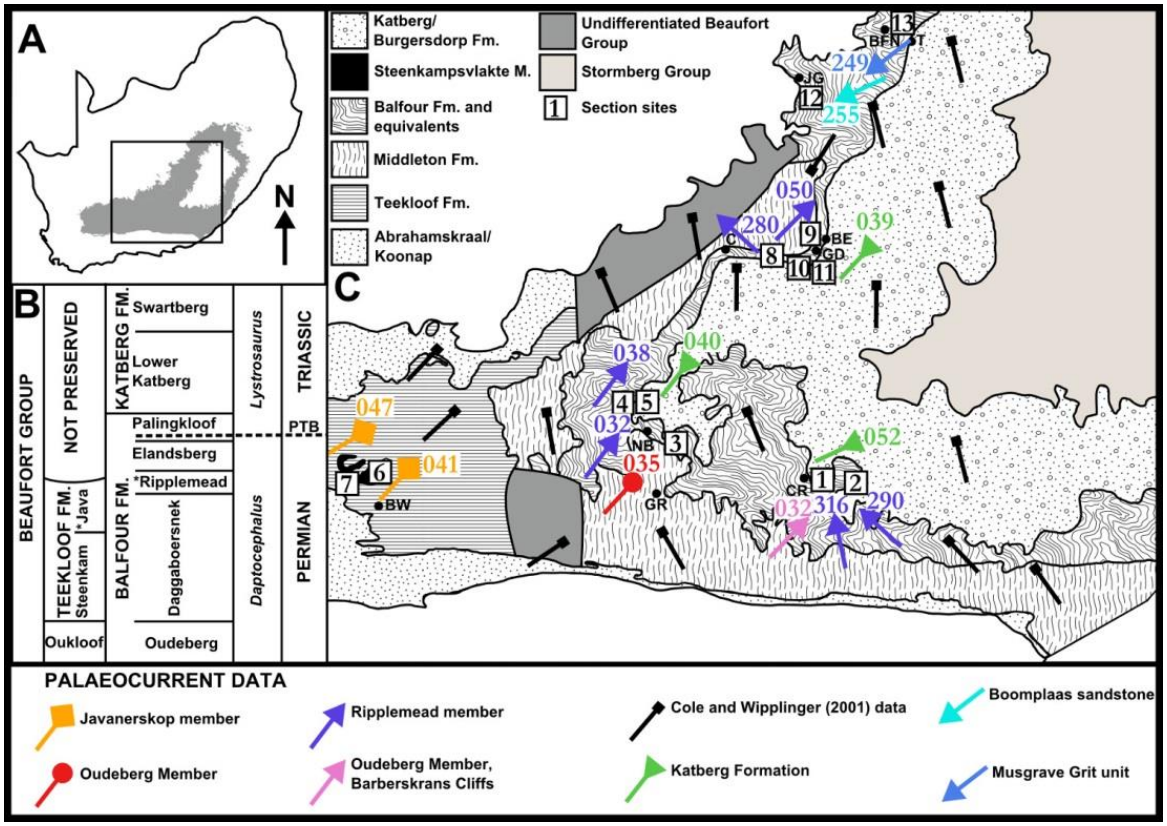

Figure 3.31: Mean palaeocurrent vectors collected from the Javanerskop (Teekloof Formation), Oudeberg, and Ripplemead members, the Musgrave Grit unit, and the Katberg Formation. Also included are vectors of indeterminate formation collected by Cole and Wipplinger (2001).

3.5 Petrography

The results of the petrographic descriptions, classifications, and potential provenance will now be discussed for the Oudeberg, Ripplemead (RM), and Javanerskop members, the Boomplaas sandstone (BS), Musgrave Grit unit, and Lower Triassic Katberg Formation. Lithostratigraphic units were sampled from the base and top of the sandstone with exception to those from Beaufort West, Bloemfontein, Jagersfontein, Oudeberg Member, and Katberg Formation which have a single sample investigated from the base of the sandstone. The petrographic descriptions were conducted as a means to identify differing lithologies or source areas, if any, between the arenaceous lithostratigraphic units investigated in the study area. In total 13 samples were described from the field sites. Thin section descriptions were made based on quantitative observations (eg. 250 points per thin section for mineral percentages and 50 point counts for grain size determination), and semi-quantitative visual methods (eg. comparison charts for sorting, roundness, sphericity). Galehouse (1971) states that 250 point counts are satisfactory to obtain reliable percentages of the mineral components present. The applied point counting method used in this study was that of Dickinson (1985) and the classification scheme that of Pettijohn et al. (1987) and Dickinson (1985).

Overall, the sandstones are similar in their petrographic classification, ranging from litharenite to sublitharenite with the exception of two samples which plot in the subarkose field. The sandstones of the Upper Permian – Lower Triassic Beaufort Group were plotted on a provenance ternary diagram after Dickinson (1985) (Figure 3.32). This indicates that the majority of the samples plotted (A1, B1, D1, E2, G1) were mainly sourced from recycled orogen. However, all the samples from the Gariep Dam area (A2, B2, C1, C2, G2) and Jagersfontein (E1) showed continental block provenance or a mixture between continental block and recycled orogen. This is of relevance to the discussion on provenance interpretations later in the thesis (Chapter 5.4), which will be augmented by the detrital zircon investigation.

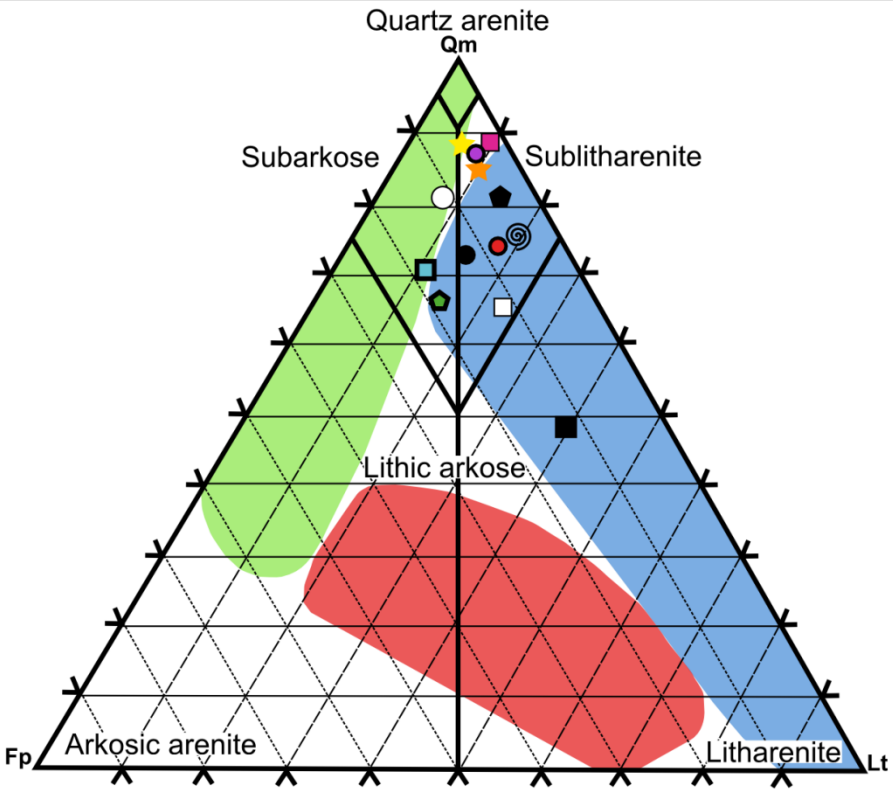

Legend

- Samples from Cradock and Baviaanrivier Valley
- Samples from Nieu Bethesda
- Sample from Beaufort West
- Samples from the Katberg Formation
- Samples from Gariep Dam
- Samples from Bloemfontein and Jagersfonein
- Sample from the Oudeberg Member

Qm Monocrystalline quartz
Fp Feldspar
Lt Total lithic fragments including polycrystalline quartz
Continental block provenance
Recycled orogen provenance
Magmatic arc provenance

Sample	Qm	Fp	Lt	Texture	Grain sphericity	Grain size (mm)	Classification	Provenance
A1	72 %	13 %	15 %	Submature	Subangular	0.1-0.2; 0.4-0.6	Sublitharenite	Recycled orogen
A2	88 %	6 %	6 %	Immature	Angular to subangular	0.1-0.2	Sublitharenite	Between recycled orogen and continental block
A3	75 %	7 %	18 %	Immature	Angular to subangular	0.1-0.3	Sublitharenite	Recycled orogen
B1	49 %	13 %	38 %	Immature	Angular to subangular	0.1-0.3	Litharenite	Recycled orogen
B2	71 %	19 %	10 %	Submature	Angular to subangular	0.1-0.2	Subarkose	Between recycled orogen and continental block
C1	75 %	6 %	18 %	Immature	Angular to subangular	0.1-0.3	Sublitharenite	Recycled orogen
D1	88 %	5 %	7 %	Immature	Subangular	0.2-0.5; 1-4	Sublitharenite/arkose	Continental block
D2	85 %	5 %	10 %	Submature	Angular to subangular	0.1-0.2	Sublitharenite	Between recycled orogen and continental block
E1	66 %	20 %	14 %	Immature	Angular to subangular	0.1-0.3; 0.5-3	Subarkose	Continental block
E2	82 %	4 %	14 %	Submature	Angular to subangular	0.25-0.6; 1-3	Sublitharenite	Recycled orogen
F1	81 %	12 %	7 %	Submature	Angular to subangular	0.1-0.2	Subarkose	Between recycled orogen and continental block
G1	66 %	11 %	23 %	Submature	Angular to subangular	0.1-0.3	Sublitharenite	Recycled orogen
G2	88 %	3 %	9 %	Submature	Angular to subangular	0.1-0.3	Sublitharenite	Between recycled orogen and continental block

Figure 3.32: Ternary diagram after Dickinson (1985) for provenance and rock classification of the 13 samples under investigation. In addition other petrographic characteristics such as texture, grain spericity, and grain size are also documented. Other descriptive features are discussed within the text.

Samples A1 and A2: Barberskrans Cliffs, N10, Cradock, Eastern Cape (section 1A)

Samples A1 and A2 are both classified as a sublitharenites and were sampled in the Oudeberg member at the site of section 1A (Figure 3.32). Similarly, the matrix content in both samples ranges from 5 to 15% component. Sample A1 also interestingly has a lot of polycrystalline quartz which was counted as part of the lithic fragments (see Figure 3.33). A2 is sampled from rippled sandstone (Sr). The ripple-cross lamination is visible in the thin sections in the form of very fine laminations and imbrication of grains, with some claystone drapes around the grains (see Figure 3.33). The fine laminations appear as mini fining-upward sequences with clay films more concentrated in the upper portion.

Sample A3: Lower Clifton farm, Baviaansriver Valley, Eastern Cape (section 2)

Sample A3 is classified as a sublitharenite with >5 % clay draped matrix and was sourced from the RM on Lower Clifton farm in the Baviaansrivier Valley (Figures 3.32 amd 3.33). A fining-upward fabric is observed and the grains are closely packed (clast-supported).

Samples B1 and B2: Krugerskraal and Ripplemead farms, Nieu Bethesda, Eastern Cape (sections 4 and 5)

These two samples are from the RM on Ripplemead farm (B1), and Krugerskraal farm (B2) near Nieu Bethesda (Figure 3.32 and 3.34). B1 is classified as a litharenite and comes from the sandstone base. Localized calcite cement is present between grains in places, which is probably diagenetic. There is a massive fabric in the sample, and this is likely due to the sample coming from the base of the sandstone, where upper-flow regime conditions would have been present during its deposition. Sample B2 is classified as a subarkose fine-grained sandstone from the top of the RM on Krugerskraal farm. Matrix is >5% and localized calcite cement is also present between grains in places, which is probably diagenetic. There is some lineation of the mica grains in the sample (Figure 3.34).

Sample C1: Javanerskop, Oukloof Pass, Beaufort West (section 7)

Sample C1 is classified as a sublitharenite and is sourced from the base of the Javanerskop member near the summit of Javanerskop (section 7). Large mud chips are common in the sample and have jagged edges due to compaction of the grains in the sample (Figure 3.34).

Samples D1 and D2: Inhoek farm, Gariep Dam, Free State Province (section 9)

Sample D1 and D2 come from the base and top of the RM on Inhoek farm respectively. Sample D1 could be classified as either a sublitharenite or a subarkose. A fining-upward fabric can be

observed with many of the clay chips which show iron oxide rim staining and the quartz grains exhibit a kind of surface etching (Figure 3.35). Sample D2 is classified as a sublitharenite.

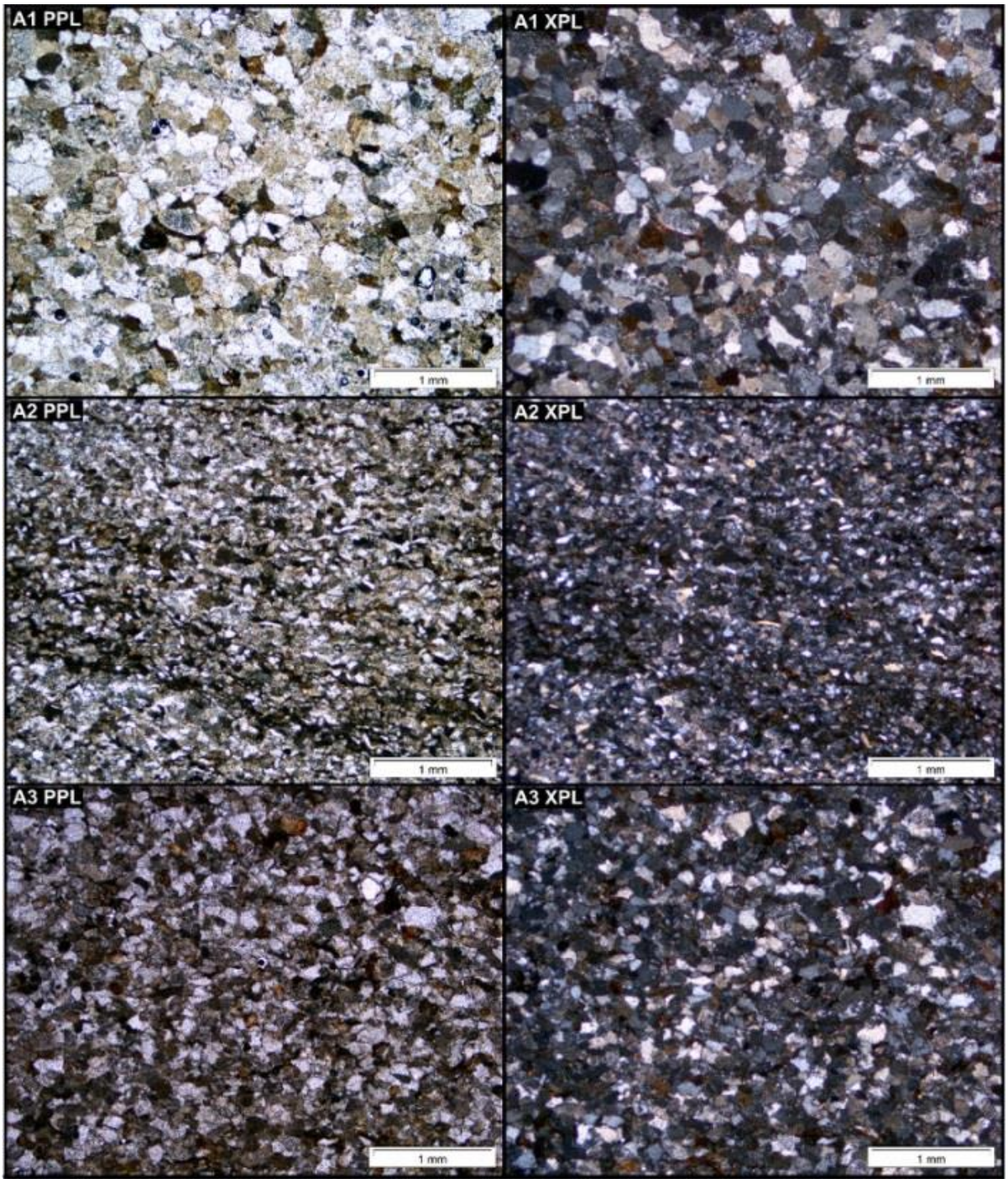

Figure 3.33: Thin section micrographs of samples A1 and A2 from the Oudeberg Member at its type locality (section: 1A) and sample A3 from Lower Clifton farm, Baviaanrivier Valley (section 2). Note the cross-bedding and grain imbrication in A2. Each sample is shown under plane polarized light (PPL) and cross polarized light (XPL). Magnification in all photographs is 4 X.

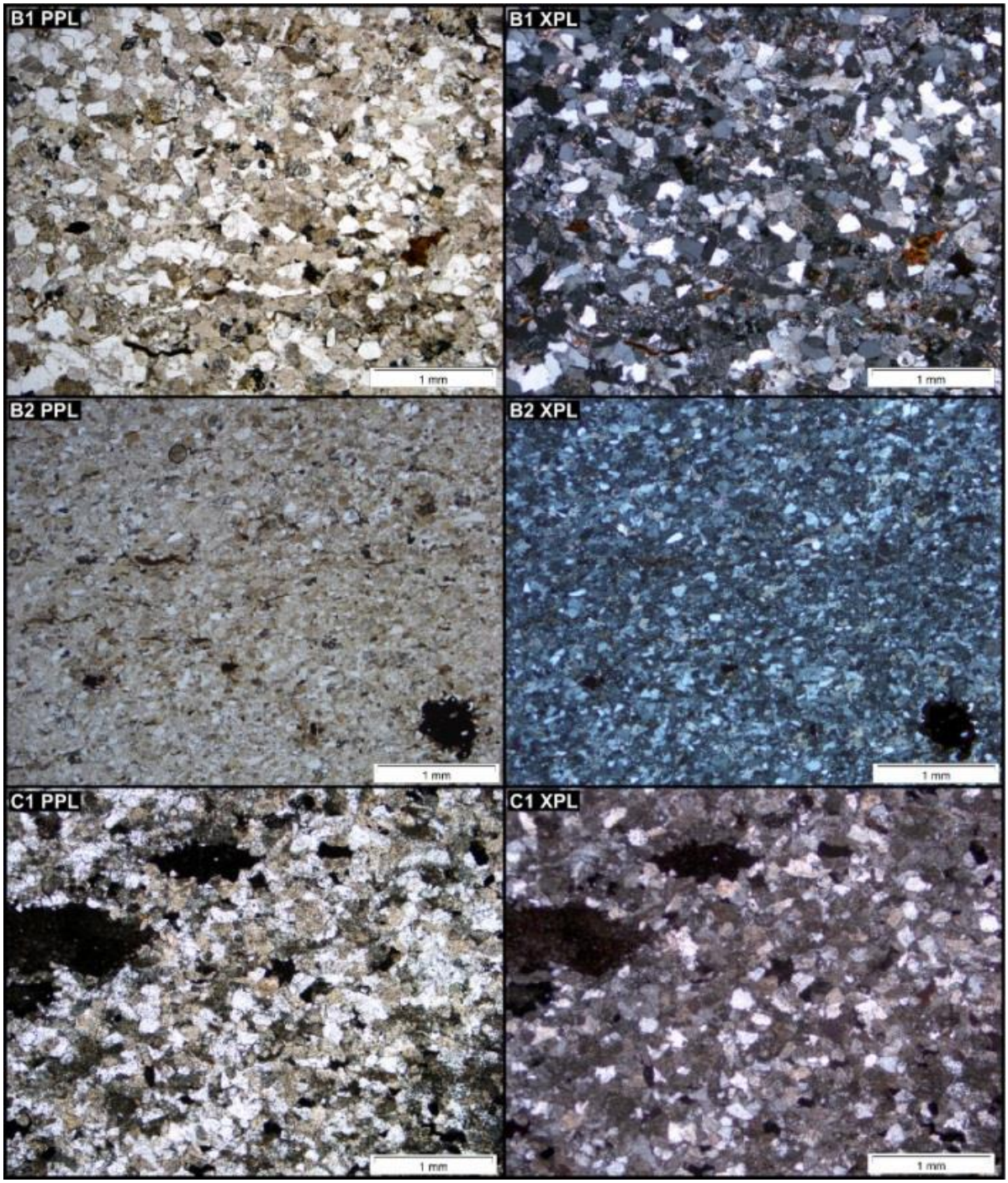

Figure 3.34: Thin section micrographs of samples B1 and B2 from Ripplemead and Krugerskraal farms, Nieu Bethesda respectively (sections 4 and 5) and sample C1 from the Javanerskop member on Javanerskop (section 7). Each sample is shown under plane polarized light (PPL) and cross polarized light (XPL). Magnification of the photographs is 4 X.

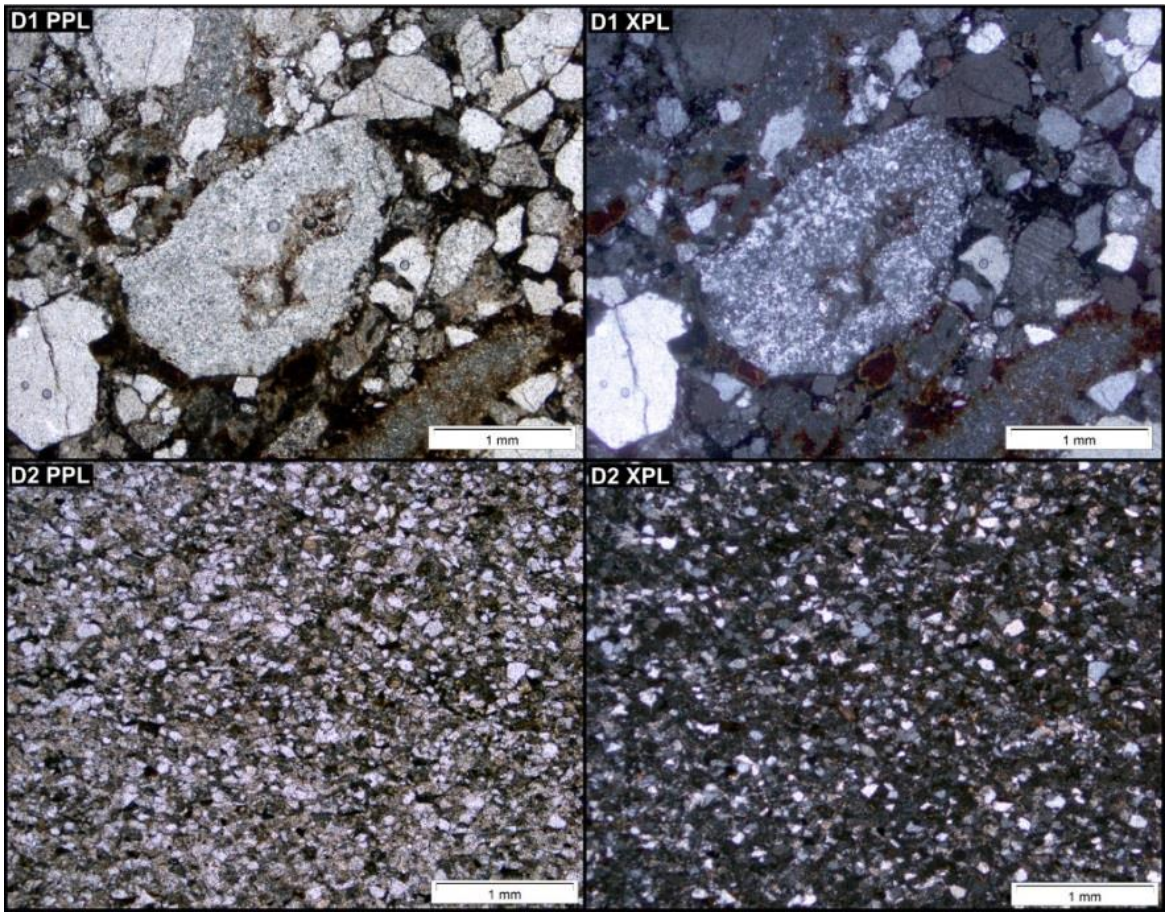

Figure 3.35: Thin section micrographs of samples D1 and D2 from Inhoek farm, Gariep Dam (section: 9). Each sample is shown under plane polarized light (PPL) and cross polarized light (XPL). Magnification of the photographs is 4 X. Note the large lithic fragment in D1.

Samples E1 and E2: Free State Province (sections 12 and 13)

Sample E1 is from the base of the BS on section 12 and is classified as a subarkose sandstone (Figures 3.32 and 3.36). Sample E1 shows how varied the grain sizes are in this sandstone and consists of coarse sand to gravel (granule) sized grains at its base and also fine to medium sand at the top of the thin section (Figure 3.32). Although the texture is overall immature, the fining-upward fabric in the thin section means that it ranges from immature to submature. Sample E2 comes from the Musgrave Grit unit on section 13 and is classified as a sublitharenite (Figures 3.32 and 3.36). Compaction of the grains is evident by the compression of micas between the quartz and feldspar grains (Figure 3.36).

Sample F1: Oudeberg Member, Oudeberg Pass, Graaff-Reinet, Eastern Cape

This sample is from the Upper Oudeberg Member from Oudeberg Pass and is classified as a subarkose sandstone (See Figures 3.32 and 3.37).

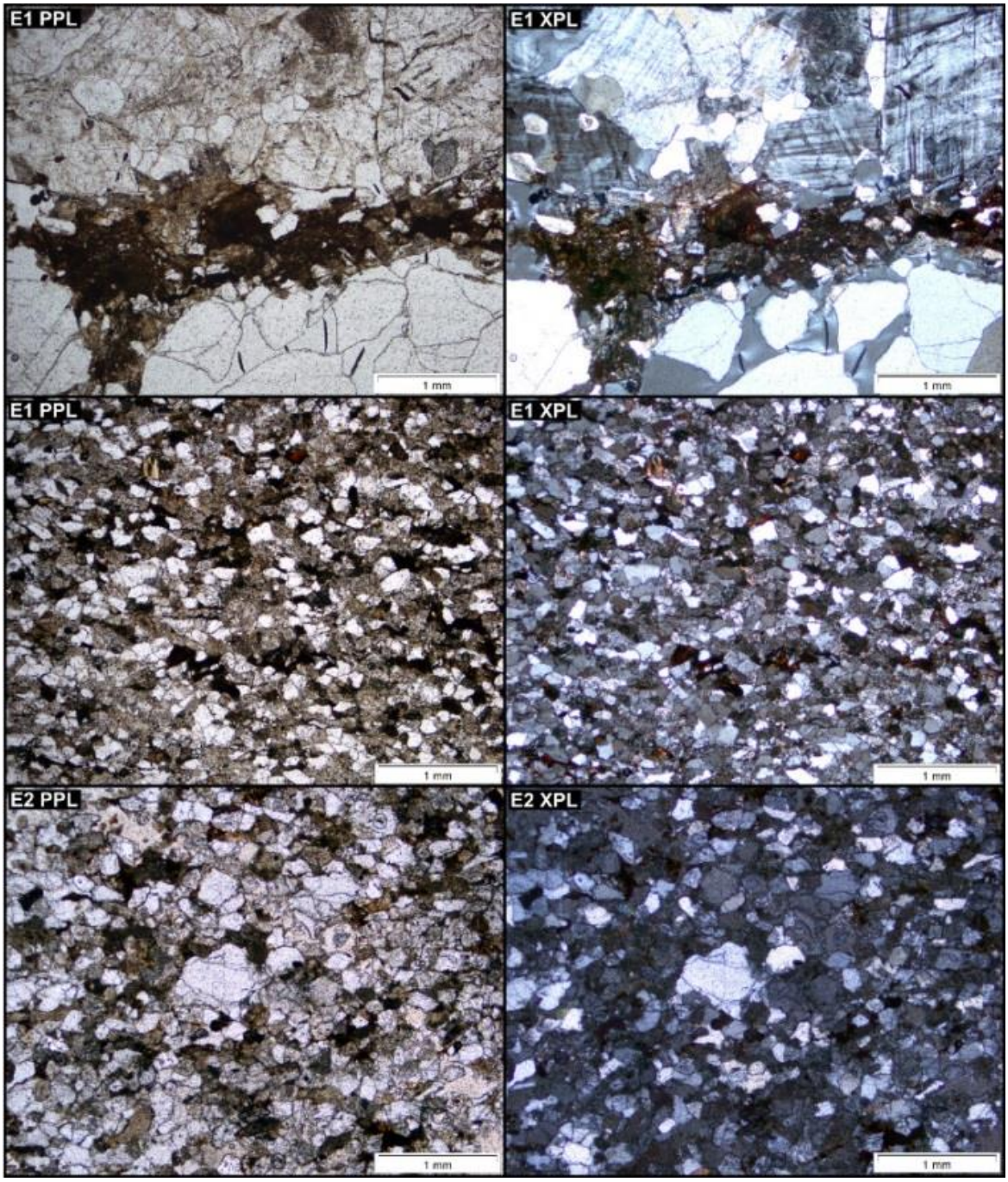

Figure 3.36: Thin section micrographs of samples E1 and E2 from the Boomplaas sandstone, Jagersfontein and the Musgrave Grit unit, Bloemfontein respectively (sections 12 and 13). Each sample is shown under plane polarized light (PPL) and cross polarized light (XPL). Magnification of the photographs is 4 X. Note the large polycrystalline quartz and feldspar grains in E1.

Samples G1 and G2: Katberg Formation

Sample G1 comes from the lowermost Katberg Formation on section 2, Lower Clifton farm and is classified as a sublitharenite (Figures 3.32 and 3.37). Interestingly many of the quartz grains contain cracks and no plagioclase feldspar is present in the sample (Figure 3.37). G2 comes from the Katberg Formation on the summit of Inhoek farm near Gariep Dam (section 9) and is classified as a sublitharenite. The Ripplemead member in the Gariep Dam area tends to be very

coarse-grained at its base for ~ 1m or so and then abruptly fine-upwards into fine-grained sandstone (see D1 and D2, Figure 3.35) and this was not the case for the Katberg Formation in the area, although a massive fabric is observed in G2 (Figure 3.37).

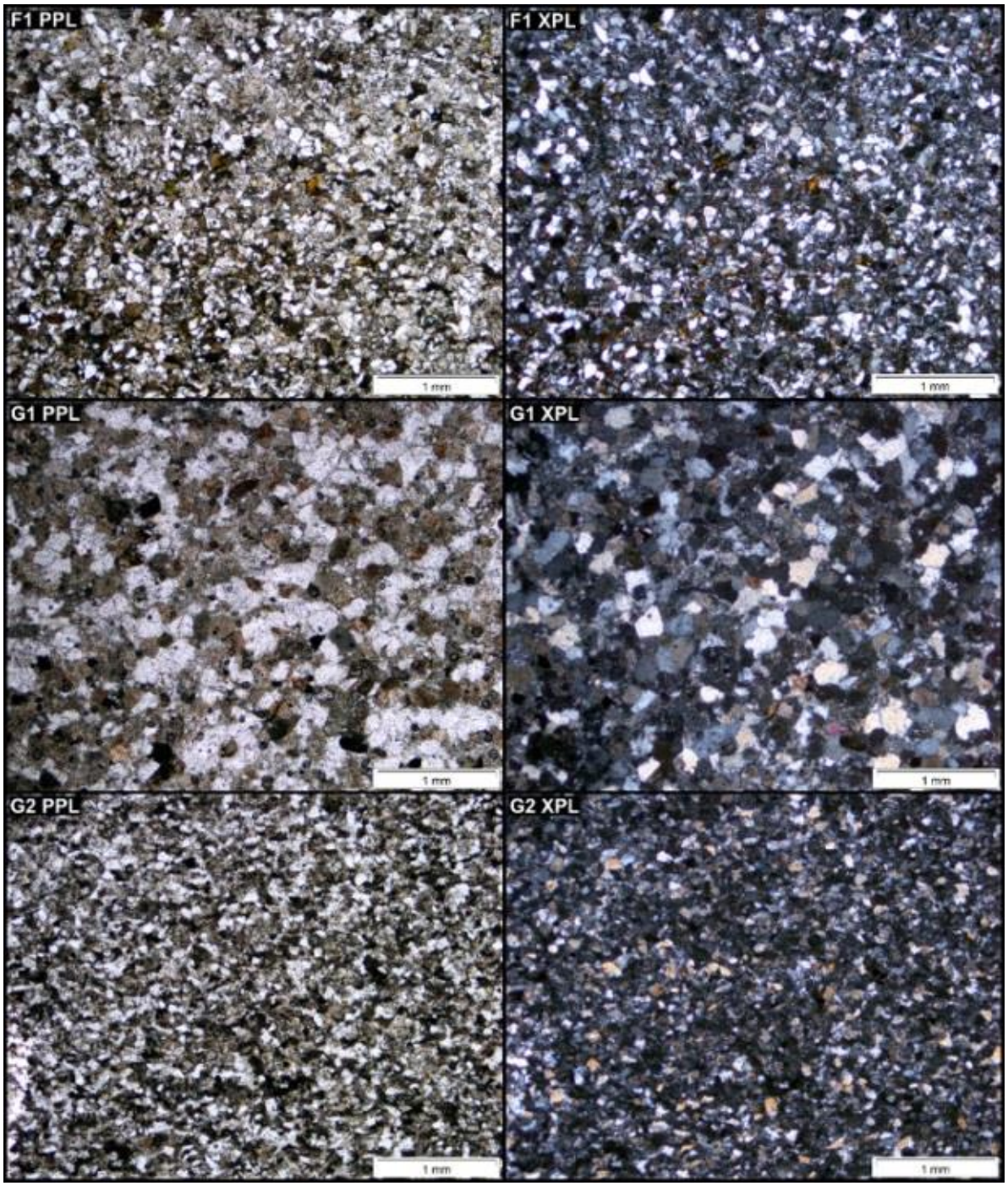

Figure 3.37: Thin section micrographs of sample F1 from the Oudeberg Member, and G1 and G2 of the Katberg Formation. Each sample is shown under plane polarized light (PPL) and cross polarized light (XPL). Each sample is shown under plane polarized light (PPL) and cross polarized light (XPL). Magnification of the photographs is 4 X.

3.6 Detrital zircon age populations of rock samples from the Beaufort Group

Detrital zircons were analysed from sandstone samples collected at all field sites. The samples were sourced from the Oudeberg, Ripplemead (RM), and Javanerskop members, the Boomplaas sandstone (BS) Musgrave Grit unit, and the Lower Triassic Katberg Formation. This investigation was conducted as a means to characterise and compare lithological units investigated at the field sites. Table 3.3 shows the numbers of grains collected for each sample from each major geological period. Data obtained from detrital zircon dating and grain analysis are summarized in Table 3.4 and discussed in detail in this section (Figures 3.38 – 3.61). A total of 1029 concordant zircon grains were analysed from the sandstone samples (Table 3.4, Appendix 1, on disc). Appendix 1 includes all the data (including discordant grain data), Wetherill Concordia diagrams, and the cathode luminescence SEM images of all grains collected from the sandstone samples. These samples are discussed in Chapter 5.4 with regards to interpretations of source areas and potential genetic relationship to one another.

Table 3.3	**Trias**	**Perm**	**Carb**	**Devo**	**Silur**	**Ordo**	**Cam**	**Neo -P**	**Meso-P**	**Paleo-P**	**Arc**
Late Permian											
Cr1	0	3	1	0	0	0	21	56	1	0	0
LC	0	34	8	0	0	0	0	13	8	4	2
NbDo1	0	61	5	0	2	1	2	13	16	2	2
H1	2	17	4	0	0	2	2	9	5	3	0
Javanerskop	0	24	11	1	0	1	5	7	9	2	1
BMIn2	0	39	2	2	0	4	3	9	7	3	0
Springfontein	0	31	3	1	1	0	7	29	12	1	0
J615	0	10	2	0	0	1	16	31	36	2	2
T28m	1	60	8	2	1	4	0	13	10	2	0
Early Triassic											
Kat2Pass	0	77	7	0	0	2	5	10	18	1	4
Venter	1	46	8	2	0	0	7	5	6	0	1
KTIn	0	33	4	0	0	2	8	26	20	1	1

Table 3.4 (next page): Age data, size of sample populations, character of zircon populations and composition of zircons with <10% discordance from rock samples of the Oudeberg, Ripplemead members, Boomplaas sandstone, and Musgrave Grit unit (Balfour Formation), Javanerskop member (Upper Teekloof Formation), and Lower Katberg Formation (Tarkastad Subgroup). Total n= total number of zircons analysed; concordant n= number of <10% concordant grains. Red= the youngest zircon population, yellow and green = intermediate zircon age population, blue= the oldest zircon population, pink = the youngest detrital zircon grain in the sample.

	Population	Internal and external textures	U, Pb, and Th content
Oudeberg Member (Balfour Formation) Barberskrans Cliffs, Cradock (PV-Cr1) Total n=118 Concordant n= 105	264 ± 3 - 304 ± 3 Ma (4%)	Only four grains in this population. Zircon grains are ~100 to 150 µm. Grains are all elongate and euhedral and exhibit oscillatory zoning.	U= 222-450 ppm Pb= 11-20 ppm Th/U=0.26-0.60
	489 ± 5 - 878 ± 24 Ma (73%)	A total of 77 grains are in this population. Zircon grains are ~100 to 300 µm. Grains range in shape. Some are elongate showing some preserved crystal structure, others are well rounded and likely pieces of once larger grains. The rest are fragments of euhedral elongate grains. Sector zoning most commonly encountered although some oscillatory zoning is observed in this population.	U= 24-1250 ppm Pb= 3-108 ppm Th/U=0.00-0.86 (*7 grains <0.07)
	1008 ± 22 - 1133 ± 29 Ma (23%)	Twenty four grains are in this population. Zircon grains are ~100 to 180 µm. Sector and oscillatory zoning are observed, and many grains are fragmentary. Some have preserved their elongate and euhedral nature although these are rare.	U= 41-1159 ppm Pb= 7-198 ppm Th/U=0.13-0.58
	1133 ± 29 Ma	The oldest grain in this sample ~130 µm. The grain is subrounded and exhibits sector zoning.	U= 203 ppm Pb= 38 ppm Th/U= 0.31
	264 ± 3 Ma	The youngest grain in this sample ~160 µm. The grain is elongate, euhedral and oscillatory zoned.	U= 322 ppm Pb= 13 ppm Th/U= 0.60

	Population	Internal and external textures	U, Pb, and Th content
Ripplemead member Lower Clifton, Baviaans River Valley (PV-LC) Total n=110 Concordant n= 73	251 ± 5 - 315 ± 6 Ma (58%)	There are 42 grains in this population. Zircon grains are ~70 to 150 µm. Grains are mostly euhedral but not always elongate. Sector and oscillatory zoning is observed, sometimes in the same grain.	U= 81-1222 ppm Pb= 3-51 ppm Th/U= 0.18-4.16
	487 ± 10 - 845 ± 25 Ma (22%)	There are 16 grains in this population. Zircon grains are ~50 to 150 µm. Grains are mostly well rounded or fragmentary, but a few euhedral grains were found. Sector zoning most commonly encountered.	U= 49-658 ppm Pb= 5-75 ppm Th/U=0.05-1.44 (*2 grains <0.07)
	948 ± 25 - 1137 ± 25 Ma (8%)	There are 6 grains in this population. Zircon grains are ~50 to 150 µm. Grains are well rounded or fragments of once larger grains. Sector zoning most commonly encountered.	U= 120-474 ppm Pb= 21-84 ppm Th/U=0.17-0.87
	1402 ± 26 - 1848 ± 20 Ma (5%)	There are 4 grains in this population. Zircon grains are ~70 to 120 µm. Two grains are well rounded with sector zoning, one is elongate and euhedral, and one is fragmentary.	U= 40-692 ppm Pb= 9-190 ppm Th/U= 0.23-0.72
	2167 ± 19 - 2780 ± 18 Ma (7%)	There are 5 grains in this population. Zircon grains are ~70 to 130 µm. Grains either well rounded or fragmentary. Sector and oscillatory zoning observed.	U= 150-668 ppm Pb= 73-258 ppm Th/U= 0.35-0.71
	251 ± 5 Ma	The youngest grain is ~50 µm. Its euhedral nature partially preserved but it has been rounded. Oscillatory zoning present.	U= 423 ppm Pb= 17 ppm Th/U= 0.44

	Population	Internal and external textures	U, Pb, and Th content
Ripplemead member Doornplaats, Nieu Bethesda (PV-NbDo1) Total n=119 Concordant n= 104	255 ± 3 - 324 ± 4 Ma (64%)	There are 66 grains in this population. Zircon grains are ~70 to 150 µm. Grains are mostly euhedral and elongate, exhibiting oscillatory zoning. Some show both sector and oscillatory zoning. Many are also fragmentary but still exhibit their euhedral nature.	U= 77-1519 ppm Pb= 3-65 ppm Th/U= 0.14-1.86
	439 ± 5 - 675 ± 7 Ma (15%)	There are 16 grains in this population. Zircon grains are ~50 to 150 µm. Grains show both oscillatory and sector zoning. Most grains are elongate with sector zoning, but some are well rounded. A few are fragments of once larger grains.	U= 130-1992 ppm Pb= 13-140 ppm Th/U= 0.05-0.72 (*1 grain <0.07)
	981 ± 37 - 1213 ± 23 Ma (15%)	There are 18 grains in this population. Zircon grains are ~40 to 100 µm. Both oscillatory and sector zoned grains are present, as are elongate and rounded grains. Some grains show evidence of damage, having pieces missing or chips.	U= 86-713 ppm Pb= 16-118 ppm Th/U= 0.10-2.89
	1443 ± 24 - 1774 ± 21 Ma (4%)	There are 2 grains in this population. Zircon grains are ~100 µm. One is fragmentary and shows no internal features, the other is subrounded and shows sector zoning.	U= 101-708 ppm Pb= 26-211 ppm Th/U= 0.76-0.24
	2756 ± 18 - 2760 ± 20 Ma (2%)	There are 2 grains in this population. Zircon grains are ~50 µm. Both are fragments of once larger grains, one showing poor evidence of oscillatory zoning.	U= 88-161 ppm Pb= 47-82 ppm Th/U= 0.34-0.55
	255 ± 3 Ma	The youngest grain in the population is ~100 µm. It is elongate, euhedral with oscillatory zoning.	U= 1007 ppm Pb= 41 ppm Th/U= 0.60

	Population	Internal and external textures	U, Pb, and Th content
Javanerskop member Highlands, Beaufort West (PV-H1) Total n= 84 Concordant n= 44	226 ± 3 - 316 ± 3 Ma (52%)	There are 23 grains in this population. Zircon grains are ~50 to 100 µm. Most grains are euhedral prisms that are chipped or broken. These grains show mainly oscillatory but sometimes sector zoning. Some elongate grains are also present that show sector zoning.	U= 140-981 ppm Pb= 6-43 ppm Th/U= 0.20-0.98
	399 ± 4 - 870 ± 26 Ma (29. 5%)	There are 13 grains in this population. Zircon grains are ~60 to 90 µm. Most are broken but euhedral prism shaped grains with sector zoning, although some oscillatory zoning is present in some grains.	U= 160-600 ppm Pb= 10-78 ppm Th/U= 0.01-0.99 (*1 grain <0.07)
	1044 ± 22 - 1308 ± 23 Ma (11. 5%)	There are 5 grains in this population. Zircon grains are ~40 to 60 µm. Most grains are well rounded or fragments of once larger grains. Not much of the internal structure can be observed but some zoning is visible. It is difficult to describe type of zoning.	U= 104-454 ppm Pb= 23-67 ppm Th/U= 0.25-0.84
	1943 ± 18 - 2102 ± 18 Ma (7%)	There are 3 grains in this population. Zircon grains are ~60 to 100 µm. All are fragments of once larger grains, but one is well rounded. Oscillatory zoning observed in one grain.	U= 114-559 ppm Pb= 43-197 ppm Th/U= 0.08-0.62
	226 ± 3 Ma	The youngest grain in the sample us ~60 µm. The edges of the grain are rounded but it still retains some original crystal shape. Oscillatory zoning is observed.	U= 476 ppm Pb= 17 ppm Th/U= 0.87

	Population	Internal and external textures	U, Pb, and Th content
Javanerskop member Javanerskop, Beaufort West (PV-Javanerskop) Total n= 101 Concordant n= 61	255 ± 5 - 321 ± 6 Ma (57%)	There are 35 grains in this population. Zircon grains are ~50 to 150 µm. Most grains are short or sperical prisms with oscillatory and sector zoning. Some of the prisms are chipped or fragments of larger grains, but still retain their euhedral shape.	U= 3-772 ppm Pb= 2-32 ppm Th/U= 0.23-1.40
	364 ± 7 - 869 ± 22 Ma (23%)	There are 14 grains in this population. Zircon grains are ~60 to 100 µm. Well rounded grains most common, although some are angular fragments from larger grains. Oscillatory and sector zoning observed, with sector zoning slighty more common.	U= 86-756 ppm Pb= 7-79 ppm Th/U= 0.09-0.81
	1040 ± 24 - 1253 ± 29 Ma (15%)	There are 9 grains in this population. Zircon grains are ~50 to 120 µm. These are well rounded grains that exhibit sector or oscillatory zoning.	U= 43-431 ppm Pb= 7-60 ppm Th/U= 0.21-1.01
	2026 ± 19 - 2803 ± 17 Ma (5%)	There are 3 grains in this population. Zircon grains are ~80 µm. All grains exhibit oscillatory zoning but have different external appearances. One is elongate, another sperical, and the other an angular fragment.	U= 91-639 ppm Pb= 50-239 ppm Th/U= 0.26-0.99
	255 ± 5 Ma	The youngest grain is ~80 µm. It is a sub rounded prism with oscillatory zoning.	U= 112 ppm Pb= 5 ppm Th/U= 0.75

	Population	Internal and external textures	U, Pb, and Th content
Ripplemead member Inhoek, Gariep Dam (PV-BMIn2) Total n=103 Concordant n= 69	250 ± 5 - 306 ± 6 Ma (60%)	There are 41 grains in this population. Zircon grains are ~40 to 90 µm. Grains are euhedral but show a range of shapes such as elongate, tabular, and sperical. A couple are broken or have chipped edges. Oscillatory and sector zoning observed.	U= 104-619 ppm Pb= 4-25 ppm Th/U= 0.28-2.26
	373 ± 7 - 666 ± 12 Ma (26%)	There are 18 grains in this population. Zircon grains are ~50 to 100 µm. Euhedral grains are less common but still present. None are elongate. Sector and oscillatory zoning is observed, but sector zoning most common.	U= 89-963 ppm Pb= 10-98 ppm Th/U=0.06-0.72 (*3 grains <0.07)
	1048 ± 22 - 1280 ± 21 Ma (10%)	There are 7 grains in this population. Zircon grains are ~30 to 100 µm. All grains are rounded, but some are elongate. Sector zoning observed in some grains.	U= 92-50 ppm Pb= 15-92 ppm Th/U= 0.17-0.53
	1634 ± 20 Ma - 2450 ± 17 Ma (4%)	There are 3 grains in this population. Zircon grains are ~40 to 80 µm. All are rounded fragments of once larger grains. Evidence of oscillatory zoning evident on two of the grains.	U= 155-389 ppm Pb= 56-148 ppm Th/U= 0.35-0.42
	250 ± 5 Ma	There youngest grain is ~90 µm. It is euhedral and exibits sector zoning.	U= 454 ppm Pb= 18 ppm Th/U= 1.87

	Population	Internal and external textures	U, Pb, and Th content
Ripplemead member Springfontein, Free State Province (PV-Springfontein) Total n=108 Concordant n= 84	254 ± 5 - 320 ± 7 Ma (39.2%)	There are 33 grains in this population. Zircon grains are ~50 to 120 µm. Euhedral, elongate, sperical, and fragmentary grains present, but sector zoning most common.	U= 58-947 ppm Pb= 2-41 ppm Th/U= 0.09-2.15
	407 ± 8 - 723 ± 15 Ma (37%)	There are 31 grains in this population. Zircon grains are ~70 to 200 µm. Most are elongate but rounded grains, but there are also fragmentary or broken grains. Sector and oscillatory zoning is observed.	U= 47-1580 ppm Pb= 5-108 ppm Th/U= 0.02-1.39 (*4 grains <0.07)
	910 ± 25 - 1268 ± 21 Ma (22.6%)	There are 19 grains in this population. Zircon grains are ~70 to 180 µm. Most are well rounded grains with oscillatory or sector zoning. There are also fragmentary grains that were clearly once part of larger grains.	U= 38-896 ppm Pb= 6-158 ppm Th/U=0.11-0.60
	1691 ± 22 (1.2%)	There is one grain in this population that is ~100 µm. It is a well rounded grain with sector and oscillatory zoning.	U= 80 ppm Pb= 24 ppm Th/U= 0.31
	254 ± 5 Ma	The youngest grain in the sample is ~120 µm. It is a well rounded grain exhibiting sector zoning.	U= 101 ppm Pb= 4 ppm Th/U= 1.12

	Population	Internal and external textures	U, Pb, and Th content
Boomplaas sandstone Boomplaas Hill, Jagersfontein (PV-J615) Total n=122 Concordant n= 99	252 ± 4 - 339 ± 5 Ma (12%)	There are 12 grains in this population. Zircon grains are ~80 to 120 µm. Grains are either euhedral elongate or prismatic grains. Oscillatory and sector zoning oberserved, sometimes in the same grain.	U= 87-779 ppm Pb= 4-43 ppm Th/U= 0.08-1.68
	477 ± 8 - 819 ± 28 Ma (43%)	There are 43 grains in this population. Zircon grains are ~80 to 150 µm. A number of different grain types are observed, some elongate, other prismatic. A single well rounded grain was also observed. All show combinations of sector and oscillatory zoning, sometimes in the same grain.	U= 51-1265 ppm Pb= 4-140 ppm Th/U= 0.02-1.51 (*2 grains <0.07)
	908 ± 24 - 1252 ± 22 Ma (41%)	There are 41 grains in this population. Zircon grains are ~60 to 100 µm. Grains are either prismatic or well rounded. A few are fragments of larger grains. Oscillatory and sector zoning oberserved, sometimes in the same grain.	U= 33-603 ppm Pb= 6-104 ppm Th/U= 0.11-0.92
	1753 ± 21 - 2712 ± 18 Ma (4%)	There are 3 grains in this population but 4 dates were retrieved. Zircon grains are ~60 to 100 µm. The grains are prisms with some of their euhedral nature preserved. Two show oscillatory zoning, and one sector and oscillatory zoning.	U= 162-297 ppm Pb= 52-196 ppm Th/U= 0.27-0.92
	252 ± 4 Ma	The youngest grain in the population is ~100 µm. It is a euhedral prism shaped grain with oscillatory zoning.	U= 233 ppm Pb= 9 ppm Th/U=0.67

	Population	Internal and external textures	U, Pb, and Th content
Musgrave Grit unit (Balfour Formation) Tafelkop, Bloemfontein (PV-T28m) Total n=130 Concordant n= 101	248 ± 3 - 325 ± 6 Ma (69%)	There are 70 grains in this population. Zircon grains are ~100 to 150 µm. Elongate prisms most common grain type although shorter prisms are present. Some grains are broken. Oscillatory and sector zoning common.	U= 93-1387 ppm Pb= 5-57 ppm Th/U= 0.10-1.17
	375 ± 4 - 770 ± 8 Ma (17%)	There are 18 grains in this population. Zircon grains are ~80 to 180 µm. Euhedral elongate grains and prisms common. Some sperical and well rounded grains are also present. Oscillatory and sector zonging observed.	U= 84-765 ppm Pb= 10-58 ppm Th/U= 0.05-1.07 (*2 grains <0.07)
	941 ± 22 - 1312 ± 23 Ma (11%)	There are 11 grains in this population. Zircon grains are ~100 to 120 µm. Elongate prisms and well rounded grains are observed. the Elongate grains are often broken or fragments of larger grains. Sector zoning most common.	U= 68-606 ppm Pb= 15-113 ppm Th/U= 0.06-0.58 (*1 grain <0.07)
	1422 ± 21 - 1770 ± 19 Ma (3%)	There are 3 grains in this population. Zircon grains are ~80 to 100 µm. One grain is a damaged, sub rounded prism with oscillatory zoning. The second grain is clearly a fragment of a larger grain.	U= 88-242 ppm Pb= 26-76 ppm Th/U= 0.56-0.71
	248 ± 3 Ma	The youngest grain in the population is ~100 µm. It is an euhedral prism with oscillatory zoning.	U= 706 ppm Pb= 28 ppm Th/U= 0.49

	Population	Internal and external textures	U, Pb, and Th content
Katberg Formation Baviaans River Valley (Kat2Pass) Total n=132 Concordant n= 124	252 ± 5 - 313 ± 6 Ma (68%)	There are 84 grains in this population. Zircon grains are ~70 to 150 µm. Grains are mostly euhedral and elongate, exhibiting oscillatory zoning. Some show both sector and oscillatory zoning. Many are also fragmentary but still exhibit their euhedral nature.	U= 92-886 ppm Pb= 4-39 ppm Th/U=0.23-2.03 (*10.24 single grain)
	442 ± 8 - 625 ± 11 Ma (10%)	There are 13 grains in this population. Zircon grains are ~100 to 150 µm. Grains are similar to the previous populatoin, although more fragments of once larger grains are evident. Oscillatory and sector zoning both observed.	U= 27-574 ppm Pb= 6-103 ppm Th/U=0.16-0.85
	929 ± 23 - 1463 ± 20 Ma (18%)	There are 25 grains in this population. Zircon grains are ~100 to 150 µm. Most grains are well rounded to subrounded but some are clearly fragments of once larger grains. Sector zoning and oscillatory zoning common.	U= 51-728 ppm Pb= 5-52 ppm Th/U=0.09-1.24
	2258 ± 18 - 3239 ± 16 Ma (4%)	There are 5 grains in this population. Zircon grains are ~100 to 150 µm. Grains are mostly fragments are once larger grains, but some are rounded elongate grains. Oscillatory and sector zoning is observed.	U= 161-441 ppm Pb= 67-250 ppm Th/U=0.05-0.90
	252 ± 5 Ma	There youngest grain is an elongate, euhedral grain ~120 µm in length. It exhibits oscillatory zoning and has preserved much of its original crystal structure.	U= 238 ppm Pb= 9 ppm Th/U=0.45

	Population	Internal and external textures	U, Pb, and Th content
Katberg Formation Venterstad (PV-Venter) Total n=105 Concordant n= 76	250 ± 5 - 332 ± 6 Ma (72.4%)	There are 55 grains in this population. Zircon grains are ~80 to 150 µm. Elongate prisms and sperical grains are present. Most common is oscillatory zoning in this population.	U= 85-1034 ppm Pb= 4-43 ppm Th/U=0.24-2.19
	395 ± 7 - 647 ± 12 Ma (17.1%)	There are 13 grains in this population. Zircon grains are ~50 to 100 µm. Prismatic and sperical grains are present, some well rounded. Oscillatory and sector zoning observed.	U= 123-895 ppm Pb= 11-90 ppm Th/U=0.09-1.56
	963 ± 29 - 1087 ± 24 Ma (9.2%)	There are 7 grains in this population. Zircon grains are ~70 to 200 µm. Elongate euhedral grains are present with oscillatory zoning. The other grains are angular or rounded fragments of once larger grains. Sector and oscillatory zoning observed in these grains.	U= 72-262 ppm Pb= 13-40 ppm Th/U=0.21-0.46
	2846 ± 17 Ma (1.3%)	A single grain that is ~60 µm. It is a well rounded grain that does not show internal zoning.	U= 147 ppm Pb= 82 ppm Th/U= 0.01 *metamorphic grain
	250 ± 5 Ma	The youngest grain is ~110 µm. It is a euhedral prism that exhibits oscillatory zoning. It is mostly intact apart from a small fragment that is missing.	U= 178 ppm Pb= 7 ppm Th/U=0.52

	Population	Internal and external textures	U, Pb, and Th
Katberg Formation Inhoek, Gariep Dam (PV-KTIn1) Total n=110 Concordant n= 95	255 ± 5 - 326 ± 7 Ma (40%)	There are 37 grains in this population. Zircon grains are ~90 to 200 µm. Most are euhedral grains, or fragments of euhedral grains showing oscillatory and sector zoning. Some subrounded grains are present as well.	U= 65-623 ppm Pb= 3-26 ppm Th/U=0.06 -1.96 (*1 grain <0.07)
	457 ± 10 - 777 ± 16 Ma (33%)	There are 32 grains in this population. Zircon grains are ~80 to 200 µm. The majority of grains are well rouned but a few euhedral grains are present. Both oscillatory and sector zoning are observed.	U= 50-823 ppm Pb= 4-87 ppm Th/U=0.01-1.39 (*5 grains <0.07)
	891 ± 22 - 1172 ± 21 Ma (25%)	There are 24 grains in this population. Zircon grains are ~120 to 160 µm. Most grains are fragments of once larger grains, and in some oscillatory zoning is still preserved.	U= 40-1182 ppm Pb= 7-163 ppm Th/U=0.04-4.90 (*3 grains <0.07)
	2364 ± 18 Ma 3416 ± 31 Ma (2%)	There are 2 grains in this population. Zircon grains are ~150 µm. one grain is well rounded showing sector zoning, and the other is a tabular fragment showing sector zoning.	U= 149, 22 ppm Pb= 65, 15 ppm Th/U=0.35, 0.49
	255 ± 5 Ma	The youngest grain in the sample is ~200 µm. It is a euhedral grain that is twinned at 120 degrees (known as knee twinning, or geniculate twinning).	U= 273 ppm Pb= 11 ppm Th/U= 1.01

3.6.1 Detrital zircon samples

Cradock

Section 1A: Barberskrans Cliffs, N10, Cradock, Cradock District, Eastern Cape

The sandstone rock sample from the Oudeberg Member (PV-Cr1) at the type locality (section 1A) produced 105 zircon grains that have a discordance of less than 10% from a total of 118 grains analysed (Figure 3.38, Table 3.4). The ages of the most prominent zircon population in the sample ranges between 484 Ma and 902 Ma, a total of 77 grains or 73% of the total sample. The second most prominent population ranges from 984 Ma to 1162 Ma, a total of 24 grains or 24% of the total sample. The youngest population is also the least prominent with ages between 261 Ma and 307 Ma and only comprises 4 grains, or 4% of the population.

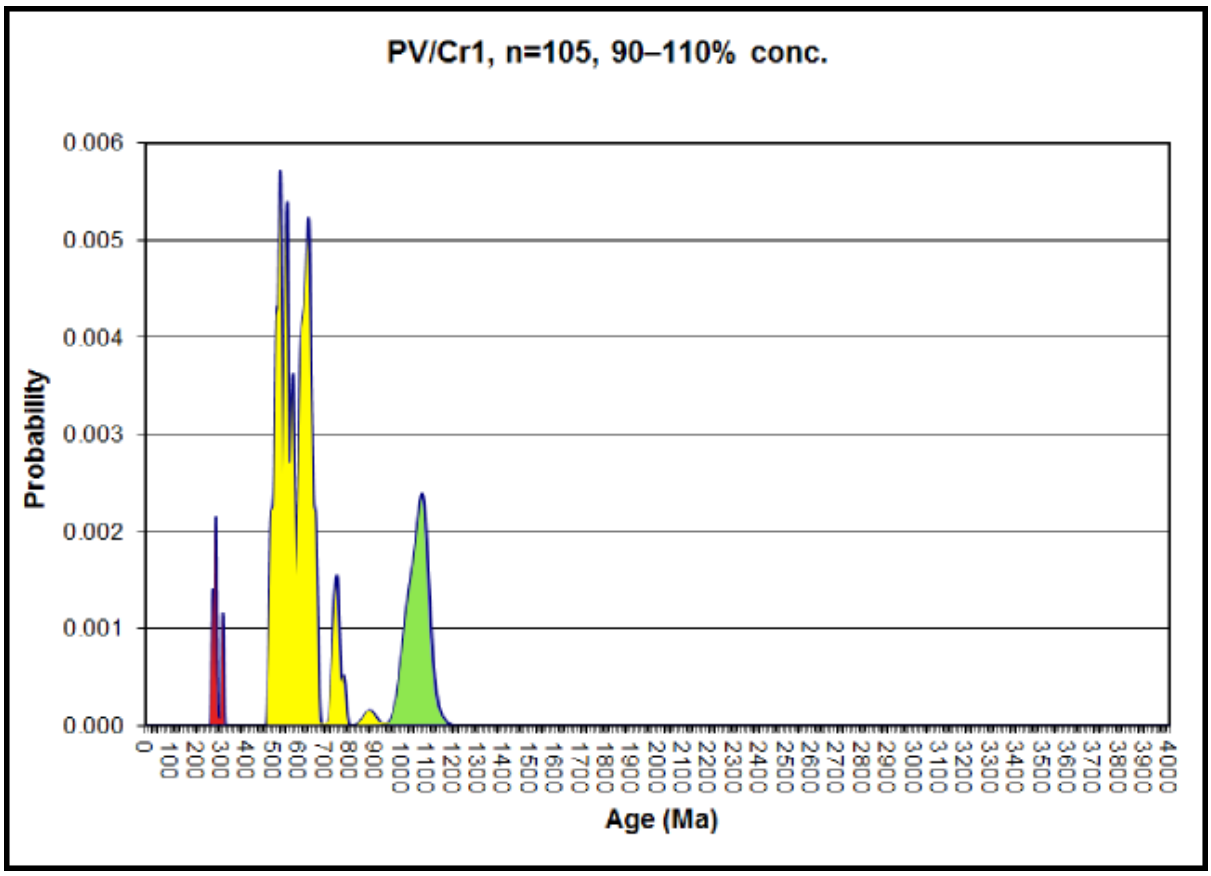

Figure 3.38: Probability density plot for sample PV-Cr1 of the Oudeberg Member (N10 highway, Cradock) revealing three prominent zircon age populations; a younger with ages 264 ± 3 to 304 ± 3 Ma (4 grains), and intermediate population with ages 489 ± 5 Ma to 878 ± 24 Ma (73 grains), and the oldest population with ages between 1008 ± 22 and 1133 ± 29 Ma (24 grains).

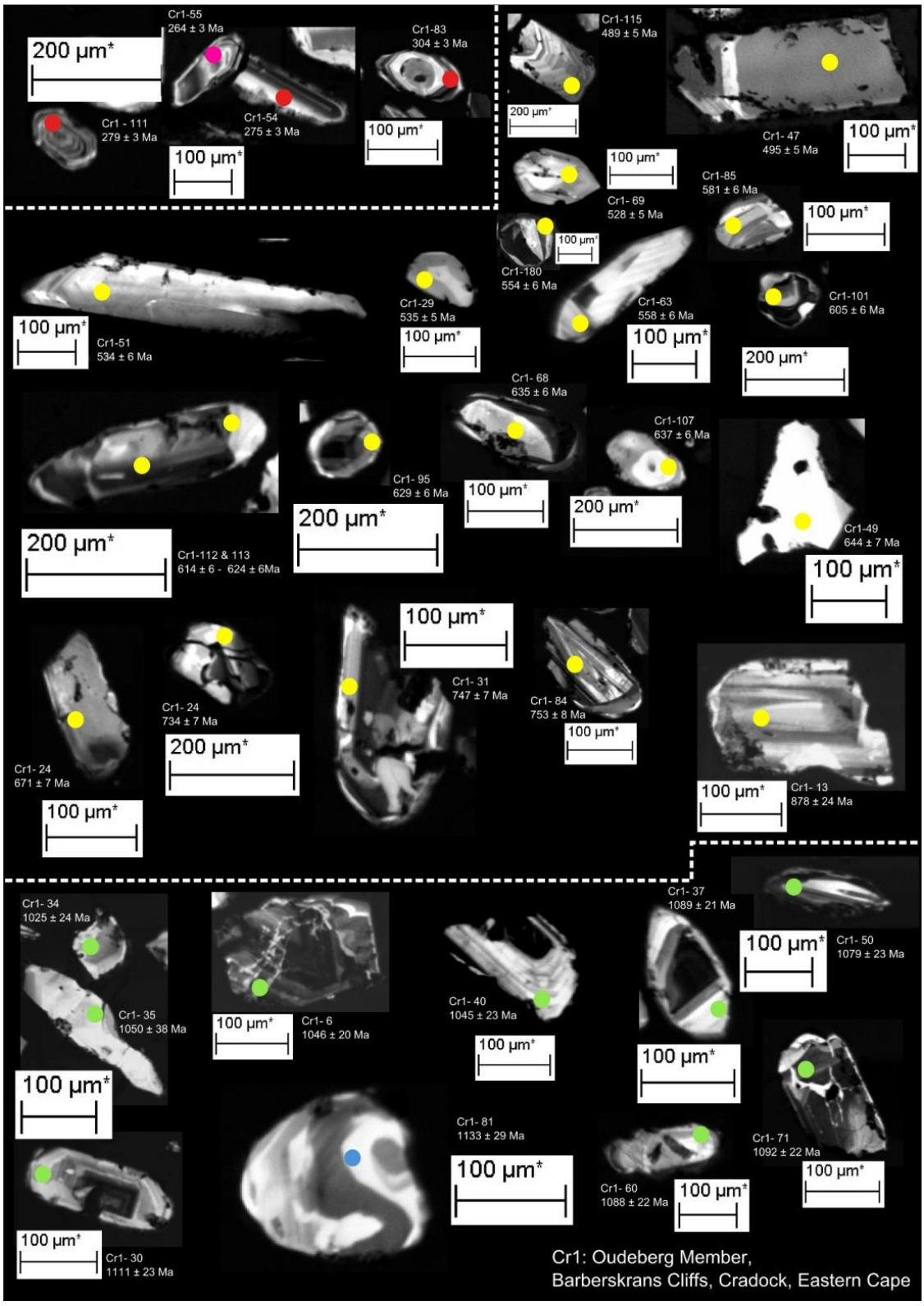

Figure 3.39: Cathode luminescence SEM images showing the internal textures of a selection of detrital grains from sample PV-Cr1 from the Oudeberg Member (N10 Highway, Cradock) (see Appendix 1A for all of the zircons used to characterize the sample). Dots indicate ablation spots. Red spots yielded aged belonging to the youngest population (264 ± 3 to 304 ± 3 Ma), yellow and green the intermediate aged populations (489 ± 5 Ma to 878 ± 24 Ma, and 1008 ± 22 and 1133 ± 29 Ma respectively). The blue dot indicates the oldest zircon identified with an age of 1133 ± 29 Ma. The pink dot indicates the youngest zircon identified with an age of 264 ± 3 Ma.

The youngest zircon grain in the sample has an age of 264 ± 3 Ma (Table 3.4) with a discordance of 1.97% and a Th/U ratio of 0.60 (ablation pit Cr1-55, Appendix 1A) and represents the upper age limit of the youngest zircon population, which was also the least prominent. An igneous zircon with an age 304 ± 3 Ma (6.46 discordant, ablation pit Cr1-83, Th/U of 0.46, Appendix 1A) represents the population's lower age limit. Zircon grains with the ages of 878 ± 24 (8.4% discordant, Th/U of 0.20, ablation pit Cr1-13) and 1133 ± 29 (2.5% discordant, Th/U of 0.31, ablation pit Cr1-81) define the upper and lower boundaries of the oldest population.

The two younger populations show similarity concerning internal and external characteristics of the grains with elongate, euhedral grains (Table 3.4, Figure 3.39). The only difference is that the intermediate population (489 ± 5 Ma to 878 ± 24 Ma) has more elongate grains that are broken or fragmentary, and there are some spherical and has well-rounded grains. Sector zoning is also more common in this population. The oldest population (1008 ± 22 and 1133 ± 29 Ma) is dominantly fragmentary and well-rounded grains that exhibit oscillatory and sector zoning (Figure 3.39).

Section 2: Lower Clifton farm, Baviaansriver Valley, Eastern Cape

The sandstone rock sample from the RM (PV-LC) from Lower Clifton farm (section 2) in the Baviaansrivier Valley, Eastern Cape produced 73 zircon grains that have a discordance of less than 10% from a total of 110 grains analysed (Figure 3.40, Table 3.4). The most prominent zircon population in the sample ranges between 251 ± 5 Ma and 315 ± 6 Ma, a total of 42 grains or 58% of the total sample. The second most prominent population ranges from 487 ± 10 Ma to 845 ± 25 Ma, a total of 16 grains or 22% of the total sample. The third most prominent population ranges from 948 ± 25 Ma to 1137 ± 25 Ma, a total of 6 grains or 8 % of the total sample.

The youngest population (251 ± 5 Ma and 315 ± 6 Ma) consists mainly of euhedral grains with oscillatory zoning, although sector zoning is also observed, sometimes in association with oscillatory zoning (Table 3.4, Figure 3.41). The second youngest population (487 ± 10 Ma to 845 ± 25 Ma) consists of more broken or fragmentary grains that are well-rounded, and there are some spherical and well-rounded grains. Sector zoning is also more common in this population.

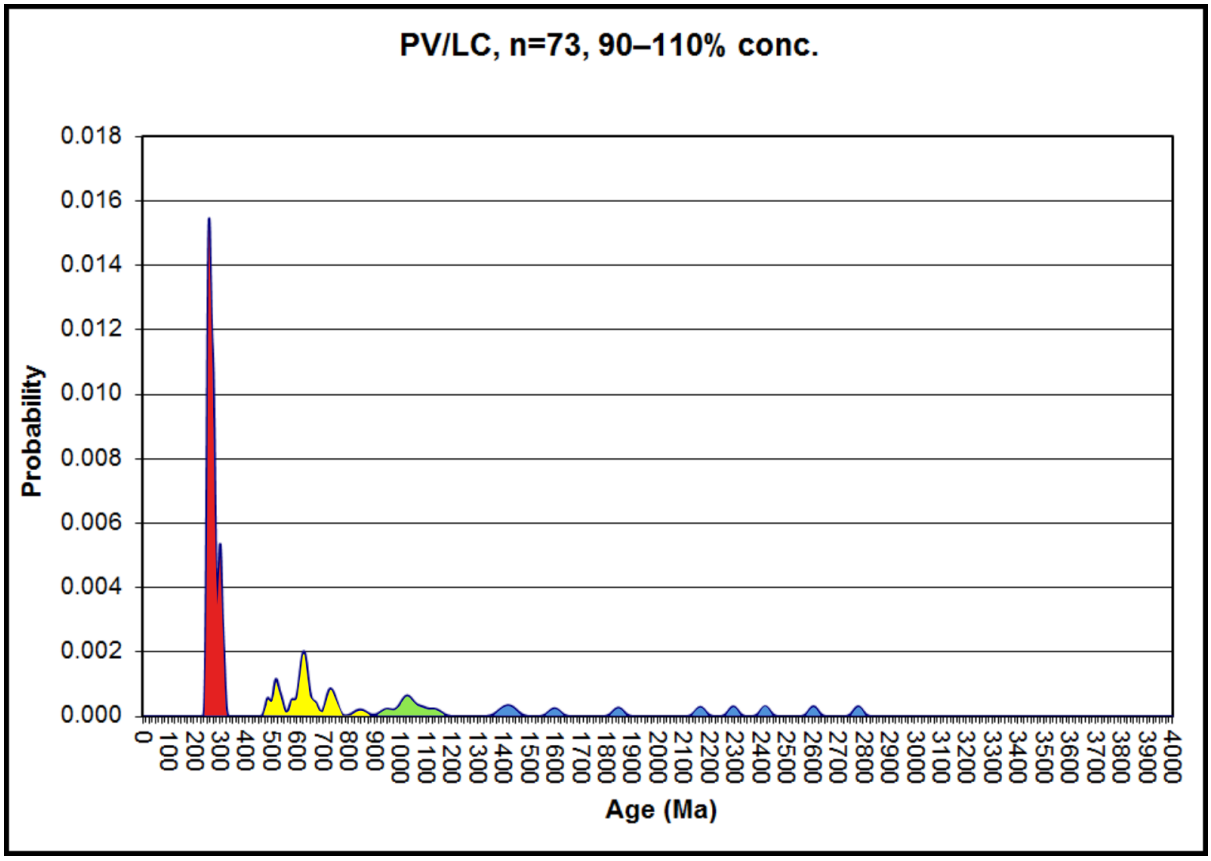

Figure 3.40: Probability density plot for sample PV-LC from the Ripplemead member (Lower Clifton, Baviaansrivier Valley) revealing one very prominent zircon age population which is also the youngest population, ranging between 251 ± 5 Ma and 315 ± 6 Ma (42 grains). The other three populations range in ages between 487 ± 10 Ma to 845 ± 25 Ma (16 grains), 948 ± 25 Ma to 1137 ± 25 Ma (6 grains), and finally the oldest population with 4 grains ranging in ages between 1402 ± 26 and 1848 ± 20 Ma and 5 grains ranging in ages between 2167 ± 19 and 2780 ±18 Ma.

The second oldest population (948 ± 25 Ma to 1137 ± 25 Ma) is dominantly well-rounded grains that exhibit sector zoning. The grains from the oldest populations 1402 ± 26 and 1848 ± 20 Ma and 2167 ± 19 and 2780 ±18 Ma) are either well rounded or angular fragments of once larger grains. Sector and oscillatory zoning observed.

The youngest zircon grain in the sample has an age of 251 ± 5 Ma (Table 3.4) with a discordance of 4.2 % and a Th/U ratio of 0.44 (ablation pit LC-7, Appendix 1B) and represents the upper age limit of the youngest zircon population, which is also the most prominent population. A zircon grain with the age 315 ± 6 Ma (8.8% discordant, ablation pit LC-19, Th/U of 0.97, Appendix 1B) represents the population's lower age limit. Zircon grains with the ages of 2167 ± 19 (0 % discordant, Th/U of 0.50, ablation pit LC-79) and 2780 ± 18 (3.1 % discordant, Th/U of 0.41, ablation pit LC-61) define the upper and lower boundaries of the oldest population.

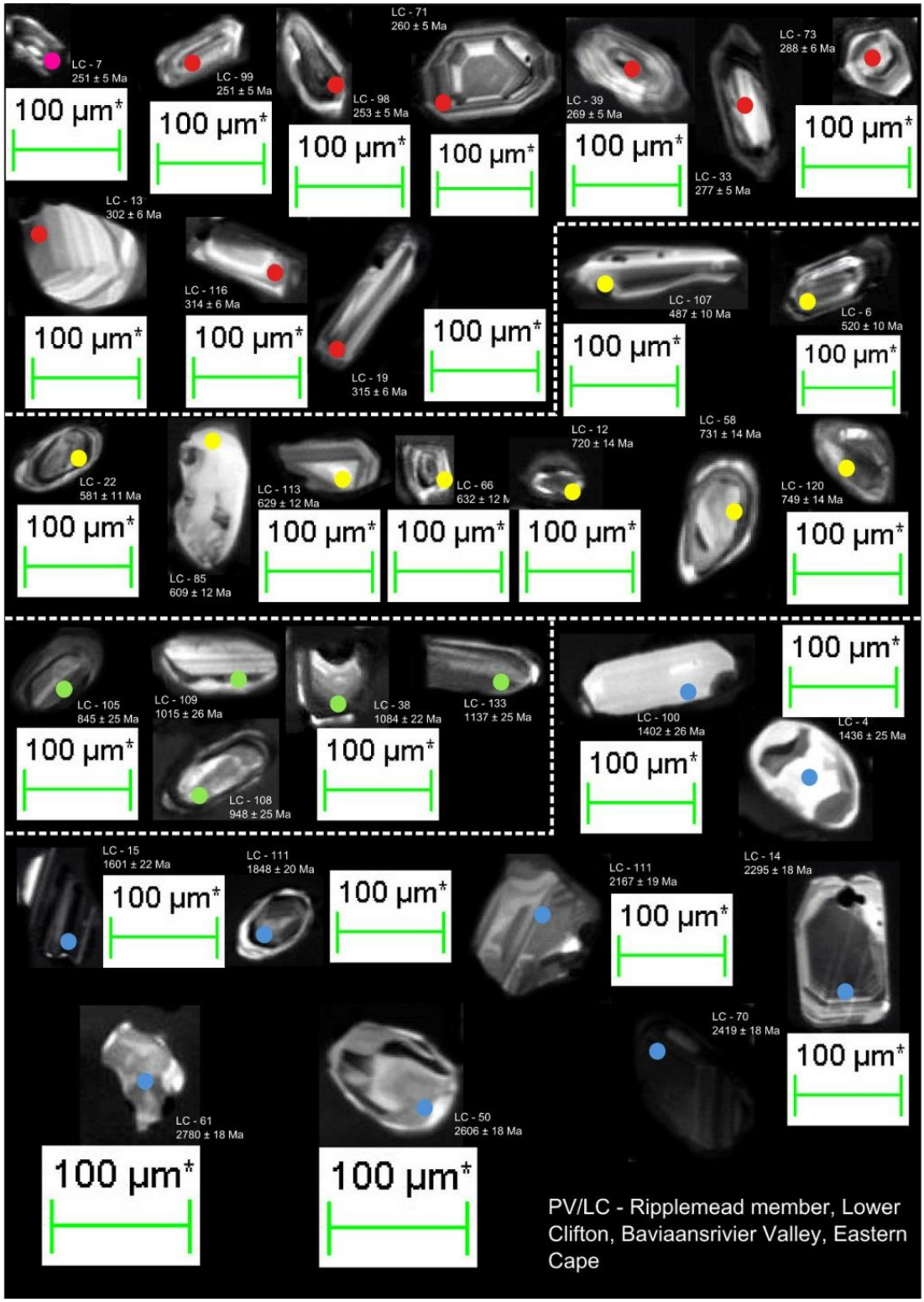

Figure 3.41: Cathode luminescence SEM images showing the internal textures of a selection of detrital grains from sample PV-LC from the Ripplemead member (Lower Clifton, Baviaansrivier Valley) (see Appendix 1B for all of the zircons used to characterize the sample). Red spots yielded aged belonging to the youngest population (251 ± 5 Ma and 315 ± 6 Ma), yellow and green the intermediate aged populations (487 ± 10 Ma to 845 ± 25 Ma; and 948 ± 25 Ma to 1137 ± 25 Ma respectively). The blue dots indicates the oldest zircon populations that range ages between 1402 ± 26 and 1848 ± 20 Ma and 2167 ± 19 and 2780 ±18 Ma. The youngest zircon (pink dot) is 251 ± 5 Ma.

Nieu Bethesda

Section 3: Doornplaats farm, Graaff-Reinet, Eastern Cape

The sandstone rock sample from the RM (PV-NbDo1) from the highest point on Doornplaats farm (section 3), Eastern Cape produced 104 zircon grains that have a discordance of less than 10% from a total of 119 grains analysed (Figure 3.42, Table 3.4). The most prominent zircon population in the sample ranges between 255 ± 3 Ma and 324 ± 4 Ma, a total of 66 grains or 64% of the total sample. The second most prominent populations range from 439 ± 5 Ma to 675 ± 7 Ma, a total of 16 grains or 15 % of the total sample; and 981 ± 37 Ma to 1213 ± 23 Ma, 16 grains or 15 % of the total sample. The oldest populations in the sample range from ages between 1443 ± 24 to 1774 ± 21 Ma, a total of 4 grains (4% of total sample); and 2756 ± 18 to 2760 ± 20 Ma, a total of 2 grains (2% of total sample).

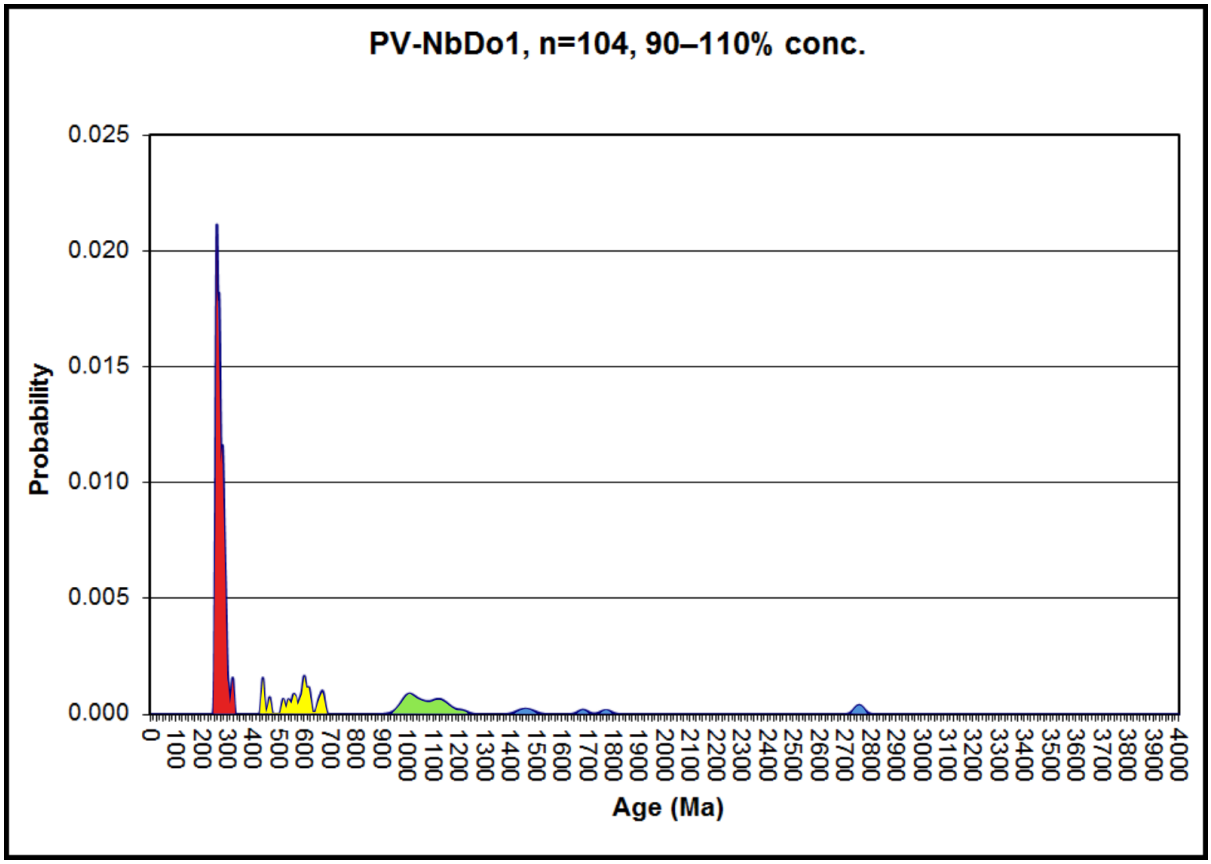

Figure 3.42: Probability density plot for sample PV-NbDo1 from the Ripplemead member (Doornplaats, Nieu Bethesda) revealing one very prominent zircon age population which is also the youngest population, ranging between 255 ± 3 Ma and 324 ± 4 Ma (66 grains). The other three populations range in ages between 439 ± 5 Ma to 675 ± 7 Ma (16 grains), 981 ± 37 Ma to 1213 ± 23 Ma (16 grains). The third and oldest population ranges from ages between 1443 ± 24 to 1774 ± 21 Ma (4 grains) and 2756 ± 18 to 2760 ± 20 Ma (2 grains).

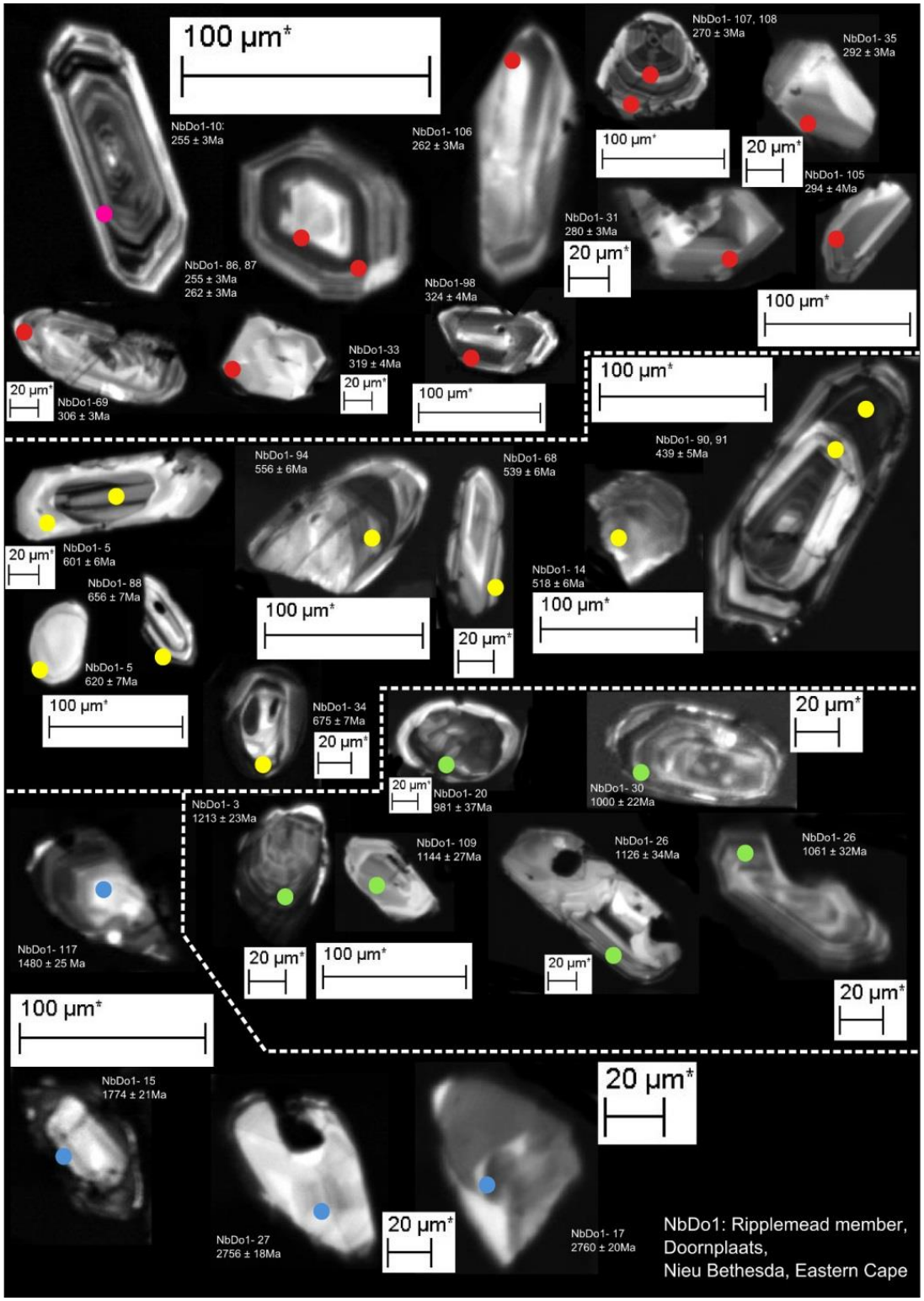

Figure 3.43: Cathode luminescence SEM images showing the internal textures of a selection of detrital grains from sample PV-NbDo1 from the Ripplemead member (Doornplaats, Nieu Bethesda) (see Appendix 1C for all of the zircons used to characterize the sample). Red spots yielded aged belonging to the youngest population (255 ± 3 Ma and 324 ± 4 Ma), yellow and green the intermediate aged populations (439 ± 5 Ma to 675 ± 7 Ma and 981 ± 37 Ma to 1213 ± 23 Ma). The blue dots indicates the oldest zircon populations that range in ages between 1443 ± 24 to 1774 ± 21 Ma and 2756 ± 18 to 2760 ± 20 Ma. The youngest zircon (pink dot) is 255 ± 3 Ma.

The youngest zircon grain in the sample has an age of 255 ± 3 Ma (Table 3.4) with a discordance of 0 % and a Th/U ratio of 0.60 (ablation pit A-27, Appendix 1C) and represents the upper age limit of the youngest zircon population, which is also the most prominent population. The lower age limit of the youngest population is defined by a zircon grain with an age of 324 ± 4 Ma (8.7% discordant, ablation pit A-120, Th/U of 0.19, Appendix 1C. Zircon grains with the ages of 2756 ± 18 (0 % discordant, Th/U of 0.55, ablation pit A-34) and 2760 ± 20 (4.2 % discordant, Th/U of 0.34, ablation pit A-24) define the upper and lower boundaries of the oldest population.

The youngest population (255 ± 3 Ma and 324 ± 4 Ma) are elongate, euhedral grains exhibiting oscillatory zoning (Table 3.4, Figure 3.43). The second youngest population (439 ± 5 Ma to 675 ± 7 Ma and 981 ± 37) are similar to the previous population, only there are more rounded grains in the population. Some are broken fragments of once larger grains. The second oldest population (981 ± 37 Ma to 1213 ± 23 Ma) consists of elongate and rounded grains with oscillatory zoning, sector zoning, or both. Many are damaged grains with chips or pieces missing. The grains from the oldest populations (1443 ± 24 to 1774 ± 21 Ma and 2756 ± 18 to 2760 ± 20 Ma) are mostly fragmentary with some showing poor evidence of oscillatory zoning.

Beaufort West

Section 6: Highlands farm, Beaufort West, Western Cape

This rock sample (PV-H1) is from the base of the Javanerskop member, upper Teekloof Formation, Highlands farm (section 6) near Beaufort West, Western Cape. This sample produced 44 zircon grains that have a discordance of less than 10% from a total of 84 grains analysed (Figure 3.44, Table 3.4). The most prominent zircon population in the sample ranges between 226 ± 3 Ma and 316 ± 3 Ma, a total of 23 grains or 52 % of the total sample. In joint second the next most prominent populations range from 399± 4 Ma to 870 ± 26 Ma, a total of 13 grains or 29.5 % of the total sample; and 1044 ± 22 Ma to 1308 ± 23 Ma, 5 grains or 11.5 % of the total sample. The oldest population in the sample consists of 3 grains that range in age between 1943 ± 18 Ma and 2102 ± 18 Ma (7 % of total sample).

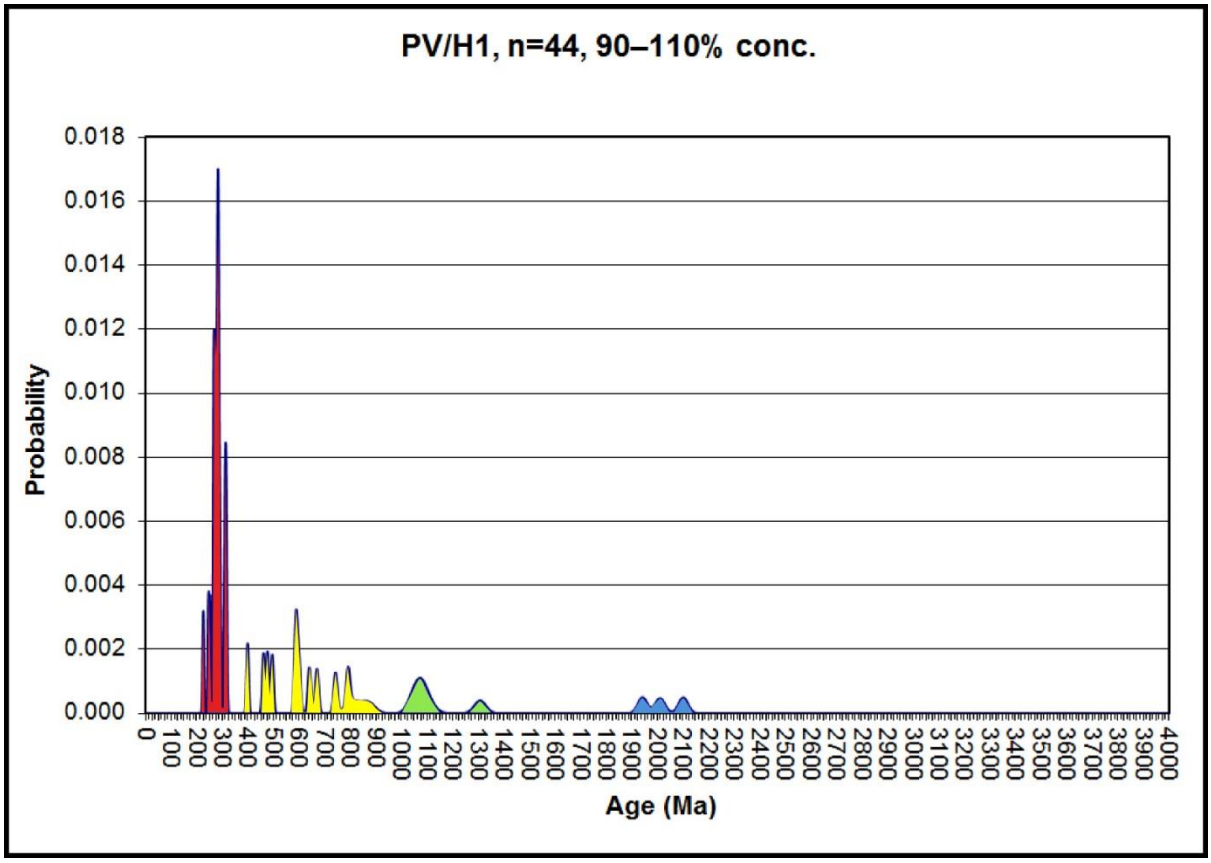

Figure 3.44: Probability density plot for sample PV-H1 from the Javanerskop member (Highlands, Beaufort West) revealing three prominent zircon age populations which range between 226 ± 3 Ma to 316 ± 3 Ma (23 grains), 399± 4 Ma to 870 ± 26 Ma (13 grains), and 1044 ± 22 Ma to 1308 ± 23 Ma (5 grains). The oldest population consists of 3 grains that range in age between 1943 ± 18 Ma and 2102 ± 18 Ma respectively.

The youngest zircon grain in the sample (226 ± 3 Ma) (Table 3.4) has a discordance of 2.3 %, Th/U ratio of 0.87 (ablation pit A-059, Appendix 1H), and represents the upper age limit of the youngest zircon population. It is a very young grain (Early Triassic) which is not expected in Upper Permian strata. An explanation for the young grains is discussed in Chapter 5.4. The lower age limit of the youngest population is defined by a zircon grain with an age of 316 ± 3 Ma (9.5 % discordant, ablation pit A-006, Th/U of 0.76, Appendix 1H. The oldest zircon grain is dated to 2102 ± 18 Ma (0.7 % discordant, Th/U of 0.62, ablation pit A-004) defines the lower boundary of the oldest population.

The youngest grains (226 ± 3 Ma to 316 ± 3 Ma) are mostly euhedral prisms that are sometimes chipped or broken and show mainly oscillatory zoning (Table 3.4, Figure 3.45). The second youngest population (399± 4 Ma to 870 ± 26 Ma) are mostly broken with some preservation of their euhedral shape and sector zoning. The second oldest population (1044 ± 22 Ma to 1308 ± 23 Ma) are mostly fragments of once larger grains. The oldest population (1943 ± 18 Ma to 2102 ± 18 Ma) consist of fragments of once larger grains although one is well rounded.

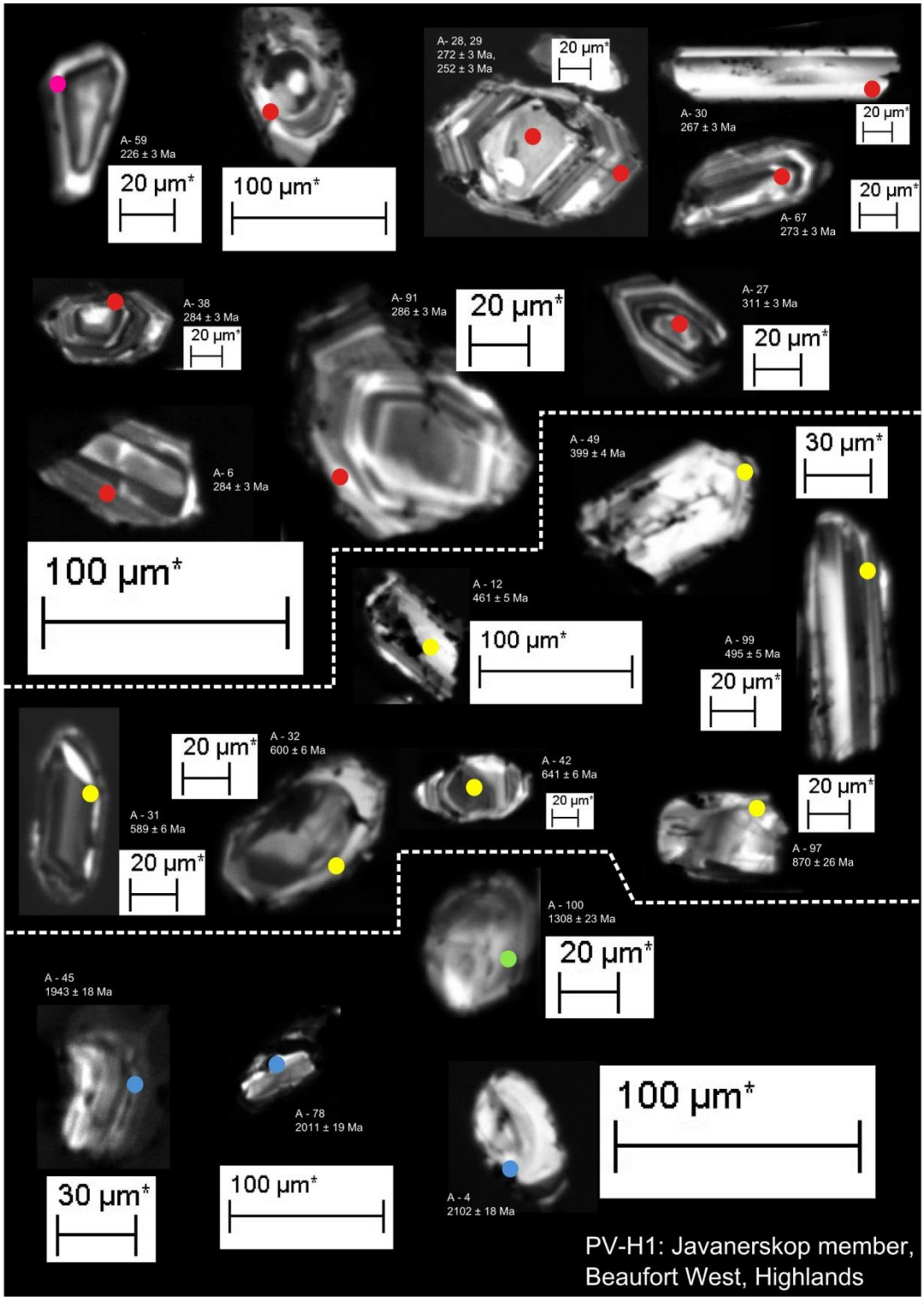

Figure 3.45: Cathode luminescence SEM images showing the internal textures of a selection of detrital grains from sample PV-H1 from the Javanerskop member (Highlands, Beaufort West) (see Appendix 1H for all of the zircons used to characterize the sample). Red spots yielded aged belonging to the youngest population (226 ± 3 Ma to 316 ± 3 Ma), yellow and green the intermediate aged populations (399± 4 Ma to 870 ± 26 Ma and 1044 ± 22 Ma to 1308 ± 23 Ma). The blue dots indicate the oldest zircon population that consists of 3 grains that range in age between 1943 ± 18 Ma and 2102 ± 18 Ma. The youngest zircon (pink dot) is 226 ± 3 Ma.

Section 7: Javanerskop, Oukloof Pass, Northern Cape

This rock sample (PV-Javanerskop) is from the base of the Javanerskop member, upper Teekloof Formation from Javanerskop (section 7) in Oukloof Pass near Beaufort West, Western Cape. This sample produced 61 zircon grains that have a discordance of less than 10% from a total of 101 grains analysed (Figure 3.46, Table 3.4). The most prominent zircon population in the sample ranges between 255 ± 5 Ma and 321 ± 6 Ma, a total of 35 grains or 57 % of the total sample. The second most prominent population ranges in age between 364± 47 Ma to 869 ± 22 Ma, a total of 14 grains or 23 % of the total sample. The third most prominent population ranges in age between and 1040 ± 24 Ma to 1253 ± 29 Ma, 10 grains or 15 % of the total sample. The oldest population in the sample consists of 3 grains that range in age between 2026 ± 22 Ma and 2803 ± 17 Ma (5 % of total sample).

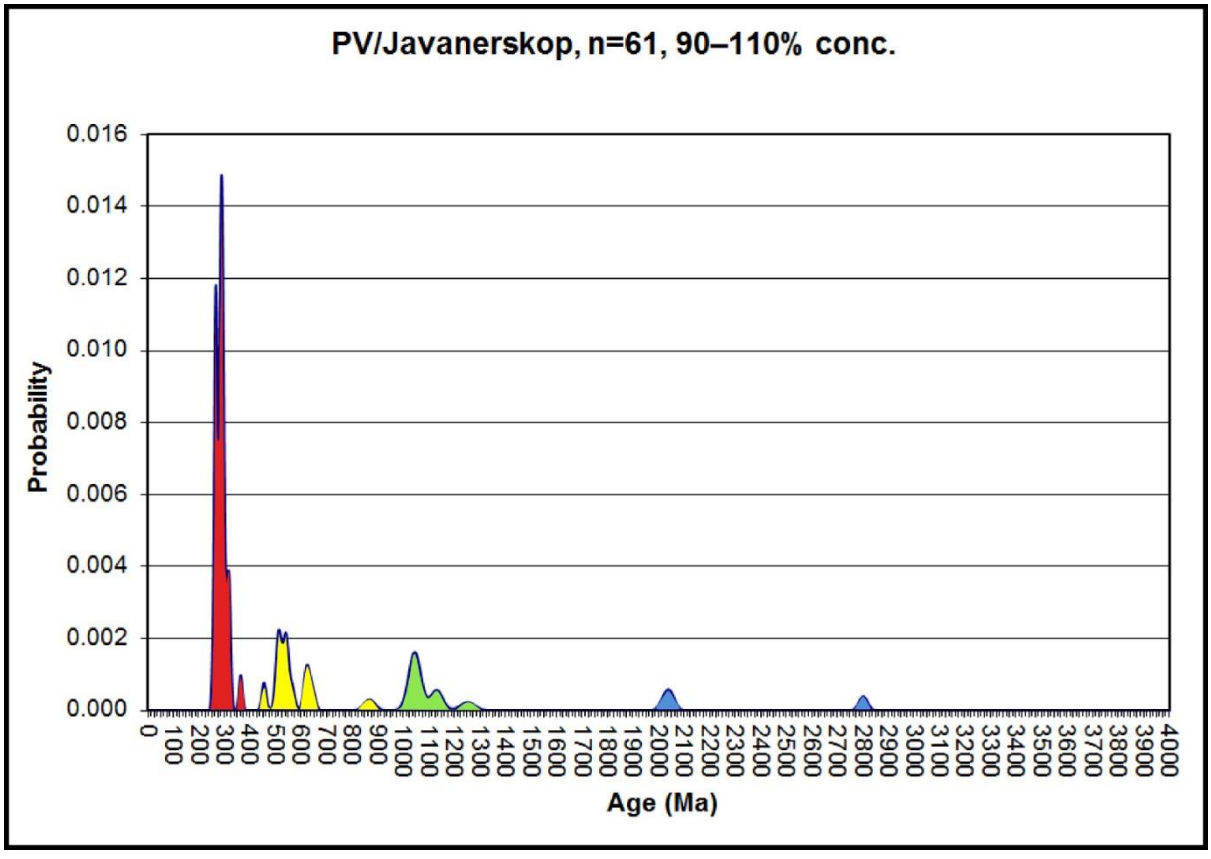

Figure 3.46: Probability density plot for sample PV-Javanerskop from the Javanerskop member (Oukloof Pass, Fraserburg) revealing three prominent zircon age populations which range between 255 ± 5 Ma to 321 ± 6 Ma (35 grains), 364± 47 Ma to 869 ± 22 Ma (14 grains), and 1040 ± 24 Ma to 1253 ± 29 Ma (9 grains). The oldest population consists of 3 grains that range in age between 2026 ± 22 Ma and 2803 ± 17 Ma.

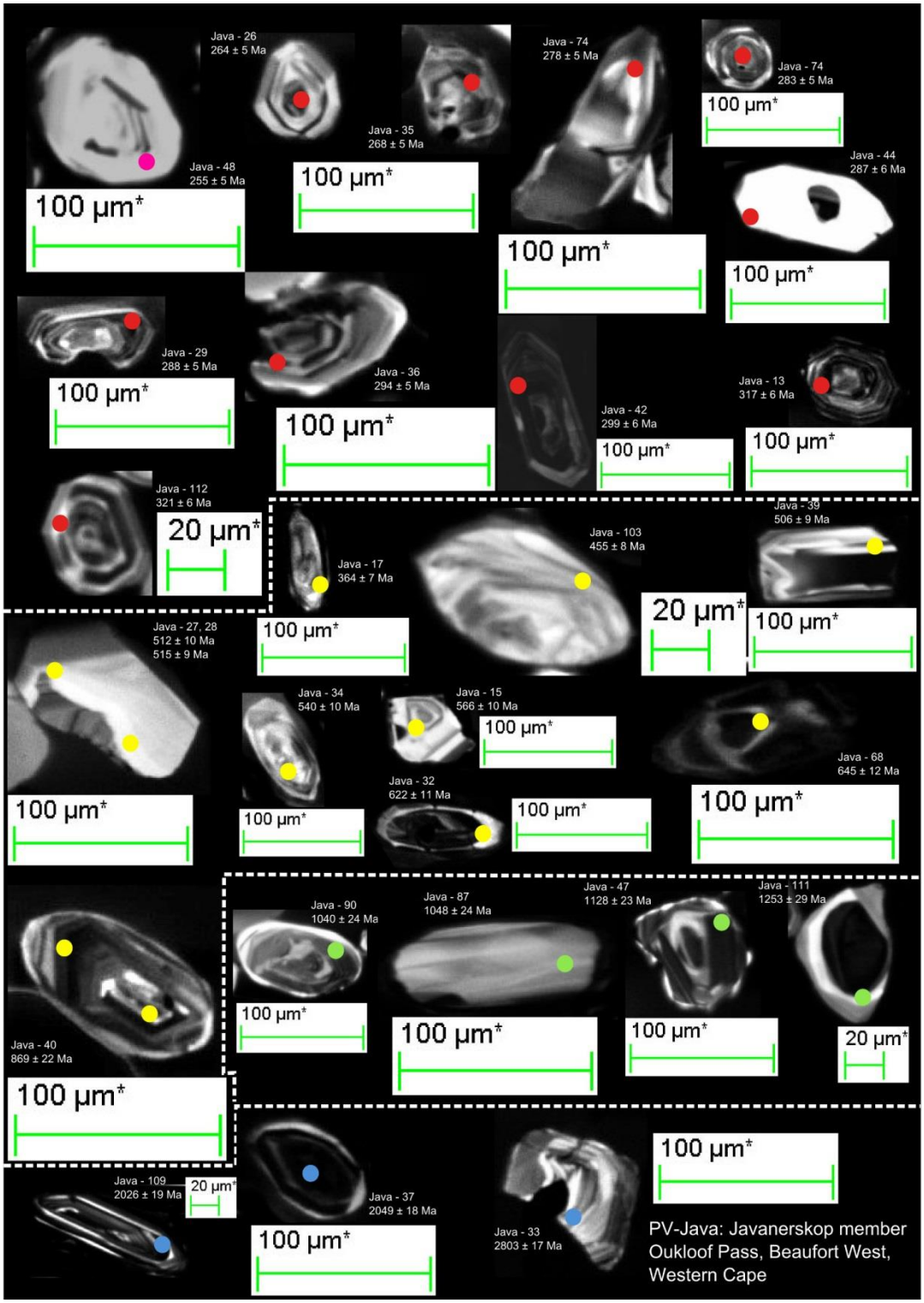

Figure 3.47: Cathode luminescence SEM images showing the internal textures of a selection of detrital grains from sample PV-Javanerskop from the Javanerskop member (Oukloof Pass, Fraserburg) (see Appendix 1I for all of the zircons used to characterize the sample). Red spots yielded aged belonging to the youngest population (255 ± 5 Ma to 321 ± 6 Ma), yellow and green the intermediate aged populations (364± 47 Ma to 869 ± 22 Ma and 1040 ± 24 Ma to 1253 ± 29 Ma). The blue dots indicate the oldest zircon population that consists of 3 grains that range in age between 2026 ± 22 Ma and 2803 ± 17 Ma. The youngest zircon (pink dot) is 255 ± 5 Ma.

The youngest zircon grain in the sample (255 ± 5 Ma) (Table 3.4) has a discordance of 8.7 %, Th/U ratio of 0. 75 (ablation pit Java-48, Appendix 1I), and represents the upper age limit of the youngest zircon population. The lower age limit of the youngest population is defined by a zircon grain with an age of 321 ± 6 Ma (0.62 % discordant, ablation pit Java-112, Th/U of 0.50, Appendix 1I. The oldest zircon grain is dated to 2803 ± 17 Ma (0 % discordant, Th/U of 0.99, ablation pit Java-33) defines the lower boundary of the oldest population.

The youngest population (255 ± 5 Ma to 321 ± 6 Ma) are mostly short spherical prisms that exhibit sector and oscillatory zoning (Table 3.4, Figure 3.47). The second youngest population (364± 47 Ma to 869 ± 22 Ma) are mostly well rounded grains with oscillatory and sector zoning. The second oldest population (1040 ± 24 Ma to 1253 ± 29 Ma) are mostly well rounded grains with oscillatory and sector zoning. The oldest population (2026 ± 22 Ma and 2803 ± 17 Ma) consist of one spherical and one elongate grain with oscillatory zoning. The third grain is an angular fragment with no internal features visible.

Gariep Dam

Section 9: Inhoek farm, Gariep Dam, Free State Province

The sandstone rock sample from the RM (PV-BMIn1) from Inhoek farm (section 9), Gariep Dam in the Free State Province produced 69 zircon grains that have a discordance of less than 10% from a total of 103 grains analysed (Figure 3.48, Table 3.4). The most prominent zircon population in the sample ranges between 250 ± 5 Ma and 306 ± 6 Ma, a total of 41 grains or 60% of the total sample. The second and third most prominent populations range from 373 ± 7 Ma to 666 ± 12 Ma, a total of 18 grains or 26 % of the total sample; and 1048 ± 22 Ma to 1280 ± 21 Ma, 7 grains or 10 % of the total sample. The oldest population in the sample ranges from ages between 1634 ± 20 Ma to 2450 ± 17 Ma, a total of 3 grains (4% of total sample).

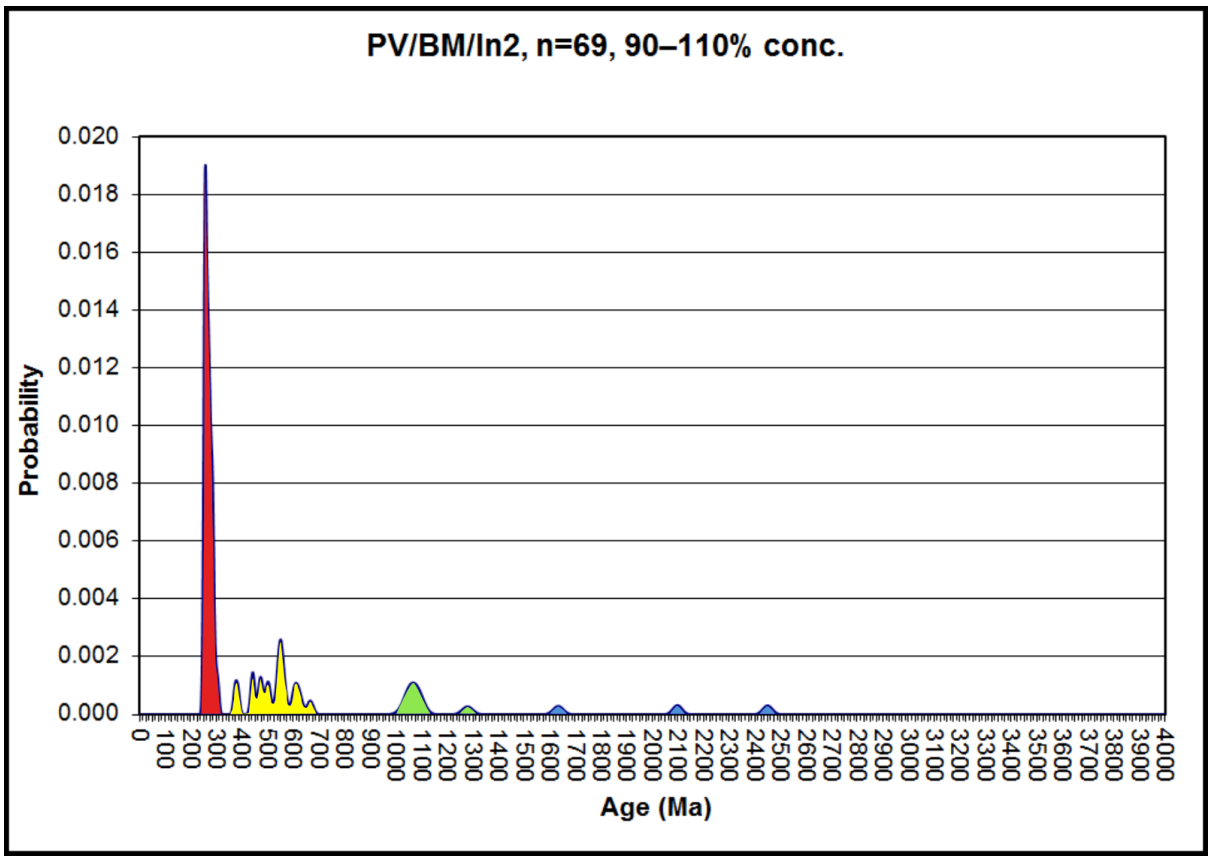

Figure 3.48: Probability density plot for sample PV-BMIn2 of the Ripplemead member (Inhoek, Gariep Dam) revealing one very prominent zircon age population which is also the youngest population, ranging between 250 ± 5 Ma and 306 ± 6 Ma (41 grains). The other three populations range in ages between 373 ± 7 Ma to 666 ± 12 Ma (18 grains) and 1048 ± 22 Ma to 1280 ± 21 Ma (7 grains). The third and oldest population ranges from ages between 1634 ± 20 Ma to 2450 ± 17 Ma (13 grains).

The youngest zircon grain in the sample has an age of 250 ± 5 Ma (Table 3.4) with a discordance of 4.3 % and a Th/U ratio of 1.83 (ablation pit BM/In2-67, Appendix 1D) and represents the upper age limit of the youngest zircon population, which is also the most prominent population. The lower age limit of the youngest population is defined by a zircon grain with an age of 306 ± 6 Ma (0 % discordant, ablation pit BM/In2-67, Th/U of 0.50, Appendix 1D. Zircon grains with the ages of 1634 ± 20 Ma (7 % discordant, Th/U of 0.35, ablation pit BM/In2-80) and 2450 ± 17 Ma (4.2 % discordant, Th/U of 0.42, ablation pit BM/In2-102) define the upper and lower boundaries of the oldest population. The youngest population (250 ± 5 Ma and 306 ± 6 Ma) are mostly euhedral grains but show a range of shapes and sizes (Table 3.4, Figure 3.49). The second youngest population (373 ± 7 Ma to 666 ± 12 Ma) does not have many euhedral grains and most or well-rounded grains. Sector and oscillatory zoning is present but sector zoning most commonly encountered. The second oldest population (1048 ± 22 Ma to 1280 ± 21 Ma) consists of elongate and rounded grains with sector zoning. The grains from the oldest populations (1634 ± 20 Ma to 2450 ± 17 Ma) are all rounded fragments of once larger grains, showing oscillatory zoning in two of the grains.

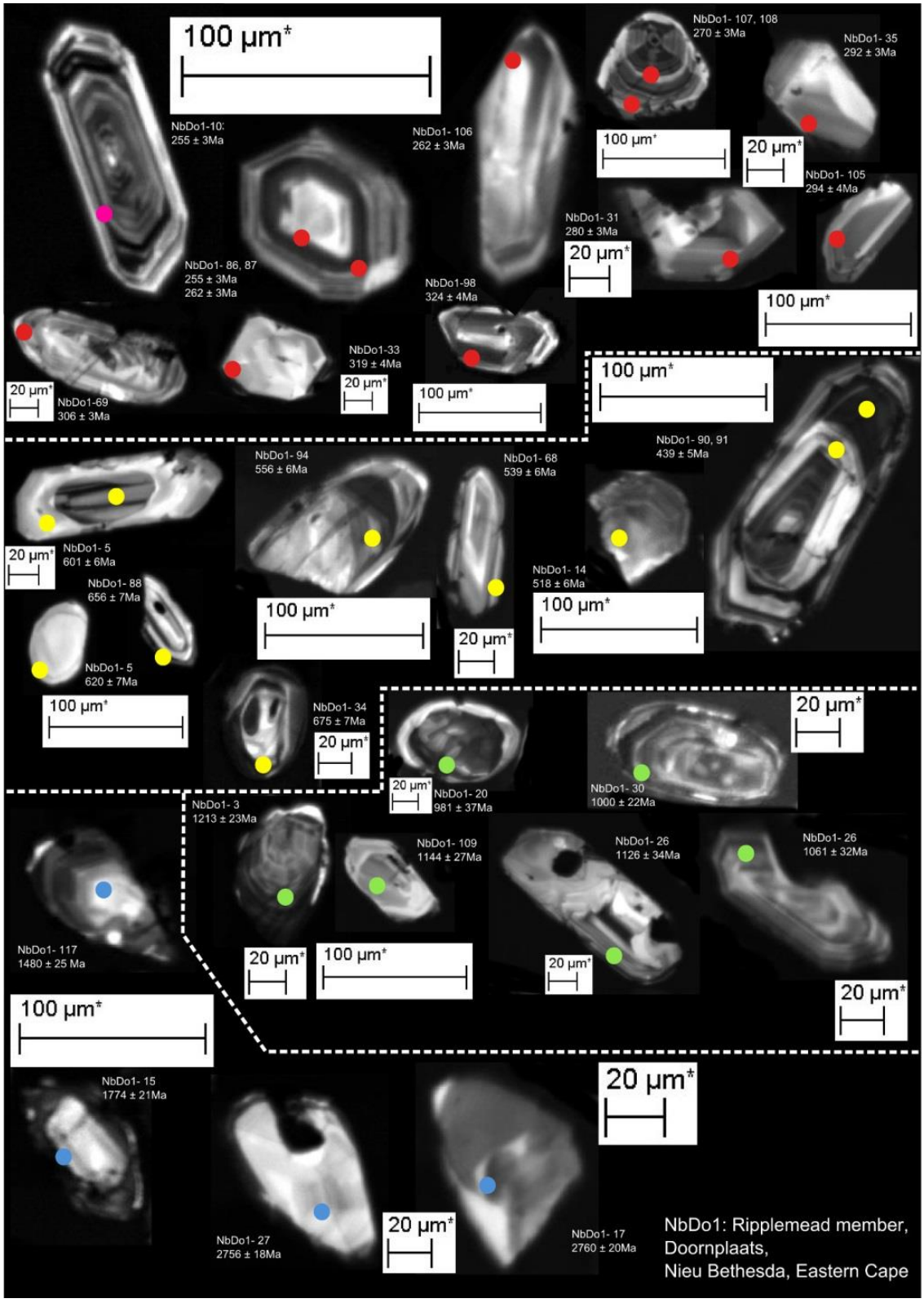

Figure 3.49: Cathode luminescence SEM images showing the internal textures of a selection of detrital grains from sample PV-BMIn2 from the Ripplemead member (Inhoek, Gariep Dam) (see Appendix 1D for all of the zircons used to characterize the sample). Red spots yielded aged belonging to the youngest population (250 ± 5 Ma and 306 ± 6 Ma), yellow and green the intermediate aged populations (373 ± 7 Ma to 666 ± 12 Ma and 1048 ± 22 Ma to 1280 ± 21 Ma). The blue dots indicate the oldest zircon population that ranges in age between 1634 ± 20 Ma to 2450 ± 17 Ma. The youngest zircon (pink dot) is 250 ± 5 Ma.

Springfontein, Free State Province

This rock sample (PV-Sprinfontein) is from the RM that outcrops close to the small town of Springfontein in the Free State Province. This sample produced 84 zircon grains that have a discordance of less than 10% from a total of 108 grains analysed (Figure 3.50, Table 3.4). The most prominent zircon population in the sample ranges between 254 ± 5 Ma and 320 ± 7 Ma, a total of 33 grains or 39.2 % of the total sample. The second and third most prominent populations range from 407 ± 8 Ma to 723 ± 15 Ma, a total of 31 grains or 37 % of the total sample; and 910 ± 25 Ma to 1268 ± 21 Ma, 19 grains or 22.6 % of the total sample. The oldest population in the sample ranges consists of a single grain with an age of 1691 ± 22 Ma (1.2 % of total sample).

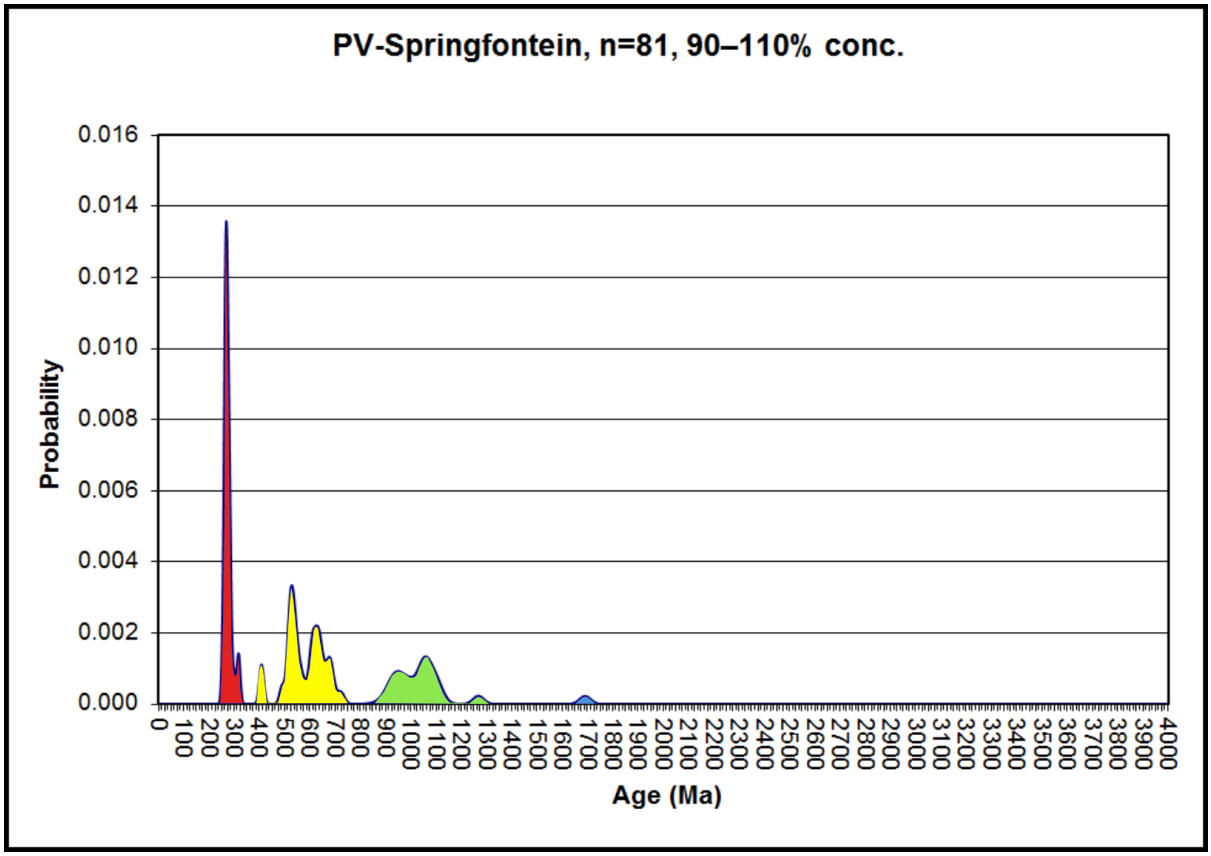

Figure 3.50: Probability density plot for sample PV-Springfontein from the Ripplemead member near Springfontein, Free State Province, revealing two prominent zircon age populations which range between 254 ± 5 Ma and 320 ± 7 Ma (33 grains) and 407 ± 8 Ma to 723 ± 15 Ma (31 grains). The second oldest population consists of 19 grains which range in ages between 910 ± 25 Ma to 1268 ± 21 Ma. The oldest population consists of a single grain with an age of 1691 ± 22 Ma.

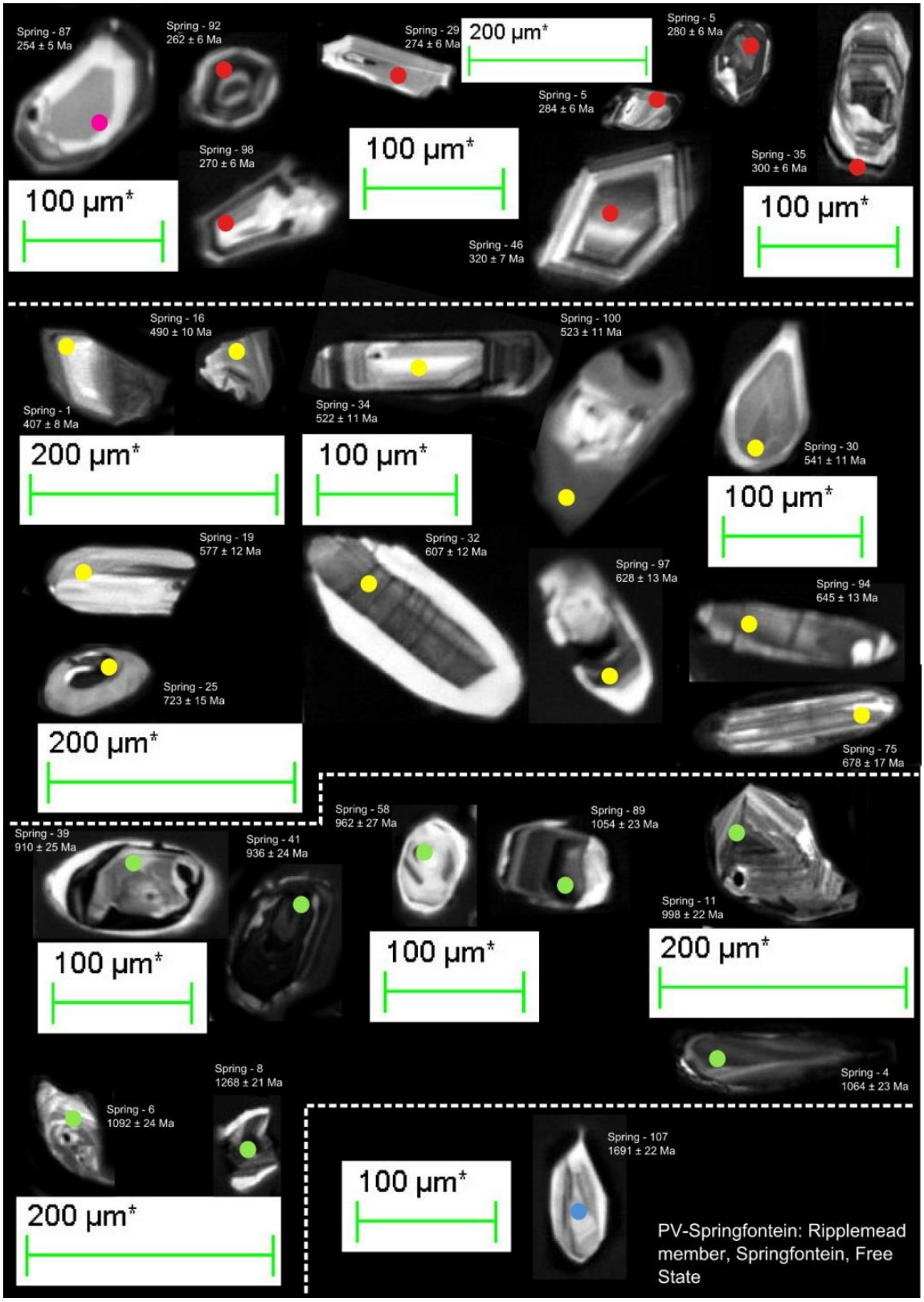

Figure 3.51: Cathode luminescence SEM images showing the internal textures of a selection of detrital grains from sample PV-Springfontein from the Ripplemead member (see Appendix 1E for all of the zircons used to characterize the sample). Red spots yielded aged belonging to the youngest population (254 ± 5 Ma and 320 ± 7 Ma), yellow and green the intermediate aged populations (407 ± 8 Ma to 723 ± 15 Ma and 1048 ± 22 Ma to 1280 ± 21 Ma). The blue dot indicates the oldest zircon population that consists of a single grain with an age of 1691 ± 22 Ma. The youngest zircon (pink dot) is 254 ± 5 Ma.

The youngest zircon grain in the sample has an age of 254 ± 5 Ma (Table 3.4) with a discordance of 8 % and a Th/U ratio of 1.12 (ablation pit SF-87, Appendix 1E) and represents the upper age limit of the youngest zircon population, which is also the most prominent population. The lower age limit of the youngest population is defined by a zircon grain with an age of 320 ± 7 Ma (2.2 % discordant, ablation pit SF-46, Th/U of 0.66, Appendix 1E. The oldest Zircon grain with the age 1691 ± 22 Ma (7 % discordant, Th/U of 0.31, ablation pit SF-107) defines the lower boundary of the oldest population.

The youngest population (254 ± 5 Ma and 320 ± 7 Ma) are mostly euhedral grains which can be elongate or spherical in shape and sector zoning is most common (Table 3.4, Figure 3.51). The second youngest population (407 ± 8 Ma to 723 ± 15 Ma) are mostly elongate, well-rounded grains but some retain some of their euhedral nature. Sector and oscillatory zoning is present. The second oldest population (1048 ± 22 Ma to 1280 ± 21) are mostly well-rounded grains with sector or oscillatory zoning but some are fragments of once larger grains. The grain from the oldest populations (1691 ± 22 Ma) is a rounded fragment of a once larger grain with oscillatory zoning.

Jagersfontein and Bloemfontein

Section 12: Boomplaas Hill, Jagersfontein, Free State Province

This rock sample (PV-J615) is from the Boomplaas sandstone on Boomplaas Hill (section 12) near Jagersfontein in the Free State Province. This sample produced 100 zircon grains that have a discordance of less than 10% from a total of 122 grains analysed (Figure 3.52, Table 3.4). The most prominent zircon population is in the sample range between 477 ± 8 Ma and 819 ± 28 Ma, a total of 43 grains or 43 % of the total sample. The second and third most prominent populations range from 908 ± 24 Ma to 1252 ± 22 Ma, a total of 41 grains or 41 % of the total sample; and 252 ± 4 Ma to 339 ± 5 Ma, 12 grains or 12 % of the total sample. The oldest population in the sample ranges consists of 3 grains with an age range between 1753 ± 21 to 2712 ± 18 Ma (4 % of total sample).

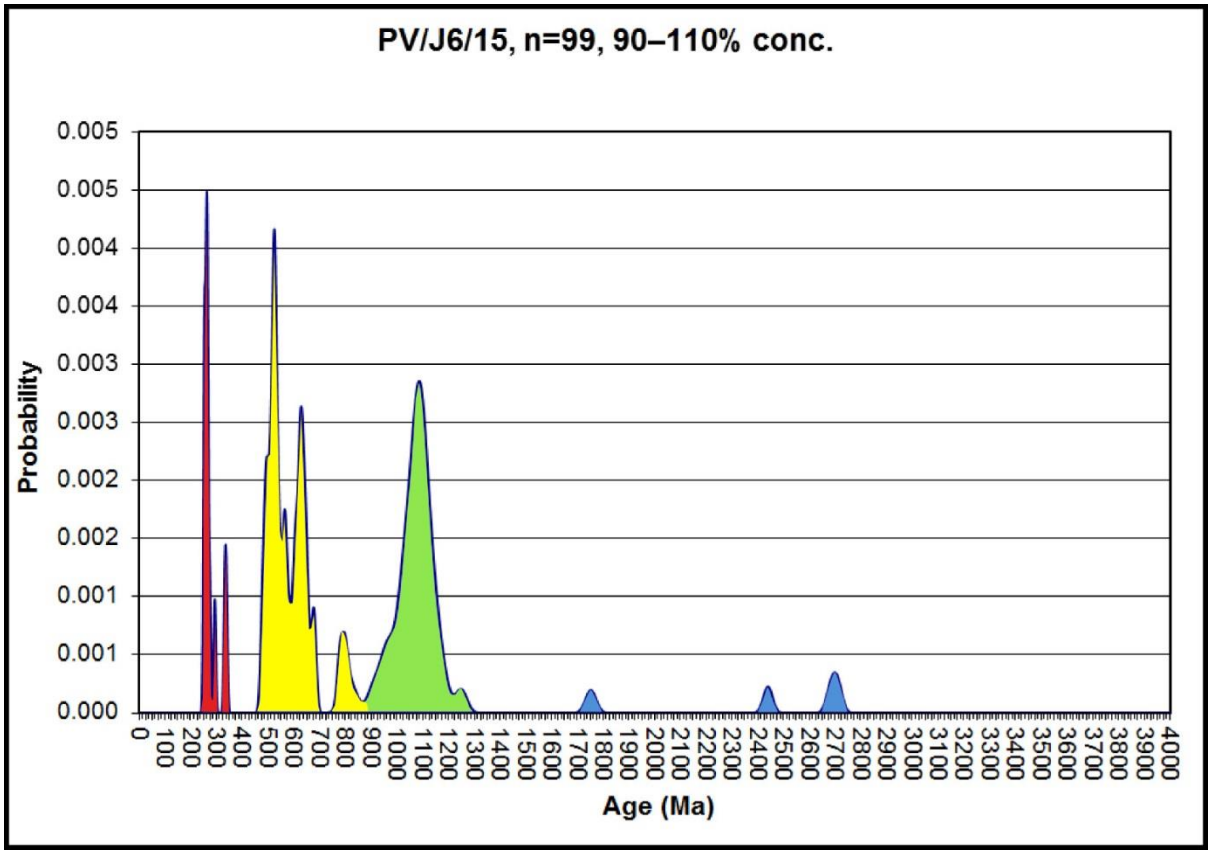

Figure 3.52: Probability density plot for sample PV-J615 from the Boomplaas sandstone (Boomplaas Hill, Jagersfontein) revealing three prominent zircon age populations which range between 477 ± 8 Ma and 819 ± 28 Ma (43 grains), 908 ± 24 Ma to 1252 ± 22 Ma (41 grains), and 252 ± 4 Ma to 339 ± 5 Ma (12 grains). The oldest population consists of 3 grains which range in ages between 1753 ± 21 to 2712 ± 18 Ma.

The youngest zircon grain in the sample has an age of 252 ± 4 Ma (Table 3.4) with a discordance of 3.1 % and a Th/U ratio of 0.67 (ablation pit 15-5, Appendix 1F) and represents the upper age limit of the youngest zircon population. The lower age limit of the youngest population is defined by a zircon grain with an age of 339 ± 5 Ma (4.9 % discordant, ablation pit 15-81, Th/U of 0.08, Appendix 1F. The oldest zircon grain with the age 2712 ± 18 Ma (0 % discordant, Th/U of 0.37, ablation pit 15-41) defines the lower boundary of the oldest population.

The youngest population (252 ± 4 Ma to 339 ± 5 Ma) are mostly euhedral prismatic grains with oscillatory and sector zoning (Table 3.4, Figure 3.53). The second youngest population (477 ± 8 Ma and 819 ± 28 Ma) are mostly elongate euhedral grains with sector and oscillatory zoning. The second oldest population (908 ± 24 Ma to 1252 ± 22 Ma) are either prismatic or well-rounded grains with sector or oscillatory zoning, sometimes in the same grain. Some are fragments of once larger grains. The grains from the oldest population (1753 ± 21 to 2712 ± 18 Ma) are prisms with some of their euhedral nature preserved, although one is a fragment of a once larger grain. Two of the grains show oscillatory zoning and one shows both in the same grain.

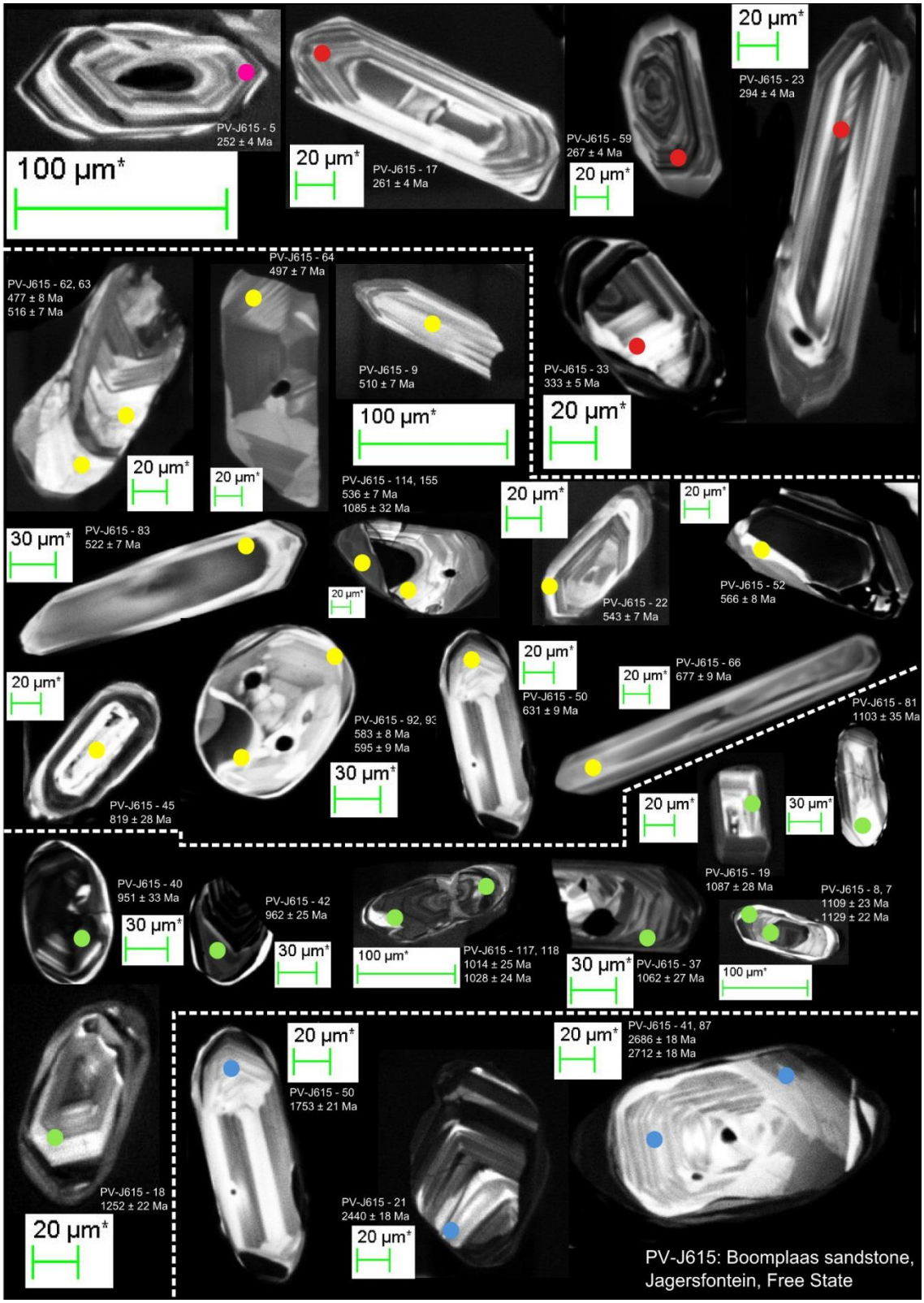

Figure 3.53: Cathode luminescence SEM images showing the internal textures of a selection of detrital grains from sample PV-J615 from the Boomplaas sandstone (Boomplaas Hill, Jagersfontein) (see Appendix 1F for all of the zircons used to characterize the sample). Red spots yielded aged belonging to the youngest population (252 ± 4 Ma to 339 ± 5 Ma), yellow and green the intermediate aged populations (477 ± 8 Ma and 819 ± 28 Ma and 908 ± 24 Ma to 1252 ± 22 Ma). The blue dots indicate the oldest zircon population that consists of 3 grains with an age range between 1753 ± 21 to 2712 ± 18 Ma. The youngest zircon (pink dot) is 252 ± 4 Ma.

Section 13: Tafelkop, Bloemfontein, Free State Province

This rock sample (PV-T28m) is from strata assigned to the Musgrave Grit unit (Balfour Formation) on Tafelkop Hill (section 13) near Bloemfontein in the Free State Province. This sample produced 101 zircon grains that have a discordance of less than 10% from a total of 130 grains analysed (Figure 3.54, Table 3.4). The most prominent zircon population in the sample ranges between 248 ± 3 Ma and 325 ± 6 Ma, a total of 70 grains or 69 % of the total sample. The second and third most prominent populations range from 375 ± 4 Ma to 770 ± 8 Ma, a total of 18 grains or 17 % of the total sample; and 941 ± 22 Ma to 1312 ± 23 Ma, 11 grains or 11 % of the total sample. The oldest population in the sample ranges consists of 3 grains that are 1422 ± 21 Ma and 1770 ± 19 Ma respectively (3 % of total sample).

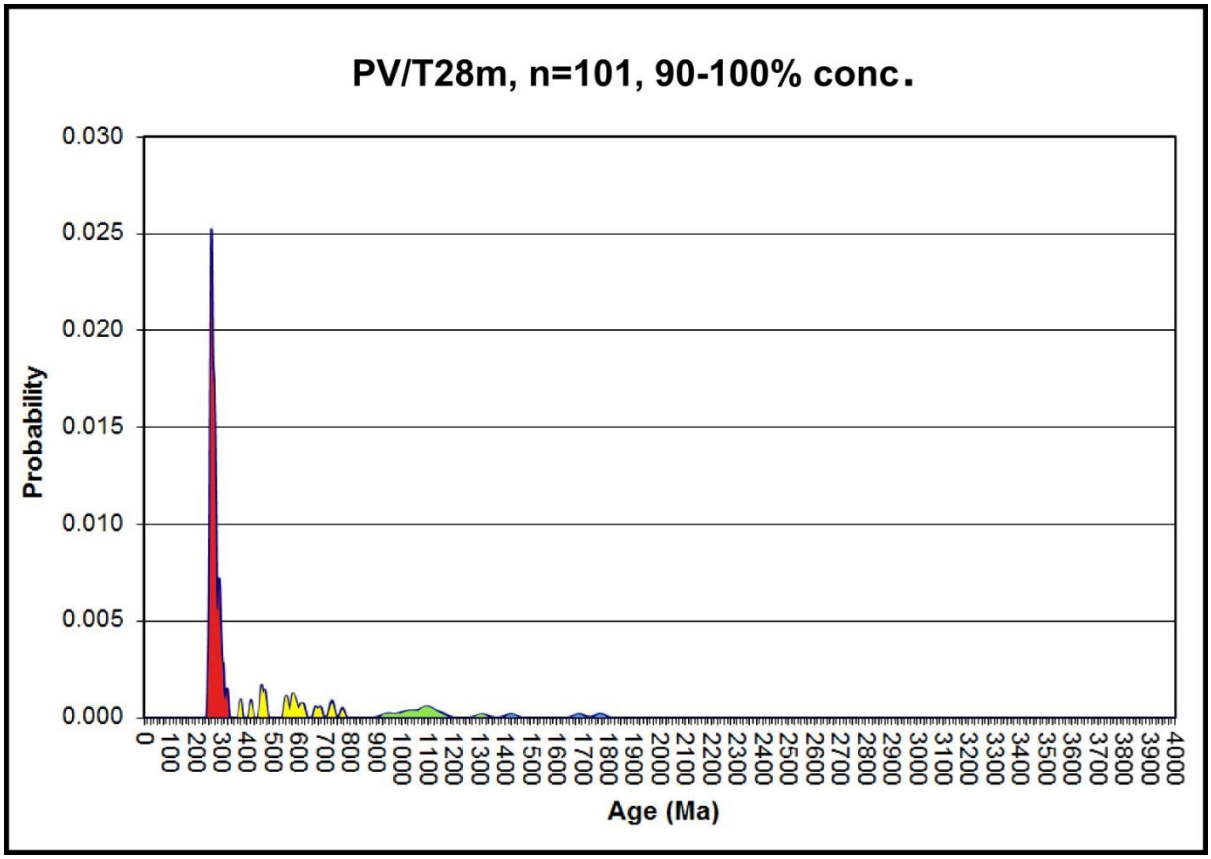

Figure 3.54: Probability density plot for sample PV-T28m from the Musgrave Grit unit (Balfour Formation) on Tafelkop near Bloemfontein, revealing three prominent zircon age populations which range between 248 ± 3 Ma and 325 ± 6 Ma (70 grains), 375 ± 4 Ma to 770 ± 8 Ma (18 grains), and 941 ± 22 Ma to 1312 ± 23 Ma (11 grains). The oldest population consists of 3 grains that are 1422 ± 21 Ma and 1770 ± 19 Ma respectively.

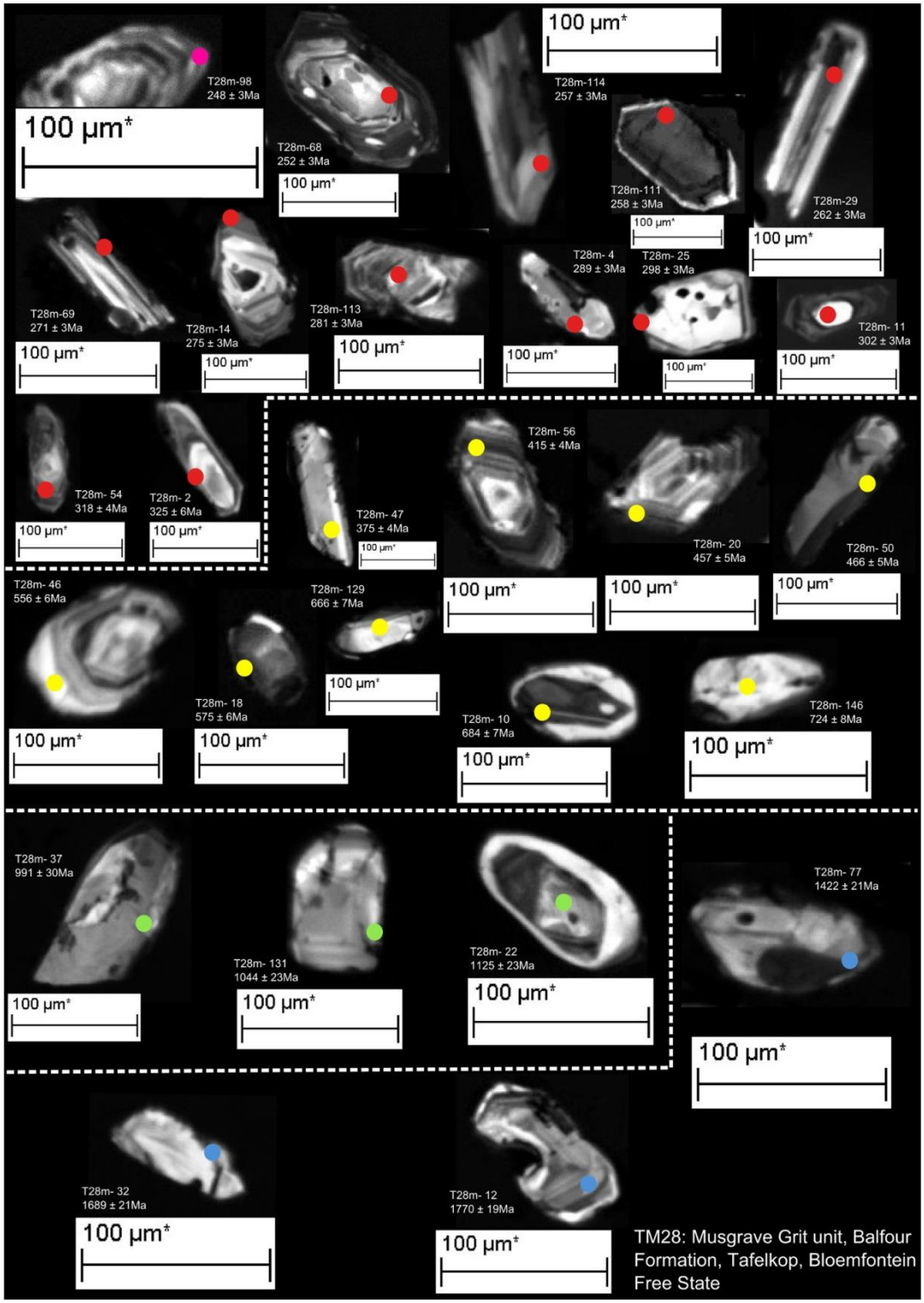

Figure 3.55: Cathode luminescence SEM images showing the internal textures of a selection of detrital grains from sample PV-T28m from the Musgrave Grit unit (Tafelkop, Bloemfontein) (see Appendix 1G for all of the zircons used to characterize the sample). Red spots yielded aged belonging to the youngest population (248 ± 3 Ma to 325 ± 6 Ma), yellow and green the intermediate aged populations (375 ± 4 Ma to 770 ± 8 Ma and 941 ± 22 Ma to 1312 ± 23 Ma). The blue dots indicate the oldest zircon population that consists of 2 grains that are 1422 ± 21 Ma and 1770 ± 19 Ma respectively. The youngest zircon (pink dot) is 248 ± 3 Ma.

The youngest zircon grain in the sample (248 ± 3 Ma) (Table 3.4) has a discordance of 3.1 %, Th/U ratio of 0.49 (ablation pit A-370, Appendix 1G), and represents the upper age limit of the youngest zircon population. The lower age limit of the youngest population is defined by a zircon grain with an age of 325 ± 6 Ma (1.3 % discordant, ablation pit A-260, Th/U of 0.51, Appendix 1G. The oldest zircon grain is dated to 1770 ± 19 Ma (0.7 % discordant, Th/U of 0.71, ablation pit A-397) defines the lower boundary of the oldest population.

The youngest population (248 ± 3 Ma to 325 ± 6 Ma) are mostly euhedral elongate or prismatic grains that exhibit oscillatory and sector zoning (Table 3.4, Figure 3.55). The second youngest population (375 ± 4 Ma to 770 ± 8 Ma) are mostly elongate euhedral prism, although some spherical and well-rounded grains are present. Sector and oscillatory zoning is present. The second oldest population (941 ± 22 Ma to 1312 ± 23 Ma) are either elongate prisms or well-rounded grains with sector zoning. Some are fragments of once larger grains. The oldest population (1422 ± 21 Ma and 1770 ± 19 Ma) consists of one damaged sub rounded grains and a sub rounded prism with oscillatory zoning.

Katberg Formation

Baviaanrivier Valley, Eastern Cape

This rock sample (Kat2Pass) is from the lower Katberg Formation (Tarkastad Subgroup) from the Tarkastad road in the Baviaansriver Valley, Eastern Cape. This sample produced 124 zircon grains that have a discordance of less than 10% from a total of 132 grains analysed (Figure 3.56, Table 3.4). The most prominent zircon population in the sample ranges between 252 ± 5 Ma and 313 ± 6 Ma, a total of 84 grains or 68 % of the total sample. The second most prominent population ranges in age between 929± 23 Ma to 1423 ± 20 Ma, a total of 25 grains or 18 % of the total sample. The third most prominent population ranges in age between 442± 8 Ma to 625 ± 11 Ma, a total of 13 grains or 10 % of the total sample. The oldest population in the sample consists of 7 grains that range in age between 2258 ± 18 Ma and 3239 ± 16 Ma (4 % of total sample).

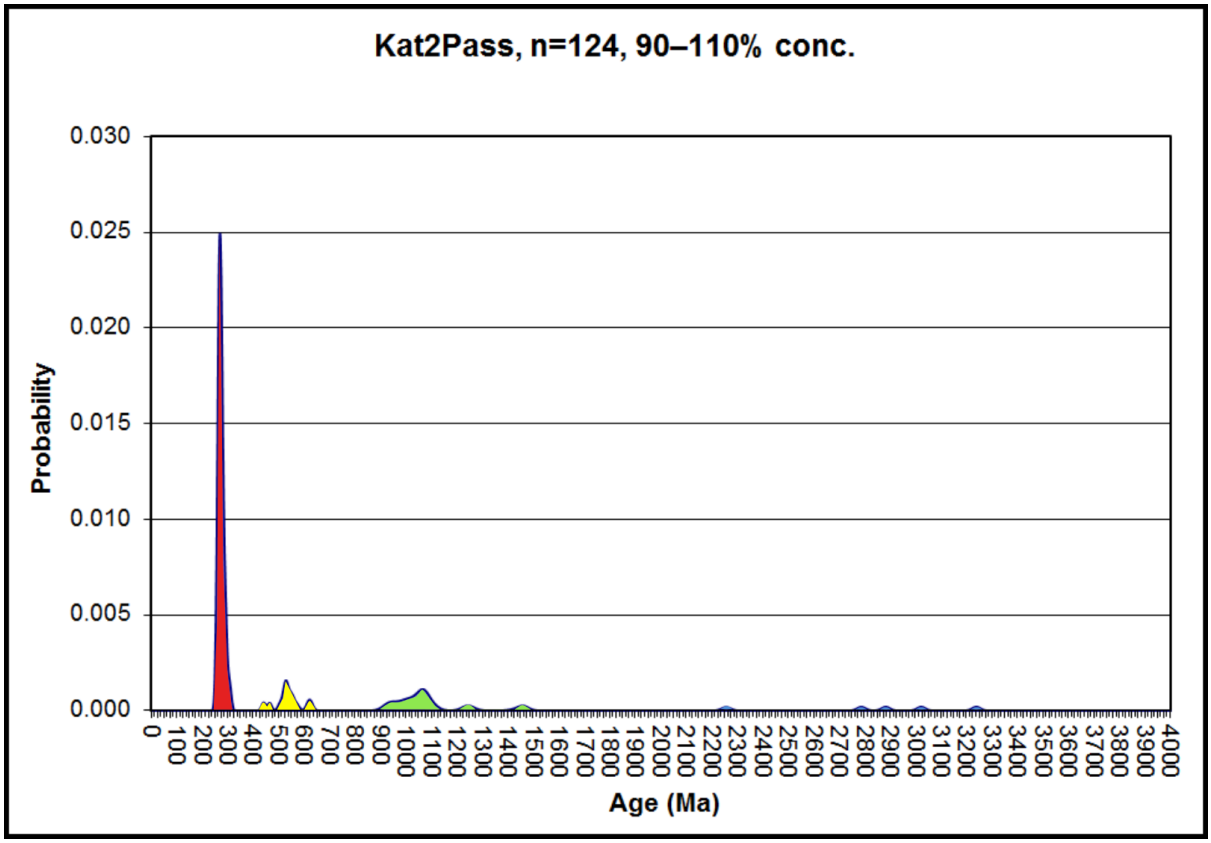

Figure 3.56: Probability density plot for sample Kat2Pass from the lower Katberg Formation (Tarkastad road) revealing three prominent zircon age populations which range between 252 ± 5 Ma and 313 ± 6 Ma (84 grains), 929± 23 Ma to 1423 ± 20 Ma (25 grains), and 442± 8 Ma to 625 ± 11 Ma (7 grains). The oldest population consists of 7 grains that range in age between 2258 ± 18 Ma and 3239 ± 16 Ma.

The youngest zircon grain in the sample (252 ± 5 Ma) (Table 3.4) has a discordance of 0.07 %, Th/U ratio of 0. 45 (ablation pit Pass-118, Appendix 1J), and represents the upper age limit of the youngest zircon population. The lower age limit of the youngest population is defined by a zircon grain with an age of 313 ± 6 Ma (4.5 % discordant, ablation pit Pass-28, Th/U of 0.34, Appendix 1J. The oldest zircon grain is dated to 3239 ± 16 Ma (0 % discordant, Th/U of 0.59, ablation pit Pass-98) defines the lower boundary of the oldest population.

The youngest population (252 ± 5 Ma and 313 ± 6 Ma) are mostly elongate euhedral grains that exhibit sector and oscillatory zoning (Table 3.4, Figure 3.57). The second youngest population (442± 8 Ma to 625 ± 11 Ma) are similar to the previous population but more fragmentary grains are encountered. The second oldest population (929± 23 Ma to 1423 ± 20 Ma) are mostly well rounded to subrounded grains with oscillatory and sector zoning. The oldest population (2258 ± 18 Ma and 3239 ± 16 Ma) are mostly fragments of once larger grains with sector or oscillatory zoning.

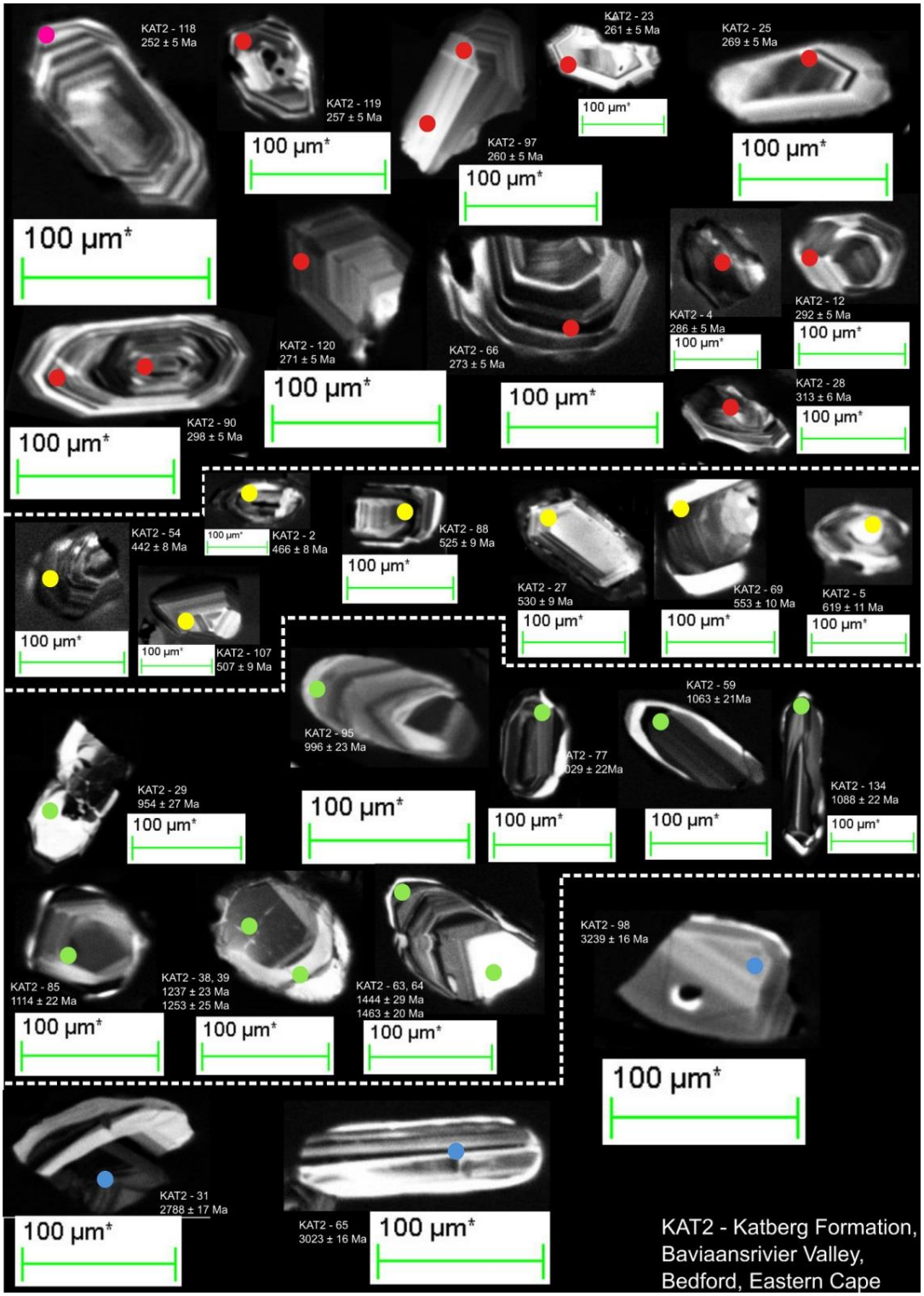

Figure 3.57: Cathode luminescence SEM images showing the internal textures of a selection of detrital grains from sample Kat2Pass from the lower Katberg Formation (Tarkastad road) (see Appendix 1J for all of the zircons used to characterize the sample). Red spots yielded aged belonging to the youngest population (252 ± 5 Ma and 313 ± 6 Ma), yellow and green the intermediate aged populations (442± 8 Ma to 625 ± 11 Ma and 929± 23 Ma to 1423 ± 20 Ma). The blue dots indicate the oldest zircon population that consists of 7 grains that range in age between 2258 ± 18 Ma and 3239 ± 16 Ma. The youngest zircon (pink dot) is 252 ± 5 Ma.

Venterstad, Eastern Cape

This rock sample (PV-Venter) is from the lower Katberg Formation (Tarkastad Subgroup) in close vicinity to Venterstad, a small town overlooking Gariep Dam and within the Eastern Cape Province. This sample produced 76 zircon grains that have a discordance of less than 10% from a total of 105 grains analysed (Figure 3.58Figure 3.58, Table 3.4). The most prominent zircon population in the sample ranges between 250 ± 5 Ma and 332 ± 6 Ma, a total of 55 grains or 72.4 % of the total sample. The second most prominent population ranges in age between 395 ± 7 Ma to 647 ± 12 Ma, a total of 13 grains or 17.1 % of the total sample. The third most prominent population ranges in age between 963 ± 29 Ma to 1087 ± 24 Ma, a total of 7 grains or 9.2 % of the total sample. The oldest population in the sample consists of a single grain that is 2846 ± 17 Ma (1.3 % of total sample).

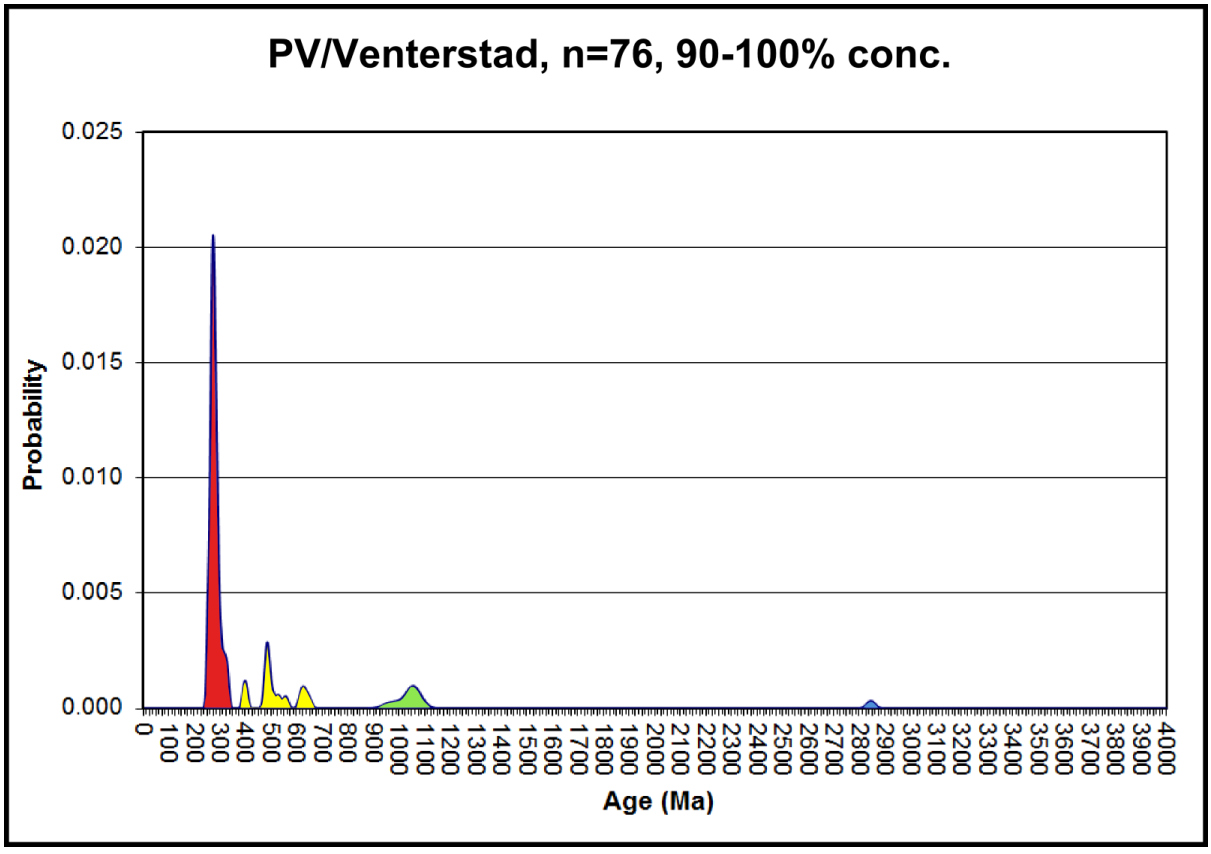

Figure 3.58: Probability density plot for sample PV-Venter from the lower Katberg Formation at Venterstad revealing three prominent zircon age populations which range between 250 ± 5 Ma and 332 ± 6 Ma (55 grains), 395 ± 7 Ma to 647 ± 12 Ma (13 grains), and 963 ± 29 Ma to 1087 ± 24 Ma (7 grains). The oldest population consists of a single grain that is 2846 ± 17 Ma.

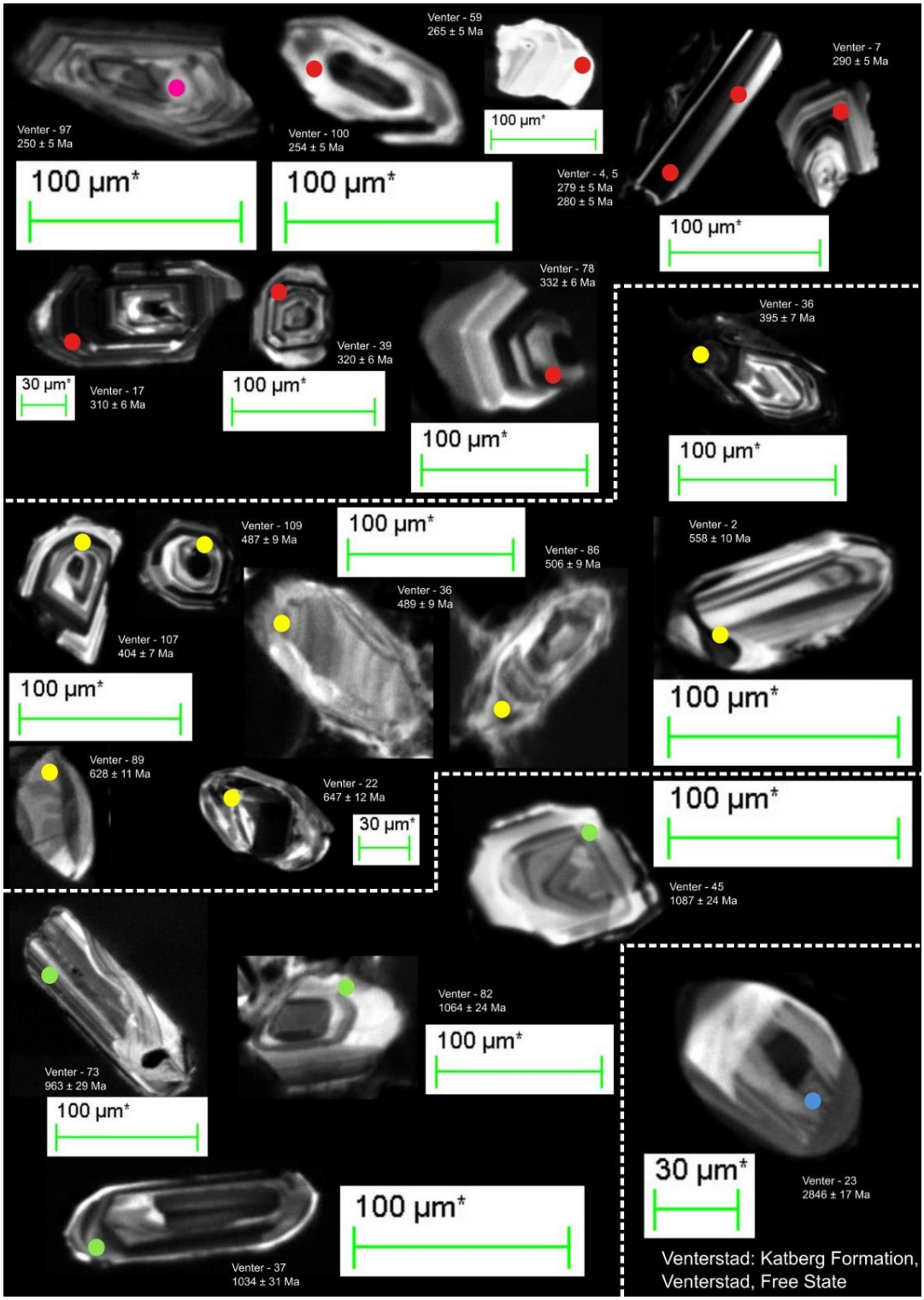

Figure 3.59: Cathode luminescence SEM images showing the internal textures of a selection of detrital grains from sample PV-Venter from the lower Katberg Formation at Venterstad (see Appendix 1K for all of the zircons used to characterize the sample). Red spots yielded aged belonging to the youngest population (250 ± 5 Ma and 332 ± 6 Ma), yellow and green the intermediate aged populations (395 ± 7 Ma to 647 ± 12 Ma and 963 ± 29 Ma to 1087 ± 24 Ma). The blue dot indicates the oldest zircon in the population, a single grain that is 2846 ± 17 Ma. The youngest zircon (pink dot) is 250 ± 5 Ma.

The youngest zircon grain in the sample (252 ± 5 Ma) (Table 3.4) has a discordance of 2.9 %, Th/U ratio of 0. 52 (ablation pit Venter-91, Appendix 1K), and represents the upper age limit of the youngest zircon population. The lower age limit of the youngest population is defined by a zircon grain with an age of 332 ± 6 Ma (3 % discordant, ablation pit Venter-78, Th/U of 0.34, Appendix 1K. The oldest zircon grain is a metamorphic grain dated to 2846 ± 17 Ma (0 % discordant, Th/U of 0.01, ablation pit Venter-23) and defines the lower boundary of the oldest population.

The youngest population (250 ± 5 Ma and 332 ± 6 Ma) are mostly elongate and spherical grains that exhibit oscillatory zoning (Table 3.4, Figure 3.59). The second youngest population (395 ± 7 Ma to 647 ± 12 Ma) are similar to the previous population but some well-rounded grains are also present. Oscillatory and sector zoning is observed. The second oldest population (963 ± 29 Ma to 1087 ± 24 Ma) consist of elongate sub rounded grains and also fragmentary prisms with either sector of oscillatory zoning. The oldest grain (2846 ± 17 Ma) is a well- rounded grain that does show internal features well.

Inhoek farm, Gariep Dam, Free State Province

This rock sample (PV-KTIn1) is from Inhoek farm, Gariep Dam, Free State Province. This sample comes from Katberg Formation that was previously mapped as Balfour Formation. This is because attenuation of the strata were not taken into account in this part of the basin up until this study and this is the first time Katberg Formation has been documented on Inhoek farm (section 9). This sample produced 95 zircon grains that have a discordance of less than 10% from a total of 110 grains analysed (Figure 3.60, Table 3.4). The most prominent zircon population in the sample ranges between 255 ± 5 Ma and 326 ± 7 Ma, a total of 37 grains or 40 % of the total sample. The second most prominent population ranges in age between 457 ± 10 Ma to 777 ± 16 Ma, a total of 32 grains or 33 % of the total sample. The third most prominent population ranges in age between 891 ± 22 Ma to 1172 ± 21 Ma, a total of 7 grains or 25 % of the total sample. The oldest population in the sample consists of 2 grains that are 2364 ± 18 Ma and 3416 ± 31 Ma respectively.

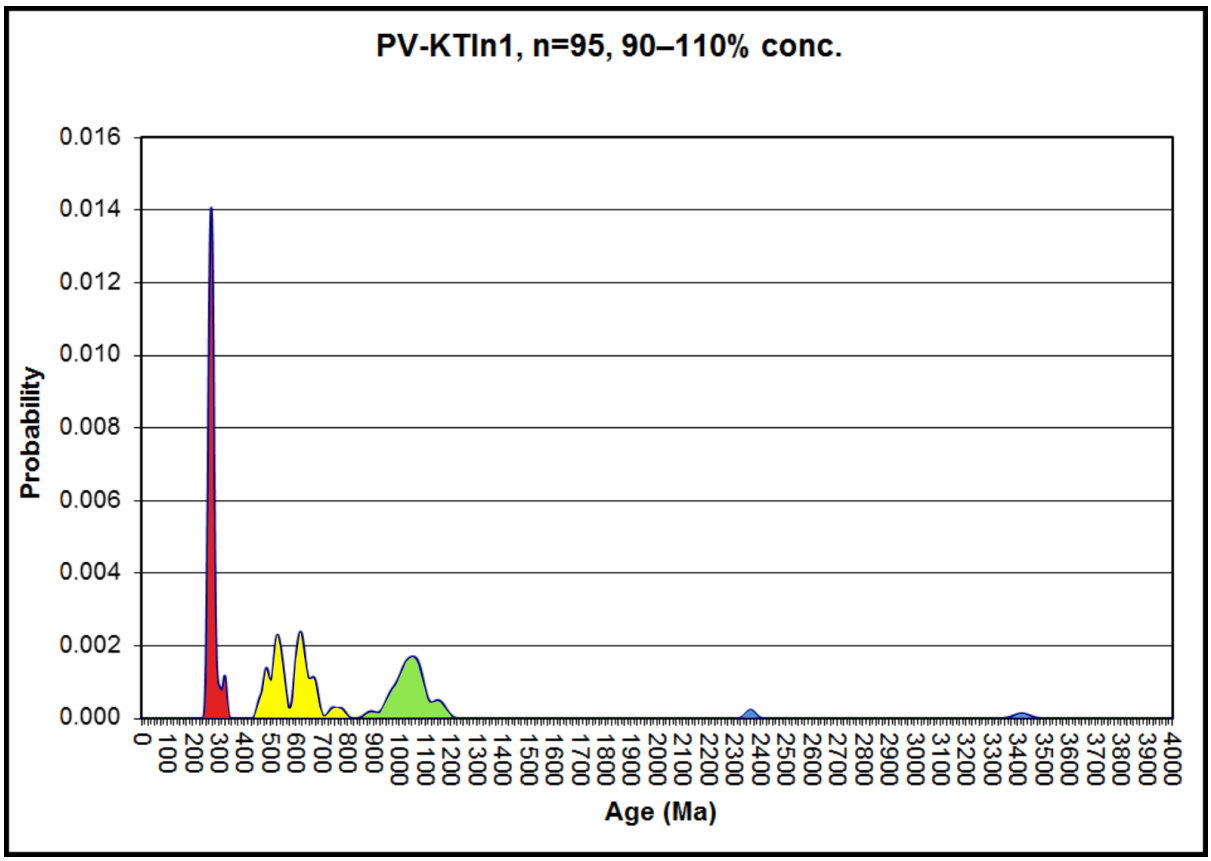

Figure 3.60: Probability density plot for sample PV-KTIn1 from the lower Katberg Formation from Inhoek Farm revealing three prominent zircon age populations which range between 255 ± 5 Ma and 326 ± 7 Ma (37 grains), 457 ± 10 Ma to 777 ± 16 Ma (32 grains), and 891 ± 22 Ma to 1172 ± 21 Ma (7 grains). The oldest population consists of 2 grains that are 2364 ± 18 Ma and 3416 ± 31 Ma respectively.

The youngest zircon grain in the sample (255 ± 5 Ma) (Table 3.4) has a discordance of 1.8 %, Th/U ratio of 1.16 (ablation pit KTIn1-93, Appendix 1L), and represents the upper age limit of the youngest zircon population. The lower age limit of the youngest population is defined by a zircon grain with an age of 326 ± 7 Ma (0 % discordant, ablation pit KTIn1-41, Th/U of 0.37, Appendix 1L. The oldest zircon grain is an igneous grain dated to 3416 ± 31 Ma (2.3 % discordant, Th/U of 0.49, ablation pit KTIn1-83) and defines the lower boundary of the oldest population.

The youngest population (255 ± 5 Ma and 326 ± 7 Ma) are mostly euhedral grains or fragments of euhedral grains that exhibit oscillatory and sector zoning (Table 3.4, Figure 3.61). The second youngest population (457 ± 10 Ma to 777 ± 16 Ma) are mostly well-rounded grains exhibiting oscillatory and sector zoning. The second oldest population (891 ± 22 Ma to 1172 ± 21 Ma) consist of fragments of once larger grains with oscillatory zoning sometimes visible. The oldest grains (2364 ± 18 Ma and 3416 ± 31 Ma) are both fragments of once larger grains. One is well rounded with sector zoning, and the other is an elongate, tabular fragment showing sector zoning.

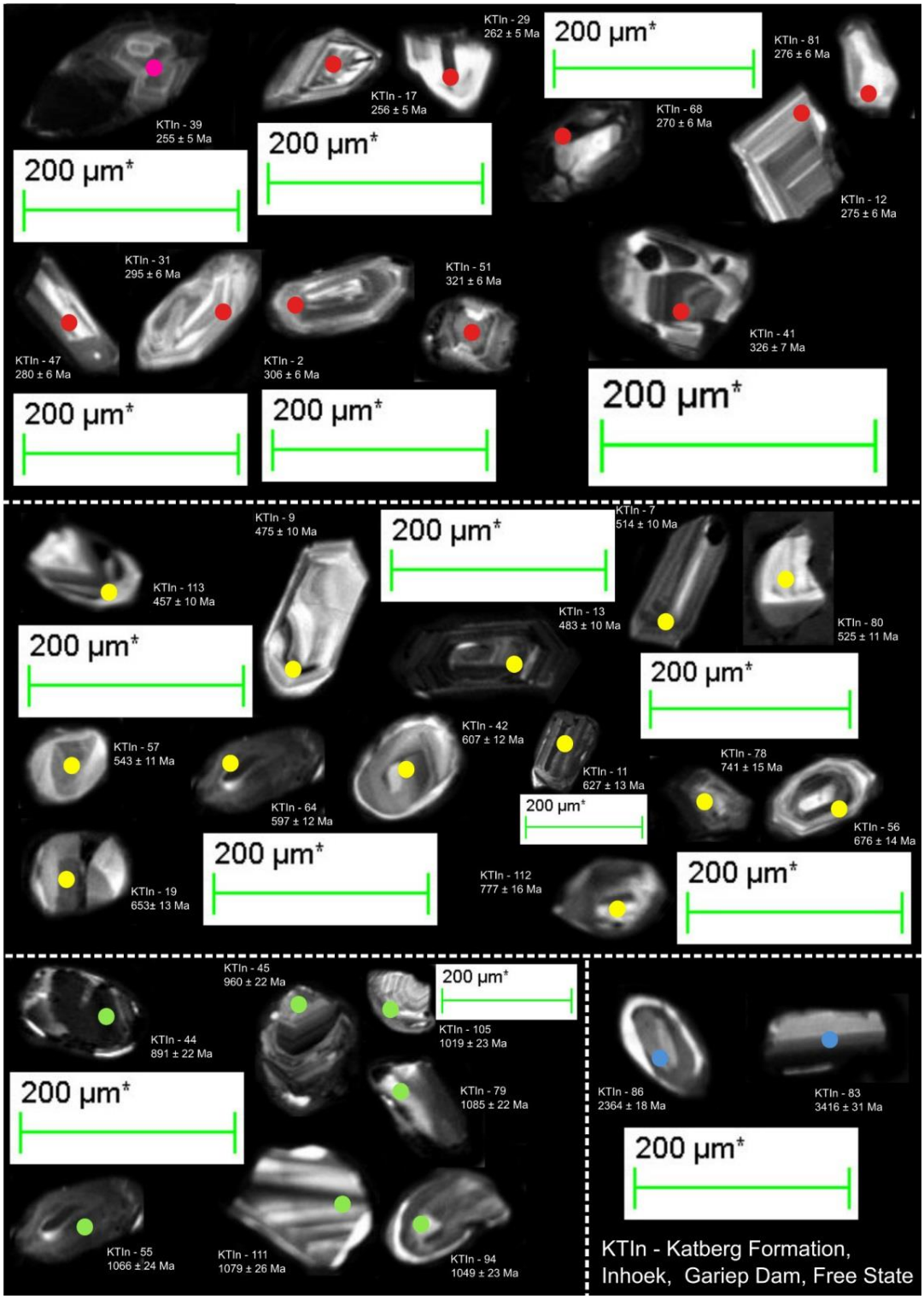

Figure 3.61: Cathode luminescence SEM images showing the internal textures of a selection of detrital grains from sample PV-KTIn1 from the lower Katberg Formation from Inhoek farm (see Appendix 1L for all of the zircons used to characterize the sample). Red spots yielded aged belonging to the youngest population (255 ± 5 Ma and 326 ± 7 Ma), yellow and green the intermediate aged populations (457 ± 10 Ma to 777 ± 16 Ma and 891 ± 22 Ma to 1172 ± 21 Ma). The blue dots indicates the oldest zircons in the population, 2 grains that are 2364 ± 18 Ma and 3416 ± 31 Ma respectively. The youngest zircon (pink dot) is 255 ± 5 Ma.

3.6.2 Summary

Signatures of the lithostratigraphic units

The twelve sandstone samples yielded detrital zircon ages that could be ordered into three main populations, a latest Carboniferous to latest Permian population (250 ± 5 Ma – 332 ± 6 Ma), a earliest Devonian to Neoproterozoic (364 ± 7 Ma to 878 ± 24 Ma), and latest Neoproterozoic to Mesoproterozoic (908 ± 22 Ma to 1308 ± 23) (see Chapter 5.4). The oldest grains in the samples are split into two groups that range from late Mesoproterozoic to late Palaeo-Proterozoic (1402 ± 26 Ma to 2450 ± 17 Ma) and a trace Archean (2756 ± 18 to 3416 ± 31) population. The zircon signatures of the samples collected from the RM (PV-LC, PV-NbDo1, PV-BMIn2, PV-Springfontein), Javanerskop member (PV-H1, PV-Javanerskop), Musgrave Grit unit (PV-T28m), and Katberg Formation (PV-Kat2Pass, PV-Venter, PV-KTIn) are the same. In these samples the dominant population is always the youngest detrital zircon population (250 ± 5 Ma – 332 ± 6 Ma). Two samples are different to the rest of the samples but similar to one another and they are the sample from the Oudeberg Member (PV-Cr1) and the sample from the Boomplaas sandstone from Boomplaas Hill, Jagersfontein (PV-J615). In both these cases the youngest detrital zircon population is the least dominant with only 4 and 12 grains in this population for the two samples respectively. In addition the density plots for the other dominant populations show similar ditributions (see Figures 3.38 and 3.52). Therefore they are tentatively correlated to the same stratigraphic horizon (Figure 3.62).

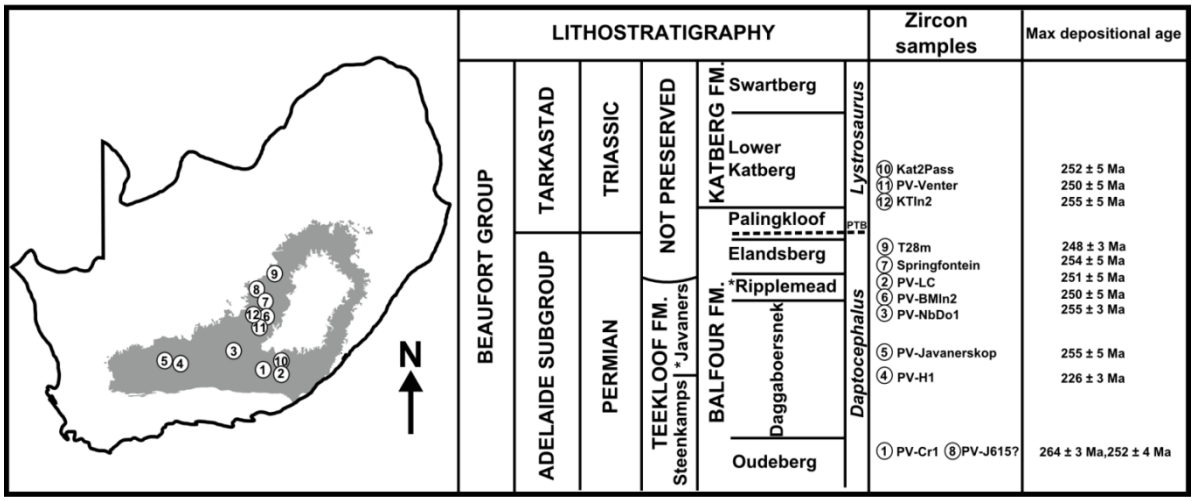

Figure 3.62: Maximum depositional ages for the twelve sandstone samples. Geographic position in the Karoo Basin and stratigraphic position are both shown.

Maximum depositional age of the lithostratigraphic units

The radiometric age obtained for the youngest zircon grain within a population of detrital zircons is considered to be a good indication as to the maximum age of the deposition of the sedimentary layer

itself (Zeh et al. 2008; Vorster, 2013). Therefore the maximum depositional ages for each sample were compared to one another, relative to their stratigraphic position (Figure 3.62).

The youngest zircon in each sample mostly agree with Late Permian maximum depositional age for samples from the Oudeberg, Ripplemead, and Javanerskop members, and early Triassic maximum depositional age for the samples sourced from the Katberg Formation. However, it is interesting to note the sample from the Oudeberg Member (PV-Cr1) near Cradock shows the oldest maximum depositional age. While does not prove it is an older unit, combined with the very small young detrital zircon population, does support a lower stratigraphic position for the this unit in comparison to the RM. Additionally, some of the samples from Upper Permian strata do contain early Triassic grains (PV-H1, PV-T28m). These are not considered to be true maximum depositional ages for reasons now outlined in the next section.

Reliability of the data and problems

The youngest grains present in the samples range in age from 250 ± 5 Ma to 264 ± 3 Ma however three Triassic-aged grains were obtained from PV-H1 (226 ± 3 Ma; 246 ± 3 Ma) and T28 m (248 ± 3 Ma). Although these grains are concordant they are not regarded as a true reflection of the maximum depositional age for this sample. This is due to a number of factors that include Pb-loss not revealed by resolvable discordance on the Concordia curve (Vorster, 2013). When one reaches the section of the Concordia curve that is straight, the Discordia line will nearly coincide with the Concordia (see Vorster, 2013 and Appendix 1). In this situation the error ellipses of individual data points will encircle both the Concordia curve and the Discordia curve (Vorster, 2013). As a result Pb-loss in some grains would not be revealed by resolvable discordance within the error limits of LA-ICP-MS. Previous studies by Bowden (2013) for example do not take this into account when estimating the maximum ages of deposition for their samples on the Beaufort and Stormberg Groups.

Additionally, the metamict nature of the detrital zircon grain also needs to be taken into account. The metamictization of a natural zircon results from accumulated radiation damage to the crystal structure due to radioactive decay of U and Th that substitute for Zr in the crystal structure (Holland and Gottfried, 1955; Headley et al. 1982; Woodhead et al. 1991). Additionally metamictization can be exacerbated by extremely high U or Th content of a zircon crystal (Soman et al. 2010; White and Ireland, 2012; Deng et al. 2013). Metamict detrital zircons under cathode luminescence images include misorientated crystallites, mixed crystalline and amorphous domains, or the general loss of crystal structure (Woodhead et al. 1991; Corfu et al. 2003).

The grains in question from samples of the Javanerskop member (PV-H1, A-59, A-86) and PV-(T 28 m, A-370) do not have unusually high U or Th content however little, if any crystal structure is preserved. Moderate zoning is present in two of the Triassic grains (A-59, A-370) but that they are not euhedral in appearance with well-developed sector or oscillatory zoning which is unusual for the young population. Additionally, the quality of zircons retrieved from sample PV-H1 is exceptionally poor and as a result only 44 showed concordance. Sample PV-Javanerskop is stratigraphically above PV-H1 by ~ 70 m and has a maximum depositional age of 255 ± 5 Ma. Therefore these Triassic grains are not regarded as the true maximum depositional age for PV-H1 and PV-T 28 m.

This does not imply that all of the young grains cannot be trusted to present an accurate maximum depositional age due to the prevalence of this population as presented in the population density plots and the tables in this section. Therefore it is very unlikely all of them are the result of Pb-loss. This is what Vorster (2013) identified in samples from the Ecca Group and Cape Supergroup. These young ages are also in agreement with the estimated stratigraphic age of the rocks (Upper Permian) due to relative dating of fossil fauna and thus are considered to mostly reflect actual ages.

Work conducted by Andersen (2005) and Andersen et al. (2015) also concludes that the current detrital zircon analytical methods assume an uninterrupted and direct pathway between a clastic sediment at its site of deposition, and its original source in crystalline bedrock. They suggest this "source to sink" relationship has been obscured in many cases by repeated events of sediment recycling. This has been alluded to by Vorster (2013) who suggested that similarities in population signatures between the Ecca Group and Cape Supergroup by large Neoproterozoic population over a trace Archean population shows that a significant sediment recycling of the Cape Supergroup rocks into the Karoo Basin. It is this significant sediment recycling that is argued by Andersen et al. (2015) to be obscuring the signal from any freshly eroded primary crystalline (Archean) basement sources. The second largest population in most of the 12 samples in this study, and present in all samples, is a Neoproterozoic-Mesoproterozoic population. Archean grains are also scarce in all samples. This means significant sediment recycling is also very likely obscuring primary source rocks to the Beaufort Group. Chapter 5.4 discusses the potential source areas of the grains present in the 12 samples analysed in this study.

Chapter 4: Facies and architectural element analysis

This chapter provides an overview of the facies, facies associations and architectural elements at the field sites, and combines these data to interpret the changing palaeoenvironments of the Upper Permian Balfour and Teekloof formations. Of particular interest are the sandstone-rich units of the Oudeberg, Ripplemead (RM), and Javanerskop members, and the Musgrave Grit unit. Facies associations are used to describe suites of different lithofacies that commonly occur together and when combined with analyses of the architectural elements of the Oudeberg, Ripplemead, and Javanerskop members, and the Musgrave Grit can lead to an interpretation of their palaeoenvironments and fluvial styles.

4.1 Lithofacies

Facies analyses were carried out using a modified version of Miall's (1977, 1978, 1996, 2014) lithofacies classification which is based on a letter coding system described in Chapter 2.3.4. The facies were identified principally on grain size and sedimentary structures and then further divided into three main groups based on lithology such as gravels or conglomerates (G), sandstones (S), and mudstones (F). The interpretation and characterization of the facies uses the nomenclature and process of Reading (1978), Friend (1979) and Miall (1985, 1994, 1996, 2014) and additional sources (Ashworth and Lewin, 2012; Colombera et al. 2013; Wilson et al. 2014). These are summarized and briefly described in Table 4.1. Figures 4.1-4.7 are photographs of the most common lithofacies encountered at the field sites.

Table 4.1: Facies classification and descriptions encountered during the study.

Facies Names and Code	Grain size	Description	Geometry	Occurrence	Interpretation
Gm1 Scour-fill lag	Very coarse sand to granule sized clasts.	Mudstone or quartz, rare lithic, feldspar clasts, bone, carbonate nodule and plant fragments. Forms poorly sorted, clast-supported pods or lenses. Mudstone clasts are well-rounded, and quartz, feldspar clasts and bone, angular to subrounded. May be weakly normally graded and weathers recessively (ie. faster than overlying sandstone).	Discontinuous beds, forming lenses or pods within erosional scours. Thickness varies but never greater than 2 m.	Occurs in the basal parts of sand bodies, and sometimes within erosional boundaries between sandstone storeys. Most frequently as filling scours into underlying mudstones. See Figures 4.3 (A), 4.5 (B), and 4.6 (A).	Lag deposit from rapidly waning flow close to position of the thalweg. Rounded mudstone clasts and angular lithic fragments indicate relatively short transport in pulsatory rapid-flows. Calcareous nodules and fossil material are evidence for erosion of floodplain deposits.

Gm2 Sandstone matrix with rip-up mudstone clasts	Fine to coarse-grained sand with mudrock clasts 0.5-10 cm in diameter.	Colour ranges from greyish brown (5YR 3/2) to pale olive (10Y 6/2). Contains matrix supported mudrock fragments that can be well-rounded to subrounded (friable). They are normally dark greenish grey (5GY 4/1) but also moderate brown (5YR 3/4) are found. Broken up plants fragments on the millimetre and centimetre scale are often associated and stem and leaf impressions that are reasonably intact.	Heterolithic units below other sandstone facies or as isolated pods or lenses. Average thickness is ~ 25 cm but it can occur as deposits less than 10 cm and greater than 1 m.	This facies is laterally restricted, occurring in close proximity to Gm1 as pods (1-2 m long, 20-50 cm thick) or small isolated (<1 m) lenses. See Figures 4.1 (A, C, E), 4.2 to 4.5 (A), 4.6 (B), and 4.7 (A).	Chaotic fabric indicates deposition during rapidly waning flow in the channel or in a point sourced splay on the proximal floodplain and adjacent to broken levees.
Sp Planar cross–bedded sandstone	Fine to coarse sand.	Weathers yellowish-grey (5Y 7/2) but otherwise pale olive (10Y 6/2) and sometimes greenish-grey (5GY 6/1). Cross-bedding angle normally 20-30 degrees, cross-bed foresets are often silt draped and sometimes fine upwards. Rare in comparison to St.	Small tabular or wedge shaped beds less than 1 m thick with small foresets greater than 1 cm. Can be classed as planar cross-laminae in some instances.	Rare but observed in the middle to lower portions of sandstone bodies. In some cases is associated with Sr. See Figures 4.3 (D), 4.4 (D, H), and 4.7 (B, D, E).	Small dunes with linear or slightly sinuous crests formed in deeper/faster flowing parts of the channel. Rarely preserved as 3D bedforms as part of unconfined deposition on proximal floodplain.
Sl Low angle cross–bedded sandstone	Fine to coarse sand.	Low angle cross-beds or laminae similar to Sp except for the low angle of deposition occurring on the foresets (5-10 degrees). Normally pale olive (10Y 6/2) but sometimes greenish-grey (5GY 6/1)..	Ribbon or wedge shaped layers up to 1 m thick and a few metres across. Truncated on lower and upper bounding surfaces by St and often changes laterally into St.	More common than Sp. In some cases likely mistaken for truncated St. Found in the middle to lower portions of the sandstone bodies in association with St. See Figures 4.1-4.6.	Represents deposition in low relief downstream migrating large wavelengths/low amplitude sand waves.
Sh Horizontally laminated sandstone	Fine to medium sand.	Thinly-laminated (< 1 cm) and thinly-bedded (> 1 cm) fine-grained pale olive (10Y 6/2) sand. Often fines upward between laminae. Lower bounding surfaces commonly sharp.	Tabular sheets 1-3 m thick. Over a few metres often changes into Sl (vertically or laterally).	Common. Parting lineation and obstacle marks, such as currents crescents are observed on the upper bounding surfaces where exposed. See Figures 4.1-4.6	Upper flow regime conditions in any part of the channel where stable bedforms are unable to form.

St Trough cross–bedded sandstone	Fine to coarse sand.	Cross-bedded greenish-grey (5GY 6/1) units in which one or both bounding surfaces are curved. Often this is in the form of truncating another facies. Sometimes silt draping is visible between foresets. The most common facies encountered in the sandstone bodies during this study.	Lateral and vertical size variation. Minimum thickness of between 9 and 15 cm in the axis pinching out laterally. Maximum size ~ 50 to 85 cm. The lower and upper contacts are erosional, creating the pinching and swelling shapes.	Occur in the lower to middle portions of sandstones. Laterally the larger St can become large ribbons where multiple beds truncate one another (Figure 4.15). The bases of these ribbons are St whereas the upper bed is Sh or comprises Sl. See Figures 4.1-4.7.	Three dimensional sinuous crested dunes which form in the deeper and/or faster flowing sections of the channel. The troughs are scoured into the sand bed during peak flood and then filled by migrating dunes during waning flow..
Sm Massive/weakly graded sandstone	Fine to coarse sand.	Massive, apparently structure-less medium to fine-grained pale olive (10Y 6/2) or greenish grey (5GY 6/1) sandstone. Sometimes mud drapes or mud chip layers are present. Bioturbation features have been observed in some cases on upper bounding surfaces. Lower bounding surfaces often erosional but can be flat or sharp. Weathering of the rock surface obscures faint sedimentary features.	Forms tabular beds or sheets within channel sandstone storeys and smaller (< 2 m) overbank sandstone bodies. Can be several metres in thickness and width.	Occurs in the channel fill deposits and common in the floodplain facies associations. See Figures 4.1 (E), 4.2 (C), 4.4 (E, H), and 4.5 (E).	Deposited in proximal parts of unconfined point sourced splays or debris flows in fluvial channels. Bioturbation by plant roots and invertebrates can also cause the lack of structure.
Sr Ripple cross laminated sandstone	Coarse silt to fine sand.	Greenish grey (5GY 6/1) but also dusky yellow green (5GY 5/2) or brownish grey (5YR 4/1). Frequent asymmetrical rippled surfaces with siltstone drapes present throughout sandstone bodies. Occasionally changes vertically into trough cross lamination (Rib and furrow) and laterally into climbing ripples.	Occurs in two forms: 1) Laterally and vertically extensive tabular to wedge shaped beds for tens of metres. 2) Sheet-like ~ 1 m thick laterally restrictive beds beds. Can be preserved by silt draping on upper bounding surfaces.	Common in all the facies associations. Symmetrical and planed off ripples frequent in the floodplain facies associations. See Figures 4.2 (C, D, E), 4.3 (F), 4.5 (D), 4.6 (C, E, F), and 4.7 (B, E).	Indicative of sustained unidirectional flow in waning energy or water depth conditions. In the case of climbing ripples, rapid deposition of inclined bar forms. Planed off ripples can mean subaerial exposure or wind action in shallow ponds or lakes.

Sdef Soft sediment deformed sandstone	Fine to medium sand.	Medium to fine-grained sandstone with slump structures, boundins, sandstone pillows, flames, and hummocks.	Not common but when present can be laterally continuous over tens of metres.	Common at the type locality of Tordiffe's (1978) Barberskrans Member where it is laterally extensive within the Oudeberg Member sandstone (> 50 m). See Figures 4.1 (G), 4.3 (A), 4.5 (E), and 4.6 (C, E).	Represents physicaldisturbance of sediment before consolidation. It is locally caused by storm discharge but where it is more extensive seismic activity and subsequent dewatering may be the cause.
Fm Massive coarse siltstone	Medium to coarse silt.	Mostly greenish grey (5GY 6/1) but sometimes dusky yellow green (5GY 5/2) or brownish grey (5YR 4/1). Mud chips, invertebrate burrows, rootlets, carbonate nodules, fossils are encountered in this facies. Sometimes is locally sandy (flaser bedding) or locally muddy (lenticular bedding).	Laterally extensive on the scale of hundreds of metres as tabular, lense, or sheet shaped bodies ranging from 1-10 m thick.	Occurs most commonly in the floodplain facies association, but also close to the bases of the channel facies. See Figures 4.1 (D), 4.2 (F, G), 4.3 (G, H), 4.4, 4.5 (G), and 4.7 (F).	Fm represents floodplain with high water table. Waterlogged or marshy conditions, such as vegetated wetland environments of the floodplain.
Fl Finely laminated siltstone	Fine silt to coarse silt.	Frequently alternating beds of greenish grey and dusky yellow green (5GY 6/1, 5GY 5/2), or brownish grey (5YR 4/1) siltstone. Colours often indicate slightly differing grain sizes, brownish grey normally being fine-grained and fissile. Mottling and disturbance of the laminations often associated with worm trails, burrows, rootlet horizons, carbonate nodules, and fossil remains.	Laterally extensive on the scale of hundreds of metres as tabular or sheet shaped bodies ranging from 1-10 m thick.	Occurs in close association with Fm and Fr. See Figures 4.2 (F, H), 4.3 to 4.5 (G), 4.6 (H), and 4.7 (F).	Suspension settling in ephemeral floodplain ponds where the water table seasonally intersects the surface.

N Carbonate nodules		This code documents five carbonate nodule types observed during this study. This distinction is made by symbols used on the sections (see Figure 2.2 for symbols).	Irregular in shape and size. Pedogenic nodules often only a few centimetres across but the larger diagenetic ones can range in size from ~20 cm in length all the way to >10 m across. Most commonly they range in size from 0.2 m to 1 m.	Found throughout the Balfour and Teekloof formations in palaeosol horizons and sandstone bodies for the diagenetic ones. See Figures 4.1 (H), 4.3 (G), and 4.5 (H).	Diagenetic and pedogenic origin to the carbonate nodules. Pedogenic nodules associated with palaeosols are precipitated in the soil horizon during seasonal rise and fall of the water table.

4.2 Facies associations

The lithofacies identified in sections 1-13 were grouped into four facies associations using the methodology of Miall (1996), Bordy and Catuneanu (2002b, 2002a), Colombera et al. (2013), and Wilson et al. (2014) (Table 4.2). They will be useful in defining the architectural elements that are facies associations with a distinct 3D geometry and palaeoenvironments of the *Daptocephalus* Assemblage Zone through time later in the chapter (Chapter 4.3). The distinguishing features of the facies associations are discussed below, using examples documented from the field sites and vertical sections.

Table 4.2: Facies associations from the study areas

Facies Association	**Major Facies Types**	**Interpretation**
F1	Gm1, Gm2, Sm, Sh, St, Sl, Sr, N	Confined channelized system.
F2	Fm, Fl, N,Sr	Suspension settling on floodplain.
F3	Gm1, Gm2, Sh, Sr, Fm	Unconfined overbank deposition.
F4	Fm, Fl, Sr, Gm1, Gm2	Lacustrine system.

Facies association 1 (confined channelized system)

Multi- or single-storey units of cross-bedded or cross-laminated sandstone dominate facies association 1 (F1) and examples of F1 from the field sites are shown in Figure 4.8. Average thickness of F1 varies but normally outcrops reach ~ 25 m, with each storey being on average 5-10 m thick. Within the overall argillaceous Balfour and Teekloof formations, F1 is conspicuous, laterally continuous over tens of kilometres, is fairly resistant to weathering, occuring as indurated outcrops (Figure 4.8, C and E). Colours associated with this facies association are mainly greenish grey and pale olive.

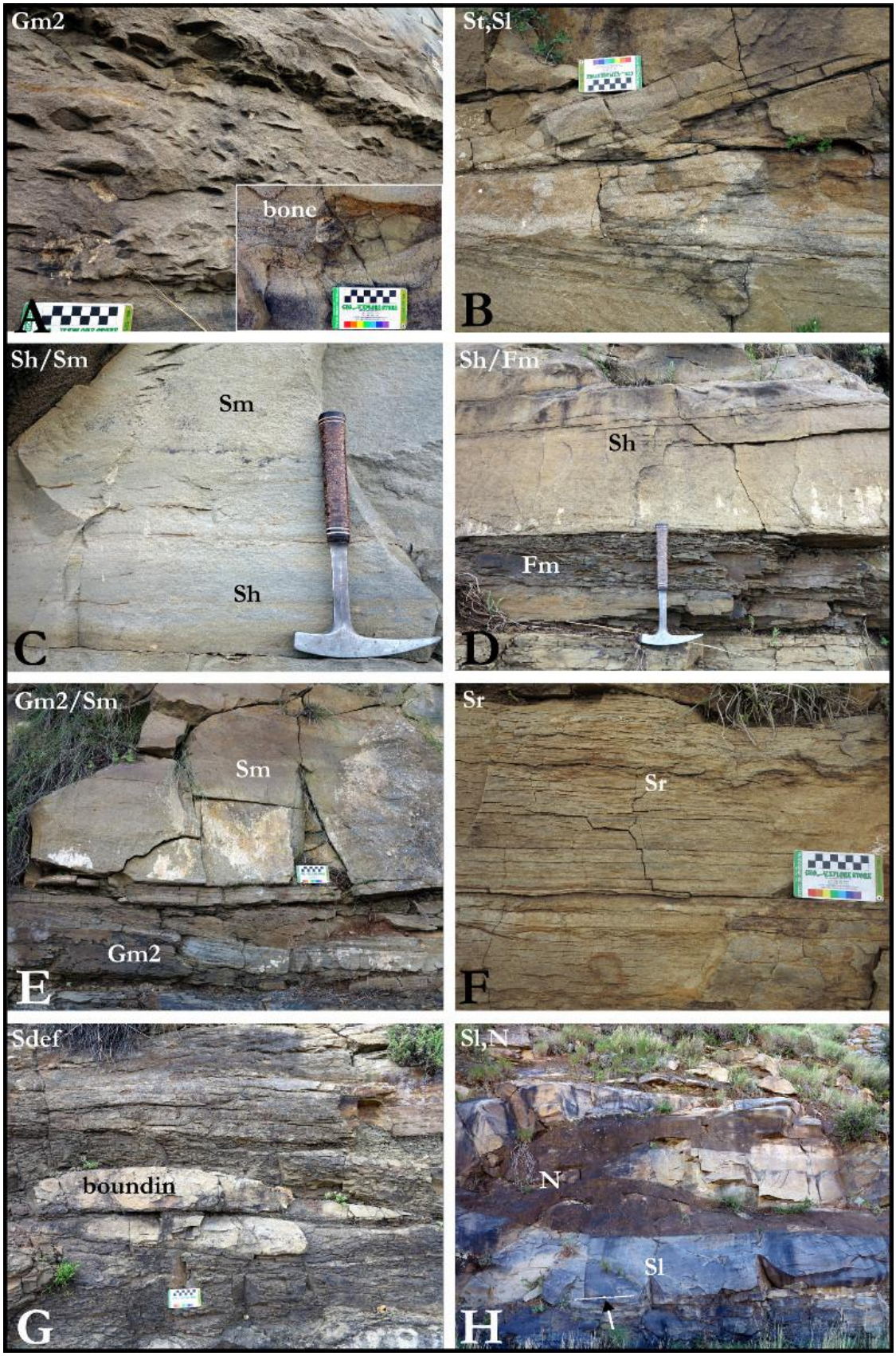

Figure 4.1: Examples of facies in the Oudeberg Member at the Barberskrans Cliffs (section 1A). Since overbank lithofacies are poorly exposed at this site, few examples are shown. The boudin in (G) indicates soft sediment deformation (Sdef). Note hammer for scale (C, D), 8 cm (A, B, E, F, G) and arrow pointing to 1 m scale in H.

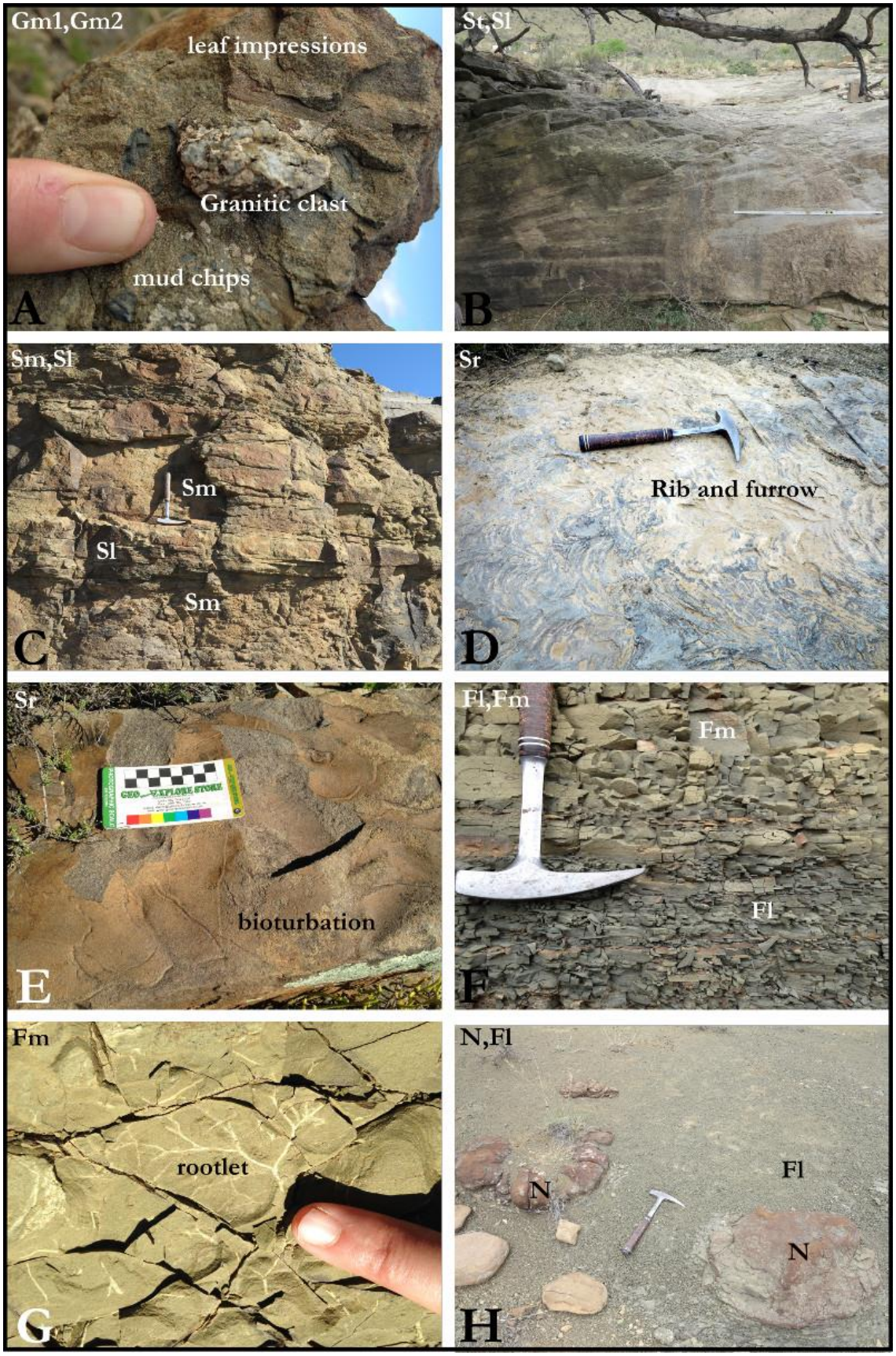

Figure 4.2: Examples of facies present in the Ripplemead member on Hales Owen (section 1B) and Lower Clifton farms (section 2). A, C, E, and F are examples from Hales Owen, and B, D, G, and H are examples from Lower Clifton farm. Note hammer for scale (C, D, F), 8 cm (E), and 1 m scale (B).

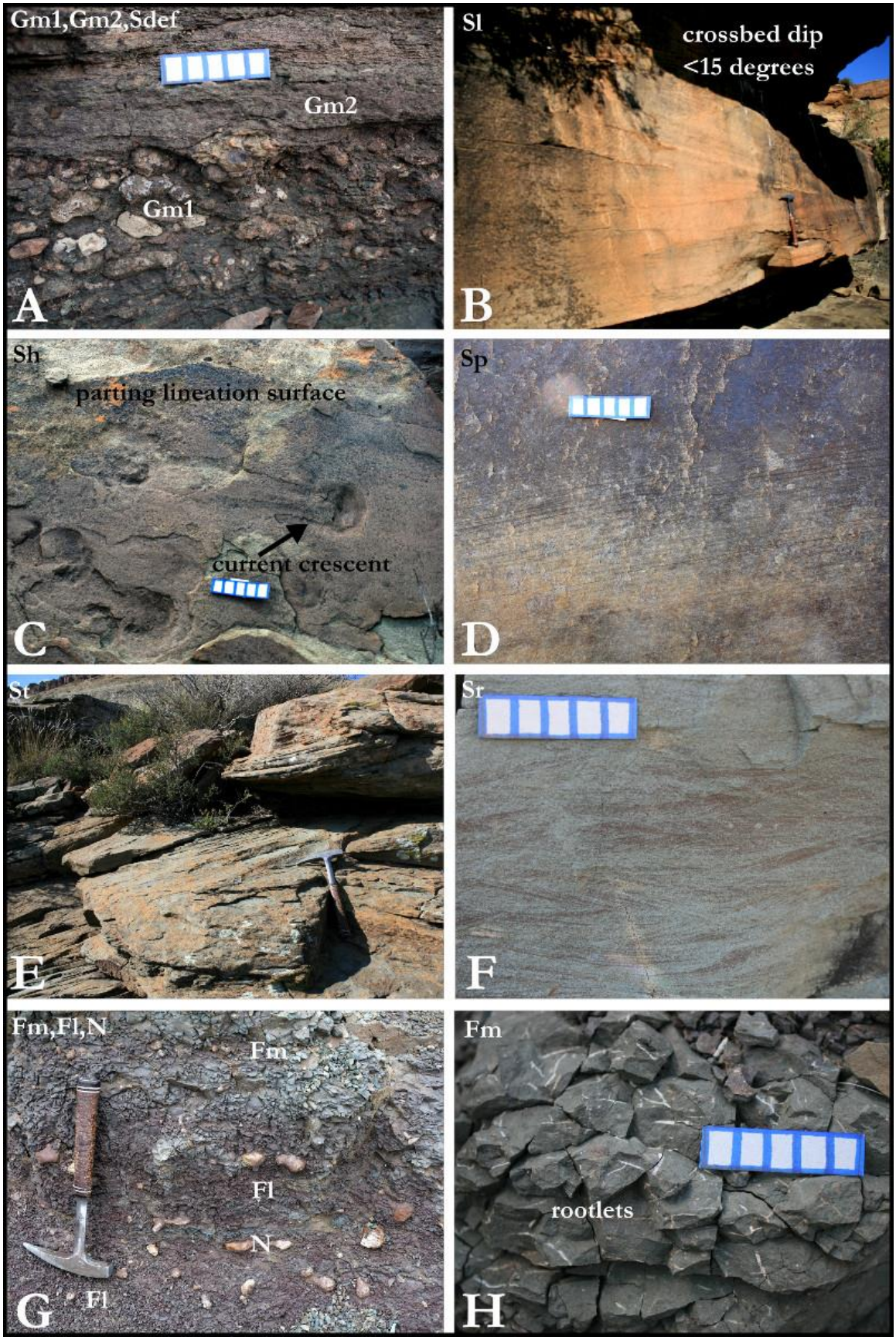

Figure 4.3: Examples of facies present in the Ripplemead member member at Nieu Bethesda. G is from Doornplaats (section 3), C, D, E, and F are from Krugerskraal (section 4), and A, B, and H are from Ripplemead (section 5). Note hammer for scale, and 5 cm scale in A, C, D, F, and H.

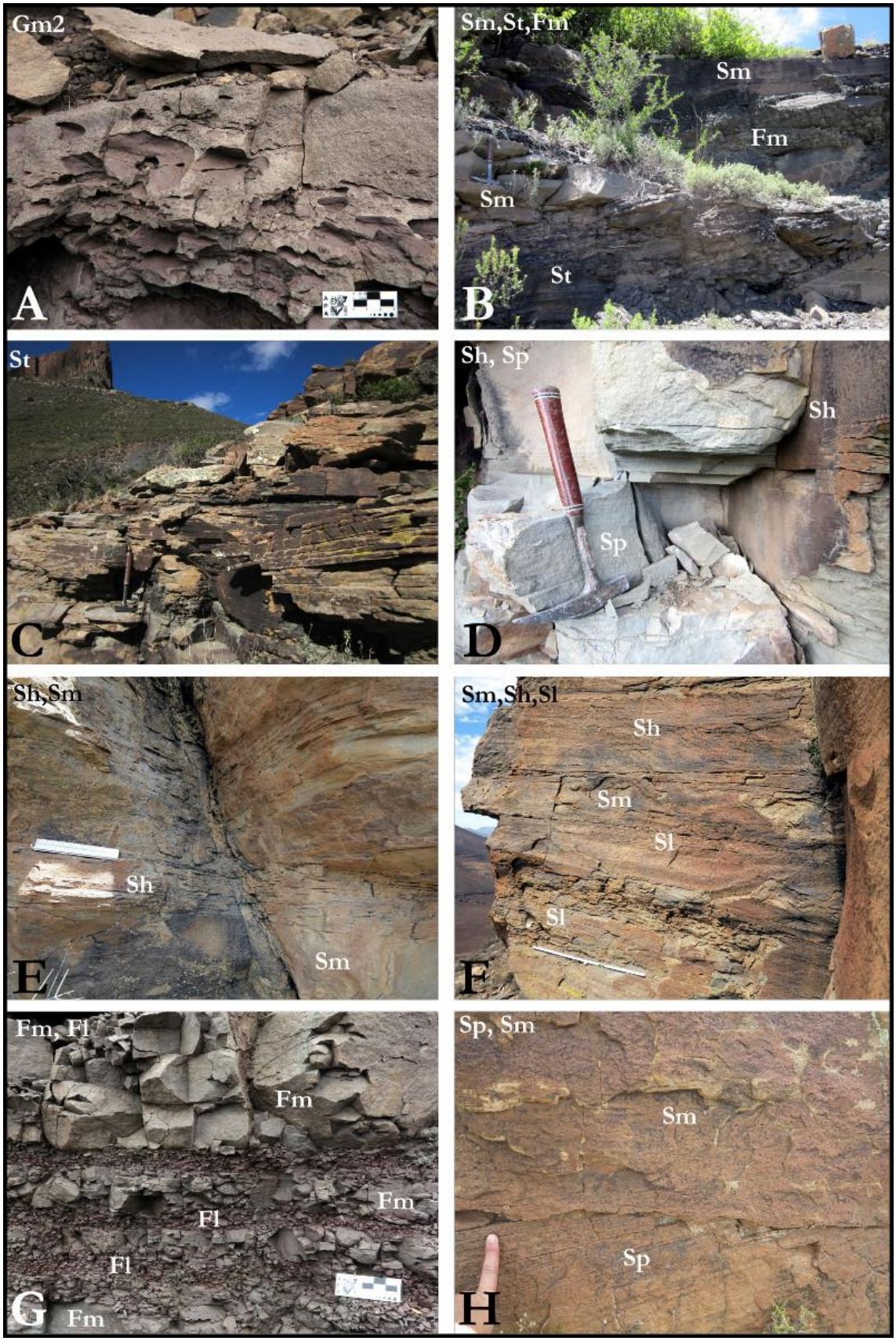

Figure 4.4: Examples of facies present in the Javanerskop member at the Beaufort West and Fraserberg field site. A, B, C, D, and G are examples from Highlands farm (section 6). E, F, and H are examples from Javanerskop, Oukloof Pass (section 7). Note the 5 cm (A, G), 25 cm (E), and 1 m scales (F), and hammer (B, C, D).

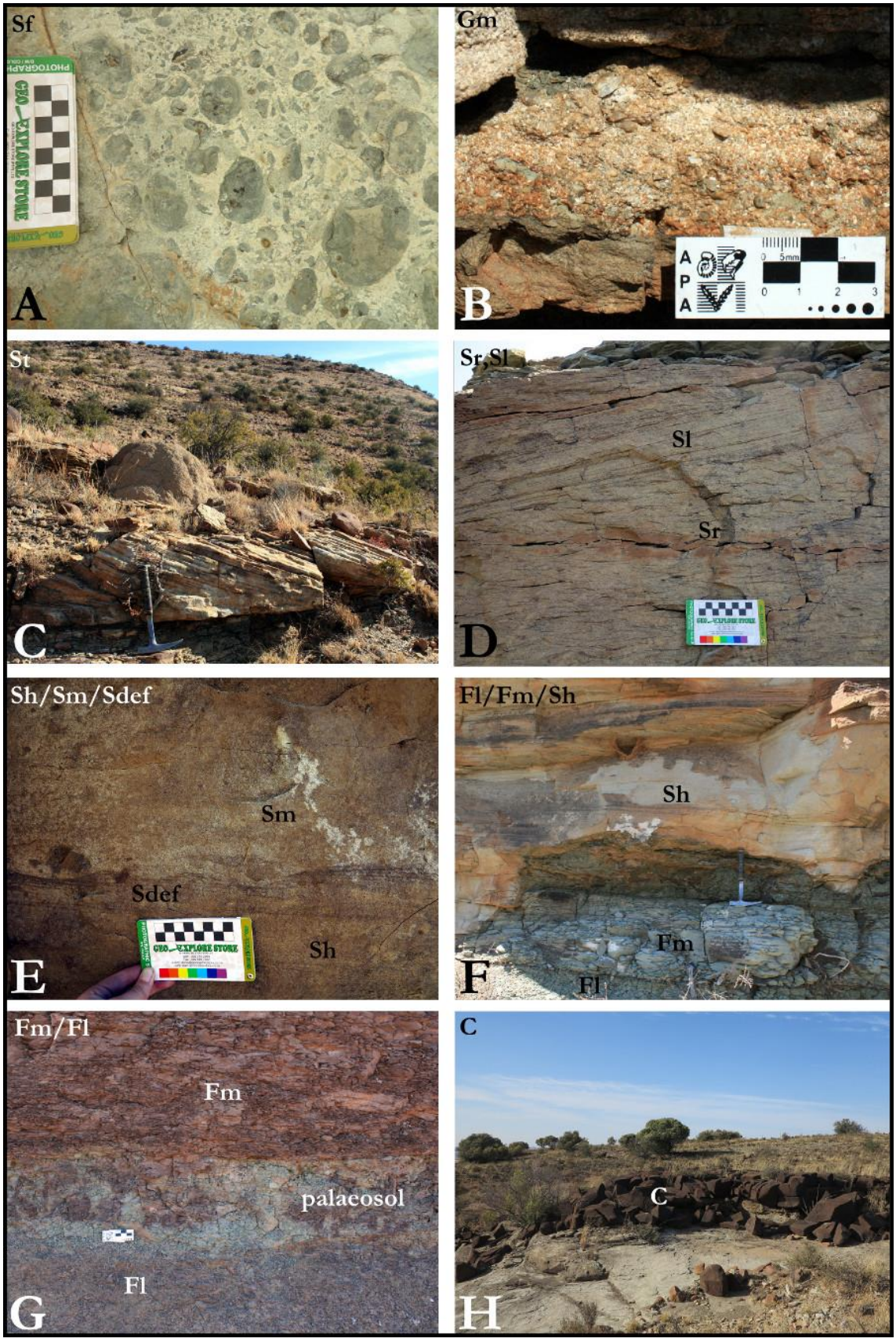

Figure 4.5: Examples of facies present in the Ripplemead sandstone member at Gariep Dam. B, C, F, and G are from van Wyksfontein (section 8), D is from Inhoek (section 9), H is from Schalkwykskraal (section 10), and A, and E are from Tierhoek (section 11). Note hammer and 8 cm, and 4 cm scale where appropriate.

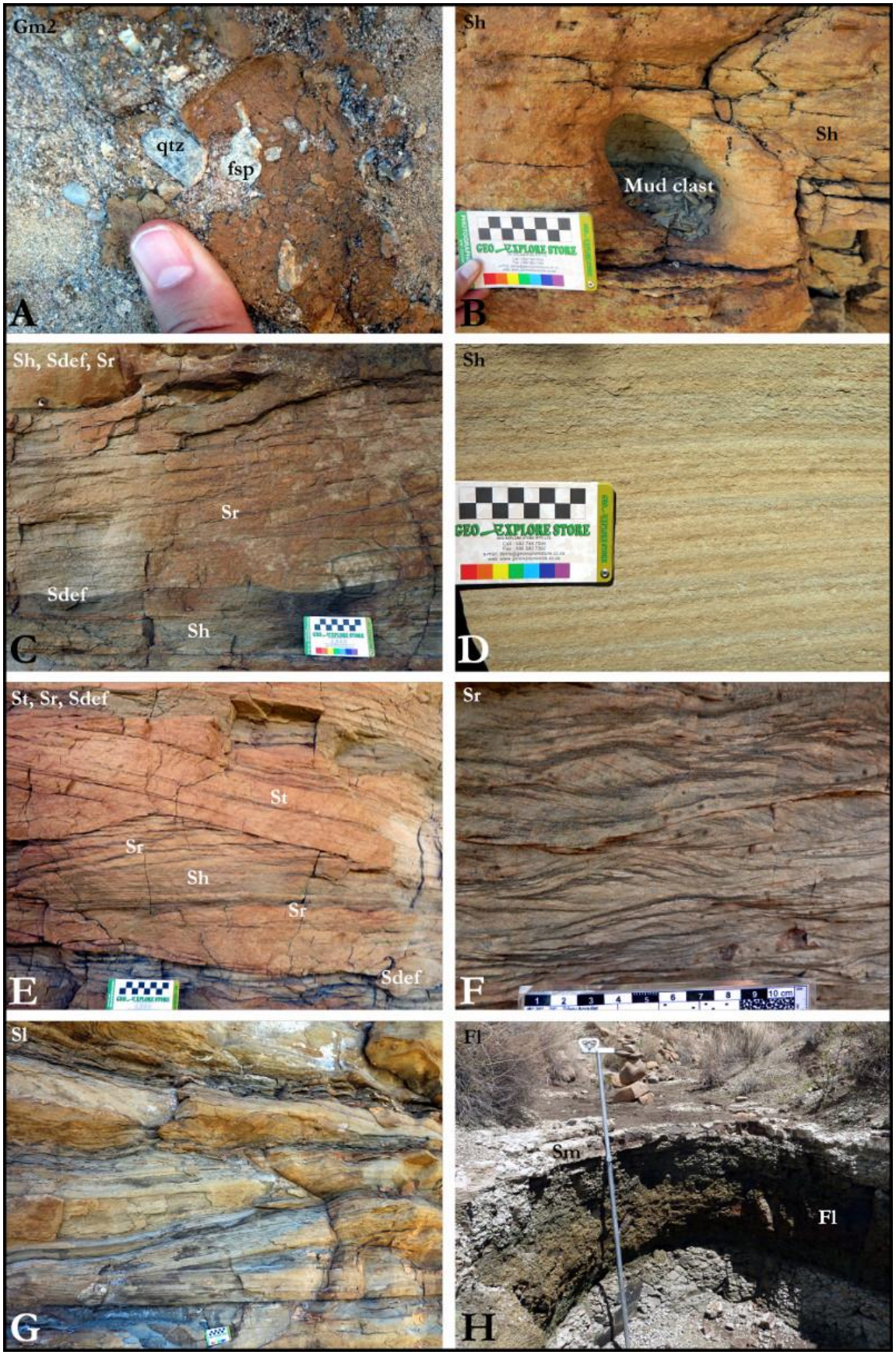

Figure 4.6: Examples of facies present in the Boomplaas sandstone at the Boomplaas Hill, near Jagersfontein (section 12). Note 1 cm scale and Jacob Staff for scale where appropriate.

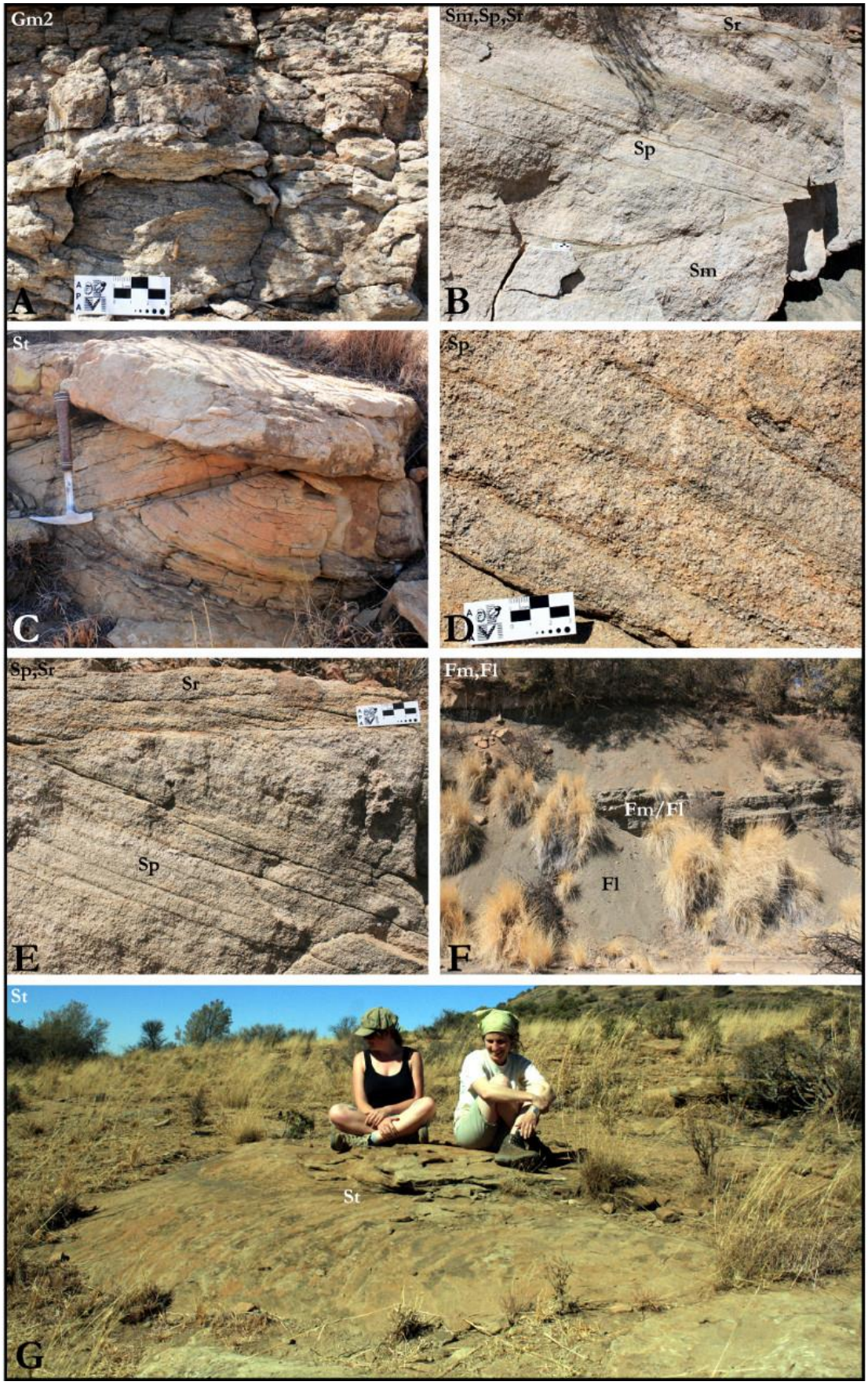

Figure 4.7: Examples of facies present in the Musgrave Grit unit on Tafelkop, near Bloemfontein (section 13). Note 4 cm scale (A, D, E) and hammer (C) and where appropriate.

The lower contacts of F1 can be flat but are normally undulating or erosional with gutter casts or gullied bases (Figure 4.8, A and D). Sole and tool markings can rarely be identified due to the steepness of the sandstone outcrops. Upper bounding surfaces are normally flat, sometimes concave up with minor undulations and rippled surfaces, sharply contacting the overlying and underlying argillaceous deposits (Figure 4.8, F). Single-storey sandstone units are mostly tabular in appearance but commonly pinch out as large lenses over tens or hundreds of metres. Dominant facies are the gravel facies with chaotic fabric (Gm1, Gm2) or the sand facies that normally fines upwards from coarse/medium sand to fine sand in the following order:Sm→Sh→Sl, Sh/Sm→St→Sr (vertical sections 1-13 in Chapter 3.2). Similar facies are present in the single-storey sandstones, although there is a higher preponderance of Sh and Sr.

The fining-upward sequences are commonly truncated (Figure 4.8, B) and mudstone rip-up clasts and mud chip conglomerates (Gm2) are common along these truncation surfaces. Lateral facies changes can be observed in places along strike and this is particularly true with the Sh, St, Sl and Sp facies. Sl and Sp may be lateral equivalents to Sh and St. In places thin beds of floodplain sediments (Fm, Fl, Fr) are present between stories (Figure 4.8, A, B). F1 dominates the Oudeberg, Ripplemead, and Javanerskop members, and Musgrave Grit unit.

Based on the observations of upward-fining sandstone-dominated lithosomes deposited in rapidly eroded semi-consolidated floodplain surfaces, F1 is interpreted to represent confined channelized systems with fluctuating discharge that was likely due to seasonal changes in a semi-arid climate (Stear, 1983, 1985; Smith, 1995; Haycock et al. 1997; Smith and Botha, 2005; Viglietti et al. 2013). Gullied bases encountered in F1 may indicate rapidly dumped sandy sediment during flood events (Myrow, 1992; Smith, 1995). Sedimentary structures overlying these scoures also indicate vertical or lateral accretion in the waning flow following flash flood events. Truncation surfaces in multi-storey sandstones could indicate erosion and waning flood cycle deposits in active river channels, whereas single-storey units could represent failed avulsion events (Sambrook-Smith et al. 2006; Horn et al. 2012).

Aggradation in fluvial systems is the result of bars migrating either downstream (vertical accretion) or lateral to the downstream direction (lateral accretion) and this depends on the channel type (eg. braided or meandering). There are a number of allogenic and autogenic factors that determine fluvial style (eg. discharge, sediment load, channel width, depth, flow velocity, and gradient, vegetation etc.) (Leopold and Wolman, 1957; Schumm, 1968; Tooth, 2000; Long, 2006) (Chapter 5.4).

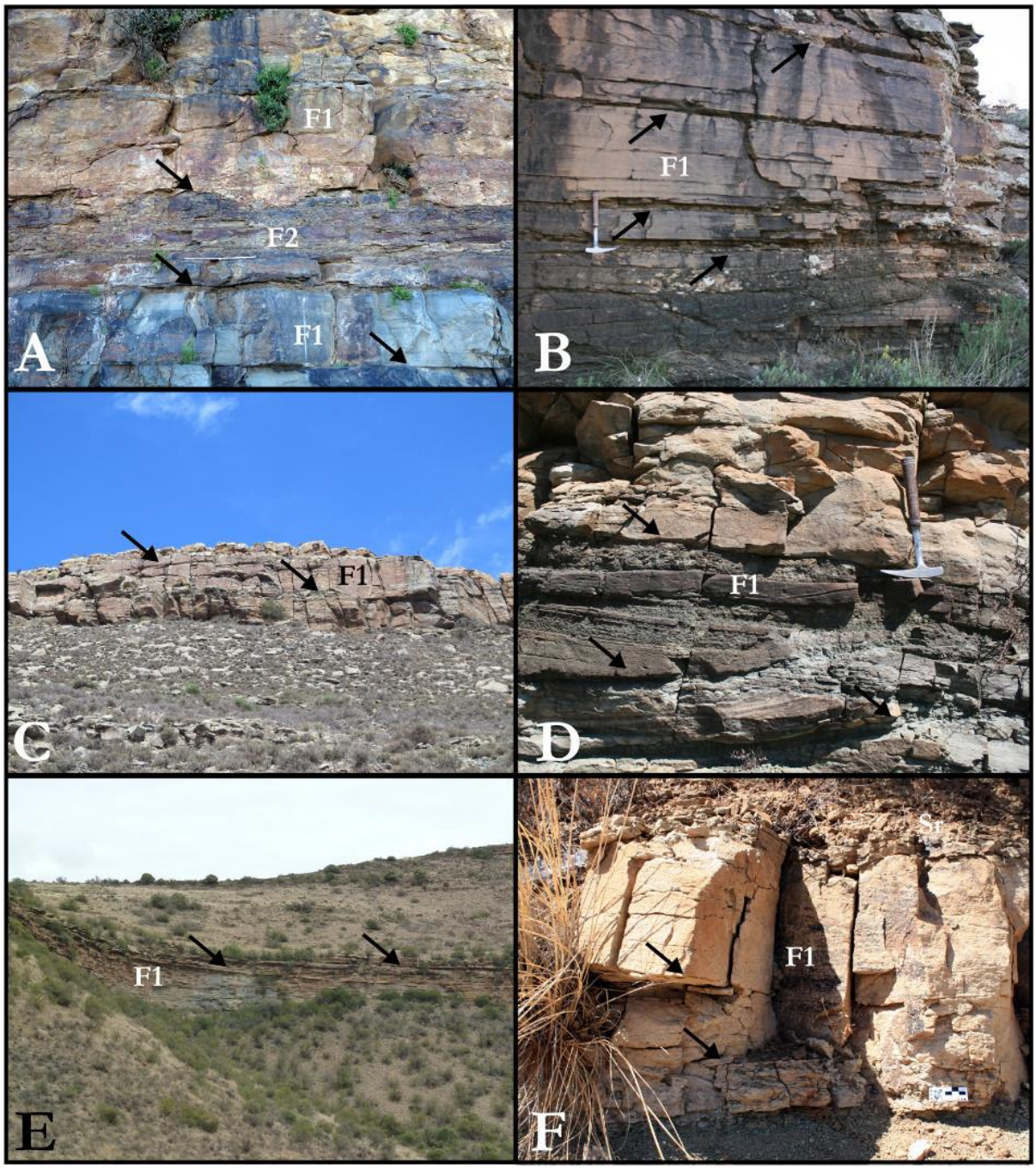

Figure 4.8: Examples of facies association 1 (confined channelized system) from the field sites. Black arrows point to truncation surfaces that are common on the macro and micro scale in F1. A) This F1 example is from the Oudberg Member at the Barberskrans Cliffs (section 1A, Figure 3.6). Note the presence of thin beds of facies association 2 between the F1. It was probably once a much thicker unit because the contacts with the F1 units are sharp and erosional. B) A well preserved example of the multiple truncation surfaces present within the F1 units. They represent multiple sedimentation events during waning flood cycles and subsequent erosion. This example comes from the Ripplemead member on Ripplemead (section 5, Figure 3.13). C) The Javanerskop member on section 7 (Figure 3.18) showing the indurated appearance of F1 in outcrop. D) An example of the erosional bases of F1 in the RM from Inhoek farm (section 9, Figure 3.22). E) The prominent Boomplaas sandstone (section 12, Figure 3.27) showing with arrows pointing to large truncation surfaces. F) The Musgrave Grit unit on Tafelkop (section 13, Figure 3.28) showing smaller truncation surfaces, and the rippled top which F1 deposits commonly have.

Facies Association 2 (suspension settling on floodplain)

Facies association 2 (F2) is the most commonly encountered facies association on the vertical sections (see vertical sections 1-13, and Figure 4.9). F2 comprises lithofacies Fl, Fr, and Fm is locally in association with C or rarely ash layers which have been documented in the Beaufort Group (Rubidge et al. 2013; Day et al. 2015; Gastaldo et al. 2015; McKay et al. 2015) but not during this study. Normally the F2 deposits are sheet like in geometry and laterally continuous (Figure 4.9, B and D). The fine siltstones and mudstones are mainly greenish grey or dusky yellow green particularly in close association to the F1 deposits, although brownish red is present in someplaces (Figure 4.9). The brownish red siltstone colour is abundant in the Teekloof Formation (sections 6 and 7, Figures 3.18 and 3.19), Balfour Formation at Nieu Bethesda (sections 3 to 5, Figures 3.11-3.13), Gariep Dam (sections 8-11; Figures 3.21-3.24), and Jagersfontein (section 12, Figure 3.27) field areas, but absent from Cradock (sections 1A and 1B; Figures 3.6 and 3.7) and Bloemfontein (section 13, Figure 3.28). Exception to this is on Lower Clifton farm in the Baviaansrivier Valley (section 2, Figure 3.8) close to the Permo-Triassic Boundary and the Katberg Formation.

Slickensides, blocky to fissile weathering features (Figure 4.9, C), desiccation cracks, silicified gypsum roses, vertebrate fossils (Figure 4.9, E), and palaeosols are also common in F2. Palaeosols can be recognized by the localized rootlet horizons, colour mottling, and laminae distortion by burrowing invertebrates or vertebrates, and carbonate nodules (Figure 4.9, A, C-E). Additionally many of the fine-grained facies (Fl, Fm) grade laterally into coarser siltstone or sandstone lenses (Fm) which are thin and discontinuous (Figure 4.9, B). F2 is a dominant component of the Daggaboersnek Member, but is also present in the Elandsberg and Palingkloof members. In the Cradock area F2 is rare in comparison to F4 which will be discussed later in the section. F2 normally has sharp lower and upper bounding contacts with the other facies associations (F1 and F3, Figure 4.9, A). Examples of F2 deposits from the field sites are shown in Figure 4.9 but also refer to the lithofacies photographs for examples of the F2 outcrops (Figures 4.1-4.7).

F2 is interpreted as suspension settling on the floodplain due to the evidence described above. Slow accretion of fines on the floodplain is the norm where fine-grained sediment is safe from erosion by the active channels (Walker, 1984). Among others, if floodplain accretion occured over long periods of time, plants could take hold and soil forming processes could begin.

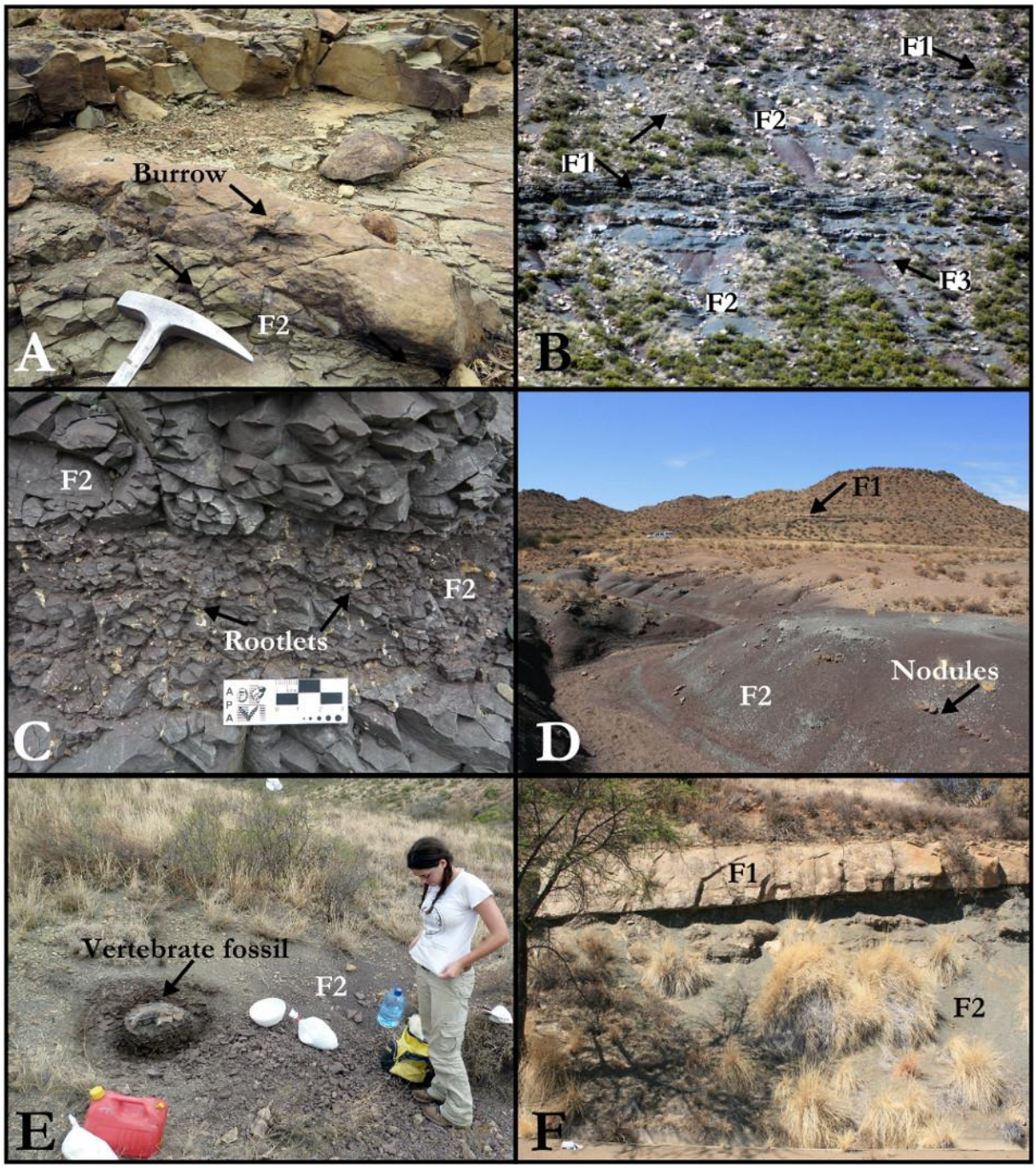

Figure 4.9: Examples of facies association 2 (suspension settling on floodplain) from the study sites. A) Example of F2 on Eildon farm that correlates to the Ripplemead member on section 2 (Figure 3.8) measured on Lower Clifton. Note the vertebrate burrow infilled with fine sandstone. B) Ripplemead farm (section 5, Figure 3.13) shows a good example of the F2 geometry in outcrop within the Elandsberg Member. C) Close up of F2 on Highlands farm in the Upper Steenkampsvlakte Member (section 6, Figure 3.17). Arrows point to calcified fossil rootlets. Note the blocky and fissile weathering. D) Low undulating F2 outcrop on van Wyksfontein at the Middleton-Balfour formation boundary (section 8, Figure 3.21). E) F2 on Boomplaas Hill (section 12, Figure 3.27) with in situ dicynodont fossil (PV/J1, Appendix 2). F) F2 on Tafelkop (section 13, Figure 3.28) with associated F1 deposit from the Musgrave Grit unit.

Evidence of this in the study area include locally common palaeosol horizons, which are common as horizons containing carbonate nodules, slickensides (evidence of soil movement according to Khadkikar et al. (1998)), and colour mottling of deposits in the field areas (Smith, 1995, 2005). Commonly these floodplain deposits are eroded by an overlying F1 or facies association 3 deposit into the immediate area following a flood, as is evidenced by the interruption by F1 or F3 deposits in the study areas (Viglietti et al. 2013).

Facies Association 3 (unconfined overbank deposition)

F3 represents unconfined high energy deposition onto the overbank environments (Figure 4.10). F3 are rarely thick deposits (between 0.5-3 m thick) and include some of the siltstone facies (Fm, Fl) (Figure 4.10, A and B) but also the sandstone facies (Sm, Sh, Sr, St) (Figure 4.10, C and D). F3 are laterally continuous lense or pod shaped bodies over tens to hundreds of metres (Figure 4.10). The most common colour for the deposits is greenish grey and pale olive. Basal contacts with other facies associations are sharp, whereas upper bounding surfaces can be sharp, even or gradational (Figure 4.10, A, C, and D). Sometimes undulatory upper contacts are present if erosion occurred prior to burial. Bioturbation, fossil fishes, rootlets and fossil plants are common in the facies association at Nieu Bethesda (sections 3-5; Figures 3.6-3.9) and Cradock (sections 1B and 2). Bivalves have also been documented in F3, but only near Cradock and the site of section 2 (see Figure 4.12).

Based upon the juxtaposition to F1 deposits, lack of sedimentary structures that indicate channelized flow (Sm, Sh, Sr) and general fine sand to coarse silt grain size, F3 is interpreted to represent unconfined overbank deposition. F3 may also represent crevasse-splay deposits as they bear similarities with decimetre thick sheet sandstones from the Oligocene Guadalop-Matarranya System (northern Spain) described by Mohrig et al. (2000) and also sheetfloods described by Graf and Lecce (1988) and Long (2006).

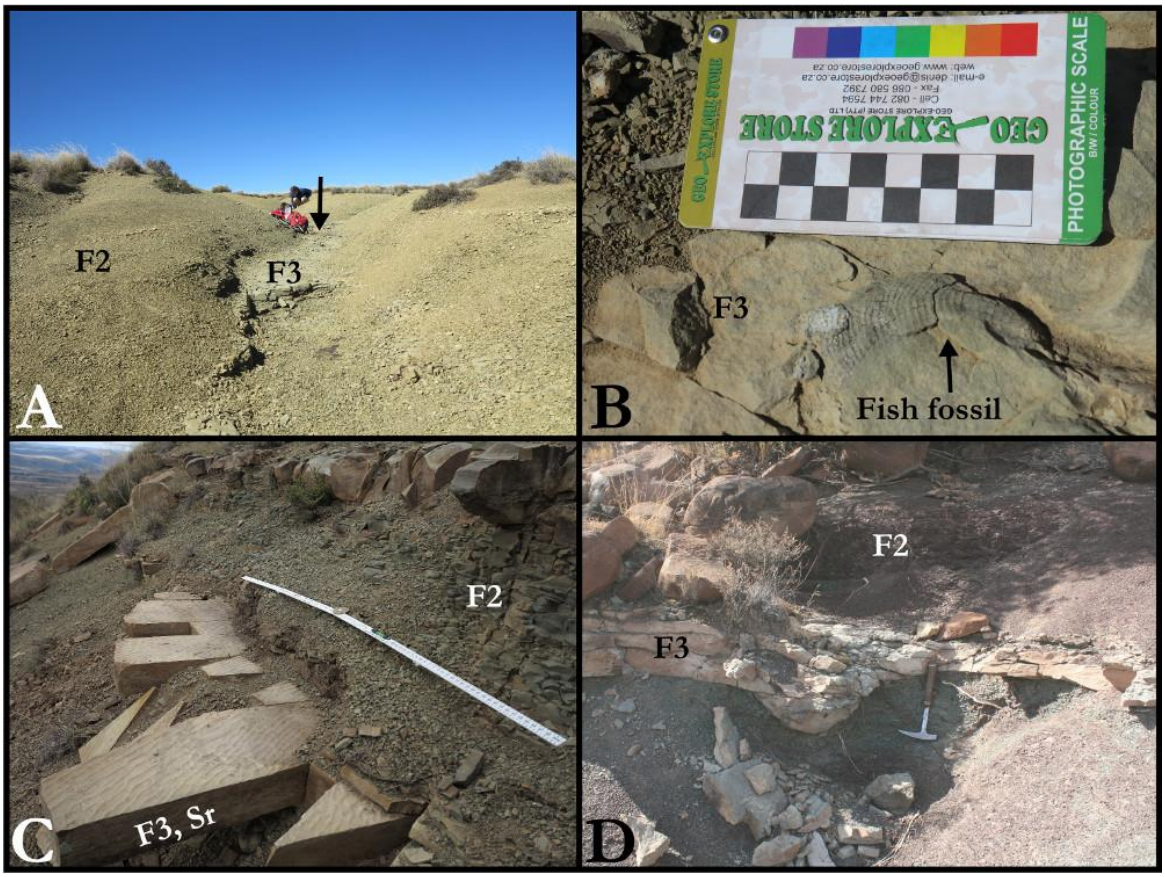

Figure 4.10: Examples of facies association 3 (unconfined overbank deposition). A and B) F3 siltstone containing fragmentary palaeoniscid fish (Actinopterygii). Arrow indicates where the fossil fish were found on Eildon farm (Baviaansrivier Valley) in Lower Elandsberg Member. C) F3 with rippled top on Doornplaats farm (section 3, Figure 3.11) Scale is 1 m long. D) F3 deposit with large gutter cast on Inhoek farm (section 9, Figure 3.22).

Facies Association 4 (lacustrine system)

F4 occurs locally in association with F1, F2, and F3 (Figure 4.11). This facies association has only been documented abundantly in the Daggaboersnek Member (Lower *Daptocephalus* Assemblage Zone) in the Cradock area where it is a laterally continuous and ubiquitous facies association, consisting of up to 20 m thick sheet like bodies of finely laminated and interbedded mudstone and siltstone (Fl) (Figure 4.11, A, B). This is particularly the case in section 1B (Figure 3.7) on Hales Owen farm. In many cases thin (< 10 cm) rippled sandstone beds (Sr) or coarse massive siltstone (Fm) can be observed (Figure 4.11, A, B). The most common colours for this facies association are dark greenish grey and dusky yellow green. The former colour is most common in the Cradock area where this facies association is best developed. In the Cradock area plant fossils, leaf and stem impressions, fish bones, and rare bivalves have been identified from this facies association (Figure 4.12). The bivalves occur in both F3 deposits and carbonaceous pods in the F4 deposits. The lack of pedogenic nodules, and laterally extensive laminated varve-like

mudstone and sandstone are indicators of lacustrine conditions (Reading, 1978; Boggs Jr, 2006) (Figure 4.11, C). Johnson (1976) also interpreted the Daggaboersnek Member in this part of the basin as representing lacustrine environments based upon the following. He noted this unit consists of regular bedding of thin tabular sandstones and moderately developed varved rhythmitites of fine sandstone and dark green shales. The sandstones commonly have large wavelength (7cm, ripple index 9) wave ripple surfaces preserved which trend at a right angle to the palaeocurrent vectors collected from overlying and underlying strata (ENE-WSW). In addition Johnson (1976) also noted that the dark green shales with locally abundant leaf impressions was additional evidence for the presence of either coastal marshes or swamps adjacent to a large water body capable of generating large enough wave systems to produce the wave rippled sandstones.

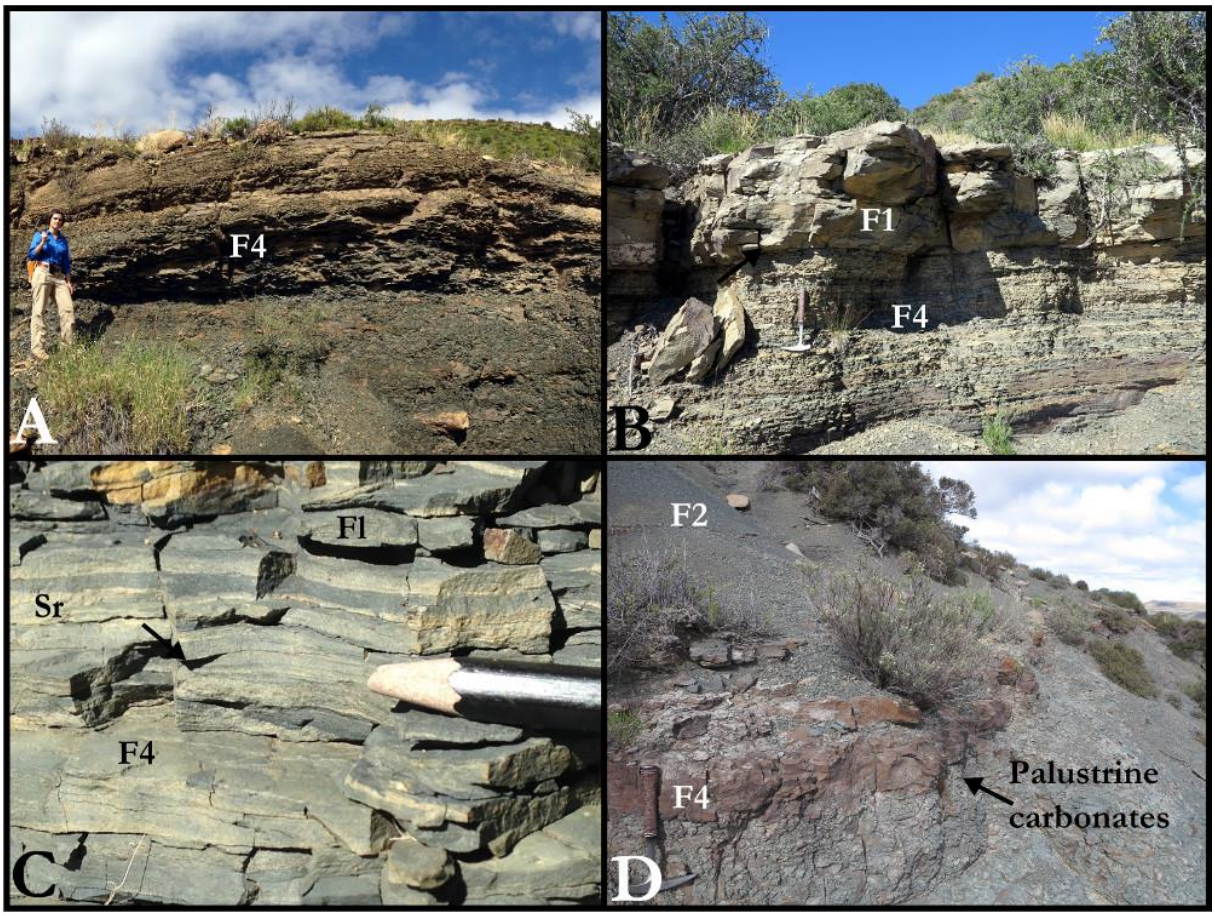

Figure 4.11: Examples of facies association 4 (lacustrine system). A) Typical F4 outcrop on Hales Owen farm (section 1B, Figure 3.7) showing the well laminated fine dark green siltstone and fine sandstone. B) F4 beds overlain by small single story F1 deposit on Hales Owen (section 1B, Figure 3.7). Hammer for scale. The bases of these F1 deposits are commonly gulleyed contain fossil plant material, gravel-sized clasts, fossil bone. C) Close up of the varve-like laminations of siltstone and fine sandstone in F4 on Hales Owen, pencil for scale. Fossils plant material and worm trails are common on these horizons. D) Carbonaceous layer on Doornplaats (section 3, Figure 3.11) that is laterally continuous over a couple tens of metres. It is possible that this layer formed under waterlogged or palustrine conditions on the floodplain (Smith, 1990, 1995; Tabor et al. 2007). Rock hammer for scale.

F4 has been documented in Nieu Bethesda but they are not as well developed as in Cradock (section 1B). On the Doornplaats farm section (section 3, Figures 3.11 and 4.11, D) F4 grades laterally to F2 and it is rarely more than a few metres thick and is mostly dusky yellow green (5GY 5/2) in colour. Here F4 is also associated with thin ripple-topped F3 sandstones (Figure 3.10, C). Additionally, laterally continuous smooth-surfaced carbonate nodule-rich horizons documented on Doornplaats farm (section 3, Figure 3.11) in this study have been interpreted previously to have formed under palustrine conditions (Smith, 1990, 1995; Tabor et al. 2007) (Figure 4.11, D). Thus the thicker more laterally continuous F4 units in the Daggaboersnek of the Cradock area may representative deposits of larger and more permanent and waterbodies than the Daggaboersnek Member in the Nieu Bethesda area.



Figure 4.12: Examples of F3 and F4 deposits from the Baviaansrivier Valley, Eastern Cape in the Lower Daggaboersnek Member. In these examples the association of fossil bivalves is shown from Lyndoch farm which is close to the horizon of the Oudeberg Member in the valley. A) F3 rippled sandstone that overlies very finely laminated siltstone and mudstone. B) The site where bivalve fossils were recovered from within the F3 and F4 layer. Rock hammer for scale. C) An example of one of the larger bivalve shells recovered from the F3 deposit. D) Thin section micrograph showing the size range of the bivalve remains recovered from the base of the F3 deposit shown in (B). Note the associated presence of tiny bones, possibly from fish or other small tetrapods. Photograph is in cross polarised light (XPL) at 4 X magnification.

4.3 Architectural element analysis

Architectural elements, as discussed in Chapter 2.3.4, represent facies associations with distinct 3D geometry than can be defined as components of a fluvial depositional system with characteristic facies associations (eg. confined channelized system) that are interpretable subenvironments. Since architectural element analyses are mainly conducted on channelized systems (Miall, 1996), this section investigates the architectural elements identified in the sandstone-rich horizons of the Oudeberg, Ripplemead (RM), and Javanerskop members, the Boomplaas sandstone (BS) and the Musgrave Grit unit (eg. F1 deposits). The investigation was conducted in order to discern whether fluvial style changes occurred in the sandstone-rich horizons through time in the Balfour and Teekloof formations, and if so did these occur at the same stratigraphic intervals at all study sites, or were the fluvial style changes a reflection of their position in the distributive fluvial systems within the proximal or distal foredeep of the Karoo Basin in the Lopingian.

Reference is made to panel sections and field photographs from each study site which are annotated to show different architectural features. Nine main architectural elements were identified using the revised architectural element classification of Miall (1985, 1996, 2014) which is based on a letter coding system. The methodology of Colombera et al. (2013) and Wilson et al. (2014) was also followed. Previous works of Leopold and Wolman (1957); Allen (1963a, b, 1970); Friend (1977); McCabe (1977); Miall (1977); Reading (1978); Rust (1981); Goldring and Aigner (1982); Allen (1983); Mossop and Flach (1983); Miall (1985); Stear (1985); Bridge et al. (1986); Reading (1986); Bristow (1987); Olsen (1988); Wizevich (1992, 1993); Miall (1994, 1996); Nanson and Knighton (1996); Reading (1996); Tooth (2000); Sambrook-Smith et al. (2006); Friend (2009); Sambrook-Smith et al. (2009); Sambrook-Smith et al. (2010); Ashworth and Lewin (2012); Horn et al. (2012); Miall (2014) helped to identify the nine architectural elements in the Oudeberg, Ripplemead, Javanerskop member, and Musgrave Grit unit, into five architectural types (A to E). The five architectural types, alongside the facies associations and architectural elements used to identify them, are compiled in Table 4.3.

Table 4.3: Architectural elements identified in this study				
Element name and code	**Key characteristics**	**Interpreted subenvironment**	**Facies association**	**Architectural type**
CH (aggradational channel fill)	Characterized by concave upward geometry, erosional bases and vertically stacked facies units separated by erosional 2nd or 3rd order bounding surfaces. This element code is used only when channel fill lacks evidence for bedding grown through inclined accretion such as by LA or DA (Reading, 1978; Miall, 1996; Colombera et al. 2013).	Aggradational channel fill in active channels.	F1,F3	A,B,C,D
DA (downstream–accretion barform)	Identified by horizontal basal (5th order) and convex up upper (4th order) bounding surfaces along with internal 3rd order bounding surfaces that incline downcurrent at a low angle (<10˚) (Miall, 1994, 1996).	Infill of active channel by downstream migrating bars.	F1	A,B
LA (lateral–accretion barform)	Characterized by the dip direction of the inclined (~25˚) accretionary surfaces, which is roughly normal to the palaeoflow. These elements have slightly concave upward bases which are often erosional. (Allen, 1963; Miall, 1985; Colombera et al. 2013).	This element has traditionally been used to represent the channel infill by laterally migrating point bars in a meandering river system.	F1	A,C,D
DLA (downstream and lateral–accretion barform)	This element type was used by Colombera et al. (2013) in their study and it characterizes elements that accrete obliquely to the palaeoflow.	DLA has been identified by a number of authors who refer to these elemenys as representing alternate bars that accrete both downstream and laterally (McCabe, 1977; Bridge et al. 1986; Olsen, 1988; Wizevich, 1992; Miall, 1996).	F1,F3	A
AC (abandoned channel–fill)	Similar to CH but infilled by finer grained material (Hopkins, 1985; Miall, 1996).	Often identified in high sinuosity systems where channels are abandoned by chute or neck cut-off.	F1,F3,F2	A

CS (crevasse splay or lacustrine delta)	Ribbon shaped bodies that coarsen upwards. They have sharp bases and gradational tops and are normally a feature of the floodplain environment.	Interpreted as mini channels that have a point source from the active channel. They either show confined or unconfined flow during flood events. (Colombera et al. 2013).	F3,F4	B,C,D
SB (sandy bedform)	Represent tabular sheets or lenticular sandbodies with flat bases and tops that are sharp. They are identified when LA or DA cannot be identified and by the presence of purely vertical aggradation. Normally infilled by Sh or St, sometimes Sr.	SB are commonly identified as unconfined flows such as in distal braid plain environments (Miall, 1996). Alternatively they have also been interpreted as sheet floods in ephemeral streams during flood events (Stear, 1985).	F3	B
LV (levee)	Tapering wedges that dip (2-4˚) and thin away from the channel margin (Colombera et al. 2013). Palaeoflow normally orientated perpendicular to the channel or obliquely downstream from the channel margin (Miall, 1996).	Proximal overbank deposition by sheetfloods next to channel belt margins. Often represented high points on the overbank environment (Miall, 1996).	F1	A,D
FF (overbank fines)	Tabular geometry and dominated by vertical aggradation. Palaeosols, rooted horizons, and vertebrate fossils common.	Suspension settling of mud and silt during floods on the flooplain environments adjacent to major channel systems.	F2,F4	A,B,C,D

4.4 Recognition of architectural types in the study area

The five architectural types (A, B, C, D, and E) were identified based on the co-occurance of particular architectural elements (see Table 4.3) at the field sites and were documented using photomosaic panels. Where appropriate the position of individual figures is shown on the photomosaic panels. The description of the architectural types is followed by an interpretation of each architectural type and an inferred fluvial style.

Type A: Channel belt dominated by DA

Type A consists of stacks of channel forms (CH) comprising multi-storey ribbons and sheets that are dominantly downstream accreting (DA) but downstream and lateral-accreting barforms (DLA) are present too. The DA barforms are identified by their horizontal basal (5th or 4th order) and convex up upper (4th order) bounding surfaces along with internal 3rd order bounding surfaces that incline parallel to palaeocurrent flow (normally at $<10^{0}$). At all outcrops, palaeocurrent measurements were taken from cross-bedded sandstone (St, Sl, Sr) or from tool

markings or other trend marking sedimentary structures. The DA and LA features are present within 12-15 m wide but 75–100 cm thin nested channel forms (CH) that truncate one another, creating pinch and swell structures and ribbon features. Many of these shallow wide CH are positioned alongside one another on the same level, are infilled with St in their bases, and laterally and vertically change into Sl or Sh, then finally Sr at their upper bounding surfaces. Dusky yellow green (5GY 5/2) overbank fines (FF) are present in places underlying CH or as thin drapes between truncation surfaces (Figure 4.8, A, B). Associated with these contacts are heterolithic lithologies of F1, including Gm or Sf (Figure 4.1, A, C-E).

Type A is the main architectural style present at the Oudeberg Member at the Barberskrans Cliffs (section 1A) south of Cradock (Figure 4.13, see disc for high resolution version). Examples of the architectural elements and features described in Table 4.3 are shown in Figures 4.14-4.16. Figure 4.14 shows examples of the smallest nested channels identified at ~ 110-130 m on Figure 4.13. They likely represent small channels (~3 m wide and 0.5 m high). These channels are infilled with trough cross-bedded sand with many internal 2nd and 3rd order bounding surfaces. Figure 4.15 shows examples of the DA macroforms present at ~ 170 m and 350 m on Figure 4.13. These macroforms are larger but show the same ribbon shapes as the previous smaller channels. The pinch and swell features are caused by topographic highs between channels (Friend, 1977). Some show examples of being truncated and eroded and these are pointed out in the photographs. Figure 4.16 is an example of one of the better preserved large channel forms in the panel and is present at ~310 m on Figure 4.13. This channel shows examples of truncating previous DA macroforms, and also channel piracy, which is likely the result of some macroforms accreting obliquely (DLA) to the current flow (Bridge et al. 1986; Miall, 1996; 2014) (Figure 4.16, A, B, and D).

Figure 4.13: Panel section of the Oudeberg Member, Barberskrans Cliffs, Cradock (section 1A). See disc for high resolution version.

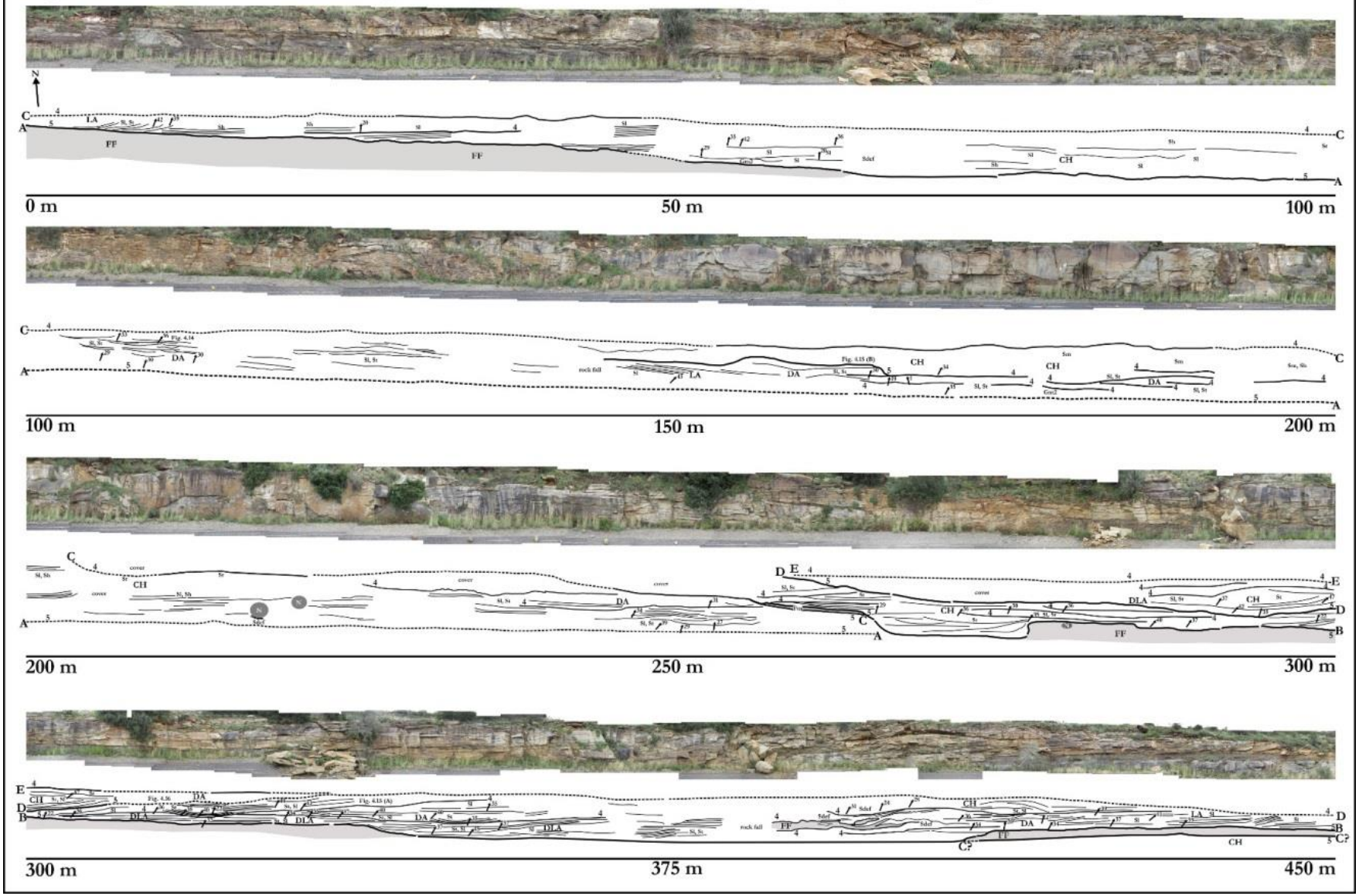



Figure 4.14: A) Small wide distributary channels and their low angle scours are pointed out by Cameron Penn-Clarke at ~110 m to 130 m on the panel section constructed at the Barberskrans Cliffs (Figure 4.13). B) Scours shown close up and 3rd order bounding surfaces indicated by black arrows. Scale in photograph represents 1 m.



Figure 4.15: DA macroforms as present in the Oudberg Member panel at the Barberskrans Cliffs (Figure 4.13) at (B) ~ 170 m and (A) 350 m on Figure 4.13. Note the truncations of the sand ribbons in (B) by a large channel form (CH) (5th order arrows).

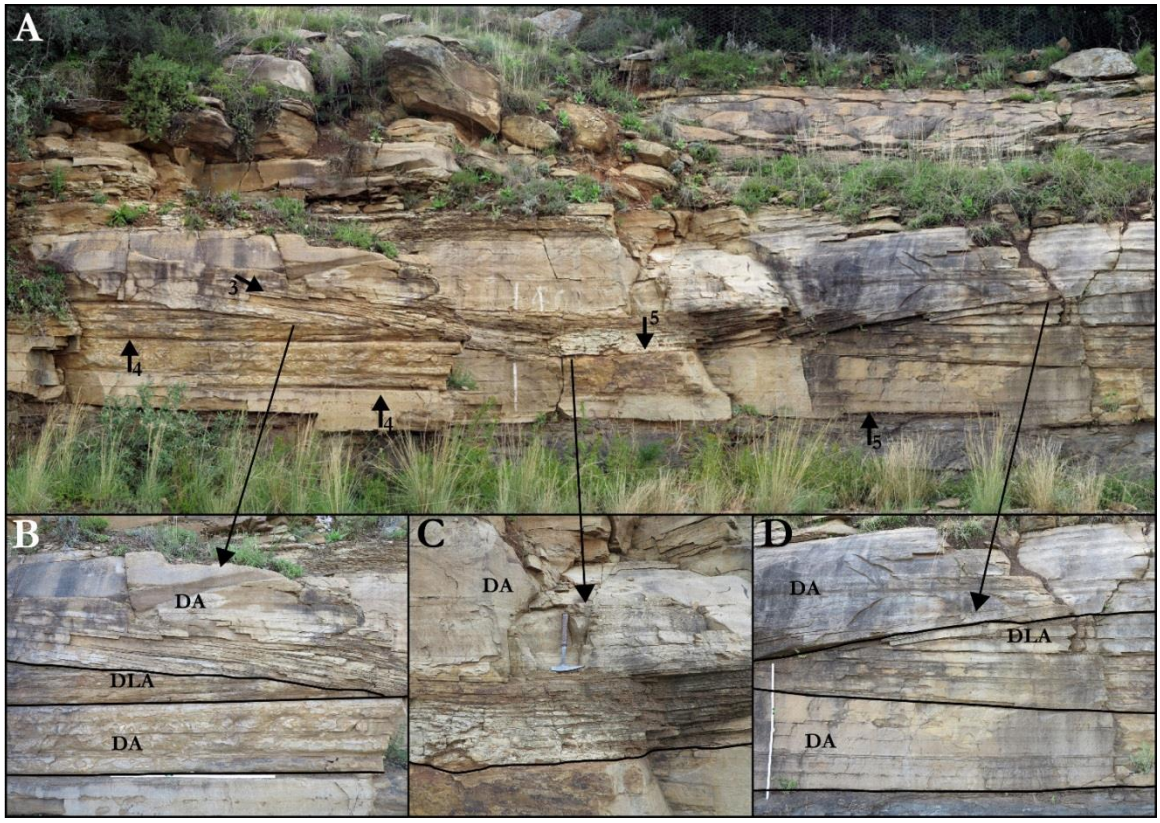

Figure 4.16: A) One of the better preserved channel forms from Figure 4.13 which is 12 m across and 0.75 m high. This channel occurs ~310 m on Figure 4.13 and shows examples of DA, DLA (B, D), and truncations into previous DA barforms by the central channel (C). It is an example of channel piracy, which is likely the result of some macroforms accreting obliquely to the current flow (DLA). Scale bar represents 1 m.

Type A is also identified on Ripplemead farm (section 5, Figure 3.13) near Nieu Bethesda in the RM sandstone (Figure 4.17). Figure 4.17 is located ~ 38 m on section 5 and here the DA macroforms (~ 5 m high, 20 m wide) are larger than those in the Barberskrans Cliffs panel (Figure 4.13). LA macroforms are not abundant however, evidence for some higher sinuosity components are evident. Figure 4.18 depicts an example of components reflecting higher sinuosity in the lowermost RM sandstone and shows evidence of slight changes in accretion direction. Here the lower barforms are typical DA bars, accreting in the flow direction. This is evident from the orientation of the barforms in the outcrop relative to the palaeocurrent direction (Figure 4.18). Above these DA barforms are DLA barforms because they show features that indicate some lateral accretion juxtaposition to downstream accretion.

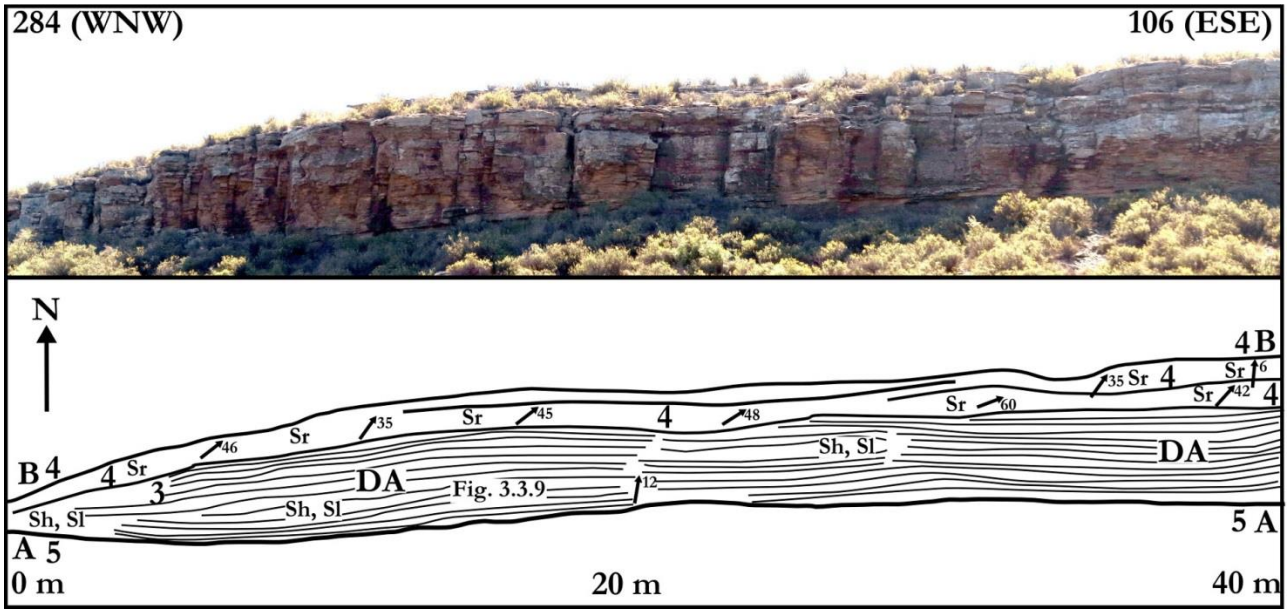

Figure 4.17: Panel section in the Ripplemead member on Ripplemead farm. The DA macroforms are present on the second single story RM sandstone on Ripplemead (section 5, Figure 3.13).

Truncation by the younger channel shows evidence of accretion that occurred obliquely to the current flow (Figure 4.18). This means some attachment of the bar to the side of the channel is evident, which is not typical of DA barforms (McCabe, 1977; Bridge et al. 1986; Miall, 1996, 2014). At 55 m on section 5 (Figure 3.19) is an abandoned channel-fill (AC) architectural element (Figure 4.19). According to Hopkins (1986) and Miall (1996) these elements are encountered in higher sinuosity systems where channels are abandoned by chute or neck cut-off and have also been interpreted in this manner by Smith (1993, 1995) in the Beaufort Group. Additionally Colombera et al. (2013) suggest they represent the infill of ponded water bodies developed in abandoned reaches. Therefore the fluvial style of the RM in the Nieu Bethesda area may represent higher sinuosities than identified at Cradock in the Oudeberg Member, but are still considered low sinuosity. Since neither of these sites manifests typical features of true braided or meandering systems, they still fit the criteria that define architectural Type A which comprises vertically stacked channels dominated by DA elements with minor DLA or LA elements.

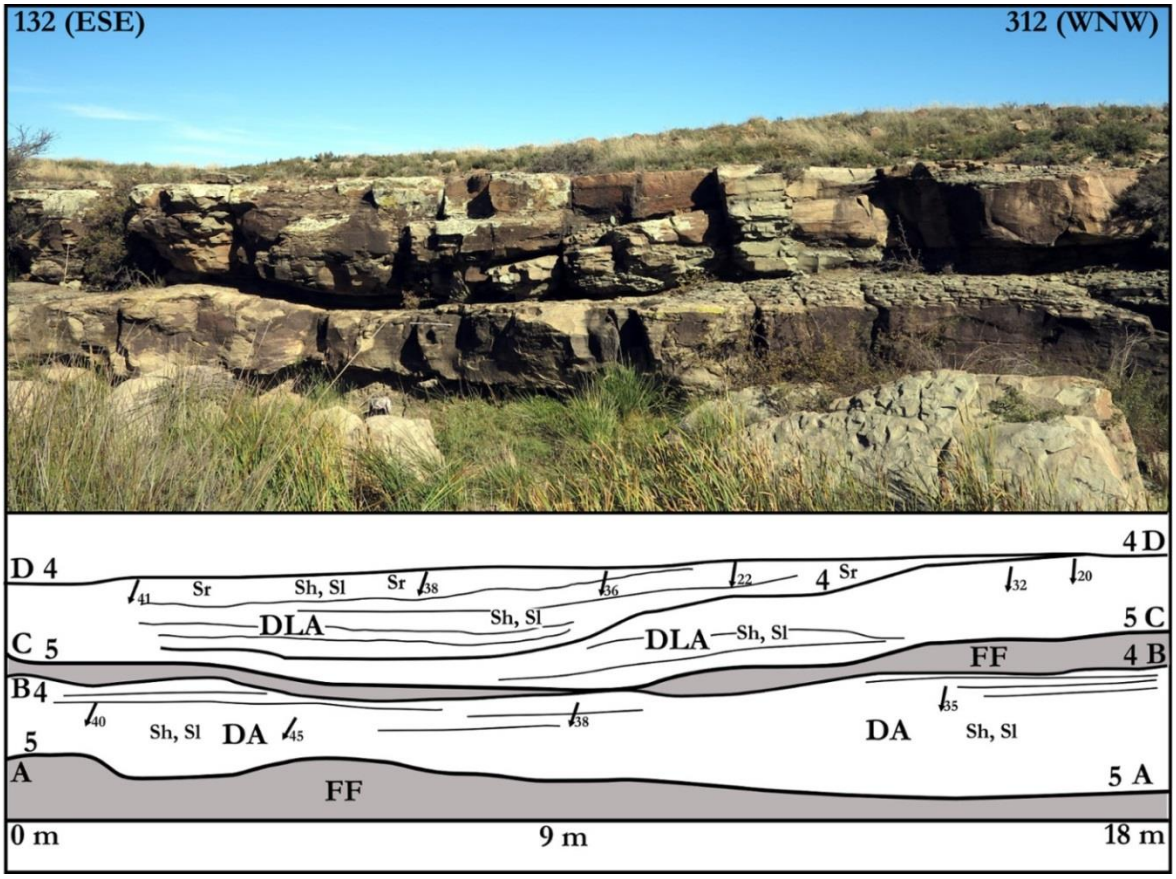

Figure 4.18: The lowermost Ripplemead member sandstone at the base of the Ripplemead farm section (section 5, Figure 3.13). The panel above depicts a slight change in accretion direction in the barforms from the bottom of the panel to the top. At the base the barforms are accreting downstream and parallel to flow (DA). However the upper barforms show some oblique accretion to the current by the presence of gently dipping accretion foresets dipping towards the left of the photograph. Since the foresets are at a high angle but not normal to the current, they are not true LA surfaces which means they are classed as DLA barforms.

Type B: SB dominated channel-belt fills

The main architectural component of Type B is laterally extensive sheets of plane beds (Sh) or 3D dunes (St) identified as SB elements by flat 5th order lower, irregular 4th order upper and low angle 3rd order internal bounding surfaces (Miall, 1996; Reading, 1996). In places the SB are disrupted by an erosional cutbank of a channel (CH) which are usually infilled by large scale St or Sh (Figures 4.22, and 4.23). The lowermost bounding surfaces for Type B can be highly erosive and gullied (Figure 4.24, A, B). Lenticular or wedge-shaped channel fills and cut banks are normally infilled with St or Sl with erosive bases that have high relief. Upper bounding surfaces can be sharp or gradational. SB and CH are frequently draped with fine-grained rippled (Sr) sand or siltstone (Figure 4.24, B). Type B has been recognized mainly in the RM sandstones of the

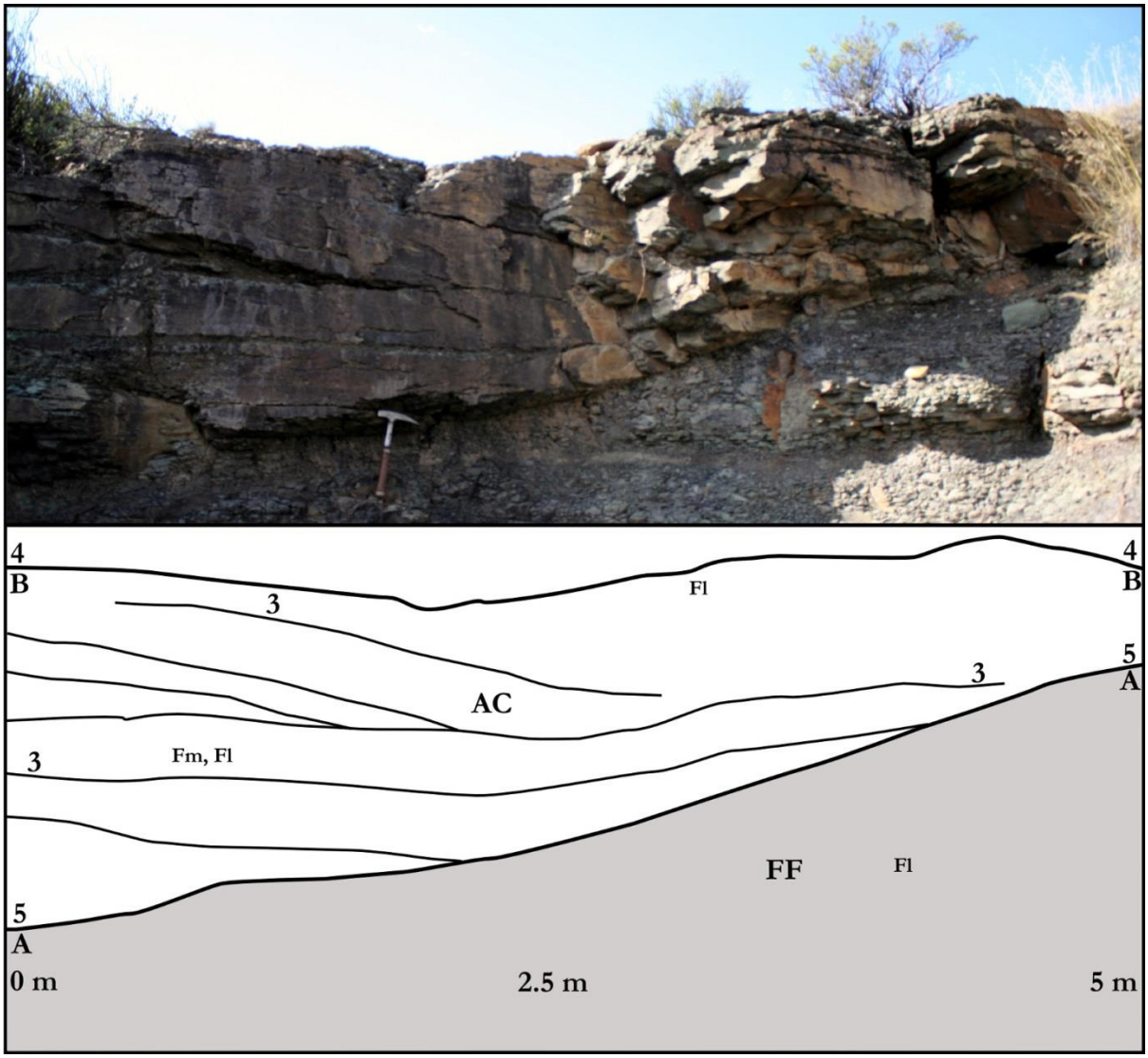

Figure 4.19: The abandoned channel element (AC) that is located 55 m on section 5 (Figure 3.13). This channel fill comprises only coarse siltstone (Fm, Fl) thus is interpreted as an abandoned channel (AC) element. Although these are typical of higher sinuosity rivers, (Miall, 1996), AC elements are not restricted to any particular fluvial style setting.

Gariep dam area on van Wyksfontein (section 8, Figure 3.21) and Inhoek farms (section 9, Figure 3.22), although it has also been identified on Krugerskraal farm (section 4, Figure 3.12), Nieu Bethesda. Figure 4.20 shows SB elements in the RM sandstone on Krugerskraal farm at ~ 129 m on section 4 (Figure 3.12). The elements were defined SB because they could not be assigned to elements LA, DA, or DLA, however they are dominated by vertical aggradation due to the very low angle of the 4th order scoured bounding surfaces which are likely the result of multiple flood cycles. A close up of these SB elements is shown in Figure 4.21. The RM sandstone at van Wyksfontein (Figure 4.22) and Inhoek (Figure 4.23) show good examples of

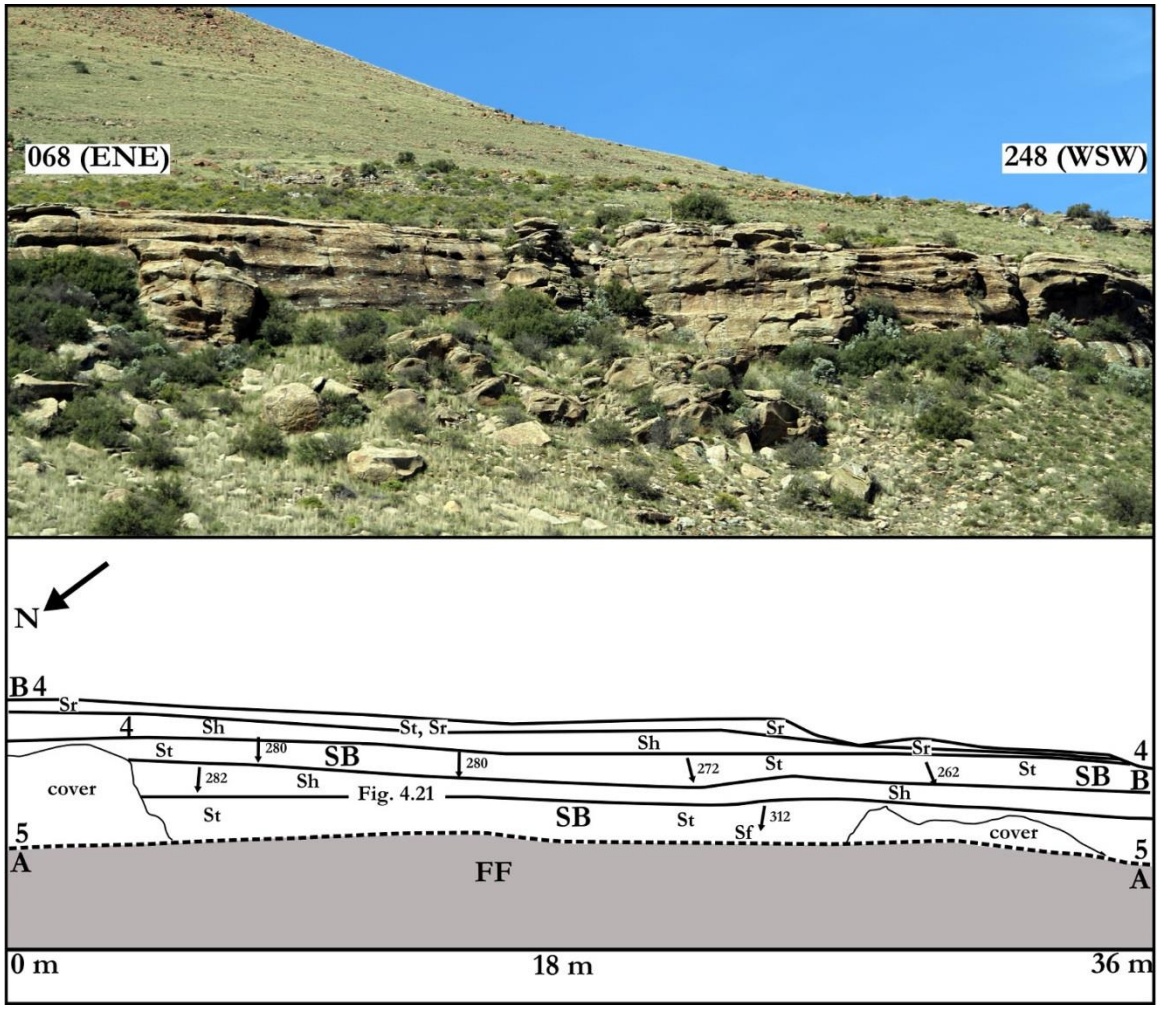

Figure 4.20: Panel section shows examples of element SB in the Ripplemead member on Krugerskraal farm (section 4, Figure 3.12), Nieu Bethesda, Eastern Cape.

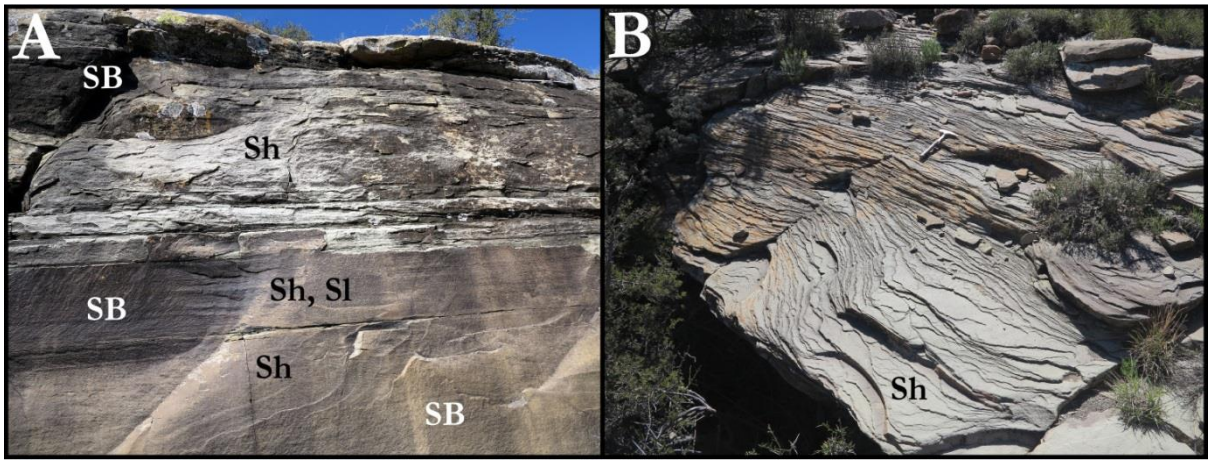

Figure 4.21: A) A close up of the SB elements on Figure 4.20, note the low angle of the elements. Scale in top right corner is 1 m B) An example of how finely laminated the SB elements are on Krugerskraal farm (section 4, Figure 3.12). Note rock hammer for scale.

multi-story sandstone sheets (SB). The only difference between the Krugerskraal panel (Figure 4.20) and this site is the presence of cutbanks at van Wyksfontein and Inhoek farms. At each site the SB are either dominated by trough cross-bedded sandstone (St) or horizontally laminated sandstone (Sh), but each SB element is capped by ripple cross-laminated sandstone (Sr). These Sr units in the SB can take up more than 50 % of the SB element. The SB elements at each site continue laterally over tens of metres but do not reach more than 5 m in thickness. The CH elements on each panel are also similar in size, with the CH in Figure 4.22 measuring ~ 70 m x 5 m and the CH on the Inhoek panel (Figure 4.23) measuring ~ 50 m x 12 m. Thus these channels have a relatively large width to depth ratio.

The channel bases are eroded (Figure 4.24, A, B) and include gutter casts and thin veneers of eroded floodplain deposits (Fm, Fl) which provide evidence of floodplain scouring. Also evident is rapid fluctuation in flow velocity as shown by the mini-fining upward cycle in Figure 4.24 (B-D). Between the SB elements (eg. 4th order bounding surfaces) scour lags (Gm1) or mud rip-up clasts (Gm2) are present signifying the cyclic nature of sedimentation in this fluvial system.

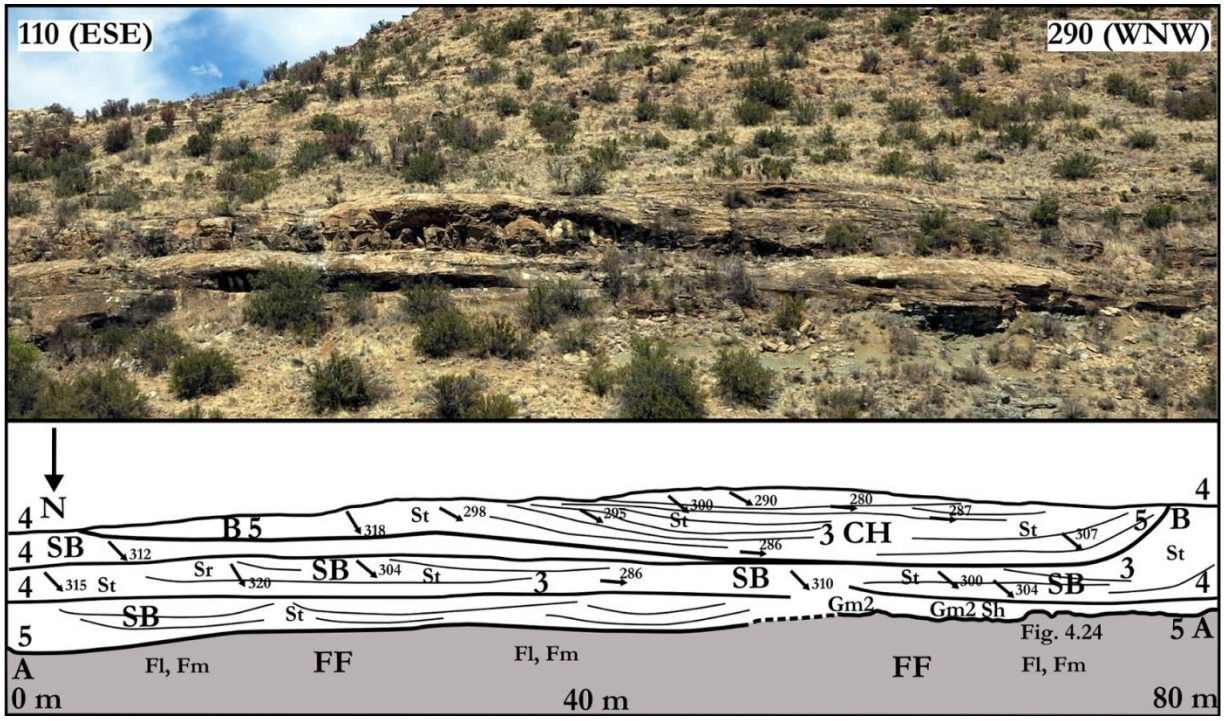

Figure 4.22: Panel section on van Wyksfontein showing examples of element SB and CH in the Ripplemead member on section 8 (Figure 3.21), near Colesburg, Free State Province.

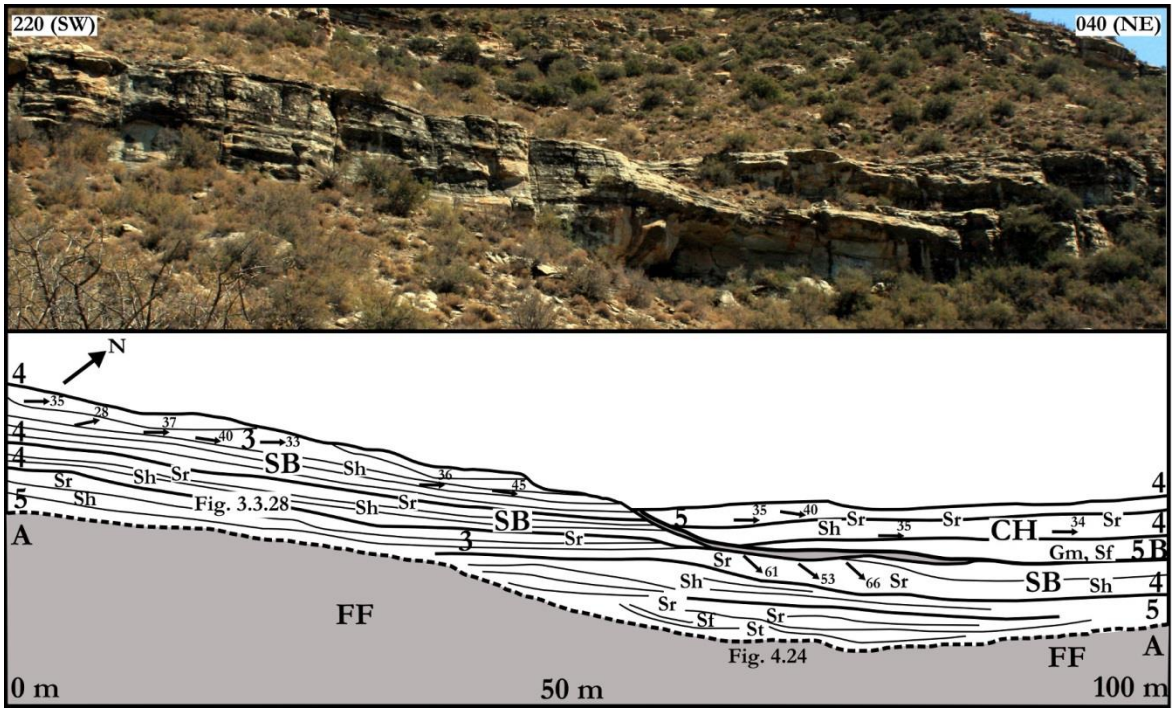

Figure 4.23: Panel section on Inhoek farm showing examples of element SB and CH in the Ripplemead member on section 9 (Figure 3.22) near Gariep Dam, Free State Province.

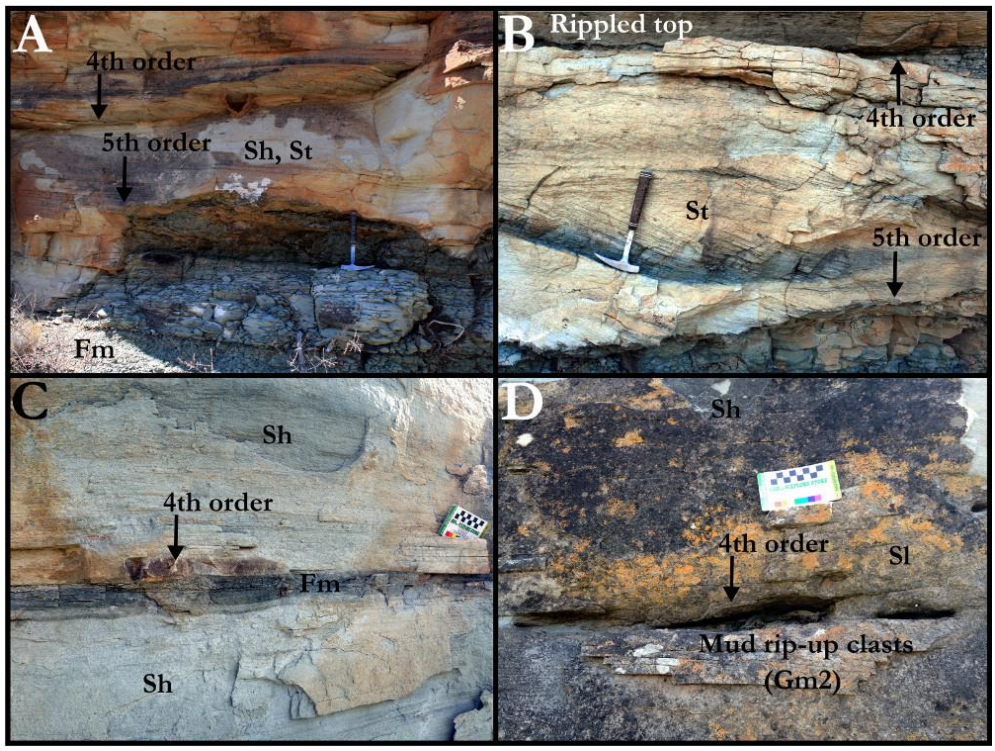

Figure 4.24: Channel bases and truncation surfaces from Figure 4.22 (A) and 4.23 (B, C, D). Note the pronounced gutter casts present in A. B is evidence for sudden deposition by the presence of rapid changes in flow regime. In a thin succession there is St and Sr, and this is capped by a ripple surface and Fm which is then eroded by another cycle. C and D are examples of truncation surfaces between SB elements on Figure 4.23. C massive siltstone (Fm) lining a 4th order truncation surface in Figure 4.23. Note the ubiquitous horizontally laminated sandstone (Sh). D shows examples of large (maximum 20 cm across) mud rip-up clasts along a 4th order truncation surface in Figure 4.23. Some low-angle cross-bedded sandstone (Sl) is associated along the truncation surface.

Type C: Multi-storey sheets dominated by LA

Type C is identified in the field as large LA surfaces (tens of metres long) with high angle of dip (~20^0) that cross the entire thickness of the exposed sandstone body as shown in Figure 4.25 (section 12). LA barforms are identified by inclined (>20^0) lower bounding surfaces, flat or mildly concave upper bounding surfaces, and palaeocurrents that are normal to dip of the barform (Reading, 1978; Miall, 1994, 1996). The dip directions of the inclined accretionary bedforms in Figure 4.25 are at a high angle to the palaeoflow direction measured from cross-bedded sandstone (> 75^0) and therefore are identified as LA elements. Upper bounding surfaces with the overlying fine-grained overbank fines (FF) are gradational and in places interbedded. The Type C sandstone complex is dominated by truncation surfaces at steep angles (> 20^0) (Figure 4.26, A, B) which in many places are lined with poorly-sorted lag deposits containing large rounded mud chips (Gm), and gravel sized quartz and feldspar grains in places. Most of the LA surfaces truncate fine-grained siltstone of facies association 2 (Fl, Fm) (~ 5 m thick) which overlies a sandstone comprising poorly-sorted, gravel sized clasts up to 1 cm in diameter which is documented as Gm1. It also manifests as trough cross-bedded Gm1 in some places.

Type C has been recognized at Boomplaas Hill near Jagersfontein (Figure 4.25). Here LA macroforms are large (> 100 m across) but are only at most ~ 5 m in maximum thickness. The macroforms interfinger with FF on their upper bounding surfaces (Figure 4.26, D) and this arrangement has been identified as scroll bars by Stear (1983) and Smith (1993b) in previous studies on sandstones of the Beaufort Group. The basal-most portions of the sandstone are coarse-grained and consist of gravel-sized clasts of feldspar and quartz (Figure 4.26, C). Internal 3rd order bounding surfaces within the LA elements are frequent and often have sharp contacts (Figure 4.26, A and B). These erosional cycles are indicative of falling stage erosion where the bar can be subaerially exposed (Miall, 1996). Additionally, the presence of feldspars means a source area must have been fairly close to this fluvial system and possibly a dry climate since feldspars are notoriously sensitive to tropical weathering (Nesbitt et al. 1997).

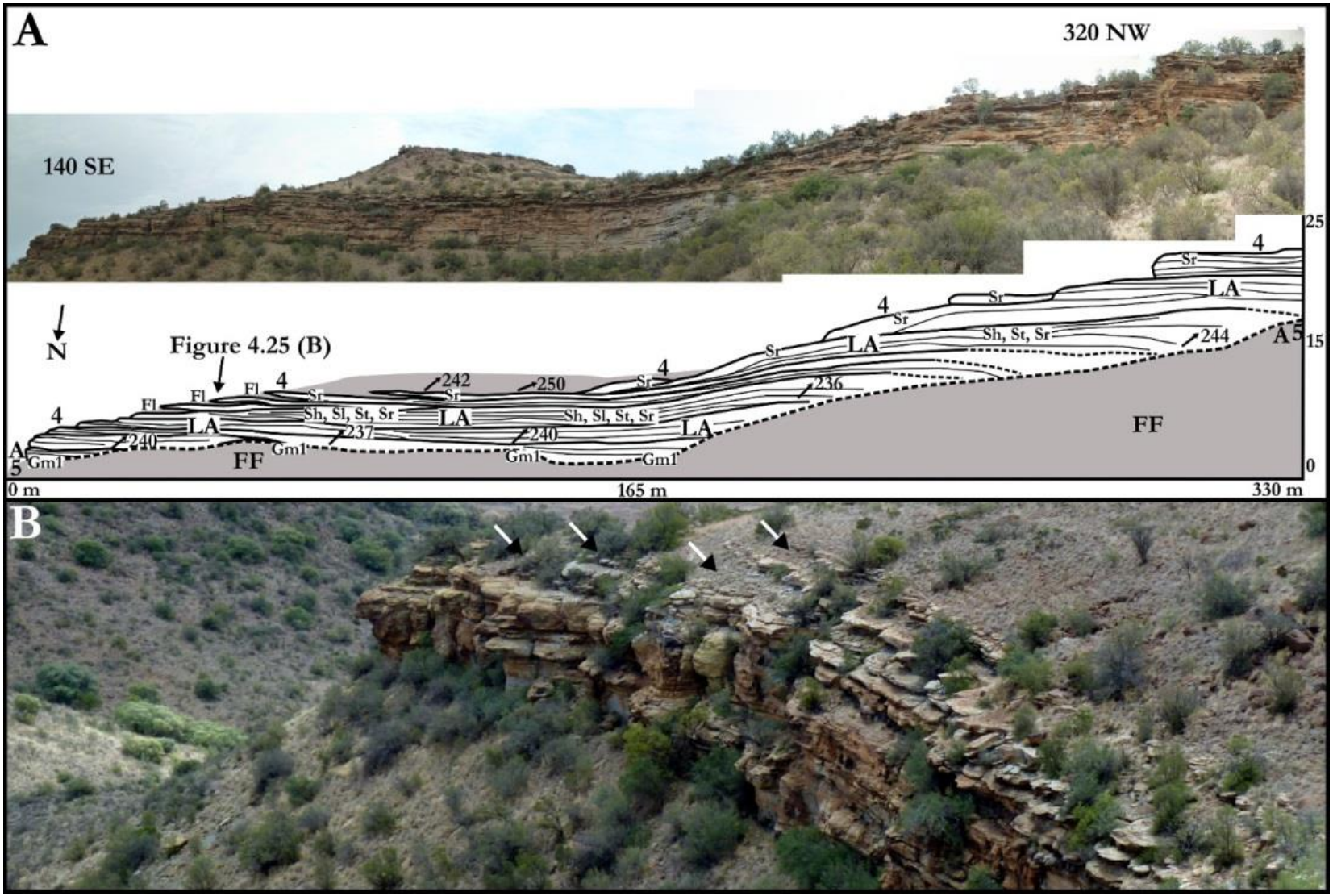

Figure 4.25: A) Panel section on Boomplaas Hill, section 12 (Figure 3.27) showing LA surfaces within the Boomplaas sandstone. B) Looking above the panel section, arrows point to scroll bars.

Type D: Weakly amalgamated convex up ribbons

Type D comprises weakly amalgamated channel belts that are dominated by St and Sr and manifest as wedge-shaped, convex up characters in outcrop. These sandstones are in most places paired but locally may amalgamate into a single sandstone (Figures 4.26 and 4.27). Laterally the sandstones grade to siltstone units that dip away from the channel deposit at a low angle and may represent levee (LV) deposits. Individual sandstone rich horizons are <10 m thick and are only laterally for a few hundred metres.

Type D is identified on Highlands farm (section 6, Figure 3.17) near Beaufort West. The panel shows three convex up channels with wings of sand that grade into laminated floodplain fines which are interpreted to represent LV elements. These elements on the panel are tapering, wedge-shaped deposits consist of rhythmically bedded units of silty, ripple cross-laminated sandstones with coarse siltstones which are all distinctive features of levees (Miall, 1996). Although palaeocurrent vectors could not be taken on these deposits, flow typically is oblique or downstream to the channel margin in levee deposits (Coleman, 1969; Miall, 1996). Elements LA, DA, and DLA cannot be identified at this panel section, however a lack of amalgamation is present in the sandstone bodies as shown in Figure 4.27. This photograph shows how the CH elements on the eastern outcrop interfingers laterally with FF.

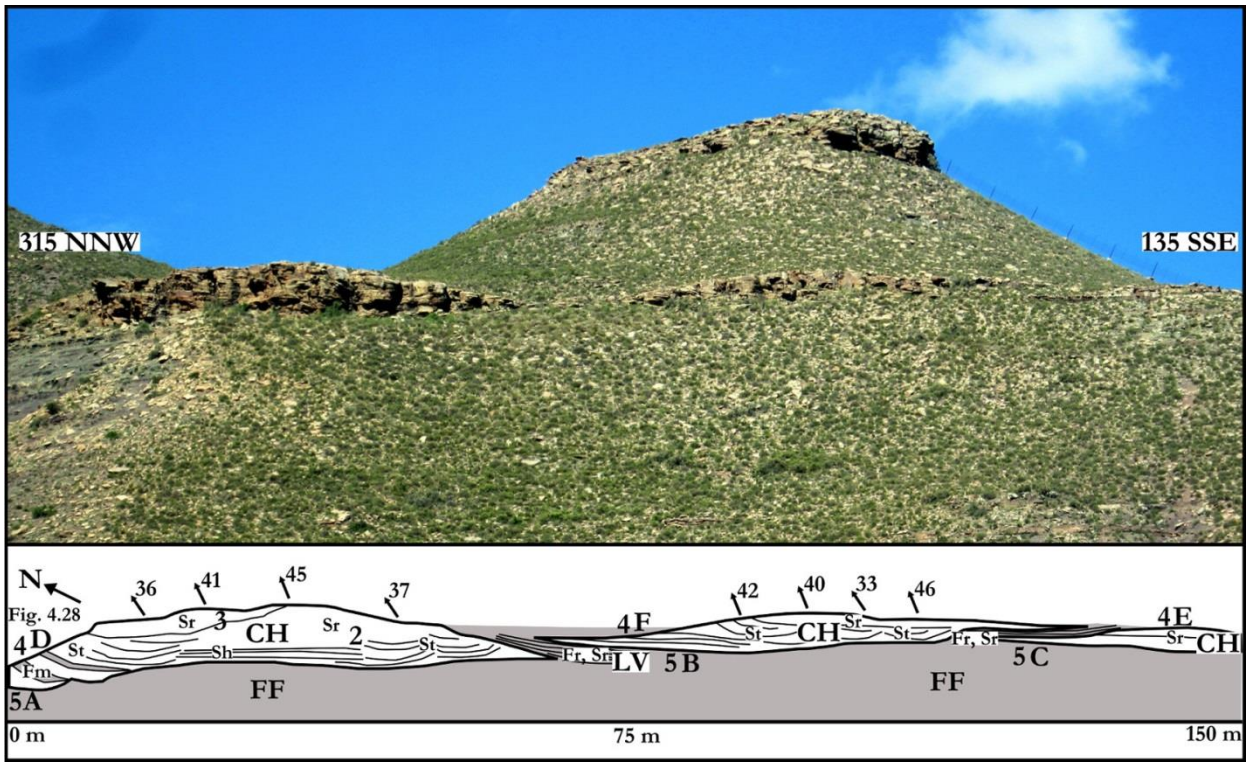

Figure 4.26: Panel section on section 6 (Figure 3.17) showing CH and LV elements in the Javanerskop member on Highlands farm near Beaufort West.



Figure 4.27: Photograph of the same Javanerskop member sandstone in Figure 4.27 taken at 90 degrees to the previous photograph showing the lack of amalgamation present within the channel bodies on Highlands farm (section 6, Figure 3.17).

Type E Crevasse splay/lacustrine delta sequence

Type E was identified in the Musgrave Grit unit on Tafelkop, Bloemfontein (section 13, Figure 3.28). Because CS elements are normally rare in low sinuosity systems (Miall, 1996), it may mean the Musgrave Grit unit on Tafelkop is part of a high sinuosity, or anastomosing fluvial system, and could either be Type C or Type D. However, due to poor outcrop at the panel site, the fluvial style cannot be determined and thus the outcropping unit has been defined by a separate architectural type.

CS elements are identified on the panel and have the following features. 1) Lens-shaped sandstone and siltstone bodies that are continuous on the outcrop for ~ 50 m. 2) Are 2-6 m thick and contain many internal 3rd order bounding surfaces, and interfinger at their margins with FF (Miall, 1996). 3) Show small internal low angle accretion surfaces which result in coarsening-upward cycles (Figure 4.29). 4) Upper bounding surfaces of the elements often become upward-fining as the splay is abandoned. 5) They also comprise interbedded laminae of siltstone and mudstone, or siltstone and fine sandstone. Therefore this panel is interpreted as containing a CS element sequence because the features of these elements fit with descriptions of crevasse splay deposits outlined by Miall (1996).

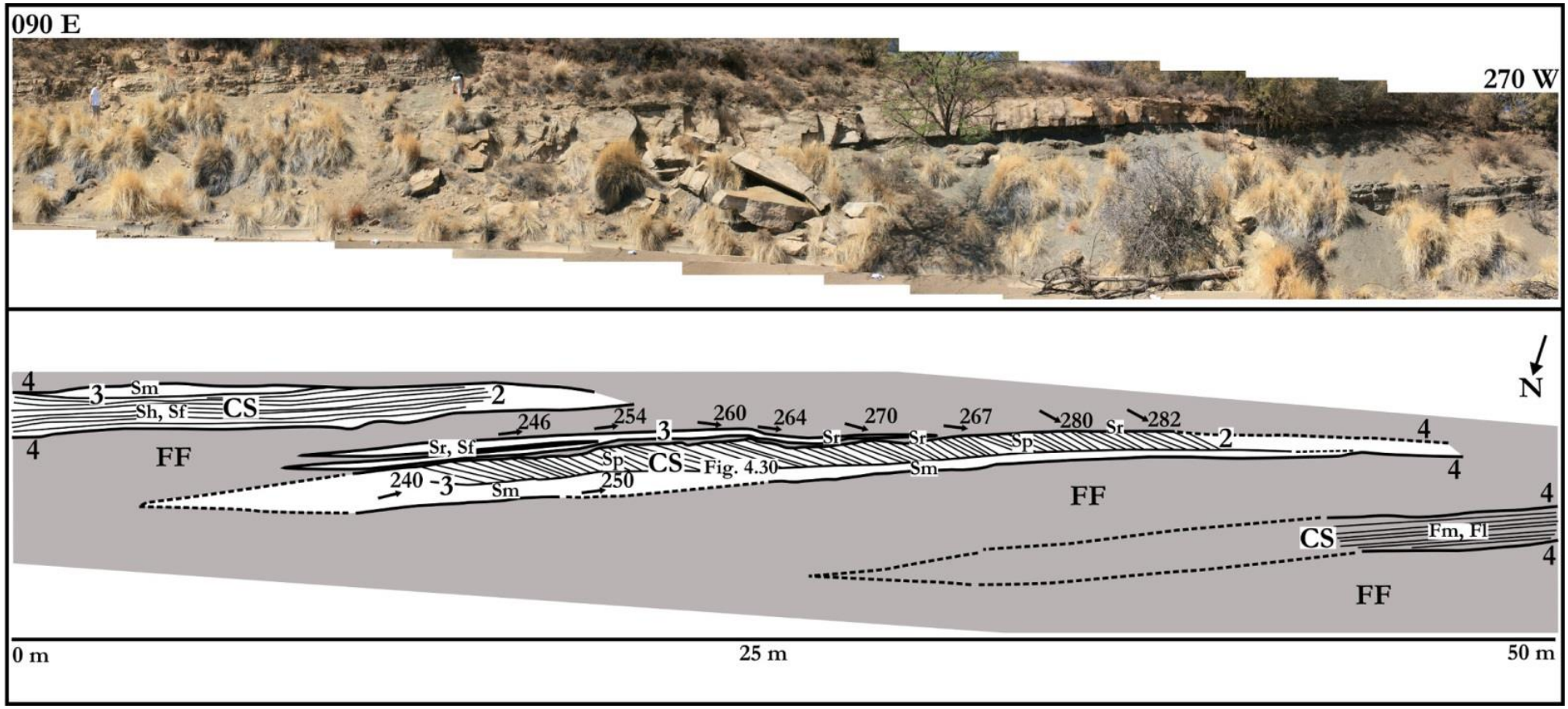

Figure 4.28: Panel section from section 13 (Figure 3.28) showing CS elements in the Musgrave Grit unit on Tafelkop Hill near Bloemfontein, Free State Province. Aurore Val and Paloma De la Peña are scale in this panel.

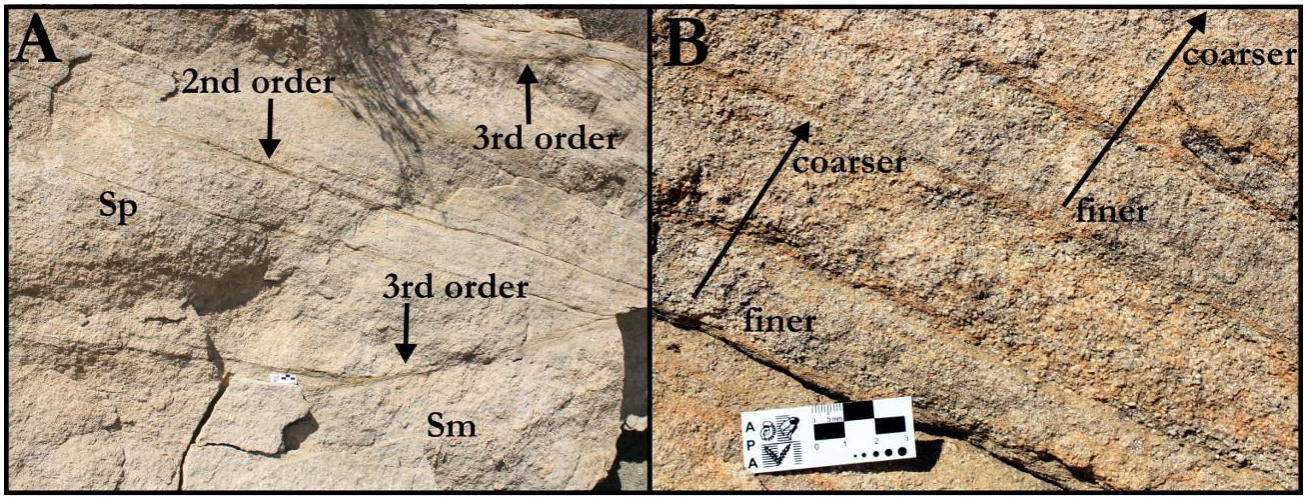

Figure 4.29: A) Close up of the large CS element on Figure 4.29. Note the two internal 3rd order bounding surfaces and 2nd order low angle accretion surfaces (large crossbeds). B) A close up of the large crossbeds in (A). Note the mini coarsening upward sequences.

4.5. Interpretation of identified architectural types

Figure 4.30 shows reconstructions of the fluvial styles represented by architectural types A, B, C, and D. These fluvial styles will now be discussed in greater detail.

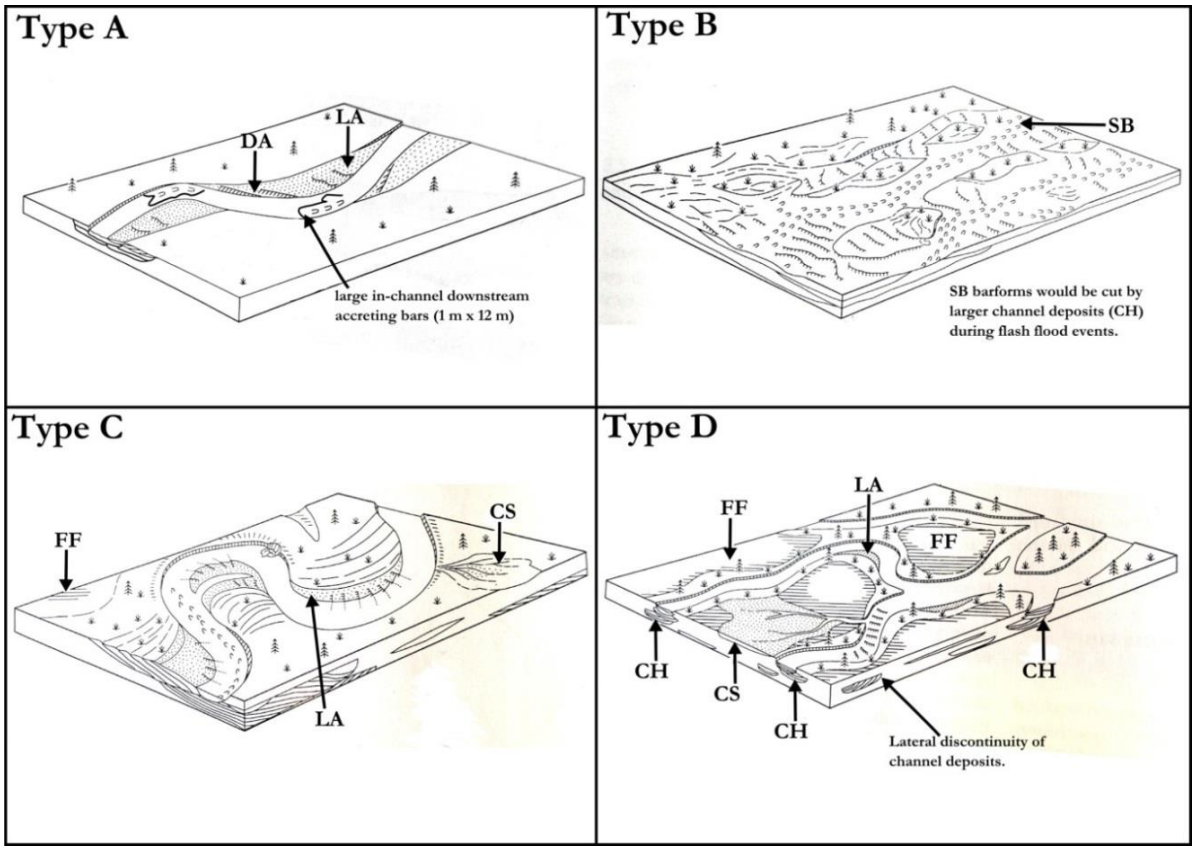

Figure 4.30: Architectural types A, B, C, and D are illustrated here with block diagrams (modified from Miall 1985, 1996). Note a reconstruction for type E might have formed could not be done due to insufficient data.

Type A: Channel belt dominated by DA

Type A was identified on section 1A (Figure 3.6) in the Oudeberg Member at the Barberskrans Cliffs (Figure 4.13), and in the RM sandstones on section 5 (Figure 3.13) on Ripplemead farm near Nieu Bethesda (Figures 4.17 and 4.18). This architectural type is interpreted as representing a low sinuosity fluvial style intermediate to the braided and meandering condition because it contains features that are common to both of these fluvial systems. The preponderance of DA has traditionally been interpreted as indicating a fluvial system closest to the braided condition (Miall, 1985) however revisions on fluvial systems now indicate that DA can be found in any kind of river type (Miall, 1996, 2014; Colombera et al. 2013). At the Barberskrans Cliffs, between some of the nested DA barforms within the channel fills there is evidence of slight changes in palaeocurrent direction and dip of fairly large (up to 2 m high) cross-bedded foresets. Bidirectionality is also evident by high angle ($>10^0$) truncations which facies in opposing dip directions (see Figures 4.16 and 4.18). As a result palaeocurrent directions are not always locally parallel to the vectors of the DA macroforms which means some point bars were possibly attached to the banks and migrating obliquely downstream alongside the in-channel DA barforms. This has been identified by a number of authors who refer to them as alternate bars (McCabe, 1977; Bridge et al. 1986; Olsen, 1988; Wizevich, 1992; Miall, 1996), and these have been used as evidence for intermediate fluvial styles to the true braided or meandering systems.

McCabe (1977) described giant cross-beds that are the major channel infill facies of the Kinderscoutian (Upper Namurian Carboniferous), deltaic sediments of the Central Pennines, Northern England. In places the channel sandstones are up to 40 m thick and 1.6 km across and grade upwards into Sh then smaller laminated Sp or Sr. McCabe (1977) interpreted the giant cross-bed filled channels as accretion on slip faces of alternate bars in a straight channel rather than typical lateral accretion due to the oblique orientation of the foresets and their high dip (maximum 25^0). Bridge et al. (1986) and Olsen (1988) described a process where alternate bars and point bars can become in-channel DA bars by the development of chute channels that over time can change the geometry of the channel. These observations could help explain the association of LA and DA in the type locality panel and how DA increases in abundance towards the centre of the outcrop, where the master channels are dominated by DA (see Figure 4.13).

The fluvial style of Type A is therefore interpreted as being similar to Miall's (1996) low sinuosity river with alternate bar model, although the suite of architectural elements is also shared with Miall's (1985) model 10 and Wilson et al.'s (2014) type 5 and 6. In comparison to the Katberg Formation, which is regarded as a typical ephemeral, flash flood dominated braided system by a

number of authors (Smith, 1995; Smith and Ward, 2001; Smith and Botha, 2005; Viglietti et al. 2013; Smith and Botha-Brink, 2014), the DA elements Oudeberg Member contain less interbedded overbank fines, and indicate more confined flow conditions (Figure 4.31).

Type B: SB dominated channel belt fills

Type B was identified on section 4 (Figure 3.12) in the RM on Krugerskraal farm (Figure 4.20), in the RM on section 8 (Figure 3.21) from van Wyksfontein farm (Figure 4.22), and in the RM on section 9 (Figure 3.22) from Inhoek farm (Figure 4.23). These elements can be interpreted as representing trains of bedforms in unconfined flows that accumulated by vertical aggradation (Miall, 1996; Reading, 1996; Colombera et al. 2013) and can form under upper (Sh) or lower flow regime (St, Sp) conditions. These different facies do not appear together because they represent distinct flow regime conditions or barform types, however vertical stacking of different bedform types indicates long or short term changes in flow regime (Miall, 1996) (Figure 4.21). Short term changes could be attributed to flash flood events or other seasonal fluctuations (such as seasonal snowmelt from the Gondwanides) (Haycock et al. 1997) (Figure 4.24), whereas longer term changes could be reduction of water depth on the scale of many years (Miall, 1996).

Miall (1996) describes several examples of SB such as those formed by channel floor dune fields (St dominated), shallow channel fill assemblages (Sp dominated) or bar top assemblages (Sr dominated) and distal braid plain channel sheets (Sh and St). Since the RM sandstones show a paucity of Sp and dominance of Sh and St, the interpretation for this architectural type is that these deposits represent Miall's (1996) distal braid plain sandstone sheets (Miall, 1985; Model 11). Thick layers of Sr are abundant, but bar top assemblages occur in many fluvial environments and are therefore not diagnostic of any particular fluvial style (Miall, 1996) (Figure 4.31). Stear (1985) interpreted multi-storeyed sandstone bodies composed mainly of Sh in the Middle Permian Lower Beaufort Group as the product of a complex series of ephemeral flooding events. Since this architectural type is most abundant in the northerly sector of the study area (Gariep Dam), it appears to fit with the model that this is the far distal reaches of fluvial systems propagating from a southerly source area as the strata in this part of the basin are younger and more incomplete than in the south. The erosional relationship of elements CH and SB also fit the model, and the former has been intepreted as sediments of flash floods in semi-arid climates (e.g. Kanyeta Formation, Arizona, USE - Miall, 1996). The deposits of the Beaufort Group have a long been considered to have accumulated in a highly seasonal semi-arid climate (Johnson, 1976; Smith 1987, 1989, 1993b, 1995; Stear, 1985; Smith and Ward, 2001; Botha and Smith, 2006; Smith and

Botha-Brink, 2014), and therefore it is expected that flash flood processes influenced the supply and preservation or erosion of sediments in the Karoo Basin during the Lopingian.

Type C: Multi-storey sheets dominated by LA

Type C is documented in indeterminate Balfour Formation in section 12 (Figure 3.27) from Boomplaas Hill, Jagersfontein (Figure 4.25). LA deposits have long been recognized as the record of point bar deposition in ancient meandering rivers (Willis, 1993). Therefore, Type C is interpreted as sedimentary product of a highly sinuous system for reasons explained below. Firstly, there is a decrease in grain size from the base of the outcrop to the top. An up to ~5 m thick conglomarate (facies Gm) is present at the base of the outcrop containing igneous clasts along with angular quartz and feldspar (Figure 4.26, C). Similar erosively based, coarse-grained facies at the base fining upward sussessions has been observed in other ancient meandering systems (Allen, 1970; Reading, 1978; Mossop and Flach, 1983; Miall, 1996). Secondly, the near perpendicular direction of palaeoflow to the accretion direction of the LA surfaces shows that bars were side attached to the meander bend, although this could also be interpreted as lateral shifting of compound bars in braided systems (Allen, 1983; Bristow, 1987; Miall, 1994). LA surfaces terminate down dip into FF, which could indicate cut off of the active meander (Figures 4.25) (Reading, 1978). Thirdly, chute cut off is also evident in the outcrop by the presence of exposed scroll bars infilled with finer sediment (Figure 4.26, D) (Smith, 1993b). Finally, high angle (>20°) truncation surfaces indicate subtle internal change in accretion direction of the LA surfaces on the attached bar (Figure 4.26, A and B). Type C represents a meandering system showing similarities to Miall's (1996) sand-bed meandering river (Miall's 1985 Model 6) (Figure 4.31). Additionally Type C is also interpreted to have similarities with Mossop and Flach's (1983) deep channel meandering system due to the large scale LA forests, which they interpret as giant point bar deposits in a meandering system with channel depth up to 25-40 m.

Type D: Weakly amalgamated convex up ribbons

Type D was only identified in the Javanerskop member on section 6 (Figure 3.17), Highlands farm near Beaufort West. Large convex up sand bodies (10 m high, 90 m wide) filled with St and Sr defines this type of fluvial architecture. Minor wings of sand split into laminated floodplain fines that could indicate LV elements (Figures 4.27). The sandstones are not well amalgamated and continue laterally for only a couple kilometres (Figure 4.28). Anastomosed channel systems comprise ribbon sandstones (Friend, 1977) that have moderate to poor lateral or vertical interconnectedness, and are commonly separated by FF (Miall, 1996). Due to the convex up nature of the sandstone bodies and ribbon shape, it is possible that this architectural type is

representative of an anastomosed river system. Smith (1980) recognized that channel evolution in anastomosing systems may take the form of crevassing and development of stable crevasse channels which were not observed in outcrop, however Rust (1981) did not observe crevasse splays in his study of modern anastomosed systems in Cooper's Creek Australia, and argued that the discontinuous nature of the levees allows for new channels to form without the need for crevassing. Rust (1981) also observed a series of relict braids among the active anastomosed channels that he interprets as an adjustment to a more arid climate. Although DA and LA elements could not be identified in outcrop on Highlands, the lack of amalgamation of the sandstone bodies and presence of levees permit the interpretation of Type D as sedimentary products of an anastomosed river system similar to Miall's 1985 Model 8 (Figure 4.31).

Type E: Crevasse splay sequence

Type E was identified in the Musgrave Grit unit on section 13 (Figure 3.28) on Tafelkop near Bloemfontein (Figure 4.29). CS elements are common components in meandering and anastomosing fluvial systems (Miall, 1996; 2014). Although CS elements are rare in braided or low sinuosity fluvial systems, they are not absent due to being identified in the Precambrian braided fluvial deposits by Long (2006), and also in the Katberg Formation Smith by Botha-Brink (2014). Thus these fluvial systems cannot be entirely ruled out either in the interpretation of the depositional environment of Type E. Since CS elements can be found in many different fluvial systems (Miall 1996; 2014; Long, 2006) they are not diagnostic of a definitive fluvial style therefore, Type E cannot be given an interpreted fluvial style. It is possible it could be representative of Type C or D but without more outcrop data, this could not be proven.

4.3.1 Stratigraphic distribution of fluvial style

The aim of the facies analysis was to determine if there was a distinct change in fluvial style through the *Daptocephalus* Assemblage Zone. Therefore the results are now presented in their stratigraphic context in Figure 4.32. The stratigraphic positions of high sinuosity types (C, D) and low sinuosity types (A, B, D) are shown where appropriate on the composite sections. Stratigraphic context for Types C is not given due to insufficient stratigraphic and sedimentological information for these units as demonstrated in Chapter 3.1.1.

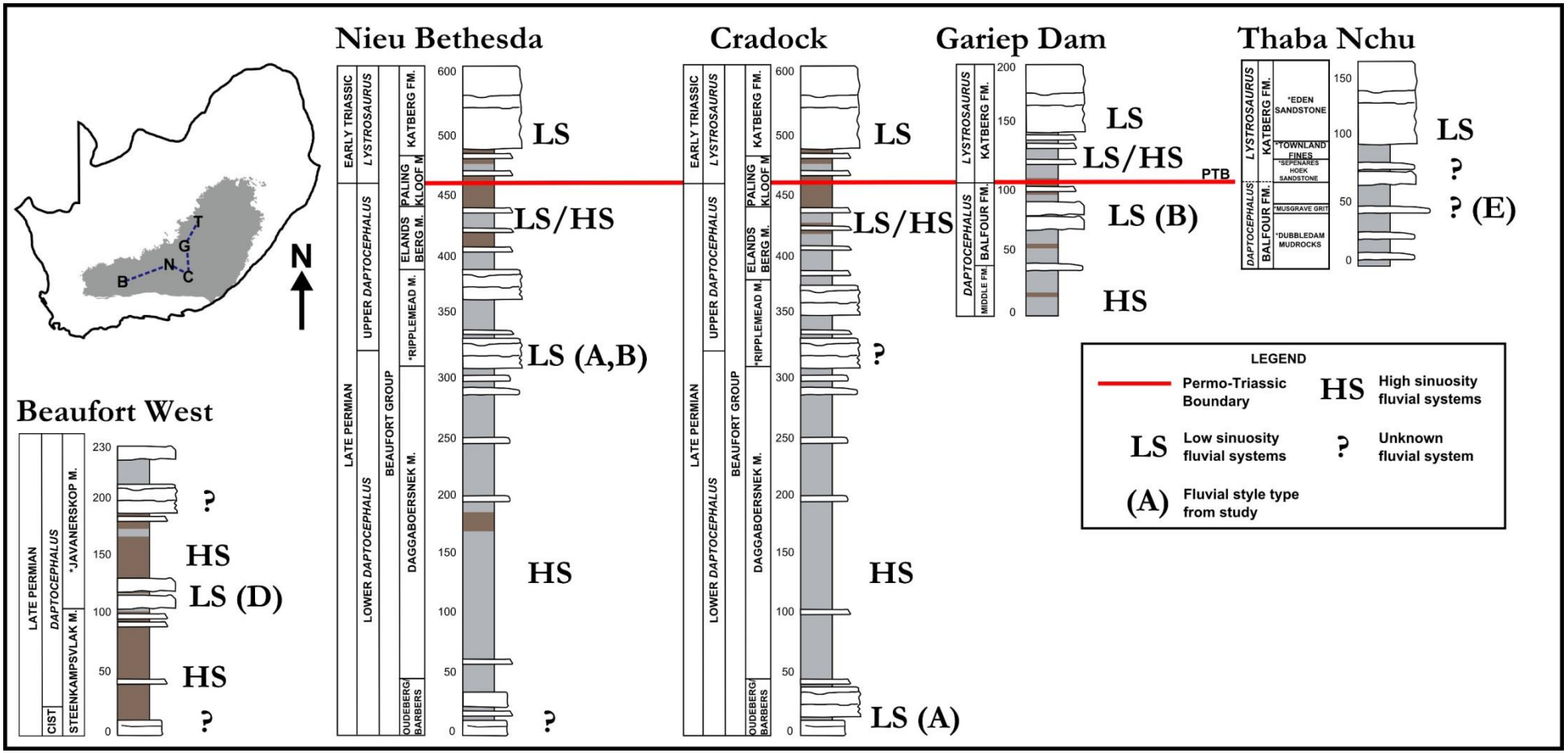

Figure 4.32: Stratigraphic distribution of high sinuosity (HS) and low sinuosity (LS) fluvial systems studied during this investigation. The stratigraphic position of fluvial style types identified during this study (A, B, C, D) are indicated where appropriate. Interpretations on fluvial style were also taken from the literature for the Steenkampsvlakte and Daggaboersnek members, Elandsberg and Palingkloof members, Katberg Formation, and distal fordeep (see text for references). Question marks indicate missing information that did not allow for an interpretation on fluvial style. What the data demonstrate is that the LS systems commonly coincide with the more arenaceous lithostratigraphic subdivisions on the composite sections, whereas the HS systems commonly coincide with the argillaceous lithostratigraphic subdivisions on the composite sections which has been identified by previous workers (Visser and Dukas, 1979; Catuneanu et al. 1998). The implications of this are discussed in Chapter 5.3.

The literature was also referred to for lithostratigraphic units where fluvial style was not directly investigated during this study. This included the Daggaboersnek and Steenlampsvlakte members (Johnson, 1966, 1976; Visser and Dukas, 1979; Rubidge et al. 1995), Elandsberg and Palingkloof members (Smith, 1995; Smith and Ward, 2001; Smith et al. 2012; Smith and Botha-Brink, 2014), the Katberg Formation (Neveling, 2002; Smith and Botha, 2005; Botha and Smith, 2006; Viglietti et al. 2013), and the Musgrave Grit unit in the vicinity of Bloemfontein and Thaba Nchu (Rutherford, 2009; Rutherford et al. 2015). Visser and Dukas (1979) and Catuneanu et al. (1998) hypothesized that the sandstones of the RM and Oudeberg Member were low sinuosity, however for the first time an interpretation of fluvial style for the Oudeberg Member and RM has been conducted in this study. Insufficient information did not allow for the determination of the fluvial style for these units in all of the composite sections (question marks on Figure 4.32)..

Stratigraphic positioning of the fluvial styles recognised in the study area confirms work conducted by previous workers (eg. Visser and Dukas, 1979; Catuneanu et al. 1998; Smith and Ward, 2001; Neveling, 2002) that in most cases the low sinuosity systems coincide with the more arenaceous lithostratigraphic subdivisions on the composite sections, whereas the high sinuosity systems commonly coincide with the argillaceous lithostratigraphic subdivisions on the composite sections. This highlights the ever difficult question as to whether or not documented changes in lithology and fluvial style in the Karoo Basin were controlled by allogenic or autogenic changes, or a combination of both. The implications of these influences will be addressed in the discussion section of this investigation (chapters 5.3 and 5.4).

Chapter 5: Discussion

This chapter explores the implications of the data collected during the course of this study, and presented in chapters 2, 3, and 4. As this is a multidisciplinary study, this data comes from a number of different disciplines such as lithology, stratigraphy, petrography, palaeocurrent analysis, geochronology and provenance of detrital zircons, facies and architectural element analysis. The main implications for the data presented are as follows.

A new lithostratigraphic scheme has been compiled for the Balfour and uppermost Teekloof formations. Tordiffe's Barberskrans Member (BM) is renamed the Ripplemead member (RM) because the Oudeberg Member is identified at Tordiffe's (1978) type locality for this unit (Barberskrans Cliffs) and new type locality (Ripplemead farm, Nieu Bethesda) is identified. It has been demonstrated in this study that the geographic distribution of the RM extends from Cradock in the south to Springfontein in the north (southern Free State Province) but the unit is significantly attenuated at this northerly juncture. The informal arenaceous Javanerskop member is present in the western basin could not be correlated temporally to the RM (see chapters 5.1 and 5.2), but it may be related to the same tectonic event (see Chapter 5.5). This study has also recognized that the Javanerskop member is a distinct and mappable unit which should receive formal recognition due to its distinct lithological properties and traceable stratigraphic position. The *Daptocephalus* Assemblage Zone (DaAZ) has been revived and refined to address the shortcomings of the current *Dicynodon* Assemblage Zone (DiAZ). This was done by refining the stratigraphic ranges of biozone indicating taxa (*Daptocephalus leoniceps*, *Dicynodon lacerticeps*, *Theriognathus microps, Procynosuchus delaharpeae*) as well as other taxa from the DaAZ (*Lystrosaurus maccaigi*).

The RM is discussed within the context of the new lithostratigraphic and biostratigraphic scheme compiled during this investigation and interpretations are made concerning palaeoenvironmental changes of the DaAZ through time by use of facies and architectural element analysis data. Provenance interpretations are discussed for the Upper Permian Balfour, uppermost Teekloof formations, Boomplaas sandstone (BS), Musgrave Grit unit, and Lower Triassic Katberg Formation by referral to the results of the palaeocurrent and detrital zircon analyses. Finally an interpreted basin development model for the Late Permian Karoo Basin is discussed by comparison of observations in this study with previous basin models for the Karoo Basin.

5.1 New stratigraphic framework for the Upper Permian Karoo Basin

This study provides a new litho- and biostratigraphic framework for the Upper Permian Balfour and uppermost Teekloof formations (Figure 5.1). The new stratigraphic framework highlights that arenaceous units identified in this study (eg. Ripplemead and Javanerskop members, and Musgrave Grit unit) do not represent a single traceable unit, and were not deposited synchronously. Evidence for and implications of this will be discussed in the proceeding sections (Chapter 5.5). The Ripplemead member (RM) is the new name for Tordiffe's (1978) Barberskrans Member and is renamed because the Oudeberg Member was identified at the Tordiffe's (1978) type locality for this unit. Therefore Ripplemead farm in Nieu Bethesda is the new type locality for the unit and thus it is now the RM.

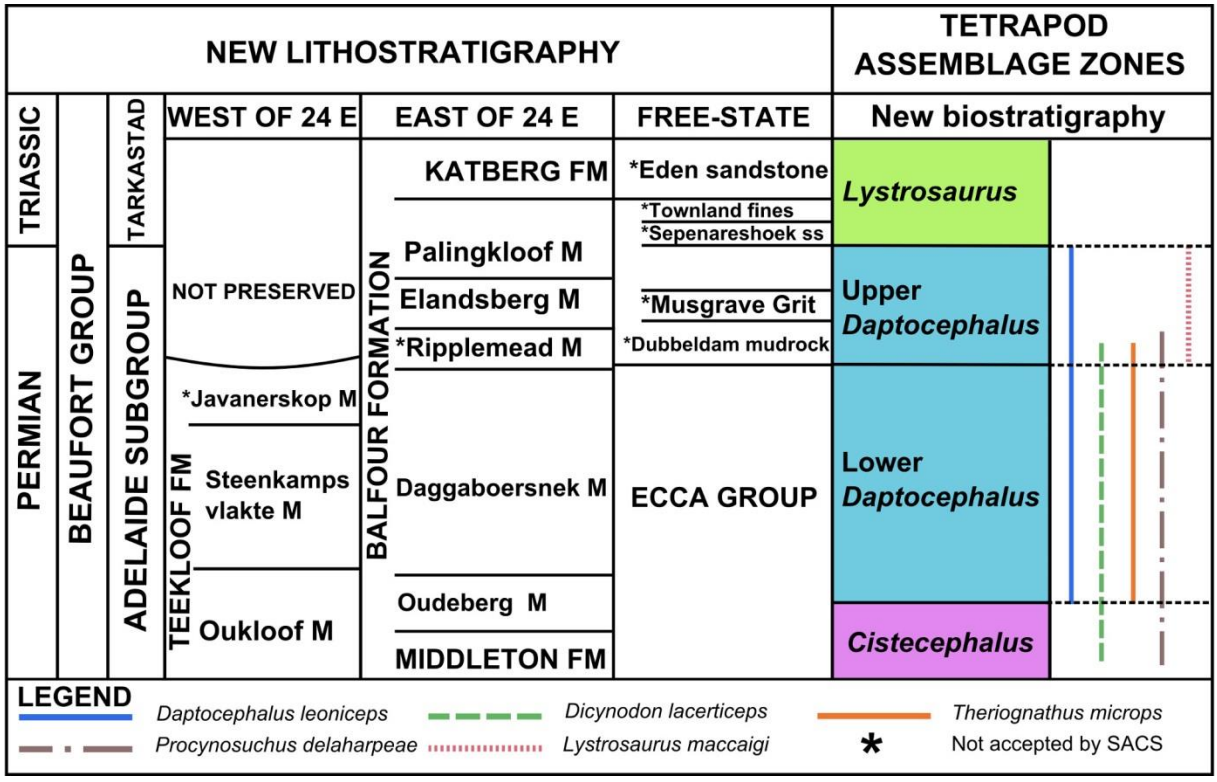

Figure 5.1: Proposed stratigraphic framework for the newly proposed *Daptocephalus* Assemblage Zone (Viglietti et al. 2016). Note that the Barberskrans Member is renamed the Ripplemead member. Also note proposed names for the new arenaceous units identified within the Balfour and uppermost Teekloof Formation in this study, by Le Roux (1985) (Javanerskop member), and Rutherford et al. (2015) (Musgrave Grit). Although the Musgrave Grit unit is shown as a single unit overlying the Dubbeldam mudrock (Rutherford, 2009), it comprises a series of coarse-grained sandstones within this unit (see chapters 1.2 and 2.2). While these sandstone units across the field site are not present at the same stratigraphic position, some may relate to the same tectonic event which is discussed in Chapter 5.5.

The Javanerskop member, first described by Le Roux (1985) on Oukloof Pass near Beaufort West, was never officially adopted into the lithostratigraphic framework of SACS (1980). Two sections measured in this part of the basin during this study (sections 6 and 7) document an arenaceous inverval in the highest points of the escarpment in the western basin. It is

lithologically distinct from the Steenkampsvlakte member due to its higher sandstone content and lower red mudstone content (see Table 1.1) which is why this study recommends it has member status.

The Boomplaas sandstone, Jagersfontein (section 12) and the Musgrave Grit unit identified on Tafelkop near Bloemfontein (section 13) are also not considered to be synchronous with the deposition of the RM. The outcrop where section 12 was measured is very isolated and therefore no composite section for this part of the basin could be created, so for now the exact stratigraphic position of this sandstone is undetermined but is estimated to be at the stratigraphic positon of the Oudeberg Member due to the results of the detrital zircon analysis (see chapters 3.6 and 5.4). Section 13 was placed on a composite section due to the work of Rutherford et al. (2015) conducted near Thaba Nchu and is regarded to be part of the Mugrave Grit unit.

Thicknesses

Thicknesses of the strata assigned to the *Daptocephalus* Assemblage Zone strata that were part of this investigation are shown in the composite sections created during this study (see Figure 3.29, Chapter 3.2.1). They demonstrate that accommodation in the main Karoo Basin varied greatly in the west, central, and northwestern portions of the proximal Karoo Basin (eg. foredeep). They also indicate that correlation of lithostratigraphic units westward and northward is problematic due to varied periods of nondeposition or out-of-phase deposition. The marked changes in thickness of the RM are testament to the fact that the different lithostratigraphic units identified in this study do not only reflect changes in depositional rates in different parts of the basin, but also the diachronous nature of deposition in the Karoo Basin. In the past attempts have been made to locate marker horizons in the lithostratigraphic succession of the Beaufort Group for use in correlation but this has not always been possible (Broom, 1907b, 1909; Haughton and Brink, 1954; Haughton, 1963, 1969; Keyser, 1979; Keyser and Smith, 1979b; Rubidge et al. 1995).

This is why the biozonation of the Karoo Supergroup has been a useful tool for correlating the lithostratigraphic subdivisions as they represent more fixed time lines than the lithostratigraphic boundaries (Rubidge et al. 1995; van der Walt et al. 2011). The diachronous nature of the Ecca-Beaufort contact is well-demonstrated around the Karoo Basin (Rubidge, 1988; Rubidge et al. 2000; Catuneanu et al. 2002; Rubidge, 2005) as well as several other major lithological boundaries that have been traced throughout the basin (Keyser, 1979; Catuneanu et al. 1998; Hancox, 1998; Neveling, 2002).

Recognition of this northward thinning of the stratigraphic succession demonstrates that accommodation in the Karoo Basin was variable in the Lopingian with more accommodation available in the south than in the north due to less frequent and shorter periods of nondeposition in the south. Progradation of sediment northwards was also not synchronous, leading to multiple events of nondeposition in the distal foredeep of the basin. Also, older Beaufort Group strata and biozones are mainly confined to the south (*Eodicynodon*, *Tapinocephalus*, *Pristerognathus*, *Tropidostoma*, and *Cistecephalus* AZ), and younger in the north *Daptocephalus*, *Lystrosaurus*, *Cynognathus* AZ) (van der Walt et al. 2011). The exception to this rule is strata correlated to the *Pristerognathus* Assemblage Zone near Phillipolis and Jagersfontein in the southern Free State Province by Welman et al. (2001), Rubidge et al. (2015), and during this study. This suggests that there may be some exceptions to this rule as more work is conducted in the northwestern Free State Province.

5.2 Distribution of Lopingian fauna within the Balfour and Teekloof formations

The new biostratigraphic framework constructed during this study replaces the *Dicynodon* Assemblage Zone with the Lower and Upper *Daptocephalus* Assemblage Zone. This is to satisfy the new stratigraphic ranges of the old index fossils for the DiAZ (*Dicynodon lacerticeps*, *Theriognathus microps*, *Procynosuchus delaharpeae*) which extend the lower boundary of the old biozone but disappear well below the upper boundary (Figure 5.2). The range of *Daptocephalus leoniceps* extends throughout the temporal range of the new biozone, and the Upper DaAZ subdivision was erected to satisfy the appearance of *Lystrosaurus maccaigi* (Chapter 3.2, Figures 1 and 2). *Lystrosaurus maccaigi* is excluded from the *Lystrosaurus* Assemblage Zone because it remains part of a Permian assemblage zone fauna just prior to the major faunal turnover observed at the PTB (Smith and Botha, 2005; Smith and Botha-Brink, 2014).

Figure 5.2 demonstrates that the distribution of DaAZ defining fauna through the Balfour and Teekloof formations is different for most of the composite sections. Lithostratigraphic units correlate with either the Lower DaAZ or Upper DaAZ by the stratigraphic of *Lystrosaurus maccaigi* in the composite sections. This suggests that the Javanerskop member, which is the uppermost unit in the DaAZ of the Teekloof Formation, correlates with the Lower DaAZ because *L. maccaigi* has yet to be found the western part of the basin. Since there has been regional erosion down to the uppermost DaAZ strata in this part of the basin, it is difficult to estimate how much more of the succession was once present. Karoo sills cap this erosional surface at many places and since they are hypabyssal intrusions that emplace in the shallow crust (Duncan et al. 1997), it could be estimated that between 2 and 3 km of strata once lay above this

erosional boundary (Hanson et al. 2009). Therefore Upper DaAZ strata and the Katberg Formation may have been present in this part of the basin, but have since been eroded.

In the Nieu Bethesda area the appearance of *L. maccaigi* is close to the base of the RM (~ 130 m below the PTB). This indicates that strata assigned to both Lower and Upper DaAZ are present here. Although palaeontological evidence is lacking in the Cradock area, the similar stratigraphic thicknesses, and similar fossil fauna above the RM in the Elandsberg and Palingkloof members as observed in Nieu Bethesda (see Appendix 2) does make it tempting to theorize that these field sites and their lithostratigraphic subdivisions roughly correlate in time. However fossil evidence and more robust absolute dates would be needed to confirm this. At Gariep Dam, *L. maccaigi* also appears near the base of sandstones defined as the RM, but this unit is much thinner (eg. appears ~ 30 m below the PTB) because the stratigraphy is incomplete in this part of the basin. At Thaba Nchu only Upper DaAZ strata are present because *L. maccaigi* ranges throughout the Upper Permian portion of the section of Rutherford et al. (2015). Since the sandstones near Bloemfontein were correlated to the Musgrave Grit unit using Rutherford et al.'s (2015) section, this field site is also considered to only represent Upper DaAZ strata. This shows that there is a northward younging of DaAZ strata as suggested by Catuneanu et al. (1998) and also that lithostratigraphic units identified in this study do not represent the same period of time. Miall (1996) stresses sandstone-rich units should not be used as regional marker horizons by the fact that their deposition is defined and controlled by multiple events of incision and erosion and as a result can represent significant missing time. Locally lithostratigraphic members could serve as marker horizons (Smith, 1990; Smith and Botha-Brink, 2014; Day et al. 2015), but at regional scale, across the Karoo Basin their utility for correlation is dubious. Correlation of lithostratigraphic units identified in this study, and other proxies (biostratigraphy, detrital zircon populations) have heped to create a basin evolution model for this study, which will be discussed later in this chapter.

The roughly coeval appearance of *L. maccaigi* and disappearance of *Di. lacerticeps*, *P. delarharpeae*, and *T. microps* may represent palaeoclimatic changes occurring between the Lower and Upper DaAZ. Additionally, the stratigraphic placement of Smith and Botha-Brink's (2014) phased extinctions fits with the disappearance of these taxa in the Gariep Dam area in the north but not in the south. This suggests preservation of extinction event in the north is a compressed record in comparison to the south and that the climatic changes that culminated in the Permo-Triassic mass extinction (PTME) were begining at the start of the Upper DaAZ with the disappearance of the three index fossils for the old DiAZ.

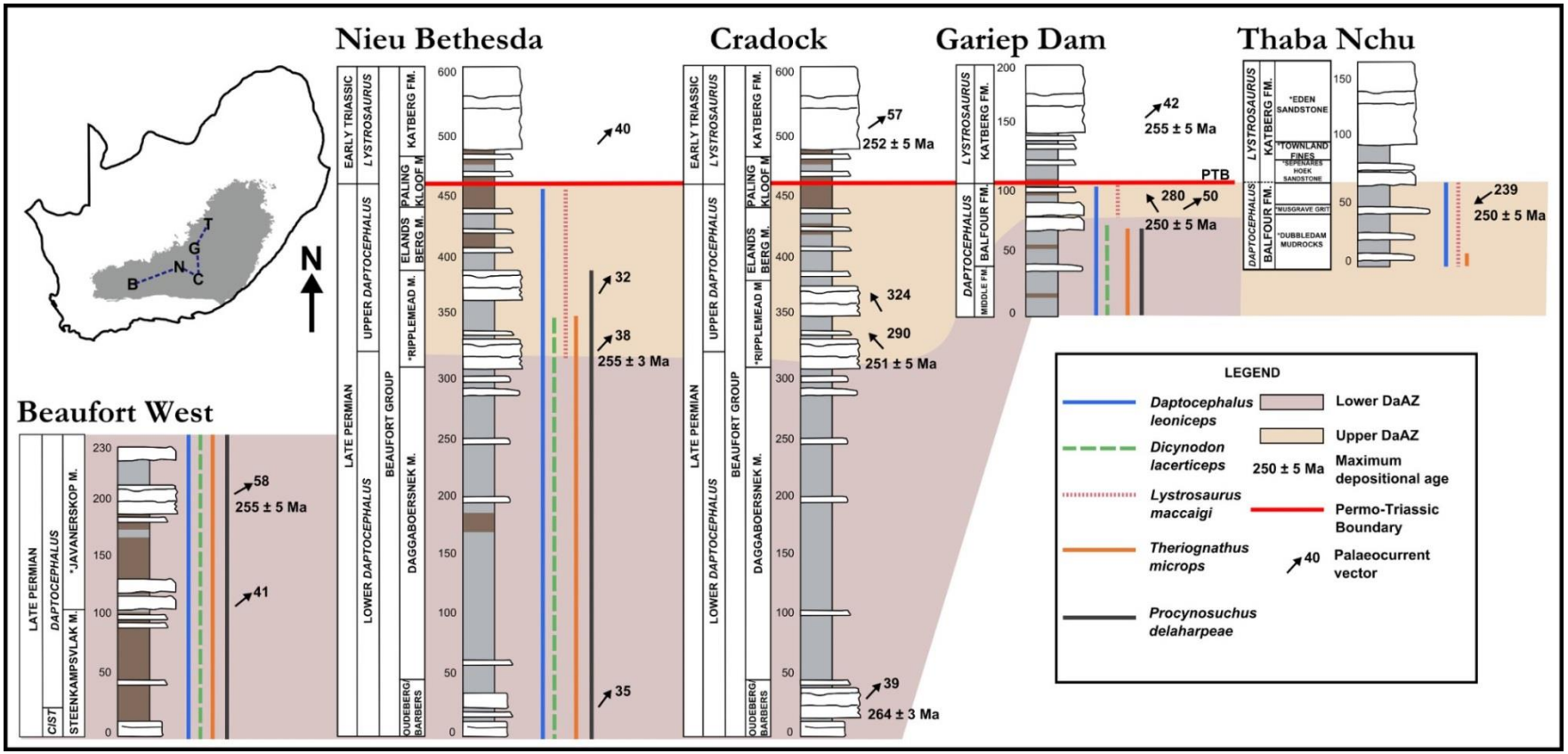

Figure 5.2: Composite sections created at the field sites of this study. In this example, palaeocurrent vectors, the Permo-Triassic Boundary, and distribution of *Daptocephalus* Assemblage Zone fauna are shown in each of the composite sections. By default, the distribution of strata assigned to Lower DaAZ and Upper DaAZ is also shown by use of the first appearance datum of *Lystrosaurus maccaigi*. The distribution of fauna in the Balfour and Teekloof formations shows that strata in the Beaufort West area (Teekloof Formation) are considered the oldest due to the current absence of *L. maccaigi* in this part of the basin. In the Nieu Bethesda area *L. maccaigi's* appearance is close to the base of the Ripplemead member. Although palaeontological evidence is lacking in the Cradock area, the similar thicknesses for lithostratigraphic units, similar fossils fauna found in the Elandsberg and Palingkloof members (see Appendix 2), and maximum ages of deposition means these field sites are tentatively correlated in time however, more robust fossil evidence and abosulte dates will be required to prove this. At Gariep Dam, *L. maccaigi* appears at a similar stratigraphic position in the sandstone defined as the RM, but this unit is much thinner than in Nieu Bethesda. In the vicinity of Thaba Nchu and Bloemfontein only Upper DaAZ strata are present. This implies is that there is a northward younging of DaAZ strata and also importantly that the Javanerskop member, the RM, and Musgrave Grit unit are not contemporaneous.

5.3 Palaeoenvironmental interpretation of the *Daptocephalus* Assemblage Zone

This section is discussed in the context of four block diagrams that explain the observed palaeoenvironmental changes that occurred through the *Daptocephalus* Assemblage Zone prior to the onset of the PTME (Figure 5.3). Causes for palaeoenvironmental change, namely allogenic (tectonics, climate) vs autogenic (gradient, discharge rate, aggradation, avulsion) forces, are often difficult to distinguish from one another in the ancient rock record, because these commonly operate simultaneously, and in many instances can be interconnected (Miall, 1996; Catuneanu, 2006; Catuneanu et al. 2011). Therefore this section will conclude on assessment of the potential allogenic and autogenic causes of the observed palaeoenvironmental change in this study.

The block diagrams in Figure 5.3 represent changes in environment and fluvial style between the Lower and Upper DaAZ in the context of the lithostratigraphic units within the Balfour and Teekloof formations. The reconstructions reflect the synthesis of results obtained during this study, but where appropriate have also referred to the literature (Johnson, 1966, 1976; Visser and Dukas, 1979; Smith, 1993b, 1995; Shanley and McCabe, 1994, 1995; Rubidge et al. 1995, 2000; DeCelles and Giles, 1996; Catuneanu et al. 1997, 1998, 2004, 2011; Heller et al. 1998; Smith and Ward, 2001; Catuneanu and Elango, 2001; Weissmann et al. 2010, 2015; Fielding et al. 2012; Smith et al. 2012; Smith and Botha-Brink, 2014; Rutherford et al. 2015). The four block diagrams (Figure 5.3) demonstrate that the arenaceous units of the Lower *Daptocephalus* Assemblage Zone were initially deposited by low sinosity fluvial systems that then fine-upwards into argillaceous units deposited in high sinuosity systems. This cycle is then repeated in the Upper DaAZ and has also previously been documented for the Beaufort Group by and Visser and Dukas (1979) and Catuneanu and Elango (2001).

Block 1 represents depositional conditions at the base of the DaAZ (Lower DaAZ) whereby in the proximal foredeep the base of the Balfour and upper Teekloof formations were represented by arenaceous units (eg. Oudeberg, and Oukloof members). Distally (Bloemfontein, Jagersfontein), these units are conformable with the uppermost Ecca Group (Volksrust and Tierberg formations) (Catuneanu et al. 1998) but between these two depocentres there was either non-deposition, or incision and erosion of the Lower DaAZ strata, because it is not preserved in this part of the basin (Gariep Dam). The presence of the *Pristerognathus* Assemblage Zone in the southern Free State Province and the absence of the *Tropidostoma* and *Cistecephalus* assemblage zones does point to a period of non-deposition between the PAZ and DaAZ in the distal foredeep (Welman et al. 2001; Rubidge et al. 2015). Although the fluvial style of the

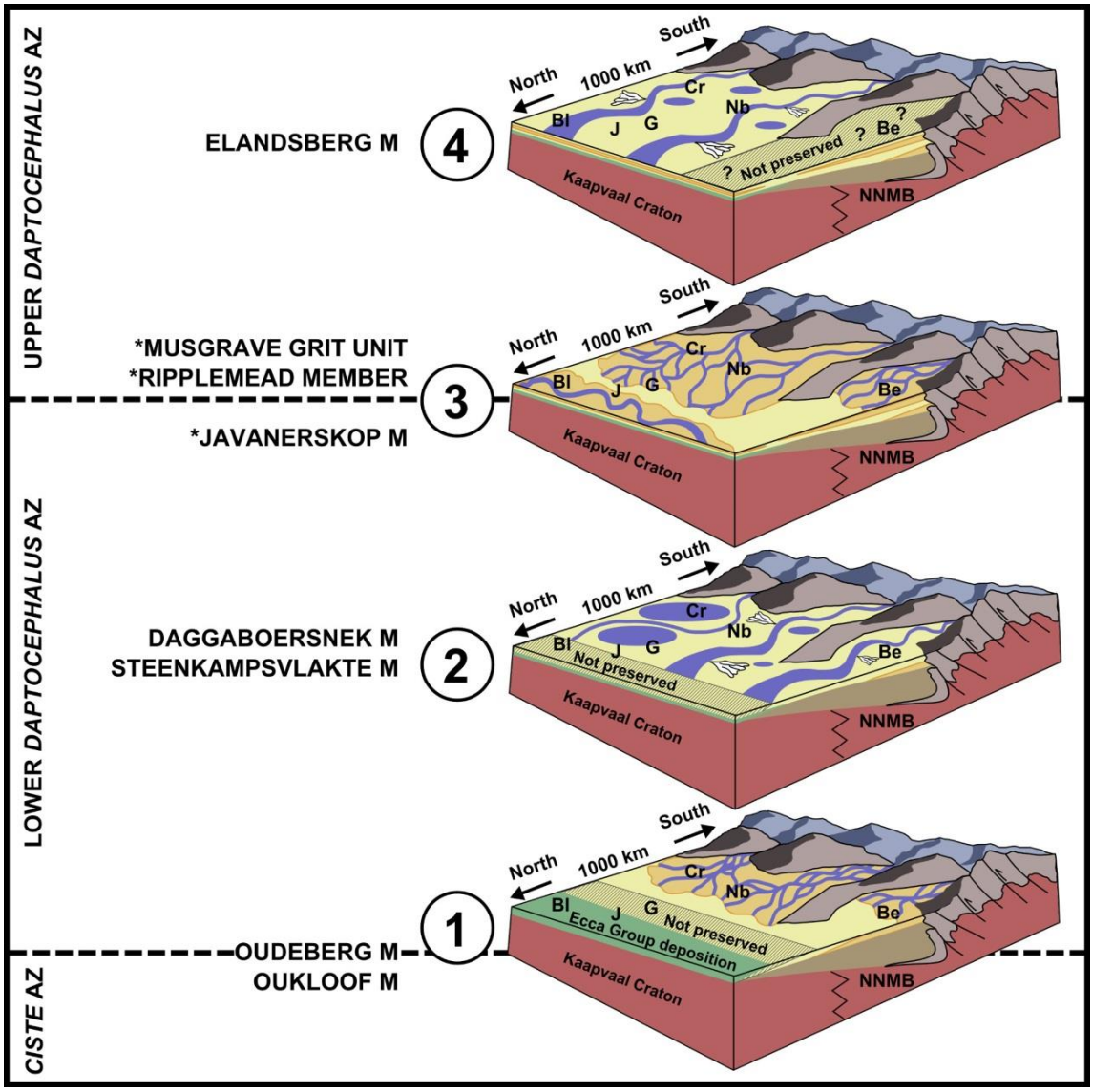

Figure 5.3: Palaeolandscape reconstructions (not to scale) for the Late Permian foredeep of the Karoo Basin (*Daptocephalus* Assemblage Zone). They are the synthesis of results from this study, but also incorporate those from previous studies. Abbreviations on the block diagram are: Beaufort West (Be), Bloemfontein (Bl), Cradock (Cr), Gariep Dam (G), Jagersfontein (J), Nieu Bethesda (Nb), and the Namaqua-Natal Metamorphic Belt (NNMB). Numbered 1-4, the block diagrams depict changes in fluvial style, distribution of sedimentation and non-deposition or erosion. Block 1 represents the lowermost Lower DaAZ and depicts low sinuosity rivers distributing sediment of the Oudeberg and Oukloof members only in the most proximal portions of the foredeep because these units are not preserved distally. This could be due to non-deposition or subsequent erosion. Block 2 represents the palaeoenvironment of the Daggaboersnek and Steenkampsvlakte members. Perennial Mississippian-style rivers have been interpreted for these lithostratigraphic units (Smith 1993b; Johnson, 1976; Rubidge et al. 1995; Smith et al. 2012). Lacustrine conditions were documented in the Cradock area for the Daggaboersnek Member during this study and by Johnson (1976) and therefore this is depicted in the Cradock area on Block 2. Block 3 depicts the return of low sinuosity distributory fluvial systems for the Javanerskop and Ripplemead members. Slightly after, a northeasterly source area in the distal foredeep deposits the Musgrave Grit unit in a higher sinuosity fluvial system. Block 4 depicts interpretations for the Elandsberg Member by Smith (1995), Smith and Ward (2001), and Smith and Botha-Brink (2014) just prior to the Permian-Triassic mass extinction. At this stage there is accommodation available throughout the foredeep although amount decreases northwards. In the Beaufort West portion, the Upper DaAZ is not preserved and thus interpretations cannot be made for the western basin.

Oudeberg and Oukloof members was not investigated in this study, Catuneanu et al. (1998) suggest that both the Koonap-Middleton formations and Oudeberg-Daggaboersnek members of the Balfour Formation represent fining-upward cycles whereby low sinuosity systems grade into high sinuosity fluvial systems. In addition to the low sinuosity fluvial style demonstrated for the Oudeberg Member in this study (Figures 4.13-4.16 in Chapter 4.3), the depositional environment of the Oudeberg and Oukloof is interpreted to be low sinuosity fluvial systems in addition to Catuneanu et al.'s (1998) hypothesis.

Block 2 represents the depositional environment of the Lower DaAZ whereby much of the foredeep accommodated high sinuosity systems that are represented by the Daggaboersnek (Balfour Formation) and Steenkampsvlakte (Teekloof Formation) members. Although significantly attenuated as the unit is followed northwards (Gariep Dam), the Daggaboersnek Member is present but not much further north of the Orange River. In the most distal portions of the foredeep (Jagersfontein, Bloemfontein) there was either marine deposition, erosion, or non-deposition occurring during this time due to the lack of Lower DaAZ strata in the portion of the basin. The previous distribution of the Steenkampsvlakte Member in the Karoo Basin is more difficult to infer due to post-Karoo erosion. Noteworthy in this block diagram is the predominatly subaqueous or lacustrine conditions in the Cradock area (Figure 5.3, Block 2), which, in line with the results of this study and Johnson (1976), demonstrate the preponderance of lacustrine conditions of the Daggaboersnek Member in this part of the Karoo Basin. The potential reasons for lacustrine conditions around Cradock will be discussed in chapters 5.3.1 and 5.3.2.

Block 3 represents the beginning of another fining-upward cycle in the Balfour Formation, and roughly the base of the Upper DaAZ, represented by the RM (Cradock, Nieu Bethesda, Gariep Dam). In the Teekloof Formation, the Javanerskop member represents an arenaceous unit located near the upper part of the escarpment in the Beaufort West area. Biostratigraphic evidence place this unit stratigraphically below the RM, in the Lower DaAZ, which is why this block diagram straddles the boundary of the Lower and Upper DaAZ (Figure 5.3). The low sinuosity nature of the Javanerskop member and the RM is demonstrated in this study by the identification of the fluvial style Type D in Beaufort West, and Type A and B near Nieu Bethesda and Gariep Dam for these units, respectively (Figures 4.16, 4.17, 4.19, 4.21, 4.22, 4.27, and 4.28 in Chapter 4.3). Although not demonstrated in this study, the RM in Cradock is also tentatively given a low sinosity fluvial style due to the general pattern of low sinuosity deposition of arenecoues units in the Beafort Group (Visser and Dukas, 1979).

The record of the Upper DaAZ near Bloemfontein suggests that accommodation occurred in the distal foredeep during this time. Biostratigraphic evidence places the Musgrave Grit unit in the Upper DaAZ by the presense of *Lystrosaurus maccaigi* (Viglietti et al. 2016). The Boomplaas sandstone stratigraphic position cannot be determined at this stage but geochemical similarities (Chapters 3.6 and 5.4) do indicate it may have some relationship with the Oudeberg Member. The fluvial style for this part of the basin was tentatively reconstructed as high sinuosity due to the presence of Type C at Jagersfontein (Figures 4.25 and 4.26 in Chapter 4.3) and Type E at Bloemfontein which represents crevasse splay elements (Figures 4.29 and 4.30). Crevasse splay elements can occur in all fluvial styles however they are rare in low sinuosity systems (Miall, 1996). The northeasterly source area for these rocks is noteworthy, and possibly indicates incision in the distal parts of the basin (forebulge and backbulge) which would occur when accommodation is created in the foredeep during times where orogeninc loading dominates as was the case during the latest Permian (Catuneanu et al. 1998).

Block 4 represents the depositional environment of the Elandsberg Member in the argillaceous phase of the second fining-upward cycle of the Balfour Formation (Figure 5.3). By this time in the latest Permian the DaAZ occupied the entirety of the main Karoo Basin, as is demonstrated by the contemporaneous deposition of the Normandien Formation in the backbulge but not shown in Figure 5.3 (Catuneanu et al. 1998). Accommodation was also present throughout the fordeep by this time because all composite sections contain the Elandsberg Member of the uppermost Balfour Formation (Upper DaAZ). This block diagram does not include the Palingkloof Member-Katberg Formation transition and strata preserving the PTME. Fluvial style and palaeoenvironment during the formation of the Elandsberg Member were mostly inferred from the literature (Smith 1995, Smith and Ward, 2001; Smith et al. 2012; Smith and Botha-Brink, 2014), which shows the return of perennial, Mississipian-style meandering rivers that occupied the foredeep. In Beaufort West region, this part of the stratigraphy is not preserved after the post-Karoo erosion (Hanson et al. 2009) and as a result reconstruction of the palaeoenvironment is not possible for the southwestern Karoo Basin during this time.

5.3.1 Allogenic vs autogenic controls

To date, allogenic controls on the development of the Karoo Basin are better understood than autogenic controls (Catuneanu et al. 1998; Rubidge et al. 2000; Smith 1993b, 1995; Smith and Botha-Brink, 2014) however, autogenic controls also probably influenced the palaeolandscape at the local level. For instance, upward-fining cycles seen in both the micro (eg. bed scale) and macro scale (eg. member scale) on the vertical sections could be related to localized decreased

flow energy with time due to decreasing accommodation, which would decrease the gradients and lead to lateral migration of the channels and amalgamated channel bodies being preserved (Allen, 1983; Miall, 1985, 1996; Wright and Marriot, 1993; Shanley and McCabe, 1994, 1995). Wright and Marriot (1993) explain that the floodplains, which act as sinks for fine grained sediments, have asymptotic rates of accretion whereby their ability to store sediment decreases rapidly with time and elevation. If the floodplains become elevated to a point where few floods are able to reach they will confine the channel which results in incision and erosion of the floodplain sediments as the channel avulses. Thus the ratio of preserved channel to floodplain sediment does depend on the system to store floodplain sediments.

Increases in gradient (and accommodation), and in combination with the recurrence of the same types of sedimentation through geologic time demonstrates how cycles of change in accommodation, sediment supply/discharge rates (allogenic change), and local ability to store sediment (autogenic change) are intertwined in foreland basin stratigraphy (Catuneanu et al. 1997; 2011) (Figure 5.3). Holbrook et al. (2006) introduced Butress and Buffer terms to describe the available fluvial preservation space for fluvial sediments in a basin. The Buttress refers to the longitudinal profile of the river which is controlled down dip by a physical barrier (eg. sea or lake in non-marine system) while the Buffer refers to the river's latitudinal profile which is the maximum aggradation or inscion profile. These profiles which describe autogenic responses are controlled by allogenic effects in the source area (eg. sediment supply and discharge rates, tectonic uplift) or at the Buttress boundary (eg. local sea level or base level changes).

During the Lopingian, orogenic loading was the dominant tectonic setting and gradients were increased by the creation of accommodation in the foredeep (Catuneanu et al. 1998). Additionally, the northward progradation of the DaAZ deposits also indicates a significant tectonic influence on sedimentation and potentially the palaeolandscape of the Lopingian Karoo Basin because orogenic unloading would cause the progradation of accommodation distally (eg. northwards). These observations from the Lopingian Karoo Basin could be explained by the Distributive Fluvial Systems (DSF) term coined by Weissmann et al. (2010, 2015) who describes many aggradational systems in ancient and modern foreland basins as patterns of channel and floodplain deposits which radiate outward from an apex located where the river enters the basin. At this location the river becomes unconfined depositing the sediment in a wedge that progrades and thins away from the apex. Although criticised by Fielding et al. (2012) these descriptions fit with many observations in this study as to how lithostratigraphic units have been deposited and distributed in the main Karoo Basin.

Climate is another allogenic control that could have influenced the fluvial style of the Karoo Basin even if the climatic influences were not within the Karoo Basin itself, but rather in the upland source areas (Catuneanu et al. 2006). This is because seasonal changes, such as snow melt, or increased erosion rates in the source areas can control discharge and amount of sediment load, and consequently the fluvial style of the rivers transporting the sediment into the basin (Leopold and Wolman, 1957; Haycock et al. 1997). In the past, little evidence for significant climatic change has been documented during the *Daptocephalus* Assemblage Zone times (Catuneanu and Elango, 2001), at least until the onset of the PTME (Smith 1995; Smith and Ward, 2001; Smith and Botha-Brink, 2014). Most of the changes to the palaeolandscape have been attributed to the dynamic tectonic setting of the Karoo Basin, which will be discussed in the next section. However faunal changes documented between the Lower and Upper DaAZ have been identified during this study and the potential reasons for this are now discussed.

5.3.2 Implication for Lopingian fauna of the *Daptocephalus* Assemblage Zone

The change from the Lower to Upper *Daptocephalus* Assemblage Zone is defined by the first appearance datum (FAD) of *Lystrosaurus maccagi* (Viglietti et al. 2016) and roughly coincides with the disappearance of the dicynodont *Dicynodon lacerticeps*, the therocephalian *Theriognathus microps*, and the cynodont *Procynosuchus delarharpeae*. Although these disappearances do occur low in the Upper DaAZ, rarefaction analysis demonstrates that no significant changes in faunal abundance occurs between the Lower and Upper DaAZ (Viglietti et al. 2016).

One factor that cannot be entirely explained by tectonic influences is the more common occurrence of facies association 4 (lacustrine/subaqueous systems) in the Lower DaAZ in comparison to the Upper DaAZ. This is particularly the case at the Cradock field site, where there is evidence for significant lacustrine and subaqueous conditions adjacent to the channelized river systems (Figures 4.11 and 4.12 in Chapter 4.2). Increased accommodation in the east by tectonics could explain the lacustrine conditions in this part of the basin, but overall the evidence for wetter floodplain systems may be due to greater groundwater availability during Lower DaAZ times (Smith, 1995; Smith and Ward, 2001). Smith et al. (2012) reconstruct the DaAZ as comprising waterlogged floodplains with high water tables, and perhaps in the Lower DaAZ this resulted in the presence of large lakes and swamps. These conditions have also been documented in the Upper Permian Emakwezini Formation in the Lembombo Basin (Bordy and Prevec, 2008). However minor climatic changes between the Lower and Upper DaAZ meant the loss of lacustrine settings, possibly due to lowering of the watertable as groundwater availability waned. These data indicate significant faunal and climatic changes were already occurring across the

boundary of the Lower and Upper DaAZ and could be evidence for the beginning of climatic changes terminating in the PTME. This is due to same patterns of disappearance being observed at the same stratigraphic interval throughout the basin, despite the thinning of strata northward. Sedimentation rates varied greatly in the Karoo Basin and in the past this thinning was not taken into consideration for studying the PTME (Smith and Botha-Brink, 2014).

Lystrosaurus has been demonstrated to be a genus of dicynodont that was either well adapted to drier conditions, or more able to cope with the increased drying of the Karoo Basin during the onset of the PTME (Smith, 1995; Botha and Smith, 2007; Viglietti et al. 2013). There is some evidence, based on one specimen of *L. maccaigi* from the Fremouw Formation of Antarctica that it lived in the earliest Triassic in the southernmost part of Gondwana (Collinson et al. 2006). However, the multiple specimens from South Africa suggest that it did not survive the extinction event in the main Karoo Basin (Smith and Botha-Brink, 2014; Viglietti et al. 2016). Thus its appearance in the Karoo Basin may explain the onset of seasonally drier floodplains in the Upper DaAZ than existed in the Lower DaAZ.

The causes and timing of the PTME are still hotly debated (Wignall and Hallam, 1992; Erwin, 1993; Renne et al. 1995; Bowring et al. 1998; Benton and Twitchett, 2003; Heydari and Hassanzadeh, 2003; Bottjer, 2012; Sun et al. 2012; Viglietti et al. 2013; Botha-Brink et al. 2014; Gastaldo et al. 2015; McKay et al. 2015; Rey et al. 2015), and although this study and others (e.g. Hancox et al. 2002) suggests that the extinction event may not be fully represented in the north due to the significant missing strata in this part of the basin, this does not mean that the time represented by the extinction phases will need to be reconsidered. The thicker lithostratigraphy in the proximal foredeep was due to fewer and shorter non-depositional periods than in the distal foredeep and in combination with significant faunal and climatic changes were already occurring below the inferred PTME this study supports the presence of a phased terrestrial PTME in the Karoo Basin. Determining whether the Karoo PTME was synchronous with the marine event will require dated strata closer to the inferred PTB and a full consideration of the complexities of the geological and fossil records in the basin.

The construction of a basin evolution model for the DaAZ through time relies not only on thicknesses and palaeoenvironmental changes but also provenace changes between the Upper Permian and Lower Triassic Beaufort Group as discerned from the palaeocurrent, petrographic and detrital zircon studies. Thus the provenance data is first discussed in order to determine if any changes in source area can be identified through the DaAZ.

5.4 Provenance of the Upper Permian – Lower Triassic Beaufort Group

In this section the most likely source areas for detrital zircon populations obtained from the samples collected from sandstones in the Oudeberg Member, Ripplemead member (RM), Javanerskop member, Boomplaas sandstone (BS), Musgrave Grit unit, and the Katberg Formation are evaluated. This is done in conjunction with palaeocurrent and petrographic data compiled during this study and in comparison with the literature. The degree of roundness and general appearance of zircon grains themselves are also considered in making decisions on possible provenance regions (Vorster, 2013; Bowden, 2013). The location of the dominant source areas at various positions in the stratigraphic record of the Upper Permian and Lower Triassic Beaufort Group is useful in gaining insight into the basin development of the Lopingian Karoo Basin later in the chapter. Finally, the youngest detrital zircon grain in each sample is used to estimate the timing of deposition for the different stratigraphic units that make up the Oudeberg Member, RM, Javanerskop member, BS, Musgrave Gritu unit, and Katberg Formation at each field site. At the time of deposition of the Beaufort Group, southern Africa was part of Pangea (e.g. Stampfli et al. 2013) implying that source areas available to the Karoo Basin are likely now on other continents that were once part of the supercontinent (Figure 5.4). For ease of comparison and explanation, the probability density plots from each sample, presented in Chapter 3.5 are summarized in Figures 5.5 and 5.6. Upper Permian and Lower Triassic samples will be discussed separately.

Upper Permian Beaufort Group (Adelaide Subgroup)

The detrital zircon populations sampled from the Upper Permian Beaufort Group comprise three main populations: 1) a latest Carboniferous to latest Permian-Triassic population (250 ± 5 Ma – 339 ± 5 Ma); 2) an earliest Devonian to Neoproterozoic (364 ± 7 Ma to 878 ± 24 Ma), and 3) a latest Neoproterozoic to Mesoproterozoic (908 ± 24 Ma to 1308 ± 23) (Table 7, Figures 5.5-5.7). The oldest grains in the samples are split into two groups that range from late Mesoproterozoic to late Palaeoproterozoic (1402 ± 26 Ma to 2450 ± 17 Ma) and Archean (2756 ± 18 to 2803 ± 17). Most of the samples from the late Permian Beaufort Group share a dominant latest Carboniferous to latest Permian- earliest Triassic zircon population (250 ± 5 Ma – 339 ± 5 Ma), ranging from 39.2 % to 64% of the population (Table 5.1). An exception is the sample from the Oudeberg Member at the Barberskrans Cliffs (PV-Cr1) which had the lowest population of very young zircons – only 4 % of the total sample. The only other sample similar to PV-Cr1 is from the Boomplaas sandstone on section 12 (PV-J615) which only has 12 % of its population being part of the youngest component. This is an interesting observation because the Oudeberg Member is stratigraphically lower than the RM which may mean that the influx of

younger grains only began in the very latest Permian. Additionally the stratigraphic position of the BS near Jagersfontein is undetermined, but perhaps shares a stratigraphic relationship with the Oudeberg Member due to this similar geochemical pattern. The Free State stratigraphy is poorly correlated but due to the recent discovery that *Pristerognathus* Assemblage Zone aged strata is present near Jagersfontein (Welman et al. 2001; Rubidge et al. 2015), this may mean that other strata contemporaneous to the *Tropidostoma* and *Cistecephalus* Assemblage zones could also be present in this part of the basin.

The majority of the grains from the youngest population (250 ± 5 Ma – 339 ± 5 Ma) have Th/U ratios higher than 0.07. This means they are of magmatic and not metamorphic origin (Rubatto, 2002), and are therefore likely representative of juvenile magmatic material. Results obtained from previous workers (Vorster, 2013; Bowden, 2013) show that this young population is absent from older rocks of the Cape and Karoo basins (eg. Cape Supergroup and Dwyka Group). This is of no surprise for the Cape Supergroup, because its deposition predates this young population however; the large proportion of Carboniferous-Permian grains in the RM implies that there was an influx of material from a new source during only the latest Permian. The euhedral nature of the youngest population also indicates their origin is directly from the magmatic source and may have not been significantly reworked. This source region was most likely to the south for most samples due to either northwesterley or northeasterley palaeocurrent directions (with the exception of PV-J615 and PV-T 28m that have southwesterly palaeocurrent directions). The dominantly southerly source area for the Karoo Basin has been documented (Cole, 1992; Wickens, 1996; Cole and Wipplinger, 2001) and proposed to be a southern magmatic arc related to the subduction of the Palaeo-Pacific Plate and formation of the Gondwanides (Johnson, 1991; Milani and De Wit, 2008) (Figure 5.4).

In a study conducted by Cawood et al. (2012) detrital zircon ages reported from sedimentary rocks obtained from convergent plate margins where foreland basins form are often characterized by a large proportion of detrital zircon ages close to the estimated depositional age of the rocks, whereas samples collected from extensional and intracratonic settings contain greater proportions of older ages reflecting the underlying basement geology. Interestingly Cawood et al. (2012) also consider the large amount of zircon grains approximating time of accumulation of the host sediments as evidence for close proximity of the basin to the plate margin, which has never been considered a possibility for the Karoo foreland system. The results of their study reflect these observations and perhaps highlight that more work needs to be conducted on determining the true position of the Karoo foreland basin from the plate margin.

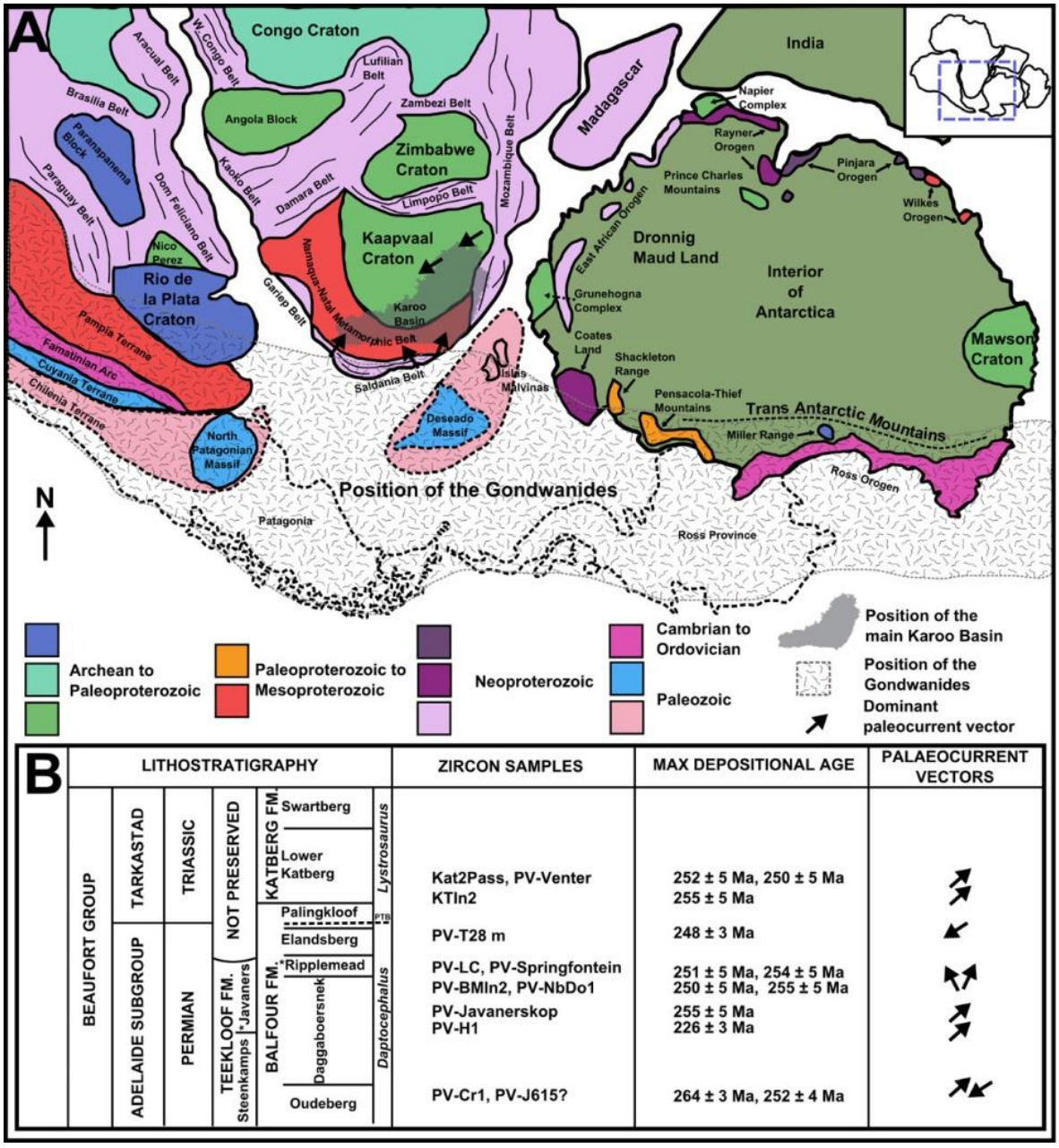

Figure 5.4: A) Proposed position of Gondwana and the Gondwanides during the deposition of the Karoo Supergroup showing possible source areas for detrital zircons indicated by colour coded age groups. These source areas include Archean to Palaeoproterozoic cratons, Neoproterozoic mobile belts, Palaeozoic volcanics, and intrusions. Not shown is the theorized Lopingian arc volcanism south of the Gondwanides that was likely a source of dominant young detrital population sampled in this study. Modified after Rapela et al. (2011); Uriz et al. (2011), Pankhurst et al. (2006), Veevers and Saeed, (2013), Vorster, (2013), and Bowden (2013). B) The stratigraphic position of the twelve sandstones sampled for detrital zircon analysis. Also shown are the maximum age of deposition for each sample (indicated by the youngest concordant grain), and the dominant palaeocurrent directions at the same stratigraphic interval. Note PV-J516 from Boomplaas Hill (section 12) has a question mark because it could not be given an exact stratigraphic position, but Upper *Cistecephalus* or Lower *Daptocephalus* Assemblage Zone is estimated.

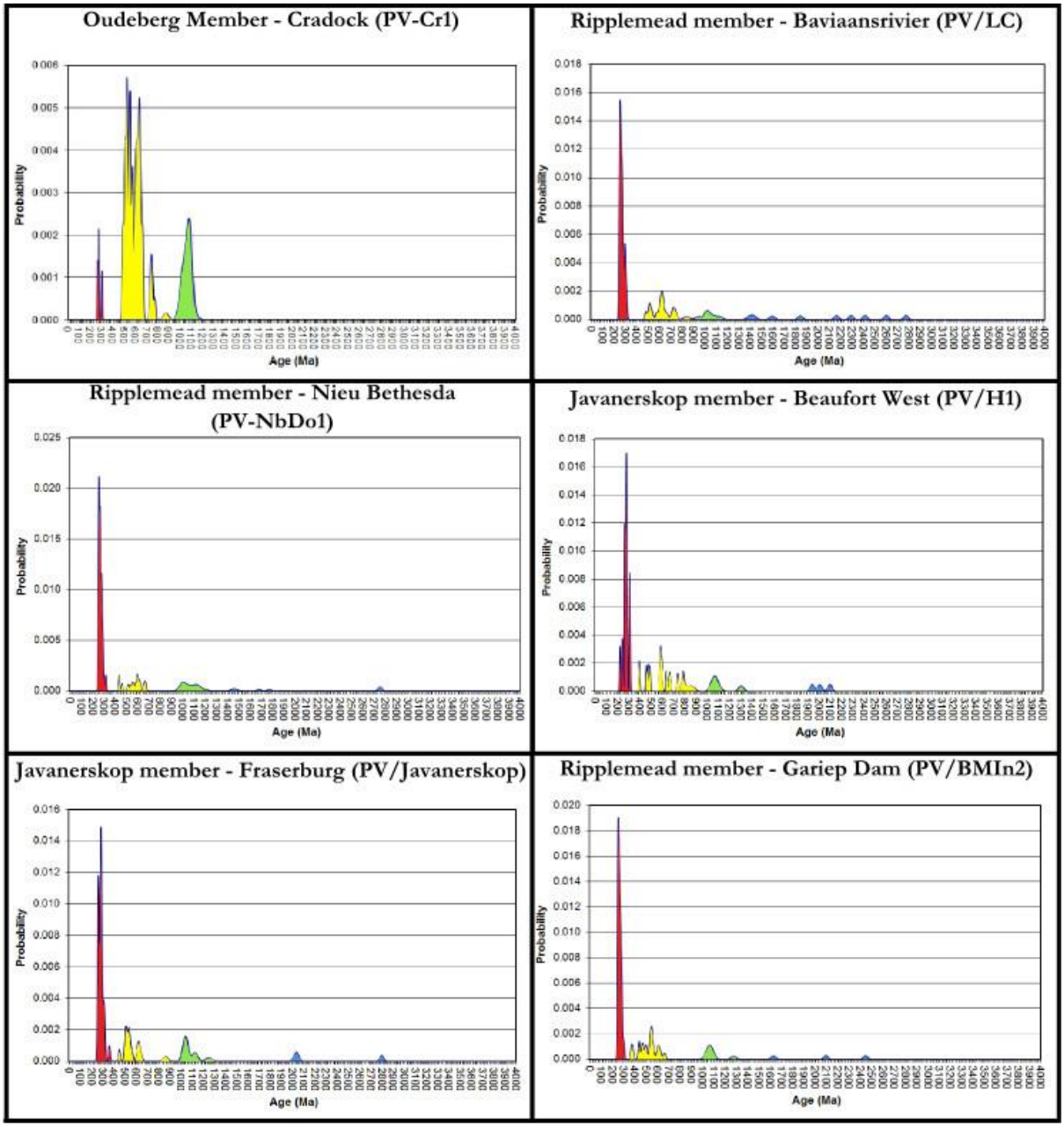

Figure 5.5: Probability density plots for the samples in this study. Red= the youngest zircon population (250 ± 5 Ma – 339 ± 5 Ma), yellow and green = intermediate zircon age population (364 ± 7 Ma to 878 ± 24 Ma), and (908 ± 24 Ma to 1308 ± 23), blue= the oldest zircon population (1402 ± 26 Ma to 2450 ± 17 Ma) and (2756 ± 18 to 2803 ± 17).

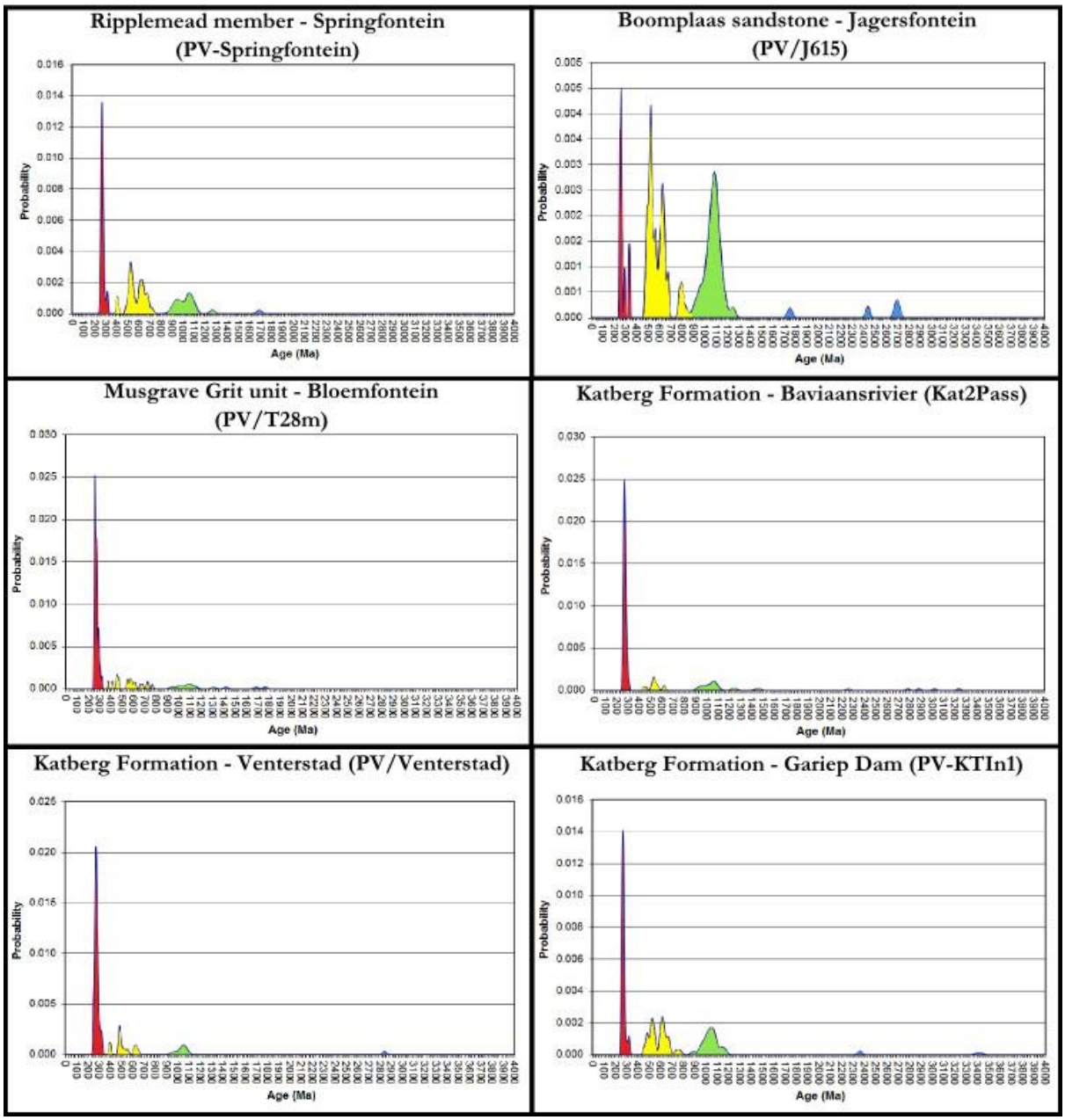

Figure 5.6: Probability density plots for the samples in this study (continued). Red= the youngest zircon population (250 ± 5 Ma – 339 ± 5 Ma), yellow and green = intermediate zircon age population (364 ± 7 Ma to 878 ± 24 Ma), and (908 ± 24 Ma to 1308 ± 23), blue= the oldest zircon population (1402 ± 26 Ma to 2450 ± 17 Ma) and (2756 ± 18 to 2803 ± 17).

Evidence for this arc system, which is no longer preserved, is the presence of ashes within the Ecca and Beaufort Group (Cole, 1992; Fildani et al. 2007; Fildani et al. 2009; Mckay et al. 2011). These ashes have been dated and show a large population of Carboniferous to Late Permian grains (Fildani et al. 2007; Fildani et al. 2009; McKay et al. 2015) and thus were likely either brought into the Karoo Basin during latest Permian period by fluvial processes or by air fall during explosive volcanic activity along the arc system (Rubidge et al. 2013; McKay et al. 2015). Air fall may also explain why samples in the distal sections of the basin (PV-J615 and PV-T 28m)

have representatives of the youngest population even though these parts of the basin were not actively sourcing sediment from the south. The sample from the Oudeberg Member (PV-Cr1) and Boomplaas sandstone (PV-J615) has the lowest young population (~4 and 12 % of the total population respectively) and the Oudeberg Memeber also has the oldest maximum age of deposition out of all the samples (264 ± 3 Ma). Although not a sure way of determining age, this data agrees with field evidence that the Oudeberg Member at the Barberskrans Cliffs is different from the RM but similar to the Boomplaas sandstone. It also points to the possibility that arc activity was less during the early late Permian than the latest Permian.

Samples from the RM (PV-LC, PV-NbDo1, PV-BMIn2, and PV-Springfontein) have similar maximum depositional ages, but they do not help to prove whether or not these sandstones are coeval within the Karoo Basin. What these data do confirm is that they are likely latest Permian in age, which fits with field observations that they are present within the upper section of the Balfour Formation. Samples from the western depocenter (PV-H1 and PV-Javanerskop) and northern most parts of the proximal basin (PV-J615 and PV-T 28m) also show similar maximum depositional ages to theRM but palaeontological evidence demonstrates they are not representative of the same period of time (see chapters 3.2 and 5.2). Additionally, some problems with the youngest grains in the samples (see discussion in Chapter 3.5.2) demonstrate that not all of the young grains are reliable to discern the maximum age of deposition of their host rock.

A small percentage of the total population in all samples have Devonian, Silurian, and Ordovician grains. Vorster (2013) and Bowden (2013) both suggest South America's Deseado Massif (DM), North Patagonian Massif (NPM), Famenian Arc, and Antarctica's Ross Orogeny as potential source areas for these grains because they would have been close to the southerly portion of the Karoo Basin during the Lopingian (Cole, 1992; Le Roux, 1995; Ben-Avraham et al. 1997; Pankhurst et al. 2003; Federico et al. 2006; Pankhurst et al. 2006; Willner et al. 2008; Fourie et al. 2011; Tibaldi et al. 2013). Since the Gondwanides may have been a significant barrier to these outcrops during Lopingian times these grains may have also been recycled from the Cape Supergroup which was involved in the Gondwanide Orogeny and active erosion during the Lopingian as demonstrated by the poor preservation of these grains (Table 3.4) (Vorster, 2013; Andersen et al. 2015).

The older populations within the samples are also likely to have also been sourced from the Gondwanides. Vorster (2013) and Bowden (2013) identified Cambrian-Neoproterozoic (50-70 % total population), Mesoproterozoic (10-25 % total population), and Palaeoproterozoic (1-3 % of total population) populations, with few or absent Archean grains, which are similar to population

abundances identified in this study. The Cape Supergroup and parts of the Dwyka and Ecca groups, formed part of Gondwanide Orogeny, thus these rocks would have been eroded and been a source of sediment for the Beaufort Group. The dominantly northerly palaeocurrents corborates this (Figures 5.2 and 5.5), however, even the samples that came from sites where southwesterly palaeocurrents dominate (PV-J615), these grains were present (Table 3.3 and Figures 5.5 and 5.6). Samples in the north of the Karoo Basin may have had direct access to Neoproterozoic sources of sediment such as the Limpopo or Mozambique Belt but it is also possible significant recycling has obscured the real source area of the Beaufort Group (Andersen, 2005; Andersen et al. 2015).

Vorster (2013) and Andersen et al. (2015) have suggested that the source of the Cape Supergroup sediments was from ex-Gondwanan continents that would have been closer to southern Africa. The large Cambrian-Neoproterozoic population was likely sourced from rocks associated with the Pan African Orogeny, preserved as a number of mobile or metamorphic belts, accreted terranes, and minor cratons during the formation of Gondwana (Gresse et al. 2006). In southern Africa, the Pan African Orogeny is represented by the Gariep and Saldanian mobile belts (Frimmel et al. 2002; Scheepers and Armstrong, 2002; Frimmel and Fölling, 2004; Gresse et al. 2006). The rounded nature of grains in this population indicates reworking and significant transport (see Chapter 3.5 cathode-luminescence images). This is corborated by the classification of the sandstones from the study area which suggest an orogenic source for the sandstones (Chapter 3.4).

Mesoproterozoic and Paleoproterozoic zircon grains are uncommon in the Cape Supergroup samples obtained by Vorster (2013) and Bowden (2013). The major Mezoproterozoic-early Paleoproterozoic source in close proximity to the Karoo Basin is the Namaqua-Natal Metamorphic Province (NNMP), although South America's Pampia terrane may have also been a potential source (Vorster, 2013, Figure 5.4). The NNMP is located to the west and south of the Kaapvaal Craton and contains igneous and metamorphic rocks that are divided into a number of accreted terranes and subprovinces (Cornell et al. 2006; Eglington, 2006; Bailie et al. 2011). All of these terranes and subprovinces are potential source of zircons to the Cape Supergroup, which later could have also been source of sediment for the Beaufort Group.

The origin of the Archean grains is more cryptic, because these grains are traced in the Cape Supergroup samples of Vorster (2013) and Bowden (2013). They are probably sourced from the Transvaal Supergroup, or by reworking of older successions in the NNMP (Vorster, 2013). All of the oldest grains in the samples are broken and fragmentary, which points to a complex

depositional history that very likely predates the formation of Pangea (see Chapter 3.5 cathode-luminescence images) and probably were derived from other older sedimentary units, obscuring the true source areas of the Beaufort Group (Andersen, 2005; Andersen et al. 2015). Nevertheless, the Gondwanides appear to have been a significant source area for all of the rocks of the Beaufort Group, even in the distal parts of the basin where palaeocurrents are from the north-northeast.

Provenance of the lowermost Katberg Formation (Early Triassic, Tarkastad Subgroup, Beaufort Group)

The zircon grains in the Katberg Formation are also grouped in three main populations: 1) a latest Carboniferous to latest Permian population (250 ± 5 Ma – 332 ± 6 Ma); 2) an earliest Devonian to Neoproterozoic (375 ± 4 Ma to 777 ± 16 Ma), and 3) latest Neoproterozoic to Mesoproterozoic (891 ± 22 Ma to 1172 ± 21). The oldest grains in the samples are split into two groups that range from late Mesoproterozoic to late Palaeoproterozoic (1422 ± 22 Ma to 2364 ± 18 Ma) and Archean (2846 ± 17 to 3416 ± 31). Zircon populations present in samples from the Katberg Formation are similar to the RM, Javanerskop member, and Musgrave Grit unit (Figures 5.6 and 5.7). This means source areas did not change significantly across the PTB and the Katberg Formation samples are very similar to the Permian samples and thus provide similar implications (eg. Cawood et al. 2012). The only minor difference noted is the presence and minor increase (1-7 %) of late Mesoarchean and early Paleoarchean grains in the population. Since the Archean grains are likely being sourced from reworking of Cape Supergroup samples, this may mean that greater erosion of these older rock units taking part in the Gondwanide Orogeny was occurring during deposition of the Katberg Formation, which corroborates the increase in sediment supply occurring at this time and increased sandstone:mudstone ratio present in the Katberg Formation (Catuneanu et al. 1998).

5.5 Basin Development model for the Lopingian Karoo Basin

All of the multidisciplinary evidence collected during this study is combined to construct a basin development model for the Lopingian Permian Karoo Basin. All evidence indicates that cyclic, out-of-phase sedimentation occurring in the Karoo Basin during the latest Permian with a strong tectonic influence and dominantly southerly sediment source (Figure 5.7).

The cyclic nature of sedimentation as fining upward mega-cycles in the Karoo Basin has been documented by many previous workers (e.g. Johnson 1966, 1976; 1991; Visser and Dukas, 1979; Smith 1989). These mega-cycles were always interpreted as having a tectonic rather than a climatic origin (Visser and Dukas, 1979; Catuneanu et al. 1998; Catuneanu and Elango, 2001) as

sporadic uplift leads to an increase in stream gradients, sediment input, and accommodation proximal to the dominantly southerly source areas. This may not be entirely true for the transition between the uppermost Balfour Formation and Katberg Formation during the onset and aftermath of the PTME as climatic and tectonic signatures overprint one another (Hiller and Stavrakis, 1984; Smith, 1995; Smith and Ward, 2001; Smith and Botha, 2005; Botha and Smith, 2006; Viglietti et al. 2013; Smith and Botha-Brink, 2014).

The retroarc foreland basin model for the Karoo Basin is pervasive because it best explains the out-of-phase deposition of lithostratigraphic units in the proximal and distal sectors, which is typical of foreland basins documented globally (DeCelles and Giles, 1996; Catuneanu et al. 1997; 2011). The key components of a retroarc foreland basin are 1) a subduction zone, 2) active orogenic belt to create accommodation and flexural partitioning (eg. into a proximal foredeep, central forebulge, and distal backbulge provinces), and 3) volcanic island arc system (Visser, 1993; Johnson et al. 1996; Johnson et al. 1997; Catuneanu et al. 1997,1998; Miall et al. 2008). Additionally sediment accumulation also begins under marine (underfilled) conditions and terminates in fluvio-lacustrine and/or aeolian (overfilled) conditions (Catuneanu et al. 1997, 1998; Uličný, 1999). The Karoo Basin system preserves evidence for all of these with the exception of the arc system. Its existence has been theorized by the presence of volcanic ash deposits, both reworked and syndepostional, throughout the Karoo Supergroup (Fildani et al. 2009; Rubidge et al. 2013; Gastaldo et al. 2015; McKay et al. 2015). Smaller en-echelon rift basins within southern Africa created by Permo-Carboniferous crustal extension in response to subduction and north-south compression also agree with the foreland basin model (Smith et al. 1993; Miall et al. 2008). The Karoo retroarc foreland system is theorized to be significantly distant from the subduction zone which has been problematic for the model in the past, but can also be explained by flat slab subduction (dynamic subsidence) which would cause the translation of deformation inland (Lock, 1980; Mitrovica et al. 1989; Gurnis, 1992; Holt and Stern, 1994; Le Roux, 1995; Burgess et al. 1997). However evidence from Cawood et al. (2012) and this study concerning detrital zircon populations, the position of the main Karoo Basin may require reconsideration (see Chapter 5.4).

While the foreland basin model for the Karoo Basin has been challenged by other workers who propose fault controlled subsidence and extension (Cloetingh et al. 1992; Turner, 1999; Tankard et al. 2009, 2012), continent-continent collision (Milani and De Wit, 2008; Lindeque et al. 2011), and asymmetrical subsidence (Fildani et al. 2009) basin models for the Karoo Basin, it is only the timing of the onset of flexural tectonics that has been seriously disputed becaused most of these

workers do recognize foreland tectonics by Beaufort Group times. However, it is now clear that by deposition of the Dwyka Group flexural tectonincs were already in place as evidenced by a foredeep transgressed by an interior seaway, a forebulge uplifted above base level with continental ice sheets, and a shallow backbulge depocenter to the north (Bordy and Catuneanu 2002; Catuneanu, 2004b; Isbell et al. 2008). A shift from marine facies in the foredeep to dominantly continental facies in the north also supports the foreland model during deposition of the Dwyka Group (Catuneanu, 2004b; Isbell et al. 2008). This means the Karoo Basin was most likely a foreland basin from its formation and these conditions continued until its termination at the end of the Stormberg Group (Catuneanu et al. 1998; Bordy et al. 2004). In addition the northward thinning, and compressed or missing stratigraphy of lithostratigraphic units away from the source area as identified in this study reflects many characterisitcs of DSFs of Weissmann et al. (2010, 2015) who have identified these aggradational fluvial systems in both modern and ancient foreland system deposits. Heller et al. (1998) also demonstrate that the asymmetrical profile in foreland systems created by advancing thrust sheet which diminished exponentially from the load contributes to the northward thining of strata in these types of basins as is identified in this study. The only problematic issue has been coinciding tectonic paroxysms with sedimentation events in the Karoo Basin (Hälbich et al. 1983). New 40Ar/39Ar age constraints on the deformation and cooling of the Cape Fold Belt (Hansma et al. 2015) do not significantly clarify this issue because the results highlight a narrower (20-25 Myr) window for the Cape Orogeny than previously considered (261 ± 3–276 ± 5 Ma to 248 ± 2–254.6 ± 2.1 Ma). These results do not reflect sedimentation events in the Karoo Basin and therefore it is these dating methods for tectonic paroxysms that likely require further refinement.

As indicated by Figure 5.7, observations from the current study support the retroarc foreland basin model as second-order subaerial unconformities (SU) have been identified at the base and top of the Balfour Formation (Catuneanu et al. 1998) and third-order SU have been identified in the Balfour Formation (Catuneanu and Elango, 2001). This has been interpreted as being caused by out-of-phase sedimentation in the Karoo Basin controlled by orogenic loading and unloading events in a retroarc foreland system. Catuneanu and Elango (2001) identify six third-order SU near Fort Beaufort (Eastern Cape) over a 2150 m interval within the Balfour Formation. In the current study a maximum thickness of only 513 m is identified in the Cradock area for the Balfour Formation, and due to the close proximity of Fort Beaufort to the field site, this investigation questions the accuracy of the total thickness obtained by Catuneanu and Elango (2001). Only one third-order SU is identified in this study, and it is theorized to represent a diachronous boundary that signalled the deposition of the Javanerskop member, RM, and

Triassic strata in the most distal foredeep (Bloemfontein and Thaba Nchu). Its stratigraphic position is highlighted in Figure 5.7. Additionally the second-order SU of Catuneanu et al. (1998) at the base of the Balfour Formation was theorized to extend west to the base of the Oukloof Member (Teekloof Formation) during this study.

The third-order SU in this study was identified by using the criteria outlined by Miall and Arush (2001). These changes identified in the RM include a relatively abrupt change in lithology (eg. from mudstone rich to sandstone rich), changes in fluvial style (from high to low sinuosity), eroded fossil material (eg. plant and bone material) or erosional coarse-grained lags on the boundaries (eg. Gm1 and Gm2 identified in RM at all field sites). Catuneanu et al. 2011 highlights that many basins are bounded by tectonically active source areas, and episodic uplift results in the rejuvenation of fluvial systems (coarsening upward cycles) or cessation of tectonic activity results in the deposition of fining-upward cycles. These repeated cycles reflect that fluvial systems are characterized by processed which produce the same depositional results but many begin with an initial pulse of high fluvial transport marked by an SU followed by increasingly fine grained sediment as is observed in the Karoo Basin. Similarly, Shanley and McCabe (1994, 1995) use the progression from amalgamated sandstone deposits to isolated meanderbelts to identify the position of SU in Upper Cretaceous deposits in southern Utah. Finally changes in faunal ranges observed as the appearance of *Lystrosaurus maccaigi* and disappearance of *Dicynodon lacerticeps*, *Theriognathus microps*, and *Procynosuchus delaharpeae* in the RM are also a possible indication of the presence of the third order SU. Although this faunal transition is not identified at the base of the Javanerskop member, it implies that the third-order SU is diachronous. Diachroneity has been identified at major lithostratigraphic boundaries of the Karoo Supergroup (Catuneanu et al. 1998; Hancox, 1998; Rubidge et al. 2000; Neveling, 2002) and is evidence of a tectonic influence controlling sediment distribution in the foredeep.

The SU identified in this study is evidence for missing time and is supported by changes in fauna across the sequence boundary and by missing or thinning of strata in the distal foredeep (eg. Gariep Dam). In Bloemfontein and Thaba Nchu, the PTB is not preserved (Rutherford et al. 2015) and therefore the third-order SU is theorized to be placed at the base of earliest Triassic strata here. The distal edge of the foredeep would have also been more sensitive to changes in accommodation or orogenic uplift in the south because of the limited available accommodation close to the rigid Kaapvaal Craton (Sloss, 1984). Gradient changes in response to an orogenic load to the south of the basin (Gondwanides) would cause changes in fluvial style, sedimentation rates, and accommodation in different sections of the basin (Figure 5.7). Evidence for this model

is substantial, thus the tectonic setting for the latest Permian Karoo Basin uses the foreland basin model to explain the distribution of the Upper Permian lithostratigraphic units. The lateral extent of the SU, attenuation of strata, and faunal ranges of DaAZ indicator taxa are used to create this new basin development model for the Lopingian Karoo Basin (Figures 5.7 and 5.8).

Inferred tectonic setting

This section will be discussed by referring to Figure 5.8 showing the interpreted changes in the tectonic setting of the Karoo Basin during the time span of the DaAZ and the role the lithostratigraphic units of the DaAZ play in this tectonic history. This model adds a new third-order detail to the mostly first and second-order framework of the Karoo Basin sedimentary fill (Catuneanu et al. 1998). Each second or third-order sequence correlates to an orogenic cycle of thrusting followed by erosional or extensional unloading (Catuneanu et al. 1998; Catuneanu and Elango, 2001). The new paroxysm dates by Hansma et al. (2015) do not provide the resolution needed to correlate individual sequences with a dated paroxysm however they do fall within the older dates of active orogenic thrusting.

It is interesting to note that although out-of-phase, the western and eastern basin (Teekloof and Balfour formations) show similar lithostratigraphic sequences which may mean they were not completely isolated from each other but were influenced by similar flexural tectonics within the same retroarc foreland system. The western and eastern sectors of the Karoo Basin could represent two distinct DSFs of Weissmann et al. (2010, 2015) and the "Willowmore arch" (Van Eeden, 1972), which a theorized topographic high that was present between these two sectors could explain their apparent stratigraphic separation. This may explain some differences between the two parts of the basin but essentially they are reflecting similar tectonic events in the foreland systems which are defined by quite repetitive depositional cycles (Catuneanu et al. 2011). The Willowmore arch and slight out of phase deposition between the east and western sectors does entertain the possibility of alternative controls on subsidence that caused the basin to be an interrupted, elongate trench. The basin likely consisted of downwarped depressions and upward arches formed by the interplay of the retroarch foreland system's compressional and flexural tectonics and the local rheology or structural integrity of the basement rocks. The Kaapvaal Craton situated north of the Orogeny in the distal basin would have been more rigid and boyant than the Namaqua-Natal Metamorphic Belt which comprises the basement rocks to the proximal foredeep and back bulge. Local structural anomalies proposed to have controlled local tectonics by Tankard et al. (2009, 2012) may have contributed to the out-of-phase deposition created by flexural tectonics of the retroarc foreland system.

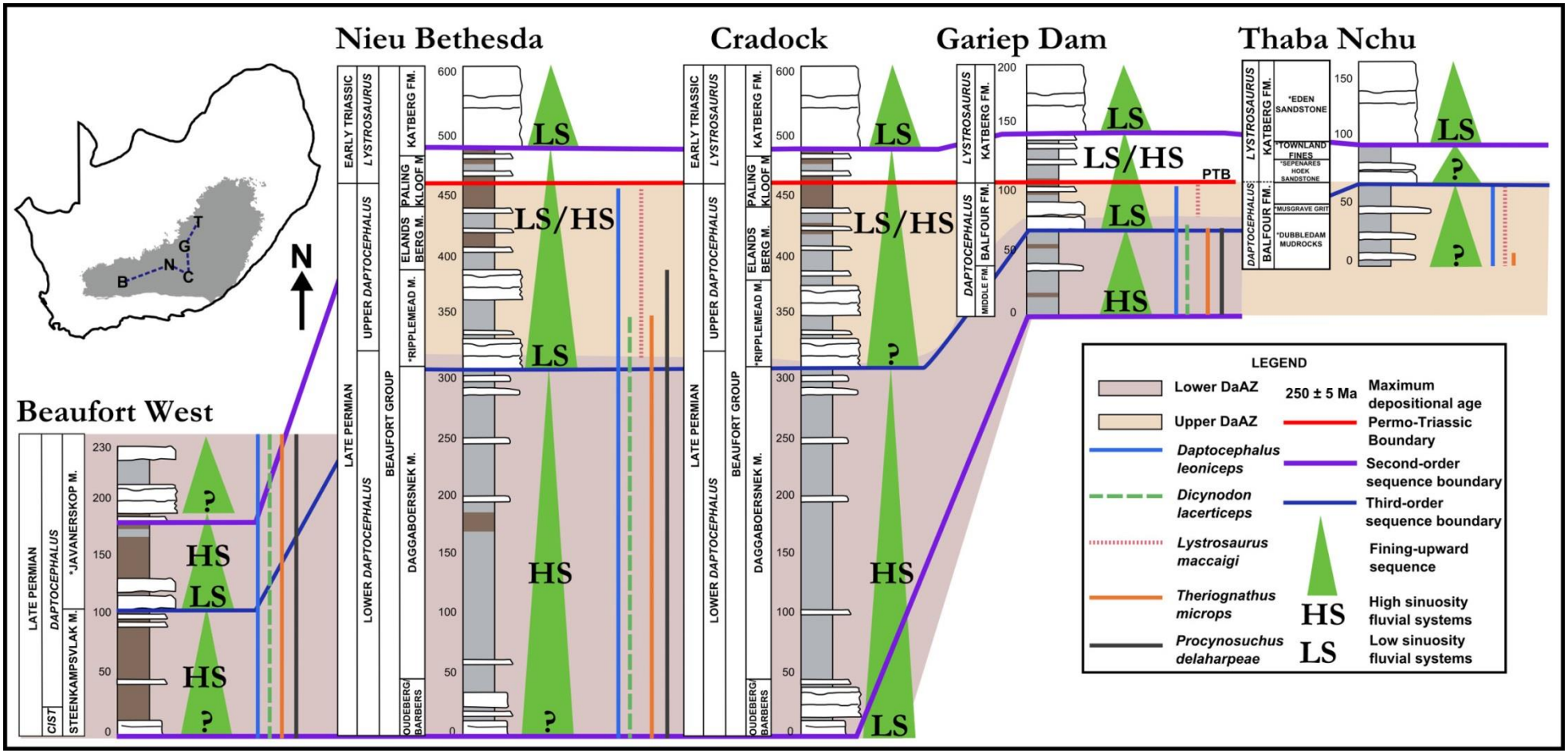

Figure 5.8: Composite sections created for the field sites of this study. In this example faunal ranges of *Daptocephalus* Assemblage Zone index taxa are shown in conjunction with stratigraphic position of low and high sinuosity fluvial systems, and interpreted second-order unconformable boundaries (SU). The second-order SU at the base and top of the Balfour Formation is theorized by Catuneanu et al. (1998) and the second-order SU at the base of the Oukloof Member (Teekloof Formation), and third-order SU drawn the base of the Javanerskop and Ripplemead sandstone members, and tentatively at the base of Triassic strata in the Bloemfontein/Thaba Nchu field site, are interpretations made in this study. The migration of this SU east and northwards fits with observations made from faunal ranges that uppermost Permian strata are more complete in the south than in the north. Therefore it can be theorized that the third-order SU will also be older in the south and younger in the north because it is a diachronous boundary.

In the basin model compiled from work during this study, four stages have been identified that explain the inferred tectonic setting of the Lopingian Karoo Basin. Explanation of the model will use these four stages as a framework for explanation, with reference to Figure 5.9 whenever appropriate.

Stage 1 depicts the onset of sedimentation of the Balfour and upper Teekloof formations which began with deposition of the first second-order cycle (Oudeberg and Oukloof members) and represents a sudden change to a low sinuosity fluvial system. Contemporaneously, sedimentation of the Ecca Group was occurring in the north, or there was nondeposition as no Lower *Daptocephalus* Assemblage Zone is documented close to the forebulge. Once sediment supply became less than available accommodation, the sequence began to fine-upward, depositing the argillaceous Steenkampsvlakte and Daggaboersnek members. Parts of the Steenkampsvlakte and Daggaboersnek members were deposited by meandering fluvial systems (Beaufort West and Nieu Bethesda) and also lacustrine conditions (Cradock) due to a combination of increased accommodation in this part of the basin and wetter palaeoclimatic conditions.

Stage 2 was initiated by another minor orogenic loading event resulting in the out-of-phase deposition of the arenaceous Javanerskop and Ripplemead members along a third-order SU. The Javanerskop member is older than the RM and is only present in the south east and central Karoo Basin. Coincidently, the decrease in sinuosity of the fluvial systems leads to reduced overbank preservation, and disappearance of the meandering fluvial and lacustrine systems.

Stage 3 is an unloading phase which results in progradation of sediment northwards as accommodation became available in the distal foredeep. This explains the attenuated but similar stratigraphy in the northern foredeep. Sedimentary input from the northeast is evidenced by deposition of the Musgrave Grit unit in the Bloemfontein area. At this time the third-order sequence began to fine upwards, terminating in the argillaceous Elandsberg and Palingkloof members. This sequence was overprinted by climatic changes during the onset of the PTME (Smith and Ward, 2001; Smith and Botha-Brink, 2014). In this study it is theorized that the third-order SU rests at the base of earliest Triassic strata in the distal foredeep (Bloemfontein/Thaba Nchu) due to the sudden change in lithology, fauna, and the fact that the PTB is not preserved in this part of the Karoo Basin (Rutherford et al. 2015).

Stage 4 marks the beginning of deposition of the early Triassic lower Katberg Formation in a new orogenic loading phase. The position of this unconformity is placed at the base of the Katberg Formation by Catuneanu et al. (1998) however Neveling (2002) identified that the

Katberg Formation comprises three distinct units that occupy different sections of the Karoo Basin. Since the second-order SU is not necessarily a synchronous boundary, the position of this unconformity at the top of the Balfour Formation may be different in the proximal basin to that in the distal basin but this was not investigated during this study. It is theorized that this second-order SU rests at the base of the Eden sandstone near Thaba Nchu (Rutherford et al. 2015), although this would require future investigation to confirm.

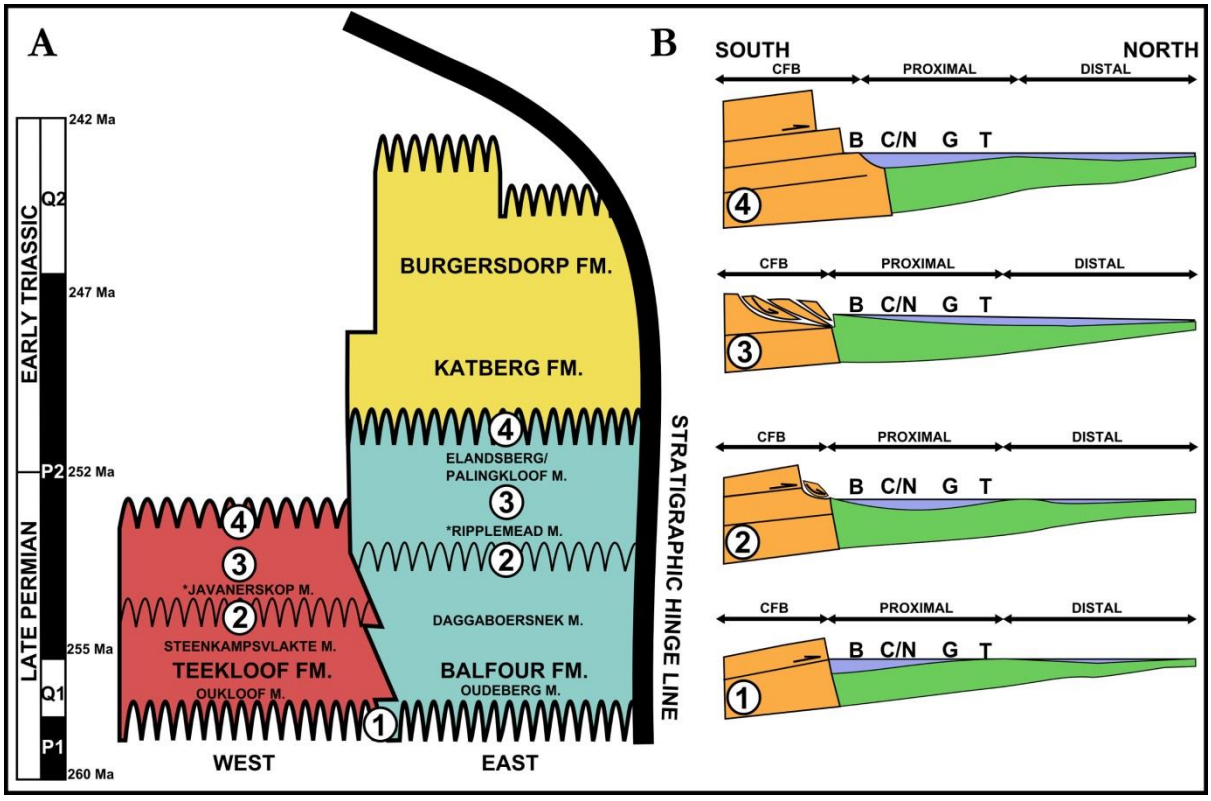

Figure 5.9: A) Sequence stratigraphic framework for the Lopingian-Lower Triassic Karoo Basin in relationship to new paroxysm dates by Hansma et al. (2015), and the stratigraphic hinge line (Catuneanu et al. 1998). Thick wavy lines depict the second-order sequence boundaries (SU) identified by Catuneanu et al. (1998) at the base and top of the Balfour Formation, and top of the Burgersdorp Formation. Theorized second-order SU are placed at the base of the Oukloof Member and top of the Teekloof Formation. Thinner wavy lines at the base of the Javanerskop and Ripplemead members were identified in this study and indicate a third-order SU. B) Schematic models for the evolution of the Karoo Basin during *Daptocephalus* Assemblage Zone times in the Lopingian to Lower Triassic. Letters represent field sites Beaufort West (B), Cradock (C), Nieu Bethesda (N), Gariep Dam (G), and Thaba Nchu/Bloemfontein (T). Numbered 1-4, the basin schematics depict changes in orogenic loading and unloading and the effect this had creation of accommodation in the retroarc foreland system. Stage 1 shows the onset of sedimentation of the Balfour and upper Teekloof Formations (beginning with the arenaceous Oudeberg and Oukloof members). In the distal foredeep Ecca Group deposits were replaced by limited accommodation, resulting in nondeposition. Once sediment supply became less than available accommodation, a fining upward sequence r esulted (Steenkampsvlakte and Daggaboersnek members). Stage 2 is another loading event which indicates deposition of the Javanerskop member and RM which occurred out of phase. This explains why the Javanerskop member is older. Stage 3 is an unloading stage which caused sedimentation and progradation of the lithostratigraphic units northwards, which is why the stratigraphy in the distal foredeep is underrepresented. Stage 4 marks the beginning of deposition of the early Triassic Katberg Formation in a new orogenic loading phase.

Chapter 6: Conclusions

This multi-disciplinary investigation draws upon results from five disciplines (lithostratigraphy, biostratigraphy and palaeontology, palaeoenvironmental interpretation, provenance, and basin development) and the conclusions are considered under these topics below:

Lithostratigraphy

This study provides a new lithostratigraphic framework for the Upper Permian Beaufort Group of South Africa's Karoo Basin. Work conducted demonstrates that the Oudeberg Member is present at the Barberskrans Cliffs south of Cradock. Since Tordiffe's (1978) Barberskrans Member could not be located at this site, it is renamed the Ripplemead member (RM) after Ripplemead farm 20 km north of Nieu Bethesda. The Oudeberg Member is not identified north of the Orange River and a compressed stratigraphic record is present in the north of the basin. The Boomplaas sandstone (BS) could not be correlated to any lithostratigraphic unit however it could correspond to Oudeberg Member aged strata. The Javanerskop member first described by Le Roux (1985) on Oukloof Pass near Beaufort West was never officially adopted into the lithostratigraphic framework of SACS (1980). Work in this study area documents an arenaceous interval in the highest most points of the escarpment in the western basin and it is recommended that the Javanerskop member should be given formal member status. The Musgrave Grit unit (Rutherford et al. 2015) is also documented near Bloemfontein and Thaba Nchu but of these sandstone horizons in the Balfour and Teekloof formations correlate temporally.

Palaeontology and biostratigraphy

This study also updates the stratigraphic ranges of Lopingian tetrapod fauna from the Karoo Basin. The current manifestation of the *Dicynodon* Assemblage Zone (DiAZ) is problematic because the three index fossils currently used to define the DiAZ, *Dicynodon lacerticeps*, *Theriognathus microps*, and *Procynosuchus delaharpeae*, first appear below the traditionally recognized lower boundary. Therefore the assemblage zone is redefined by replacing the DiAZ with the *Daptocephalus* Assemblage Zone (DaAZ) where *Daptocephalus leoniceps* is reinstated as the index taxon for the DaAZ in co-occurrence with *T. microps*. The first appearance datum of *Da. leoniceps* and *T. microps* is used to define the base of the DaAZ which incorporates strata previously defined as the uppermost *Cistecephalus* Assemblage Zone. It is further recommended that an informal two-fold lower and upper DaAZ subdivision be instated to reflect the appearance of *Lystrosaurus maccaigi*.

Dicynodon sensu lato has been used in the past to correlate various Karoo-aged basins within the Platbergian land vertebrate faunachron (LVF) yet it is now apparent it is unable to define a time unit finer than the Lopingian. This means *Dicynodon* sensu lato and the other South African dicynodontoids have little biostratigraphic utility outside of the Karoo Basin because at this time they are not known to be present in other basins, are known from very few specimens (*Euptychognathus bathyrhynchus*), and vary significantly in their temporal ranges. *Daptocephalus leoniceps* in co-occurrence with *L. maccaigi* may provide correlation with Upper Permian deposits in China (Guodikeng Formation) and the Sokolki fauna of Russia, however, further investigation is required. *Lystrosaurus maccaigi* on its own is not a useful correlation tool due to its survival into the early Triassic in Antarctica.

The stratigraphic succession in the southern field sites (Cradock/Nieu Bethesda) is much thicker than in the northern field sites (Gariep Dam/Bloemfontein). In addition the coeval appearance of *L. maccaigi* with the disappearance of *Di. lacerticeps*, *P. delarharpeae*, and *T. microps* fits the stratigraphic placement of Smith and Botha-Brink's (2014) phased extinctions in the northern field sites but not in the southern field sites. This suggests the extinction event is not fully represented by Upper Permian lithostratigraphy in the distal foredeep due to more frequent and longer periods of nondeposition, resulting in missing strata. Therefore the effects of the PTME very likely began at the base of the Upper DaAZ in association with the appearance of *L. maccaigi* in the Karoo Basin.

Palaeoenvironmental Interpretation

Palaeoenvironmental changes throughout the DaAZ can be explained by a combination of allogenic and autogenic controls. DaAZ strata comprises two fining-upward cycles that begin with arenaceous units deposited by low-sinuosity fluvial systems which were deposited when renewed accommodation was created under rapid base level fall. Decrease in river gradients through time resulted in the deposition of argillaceous material under lower energy, higher sinuosity fluvial systems. These cycles are observed in the Lower DaAZ (Oudeberg-Daggaboersnek members and Oukloof-Steenkampsvlakte members) and Upper DaAZ (Ripplemead -Elandsberg members) and are typical of continental fluvial systems (Shanley and McCabe, 1994, 1995; Catuneanu et al. 1997; 2011; Heller et al. 1998). In addition sedimentation shows similarities to the Distributive Fluvial Systems (DSF) of Weissmann et al. (2010, 2015). Importantly differnces between the Lower and Upper DaAZ were identified. Firstly facies association 4 (lacustrine/subaqueous system) is encountered more frequently in the Lower DaAZ as indicated by the presence of lacustrine conditions in the southeast (Cradock) and

palustrine conditions in the southwest (Nieu Bethesda). This demonstrates that wetter floodplains with higher water tables were present in the Lower DaAZ, whereas seasonally drier floodplains were present in the Upper DaAZ. Secondly, coinciding with the palaeoenvironmental changes is the first appearance datum of *L. maccaigi* and the last appearance datums of *Di. lacerticeps*, *T. microps*, and *P. delaharpeae*. Combined with evidence that the end-Permian extinction event may not be fully represented in the distal foredeep due to attenuated strata in this part of the basin, the transition between the Lower and Upper DaAZ is believed to preserve early palaeoclimatic changes associated with the PTME. *Lystrosaurus* is a genus of dicynodont well adapted to the drier floodplain conditions of the Karoo Basin and *L. maccaigi* is now known to survive the extinction event in Antarctica (Collinson et al. 2006).

Provenance

The detrital zircon age populations of twelve samples collected from the Balfour Formation (Oudeberg and Ripplemead members, Boomplaas sandstone and the Musgrave Grit unit), Teekloof Formation (Javanerskop member) and Katberg Formation yielded major late Carboniferous to Late Permian, secondary Neoproterzoic and Mesoproterzoic, and minor contributions from Devonian, Silurian, Ordovician, Cambrian, Palaeoproterzoic, and Archean age components. All samples were similar except the Oudeberg (PV/Cr1) and Boomplaas sandstone (PV-J615) which may mean they have some coeval stratigraphic relationship. The appearance of a dominant young detrital zircon population (250 ± 5 Ma – 339 ± 5 Ma) consisting of well preserved and euhedral grains in the RM, Javanerskop member, Musgrave Grit unit, and Katberg Formation may indicate renewed tectonism in the Gondwanides during this time and were distributed by airfall deposition. Work by Cawood et al. (2012) suggests that this large young population fits with population distributions of other samples collected from foreland basins globally and perhaps the current ideas on the distance of the main Karoo Basin from the plate margin (eg. >1500 km) requires reconsideration.

Palaeocurrent data indicate a dominant southerly source, and a recycled orogen petrography suggest that the Cape Supergroup rocks were the dominant source of older detrital zircon populations rather than primary source rocks. Similarities in composition to detrital zircon populations in the Cape Supergroup rocks sampled in previous studies supports a strongly recycled signature for the detrital zircons within the Beaufort Group (Andersen et al. 2015). These recycled grains are problematic because they are likely obscuring other potential primary source rocks of the Beaufort Group, such as primary Archean basement source rocks. Therefore

detrital zircon analyses of clastic sedimentary rocks of the Karoo Supergroup should be conducted with caution.

Basin development

Data collected for this study supports the retroarc-foreland basin model for the Lopingian Karoo Basin. Previous studies that challenge this model only really dispute the timing of flexural tectonics, which show evidence of being in place from the deposition of the Dwyka Group up until the end of Stormberg Group deposition. The retroarc foreland basin model explains the out-of-phase deposition observed in this study. Second-order sequence boundaries (subaerial unconformities, SU) have been identified at the base and top of the Balfour Formation (Catuneanu et al. 1998) and study extends the first second-order SU west to the base of the Oukloof Member (Teekloof Formation). A single diachronous third-order SU is identified at the base of the RM, Javanerskop member, and Triassic strata in the distal foredeep during this study, and is further evidence for flexural tectonics acting on the Karoo Basin during this time.

Flexural tectonics imposed phases of orogenic loading and unloading during the DaAZ. This was the major control on the distribution of accommodation in the foredeep of the Karoo Basin as demonstrated by northward thining wedge-shaped deposition of strata and cyclic sedimentation bounded by SUs (Shanely and McCabe, 1994, 1995; Weissmann et al. 2010, 2015; Catuneanu et al. 2011). Two loading and two unloading events are observed as two major fining-upward cycles (Oudeberg-Daggaboersnek members and Ripplemead-Elandsberg members) in the Balfour Formation and one in the Teekloof Formation (Oukloof-Steenkampsvlakte members). The Javanerskop member is probably the base of the second fining-upward cycle in the western basin but no strata are preserved above this unit to properly demonstrate this. A single third-order subaerial unconformity (SU) is identified at the base of the RM and Javanerskop member and tentatively at the base of earliest Triassic strata in the distal foredeep.

Reciprocal flexural tectonics meant that progradation of sediment northwards (distal foredeep) during orogenic loading and unloading was not in phase with the south (proximal foredeep) which resulted in an incomplete and attenuated stratigraphic record to the north. This shows lithostratigraphic units in the Beaufort Group cannot be used as regional marker horizons and this study recommends their use as local marker horizons only in conjunction with other proxies, such as fossils and radiometric dating. These conclusions highlight many future avenues for research on the rocks of the Lopingian Permian Beaufort Group of South Africa. The results of this work have been based on available data at the time and thus it is hoped they can serve to improve the accuracy of future investigations.

Chapter 7: References

Abdala, A., Marsicano, C. A., Smith, R. M. H., Swart, R., 2013. Strengthening Western Gondwanan correlations: A Brazilian dicynodont (Synapsida, Anomodontia) in the Middle Triassic of Namibia. Gondwana Research, 23, 1151-1162.

Allen, J. R. L., 1963a. Henry Clifton Sorby and the sedimentary structures of sands and sandstones in relation to flow conditions. Geologie en Mijnbouw, 42, 223-228.

Allen, J. R. L., 1963b. The classification of cross-stratified units. With notes on their origin. Sedimentology, 2, 93-114.

Allen, J. R. L., 1970. A quantitative model of grain size and sedimentary structures in lateral deposits. Geology, 7, 129-146.

Allen, J. R. L., 1983. Studies in fluvatile sedimentation: Bars, bar-complexes and sandstone sheets (low-sinuosity braided streams) in the Brownstones (L. Devonian), Welsh Borders. Sedimentary Geology, 33, 237-293.

Andersen, T., 2005. Detrital zircons as tracers of sedimentary provenance: limiting conditions from statistics and numerical simulation. Chemical Geology, 216, 249-270.

Andersen, T., Elburg, M., Kristofferson, M., 2015. Phanerozoic sedimentary recycling in southern Africa - The Cape and Karoo basins as "sink" and "source" for detrital zircons. In Linol, B., Miller, W., De Wit, M. J. (Eds). Proceedings of the Proceedings of the Cape-Karoo Imbizo conference. Nelson Mandela Metropolitan University, Port Elizabeth. .

Anderson, A. M., 1975. Arthropod trackways and other trace fossils from the Early Permian Lower Karoo Beds of South Africa., PhD thesis, University of the Witwatersrand, 260 pp.

Anderson, J., 1977. The biostratigraphy of the Permian and Triassic, Part 3: a review of Gondwana Permian palynology Mem. Botan. Surv. S. Africa, 41, 80.

Anderson, J. M., Cruickshank, A. R. I., 1978. The biostratigraphy of the Permian and Triassic Part 5. A review of the classification and distribution of the Permo-Triassic tetrapods. Palaeontologia Africana, 21, 15-44.

Angielczyk, K. D., Kurkin, A. A., 2003a. Phylogenetic analysis of Russian Permian dicynodonts (Therapsida: Anomodontia): implications for Permian biostratigraphy and Pangaean biogeography. Zoological Journal of the Linnean Society, 139, 157-212.

Angielczyk, K. D., Kurkin, A. A., 2003b. Has the utility of *Dicynodon* for Late Permian terrestrial biostratigraphy been overstated? Geology, 31, 363-366.

Angielczyk, K. D., Huertas, S., Smith, R. M. H., Tabor, N. J., Sidor, C. A., Steyer, J.-S., Tsuji, L. A., Gostling, N. J., 2014a. New dicynodonts (Therapsida, Anomodontia) and updated tetrapod stratigraphy of the Permian Ruhuhu Formation (Songea Group, Ruhuhu Basin) of southern Tanzania. Journal of Vertebrate Paleontology, 34, 1408-1426.

Angielczyk, K. D., Steyer, S., Sidor, C. A., Smith, R. M. H., Whatley, R. L., Tolan, S., 2014b. Permian and Triassic Dicynodont (Therapsida: Anomodontia) Faunas of the Luangwa Basin, Zambia: Taxonomic Update and Implications for Dicynodont Biogeography and Biostratigraphy. In Kammerer, C. F., Angielczyk, K. D., Fröbisch, J. (Eds): Early Evolutionary History of the Synapsida, 93-138 Springer Netherlands.

Ashworth, P. J., Lewin, J., 2012. How do big rivers come to be different? Earth-Science Reviews, 114, 84-107.

Bailie, R., Gutzmer, J., Rajesh, H. M., Armstrong, R., 2011. Age of ferroan A-type post-tectonic granitoids of the southern part of the Keimoes Suite, Northern Cape Province, South Africa. Journal of African Earth Sciences, 60, 153-174.

Bain, A. G., 1845. On the discovery of fossil remains of bidental, and other reptiles in South Africa. Transactions of the Geological Society of London, 11, 53-55.

Bain, A. G., 1856. On the geology of Southern Africa. Transactions of the Geological Society of London, 7, 175-192.

Bamford, M. K., 1999. Permo-Triassic fossil woods from the south African Karoo Basin. Palaeontologia Africana, 35, 25-40.

Bamford, M. K., 2000. Fossil woods of Karoo age deposits in South Africa and Namibia as an aid to biostratigraphical correlation. Journal of African Earth Sciences, 31, 119-132.

Bamford, M. K., 2004. Diversity of the woody vegetation of Gondwanan southern Africa. Gondwana Research, 7, 153-164.

Barbolini, N., 2014. Palynology of the South African Karoo Supergroup and correlations with coeval Gondwanan successions., PhD thesis, University of the Witwatersrand, 400 pp.

Bellanca, A., Calvo, J. P., Censi, P., Neri, R., Pozo, M., 1992. Recognition of lake-level changes in Miocene lacustrine units, Madrid Basin, Spain. Evidence from facies analysis, isotope geochemistry and clay mineralogy. Sedimentary Geology, 76, 135-153.

Ben-Avraham, Z., Hartnady, C. J. H., Kitchin, K. A., 1997. Structure and tectonics of the Agulhas-Falkland fracture zone. Tectonophysics, 282, 83-98.

Bender, P. A., 2000. Late Permian Actinopterygian (*Palaeoniscid*) fishes from the Lower Beaufort Group, South Africa., PhD thesis, University of the Witwatersrand, 300 pp.

Bender, P. A., 2001. A New Actinopterygian Fish Species From the Late Permian Beaufort Goup, South Africa. Palaeontologia Africana, 37, 25-40.

Bender, P. A., 2002. A new late Permian ray-finned (actinopterygian) fish from the Beaufort Group, South Africa.

Bender, P. A., Hancox, P. J., 2003. Fossil fishes of the *Lystrosaurus* and *Cynognathus* assemblage zones, Beaufort Group, South Africa: correlative implications. Bulletin of the council for geoscience, 136, 1-27.

Benton, M. J., Twitchett, R. J., 2003. How to kill (almost) all life: the end-Permian extinction event. Trends in Ecology and Evolution., 18, 358-365.

Benton, M. J., Tverdokhlebov, V. P., Surkov, M., 2004. Ecosystem remodelling among vertebrates at the Permian–Triassic boundary in Russia. Nature, 432, 97-100.

Benton, M. J., Newell, A. J., 2014. Impacts of global warming on Permo-Triassic terrestrial ecosystems. Gondwana Research, 25, 1308–1337.

Blanco, G., Germs, G. J. B., Rajesh, H. M., Chemale, F., Dussin, I. A., Justino, D., 2011. Provenance and paleogeography of the Nama Group (Ediacaran to early Palaeozoic, Namibia): petrography, geochemistry and U–Pb detrital zircon geochronology. Precambrian Research, 187, 15-32.

Boggs Jr, S., 2006. Principles of Sedimentology and Stratigraphy., Upper Saddle River, New Jersey, 784 pp.

Bordy, E. M., Catuneanu, O., 2002a. Sedimentology of the lower Karoo Supergroup fluvial strata in the Tuli Basin, South Africa. Journal of African Earth Sciences, 35, 503-521.

Bordy, E. M., Catuneanu, O., 2002b. Sedimentology and palaeontology of upper Karoo aeolian strata (Early Jurassic) in the Tuli Basin, South Africa. Journal of African Earth Sciences, 35, 301-314.

Bordy, E. M., Hancox, P. J., Rubidge, B. S., 2004. Basin development during the deposition of the Elliot Formation (Late Triassic-Early Jurassic), Karoo Supergroup, South Africa. South African Journal of Geology, 107, 397-412.

Bordy, E. M., Prevec, R., 2008. Sedimentology, palaeontology and palaeo-environments of the Middle (?) to Upper Permian Emakwezini Formation (Karoo Supergroup, South Africa). South African Journal of Geology, 111, 429-456.

Botha-Brink, J., Abdala, F., 2008. A new cynodont record from the *Tropidostoma* Assemblage Zone of the Beaufort Group: implications for the early evolution of cynodonts in South Africa. Palaeontologia Africana, 43, 1-6.

Botha-Brink, J., Modesto, S. P., 2009. Anatomy and relationships of the Middle Permian varanopid Heleosaurus scholtzi based on a social aggregation from the Karoo Basin of South Africa. Journal of Vertebrate Paleontology, 29, 389-400.

Botha-Brink, J., Huttenlocker, A. K., Modesto, S. P., 2014. Vertebrate paleontology of Nooitgedacht 68: A *Lystrosaurus maccaigi*-rich Permo-Triassic Boundary locality in South Africa. In Kammerer, C. F., Angielczyk, K. D., Fröbisch, J. (Eds): Early Evolutionary History of the Synapsida., 289-304 Springer Netherlands.

Botha, B. J. V., Linström, W., 1977. Palaeogeological and palaeogeographical aspects of the upper part of the Karoo Sequence in North-Western Natal. Annals of the Geological Survey of South Africa, 12, 177-192.

Botha, B. J. V., Lindstrom, W., 1978. A note on the stratigraphy of the Beaufort Group in north-western Natal. Transactions of the Geological Society of South Africa., 81, 35-40.

Botha, J., Smith, R. M. H., 2006. Rapid vertebrate recuperation in the Karoo Basin of South Africa following the End-Permian extinction. Journal of African Earth Sciences, 45, 502–514.

Botha, J., Smith, R. M. H., 2007. *Lystrosaurus* species composition across the Permo–Triassic boundary in the Karoo Basin of South Africa. Lethaia, 40, 125–137.

Bottjer, D. J., 2012. Life in the Early Triassic Ocean. Science, 338, 336-337.

Bowden, L. L., 2013. A comparative detrital zircon ages from river sediments and rocks of the Karoo Supergroup (Late Carboniferous to Jurassic), Eastern Cape Province, South Africa: Implications for the tectono-sedimentary evolution of Gondwana's southern continental margin., MSc thesis, University of Johannesburg, 321 pp.

Bowring, S. A., Erwin, D. W., Jin, Y. G., Martin, M. W., Davidek, K., Wang, W., 1998. U/Pb Zircon Geochronology and Tempo of the End-Permian Mass Extinction. Science, 280, 1039–1045.

Bridge, J. S., Smith, N. D., Trent, F., Gabel, S. L., Bernstein, P., 1986. Sedimentology and morphology of a low-sinuosity river: Calamus River, Nebraska Sand Hills. Sedimentology, 33, 851-870.

Brink, A. S., 1986. Illustrated bibliographical catalogue of the Synapsida. Vol. 10, Republic of South Africa, Department of Mineral and Energy Affairs, Geological Survey.

Bristow, C. S., 1987. Brahmaputra River: channel migration and deposition.

Broom, R., 1906a. On the Permian and Triassic Faunas of South Africa. Geological Magazine, 5, 29-30.

Broom, R., 1906b. The classification of the Karroo beds of South Africa. Geological Magazine New Series Decade, 5, 36.

Broom, R., 1907a. On some new fossil reptiles from the Karroo Beds of Victoria West, South Africa. Transactions of the South African Philosophical Society, 18, 31-42.

Broom, R., 1907b. On the geological horizons of the vertebrate genera of the Karoo formation. Records of the Albany Museum, 2, 156-163.

Broom, R., 1909. An attempt to determine the horizons of the fossil vertebrates of the Karoo. Annals of the South African Museum, 7, 285-289.

Broom, R., 1932. The mammal-like reptiles of South Africa and the origin of mammals., HF & G. Witherby.

Burgess, P. M., Gurnis, M., Moresi, L., 1997. Formation of sequences in the cratonic interior of North America by interaction between mantle, eustatic, and stratigraphic processes. Geological Society of America Bulletin, 109, 1515-1535.

Burgess, S. D., Bowring, S., Shen, S., 2014. High-precision timeline for Earth's most severe extinction. Proceedings of the National Academy of Sciences, 111, 3316-3321.

Cadle, A. B., Cairncross, B., Christie, A. D. M., Roberts, D. L., 1993. The Karoo Basin of South Africa: type basin for the coal-bearing deposits of southern Africa. International journal of coal geology, 23, 117-157.

Cairncross, B., 1989. Paleodepositional environments and tectonosedimentary controls of the postglacial Permian coals, Karoo Basin, South Africa. International journal of coal geology, 12, 365-380.

Cairncross, B., Beukes, N. J., Coetzee, L. L., Rehfeld, U., 2005. The bivalve *Megadesmus* from the Permian Volksrust Shale Formation (Karoo Supergroup), northeastern Karoo Basin, South Africa: implications for late Permian Basin development. South African Journal of Geology, 108, 547-556.

Cao, C., Wang, W., Liu, L., Shen, S., Summons, R. E., 2008. Two episodes of 13 C-depletion in organic carbon in the latest Permian: Evidence from the terrestrial sequences in northern Xinjiang, China. Earth and Planetary Science Letters, 270, 251-257.

Carroll, R. L., 1987. *Heleosuchus*: an enigmatic diapsid reptile from the Late Permian or Early Triassic of southern Africa. Canadian Journal of Earth Sciences, 24, 664-667.

Catuneanu, O., Beaumont, C., Waschbusch, P. Interplay of static loads and subduction dynamics in foreland basins: Reciprocal stratigraphies and the "missing" peripheral bulge. Geology, 12, 1087–1090.

Catuneanu, O., Hancox, J. P., Rubidge, B. S., 1998. Reciprocal flexural behaviour and contrasting stratigraphies: A new basin development model for the Karoo retroarc foreland system, South Africa. Basin Research, 10, 417-439.

Catuneanu, O., Elango, H. N., 2001. Tectonic control on fluvial styles: the Balfour Formation of the Karoo Basin, South Africa. Sedimentary Geology, 140, 291-313.

Catuneanu, O., Hancox, J. P., Cairncross, B., Rubidge, B. S., 2002. Foredeep submarine fans and forebulge deltas: Orogenic off-loading in the underfilled Karoo Basin. Journal of African Earth Sciences, 35, 489–502.

Catuneanu, O., 2004a. Basement control on flexural profiles and the distribution of foreland facies: The Dwyka Group of the Karoo Basin, South Africa. Geology, 32, 517-520.

Catuneanu, O., 2004b. Retroarc foreland systems–evolution through time. Journal of African Earth Sciences, 38, 225-242.

Catuneanu, O., Wopfner, H., Eriksson, P. G., Cairncross, B., Rubidge, B. S., Smith, R. M. H., Hancox, J. P., 2005. The Karoo basins of south-central Africa. Journal of African Earth Sciences, 43, 211–253.

Catuneanu, O., 2006. Principles of sequence stratigraphy, First edition., Elsevier.

Catuneanu, O., Galloway, W. E., Kendall, C. G. C., Miall, A. D., Posamentier, H. W., Strasser, A., Tucker, M. E., 2011. Sequence stratigraphy: Methodology and nomenclature. Newsletters on Stratigraphy, 43/3, 173–245.

Cawood, P. A., Hawkesworth, C. J., Dhuime, B., 2012. Detrital zircon record and tectonic setting. Geology, 40, 875-878.

Cisneros, J. C., Rubidge, B. S., Manson, R., Dube, C., 2008. Analysis of millerettid parareptile relationships in the light of new material of *Broomia perplexa* Watson, 1914, from the Permian of South Africa. Journal of Systematic Palaeontology, 6, 453-462.

Cloetingh, S., Lankreijer, A., De Wit, M. J., Martinez, I., 1992. Subsidence history analysis and forward modelling of the Cape and Karoo Supergroups. In De Wit, M. J., Ransome, I G D (Ed): Inversion tectonics of the Cape Fold Belt, Karoo and cretaceous basins of Southern Africa., 239-248.

Cluver, M. A., Hotton, N., 1981. The genera *Dicynodon* and *Diictodon* and their bearing on the classification of the Dicynodontia (Reptilia, Therapsida). Annals of the South African Museum, 83, 99-146.

Cluver, M. A., King, G. M., 1983. A reassessment of the relationships of Permian Dicynodontia (Reptilia, Therapsida) and a new classification fo dicynodonts. Annals of the South African Museum, 91, 195-273.

Cole, D., I., Neveling, J., Hattingh, J., Chevallier, L. P., Reddering, J. S. V., Bender, P. A., 2004. The Geology of the Middelburg Area. Explanation sheet 3124 (scale: 1:250 000). Council for Geoscience.

Cole, D. I., 1992. Evolution and development of the Karoo Basin Inversion tectonics of the Cape Fold Belt, Karoo and cretaceous basins of Southern Africa., 87-99.

Cole, D. I., Wipplinger, P. E., 2001. Sedimentology and molybdenum potential of the Beaufort Group in the main Karoo basin, South Africa. Memoir- geological survey (Pretoria).

Coleman, J. M., 1969. Brahmaputra River: channel processes and sedimentation. Sedimentary Geology, 3, 129-239.

Collinson, J. B., Thompson, D. B., 1989. Sedimentary structures. 2 ed., Unwin Hyman Ltd, Oxford Printing House, 207 pp.

Collinson, J. W., Hammer, W. R., Askin, R. A., Elliot, D. H., 2006. Permian-Triassic boundary in the central Transantarctic Mountains, Antarctica. Geological Society of America Bulletin, 118, 747-763.

Colombera, L., Mountney, N. P., McCaffrey, W. D., 2013. A quantitative approach to fluvial facies models: Methods and example results. Sedimentology, 60, 1526-1558.

Cooper, M. R., Kensley, B., 1984. Endemic South American Permian bivalve molluscs from the Ecca of South Africa. Journal of Paleontology, 1360-1363.

Corfu, F., Hanchar, J. M., Hoskin, P. W. O., Kinny, P., 2003. Atlas of zircon textures. Reviews in Mineralogy and Geochemistry, 53, 469-500.

Cornell, D. H., Thomas, R. J., Moen, H. F. G., Reid, D. L., Moore, J. M., Gibson, R. L., 2006. The Namaqua-Natal Province. In Johnson, M. R., Anhaeusser, C. R., Thomas, R. J. (Eds): The geology of South Africa, 325-379 Geological Society of South Africa.

Cosgriff, J. W., Hammer, W. R., Ryan, W. J., 1982. The Pangaean reptile, *Lystrosaurus maccaigi*, in the lower Triassic of Antarctica. Journal of Paleontology, 56, 371-385.

Croft, D. A., 2013. What constitutes a fossil mammal community in the early Miocene Santa Cruz Formation? Journal of Vertebrate Paleontology, 33, 401-409.

Csaky, A. V., Wachsmuth, W., 1971. Stratigraphy and Hydrocarbon Potential of the Dwyka, Ecca and the Beaufort Groups in the Northern Karroo. Geological Survey of South Africa, 126 pp.

Damiani, R. J., Rubidge, B. S., 2003. Temnospondyls from the Beaufort Group (Karoo Basin) of South Africa and their Biostratigraphy. Gondwana Research, 7, 165-173.

Day, M. O., 2013a. Charting the fossils of the Great Karoo: A history of tetrapod biostratigraphy in the Lower Beaufort Group, South Africa. Palaeontologia Africana, 48, 41–47.

Day, M. O., 2013b. Middle Permian continental biodiversity changes as reflected in the Beaufort Group of South Africa: A bio- and lithostratigraphic review of the *Eodicynodon*, *Tapinocephalus*, and *Pristerognathus* assemblage zones. , PhD thesis, University of the Witwatersrand, 394 pp.

Day, M. O., Ramezani, J., Bowring, S. A., Sadler, P. M., Erwin, D. H., Abdala, F., Rubidge, B. S., 2015. When and how did the terrestrial mid-Permian mass extinction occur? Evidence from the tetrepod record of the Karoo Basin, South Africa. Proceedings of the Royal Society, 282, 1-8.

DeCelles, P. G., Giles, K. A., 1996. Foreland basin systems. Basin Research, 8, 105–123.

De Wit, M. J., Jeffery, M., Bergh, H., Nicholaysen, L., 1988: Explanation to Geological Map of Sectors of Gondwana. . In: American Association of Petroleum Geologists Publications, Tulsa, Oklahoma.

Deng, X.-D., Li, J.-W., Zhao, X.-F., Hu, Z.-C., Hu, H., Selby, D., de Souza, Z. S., 2013. U–Pb isotope and trace element analysis of columbite-(Mn) and zircon by laser ablation ICP–MS: Implications for geochronology of pegmatite and associated ore deposits. Chemical Geology, 344, 1-11.

Dickinson, W. R., 1985. Interpreting provenance relations from detrital modes of sandstones. In Zuffa, G. G. (Ed): Provenance of arenites., 333-361 Springer.

Dodson, M. H., Compston, W., Williams, I. S., Wilson, J. F., 1988. A search for ancient detrital zircons in Zimbabwean sediments. Journal of the Geological Society, 145, 977-983.

Duncan, R. A., Hooper, P. R., Rehacek, J., Marsh, J. S., 1997. The timing and duration of the Karoo igneous event, southern Gondwana. Journal of Geophysical Research, 138, 127-138.

Dunn, E. J., 1887. Geological sketch map of South Africa; I inch=33 miles. Melbourne: Sands and McDougal.

Eglington, B. M., 2006. Evolution of the Namaqua-Natal Belt, southern Africa–A geochronological and isotope geochemical review. Journal of African Earth Sciences, 46, 93-111.

Erwin, D. H., 1990. The end-Permian mass extinction. Annual Review of Ecology and Systematics, 69-91.

Erwin, D. H., 1993. The great Paleozoic crisis: life and death in the Permian., Columbia University Press, New York.

Erwin, D. H., 2006. Extinction: How life on Earth nearly ended 250 million years ago., Princeton University Press, New Jersey.

Federico, L., Capponi, G., Crispini, L., 2006. The Ross orogeny of the transantarctic mountains: a northern Victoria Land perspective. International Journal of Earth Sciences, 95, 759-770.

Fedo, C. M., Sircombe, K. N., Rainbird, R. H., 2003. Detrital zircon analysis of the sedimentary record. Reviews in Mineralogy and Geochemistry, 53, 277-303.

Fielding, C. R., Ashworth, P. J., Best, J. L., Prokocki, E. W., Smith, G. H. S., 2012. Tributary, distributary and other fluvial patterns: What really represents the norm in the continental rock record? Sedimentary Geology, 261, 15-32.

Fildani, A., Drinkwater, N. J., Weislogel, A., McHargue, T., Hodgson, D. M., Flint, S. S., 2007. Age controls on the Tanqua and Laingsburg deep-water systems: new insights on the evolution and sedimentary fill of the Karoo basin, South Africa. Journal of Sedimentary Research, 77, 901-908.

Fildani, A., Weislogel, A., Drinkwater, N. J., McHargue, T., Tankard, A., Wooden, J., Hodgson, D., Flint, S., 2009. U-Pb zircon ages from the southwestern Karoo Basin, South Africa—Implications for the Permian-Triassic boundary. Geology, 37, 719-722.

Fourie, P. H., Zimmermann, U., Beukes, N. J., Naidoo, T., Kobayashi, K., Kosler, J., Nakamura, E., Tait, J., Theron, J. N., 2011. Provenance and reconnaissance study of detrital zircons of the Palaeozoic Cape Supergroup in South Africa: revealing the interaction of the Kalahari and Río de la Plata cratons. International Journal of Earth Sciences, 100, 527-541.

Friend, P., 1977. Distinctive features of some ancient river systems Fluvial Sedimentology, 5, 531-542.

Friend, P. F., 2009. Towards the field classification of alluvial architecture or sequence. In Collinson, J. D., Lewin, John (Ed): Modern and Ancient Fluvial Systems (Special Publication 6 of the IAS), 345.

Frimmel, H. E., Fölling, P. G., Eriksson, P. G., 2002. Neoproterozoic tectonic and climatic evolution recorded in the Gariep Belt, Namibia and South Africa. Basin Research, 14, 55-67.

Frimmel, H. E., Fölling, P. G., 2004. Late Vendian closure of the Adamastor Ocean: timing of tectonic inversion and syn-orogenic sedimentation in the Gariep Basin. Gondwana Research, 7, 685-699.

Fröbisch, J., 2013. Vertebrate diversity across the end-Permian mass extinction — Separating biological and geological signals. Palaeogeography, Palaeoclimatology, Palaeoecology, 372, 50-61.

Galehouse, J. S., 1971. Point counting. In Carver, R. E. (Ed): Procedures in sedimentary petrology, 385-407 Wiley-Interscience, New York, U.S.A.

Gastaldo, R. A., Adendorff, R., Bamford, M., Labandeira, C. C., Neveling, J., Sims, H., 2005. Taphonomic trends of macrofloral assemblages across the Permian–Triassic boundary, Karoo Basin, South Africa. Palaios, 20, 479-497.

Gastaldo, R. A., Kamo, S. L., Neveling, J., Geissman, J. W., Bamford, M., Looy, C. V., 2015. Is the vertebrate-defined Permian-Triassic boundary in the Karoo Basin, South Africa, the terrestrial expression of the end-Permian marine event? Geology, 43, 1-5.

Gebauer, E. V. I., 2007. Phylogeny and evolution of the Gorgonopsia with a special reference to the skull and skeleton of GPIT/RE/7113 (*Aelurognathus parringtoni*). PhD thesis, Geowissenschaftlichen Fakultät, Universität Tübingen, 328 pp.

Gehrels, G., 2014. Detrital zircon U-Pb geochronology applied to tectonics. Annual Review of Earth and Planetary Sciences, 42, 127-149.

Goldring, R., Aigner, T., 1982. Scour and fill: the significance of event separation. In Einsele, G., Seilacher, A. (Eds): Cyclic and event stratification, 354-362 Springer.

Gow, C. E., Rubidge, B. S., 1997. The oldest known procolophonid (Amniota: Parareptilis) - new Discovery from the Lower Beaufort Group of South Africa. Palaeontologia Africana, 34, 49-53.

Graf, W. L., Lecce, S. A., 1988. Fluvial processes in dryland rivers. Vol. 3, Springer Berlin.

Gresse, P. G., Von Veh, M. W., Frimmel, H. E., 2006. Namibian (Neoproterozoic) to early Cambrian successions. In Johnson, M. R., Anhaeusser, C. R., Thomas, R. J. (Eds): The geology of South Africa, 395-420.

Groenewald, G. H., 1984. Stratigrafie en sedimentologie van die Groep Beaufort in die Noordoos Vrystaat., MSc thesis, Rand Afrikaans University, 250 pp.

Groenewald, G. H., 1989. Stratigrafie en sedimentologie van die Groep Beaufort in die Noordoos-Vrystaat. Bulletin of the Geological Survey of South Africa, 96, 1-49.

Groenewald, G. H., 1990. Use of palaeontology in the correlation of lithostratigraphic units in the Beaufort Group, Karoo Sequence of South Africa. Palaeontologia Africana, 27, 21-30.

Groenewald, G. H., 1996. Stratigraphy and sedimentology of the Tarkastad Subgroup, Karoo Supergroup, South Africa, PhD thesis, University of Port Elizabeth, 341 pp.

Guinot, G., 2013. Late Cretaceous elasmobranch palaeoecology in NW Europe. Palaeogeography, Palaeoclimatology, Palaeoecology, 388, 23-41.

Gurnis, M., 1992. Rapid continental subsidence following the initiation and evolution of subduction. Science, 255, 1556-1558.

Hälbich, I. W., Fitch, F. J., Miller, J. A., 1983. Dating the Cape orogeny. In Söhnge, A. P. G., Hälbich, I W (Ed): Geodynamics of the Cape Fold Belt, 149-164.

Hammer, Ø., Harper, D. A. T., Ryan, P. D., 2001. Palaeonotlogical Satatistics software package for education and data analysis. Palaeontologia Electronica, 4, 1-9.

Hancox, P. J., Rubidge, B. S., 1997. The role of fossils in interpreting the development of the Karoo Basin. Palaeontologia Africana, 33, 41-54.

Hancox, P. J., 1998. A Stratigraphic, sedimentological and palaeoenvironmental synthesis of the Beaufort–Molteno contact, in the Karoo Basin., PhD thesis, University of the Witwatersrand, 381 pp.

Hancox, P. J., Brandt, D., Reimold, W. U., Koeberl, C., Neveling, J., 2002. Permian-Triassic boundary in the northwest Karoo basin: Current stratigraphic placement, implications for basin development models, and the search for evidence of impact. Special papers -Geological Society of America, 429-444.

Hansma, J., Tohver, E., Schrank, C., Jourdan, F., Adams, D., 2015. The timing of the Cape Orogeny: New 40 Ar/39 Ar age constraints on deformation and cooling of the Cape Fold Belt, South Africa. Gondwana Research.

Hanson, E. K., Moore, J. M., Bordy, E. M., Marsh, J. S., Howarth, G., Robey, J. V. A., 2009. Cretaceous erosion in central South Africa: Evidence from upper-crustal xenoliths in Kimberlite diatremes. South African Journal of Geology, 112, 125-140.

Haughton, S. H., Brink, A. S., 1954. A bibliographical list of Reptilia from the Karroo beds of Africa. Die Afrikaanse Pers.

Haughton, S. H., 1963. Note on the distribution of fossil reptiles of Karroo age. Palaeontologia Africana, 7, 1-11.

Haughton, S. H., 1969. Geological history of southern Africa. Geological Society of South Africa, 348-356.

Haycock, C. A., Mason, T. R., Watkeys, M. K., 1997. Early Triassic palaeoenvironments in the eastern Karoo foreland basin, South Africa. Journal of African Earth Sciences, 24, 79-94.

Headley, T. J., Ewing, R. C., Haaker, R. F., 1982. TEM study of the metamict state. Physics of Minerals and Ore Microscopy, Proceedings of the l3th general meeting ofthe International Mineralogical Association at Varna, Bulgaria, September 19-25, 281-289.

Heller, P. L., Angevine, C. L., Winslow, N. S., Paola, C., 1998. Two-phase stratigraphic model for foreland-basin sequences. Geology, 16, 501-504.

Heydari, E., Hassanzadeh, J., 2003. Deev Jahi model of the Permian–Triassic boundary mass extinction: a case for gas hydrates as the main cause of biological crisis on Earth. Sedimentary Geology, 163, 147-163.

Hiller, N., Stavrakis, N., 1984. Permo-Triassic fluvial systems in the southeastern Karoo basin, South Africa. Palaeogeography, Palaeoclimatology, Palaeoecology, 45, 1-21.

Holbrook, J., Scott, R. W., Oboh-Ikuenobe, F. E., 2006. Base-level buffers and buttresses: a model for upstream versus downstream control on fluvial geometry and architecture within sequences. Journal of Sedimentary Research, 76, 162-174.

Holland, H. D., Gottfried, D., 1955. The effect of nuclear radiation on the structure of zircon. Acta Crystallographica, 8, 291-300.

Holt, W. E., Stern, T. A., 1994. Subduction, platform subsidence, and foreland thrust loading: The late Tertiary development of Taranaki Basin, New Zealand. Tectonics, 13, 1068-1092.

Horn, J., D, Fielding, C. R., Joeckel, R. M., 2012. Revision of the Platte River alluvial facies model through the observations of extant channels and barforms, and subsurface alluvial valley fills. Journal of Sedimentary Research, 82, 72–91.

Hotton, N., Kitching, J. W., 1963: Speculations on upper Beaufort deposition. In.

Huttenlocker, A. K., Sidor, C. A., Smith, R. M. H., 2011. A New Specimen of *Promoschorhynchus* (Therapsids: Therocephalia: Akidnognathidae) from the Lower Triassic of South Africa and its implications for theriodont survivorship across the Permo-Triassic boundary. Journal of Vertebrate Paleontology, 31, 405–421.

Huttenlocker, A. K., 2014. Body size reductions in non-mammalian eutheriodont therapsids (Synapsida) during the end-Permian mass extinction. PloS one, 9, e87553.

Irmis, R. B., Whiteside, J. H., Kammerer, C. F., 2013. Non-biotic controls of observed diversity in the paleontologic record: An example from the Permo-Triassic Karoo Basin of South Africa. Palaeogeography, Palaeoclimatology, Palaeoecology, 372, 62-77.

Isbell, J. L., Cole, D. I., Catuneanu, O., 2008. Carboniferous-Permian glaciation in the main Karoo Basin, South Africa: Stratigraphy, depositional controls, and glacial dynamics Geological Society of America Special Papers, 441, 71-82.

ISSC. 1976. International Stratigraphic Guide (1st edition). New York, John Wiley and Sons.

ISSC. 1994. International Stratigraphic Guide (2nd edition). Boulder, Geological Society of America.

Jalil, N. E., Janvier, P., 2005. Les pareiasaures (Amniota, Parareptilia) du Permien supérieur du Bassin d'Argana, Maroc. Geodiversitas, 27, 35-132.

Jirah, S., 2013. Stratigraphy and sedimentology of the middle Permian Abrahamskraal formation (*Tapinocephalus* Assemblage Zone) in the southern Karoo around Merweville, South Africa., MSc thesis, University of the Witwatersrand, 143 pp.

Johnson, M. R., 1966. Stratigraphy and sedimentology of the Cape and Karoo sequences in the Eastern Cape Province., MSc thesis, Rhodes University, 336 pp.

Johnson, M. R., 1976. Stratigraphy and sedimentology of the Cape and Karoo sequences in the Eastern Cape Province., PhD thesis, Rhodes University, 351 pp.

Johnson, M. R., Keyser, A. W., 1976. Explanatory notes. 1: 250 000 Geological Series 3226 King Williams Town. Government Printer, Pretoria.

Johnson, M. R., 1991. Sandstone petrography, provenance and plate tectonic setting in Gondwana context of the southeastern Cape-Karoo Basin. South African Journal of Geology, 94, 137-154.

Johnson, M. R., van Vuuren, C. J., Hegenberger, W. F., Key, R., Show, U., 1996. Stratigraphy of the Karoo Supergroup in southern Africa: an overview. Journal of African Earth Sciences, 23, 3-15.

Johnson, M. R., Van Vuuren, C. J., Visser, J. N. J., Cole, D. I., Wickens, H. d. V., Christie, A. D. M., Roberts, D. L., 1997. The foreland Karoo Basin, South Africa. African basins. Sedimentary basins of the World, 3, 269-317.

Johnson, M. R., Van Vuuren, C. J., Visser, J. N. J., Cole, D. I., Wickens, H. d. V., Christie, A. D. M., Roberts, D. L., Brandl, G., 2006. Sedimentary rocks of the Karoo Supergroup., Geological Society of South Africa, Council for Geoscience.

Jordaan, M. J., 1990. Basin analysis of the Beaufort Group in the western part of the Karoo Basin., PhD thesis, University of the Orange Free State, 272 pp.

Kammerer, C. F., Angielczyk, K. D., Fröbisch, J., 2011. A comprehensive taxonomic revision of *Dicynodon* (Therapsida, Anomodontia) and its implications for dicynodont phylogeny, biogeography, and biostratigraphy. Society of Vertebrate Paleontology Memoir 11, 31, 1–158.

Kammerer, C. F., 2015. Cranial osteology of *Arctognathus curvimola*, a short-snouted gorgonopsian from the late Permian of South Africa. Papers in Palaeontology, 1, 41-58.

Keyser, A. W., 1973. A preliminary study of the type area of the *Cisticephalus* zone of the Beaufort series and a revision of the anomodont family Cisticephalidae. Memoirs of the Geological Survey of South Africa, 62, 1-71.

Keyser, A. W., 1979. A review of the biostratigraphy of the Beaufort Group in the Karoo Basin of South Africa Geocongress Abstracts II, Johannesburg. Geological Society of South Africa, 13-29.

Keyser, A. W., Smith, R. M. H., 1979a. Vertebrate biozonation of the Beaufort Group with special reference to the Western Karoo Basin. Annals of the Geological Survey of South Africa., 12, 1-36.

Keyser, A. W., Smith, R. M. H., 1979b. Vertebrate biozonation of the Beaufort Group with special reference to the western Karoo Basin. Annual Geological Survey of South Africa, 12, 1-36.

Khadkikar, A. S., Merh, S. S., Malik, J. N., Chamyal, L. S., 1998. Calcretes in semi-arid alluvial systems: formative pathways and sinks. Sedimentary Geology, 116, 251-260.

King, G. M., 1988. Anomodontia. . Vol. 17C, Handbuch der Paläoherpetologie

King, G. M., 1992. The palaeobiogeography of Permian anomodonts. Terra Nova, 4, 633-640.

Kitching, J. W., 1970. A short review of the Beaufort zoning in South Africa. In. Proceedings of the Second Gondwana Symposium Proceedings and Papers, 309-312.

Kitching, J. W., 1977. The distribution of the Karroo vertebrate fauna. Bernard Price Institute for Palaeontological Research Memoir 1., 1-131 pp.

Kitching, J. W., Raath, M. A., 1984. Fossils from the Elliot and Clarens Formations (Karoo Sequence) of the northeastern Cape, Orange Free State and Lesotho, and a suggested biozonation based on tetrapods. Palaeontologia Africana, 25.

Košler, J., Sylvester, P. J., 2003. Present trends and the future of zircon in geochronology: laser ablation ICPMS. Reviews in Mineralogy and Geochemistry, 53, 243-275.

Košler, J., 2007. Laser ablation ICP—MS—a new dating tool in Earth science. Proceedings of the Geologists' Association, 118, 19-24.

Košler, J., 2012. U-Pb Geochronology and Hf isotope geochemistry of detrital zircon in sedimentary systems. In Sylvester, P. (Ed): Quantitative Mineralogy and Microanalysis of Sediments and Sedimentary Rocks., 42, 185–202 Mineralogical Association of Canada.

Krebs, C. J., 1989. Ecological methodology. Harper and Row, New York, 624 pp.

Latimer, E. M., Hancox, P. J., Rubidge, B. S., Shishkin, M. A., Kitching, J. W., 2002. The temnospondyl amphibian *Uranocentrodon*, another victim of the end-Permian extinction event: research letter South African Journal of Science, 98, 191-193.

Le Roux, J. P., 1985. Palaeochannels and Uranium mineralisation in the main Karoo Basin of South Africa., PhD thesis, University of Port Elizabeth, 250 pp.

Le Roux, J. P., 1993. Genesis of stratiform U-Mo deposits in the Karoo Basin of South Africa. Ore Geology Reviews, 7, 485-509.

Le Roux, J. P., 1995. Heartbeat of a mountain: diagnosing the age of depositional events in the Karoo (Gondwana) Basin from the pulse of the Cape Orogen. Geologische Rundschau, 84, 626-635.

Lee, M. S. Y., 1997. A taxonomic revision of pareiasaurian reptiles: implications for Permian terrestrial Palaeoecology. Modern Geology, 21, 231-298.

Leopold, L. B., Wolman, M. G., 1957. River channel patterns: Braiding, meandering and straight. Geolgical Survey professional paper, United States Government printing office, Washington., 1-85.

Lindeque, A., Ryberg, T., Stankiewicz, J., Weber, M. and de Wit, M.J., 2007. Deep crustal reflection experiment across the southern Karoo Basin, South Africa. South African Journal of Geology, 110, 419-438.

Lindeque, A., De Wit, M. J., Ryberg, T., Weber, M., Chevallier, L., 2011. Deep crustal profile across the southern Karoo Basin and Beattie Magnetic Anomaly, South Africa: an integrated interpretation with tectonic implications. South African Journal of Geology, 114, 265-292.

Lindsey, E. L., Seymour, K. L., 2015. "Tar pits" of the western Neotropics: Paleoecology, taphonomy, and mammalian biogeography. In Harris, J. M. (Ed): La Brea and Beyond: The paleontology of asphalt-preserved Biotas. Natural History Museum of Los Angeles County. Science Series., 42, 111-123.

Lock, B. E., 1978. The Cape Fold belt of South Africa; tectonic control of sedimentation. Proceedings of the Geologists' Association, 89, 263-281.

Lock, B. E., 1980. Flat-plate subduction and the Cape Fold Belt of South Africa. Geology, 8, 35-39.

Long, D. G. F., 2006. Architecture of pre-vegetation sandy-braided perennial and ephemeral river deposits in the Paleoproterozoic Athabasca Group, Northern Saskatchewan, Canada as indicators of Precambrian fluvial style. Sedimentary Geology, 190, 71–95.

Loock, J. C., 1993. The stratigraphy of the Beaufort Group in the Moordenaarskaroo. Confidential report to the Atomic Corporation of South Africa Ltd., University of the Orange Free State, Bloemfontein, 1-48.

Lucas, S. G., 1997: *Dicynodon* and Late Permian Pangaea. In Wang, N., Remane, J (Ed): Proceedings of the 30 International Geological Congress. VSP, Utrecht.

Lucas, S. G., 1998a. Global Triassic tetrapod biostratigraphy and biochronology. Palaeogeography, Palaeoclimatology, Palaeoecology, 143, 347–384.

Lucas, S. G., 1998b. Toward a tetrapod biochronology of the Permian. New Mexico Museum of Natural History and Science Bulletin, 12, 71-92.

Lucas, S. G., 2001. Chinese fossil vertebrates., Columbia University Press, New York.

Lucas, S. G., 2002: Tetrapods and the subdivision of Permian time. In Hills, L. V., Hnderson, C. M., Bamber, E. W. (Eds): Memoir - Canadian Society of Petroleum Geologists., 19, 479-491.

Lucas, S. G., 2005: Permian tetrapod faunachrons. In Lucas, S. G., Zeigler, K E (Ed): New Mexico Museum of Natural History and Science Bulletin, 30, 197-201.

Lucas, S. G., 2006. Global Permian tetrapod biostratigraphy and biochronology. In Lucas, S., G., Cassinis, G., Schneider, J., W. (Eds): Non-Marine Permian Biostratigraphy and Biochronology., 265, 65-93 The Geological Society of London. London.

Marsicano, C. A., Latimer, E. M., Rubidge, B. S., Smith, R. M. H., 2015. The Rhinesuchidae and early history of the Stereospondyli (Amphibia, Temnospondyli) at the end of the Palaeozoic . Unpublished.

McCabe, P. J., 1977. Deep distributary channels and giant bedforms in the Upper Carboniferous of the Central Pennines, northern England. Sedimentology, 24, 271-290.

Mckay, M. P., Weislogel, A. L., Rawcliffe, H., Brunt, R., Hodgson, D. M., Flint, S., 2011. Evolution and petrogenesis of Gondwanan volcanism from ashes within the Ecca and Beaufort Groups: Karoo Basin, South Africa. In. Proceedings of the AGU Fall Meeting Abstracts, 2597.

McKay, M. P., Weislogel, A. L., Fildani, A., Brunt, R. L., Hodgson, D. M., Flint, S. S., 2015. U-PB zircon tuff geochronology from the Karoo Basin, South Africa: implications of zircon recycling on stratigraphic age controls. International Geology Review, 57, 393-410.

Metcalfe, I., Nicoll, R. S., Mundil, R., Foster, C., Glen, J., Lyons, J., Xiaofeng, W., Cheng-yuan, W., Renne, P. R., Black, L., 2001. The Permian-Triassic boundary & mass extinction in China. Episodes, 24, 239-244.

Miall, A. D., 1977. A review of the braided-river depositional environment. Earth-Science Reviews, 13, 1-62.

Miall, A. D., 1985. Architectural-element analysis: A new method of facies analysis applied to fluvial deposits. Earth-Science Reviews, 22, 261-308.

Miall, A. D., 1988. Architectural elements and bounding surfaces in fluvial deposits: anatomy of the Kayenta Formation (Lower Jurassic), southwest Colorado. Sedimentary Geology, 55, 233-262.

Miall, A. D., 1994. Reconstructing fluvial macroform architecture from two-dimensional outcrops: examples from the Castlegate Sandstone, Book Cliffs, Utah. Journal of Sedimentary Research, 64.

Miall, A. D., 1996. The geology of fluvial deposits., Springer, 582 pp.

Miall, A. D., Arush, M., 2001. Cryptic sequence boundaries in braided fluvial successions. Sedimentology, 48, 971-985.

Miall, A. D., Catuneanu, O., Vakarelov, B. K., Post, R., 2008. The Western interior basin. Sedimentary basins of the world, 5, 329-362.

Miall, A. D., 2014. The facies and architecture of fluvial systems. In: Fluvial depositional systems, 9-68.

Milani, E. J., De Wit, M. J., 2008. Correlations between the classic Paraná and Cape–Karoo sequences of South America and southern Africa and their basin infills flanking the Gondwanides: du Toit revisited. Geological Society, London, Special Publications, 294, 319-342.

Mitrovica, J. X., Beaumont, C., Jarvis, G. T., 1989. Tilting of continental interiors by the dynamical effects of subduction. Tectonics, 8, 1079-1094.

Mohrig, D., Heller, P. L., Paola, C., Lyons, W. J., 2000. Interpreting avulsion process from ancient alluvial sequences: Guadalope-Matarranya system (northern Spain) and Wasatch Formation (western Colorado). Geological Society of America Bulletin, 112, 1787-1803.

Mossop, G. D., Flach, P. D., 1983. Deep channel sedimentation in the Lower Cretaceous McMurray Formation, Athabasca Oil Sands, Alberta. Sedimentology, 30, 493-509.

Mountain, E. D., 1946. The Geology of an Area East of Grahamstown: An Explanation of Sheet No. 136 (Grahamstown). Geological Survey of South Africa, Pretoria, 56.

Myrow, P. M., 1992. Pot and gutter casts from the Chapel Island Formation, southeast Newfoundland. Journal of Sedimentary Research, 62, 992-1007.

Nanson, G. C., Knighton, A. D., 1996. Anabranching rivers: their cause, character and classification. Earth surface processes and landforms, 21, 217-239.

Nesbitt, H. W., Fedo, C. M., Young, G. M., 1997. Quartz and feldspar stability, steady and non-steady-state weathering, and petrogenesis of siliciclastic sands and muds. The Journal of geology, 105, 173-192.

Neveling, J., 2002. Biostratigraphic and sedimentological investigation of the contact between the *Lystrosaurus* and *Cynognathus* Assembalge Zones (Beaufort Group; Karoo Supergroup). 232 pp., PhD thesis, University of the Witwatersrand, 232 pp.

Newell, A. J., Sennikov, A. G., Benton, M. J., Molostovskaya, I. I., Golubev, V. K., Minikh, A. V., Minikh, M. G., 2010. Disruption of playa–lacustrine depositional systems at the Permo-Triassic boundary: evidence from Vyazniki and Gorokhovets on the Russian Platform. Journal of the Geological Society, 167, 695-716.

Nicolas, M., 2007. Tetrapod biodiversity through the Permo–triassic Beaufort group (Karoo Supergroup) of South Africa. , PhD thesis, University of the Witwatersrand, 488 pp.

Norton, L. A., 2012. Relative growth and morphological variation in the skull of *Aelurognathus* (Therapside: Gorgonopsia). MSc thesis, University of the Witwatersrand, 185 pp.

Olsen, H., 1988. The architecture of a sandy braided-meandering river system: an example from the lower triassic Soiling Formation (M. Buntsandstein) in W-Germany. Geologische Rundschau, 77, 797-814.

Oreska, M. P. J., Carrano, M. T., Dzikiewicz, K. M., 2013. Vertebrate paleontology of the Cloverly Formation (Lower Cretaceous), I: faunal composition, biogeographic relationships, and sampling. Journal of Vertebrate Paleontology, 33, 264-292.

Owen, R., 1845. III.—Report on the Reptilian Fossils of South Africa: PART I.—Description of certain Fossil Crania, discovered by AG Bain, Esq., in Sandstone Rocks at the South-eastern extremity of Africa, referable to different species of an Extinct genus of Reptilia (*Dicynodon*), and indicative of a new Tribe or Sub-order of Sauria. Transactions of the Geological Society of London, 59-84.

Paiva, F., 2015. Fluvial facies architecture and provenance history of the Abrahamskraal-Teekloof Formation transition (Lower Beaufort Group) in the main Karoo Basin. , MSc thesis, University of Cape Town, 98 pp.

Pankhurst, R. J., Rapela, C. W., Loske, W. P., Márquez, M., Fanning, C. M., 2003. Chronological study of the pre-Permian basement rocks of southern Patagonia. Journal of South American Earth Sciences, 16, 27-44.

Pankhurst, R. J., Rapela, C. W., Fanning, C. M., Márquez, M., 2006. Gondwanide continental collision and the origin of Patagonia. Earth-Science Reviews, 76, 235-257.

Parrish, J. T., 1993. Climate of the supercontinent Pangea. The Journal of geology, 215-233.

Pemberton, S. G., Spila, M., Pulham, A., Saunders, T., MacEachern, J. A., Robbins, D., Sinclair, I. K., 2003. Ichnology and sedimentology of shallow marine to marginal marine systems: Ben Nevis and Avalon reservoirs, Jeanne D'arc Basin. Bulletin of Canadian Petroleum Geology, 51, 206-211.

Pettijohn, F. J., Potter, P. E., Siever, R., 1987: Sand and Sandstone. 2nd edition. In, 553, Springer-Verlag, New York.

Platt, N. H., Wright, V. P., 2009. Lacustrine carbonates: facies models, facies distributions and hydrocarbon aspects. Lacustrine Facies Analysis, 57-74.

Prevec, R., Labandeira, C. C., Neveling, J., Gastaldo, R. A., Looy, C. V., Bamford, M., 2009. Portrait of a Gondwanan ecosystem: a new late Permian fossil locality from KwaZulu-Natal, South Africa. Review of Palaeobotany and Palynology, 156, 454-493.

Prevec, R., Gastaldo, R. A., Neveling, J., Reid, S. B., Looy, C. V., 2010. An autochthonous glossopterid flora with latest Permian palynomorphs and its depositional setting in the *Dicynodon* Assemblage Zone of

the southern Karoo Basin, South Africa. Palaeogeography, Palaeoclimatology, Palaeoecology, 292, 391-408.

Pysklywec, R. N., Mitrovica, J. X., 1999. The role of subduction-induced subsidence in the evolution of the Karoo basin. Journal of Geology, 107, 155-164.

Reading, H. G., 1978. Facies in sedimentary environments and facies., Blackwell, Oxford.

Reading, H. G., 1986. Sedimentary environments and facies. 2nd ed., Blackwell, Oxford.

Reading, H. G., 1996. Sedimentary environments: Processes, facies and stratigraphy., Oxford (Blackwell), 688 pp.

Reid, D. L., Erlank, A. J., Welke, H. J., Moyes, A., 1987. The Orange River Group: a major Proterozoic calcalkaline volcanic belt in the western Namaqua Province, southern Africa. Geological Society, London, Special Publications, 33, 327-346.

Reid, D. L., Smith, C. B., Watkeys, M. K., Welke, H. J., Betton, P. J., 1997. Whole-rock radiometric age patterns in the Aggeneys-Gamsberg ore district, central Bushmanland, South Africa. South African Journal of Geology, 100, 11-22.

Reineck, H. E., Singh, I. B., 1975. Depositional sedimentary environments. With reference to terrigenous clastics. 1 ed., Springer-Verlag New York Inc., Germany, 439 pp.

Renne, P. R., Zichao, Z., Richards, M. A., Black, M. T., Basu, A. R., 1995. Synchrony and causal relationships between Permian-Triassic Boundary crises and Siberian Flood Volcanism. Science, 269, 1413-1416.

Rey, K., Amiot, R., Fourel, F., Rigaudier, T., Abdala, F., Day, M. O., Fernandez, V., Fluteau, F., France-Lanord, C., Rubidge, B. S., Smith Roger, M. H., Viglietti, P. A., Zipfel, B., Lécuyer, C., 2015. Global climate perturbations during the Permo-Triassic mass extinctions recorded by continental tetrapods from South Africa. Gondwana Research.

Roopnarine, P. D., Angielczyk, K. D., Wang, S. C., Hertog, R., 2007. Trophic network models explain instability of Early Triassic terrestrial communities. Proceedings of the Royal Society Series B, 274, 2077-2086.

Rossouw, P. J., 1970. Freshwater mollusca in the Beaufort Series of southern Africa. In. Proceedings of the Proceedings 2nd IUGS Symposium on Gondwana Stratigraphy and Palaeontology. CSIR, Pretoria, 615-616.

Rubatto, D., 2002. Zircon trace element geochemistry: partitioning with garnet and the link between U–Pb ages and metamorphism. Chemical Geology, 184, 123-138.

Rubidge, B. S., 1988. A palaeontological and palaeoenvironmental synthesis of the Permian Ecca-Beaufort contact in the southern Karoo between Prince Albert and Rietbron, Cape Province, South Africa., PhD thesis, University of Port Elizabeth, 290 pp.

Rubidge, B. S., 1990. A new vertebrate biozone at the base of the Beaufort Group, Karoo Sequence (South Africa). Palaeontologia Africana, 27, 17-20.

Rubidge, B. S., Johnson, M. R., Kitching, J. W., Smith, R. M. H., Keyser, A. W., Groenewald, G. H., 1995. Biostratigraphy of the Beaufort Group (Karoo Supergroup). Biostratigraphic series 1, South African Committee for Stratigraphy.

Rubidge, B. S., Hancox, J. P., Catuneanu, O., 2000. Sequence analysis of the Ecca-Beaufort contact in the southern Karoo of South Africa. South African Journal of Geology, 103, 81-96.

Rubidge, B. S., 2005. 27th Du Toit Memorial Lecture: Re-uniting lost continents – fossil reptiles from the ancient Karoo and their wanderlust. South African Journal of Geology, 108, 135-172.

Rubidge, B. S., Erwin, D. H., Ramezani, J., Bowring, S. A., de Klerk, W. J., 2013. High-precision temporal calibration of Late Permian vertebrate biostratigraphy: U-Pb zircon constraints from the Karoo Supergroup, South Africa. Geology, 10, 1-4.

Rubidge, B. S., Day, M. O., Viglietti, P. A., Abdala, A., 2015. Recognising stratigraphic gaps in the Beaufort Group - consequences for basin modelling. In Linol, B., Miller, W., De Wit, M. J. (Eds). Proceedings of the Proceedings of the Cape-Karoo Imbizo conference. Nelson Mandela Metropolitan University, Port Elizabeth. .

Rust, B. R., 1981. Sedimentation in an arid-zone anastomosing fluvial system: Cooper's Creek, Central Australia. Journal of Sedimentary Research, 51, 745-755.

Ruta, M., Angielczyk, K. D., Fröbisch, J., Benton, M. J., 2013. Decoupling of morphological disparity and taxic diversity during the adaptive radiation of anomodont therapsids. Proceedings of the Royal Society of London B: Biological Sciences, 280, 1071-2013.

Rutherford, A. B., 2009. The sedimentology and stratigraphy of the Beaufort Group of the Karoo Supergroup in the vicinity of Thaba Nchu, central Free State Province.

Rutherford, A. B., Rubidge, B. S., Hancox, J. P., 2015. Sedimentology and palaeontology of the Beaufort Group in the Free State Province supports a reciprocal foreland basin model for the Karoo Supergroup, South Africa. South African Journal of Geology, 118, 355-372.

SACS. 1980. Stratigraphy of South Africa, Part 1 (Compiler LE Kent), Lithostratigraphy of the Republic of South Africa, South West Africa/Namibia, and the Republics of Boputhatswana, Transkei and Venda Geological Survey of South Africa Handbook, 8, 1-690.

Sahney, S., Benton, M. J., 2008. Recovery from the most profound mass extinction of all time. Proceedings of the Royal Society of London B: Biological Sciences, 275, 759-765.

Sahney, S., Benton, M. J., Falcon-Lang, H. J., 2010. Rainforest collapse triggered Carboniferous tetrapod diversification in Euramerica. Geology, 38, 1079-1082.

Sambrook-Smith, G. H., Ashworth, P. J., Best, J. L., Woodward, J., Simpson, C. J., 2006. The sedimentology and alluvial architecture of the sandy braided South Saskatchewan River, Canada. Sedimentology, 53, 413-434.

Sambrook-Smith, G. H., Ashworth, P. J., Best, J. L., Lunt, I. A., Orfeo, O., Parsons, D. R., 2009. The sedimentology and alluvial architecture of a large braid bar, Río Paraná, Argentina. Journal of Sedimentary Research, 79, 629-642.

Sambrook-Smith, G. H., Best, J. L., Ashworth, P. J., Lane, S. N., Parker, N. O., Lunt, I. A., Thomas, R. E., Simpson, C. J., 2010. Can we distinguish flood frequency and magnitude in the sedimentological record of rivers? Geology, 38, 579–582.

Scheepers, R., Armstrong, R., 2002. New U-Pb SHRIMP zircon ages of the Cape Granite Suite: implications for the magmatic evolution of the Saldania Belt. South African Journal of Geology, 105, 241-256.

Scheiber-Enslin, S.E.; Ebbing J. and Webb S.J. 2015. New depth maps of the main Karoo Basin, used to explore the Cape Isostatic Anomaly, South Africa. South African Journal of Geology, 118.3, 225-248.

Schumm, S. A., 1968. Speculations Concerning Paleohydrologic Controls of Terrestrial Sedimentation. Geological Society of America, 79, 1573-1588.

Seeley, H. G., 1892. Researches on the structure, organization, and classification of the Fossil Reptilia. Philosophical Transactions of the Royal Society of London, 182, 311-370.

Shanley, K. W., McCabe, P. J., 1994. Perspectives on the sequence stratigraphy of continental strata. AAPG Bulletin, 78, 544-568.

Shanley, K. W., McCabe, P. J., 1995. Sequence stratigraphy of Turonian-Santonian strata, Kaiparowits Plateau, southern Utah, USA: Implications for regional correlation and foreland basin evolution. In Van Wagoner, J. C., Bertram, G. T. (Eds): AAPG special volumes: Memoir 64, 103-136.

Shen, S., Crowley, J. L., Wang, Y., Bowring, S. A., Erwin, D. H., Sadler, P. M., Cao, C., Rothman, D. H., Henderson, C. H., Ramezani, J., Zhang, H., Shen, Y., Wang, X., Wang, W., Li, W., Tang, Y., Liu, X., Liu, L., Zeng, Y., Jiang, Y., Jin, Y. G., 2011. Calibrating the End-Permian mass extinction. Science, 334, 1367-1372.

Shishkin, M. A., Rubidge, B. S., 2000. A relict rhinesuchid (Amphibia: Temnospondyli) from the Lower Triassic of South Africa. Palaeontology, 43, 653-670.

Sloss, L. L., 1984. Comparative anatomy of cratonic unconformities. In Sloss, L. L. (Ed): Interregional Unconformities and Hydrocarbon Accumulation., 1-6.

Smith, R. M. H., 1980. The lithology, sedimentology and taphonomy of flood-plain deposits of the Lower Beaufort (Adelaide Subgroup) strata near Beaufort West. Transactions of the Geological Society of South Africa., 83, 399-413.

Smith, R. M. H., 1981. Sedimentology and taphonomy of the Lower Beaufort strata near Beaufort West, (Cape Province). MSc thesis, University of the Witwatersrand, 121 pp.

Smith, R. M. H., 1987. Helical burrow casts of therapsid origin from the Beaufort Group (Permian) of South Africa. Palaeogeography, Palaeoclimatology, Palaeoecology, 60, 155-169.

Smith, R. M. H., 1989. Fluvial facies, vertebrate taphonomy, and palaeosols of the Teekloof Formation (Permian) near Beaufort West, Cape Province, South Africa., PhD thesis, University of Cape Town, 450 pp.

Smith, R. M. H., 1990. Alluvial paleosols and pedofacies sequences in the Permian Lower Beaufort of the southwestern Karoo Basin, South Africa. Journal of Sedimentary Research, 60.

Smith, R. M. H., 1993a. Sedimentology and ichnology of floodplain paleosurfaces in the Beaufort Group (Late Permian), Karoo sequence, South Africa. Palaios, 8, 339-357.

Smith, R. M. H., 1993b. Vertebrate taphonomy of Late Permian floodplain deposits in the southwestern Karoo Basin of South Africa. Palaios, 8, 45-67.

Smith, R. M. H., Eriksson, P. G., Botha, W. J., 1993. A Review of the Stratigraphy and Sedimentary Environments of the Karoo-Aged Basins of Southern Africa. Journal of African Earth Sciences, 16, 143-169.

Smith, R. M. H., 1995. Changing fluvial environments across the Permian-Triassic boundary in the Karoo Basin, South Africa and possible causes of tetrapod extinctions. Palaeogeography, Palaeoclimatology, Palaeoecology, 117, 81-104.

Smith, R. M. H., Evans, S. E., 1996. New material of *Youngina*: Evidence of juvenile aggregation in Permian diapsid reptiles. Palaeontology, 39, 289-303.

Smith, R. M. H., Ward, P. D., 2001. Pattern of vertebrate extinctions across an event bed at the Permian-Triassic boundary in the Karoo Basin of South Africa. Geology, 29, 1147–1150.

Smith, R. M. H., Botha, J., 2005. The recovery of terrestrial vertebrate diversity in the South African Karoo Basin after the end-Permian extinction. Comptes Rendus Palevol, 4, 623-636.

Smith, R. M. H., Rubidge, B. S., Van der Walt, M., 2012. Therapsid Biodiversity Patterns and Paleoenvironments of the Karoo Basin, South Africa. In Chinsamy-Turan, A. (Ed): Forerunners of Mammals., 31-62 Indiana University Press, Bloomington.

Smith, R. M. H., Botha-Brink, J., 2014. Anatomy of a mass extinction: sedimentological and taphonomic evidence for drought-induced die-offs at the Permo-Triassic boundary in the main Karoo Basin, South Africa. Palaeogeography, Palaeoclimatology, Palaeoecology, 396, 99–118.

Söhnge, A. P. G., Hälbich, I. W., 1983. Geodynamics of the Cape Fold Belt: A Contribution to the National Geodynamics Programme. In.

Soman, A., Geisler, T., Tomaschek, F., Grange, M., Berndt, J., 2010. Alteration of crystalline zircon solid solutions: a case study on zircon from an alkaline pegmatite from Zomba–Malosa, Malawi. Contributions to Mineralogy and Petrology, 160, 909-930.

Stampfli, G. M., Hochard, C., Vérard, C., Wilhem, C., 2013. The formation of Pangea. Tectonophysics, 593, 1-19.

Stear, W. M., 1980. Channel sandstone and bar morphology of the Beaufort Group uranium district near Beaufort West. Transactions of the Geological Society of South Africa., 83, 391-398.

Stear, W. M., 1983. Morphological characteristics of ephemeral stream channel and overbank splay sandstone bodies in the Permian Lower Beaufort Group, Karoo Basin, South Africa. In Collinson, J. D. (Ed): Modern and ancient fluvial systems, Blackwell scientific publications. United Kingdom.

Stear, W. M., 1985. Comparision of bedform ditribution and the dynamics of the moderns and ancient sandsy ephemeral flood deposits in the southwestern karoo region, South Africa. Sedimentary Geology, 45, 209-230.

Sumida, S. S., Martin, K. L. M., 1997. Amniote Origins: Completing the Transition to Land., New York: Academic, 510 pp.

Sun, Y., Joachimski, M. M., Wignall, P. B., Yan, C., Chen, Y., Jiang, H., Wang, L., Lai, X., 2012. Lethally Hot Temperatures During the Early Triassic Greenhouse. Science, 338, 366-370.

Tabor, N. J., Montañez, I. P., Steiner, M. B., Schwindt, D., 2007. δ 13 C values of carbonate nodules across the Permian–Triassic boundary in the Karoo Supergroup (South Africa) reflect a stinking sulfurous swamp, not atmospheric CO 2. Palaeogeography, Palaeoclimatology, Palaeoecology, 252, 370-381.

Tankard, A. J., Jackson, M. P. A., Eriksson, K. A., Hobday, D. K., Hunter, D. R., Minter, W. E. L., 1982. Crustal evolution of southern Africa., Springer Science & Business Media.

Tankard, A. J., Welsink, H., Aukes, P., Newton, R., Stettler, E., 2009. Tectonic evolution of the Cape and Karoo basins of South Africa. Marine and Petroleum Geolology, 26, 1379-1412.

Tankard, A. J., Welsink, H., Aukes, P., Newton, R., Stettler, E., 2012. Geodynamic interpretation of the Cape and Karoo basins, South Africa. Phanerozoic passive margins, cratonic basins and global tectonic maps, Elsevier, 869-945.

Tarailo, D. A., Fastovsky, D. E., 2012. Post-Permo-Triassic terrestrial vertebrate recovery: southwestern United States. Paleobiology, 38, 644-663.

Theron, J., 1970. Some geological aspects of the Beaufort Series in the Orange Free State., PhD thesis, University of the Orange Free State, 270 pp.

Tibaldi, A. M., Otamendi, J. E., Cristofolini, E. A., Baliani, I., Walker, B. A., Bergantz, G. W., 2013. Reconstruction of the Early Ordovician Famatinian arc through thermobarometry in lower and middle crustal exposures, Sierra de Valle Fértil, Argentina. Tectonophysics, 589, 151-166.

Tooth, S., 2000. Process, form and change in dryland rivers: A review of recent research. Earth-Science Reviews, 51, 67–107.

Tordiffe, E. A. W., 1978. Aspects of the hydrogeochemistry of the Karoo Sequence in the Great Fish River Basin, Eastern Cape Province, with special reference to groundwater quality. , pp., PhD thesis, University of the Orange Free State, 307 pp.

Turner, B. R., 1978. Sedimentary Patterns of Uranium Mineralization in the Southern Karoo (Gondwana) Basin, South Africa. In Miall, A. D. (Ed): Fluvial Sedimentology, vol, 5, Canadian Society for Petroleum Geologists. 831-848.

Turner, B. R., 1979: Excursions Guidebook, Geocongress '79. In: Geological Society of South Africa, Port Elizabeth.

Turner, B. R., 1981. Revised stratigraphy of the Beaufort Group in the southern Karoo Basin. Palaeontologia Africana, 24, 87-98.

Turner, B. R., 1999. Tectonostratigraphical development of the Upper Karoo foreland basin: Orogenic unloading versus thermally-induced Gondwana rifting. Journal of African Earth Sciences, 28, 215-238.

Uličný, D., 1999. Sequence stratigraphy of the Dakota Formation (Cenomanian), southern Utah: interplay of eustasy and tectonics in a foreland basin. Sedimentology, 46, 807-836.

van der Walt, M., Day, M. O., Rubidge, B. S., Cooper, A. K., Netterberg, I., 2011. A new GIS-based biozone map of the Beaufort Group (Karoo Supergroup), South Africa. Palaeontologia Africana, 45, 1-5.

Van Eeden, O. R., 1972. The Geology of the Republic of South Africa: An Explanation of the 1 1000 000 Map, 1970 Edition. Vol. 18, Government Printer, South Africa.

van Hoepen, E. C. N., 1934. Oor die indeling van die Dicynodontidae na aanleiding van nuwe vorme.

Viglietti, P. A., Smith, R. M. H., Compton, J., 2013. Origin and palaeoenvironmental significance of *Lystrosaurus* bonebeds in the earliest Triassic Karoo Basin, South Africa. Palaeogeography, Palaeoclimatology, Palaeoecology, 392, 9-21.

Viglietti, P. A., Smith, R. M. H., Angielczyk, K. D., Kammerer, C. F., Fröbisch, J., Rubidge, B. S., 2016. The *Daptocephalus* Assemblage Zone (Lopingian), South Africa: A proposed biostratigraphy based on a new compilation of stratigraphic ranges. Journal of African Earth Sciences, 113, 153-164.

Vila, B., Sellés, A. G., Brusatte, S. L., 2015. Diversity and faunal changes in the latest Cretaceous dinosaur communities of southwestern Europe. Cretaceous Research.

Visser, J. N. J., Dukas, B. A., 1979. Upward-fining mega-cycles in the Beaufort Group, north of Graaff-Reinet, Cape Province. Transactions of the Geological Society of South Africa., 82, 149-154.

Visser, J. N. J., 1992. Deposition of the Early to Late Permian Whitehill Formation during a sea-level highstand in a juvenile foreland basin. South African Journal of Geology, 95, 181-193.

Visser, J. N. J., 1993. Sea-level changes in a back-arc-foreland transition: the late Carboniferous-Permian Karoo Basin of South Africa. Sedimentary Geology, 83, 115-131.

von Eynatten, H., Dunkl, I., 2012. Assessing the sediment factory: the role of single grain analysis. Earth-Science Reviews, 115, 97-120.

Vorster, C., 2013. Laser Ablation ICP-MS age determination of detrital zircon populations in the Phanerozoic Cape and Lower Karoo Supergroups (South Africa) and correlatives in Argentina., PhD thesis, University of Johannesburg, 626 pp.

Walker, R. G., 1984. Facies models, Second. ed. Geological Association of Canada, Canada.

Ward, P. D., Botha, J., Buick, R., de Kock, M. O., Erwin, D. O., Garrison, G. H., Kirschwick, J. I., Smith, R. M. H., 2005. Abrupt and gradual extinctions among Late Permian land vertebrates in the Karoo Basin, South Africa. Science, 309, 709-714.

Watson, D. M. S., 1914. II.—The Zones of the Beaufort Beds of the Karroo System in South Africa. Geological Magazine, New Series, Decade 6, 1, 203-208.

Weissmann, G. S., Hartley, A. J., Nichols, G. J., Scuderi, L. A., Olson, M., Buehler, H., Banteah, R., 2010. Fluvial form in modern continental sedimentary basins: distributive fluvial systems. Geology, 38, 39-42.

Weissmann, G. S., Hartley, A. J., Scuderi, L. A., Nichols, G. J., Owen, A., Wright, S., Felicia, A. L., Holland, F., Anaya, F. M. L., 2015. Fluvial geomorphic elements in modern sedimentary basins and their potential preservation in the rock record: A review. Geomorphology, 250, 187-219.

Welman, J., Loock, J. C., Rubidge, B. S., 2001. New evidence for diachroneity of the Ecca-Beaufort contact (Karoo Supergroup, South Africa). South African Journal of Science, 97, 320-322.

Wetherill, G. W., 1956. Discordant uranium-lead ages, In. Transactions American Geophysics Union, 37, 320-326.

White, L. T., Ireland, T. R., 2012. High-uranium matrix effect in zircon and its implications for SHRIMP U–Pb age determinations. Chemical Geology, 306, 78-91.

Wickens, H. d. V., 1996. Die stratigrafie en sedimentologie van die Ecca Groep wes van Sutherland., Pretoria.

Wignall, P. B., Hallam, A., 1992. Anoxia as a cause of the Permian/Triassic mass extinction: facies evidence from northern Italy and the western United States. Palaeogeography, Palaeoclimatology, Palaeoecology, 93, 21-46.

Wignall, P. B., Twitchett, R. J., 1996. Oceanic anoxia and the end Permian mass extinction. Science, 272, 1155-1158.

Willner, A. P., Gerdes, A., Massonne, H.-J., 2008. History of crustal growth and recycling at the Pacific convergent margin of South America at latitudes 29–36 S revealed by a U–Pb and Lu–Hf isotope study of detrital zircon from late Paleozoic accretionary systems. Chemical Geology, 253, 114-129.

Wilson, A., Flint, S., Payenberg, T., Tohver, E., Lanci, L., 2014a. Architectural styles and sedimentology of the fluvial Lower Beaufort Group, Karoo Basin, South Africa. Journal of Sedimentary Research, 84, 326-348.

Wilson, G. P., de Mar, D. G., Carter, G., 2014b. Extinction and survival of salamander and salamander-like amphibians across the Cretaceous-Paleogene boundary in northeastern Montana, USA. Geological Society of America Special Papers, 503, 271-297.

Wizevich, M. C., 1992. Sedimentology of Pennsylvanian quartzose sandstones of the Lee Formation, central Appalachian Basin: fluvial interpretation based on lateral profile analysis. Sedimentary Geology, 78, 1-47.

Wizevich, M. C., 1993. Depositional controls in a bedload-dominated fluvial system: internal architecture of the Lee Formation, Kentucky. Sedimentary Geology, 85, 537-556.

Woodhead, J. A., Rossman, G. R., Silver, L. T., 1991. The metamictization of zircon: radiation dose-dependent structural characteristics. American Mineralogist;(United States), 76, 74-82.

Wright, V. P., Marriott, S. B., 1993. The sequence stratigraphy of fluvial depositional systems: the role of floodplain sediment storage. Sedimentary Geology, 86, 203-210.

Yates, A. M., Neumann, F. H., Hancox, P. J., 2012. The earliest post-Paleozoic freshwater bivalves preserved in coprolites from the Karoo Basin, South Africa. PloS one, 7, 1-9.

Zeh, A., Gerdes, A., Klemd, R., Barton, J. M., 2008. U-Pb and Lu-Hf isotope record of detrital zircon grains from the Limpopo Belt – Evidence for crustal recycling at the Hadean to early Archean transition. Geochimica et Cosmochimica Acta, 72, 5304-5329.

Zerfass, H., Chemale, F., Schultz, C. L., Lavina, E. L., 2004. Tectonics and sedimentation in Southern South America during Triassic. Sedimentary Geology, 116, 265–292.